GEM TN-93-426

GEM Collaboration Meeting

University of California, San Diego

Radisson Hotel
La Jolla, California

May 9-12, 1993

Abstract;

Agenda, attendees and presentations of the GEM Collaboration Meeting held at the Radisson Hotel in La Jolla, CA, May 9-12, 1993.

GEM COLLABORATION MEETING
University of California, San Diego
May 9 through 12, 1993

Unless otherwise noted, all meetings are at
Radisson Hotel in La Jolla

Sunday, May 9

Informal meetings

4-6 Registration, get-together with refreshments by the pool

Monday May 10 - Plenary Session

Morning session	Chair: Hans Kobrak
8:30 Welcome -	Roger Dashen
8:45 Report of the Council Chair -	Yost
9:00 The State of GEM -	Barish
9:45 Report on the TDR -	Newman
10:30 Break	
10:45 Calorimetry: Present Status, Evolutionary Path-	
Overview of Liquid Calorimeter -	
Parameters, Design Status, Expected Performance -	Lissauer (20)
Overview of Scintillating Calorimeter -	
Parameters, Design Status, Expected Performance -	Kamyshkov (10)
Calorimetry Physics Performance Overview -	Womersley (15)
Overview of the Forward Calorimetry -	Rutherfoord (20)
Muons in the Calorimeter -	Efremenko (10)
12:00 Lunch	

Afternoon session	Chair: Jenny Thomas
1:00 Muons: Present status,	
Evolutionary Path -	
Overview of System and Design Choices -	Taylor (20)
Chamber and Alignment Details -	Mitselmakher (20)
Layout of Chambers and Support Structure -	Nimblett (20)
2:00 Tracker: Present Status, Evolutionary path -	Baltay
	Lee
	Musser
3:00 GEM Cost/Schedule Baseline and SSC Stretchout Schedule -	Sanders
3:30 Configuration Management -	Gober
3:50 GEM Activation Uaing CINDER -	Waters
4:00 Adjourn Plenary Session	
4:15 Executive Committee, other meetings	

Tuesday May 11 - Parallel Sessions

Preparations for the PAC review May 24-28

Morning sessions

8-12 Magnet, muons, calorimetry, central tracker, and electronics groups prepare for the PAC presentations.

Convenors: subsystems leaders.

Afternoon sessions

1-2 Continuation of morning sessions; followed by sessions on integration and assembly schedule, detector optimization, cost/schedule, and management/resources

2-5:30 The convenors of these sessions will be named later.

6:30 Banquet 6:30 PM

Wednesday May 12 - Plenary Session

Morning session		Chair: Xiaorong Shi
8:30	Electronics, DAQ	Marlow(30)
9:00	Computing	
	Introduction -	Sheer(5)
	Future Directions in GEM Computing -	Word (25)
	GEM Detector Simulations -	Womersley (20)
	Common GEM/SDC Computing Issues -	Hilgart (10)
10:00	Break	
10:15	Physics with GEM report -	
	Physics at the SSC -	Lane (5)
	GEMFAST -	Skwarnicki (15)
	Higgs Physics -	Zhu (25)
	Top, H^+ Physics -	Yanagisawa (15)
	Jet Physics, e/h -	Womersley (15)
	Physics at 10^34 -	Lane (15)
	Missing E_T, SUSY	Vanyashin (15)
	Detector Optimization^I -	Zhou (20)
12:20	lunch	
Afternoon session		Chair: George Yost
1:30	The Incompleteness of the Higgs Sector and the Supercollider -	J. Kuti
2:30	Summaries of Working Groups' Results Calorimetry -	Willis
	Muons -	Taylor
	Tracker -	Brau
4:00	break	
4:20	N and Gamma Leakage in the Forward Calorimeter Region -	Moore
4:40	GEMGEN -	Sheer
5:00	Summary of the meeting -	Barish
5:30	Adjourn San Diego meeting	

Presentation by:

G. Yost

GEM COLLABORATION

MAY 10-12, 1993
San Diego

TDR submitted to SSCL April 30.
600+ pages

1010 Collaborators (456 @U.S.)
114 Institutions (48 U.S.)
17 Countries

Copies will be distributed here Tuesday.

- 1 copy per registrant will be distributed at the registration desk.

(Extra copies, if any, will be distributed Wednesday afternoon)

GEM Organization Plan (chapter 14 of TDR) was adopted by unanamous vote of the Council (> 30 institutions voted).

- "Permanent" Spokesman/men will be selected soon after TDR is approved
- "Permanent" Project Manager will be nominated for vote by Council in the fairly near future. Search Committee is already at work.
- Chief Engineer will be nominated for vote of Council.

A few practical matters:

- Please register, to help defray the costs of the meeting, help pay for the color covers of the TDR, and to receive a copy of the TDR.
- Meeting rooms for tomorrow's meetings will be assigned today by Holly Durden. If you are organizing a meeting, please be sure to contact her to get a room assigned. There are a few break-out rooms for small, spontaneous, meetings. All meetings will be in this hotel unless the number of meetings becomes too large.

- Please register for the banquet and get your ticket(s) today so we can tell them a head count.

Lunches:

Humphreys; Shooters in the hotel.
Capacity of Humphreys ≈ 85; reservations for lunch strongly recommended.

Walking distance (≤ 5 minutes)

El Torito
Elephant Bar
Samson's
St. Germaine's Deli
} see directions in the FYI.

TGIF (turn left, 1 block up hill)

Driving to Campus: You probably can't park. Physics Bldg is 15 minute walk from Radisson.

Reminder: Next Council Meetings

June 30 (Wed.)

Aug 5

Sep 30

Dec 2

5

B. BARISH

GEM Collaboration Meeting

SAN DIEGO

10 MAY 93

Status of GEM

- TDR Submitted April 30
  - Supplemental documents
    - Project Management Plan
    - Safety
    - Cost / Schedule

Some highlights –

			LOI
WHO	1010	Collaborators	(710)
	114	Institutions	(93)
	17	Countries	(15)
	458	U.S. Collaborators	(340
	48	" Institutions	(44)

[GEM Organization]

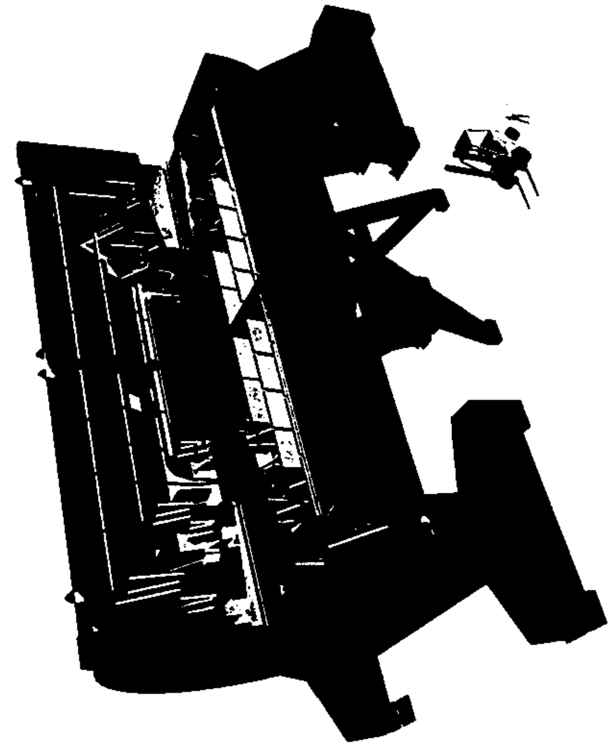

12

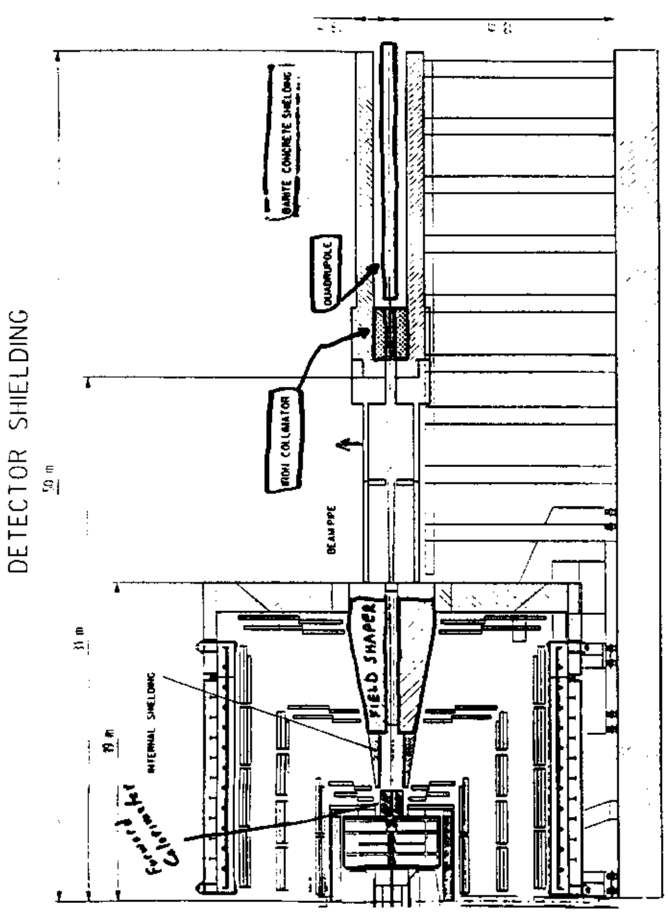

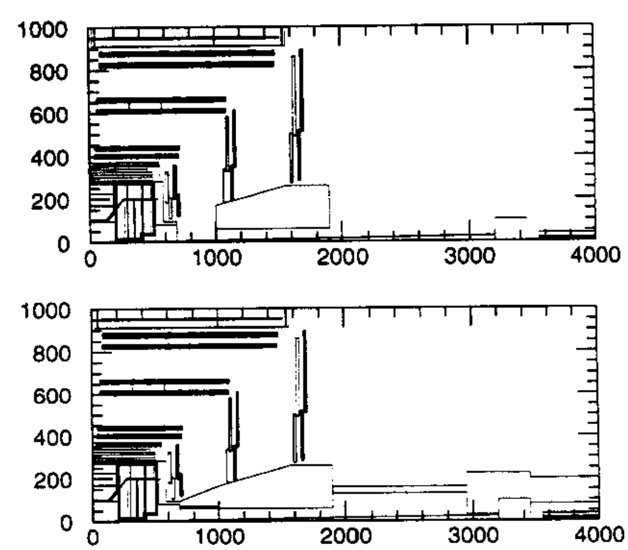

Neutrons 10^{n} cm^{-2} ssc y^{-1}

$E_n > 10^{-3}$ eV

11

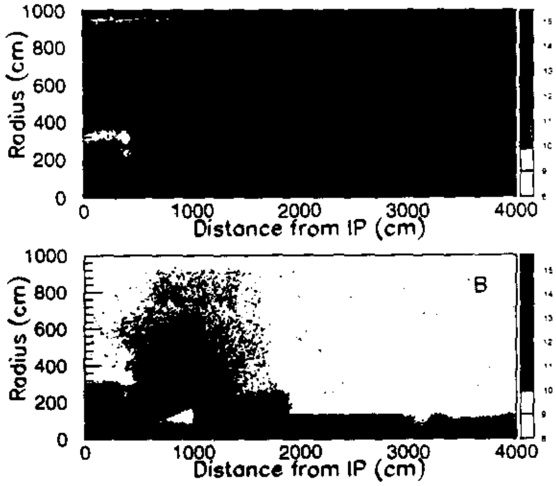

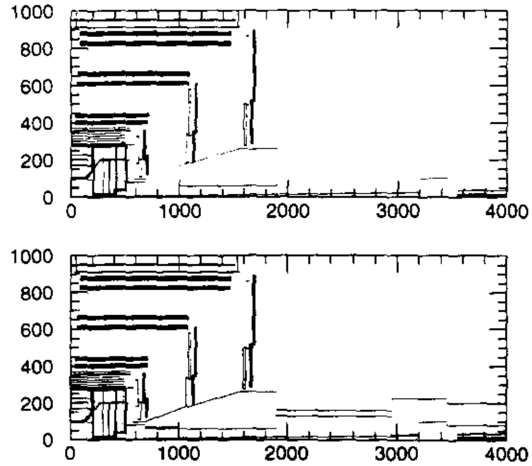

photons 10^{n} cm^{-2} $sscy^{-1}$

$E_{\gamma} > 10$ keV

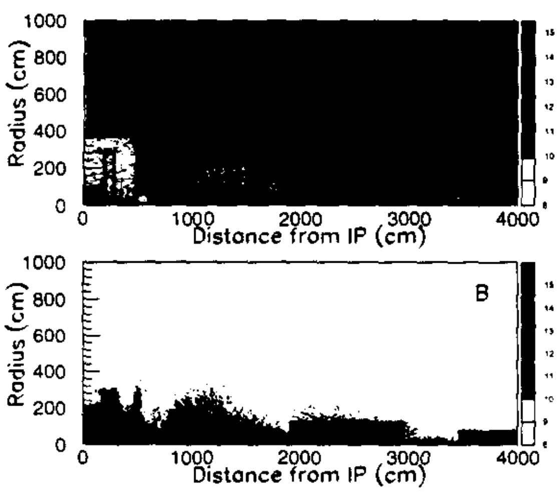

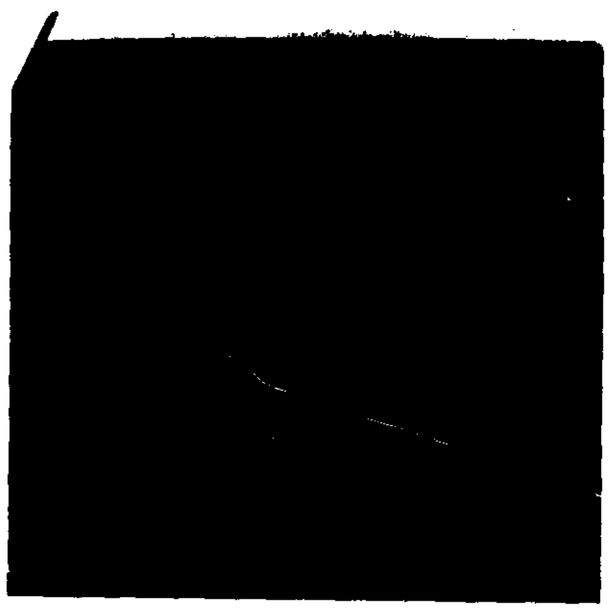

VMS
93-4-42-7

19

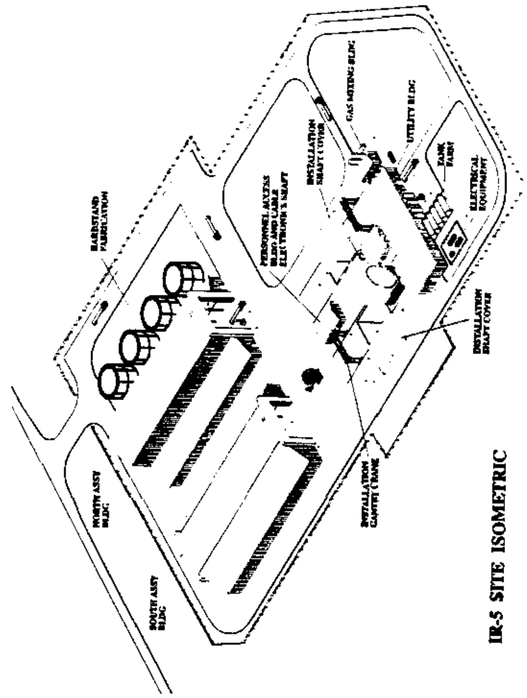

20

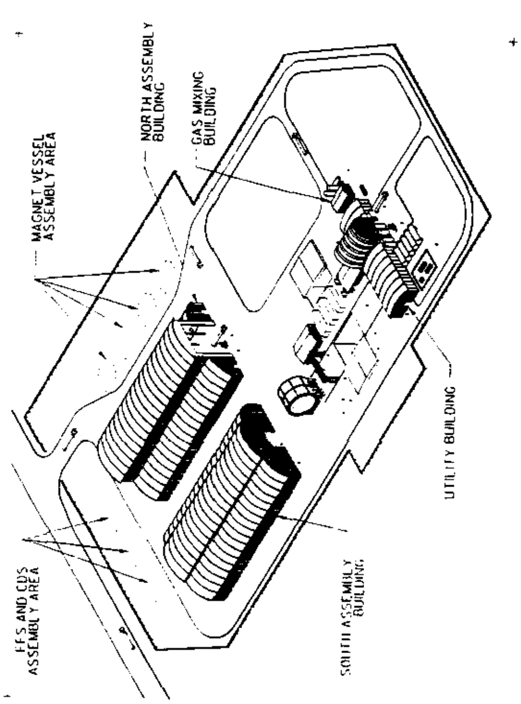

21

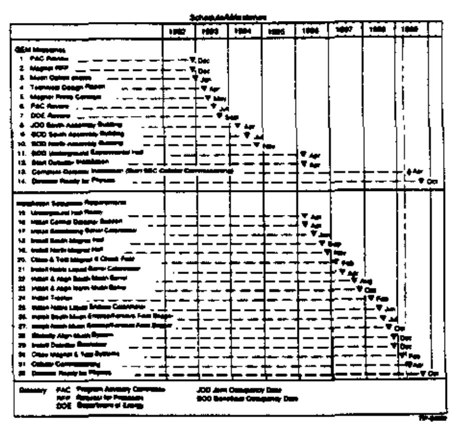

FIG. 16-1. Milestones in the GEM project.

22

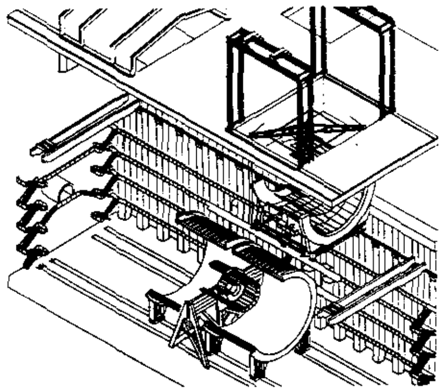

FIG. 9-15. South barrel muon installation.

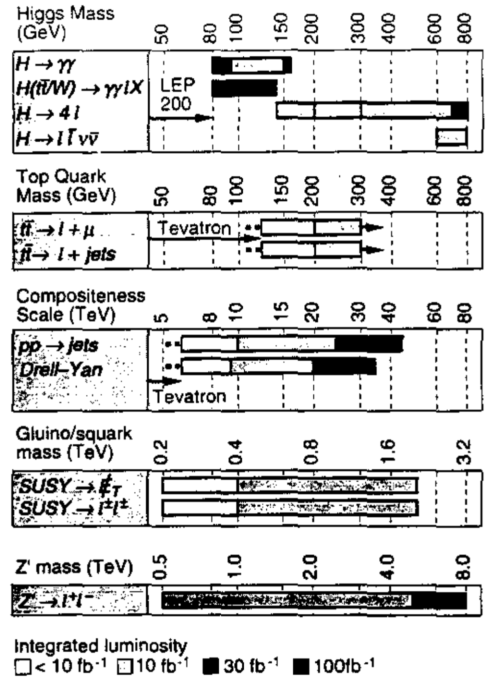

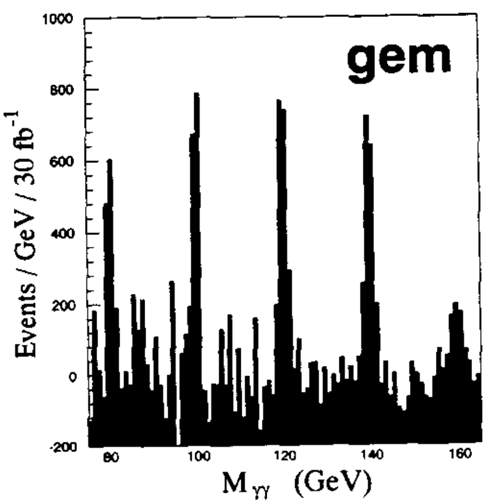

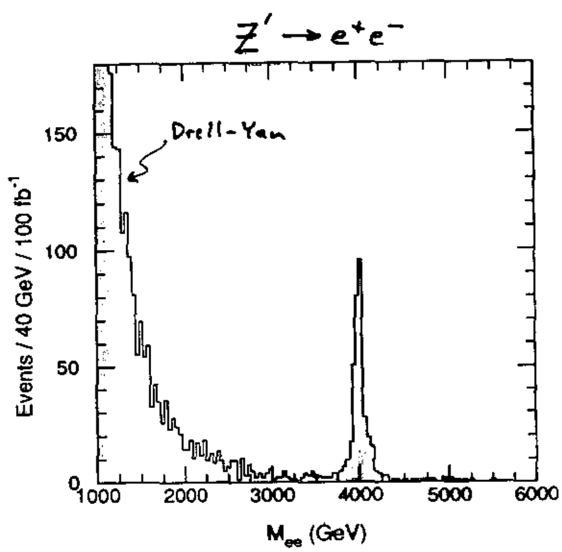

High Luminosity $\mathcal{L} = 10^{34}\ cm^{-2}s^{-1}$

Model : SO(10) Pythia width 80 GeV

$|\eta| < 2.5$ $E_e > 60$ GeV

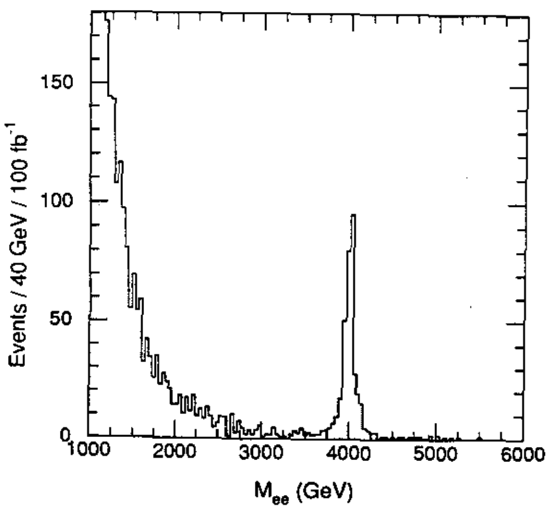

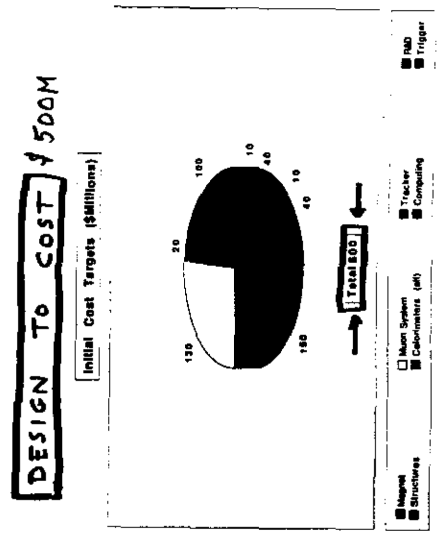

28

GEM COST REVIEW SUMMARY
December 15, 1991
(with Liquid Argon, LSDT Option)
(Costs in millions of dollars)

Procurements/Fabrication	196	
Installation/Assembly	73	
Subtotal (Procurements and Labor)	269	
EDIA	93	(34%)*
Direct Costs	362	
Contingency	112	(31%)
Subtotal	474	
R&D	37	(14%)
Total Detector FY91 $M	510	

* % of subtotal (Procurement and Labor)

GEM COST ESTIMATE SUMMARY
June 23, 1992
(with Liquid Argon, LSDT Option)
(Costs in millions of FY90 dollars)

Procurements/Fabrication	197	
Installation/Assembly	58	
Subtotal (Procurements and Labor)	255	
EDIA	113	(44%)*
Direct Costs	368	
Contingency	97	(26%)
Subtotal	465	
R&D	25	(10%)
Total Detector FY90 $M	490	

* % of subtotal (Procurement and Labor)

30

GEM DETECTOR SYSTEM COST ESTIMATE SUMMARY

22-Apr-93

(Costs in millions of FY90 dollars)

Procurements/Fabrication	228	
Installation/Assembly	51	
Subtotal (Procurements and Labor)	279	
EDIA	101	(36%)*
Direct Costs	380	
Contingency	93	(24%)
Subtotal	473	
R&D	26	(9%)*
TOTAL GEM DETECTOR SYSTEM FY90 $M	499	

* % of subtotal (Procurements and Labor)

31

WHAT'S NEXT ??

- **ES + H**: Preliminary Review
  "Good start, but ...."
- **Cost/Schedule**: Preliminary Review
  ONLY MUON, CALORIMETRY
- **TDR Review**: SSCL 24-28 May
  PAC + Consultants
  ⇓ ?
  PAC Santa Fe
  1 August
  ⇓ ?
  DoE Lehman Review
  Oct - Nov ?

32

PAC Review
24-28 May

DAY 1: Plenary Presentation of TDR

DAY 2,3: Parallel Sessions on Subsystems

- (A) Magnet (Reardon)
- (B) C.Tracking (Baltay)
- (C) Calorimeters (Willis)
- (D) Muons (Taylor)
- (E) Electronics/DAQ/Computing (Marlow)

DAY 4,5: Parallel Sessions on Global Issues

- (F) Installation/ES+H/Facilities (Harris)
- (G) Physics Performance/Detector optimization/Triggers (Barish)
- (H) Cost/Schedule (Sanders)
- (I) Organization/Management/Resources (Wi

33

Other News

- **SSC political**
- **Stretch out**
  1999 → 2002
  $8.4M → $10.3M ?
  re-baseline
  (effect on GEM)
- **Letter/Meeting**
  Willis + Barish w/ Schwitters
- **GEM Budget** FY93
  FY94 ?
- **Project Organization**
  PM Search
  Management Plan
  Subsystems organization
  ↓ timescale (evolve)
  DoE TDR Review

34

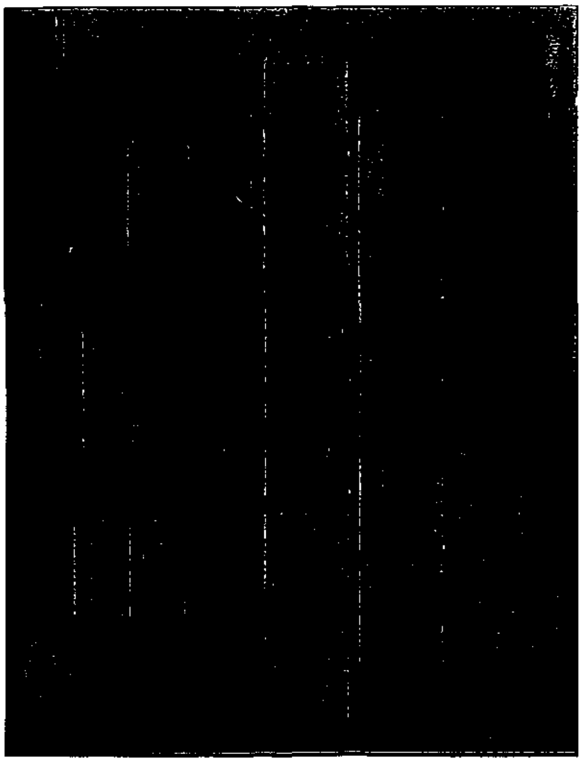

35

2-4 Summary and overview of the detector

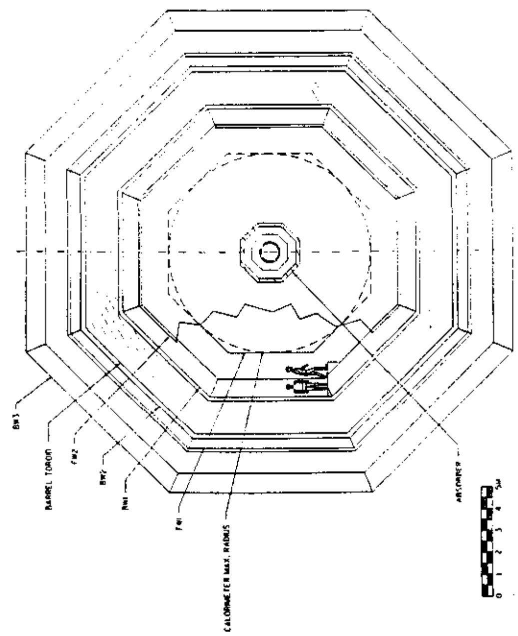

FIG. 2.3. End view of the preliminary baseline detector configuration.

36

— Future —

- TDR Represents "Baseline 2"
  - → Configuration Management (Change Control Procedures)
- MOU's with GEM groups
  - → Questionnaire / N. Baggett
- Dubna SSC Mtg (2-4 June)
  - → GEM Mtg @ ITEP 5 June (Exec Comm) 6 June (Technical)

  GEM Exec Comm + Ext Calorimeter Gp + Russian Collaborators
- Long Range Plans
  - → Magnet ⇒ prime contractor (2yr delay? Budgets)
  - → CDS + Scint Barrel Calorimeter (Early Installation)
  - → Fermilab Test Beam Program ('95 ⇒)
    - Large Scale Subsystem Tests
    - 18° Sector of GEM tracker/calorimeter/μ's

37

THIS MEETING

TDR Discussions

- Progress in Subsystems
  Project
  Physics
- Plans for PAC review
  (draft agenda tonite)
  (tomorrow planning sessions)

38

Let's do this again next year
Milind Diwan

GEM-TN-93-262

GEM

TECHNICAL DESIGN REPORT

Submitted by the

GAMMAS, ELECTRONS, AND MUONS COLLABORATION

to the

SUPERCONDUCTING SUPER COLLIDER LABORATORY*

April 30, 1993

GEM TDR

		Pages	Figures	Tables	Lead Authors
	Collaboration List	5			Barish, Yost
	Preface	3			Lane
1	Overview	17	10	7	Barish
2	Physics Performance	63	58	17	Lane, Paige
3	Magnet	32	23	9	Stroynowski
4	Muon Spectrometer	104	80	22	Taylor, Marx
5	Calorimeters	80	57	13	Gordon, Willis
6	Tracker	59	61	31	Baltay, Morgan
7	Electronics, Trigger, DAQ	86	60	26	Marlow, Shaevitz
8	Computing, Controls, Networking	38	6	9	McFarlane
9	Facilities, Assembly and Installation	31	18		Harris
10	Access, Maintenance and Operations	17	3	3	Harris
11	Detector/Beamline Interface	6	4	2	Morgan, Chapman
12	Radiation Environment and Shielding	24	17	8	Diwan, Waters, Fisyak
13	Beam Testing and Calibration	10	7	1	Yost
14	GEM Organization Plan	5			Baltay
15	Environment, Safety, and Health	25			Woolley
16	Cost/Schedule Baseline Summary	3	1	1	Sanders
	TOTALS	623	406	139	

GEM TDR SCHEDULE:

APRIL 30.

DONE !

MILESTONE DUE DATES	
Intermediate Drafts	12/18, 1/20, 2/17
GEM Internal Board Reviews Completed	1/8, 2/3, 3/1
Final Draft for Review	3/15
Final GEM Internal Review Completed	3/26
Finished Chapters: All Text and Figures	4/9
Document Complete; Submitted To SSCL	4/30

Figures Received

- > 895 Figures received for processing + ~ 50 iges files
  - Figures were provided in the following formats
    - AutoCad, Canvas, Claris CAD, Deltragraph, dgn, dxf, eps, Framemaker,iges, Intergraph Microstation, Kaleidagraph, MacDraw II, MacDraw pro, MacProject, MacSchedule, Microsoft Excel, Microsoft Word, pict, printed copies, ps, rtf
- To simplify originators work, all these formats were converted.
- This work required the use of 26 separate programs.

GEM TDR TEAM

- **PRODUCTION GROUP:**

  SSC (GEM): H. Durden, C. Thomas, L. Fowler, D. Compton;
  SSC (TIP): A. Alcorn, E. Banzon, T. Coyne, E. Engebretzen, K. Barker, S. Lee, M. McCormick
  Caltech/SSC: R. Harder

- **EDITORIAL BOARD:**

  N. Baggett, O. Fackler, K. Morgan, H. Newman, F. Paige, J. Reidy, J. Womersley, G. Yost

- **FIGURE CZARS:**

  O. Fackler, J. Reidy

- **REVIEW/EDITORIAL BOARD:**

  B. Barish, J. Brau, G. Deis, M. Diwan, Y. Fisyak, K. Freeman, V. Gavrilov, V. Glebov, H. Gordon, Y. N. Guo, M. Harris, D. Marlow, M. Marx, K. McFarlane, C. Milner, M. Mitselmakher, R. Mount, R. Panvini, R. Shypit, F. Plasil, R. Shang, M. Shaevitz, P. Slattery, R. Stroynowski, F. Taylor, J. Thomas, H. Uijterwaal, A. Vanyashin, W. Willis, C. Wuest

Figure Processing

- Figure file types were converted to Adobe Illustrator format--approximately twice the number used in the TDR. In the worst case, 3 intermediate conversion programs were required.
- Some figures required scanning followed by tracing over the scanned template in Adobe Illustrator.
- Once in Adobe Illustrator format, they were redrawn to conform with our standards. Almost all graphs required some redrawing.
- ... were converted to eps for importation
- ... cut and pasted due to file ...

47

Figure Processing Procedure

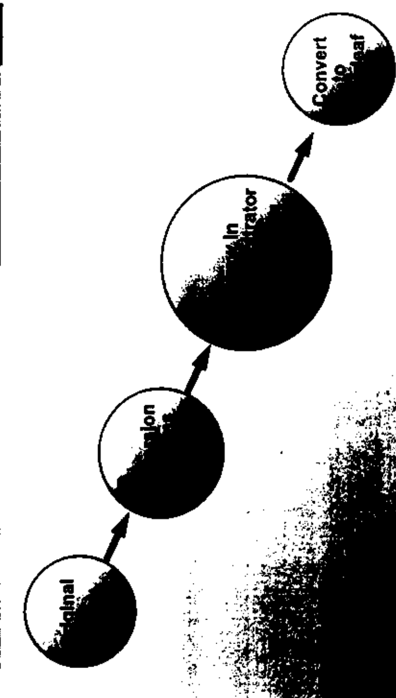

48

SEPARATE DOCUMENTS		
Project Management Plan		Sanders, Baltay
Cost/Schedule Baseline and WBS Dictionary		Sanders
Preliminary Safety Analysis Report		Woolley
Detector Upgrades and Staging Options	May 93	Willis

49

PREFACE

The theoretical elements of the standard $SU(3) \otimes SU(2) \otimes U(1)$ gauge model of strong and electroweak interactions have been in place for more than 20 years.[1,2] In all this time, the standard model has withstood extremely stringent experimental tests.[3] Down to at least 10^{-16} cm, the basic constituents of matter are spin-$\frac{1}{2}$ quarks and leptons. These interact via the exchange of spin-one gauge bosons: the massless gluons of QCD and the massless photon and massive $W^{\pm}$ and Z^0 bosons of electroweak interactions. There are six flavors each of quarks and leptons—identical except for mass, charge and color—grouped into three generations. All the fermions have been found except for the top quark and the tau neutrino.[4,5] If the number of quark-lepton generations is equal to the number N_ν of light neutrinos, then there are no more than these three. The evidence for this comes from precision measurements of the Z^0 at LEP, which give $N_\nu = 2.99 \pm 0.04$ in the standard model.[5]

The unbroken nature of the QCD gauge interaction and its ground state makes quarks and gluons almost noninteracting at small distances, while it confines them at large distances into color-singlet hadrons. Even though gauge bosons necessarily begin without mass, interactions can make them heavy. This is what happens to the $W^{\pm}$ and Z^0 bosons: electroweak gauge symmetry is spontaneously broken, a phenomenon known as the "Higgs mechanism".[6] Finally, fermions in the standard model also must start out massless. To make quarks and leptons massive, new forces beyond the $SU(3) \otimes SU(2) \otimes U(1)$ gauge interactions are required. These additional interactions explicitly break the fermions' flavor symmetry and communicate electroweak symmetry breaking to them.

Despite this great body of knowledge, the interactions underlying electroweak and flavor symmetry breakdowns remain unknown. The most important element still missing from this description of particle interactions is directly connected to electroweak symmetry breaking. This may be a single new particle—the "Higgs boson"; several such bosons; a replication of all the known particles; an infinite tower of new resonances; or something still unimagined. It is also unknown whether the new interactions required for flavor symmetry breaking need additional new particles for their implementation. Until the new dynamics are known, it seems impossible to make further progress in understanding elementary particle physics.

One very important aspect of electroweak symmetry breaking is known: its characteristic energy scale of 1 TeV. This scale is set by the decay constant of the three Goldstone bosons transformed via the Higgs mechanism into the longitudinal components, $W_L^{\pm}$ and Z_L^0, of the weak gauge bosons:

$$F_\pi = 2^{-\frac{1}{4}} G_F^{-\frac{1}{2}} = 246 \text{ GeV}.$$

New physics must occur near this energy scale. New particles produced in parton scattering processes at this energy may appear as fairly distinct resonances in weak gauge boson or fermion-antifermion final states, or only as relatively featureless enhancements of W_L and Z_L boson production or of missing energy. Whatever form they take, it is the energy scale of 1 TeV and the size of typical QCD and electroweak cross sections at this energy, $\sigma \simeq 1$ nb – 1 fb, that determine the energy and luminosity requirements of the SSC: $\sqrt{s} = 40$ Tev and $\mathcal{L} = 10^{33}-10^{34}$ cm^{-2} s^{-1}.[7]

The energy scale of flavor symmetry breaking is not known. It may lie anywhere from just above the weak scale, 1 TeV, up to the Planck scale, 10^{16} TeV. There is the possibility that the SSC will shed light on the flavor problem, but no guarantee. Several examples accessible at the SSC are introduced below and discussed in Chapter 2. Their production cross sections range from quite large ($\sim 1-10$ nb) to very small ($\sim 1-10$ fb). Finding the rare processes will require the full SSC energy and the maximum possible luminosity.

50

GEM'S STRENGTHS: PHYSICS CAPABILITY

- NEW PHYSICS: Clean, High Resolution Lepton and Photon Measurements
- Higgs Detection Over The Full Range:
  Low Mass: $H^0 \to \gamma\gamma, \ell\gamma\gamma;\ \ell^+\ell^-\ell^+\ell^-$;
  High Mass: $H^0 \to \ell^+\ell^-\ell^+\ell^-;\ \ell^+\ell^- jj, \ell^+\ell^-\nu\bar{\nu}$
- Quick Discovery of Top;
  Charged Higgs in $t \to H^+ b;\ H^+ \to \tau^+\nu$
- Squarks, Gluinos Up To the TeV Range: Jets, $\not{E}_T$; Isolated Lepton Veto for $t\bar{t}$; Like-Sign Dileptons
- Quark Substructure To $\Lambda = 25$ TeV: Jets, E_T
- Z' to 8 TeV: $Z' \to e^+e^-$ Width;
  $Z' \to \mu^+\mu^-$ F-B Asymmetry At $\mathcal{L} = 10^{34}$
- Quark-Lepton Compositeness to $\Lambda =$ 30-35 TeV:
  $q\bar{q} \to \mu^+\mu^-$ F-B Asymmetry At $\mathcal{L} = 10^{34}$

21

Several scenarios have been proposed for electroweak and flavor symmetries, and their breaking:

- Standard Higgs models, containing one or more elementary Higgs boson multiplets. These are generally complex weak doublets. The minimal model has one doublet, with a single neutral boson H^0.
- Supersymmetry. In the minimal supersymmetric standard model there are two Higgs doublets, and every known particle has a superpartner.
- Models of dynamical electroweak and flavor symmetry breaking. The most studied proposal is technicolor-plus-extended-technicolor, with one doublet or one family of technifermions.
- Composite models, in which quarks and leptons are built of more fundamental constituents.

None of these proposals is fully satisfactory. In elementary Higgs boson models, whether supersymmetric or not, there is no explanation of why electroweak symmetry breaking occurs and why it has the scale F_π. In non-supersymmetric models, the Higgs boson's mass, M_H, and its vacuum expectation value, $v \simeq F_\pi$, are unstable against radiative corrections. There is no natural reason why these two parameters should be very much less than the energy scale at which the essential physics of the model changes, e.g., a unification scale or the Planck scale.[8] This radiative instability may be cured because standard model interactions look supersymmetric down to about 1 TeV, where soft supersymmetry breaking effects become important. This is the motivation for supersymmetry at the electroweak scale.[9,10] A further problem is that elementary Higgs boson models are known to be "trivial", i.e., they cannot make sense as interacting field theories with the cutoff taken to infinity.[11] This means that elementary Higgs models are effective theories, meaningful only below some cutoff Λ at which new physics sets in. Obviously, Λ must be somewhat greater than M_H for the effective theory to make sense. For a modest separation of these energies, $M_H <$ few $\times \Lambda$, both perturbative and lattice gauge calculations give $M_H \lesssim 650$ GeV in the minimal one-doublet model with F_π fixed at 246 GeV.[12] Finally, elementary Higgs models provide no clue to the meaning of flavor symmetry and the origin of its breaking. The flavor-symmetry breaking Yukawa couplings of the Higgs boson to fermions are arbitrary free parameters.

Despite these apparent problems, the standard Higgs boson, H^0, charged Higgses, $H^\pm$, and the supersymmetric partners of all the known particles may exist and must be sought. However, if something like the standard H^0 is found and is heavier than about 700 GeV, experiments must have the capacity to discover the additional, unspecified new physics that surely exists in the same energy region, of order 1 TeV.

Dynamical theories of electroweak and flavor symmetries—technicolor and extended technicolor—address these shortcomings of the elementary Higgs boson models.[13] However, they do so at the heavy price of introducing flavor-changing neutral currents that are too large, and pseudo-Goldstone bosons (technipions) that are too light.[14] These difficulties have been mitigated, but only by invoking an unfamiliar strong dynamics.[15,16] Further, it is difficult to build realistic models; most simple technicolor models appear to be in conflict with precision tests of the electroweak interactions.[3] Realistic models of composite quarks and leptons are similarly difficult to construct.[17] Therefore, no compelling models of dynamical electroweak and flavor symmetry breaking exist. Nevertheless, model-independent phenomenological programs do exist for testing such models at the SSC.[7]

These difficulties have led to the widespread belief that none of the familiar descriptions of electroweak and flavor symmetry breaking is entirely correct. This is, in fact, the most exciting aspect of SSC physics. We know that there is new physics in the TeV energy regime and that the SSC can reach it. We do not know exactly what form it will take. The models are invaluable because they furnish a wide range of predicted signals and backgrounds. These provide a testing ground to guide the design, and to help ensure the discovery potential, of large detectors such as GEM. An overview of the GEM detector is presented in Chapter 1 and GEM's capabilities for a representative sample of processes involving photons, electrons, muons, jets and missing energy are examined in Chapter 2. Whatever physics lies in the TeV region, its signals and backgrounds are bound to be similar to some of those studied there.

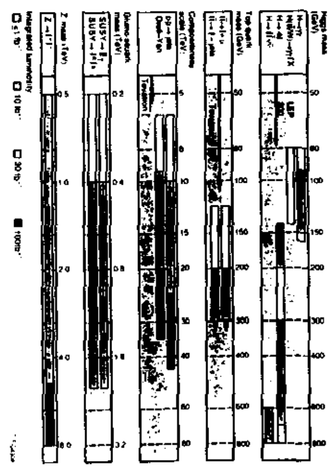

GEM TDR

- A MAJOR STEP TOWARDS GEM APPROVAL
- AN INFORMATION RESOURCE
  - For Existing GEM Groups: Greater Interaction
  - Education of New and Prospective Collaborators, Vendors and Industry
  - Figures and Tables for Presentation
- A LEARNING EXPERIENCE:
  - GEM's Strengths
  - Areas for Improvement

GEM's Sensitivity to SM Higgs

M_H	$\int \mathcal{L}dt$	$\gamma\gamma$	$\gamma\gamma\ell$	$\ell\ell\ell\ell$	$\ell\ell jj$	$\ell\ell\nu\nu$	Combined
80 GeV	30 fb^{-1}	3.9σ	4.5σ				6.3σ
90 GeV	30 fb^{-1}	4.9σ	4.9σ				7.2σ
100 GeV	10 fb^{-1}	4.6σ	2.9σ				5.8σ
120 GeV	10 fb^{-1}	7.8σ	2.7σ				8.5σ
140 GeV	10 fb^{-1}	9.0σ	2.3σ	11σ			15σ
150 GeV	10 fb^{-1}	7.3σ		13σ			15σ
160 GeV	10 fb^{-1}	3.2σ		8.1σ			8.9σ
170 GeV	10 fb^{-1}			5.7σ			5.7σ
180 GeV	10 fb^{-1}			10σ			10σ
200 GeV	10 fb^{-1}			38σ			38σ
400 GeV	10 fb^{-1}			28σ			28σ
600 GeV	10 fb^{-1}			9.7σ			9.7σ
800 GeV	10 fb^{-1}			4.7σ*	5.4σ*	11σ*	??
800 GeV	10 fb^{-1}			4σ**	2σ**	7σ***	9σ**

* Statistical only.

** Including systematic uncertainty.

*** Systematics included, assuming $\not{E}_t$ under control.

10 fb^{-1} will cover 100 GeV < M_H < 800 GeV.

30 fb^{-1} is needed to cover 80 GeV < M_H < 100 GeV.

55

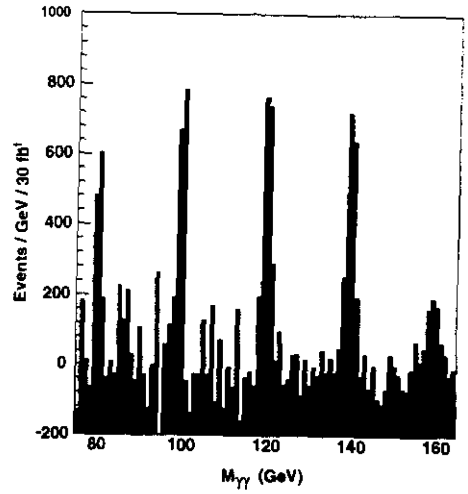

56

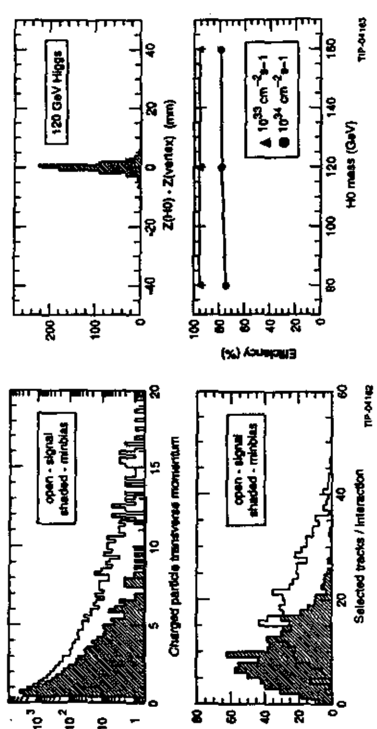

FIG. 6-23. (a) The difference in mm between the z coordinate of the true H^0 production vertex and the reconstructed primary vertex selected by choosing the vertex made up of tracks with the highest Σp_T for a 120-GeV standard model Higgs. (b) Vertex tagging efficiency as a function of the standard model Higgs mass and luminosity.

FIG. 6-22. (a) The transverse momentum spectrum for p_T > 0.5 GeV isolated charged tracks from standard model Higgs production (open histogram) for M_H = 120 GeV, and minimum bias events (hashed histogram) produced using the PYTHIA Monte Carlo. (b) The number of these tracks per event from standard model Higgs production (open) and minimum bias events (hashed).

57

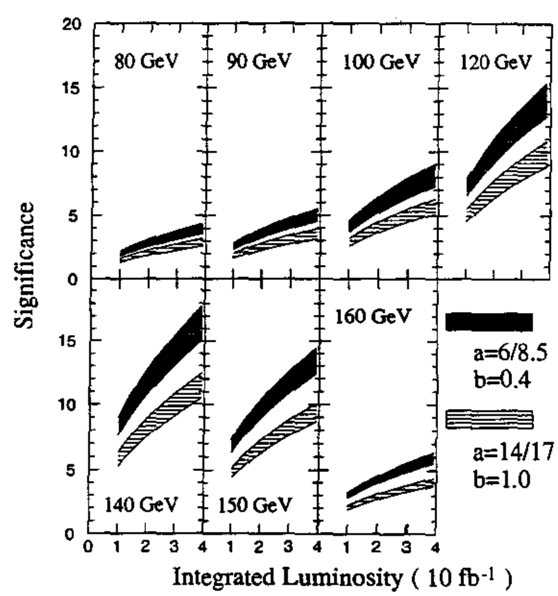

58

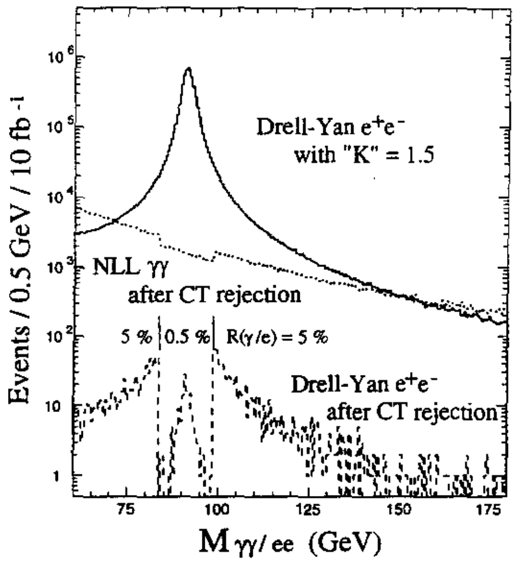

59

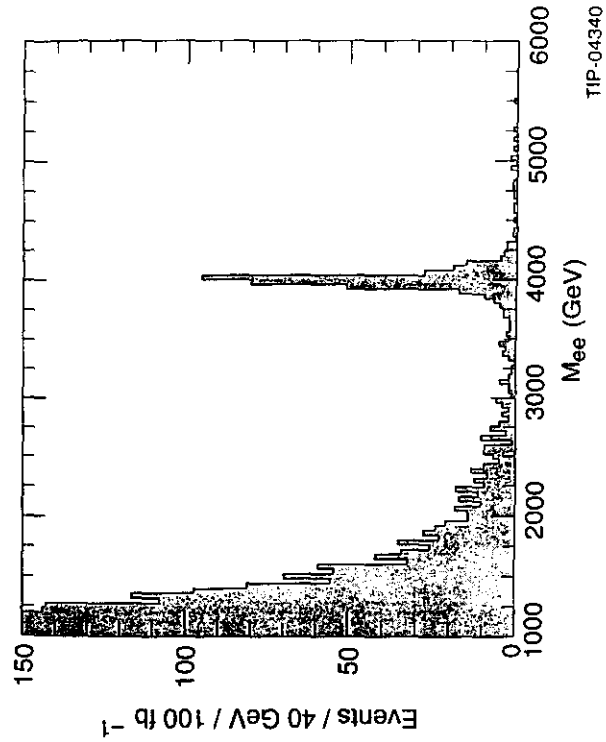

60

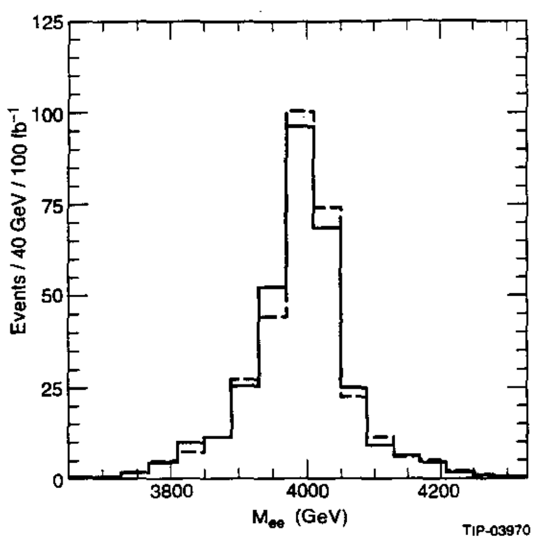

FIG. 2-45. The $M_{e^+e^-}$ distribution for a 4 TeV mass Z' of Model 2 as described in the text. Reconstructed (solid) and generated (dashed) distributions are shown.

61

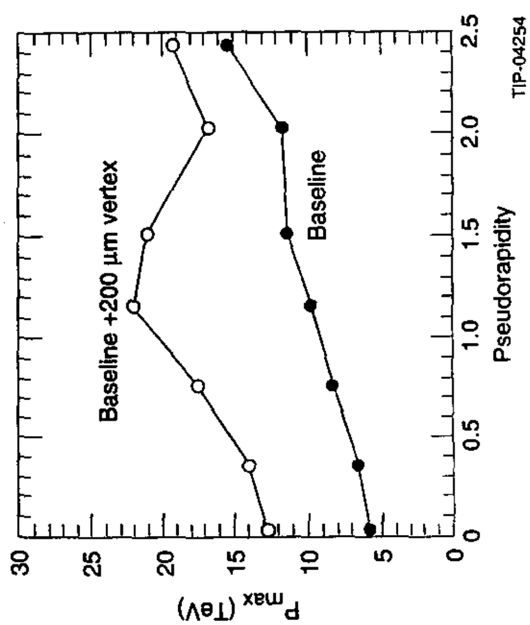

62

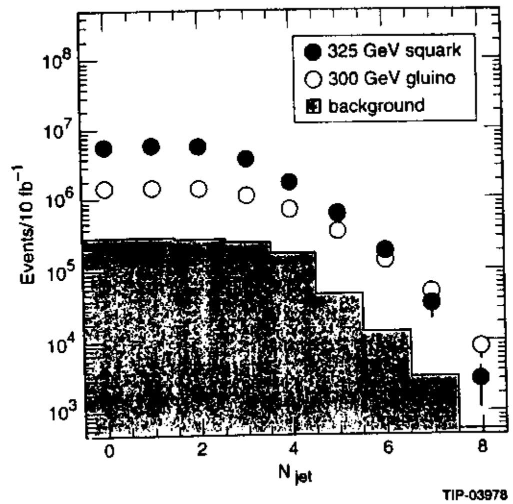

FIG. 2-56. Event numbers with $\not{E}_T > 250\,\mathrm{GeV}$ and the sphericity and lepton veto cuts described in the text vs. the minimum number $N_{\rm jet}$ of jets with $p_T > 75\,\mathrm{GeV}$. Open circles: Case I signal. Solid circles: Case II signal. Histogram: QCD background. Case II has more events with low jet multiplicity because $\tilde{q}_R \to \tilde{\chi}_1^0 q$ dominates.

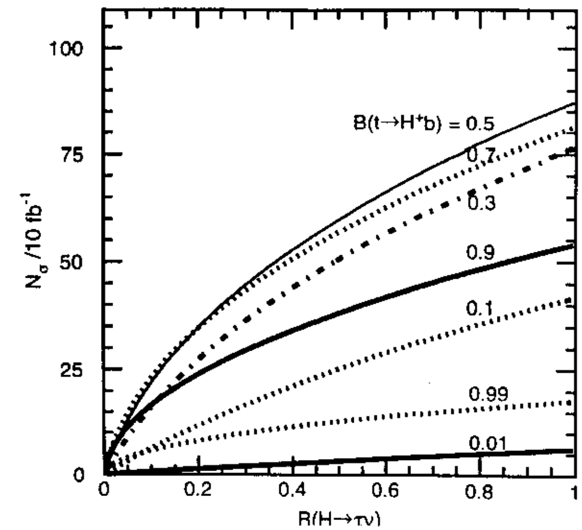

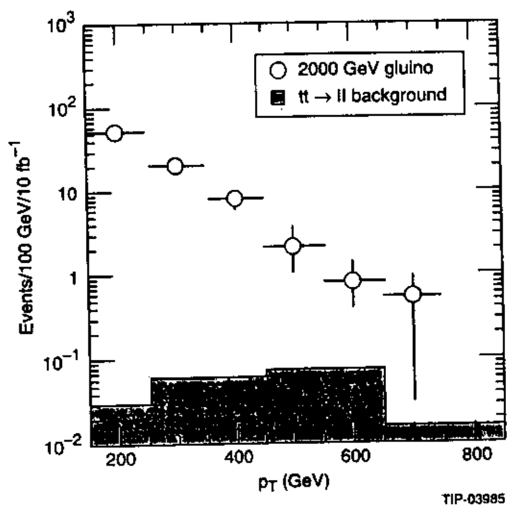

FIG. 2-58. p_T distributions for the highest-p_T isolated lepton in dilepton events containing two isolated like-sign leptons. Open circles: Signal events generated with Case III MSSM parameters. Histogram: $t\bar{t}$ background from mismeasured electrons in the GEM central tracker.

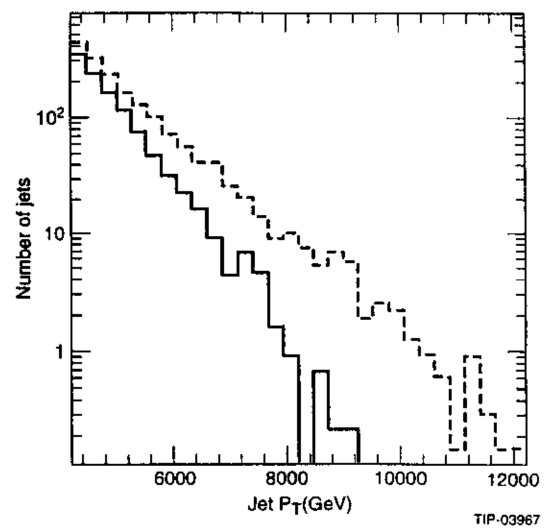

FIG. 2-42. Inclusive jet E_T spectrum for substructure at the scale $\Lambda = 25\,\mathrm{TeV}$ (dashed) and for QCD (solid).

GEM's PHYSICS GOALS

HAVE GUIDED THE DESIGN PRINCIPLES AND MAJOR TECHNICAL CHOICES FROM THE OUTSET

- **EM RESOLUTION REQUIREMENTS**
  Stochastic $(6-8\%/\sqrt{\mathrm{E}})$ *AND* Systematic $(\leq 0.4\%)$
  Terms Set By the Discovery Potential For
  $\mathrm{H}^0 \to \gamma\gamma$, $\mathrm{H}^0 \to \mathrm{ZZ}^* \to e^+e^-e^+e^-$, $\mathrm{Z}' \to e^+e^-$
- **PHOTON POINTING and ANGULAR RESOLUTION**
  $\sigma_\theta = (40-50)/\sqrt{\mathrm{E}} + 0.5$ mrad:
  For Clean ID and Measurement of $\mathrm{H}^0 \to \gamma\gamma$, $\mathrm{Z}' \to e^+e^-$;
  Event Vertex Determination at $\mathcal{L} = 10^{34}$
- **CALORIMETER SEGMENTATION**
  Precision Measurement of EM Processes;
  Rejection of Hadronic Backgrounds;
  Clean Isolation of e, μ, γ (With Tracker)
- **HIGH MUON MOMENTUM RESOLUTION**
  For All $|\eta| < 2.5$
  Detect $\mathrm{Z}' \to \mu^+\mu^-$, $\mathrm{H}^0 \to \mu^+\mu^-\mu^+\mu^-$ With High Efficiency
- **FORWARD CALORIMETER COVERAGE**
  To $|\eta| \approx 5$: $\not{E}_T$ Signatures for $H^0 \to \ell^+\ell^-\nu\bar{\nu}$ and SUSY
- **COMPACT CENTRAL TRACKER RESOLUTION**
  For Complementary SUSY Search: $\tilde{g}\tilde{g} \to \ell^\pm\ell^\pm + \mathrm{X}$
- **ADEQUATE SHIELDING: LOW n, γ FLUX**
  Low Muon Chamber Occupancies To $\mathcal{L} = 10^{34}$

67

GEM: PRECISE, ROBUST DETECTOR DESIGN MUON SPECTROMETER

- **QUIET ENVIRONMENT**
  - 11 - 16+ λ Calorimeter: Punch Through Well Below Real Muon Rate (π, K, c, b)
  - Compact Close-In FCAL + Shield: Low n, γ Flux
  - Air Gaps for Associated EM Showers: High Efficiency for Multi-TeV Muon Reconstruction
- **HIGH RESOLUTION**
  - $\Delta p_T/p_T = 5\%$ (13%) (Baseline) At $\eta = 0$ (2.5), for $p_T = 0.5$ TeV
  - Charge Determination: To 6-15 TeV (Baseline); To 13-22 TeV With 200 μm Vertex
  - CSCs: $\to \sigma_{SAG} \leq 54$ μm;
    - Intrinsic and Alignment Precision
    - 48-In-ϕ: Lorentz Angle Compensation
- **HIGH PATTERN RECOGNITION and RECONSTRUCTION EFFICIENCY**
  - CSCs $\Rightarrow$ Granularity, Near-Space Points; Two-Track Separation (Charge Profile): n, γ Occupancy 0.3 - 1.1% at $\mathcal{L} = 10^{34}$
  - 500 μm Vertex: Muon Reconstruction In 2 SL With Good Resolution

68

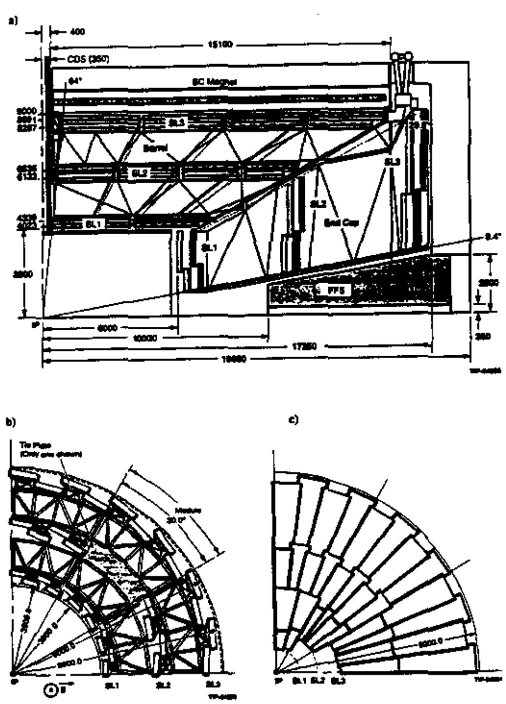

FIG. 4-1. Overview of the GEM muon system: (a) shown in quadrant view, and (b) barrel end view, (c) endcap view from IP.

69

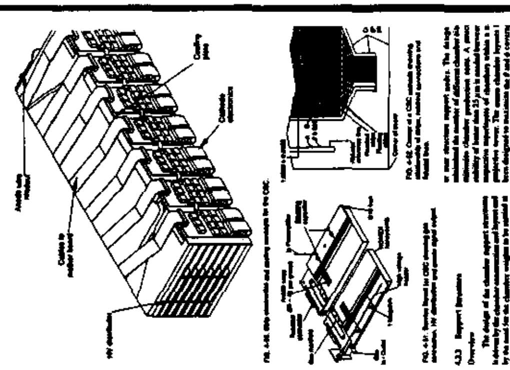

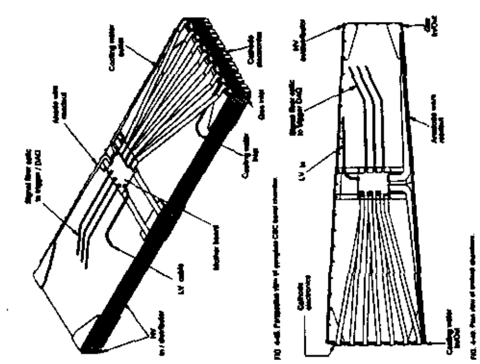

70

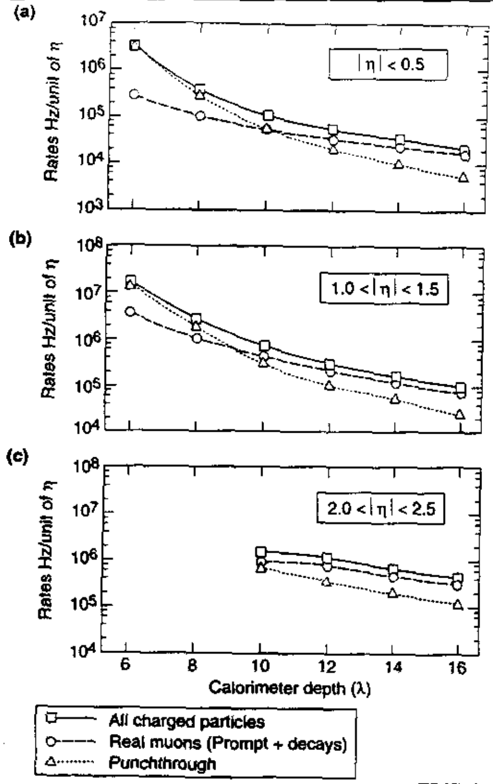

TIP-03842

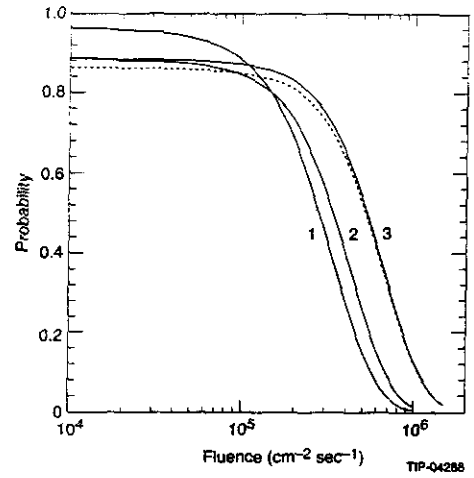

TIP-04288

	Rapidity Range		
Superlayer	0.08-1.34	1.38-1.86	1.86-2.46
Inner	0.6%	0.3%	0.3%
Middle	0.6%	0.4%	0.4%
Outer	1.1%	0.6%	0.5%

Table 4-10. Probability for having good track segments for isolated muons in:

a) all three superlayers

Muon p_T	Rapidity Range				
GeV	0.01-0.50	0.50-0.92	0.92-1.34	1.38-1.86	1.86-2.46
20	0.99	0.99	0.96	0.97	0.98
100	0.99	0.98	0.96	0.95	0.96
500	0.97	0.98	0.94	0.89	0.89
1000	0.95	0.93	0.90	0.84	0.82

b) middle and outer superlayers only

Muon p_T	Rapidity Range				
GeV	0.01-0.50	0.50-0.92	0.92-1.34	1.38-1.86	1.86-2.46
20	0.99	0.99	0.96	0.98	0.99
100	0.99	0.99	0.96	0.97	0.98
500	0.99	0.99	0.96	0.95	0.97
1000	0.97	0.95	0.93	0.94	0.96

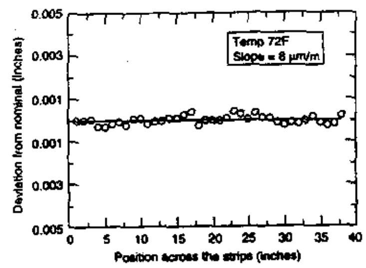

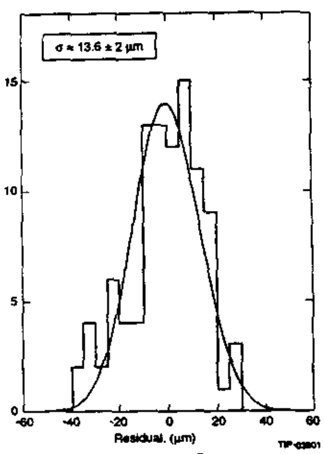

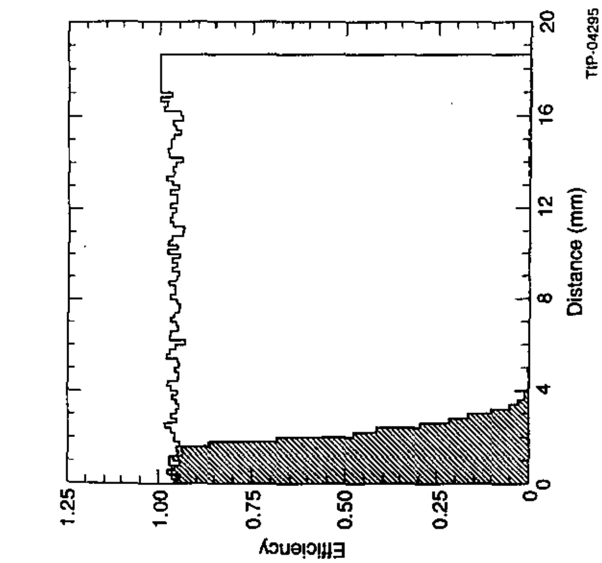

Efficiency
Distance (mm)
TIP-04295

75

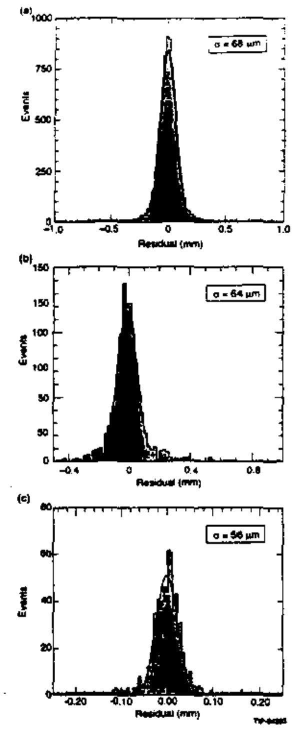

σ = 68 μm
σ = 64 μm
σ = 56 μm
Events
Residual (mm)

76

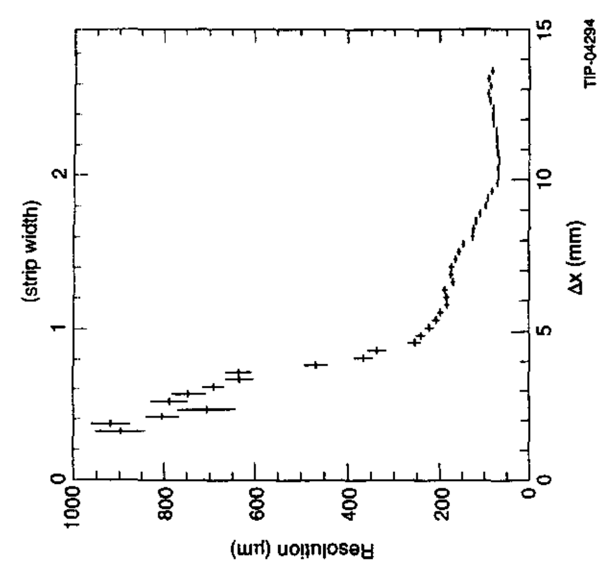

(strip width)
Resolution (μm)
Δx (mm)
TIP-04294

77

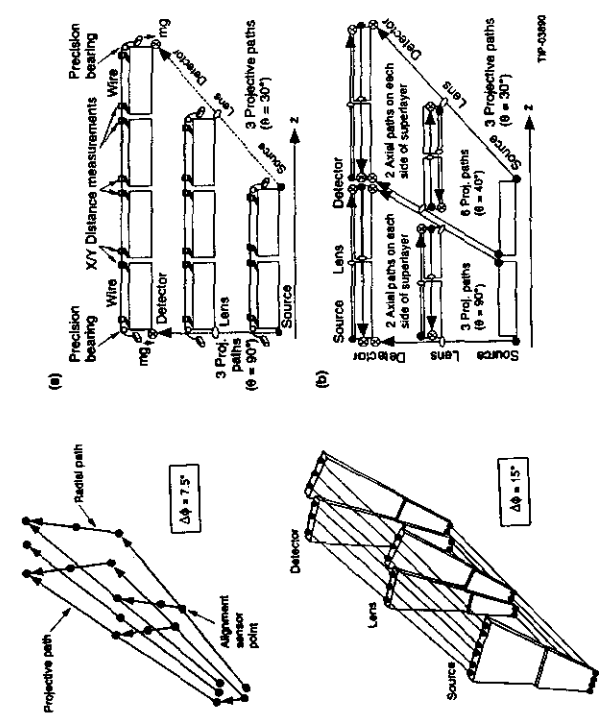

Projective path
Radial path
Alignment sensor point
Δφ = 7.5°
Δφ = 15°
Source
Lens
Detector
Precision bearing
Wire
X/Y Distance measurements
3 Projective paths (θ = 30°)
3 Proj. paths (θ = 90°)
2 Axial paths on each side of superlayer
6 Proj. paths (θ = 40°)
TIP-03890

78

TABLE 4-15. CSC material audit: thicknesses and radiation lengths.

Component	Density (g/cm^3)	cm/Xo	Thickness (cm)	Xo
NOMEX core	0.0288	1400	7 × 1.9	0.01
Circuit Boards - G10	1.7	19.4	14 × 0.05	0.0361
Copper cladding	8.96	1.43	14 × 0.0017	0.0166
Epoxy Panel Edges	1.3	31.2	7 × 1.9	0.426
G10 Gap Frames	1.7		6 × 0.8	0.2474

79

GEM CALORIMETERS

- **STABLE, ROBUST OPERATION**
  - LKr/LAr EM Accordion:
    - Intrinsically Stable ⇒ Small Systematics
    - Fast Signals ⇒ Low Noise; Clean Lepton and Photon Isolation
  - Longitudinal and Fine Transverse EM, HCAL Segmentation:
    - Photon Pointing With η-Strips: H^0 Vertex At $\mathcal{L} = 10^{34}$
    - Clean γ/Jet Separation, With Strips, Tracker: $1 - 4 \times 10^{-4}$;
    - e/Jet Separation $\sim 10^{-5}$
    - γ/e Separation With Tracker: $\mathcal{R}(\gamma/e) = 0.5\%$ for $M_H \approx M_Z$
- **HIGH EM RESOLUTION**
  - $\sigma_E/E = 6\%/\sqrt{E} \oplus 0.4\%$ (Barrel);
  - $\sigma_E/E = 8\%/\sqrt{E} \oplus 0.4\%$ (Endcap);
  - Sufficient for Higgs Discovery:
    - 10 fb^{-1} Will Cover $M_H \geq 100$ GeV
    - 30 fb^{-1} Will Cover $80 < M_H < 100$ GeV
- **GOOD JET RESOLUTION AND COVERAGE ($|\eta| < 5$)**
  - $\sigma_E/E = 60\%/\sqrt{E} \oplus 4\%$ (Weighting); Lightly Instrumented Scintillating Barrel
  - Sufficient E_T Resolution for $H^0 \rightarrow \ell^+\ell^- jj$; Discovery of Quark Substructure
  - Sufficient $\not{E}_T$ Resolution for $H^0 \rightarrow \ell^+\ell^- \nu\bar{\nu}$; Supersymmetry Signatures

80

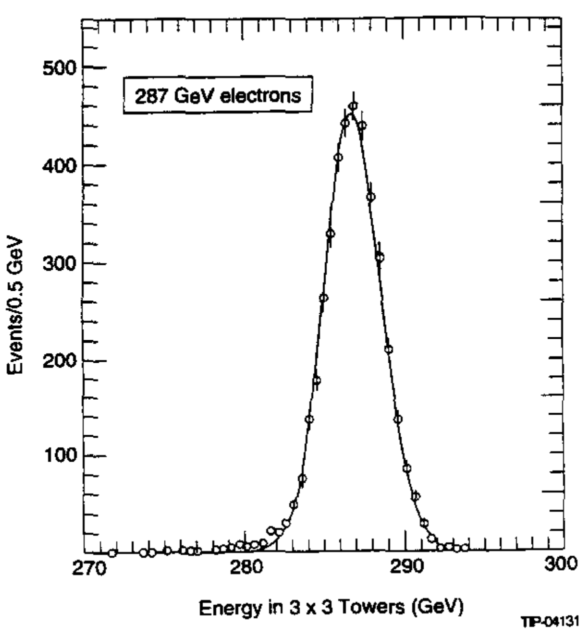

81

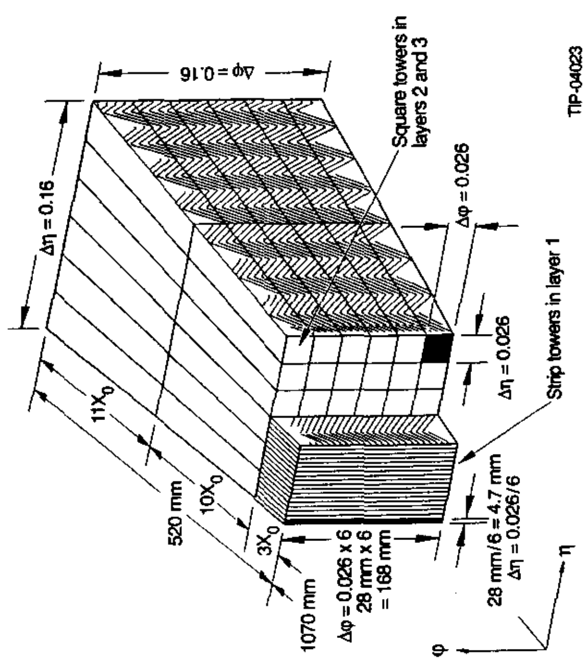

82

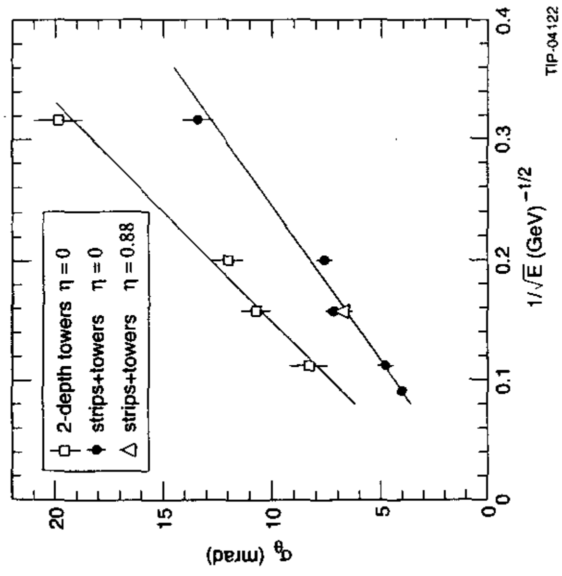

85

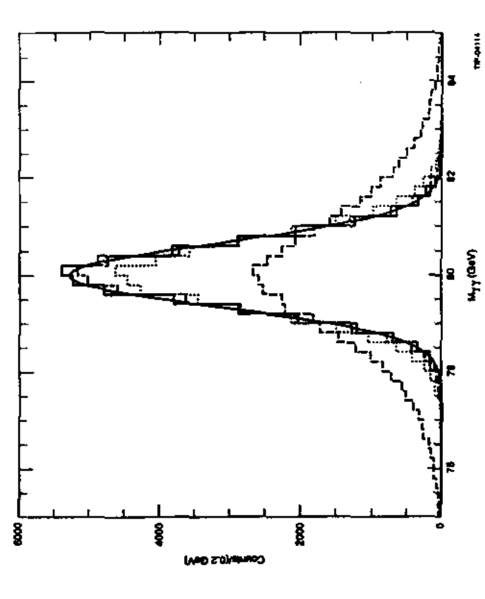

FIG. 5-10. Invariant mass of two photons from H^0 with mass of 80 GeV. Solid histogram and fitted line are with all resolution and expected noise at standard luminosity (σ = 0.65 GeV). The long dash–short dash histogram puts in the uncertainty of the vertex as determined using the pointing resolution to find the most probable Higgs vertex, out of all the vertices reconstructed by the tracker (σ = 0.68 GeV). The dotted histogram uses only the angular resolution of the calorimeter to determine the vertex (σ = 0.79 GeV). The dashed histogram is obtained when no vertex information is used (σ = 1.48 GeV).

84

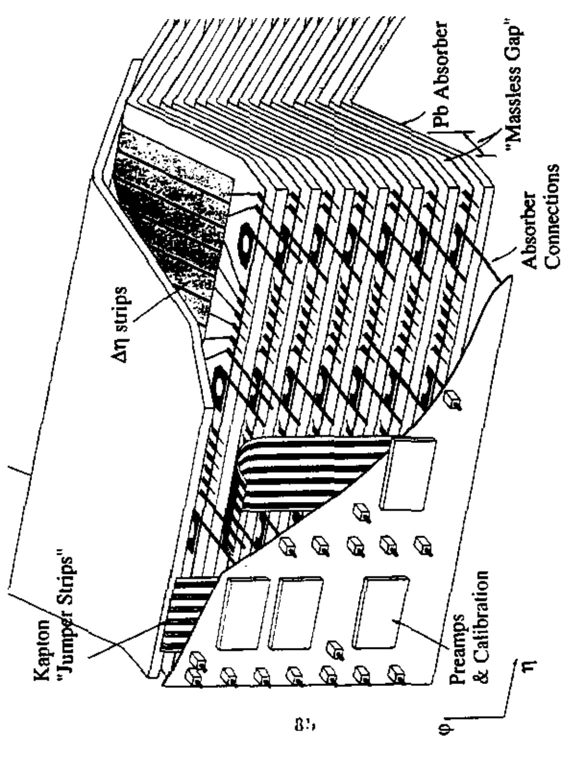

85

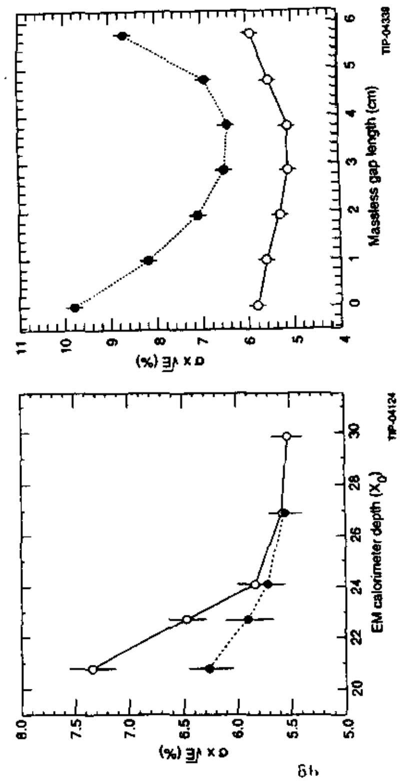

86

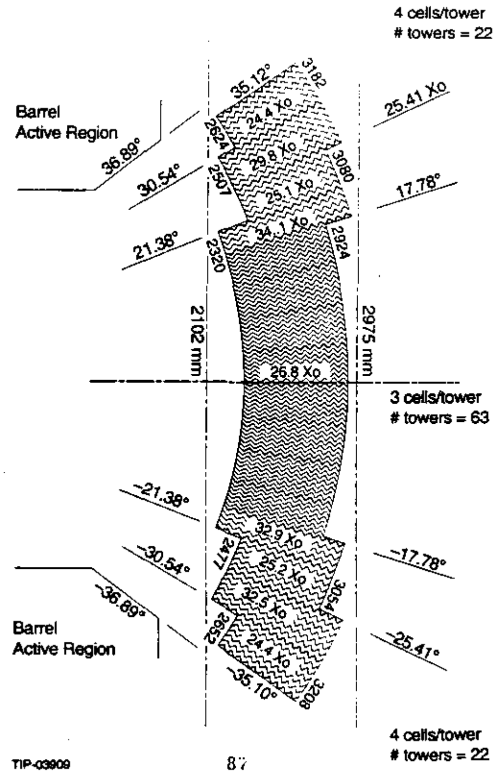

87

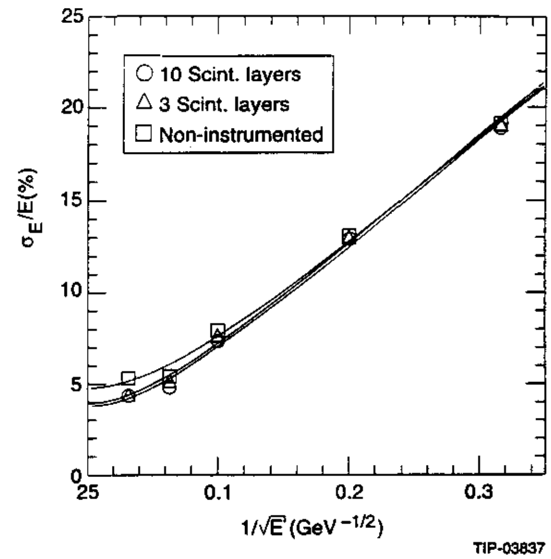

88

GEM CENTRAL TRACKER

- **COMPACT, PRECISE; DUAL TECHNOLOGIES**
  - **Si Detector: 50 μm (Standard) Pitch; 10 μm Resolution, 10 μm Alignment.**
    - **R_{min} = 10 cm: Dose < 5 Mrad/10 Years**
    - **R_{max} = 22 cm: Cost (2M/m^2)**
    - **18 cm Strips: Channel Count, Structure, Signal/Noise; Occupancy 0.1% (Typical)**
  - **IPC Detector: 50 μm Resolution, 25 μm Alignment.**
    - **Pad Sizes: Occupancy (0.5% Typical) Vs. Channel Count**
    - **R_{max}: Momentum Resol'n Vs. Cost; Matched to ECAL Tower Size**
  - **$N_{LAYERS} \approx 14$: Pattern Recognition, Resolution; e/γ Separation Vs. Space, Cost**
  - **Stereo Angles: z-Resol'n Vs. Track Ambiguity**
- **RESOLUTIONS**
  - **High p: $\Delta p_T/p_T^2 \approx 0.1\%$ (High Momentum)**
  - **Low p: $\Delta p_T/p_T \approx 3.5\%$ (10% X_0 Typical)**
  - **Improvement of Muon Resol'ns: (p < 30 GeV) and (p ~ 1 TeV or More)**
  - **Charge Determination: $p_T \leq 600$ GeV (95% CL)**
  - **$\Delta b \approx 25$ μm Above 10 GeV**
  - **$\Delta z \approx 1$ mm**

89

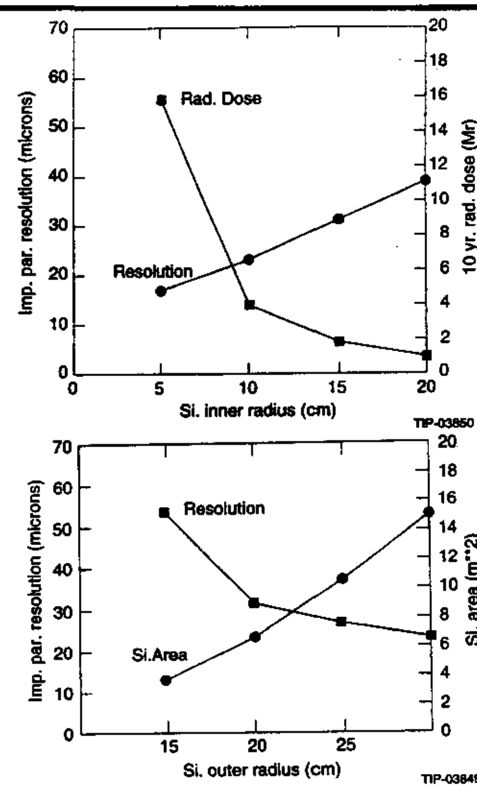

90

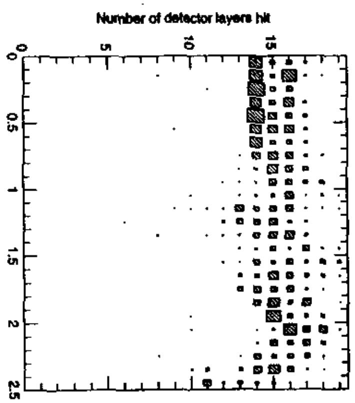

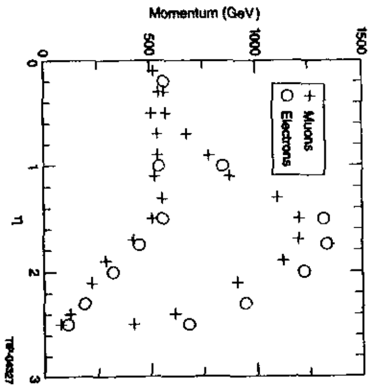

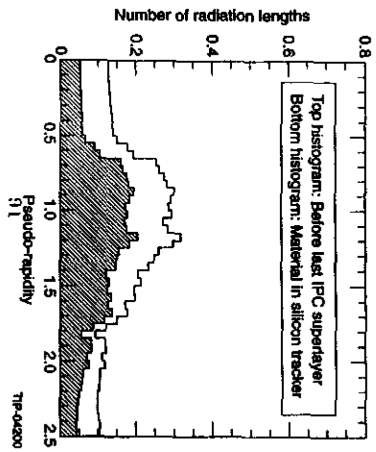

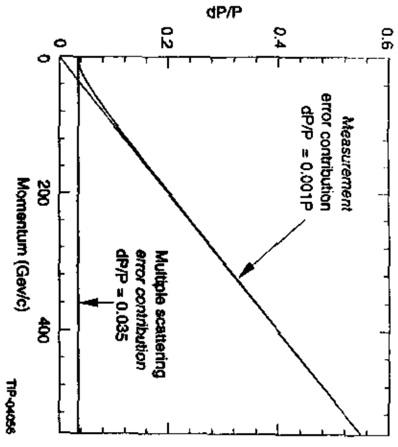

GEM CENTRAL TRACKER PHYSICS PERFORMANCE

- Electron ID: $e/\pi^0 = 0.1\%$; $e/\pi^- = 0.08\%$; $e/\mathrm{Jet} = 0.02\%$; e/Jet (Isolated) $= 0.001\%$
- $\epsilon_e \approx 97\%$; $\epsilon_\mu \approx 97\%$ in $H^0 \to \ell^+\ell^-\ell^+\ell^-$
- Correct Higgs Vtx ($\Delta z < 5$ mm): $\epsilon = 95\%$ ($L = 10^{33}$); $\epsilon = 75 - 80\%$ ($L = 10^{34}$)
- b-Tagging: Efficiency = 30 % + (Preliminary)
- $\tau \to 3$ Prong Tagging: Efficiency = 75 (33)% At $p_T = 50\,(150)$ GeV
- Momentum Resolution Sufficient For Like-Sign Dilepton Studies: $\tilde{g}\tilde{g}$; WW-Scattering.
- To Be Studied: CP Violation In $B \to J/\Psi\, K^0_s \to \mu^+\mu^-\, \pi^+\pi^-$

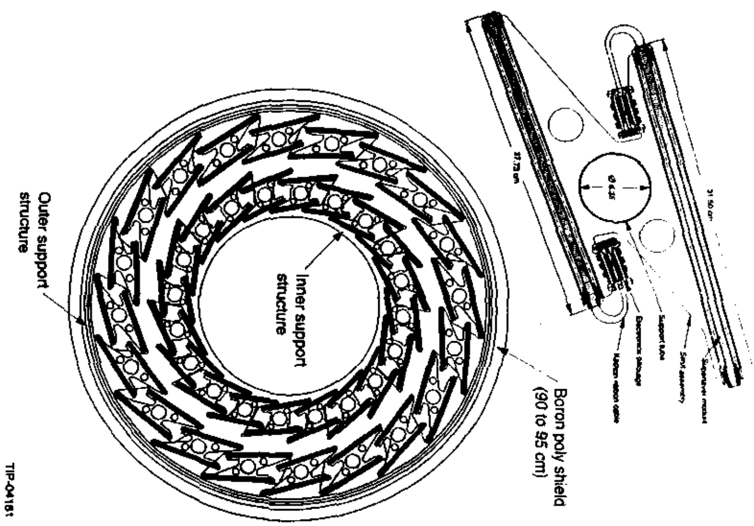

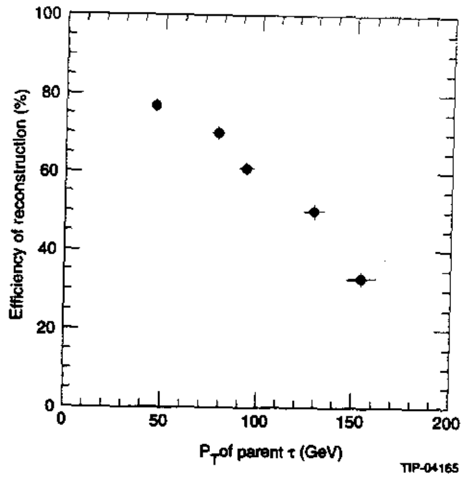

95

GEM DESIGN OPTIMIZATION STUDIES

FOLLOWING THE FIRST ROUND OF SIMULATIONS

- MUON SYSTEM ACCEPTANCE
  - Important For $Z' \to \mu^+\mu^-$, and $H^0 \to \mu^+\mu^-\mu^+\mu^-$
- REDUCE MATERIAL IN MIDDLE MUON SUPERLAYER
  - Improve Resolution For $H^0 \to \mu^+\mu^-\mu^+\mu^-$
- DETAILED ALIGNMENT PROCEDURE
  - Determine Muon System xy-Position Relative To Beam To 200μm
- DETAILED CALIBRATION STRATEGY FOR EM CALORIMETER, USING $Z^0 \to e^+e^-$
  - Important For $H^0 \to \gamma\gamma$, $Z' \to e^+e^-$
- HADRON CALORIMETER CALIBRATION PROGRAM: DETERMINE JET ENERGY SCALE
  - For Heavy Flavor Physics, $H^0 \to \ell^+\ell^-jj$, and Multi-TeV Jet Studies.
- SMALLER BEAM PIPE AT FCAL POSITION
  - For Extended η Coverage; Improved $\not{E}_T$ Resolution

96

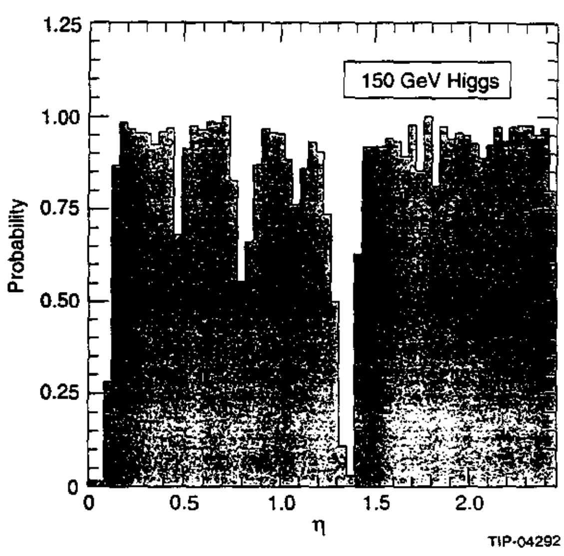

97

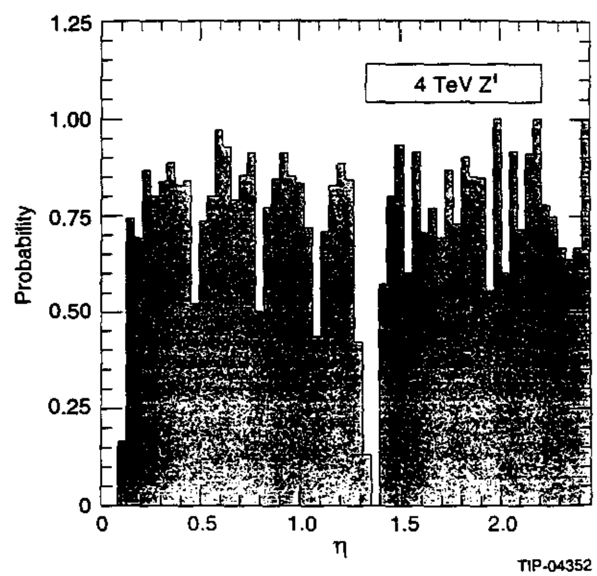

98

Table 5.6 Calibration Goals and Means

Calibration Means	Purpose	Type of Information (Quantity Defined)	Time of Calibration
Current injection into front end at the electrodes	Readout chain - gain calibration and monitoring	Absolute charge calibration; relative channel-to-channel gain, time and amplitude response	All tests and periodically during experiment runs
e's and π's Beam test at FNAL	Mapping of calorimeter response of EM and hadronic modules	Response profile (relative) for a set of modules including boundaries in φ for hadronic modules	Prototype testing in 1995
e's and π's Beam test at SSCL	Mapping of calorimeter response, mainly vs. *θ over the barrel-endcap* boundary	Response profile (relative) for the boundaries in θ	SSCL test beam operation in 1997
Z^0 mass and particles with measured momentum in tracker.	Establishing absolute energy reference points for the barrel and end caps	Charge vs. energy scale	Experiment start and during experimental runs.
α-cells in the cryostats	*Liquid purity monitoring*	*Ionization yield*, absolute charge vs. electric field for α's	Continuously during the experiment

Table 8-2 Overall model for expected rates; system capabilities will exceed these rates. Rates are given for the end of the operating year, while *integrated quantities (integrated luminosity, total storage) are assuming an exponential* increase in luminosity each year until a constant value is reached in 2003. For explanations, see text.

Parameter/Year	1999	2000	2001	2002	2003
Peak luminosity ($cm^{-2} s^{-1}$)	10^{30}	10^{31}	10^{32}	10^{33}	10^{33}
Total live time (s)	10^6	10^7	10^7	10^7	10^7
Integrated luminosity (pb^{-1})	1	40	400	4,000	10,000
Level 1 trigger level	100 μb	100 μb	100 μb	100 μb	100 μb
Level 1 trigger rate (maximum)	100 Hz	1 kHz	10 kHz	100 kHz	100 kHz
DAQ event size	1 MB	0.6 MB	0.3 MB	0.3 MB	0.3 MB
Peak data rate out of DAQ	100 MB/s	600 MB/s	3 GB/s	30 GB/s	30 GB/s
Event filter (Level 2/3) factor	1	10	100	500	500
Level 2 computational load (SSCUP)[a]	10^3	10^3	10^4	10^5	10^5
Level 3 computational load (SSCUP)	0	10^4	3×10^4	1.3×10^5	1.3×10^5
RECO rejection factor	1	1	1	2	2
RECO computational load (SSCUP)	2×10^4	2×10^5	3×10^5	4×10^5	4×10^5
Event rate stored	100 Hz	100 Hz	100 Hz	100 Hz	100 Hz
Equivalent cross section	100 μb	10 μb	1 μb	100 nb	100 nb
Initial data per event	1 MB	0.9 MB	0.6 MB	0.6 MB	0.6 MB
Rate of initial data to storage	100 MB/s	90 MB/s	60 MB/s	60 MB/s	60 MB/s
Additional event data	1.6 MB	1.6 MB	1.6 MB	1.6 MB	1.6 MB
Peak event data rate	110 MB/s	150 MB/s	130 MB/s	130 MB/s	130 MB/s
Annual event storage	0.26 PB	1 PB	0.9 PB	0.9 PB	2.2 PB
Simulation computational load (SSCUP)	1.5×10^5	3×10^5	6×10^5	6×10^5	6×10^5
Annual simulation storage	0.14 PB	0.25 PB	0.4 PB	0.4 PB	0.4 PB
Annual test beam data	0.01 PB	0.01 PB	0.01 PB	0.01 PB	0.01 PB
Total annual storage	0.5 PB	1.3 PB	1.3 PB	1.3 PB	2.6 PB
Peak rate to storage	125 MB/s	170 MB/s	155 MB/s	155 MB/s	155 MB/s

[a] The SSCUP is a unit of processing power, roughly equivalent to a DEC VAX-11/780.

Table 8-6. Technology and cost projections.

Parameter	1993	1997	1998	1999	2000	2003
Single CPU power (kSSCUP) (midrange)	0.10	0.38	0.54	0.75	1.05	2.89
Number of CPUs per box	1	2	2	4	4	8
CPU cost per box (k$)	6	7	6	11	9	13
Memory size (GB)	0.06	0.3	0.5	1	1	3
Memory Cost (k$/GB)	100	35	27	21	16	7
Disk Cost (k$/GB)	2	1	0.8	0.6	0.5	0.3
Mass (slow) memory cost (k$/GB)	25	7	5	3.5	2.4	0.9
Mass storage media cost (M$/PB)	2	0.41	0.38	0.34	0.31	0.23
Mass storage bandwidth cost (M$/GB/s) (including robots)	20	10	8	7	6	3
Number of boxes for 1 MSSCUP	10,000	1,302	930	332	237	43
Cost/MSSCUP (M$)	130	24	19	11	6	1.5

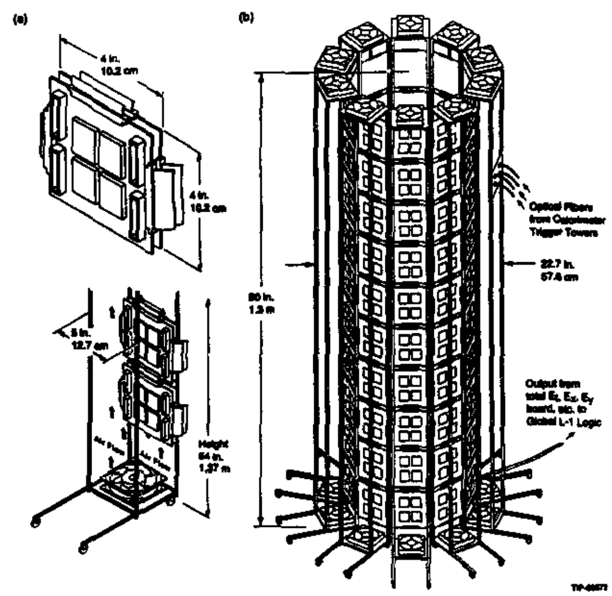

FIG. 7-7. a) Details of the 3D-Flow programmable processing system crate assembly. b) The layout and dimensions of the complete digital Level-1 trigger system.

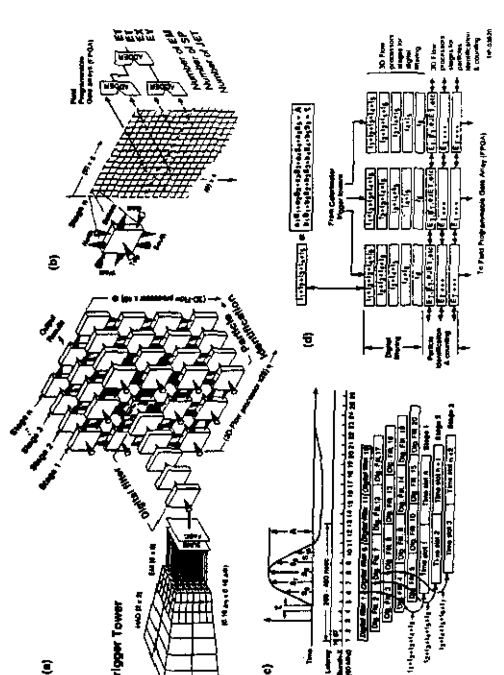

10.

GEM TDR DOCUMENT

- FIRST EDITION READY APRIL 30; SUBMITTED APRIL 30
  - TIP's First Experience With Complete Electronic Handling of Figures (R&D)
  - Color Covers: non-DOE Funds
- SECOND PRINTING: 250
- THIRD PRINTING: 1500 (Early June)
  One Copy to Each Collaborator;
  Extra Copies On Request
  - Corrections (Text, Figures) Due May 20
  - Figure and Table List (Short Captions)
  - Enlargement of Important Figures
  - Updated Covers: Decide This Week
  - "Perfect" Binding
  - Printing 2-3 Weeks
- LIBRARIES: Full-Page Tables and Figures
  - Tables in WORD
  - Figures in Adobe Illustrator or Postscript
  - Accessible by Network
- SECOND EDITION (FINAL)
  - Update Physics and Subsystem Studies; Design Work
  - Includes Response to the PAC
  - 2000+ Copies
  - Scheduled for September

10

7-6

SUMMARY SCHEDULE FOR REVIEW OF GEM

End March, 1993 — **Deadline for Cost and Schedule, draft Project Management Plan**

April 30, 1993 — **Submission of GEM TDR**

May 24 - 29, 1993 — **Review of TDR and draft plans (at SSCL)**

Focus:
- Scientific merit
- Technical feasibility
- Collaboration resources, organization, management
- Cost and schedule

Projected Results:
- Detailed evaluation of the GEM project
- Action items for further study and clarification
- Cost and schedule goals for GEM baseline

July 31 - August 6, 1993 — **PAC Meeting (tentative dates)**

Focus:
- Closure on action items from May review
- GEM in context of total SSC program

Projected Results:
- Recommendation to formulate the GEM baseline and to draft agreements with participating institutions.

10

If the August review results in a recommendation to proceed with the formulation of the GEM baseline, the tentative schedule is:

October 1, 1993 (tentative date) — **Deadline for proposed baseline Cost and Schedule and final versions of GEM Project Management Plan and Conceptual Safety Analysis Report**

October, 1993 — **DOE Project Review** (at SSCL)

Focus:
- Detailed review of GEM the baseline
- Management plan (in-depth review)
- Status of agreements & plan for institutional assignments (US and foreign)
- Operations (plans for QA, safety, acquisitions, detector operating procedures, etc.

Projected Results:
- Report to DOE/ER Management
- GEM baseline presented by Laboratory approved by DOE

10

Liquid Calorimeter Overview:

David Lissauer
BNL

Calorimeter Configuration.

Design Status:

- Barrel :
  - EM
  - Hadronic
- Endcap
  - EM
  - Hadronic.
- Cryostat
- Feedthrough
- Cryogenic Systems

GEM Calorimeter With Separate Forward Calorimeter

Note: All dimensions are in mm.

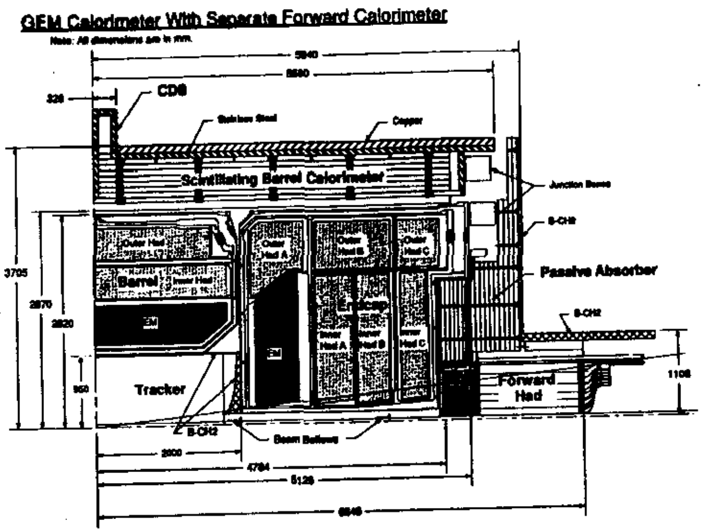

4-26-93 Jm

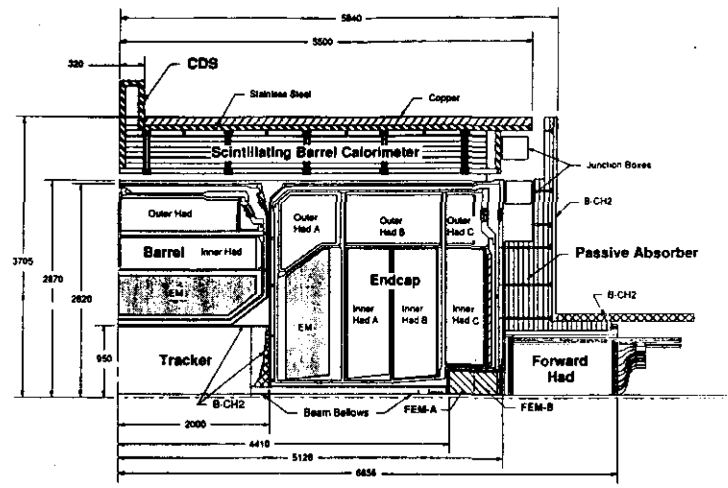

Table 5-2. GEM Calorimeter Parameters.

Physics Parameters – EM Calorimeter			
Energy resolution	– barrel	$6\%/\sqrt{E} \oplus 0.4\%$	
	– endcap	$8\%/\sqrt{E} \oplus 0.4\%$	
Liquid	– barrel	Krypton	
	– endcap	Argon	
Position resolution		$4.4\ mm/\sqrt{E}$	
Pointing resolution	– barrel	$40\ mrad/\sqrt{E} + 0.5\ mrad$	
	– endcap	$50\ mrad/\sqrt{E} + 0.5\ mrad$	
Coverage	– barrel	$\eta < 1.05$	
	– endcap	$1.15 < \eta < 3.0$	
Dynamic range		$\approx 3 \times 10^5$ (from $\approx$ 20 MeV up to $\approx$6 TeV/channel)	
Time resolution			
	Single Tower	1 GeV × ns/E	
	EM(5x5 Towers)	5 GeV × ns/E	
Speed(shaping time)		40 ns (20 ns for η >1.83)	
Noise (at $L = 10^{33}\ cm^{-2} s^{-1}$)		Thermal	Pileup
	– barrel	20 MeV/ (0.026x0.026)	13 MeV
	– endcap	$\approx$35 MeV/tower	30 MeV
Lateral segmentation (η,φ)		0.026 × 0.026	
Longitudinal segmentation			
	– barrel	3; $(3 + 10 + 11)\ X_0 = 24\ X_0$ @ $\eta = 0$	
	– endcap	3; $(4 + 10 + 13)\ X_0 = 27\ X_0$ @ $\eta = 2.5$	
EM Absorption lengths		$1.3\ \lambda$ at $\eta = 0$	

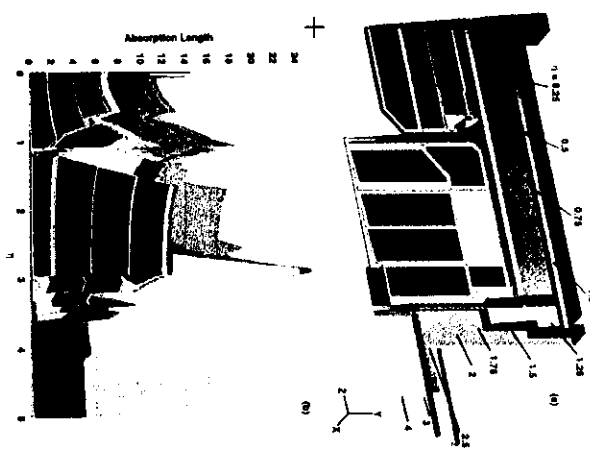

EM Accordion Segmentation

6X6 Towers

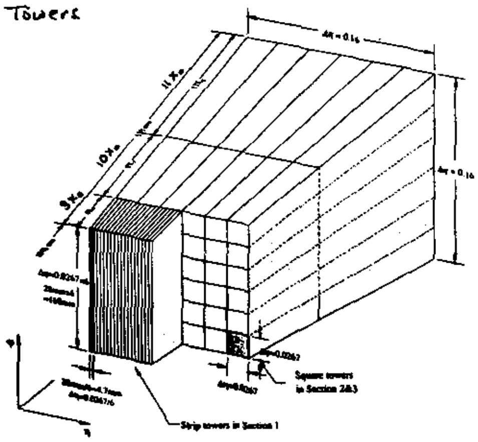

Δφ = 9°
24 cells
960 = total

115

Barrel Calorimeter:

Barrel EM Calorimeter: Design and Optimization.

Optimization:

1) Longitudinal Segmentation
   - e/π Rejection.
   - γ pointing.
   - Jet rejection.

2) *Strips in the Ist longitudinal section*
   - π^0 / Jet rejection

3) Massless Gap.
   - *Energy Resolution*

4) Transverse Segmentation. 0.026 × 0.026 ✓

6) *Total Depth of the Em calorimeter.* fixed. 25 X_0

7) Barrel to endcap transition.

8) *Dynamic Range requirements.*
   - Dynamic Range. 2^{18} non linear response.

EM Prototype Construction:

Bending Machine. (BNL/Shanghai)

Mold Press (Nevis/BNL)

Design (MM/BNL)

Assembly Concept

116

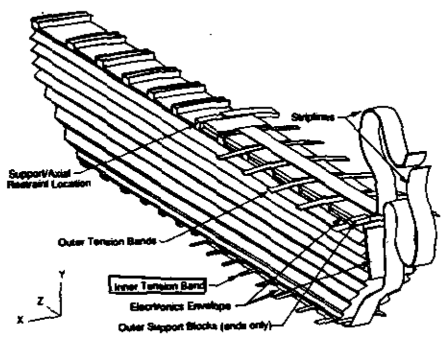

117

EM Cut Iso View

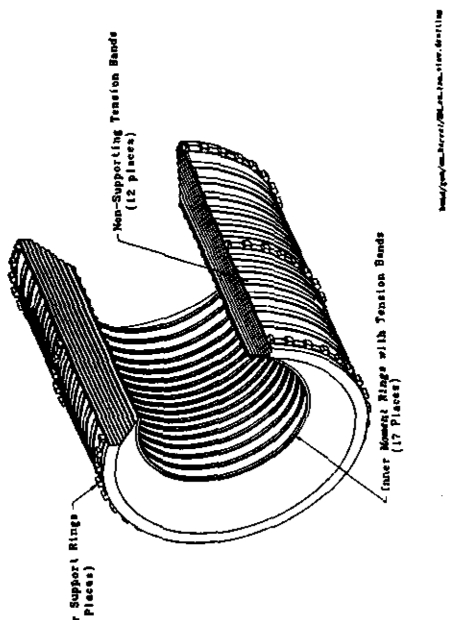

118

Barrel Hadronic Calorimeter Design and Optimization:

Optimization:

1) Transition between Liquid and Scintillator.

2) Total Depth - Hadronic Calorimeter.

3) Granularity- transverse

Matching towers to the EM , trigger towers.

4) Longitudinal Segmentation.

Ist layer EM tail catcher.
weighting for hadronic showers.

5) Cu .vs.Pb Absorber

e/π , Jet Resolution.

Hadronic Box Design:

Design (Rochester/MM) — E.S.T 9mm tile. Pb

Prototype Plans:

Endcap Calorimeter:

Endcap EM Calorimeter: Design and Optimization.

Optimization:

1) Longitudinal Segmentation

e/π Rejection.
γ pointing.
Jet rejection.

2) Strips in the Ist longitudinal section

π^0 / Jet rejection

3) Massless Gap.

Energy Resolution

4) Transverse Segmentation.

6) Total Depth of the Em calorimeter.

7) Barrel to endcap transition.

8) Dynamic Range requirements.

Dynamic Range. 2^{16} non linear response.

9) Remote Preamp region.

10) Alternative Endcap Design.

Spanish Fan
Flat wall accordion
TGT

EM Prototype Construction:

Bending Machine. (BNL/Shanghai)
Mold Press (Nevis/BNL)
Design (MM/BNL)

Assembly Concept

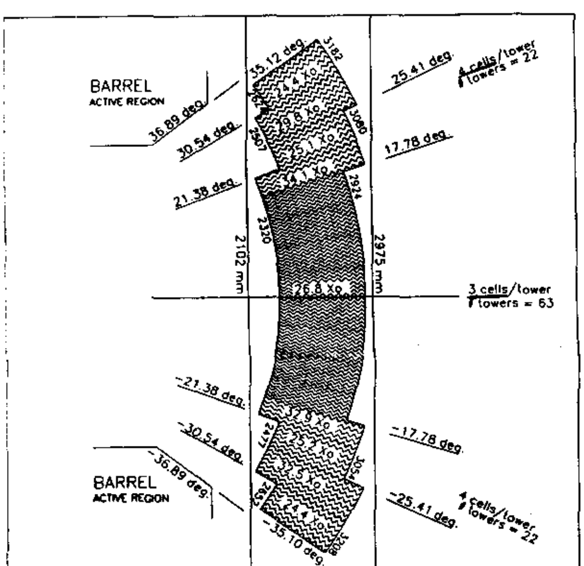

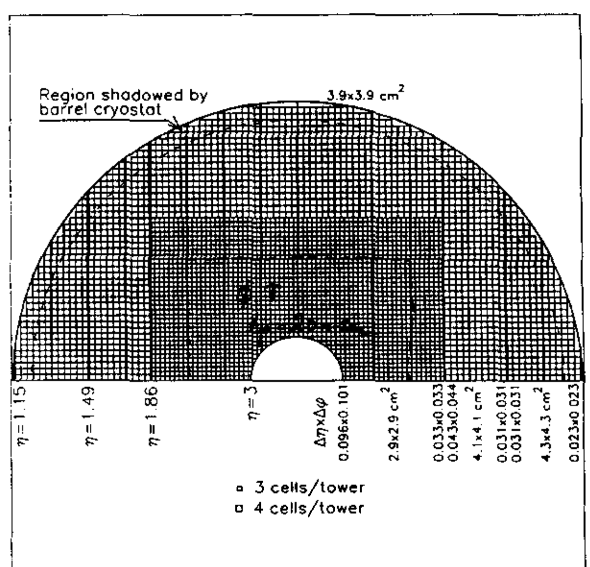

EM resolution for Et=40 GeV

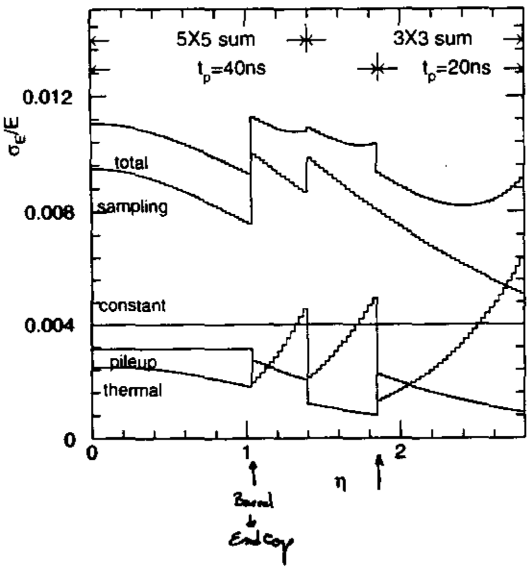

123

Endcap Hadronic Calorimeter Design and Optimization:

Optimization:

1) Transition between Liquid and Scintillator.

2) Total Depth - Hadronic Calorimeter.

3) Granularity- transverse

Matching towers to the EM , trigger towers.

4) Longitudinal Segmentation.

1st layer EM tail catcher.
weighting for hadronic showers.

5) Cu Absorber

e/π , Jet Resolution.

Hadronic Box Design:

Design (Washington/MM)

Prototype Plans:

124

ELECTROSTATIC TRANSFORMER CONFIGURATION

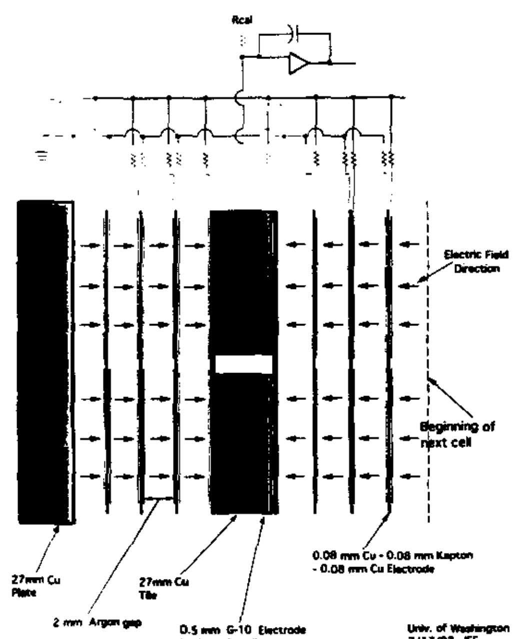

125

Hadronic Endcap Module

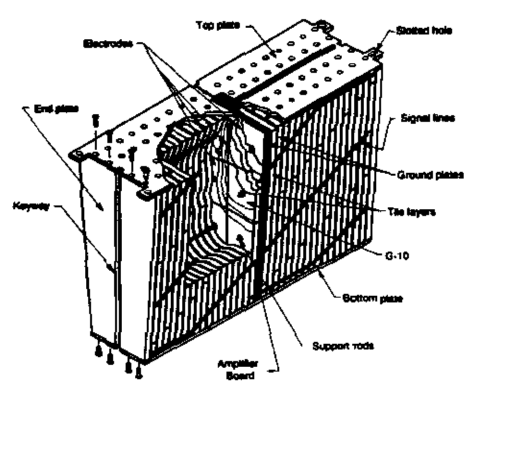

University of Washington
6/6/93 DAF

126

Calorimeter System Technology Choices:

1) Feedthrough Design

-- Design Criteria. Reliability, electrical fidelity.

2) Cryogenic System

- Fill rates,
- Operation
- Purification detail,
- fluid control
- Temperature control.
- Failure mode and safety.

127

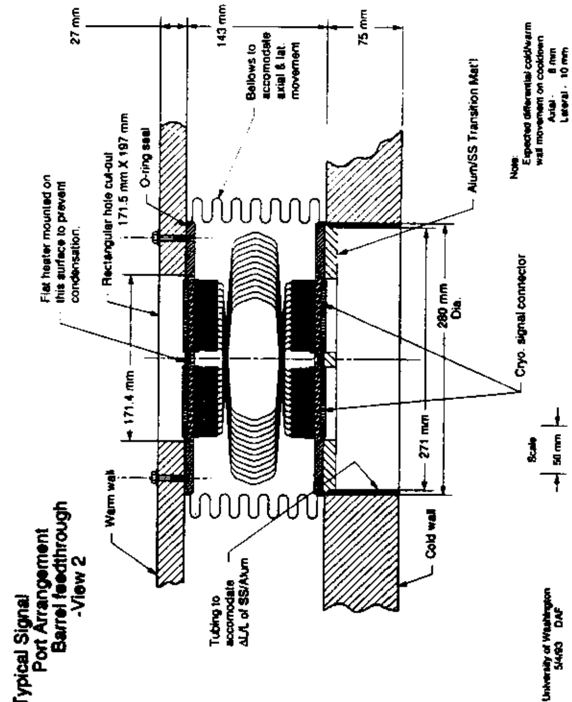

128

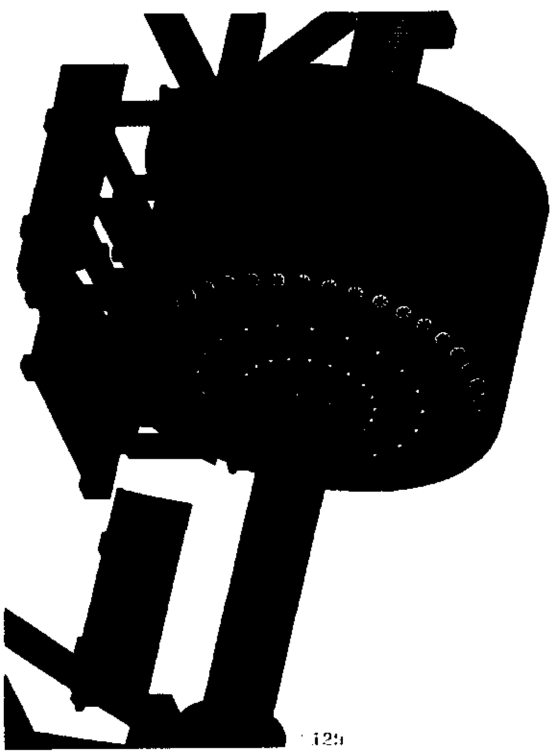

129

FNAL - Test.

1994' - 1995'

18° sector Barrel

+ some end Cap. / Barrel transition.

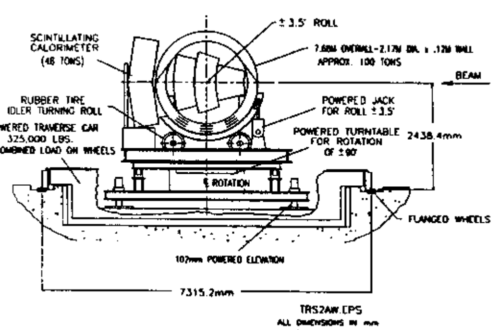

130

Liquid Calorimeter Support Documents:

1) Assembly of Liquid Barrel Calorimeter	TN-93-309
2) Assembly of Liquid Endcap Calorimeter	TN-93-310
3) Barrel Hadronic Modules	TN-93-311
4) Endcap Hadronic Modules	TN-93-312
5) Inner Barrel Cryostat Design Concept	TN-93-313
6) Endcap Cryostat Design Concept	TN-93-314
7) Feedthrough Design	TN-93-315
8) Liquid Calorimeter Thermal Design Concept	TN-93-316
9) Cryogenics System for Liquid Calorimeter	TN-93-317
10) Vacuum system for Liquid Caloriemter	TN-93-318
11) Information Flow-- Calorimeter segmentation	TN-93-319
12) Structure of Barrel EM Calorimeter	TN-93-320
13) Structure of Endcap EM Calorimeter	TN-93-321
14) EM Electrode Design	TN-93-322
15) EM Absorber production	TN-93-323
16) EM Crocodile Press (Barrel)	TN-93-324
17) EM Mold Press	TN-93-325
18) EM Module Assembly	TN-93-326
19) Liquid Calorimeter - Internal Electronics	TN-93-328
20) Installation Inside Liquid Calorimeter	TN-93-327

131

Overview

of Scintillating Barrel Calorimeter (SBC)

Yu. Kamyshkov / ORNL

May 10, 1993 San Diego

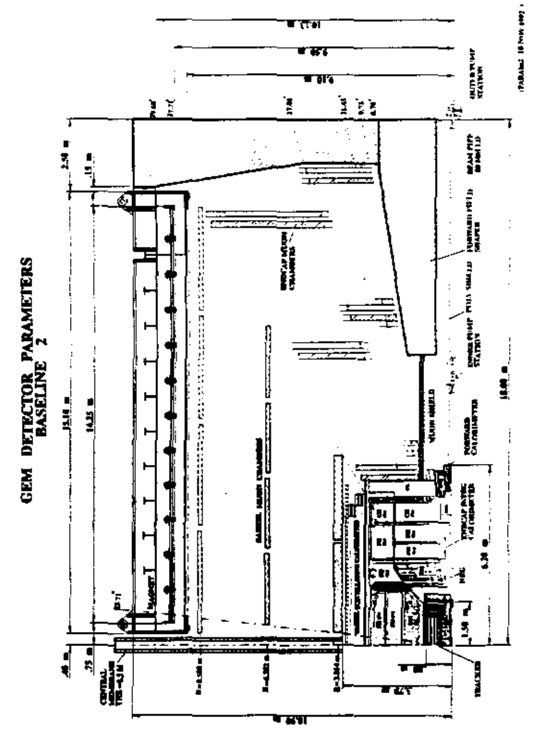

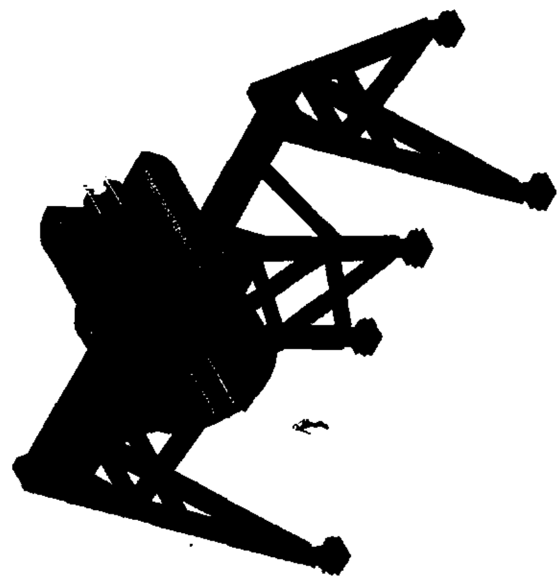

138

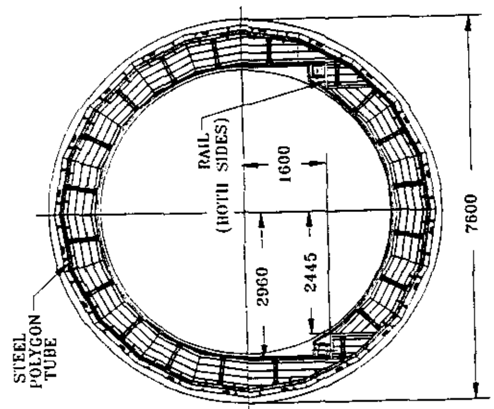

Figure 2: Scintillating Barrel Calorimeter, radial view

139

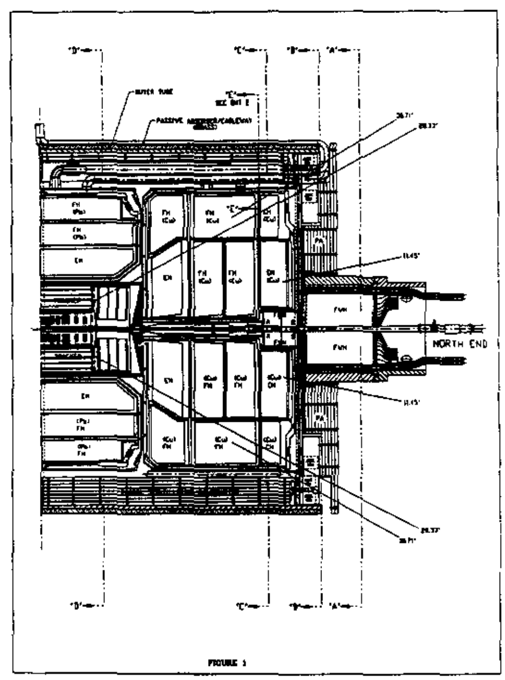

140

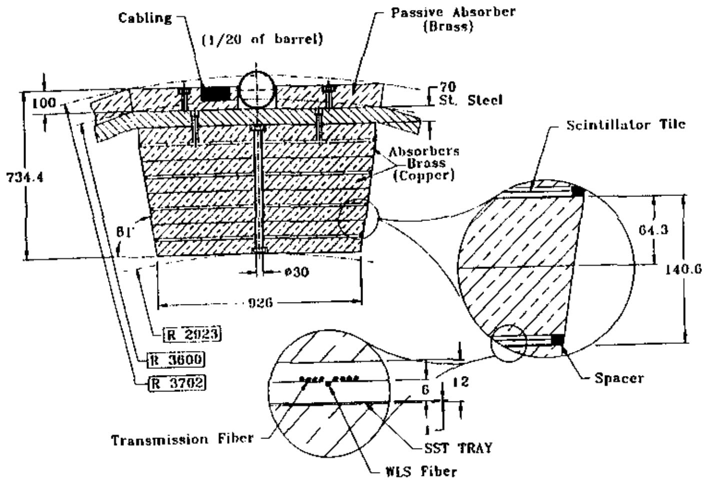

Figure 4: *Structural view of one module of Scintillating Barrel Calorimeter*

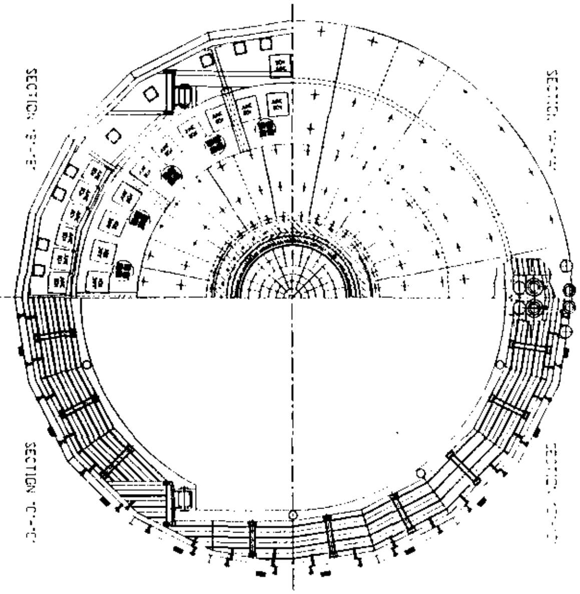

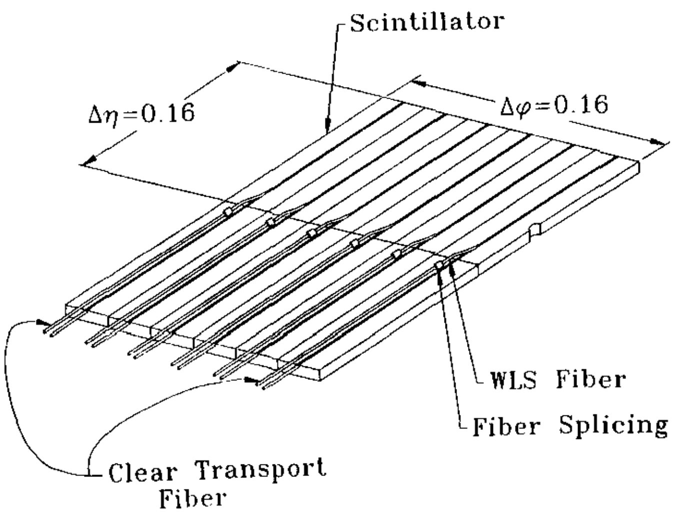

Figure 6: *The scintillating layers with WLS fibers and clear transport fibers*

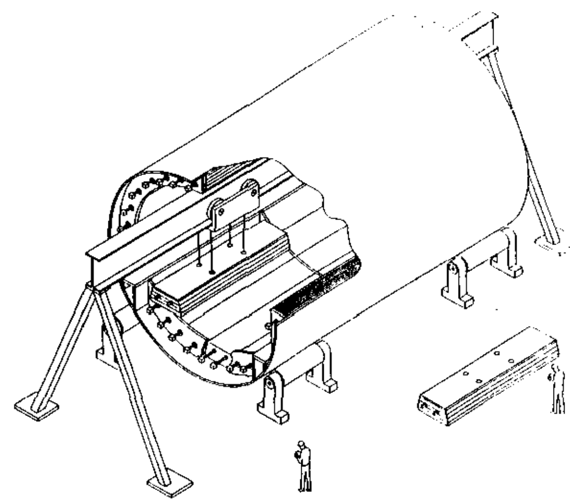

Figure 5: *Modular construction of Scintillating Barrel Calorimeter*

51

OVERALL GEM SCHEDULE MILESTONES

Complete GEM Baseline II concept and TDR	- April 1993
Complete DOE and SSCL Reviews of GEM detector	- October 1993
Receive DOE approval to begin fabrication	- May 1994
Begin Installation of GEM in experimental hall	- October 1996
GEM detector commisioning	- February 2002
SSCL Beam Line commissioning	- March 2002

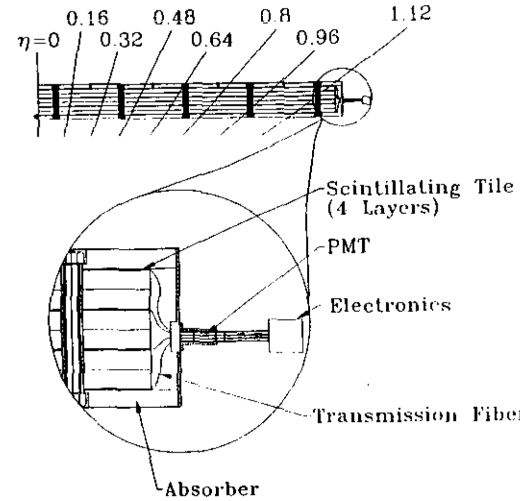

Figure 7: Fibers from 4 layers within one 0.16 x 0.16 tower, or total 24 tiles, are read-out by one photomultiplier tube

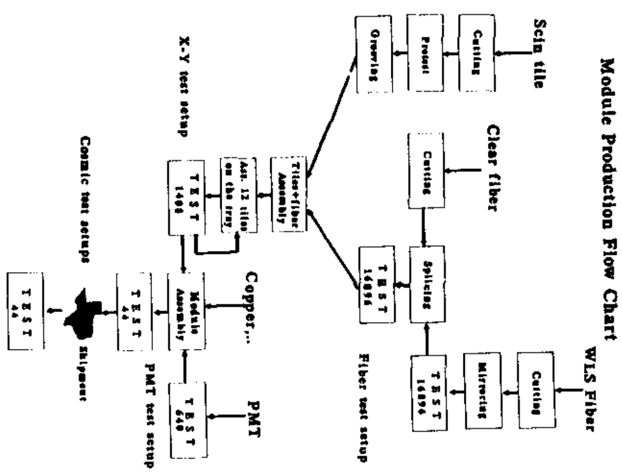

Scintillating Barrel Production Milestones:

Discuss Production Plans with Collaborators	- January-June 1993
Complete Final Production Plans with Collaborators	- June-December 1993
Complete Manufacturing Pre-Prod. Module	- November 1994
Install Module Prototype for Fermi test	- March 1995
Complete Manufacturing Design	- November 1994
Begin Full Scale Manufacturing	- April 1995
Begin Barrel Structure Assembly @ SSCL	- May 1996
Complete Scintillating Modules and Barrel Fabrication	- August 1996
Begin Module Installation	- August 1996
Complete Scintillating Barrel Assembly (at SSCL)	- July 1997
Install Barrel in Experimental Hall	- September 1997

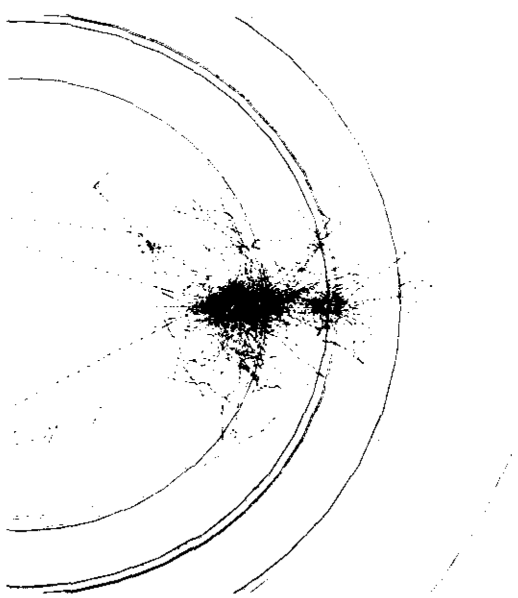

149

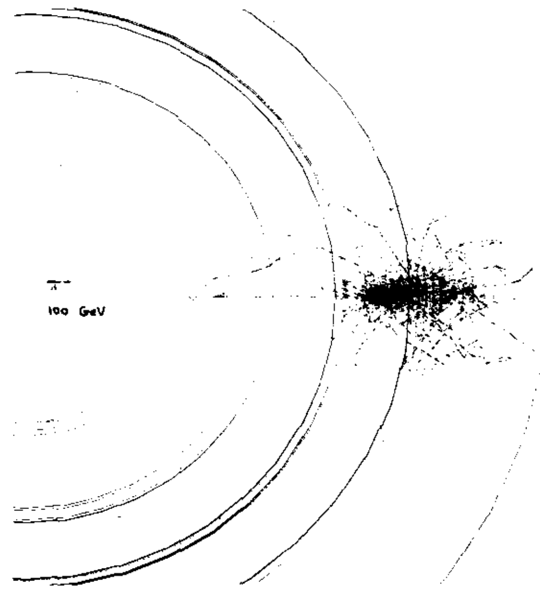

150

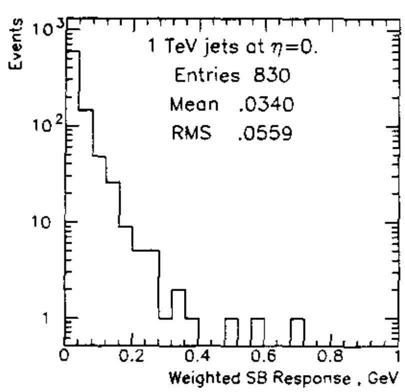

Figure 15: *SBC spectrum for 1 TeV jets*

45

151

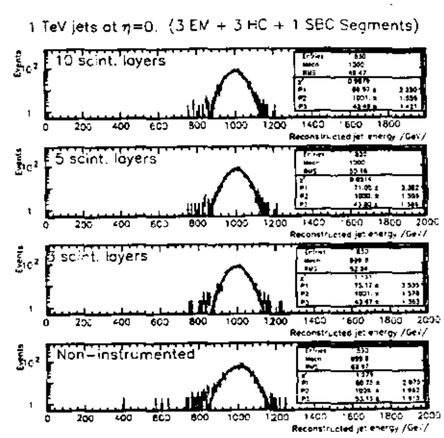

Figure 20: *Response spectrum for 1 TeV jet (3 segments in EM and 3 in HC)*

50

152

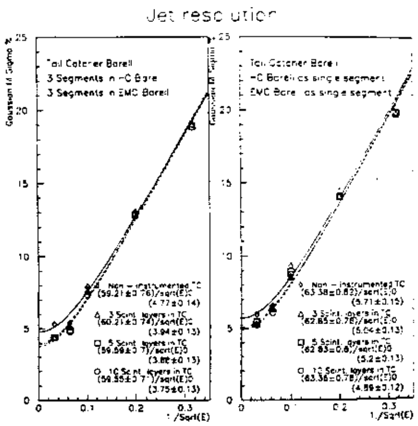

Figure 21: *Parametrization of jet resolution*

51

153

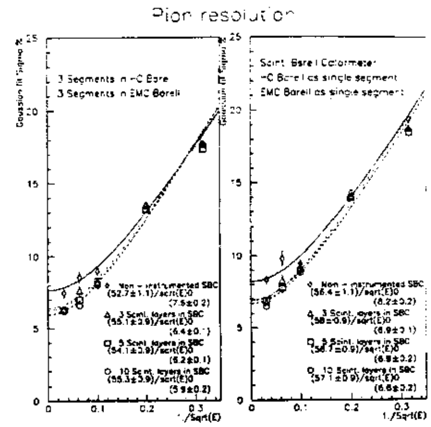

Figure 22: *Parametrization of pion resolution*

52

154

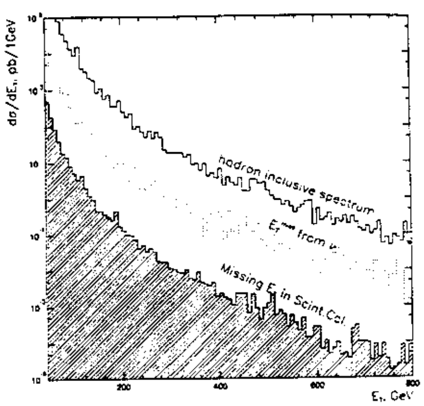

Figure 28: *E_T^{miss} spectrum originated in SBC compared to hadron inclusive cross-section from jets $|\eta| < 1.2$. Also it is shown (dotted line) E_T^{miss} Standard Model background.*

58

155

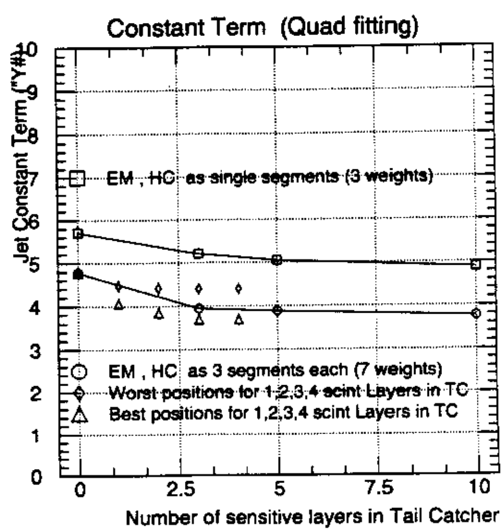

156

GEM Calorimeter With Separate Forward Calorimeter

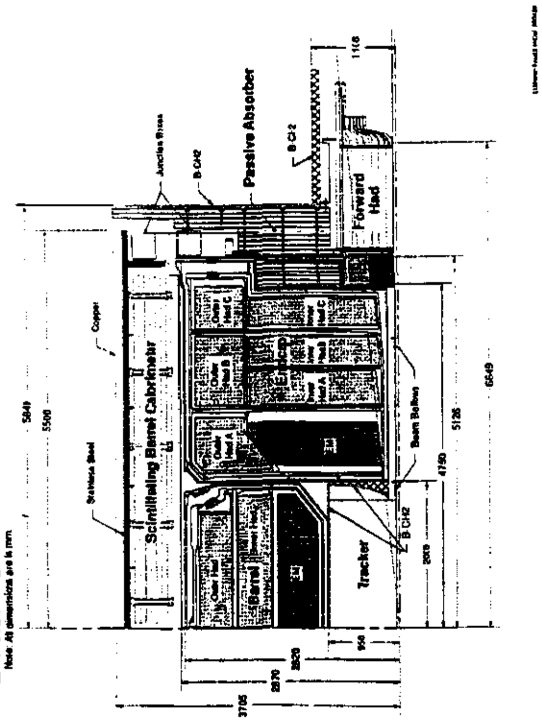

15?

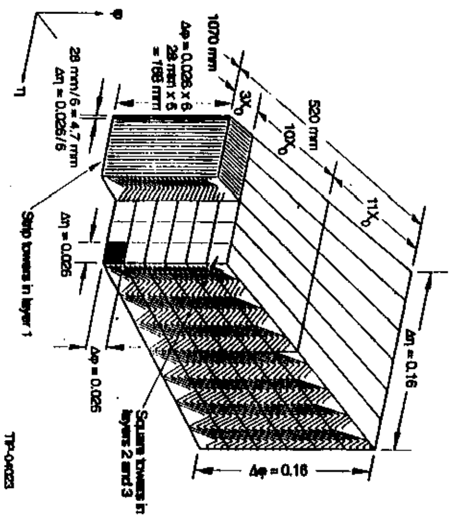

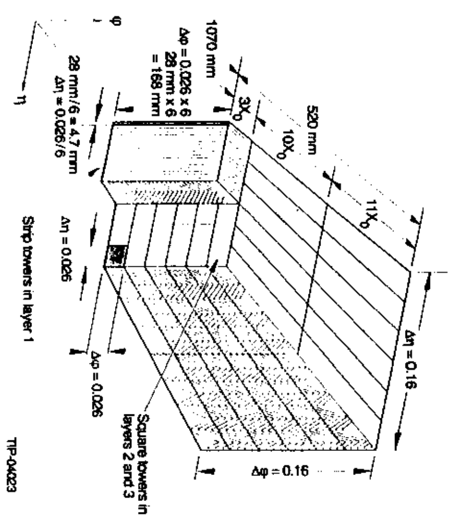

Physics Performance of the Calorimeter

Expected calorimeter performance based on detailed GEANT simulations:

- EM in complete detail with full accordion structure; similar simulation reproduces RD3 results
- Hadronic with GEANT + GHEISHA including all dead material and supports; also at mixture level in GEANT and in CALOR89.

The work of many people is summarized here:
Ma, Seman, Leitchouk, Shupe, Shmakov, Efremenko, Moore and others.

Thanks to everyone who has contributed so much time and effort.

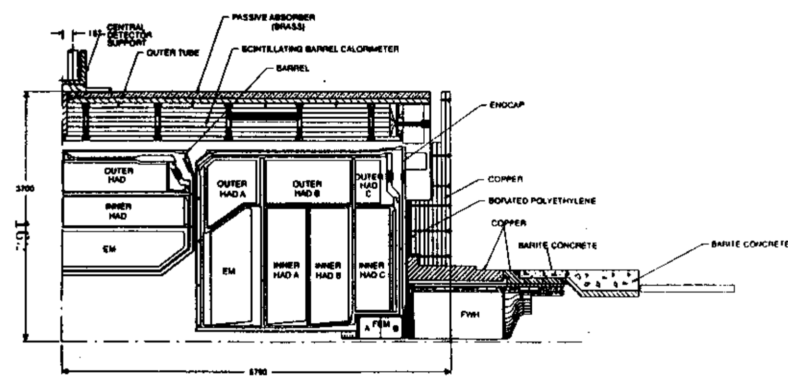

DEPTH OF CALORIMETER

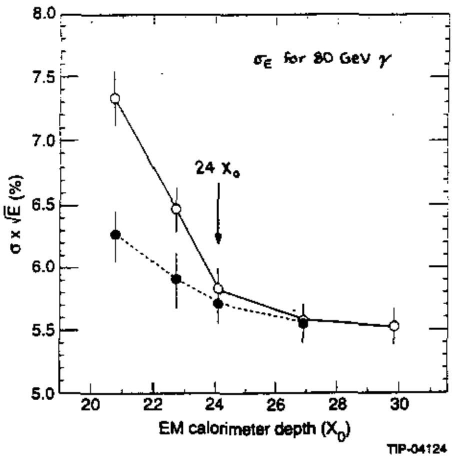

165

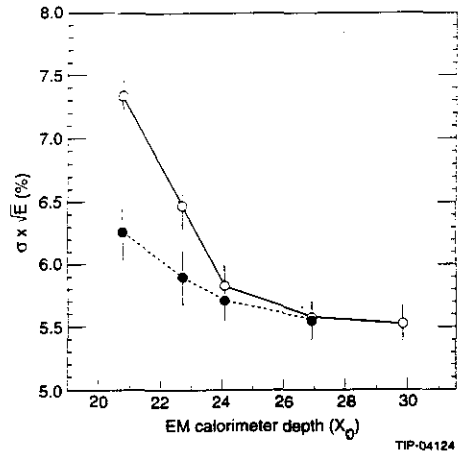

166

OPTIMIZATION OF MASSLESS GAP LENGTH
(BEHIND CRYOSTAT WALL)

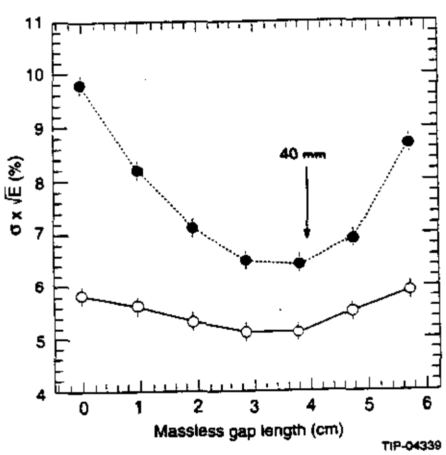

167

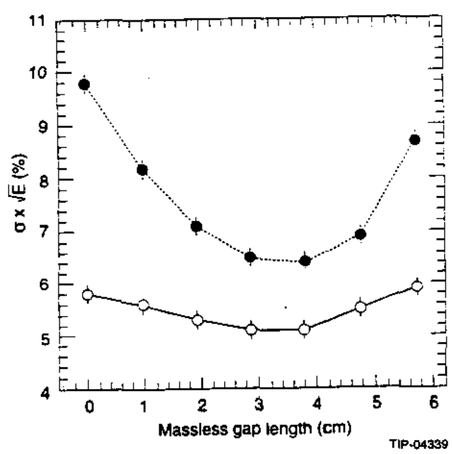

168

EM RESOLUTION LKr BARREL

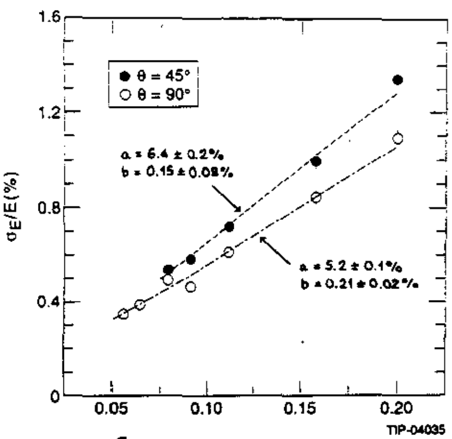

$$\frac{\sigma_E}{E} = \frac{a}{\sqrt{E}} \oplus b \oplus \frac{c}{E}$$

EFFECT OF a AND b ON $\Delta m_{\gamma\gamma}$

a =	6/8	10	15
b = 0.4	1	1.4	2.0
b = 1.0	1.4	1.7	2.3
c = 2.0	2.3	2.5	2.9

Relative to TDR Design

169

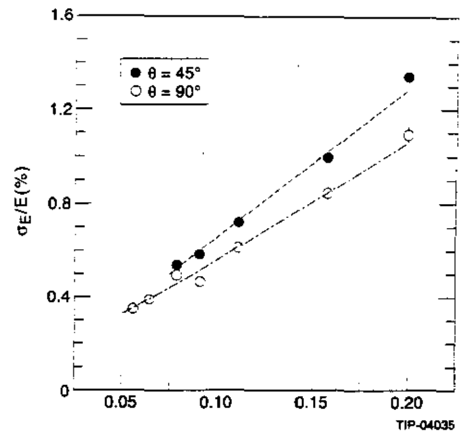

170

TRANSVERSE PHOTON SHOWER SHAPE

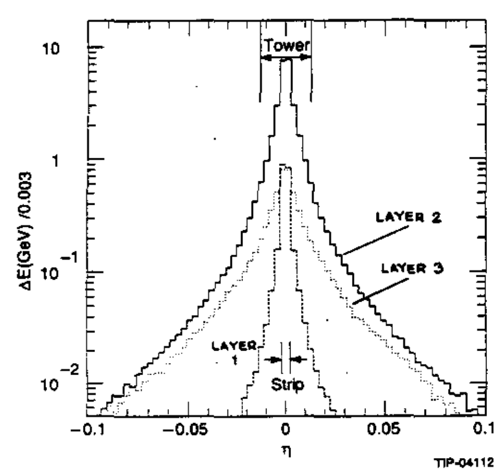

171

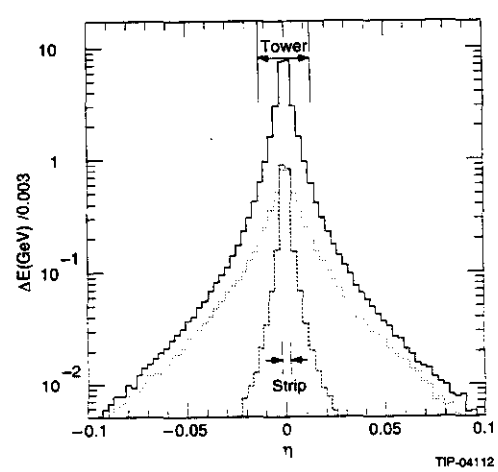

172

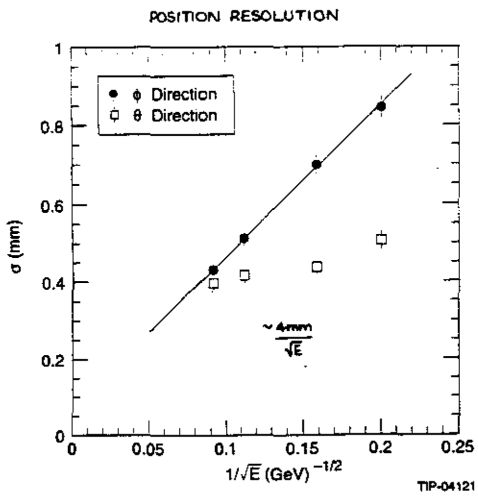

173

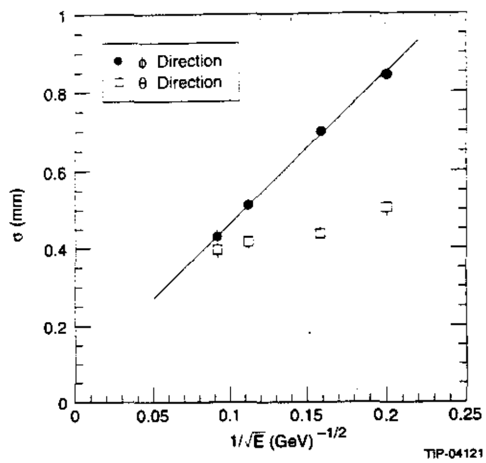

174

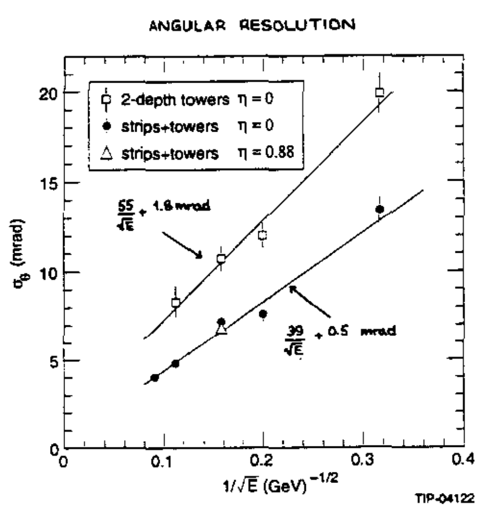

175

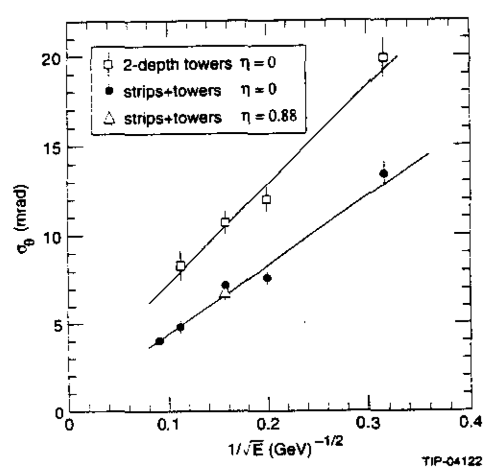

176

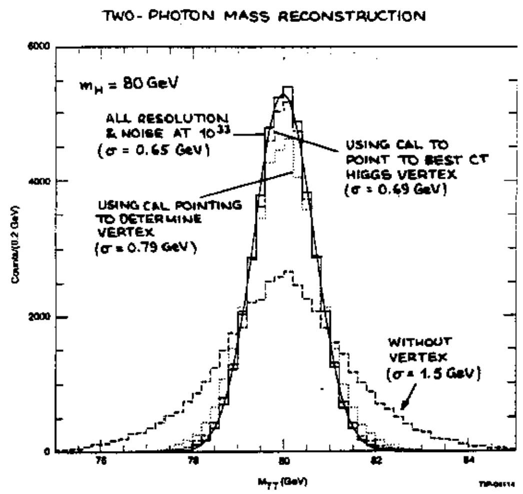

177

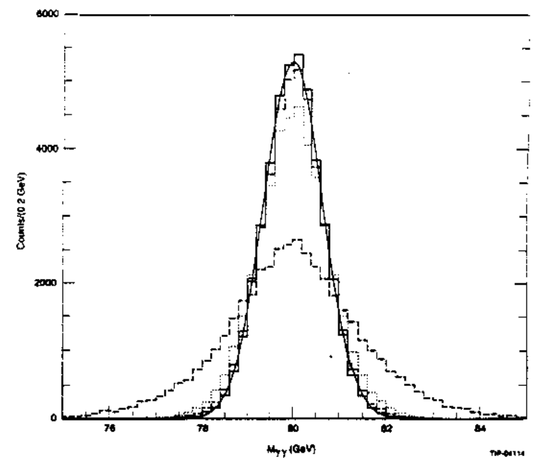

178

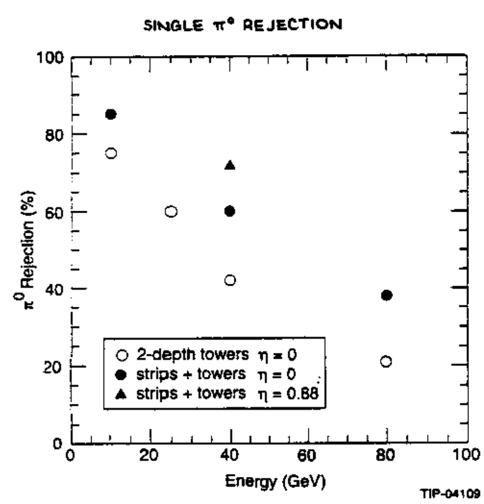

179

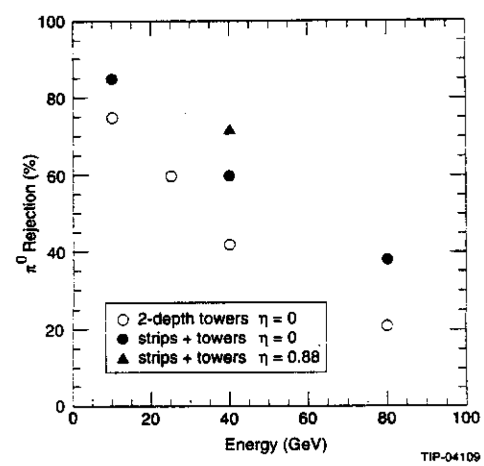

180

JET REJECTION

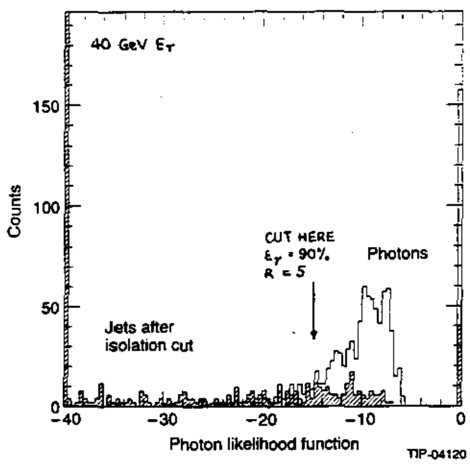

OVERALL RATE FOR JET TO MIMIC A PHOTON

$M_{\gamma\gamma}$ = 100		q jet	g jet
After isolation	:	18×10^{-4}	5×10^{-4}
After γ ID	:	4×10^{-4}	1×10^{-4}

181

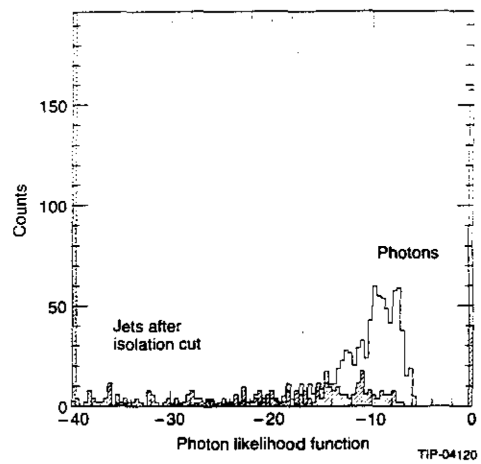

182

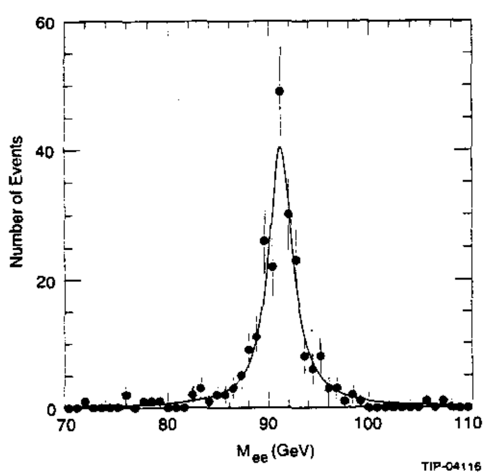

183

CALIBRATION WITH $Z \to ee$

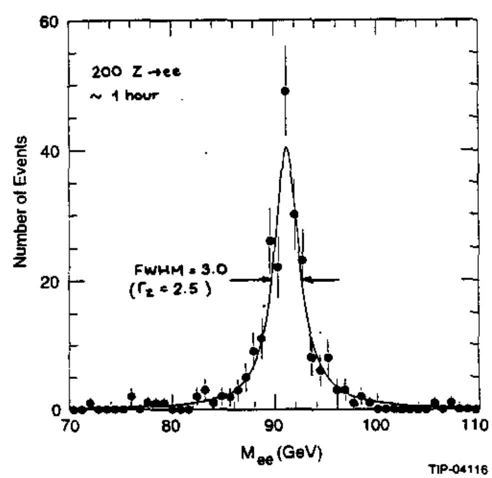

184

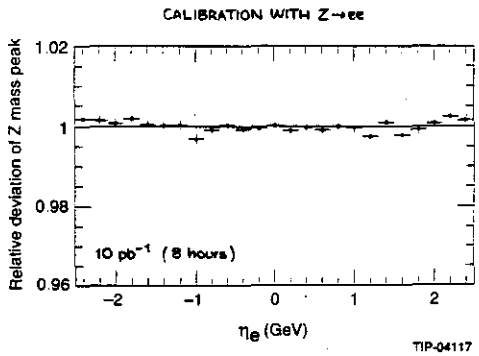

With 3 fb^{-1}, will have 400 electrons per tower, and determine tower response to ~0.4%.

Gains of preamps & readout monitored electronically to ~0.1%

185

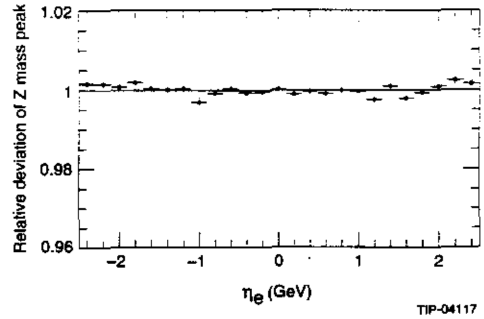

186

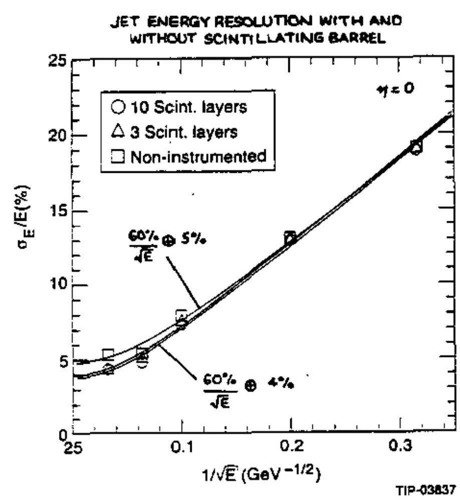

187

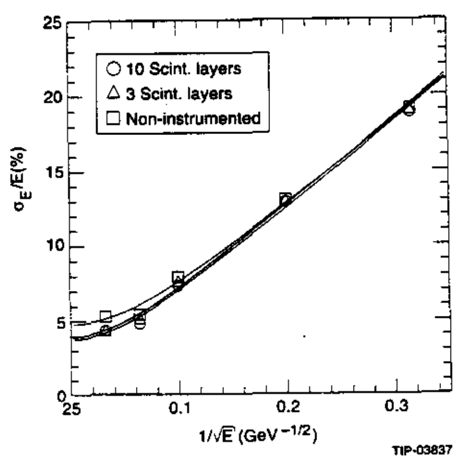

188

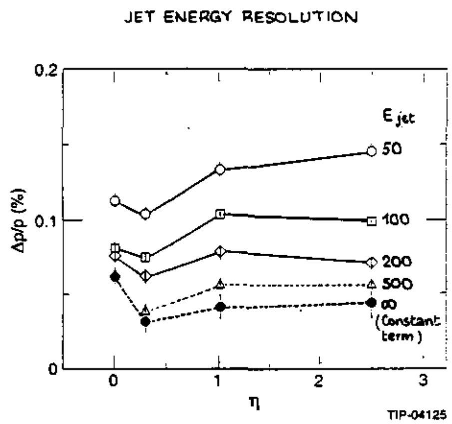

189

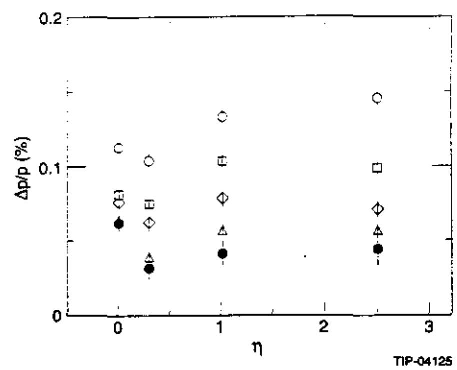

190

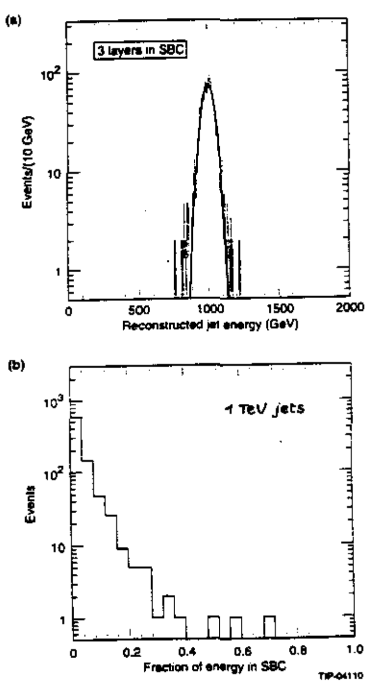

191

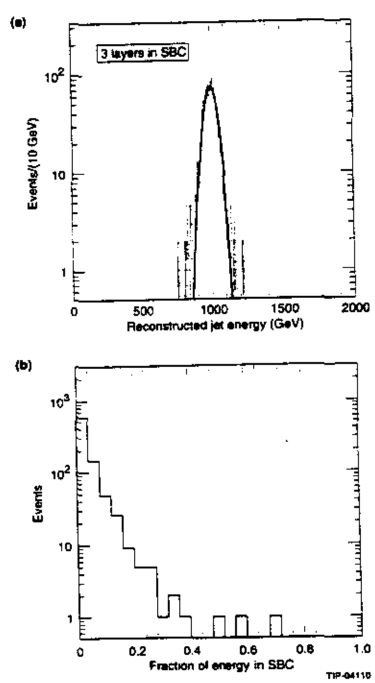

192

Functionality

The user should be able to select, either at compile-time or at run-time if suitably compiled, options such as

Overall architecture (testbeam or TDR design or some new baseline or...)
Tracker
 skip entirely — gemfast-type parametrization — full hit-level simulation
Calorimeter
 skip entirely — gemfast-type parametrization —
 mixture level GEANT simulation (a la UAZMIX) —
 full GEANT simulation
  standard cutoffs — low cutoffs — or with GFLASH showers
Muons
 skip entirely —
 gemfast-type parametrization —
 full hit-level simulation

The common data structures should allow a single piece of reconstruction code to read in any set of events generated by the package and, either reconstruct it or tell you it is inappropriate (a track finder won't work on smeared 4-vectors, for example).

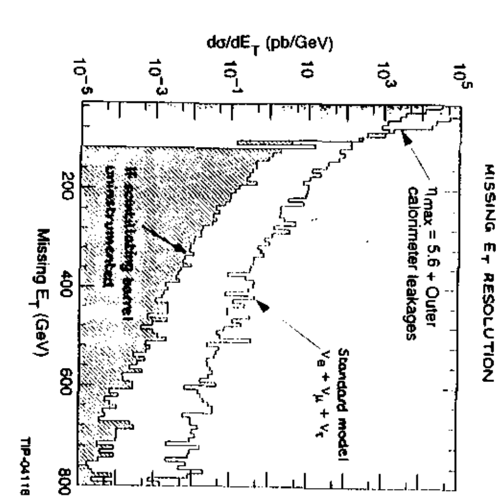

Some ground rules

- The physics simulation code must handle EM and hadronic showers and must be debugged and "trusted". This means we have no alternative but to use GEANT (which now interfaces to FLUKA and CALOR89).
- Thus we should use Fortran 77 (could use C in parts).
- And we will link with ZEBRA, (whether we use it ourselves or not)

  (all of these choices are pragmatic ones based on the need to have code working soon. Development of more adventurous solutions to simulation, using C++ for example, should continue in parallel).

- We should use as much as possible from the existing packages **gemgen**, **sigem**, **gemfast**, UAZMIX and the various detailed GEANT simulations. We don't have enough spare manpower to throw code away.
- Code should be supported on the standard 5 GEM unix platforms.
- If possible, the code should also run on VMS, though it may need to be kluged and hacked somewhat and won't be fully supported.
  This is not an absolute requirement but (I think) still a desirable feature.

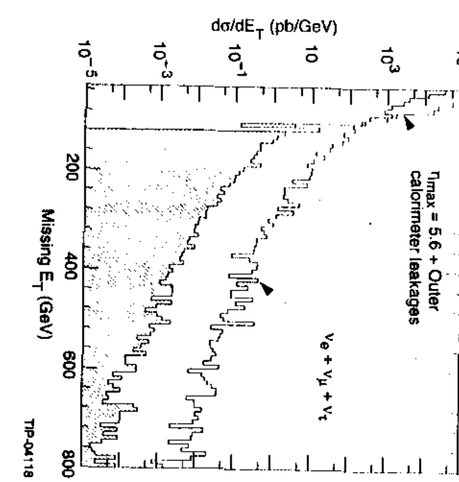

Organizational issues

The effort should be coordinated from the SSCL but must involve people from university groups and subdetector simulation experts from tracker, muon and calorimeter. Each subdetector group should assign ~1 FTE and sufficient support to this project.

There should probably be one "librarian" or "integrator" who will read codes delivered and make sure they interface correctly (the role played by Tomasz for `gemfast`).

Global simulations for GEM

It is (I hope) generally agreed that GEM simulation should evolve toward a more coherent, unified, and global simulation package.

The goal should be to have a program or suite of programs which use *common data structures* but allow selection of various levels of detail. The simulation is needed to study issues beyond the scope of gemfast-type simulations.

A few examples:

- Evolution of detector design
- Jet resolution, especially in barrel-EC, EC-FC regions.
- Forward Jet tagging
- Jet rejection
- Missing E_T resolution
- Combined detector reconstruction algorithms, eg electron and muon using tracker + calorimeter + muon system (a muon study is already underway)
- Trigger studies

All these issues must be addressed in detail over the next couple of years.

Work to be done immediately

- **Geometry input and definition package**

A front-end which will handle the parameters needed for the creation, positioning and rotation of the GEANT volumes. This should be easily edited and should support future input from CAD systems (e.g. Martin-Marietta's models) and future output to GISMO (for EGS simulations). We should have an automated system to assign material and medium numbers, rotation matrices, etc.

- **Data structures**

We will need the GEM "framework group" to provide a working solution for data structures and handling I/O which is callable from F77 and available on all 5 GEM unix platforms (plus VMS if possible) by 9/93. If this is not available we will use ZEBRA as a fall-back solution.

Milestones

I assume that the simulation and reconstruction issues listed earlier should be addressed as soon as possible, and using code that has a long life-expectancy rather than by kluging the present setup.

An additional constraint is set by the Fermilab test beam run. From D0 experience it would be extremely advantageous to have a detailed Monte Carlo simulation of the test beam in existence with events generated before the data taking begins.

I have assumed 6 months to code and debug the geometry for both the full GEM and testbeam setups and 3 months spent generating data. This leads to the following timescale:

6/93: evaluate geometry builder and data structures solutions
9/93: coding and debugging full GEM geometry
3/94: coding and debugging test beam geometry based on full detector
9/94: begin generating data
1/95: testbeam data taking starts

(This is very similar to the schedule for SDCSIM).

Forward Calorimetry

John Rutherfoord

University of Arizona

GEM Forward Calorimetry

GOALS

1) Hermetic coverage

    Measure missing E_T of event

2) Detect and measure kinematics of <u>Jets</u>

    with $\Delta E_T/E_T < 10\%$

    Not e's or isloated γs

3) Mitigate the *Neutron Problem* in muon system

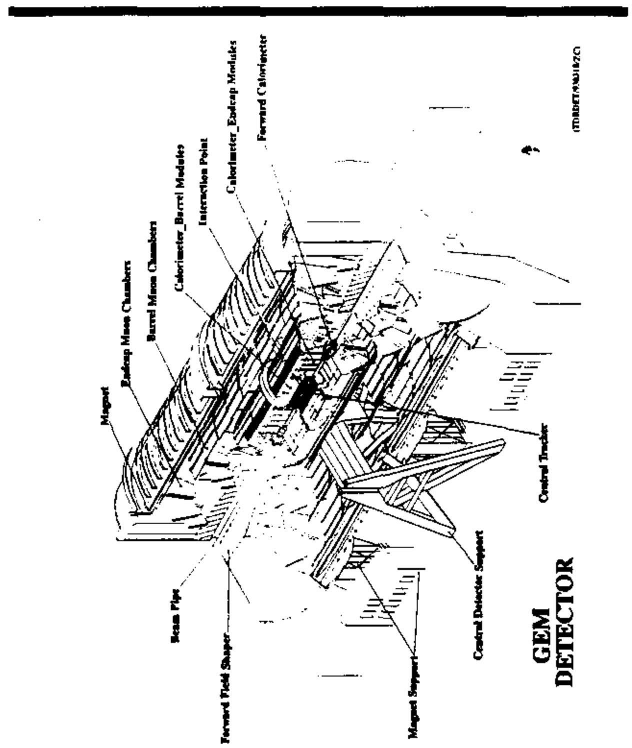

GEM Coverage

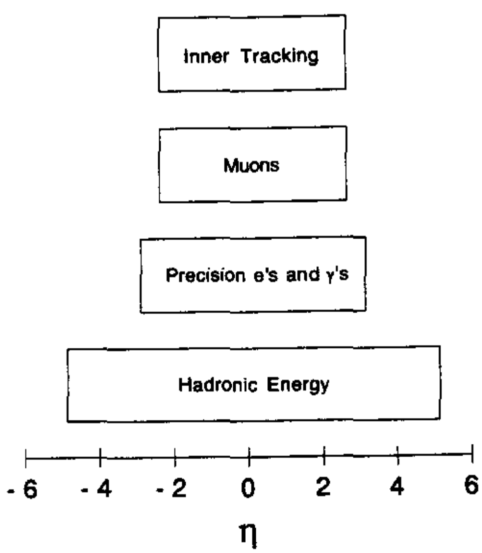

E_T Resolution

Sources

1) Hadronic Energy Resolution
    (e/h + ...)

2) Angle resolution

3) Dead material (EM/had separate manifestations)

4) Lack of coverage (beam hole, η = 1.1 cc/ec transition, ...)

5) Shower leakage out the back

6) p_T cross-over

7) Dead cells/hot cells

8) Weighting schemes

9) Extra min-bias events on top of trigger event

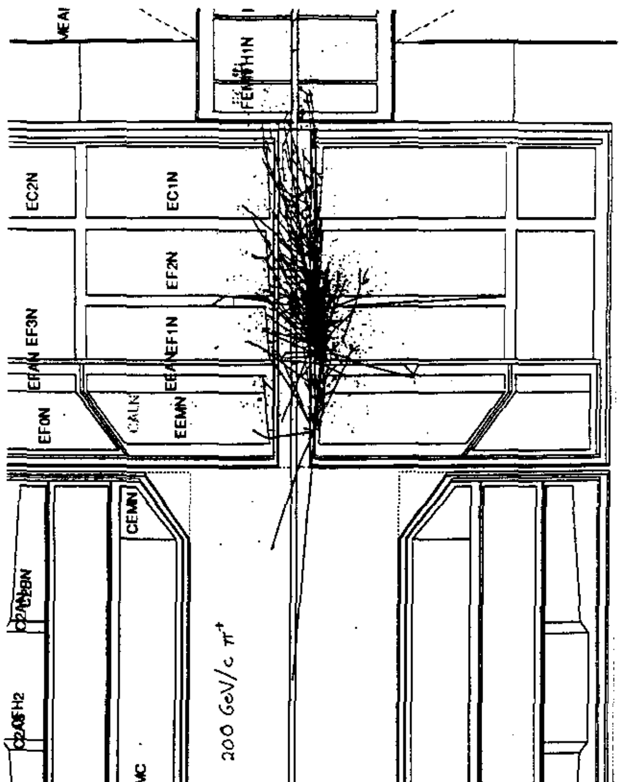

209

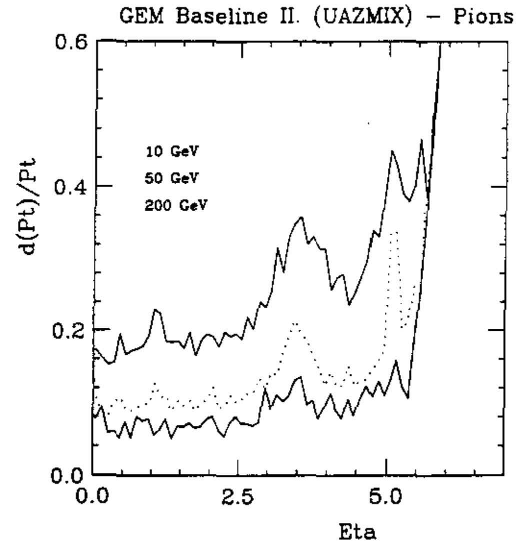

210

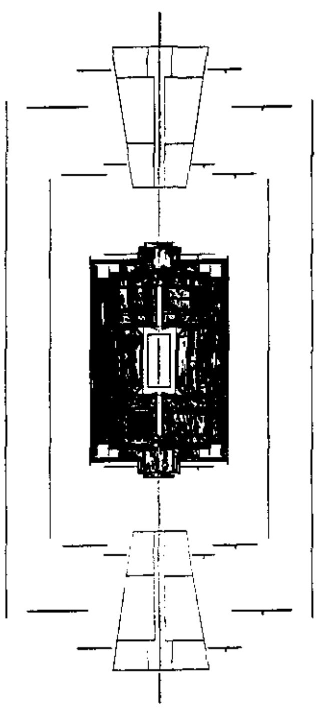

211

GEM Forward Calorimetry

CHALLENGES

1) Survive high dose rates

1 GRad/SSCyr @ 10^{34} cm^{-2} sec^{-1} and η=5

Worse at larger η

2) Protect the muon system from

Hadronic spray

Neutrons

3) Energy resolution for Jets $\Delta E/E < 7\%$

4) Angle resolution for Jets $\Delta\theta/\theta < 7\%$

5) Limit transverse spreading of showers

6) Accommodate wildly changing conditions

with *uniform* calorimetry

212

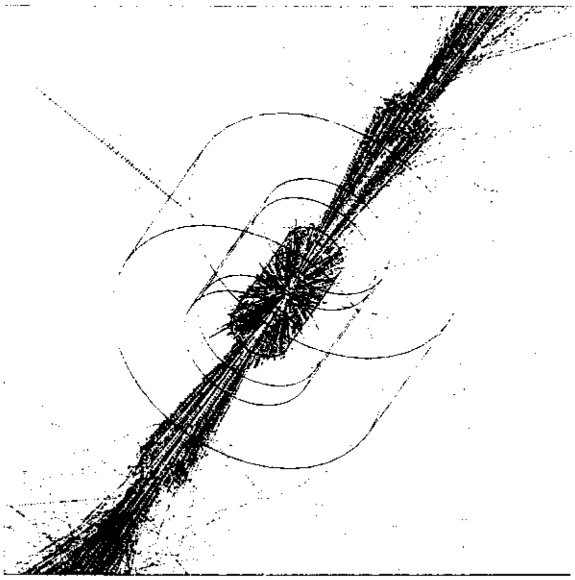

TEKTRONIX TEKTRONIX TEKTRONIX TEKTRONIX

213

Variation across the front face of the GEM FCal

η	ΔR=0.7 cone (cm)	Current Draw per 3 tubes (nA)	Physics Pileup E_T Noise (GeV)	Thermal E_T Noise (GeV)	Dose at EM Shwr Max (MRad/SSCyr)
3.4	20.5	0.03	1.1	1.7	0.9
3.8	13.8	0.09	1.1	0.8	2.8
4.2	9.2	0.3	1.2	0.4	9.3
4.6	6.2	1.0	1.8	0.3	30
5.0	4.2	3.3	2.7	0.2	96

214

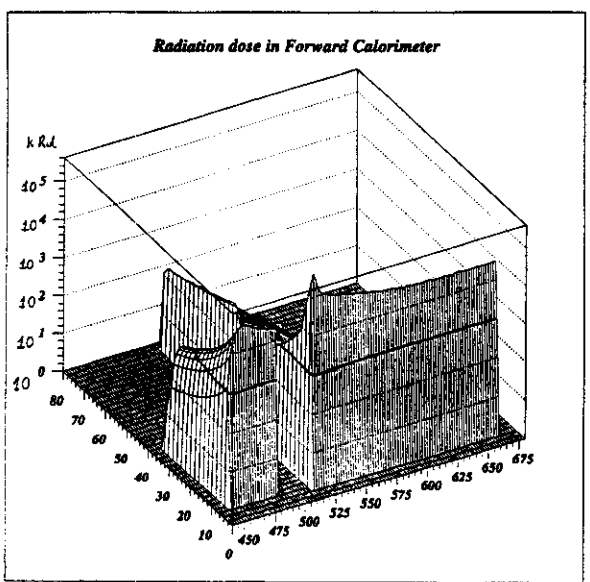

215

GEM Forward Calorimetry

GEOMETRY

1) Unique location

Integrated with end-cap

Close to IP

2) Manifestly Hermetic

Reduces *cross-over* problem

Optimal protection of muon chambers

3) Creates challenges

High rate / rad damage

Transverse shower size relatively large

Proximity to beam pipe

216

SDC

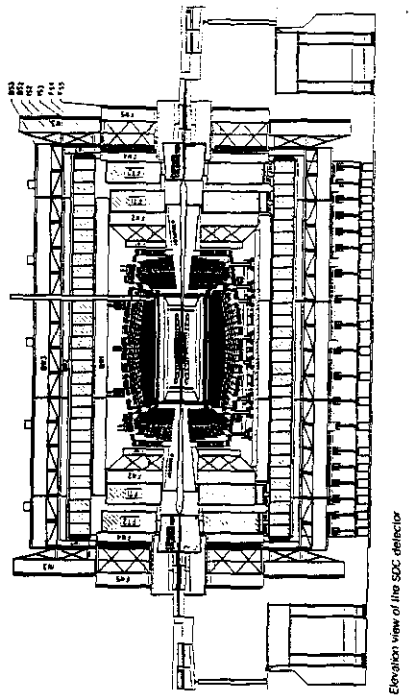

Elevation view of the SDC detector

217

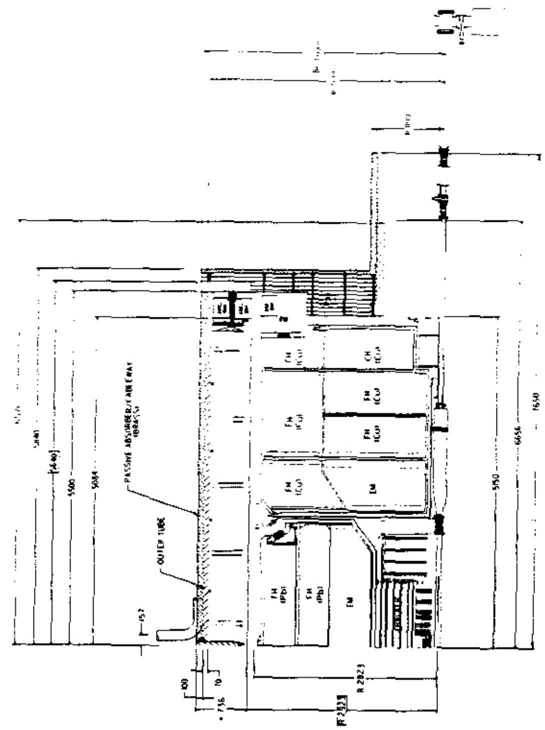

218

GEM Forward Calorimetry

LONGITUDINAL SEGMENTATION

1) Separate EM and Hadronic sections

2) Allows separate optimization for separate problems

Problems in EM section

High rad damage

Fine grained transverse segmentation for

Narrow EM showers

Precise angle determination of hadronic showers

Problems in Hadronic section

Must limit transverse spreading

3) Allows software weighting schemes for improved resolution

4) Allows cheaper/easier pseudo-projectivity

219

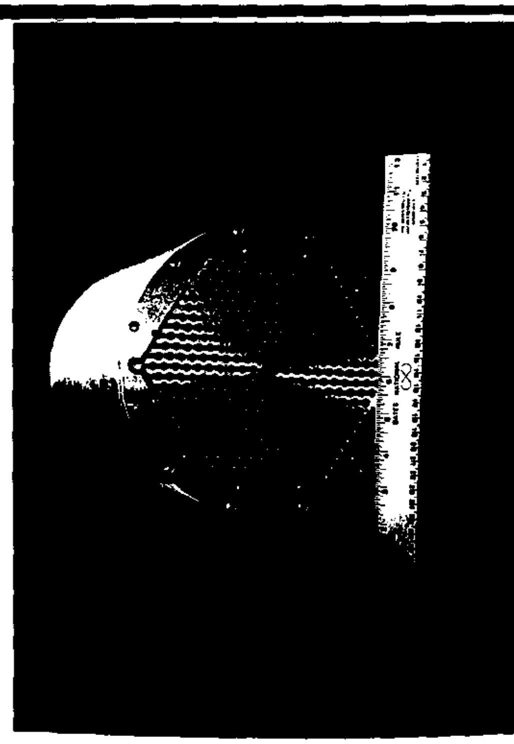

220

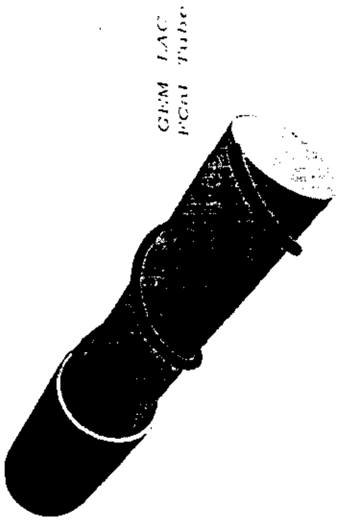

221

GEM Forward Calorimetry

EM ABSORBER MATERIAL

Choose Copper or Brass because ....

1) Less Rad damage due to longer radiation length

2) Less positive ion build-up problem

3) Larger Moliere radius for more uniform sampling

4) Easier removal of heat ~100 watts at 10^{34}

222

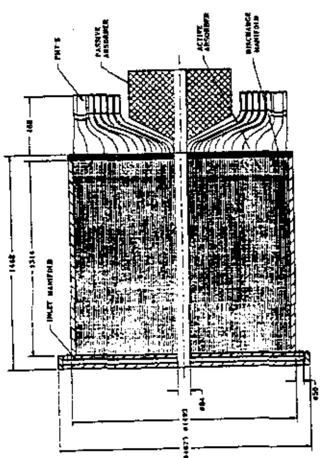

Fig. 5-23 HAD FCAL Module Arrangement

223

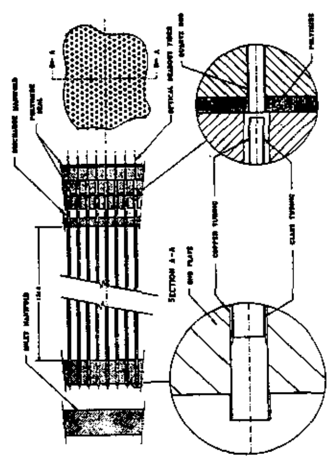

Fig. 5-24 Detail of Capillaries and Readout Section.

224

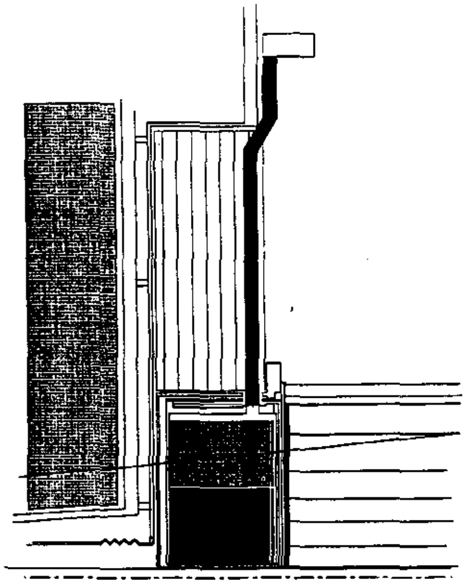

225

GEM FCal Technology Choice

Options

	TDR	Opt 1	Opt 2	Opt 3	...
"EM"	LAr	LAr	QF	LAr	
Hadronic	LScint	QF	QF	LAr	

'93 Beam Tests

LAr (EM)	BNL → CERN	UAz
LScint (Had)	BNL	TA&M
QF (Had)	BNL	Fairfield/ORNL
QF (?)	CERN	Gorodetsky

Other R&D

High Rate/Rad Damage — LAr — UAz

QF — ORNL

Time Scale of Decision

Was to be Fall '93

In time for Fermilab tests in '97

226

Muons in the calorimeter.

Y.Efremenko
ITEP/ORNL

1. Muon Pt.
2. Muon energy loss correction in calorimeter
3. Noise in calorimeter.
4. Instrumentation of SBC
5. Endcap region.
6. Conclusion

As was shown before (GEM-TN-269, 349) for muon with Pt higher,then 100 GeV the calorimeter influence on the muon resolution is negligible.

At the same time, muons with the low Pt (10-40 GeV) are very important for the Higgs detection.

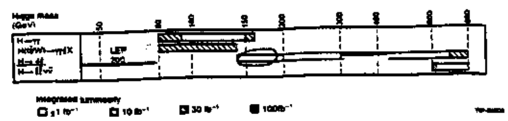

The more difficult for detection Higgs in 4μ is the Higgs with the mass 140 - 185 GeV where the Z0 mass constrain doesn't work.

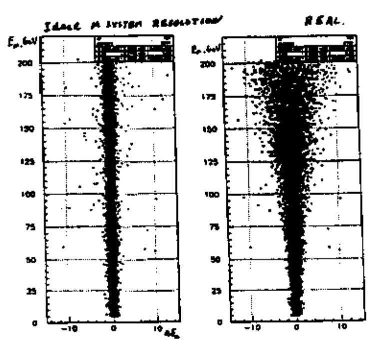

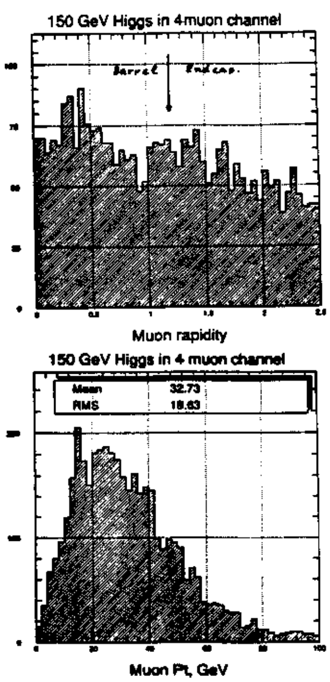

Geant simulation.

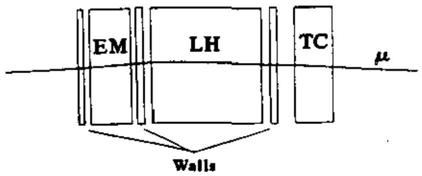

Muons Pt 10, 20, 50, 100, 500 GeV

Rapidity region near 0.0 and 0.9

One point for endcap Pt 20 GeV η 2.0

$$\Delta E_\mu = E_\mu^0 - (P_\mu + k_1 E_{EM} + K_2 E_H + K_3 E_{TC} + C)$$

Contribution from calorimeter only if $\delta P_\mu / P_\mu = 0$

233

Muon energy loss correction in calorimeter.

1. Using calorimeter information → **Combination.**
2. Using the most probable value → **Combination.**

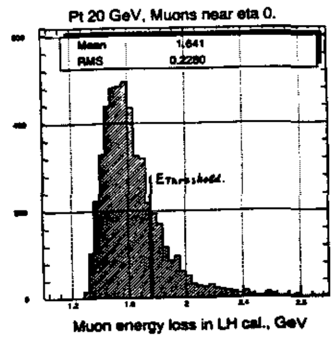

234

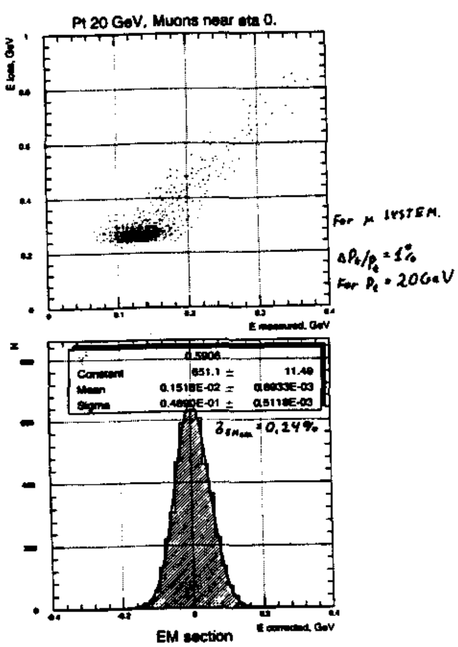

235

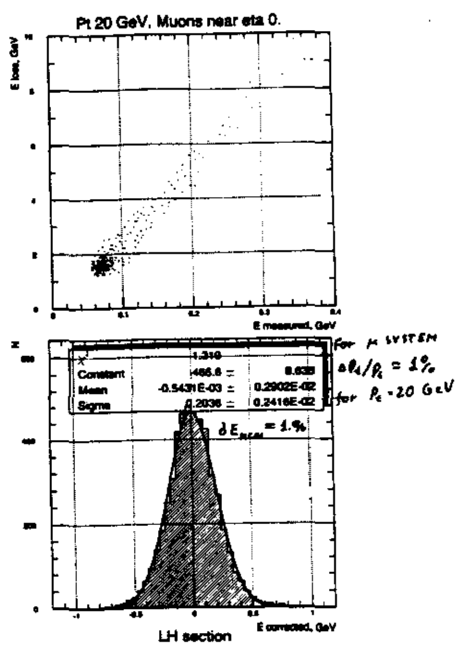

236

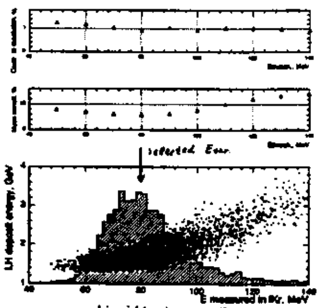

Liquid hadron section

237

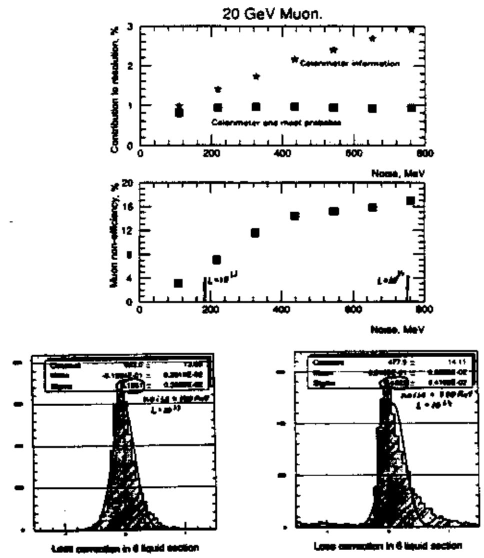

238

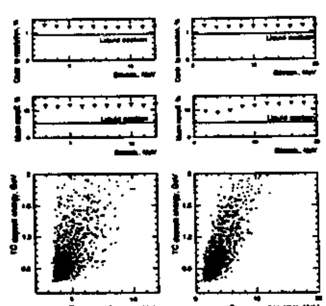

4 Sci. layers

10 Sci. Layers

239

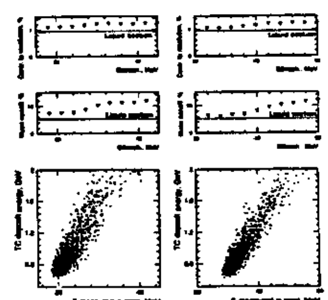

20 Sci. Layers

30 Sci. Layers

240

S.B.C.

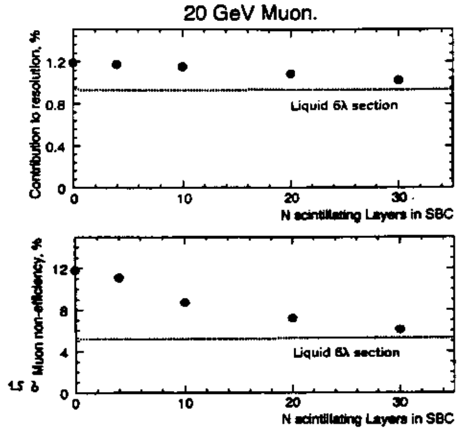

241

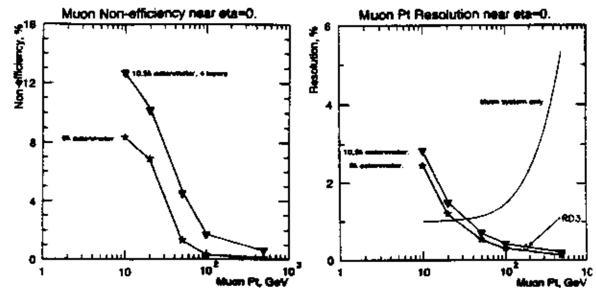

242

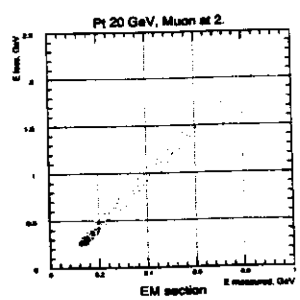

243

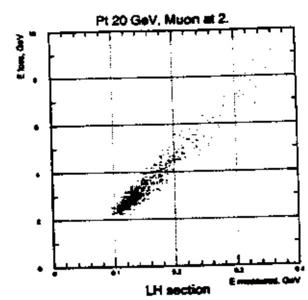

244

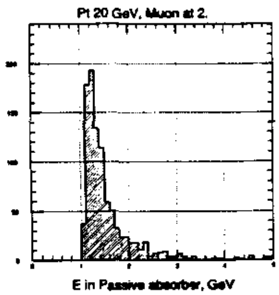

245

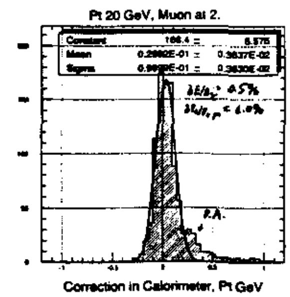

246

CONCLUSION

1. **Barrel calorimeter is strongly affect on the resolution of muons with Pt less than 30 GeV.**

2. **Influence of the Endcap calorimeter on the muon is low.**

3. **Increasing of the pileup noise at the high luminosity will strongly affect on the efficiency or resolution of the low Pt muons.**

4. **For the low momenta muon there is almost no difference how many sensitive layers (from zero to ten) are in SBC.**

   The real improvement will appear if SBC would have more than 25 sensitive layers.

247

F.E. Taylor - MIT
San Diego Review 5/10/93

GEM Muon System

- General Features
- Design Goals
- Chamber Technology
- Drivers of the Design
- System Performance

251

Speakers for GEM Muon System San Diego

- Overview

  Taylor

- Review of Chambers and Alignment

  Mitselmakher

- Layout of Chambers and Support Structure

  Nimblett

252

- **Physics Objectives - Muon System**

Examples:

Higgs searches:	$H^o \dashrightarrow \mu^+ \mu^- \mu^+ \mu^-$
	$130 < MH^o < 800$ GeV/c^2
Z' searches	$Z' \dashrightarrow \mu^+ \mu^-$
	MZ' < few TeV/c^2
W' searches	$W' \dashrightarrow \mu\, \nu$
Heavy flavor searches	$t\bar{t} \dashrightarrow \mu\, \nu\, b\, X$
The unexpected	

Note: EM calorimeter objectives complementary to Muon System

253

Features of Muon System

Design:

- **Large Superconducting magnet**

  BL^2/σ resolution figure of merit

  - radius 9 m
  - length 30 m
  - field value 0.8 T at intersection point
  - field shaper radial field component at large $|\eta|$

- **One Technology [trigger and tracking]**
  - Cathode Strip Chambers barrel and endcaps

Goals:

- **Good resolution: standalone (no CT)**
  - three-point sagitta method
    - for Pt = 25 GeV/c
      - $\delta Pt/Pt = 3\%$ at $|\eta| = 0$ ($\theta = 90^o$)
      - $\delta Pt/Pt = 1.6\%$ at $|\eta| = 2.5$ ($\theta = 9.5^o$)
    - for Pt = 500 GeV/c
      - $\delta Pt/Pt = 5\%$ at $|\eta| = 0$ ($\theta = 90^o$)
      - $\delta Pt/Pt = 12\%$ at $|\eta| = 2.5$ ($\theta = 9.5^o$)
- **Pt trigger and beam cross tag**
  - can select up to Pt > 50 GeV/c
- **Operational at $L = 10^{34}$ cm^{-2} s^{-1}**

254

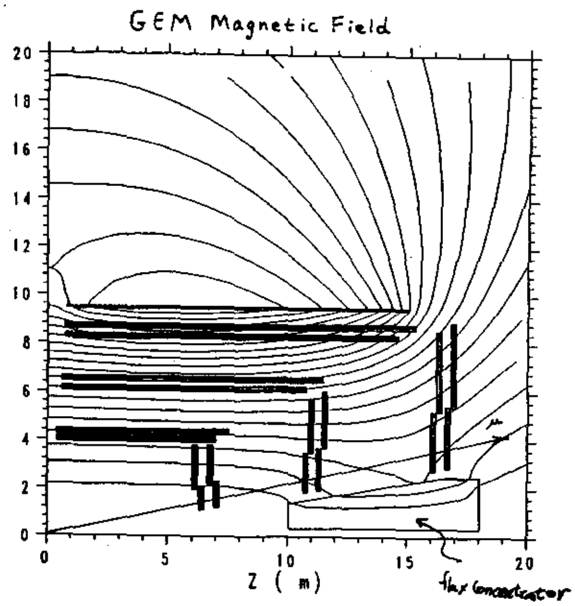

2 φ segments of chambers shown

255

Pt from Sagitta Measurement

- At $|\eta| = 0$ (90°) for $\mu \pm$

$$S = \pm \frac{0.3\, BL^2}{8 P_t}$$

- S = 1.1 mm for Pt = 500 GeV/c

- Total error "budget" at 500 GeV/c $\delta S \approx 50\ \mu m$

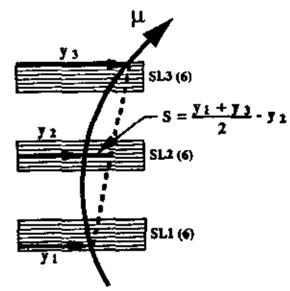

256

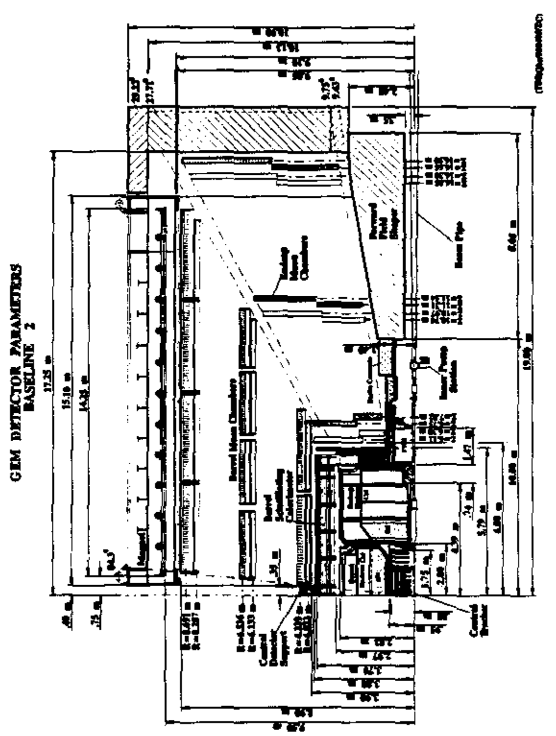

257

Chamber Technology

- Baseline for TDR:

  Trigger and Tracking Functions: barrel and endcaps

  CSC = Cathode Strip Chambers

- Considered:

  Tracking Function:

  LSDT = Limited Streamer Drift Tubes

  RDT = Round Drift Tubes (pressurized)

  Triggering Function:

  RPC = Resistive Plate Counters

- Chamber Testing Program:

  TTR = Texas Test Rig (Cosmic ray muon laboratory at SSCL)

258

Cathode Strip Chamber

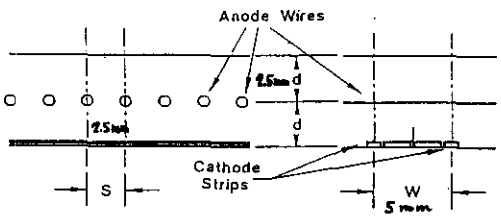

Figure 1: Geometry of the basic cell of the CSC

259

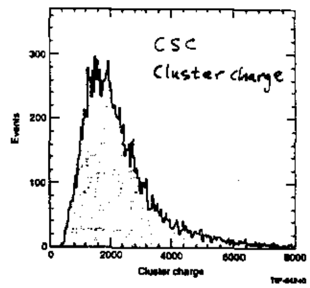

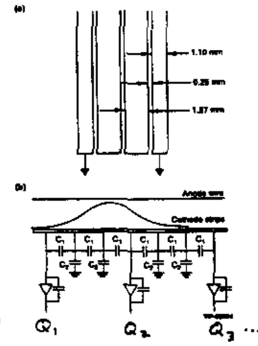

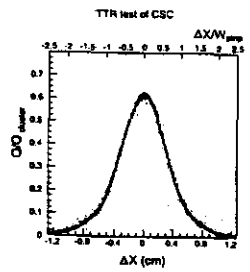

260

Properties of Cathode Strip Chambers

Property	Value
• Single layer resolution	$\sigma \leq 75\ \mu m$
• Orthogonal coordinate	anode wires $\sigma \leq 5\ cm/\sqrt{12}$
• Two track resolution	separated for $\Delta x \geq 2$ strips [e.g. $\Delta x \geq 10$ mm in SL1]
• Timing	$\sigma \leq 8$ ns (beam tag $\varepsilon \geq 99$ %) [τ–drift < 30 ns]
• Rate capability	τ–integration = 300 ns [4-strip occup. $\leq 1\%$ at 10^{34}]
• Neutron and γ sensitivities	OK for $L = 10^{34}\ cm^{-2}s^{-1}$
• Integrated function	triggering-tracking-timing
• Parameters validated	R&D program

261

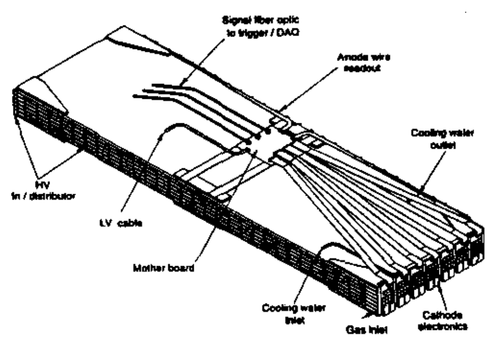

FIG. 4-48. Perspective view of complete CSC barrel chamber.

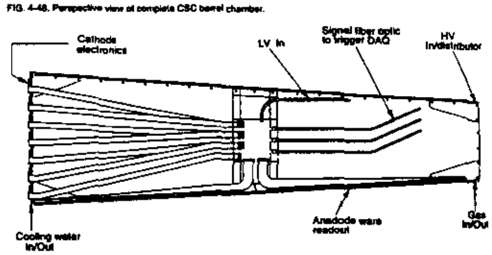

FIG. 4-49. Plan view of endcap chambers.

262

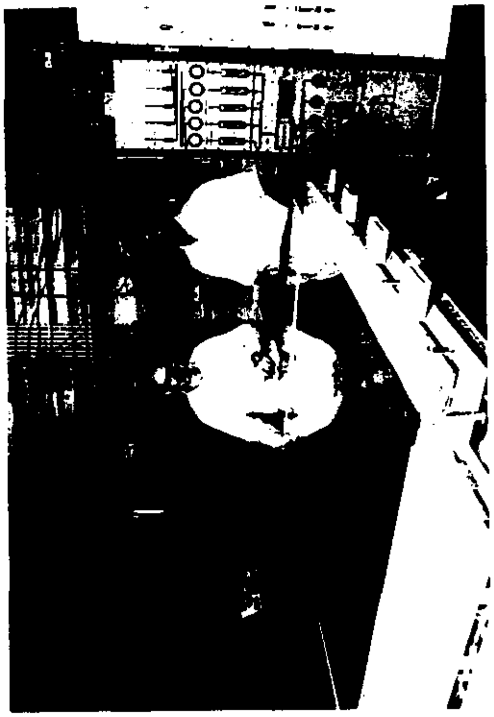

263

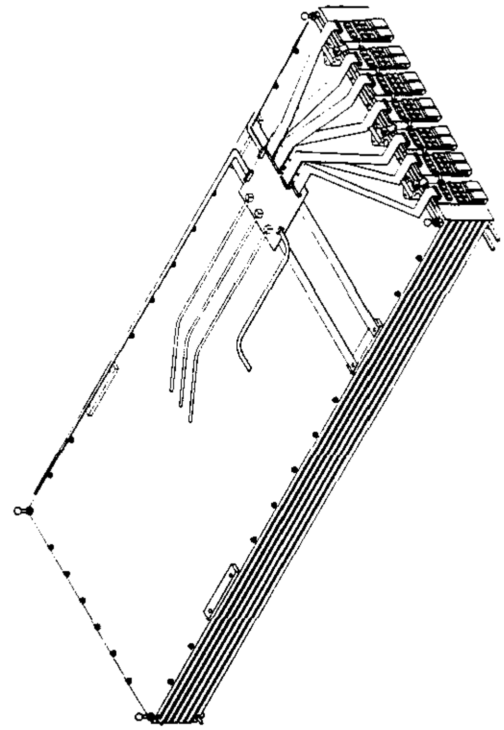

264

Drivers of GEM Muon System

- Alignment

  Projective paths
  - six per chamber tower (5 in endcap)
  - gap in middle super layer of barrel

- Support structure

  Nodes of structure
  - congruent with corners of chamber
  - chamber towers individually supported

  Separate barrel and endcaps

- Properties of Cathode Strip Chambers:

  Anode wire stability
  - width of chamber [anode wire span ≤ 1.2 m]

  Size of precision cathode panels
  - maximum length = 3.5 m
    [source capacitance and industry limit]
  - maximum width = 1.2 m
    [industry limit consistent with wire stability]

  Lorentz angle nulling
  - barrel chambers rotated by 6° to 8°
    [allows chambers to be overlapped in ϕ barrel]
  - endcap wires asymmetric to radial axis

  Radial strips in endcaps
  - trapezoidal chambers

265

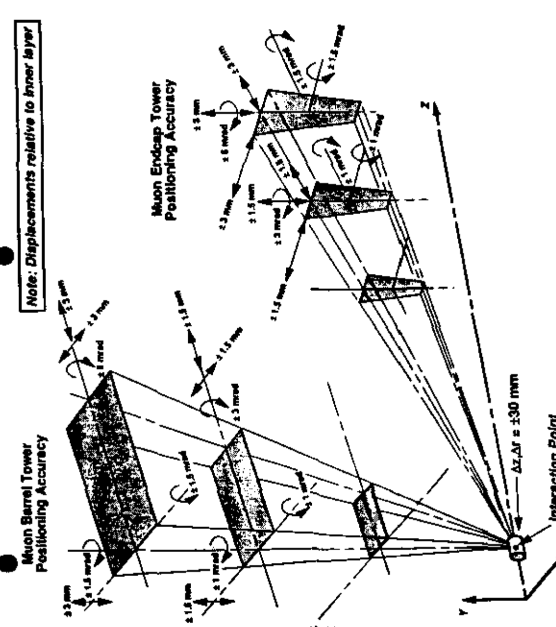

266

Chamber Support Structure

- Engineering Group:

  Draper Lab. - Cambridge, MA
  LLNL - Livermore, CA
  SGH - Arlington, MA
  SSCL /EFD - Dallas, TX

- Stable platform for chambers

  Error budget:

  $\sigma \leq 25\ \mu m$ inter - superlayer alignment
  $\sigma \leq 50\ \mu m$ intra - superlayer alignment - random
  $\sigma \leq 75\ \mu m$ single layer resolution - random

- *Considered:*

  Performance (stability to vibrations)
  Cost
  Fabrication and installation requirements
  Schedule impact on GEM construction
  Access

- Propose to build:

  Barrel: ***sectors (1/12) tied together as a monolith***
  good vibration characteristics
  ease of construction in small parts
  prototype testing possible

  Endcap: **super-wheels (one/superlayer)**
  reduces intra-layer structural elements
  monolith has good stability performance

267

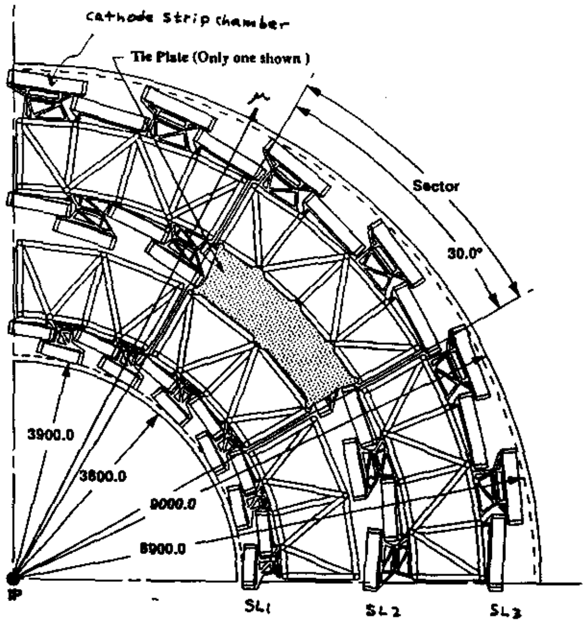

268

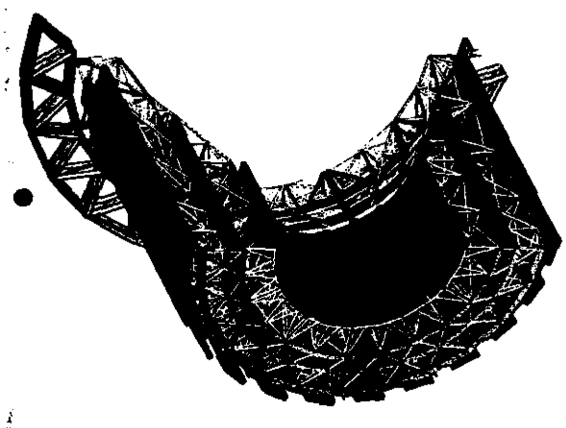

269

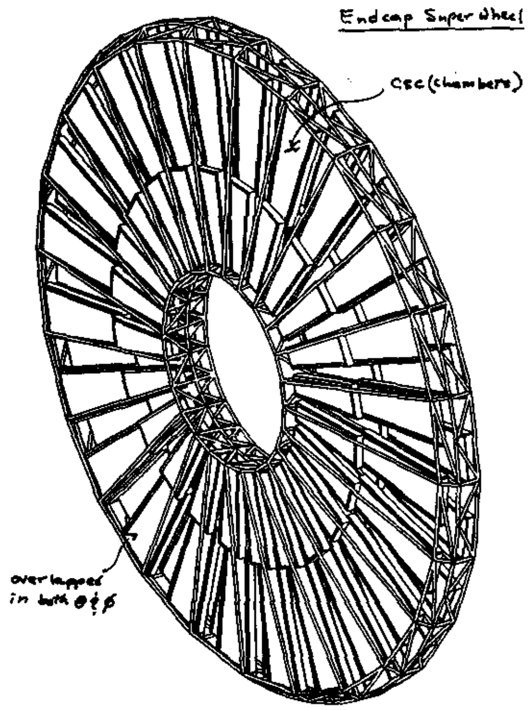

270

Endcap Support structure

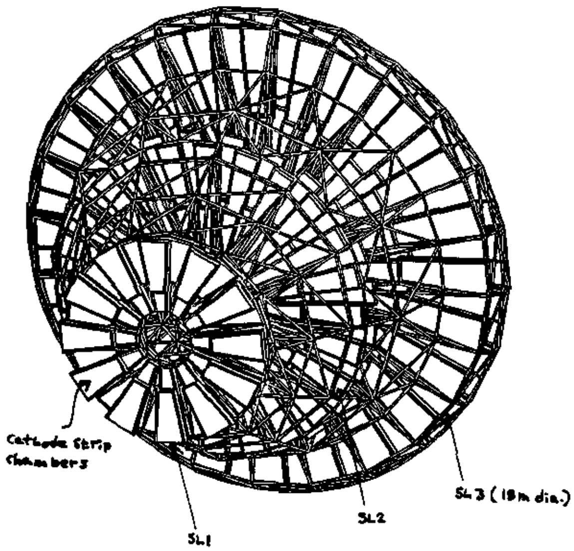

271

Projective alignment

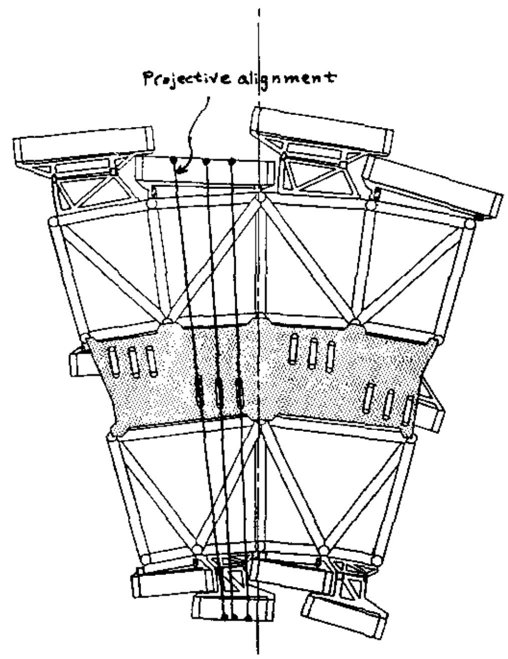

272

System Performance 1 Tev/c

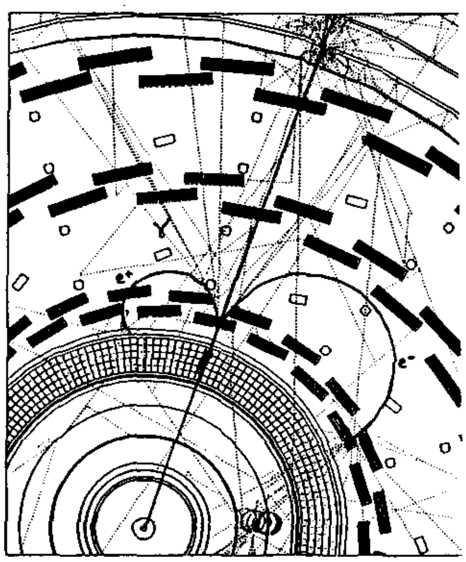

273

Chamber Configuration

Considerations:

- inner layer
  - high rate ==> fine segmentation $O_c \lesssim 1\%$
  - number of layers for local track
  - separated from calorimeter
- middle layer
  - good sagitta resolution
    small X0
    large number of layers $\sigma/\sqrt{N}$
  - employed in trigger
- outer superlayer
  - more coarse segmentation to reduce cost
  - enough layers to find local track
  - employed in trigger

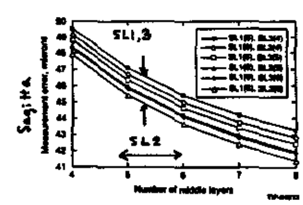

Configuration: barrel 6-6-6
endcap 8-6-6

274

Parameters of the GEM Muon System

Parameter	Value
Magnetic field at the IP 84°	0.8 T 0.1
Barrel region: (29.6° < θ < 85.8°)	0.074 < |η| < 1.33
Endcap region: (9.75° < θ < 27°)	1.43 < |η| < 2.46
Number of sectors in φ	48
Barrel lever arm	> 4.2 m
Endcap lever arm	> 8.6 m
Chamber Parameters:	
Spatial resolutions:	
Chamber single-layer resolution	75 μm (RMS)
Nonbend plane resolution	< 5 / √12 cm
Beam Crossing Tag Efficiency (6 layers)	> 99%
Internal chamber alignment	50 μm
Superlayer-to-superlayer alignment	25 μm
Radiation length/chamber layer	1.0 %
No. of chamber layers per SL (SL1:SL2:SL3)	6:6:6 barrel 8:6:6 endcap
No. of chambers in barrel	960 } 1440
No. of chambers in endcaps	480
No. of bend plane channels - barrel	645,120 } 0.92 m
No. of bend plane channels - endcaps	276,480
No. of non-bend plane channels - barrel	221,184 } 0.31 m
No. of non-bend plane - endcaps	92,160

Performance of System

- Solid angle coverage
- Triggering and tagging
- *Momentum reconstruction*
- Rate capability

The Muon System is Not Alone !

Calorimetry:

- Good γ and e± resolution

Technology	- Barrel	Pb-Liq. Kr
	- Endcap	Pb-Liq. Ar
EM-energy resolution	- Barrel	6%/√E ⊕ 0.4%
	- Endcap	8%/√E ⊕ 0.4 %
EM-pointing resolution	- Barrel	40 mr/√E ⊕ 0.5 mr
	- Endcap	60 mr/√E ⊕ 0.5 mr

- Good Hadronic Calorimetry

Technology	- Barrel	Liq. Kr + Pb + Sc
	- Endcap	Liq. Ar + Cu
Energy resolution	60%/√E ⊕ 0.4%	

- Benefit to Muon System:

Muon Filter	- Absorber: 11 λ to 16 λ *
Reconstruct ΔE_μ	- Isolated muons

* At $L = 10^{34} cm^{-2} s^{-1}$ charged particle occupancy ≤ 0.44 % in barrel, ≤ 1.0 % in endcaps for 4 adjacent strips.

Central Tracker:

- Parameters:

Radius	- 88 cm	
Technology	- Inner	Si-Microstrips
	- Outer	Interpolating Pad Ch.
Resolutions - low p	$\Delta p/p \sim 3.5$ %	
- high p	$\Delta p/p^2 = (1.2) \times 10^{-3} (GeV/c)^{-1}$	
Vertex resolution	δz ~ 1 mm δb ~ 25 μm	

- Benefit to Muon System:
  - Primary vertex constraint
  - Isolation cuts of muon track in calorimeter
  - Muon background rejection by track matching
  - Coverage of muon gaps (being evaluated)

Coverage

- Muon System:

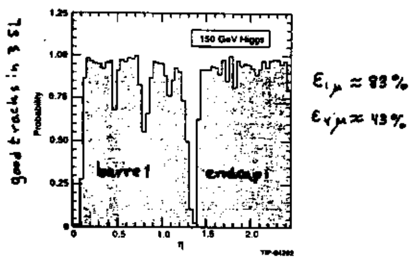

- Central Tracker:

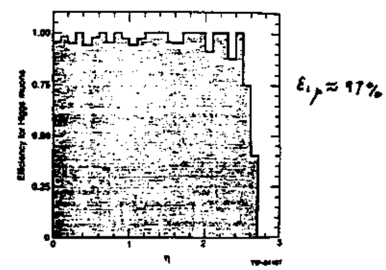

Triggering

- Sagitta and $\Delta\phi$

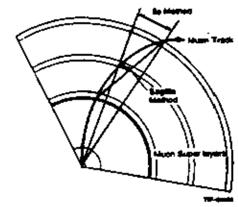

- Non-bend Plane

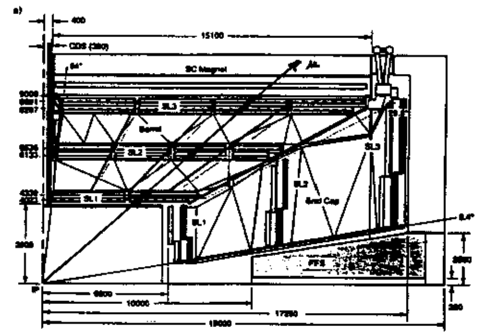

Trigger Performance

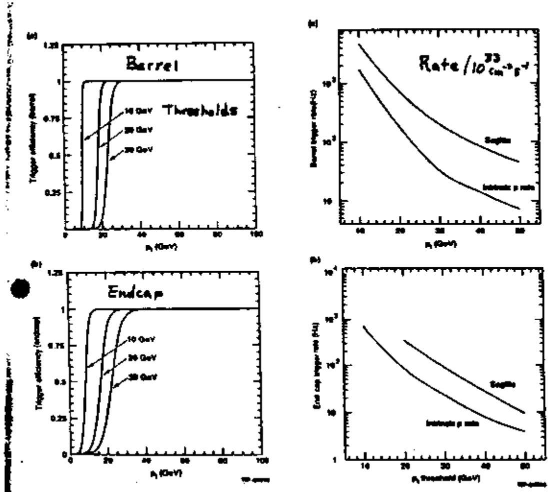

Momentum Reconstruction-1

- Muon system stand-alone:

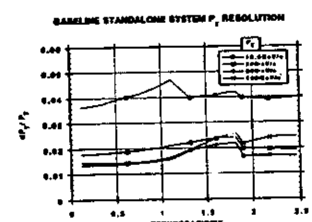

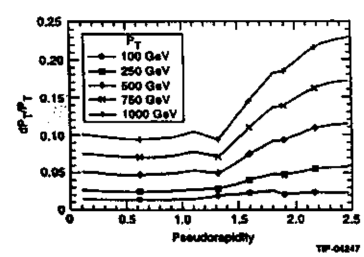

Momentum Reconstruction-2

• Muon system with vertex:

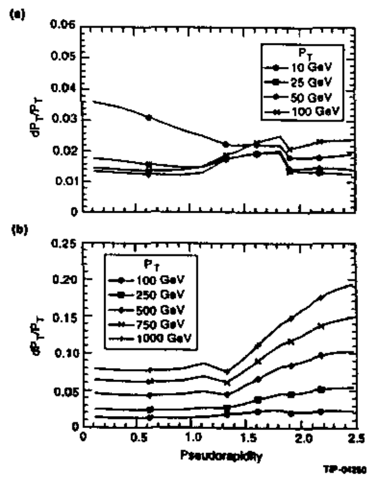

263

Momentum Reconstruction-3

• Muon system with vertex with SL2 and SL3:
limited by m.s. in Calorimeter

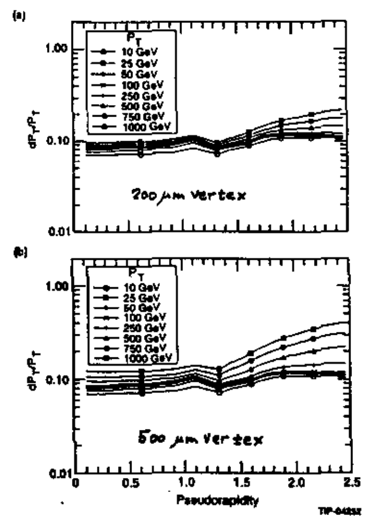

264

Momentum Reconstruction-4

• Muon system with CT:

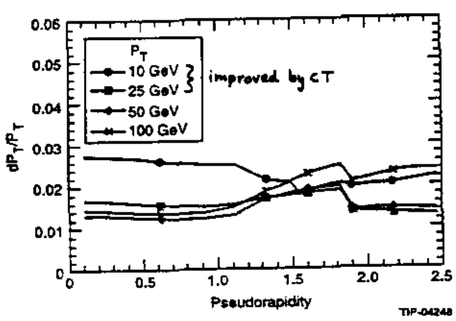

265

Rate Capability

• Charged particles

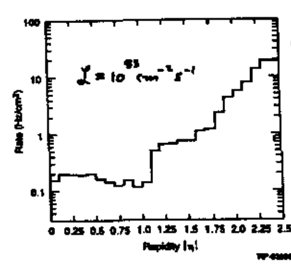

4strip Occup. at 10^{34}
0.44 % barrel
1.0 % endcap

• Neutral particles (n and γ)

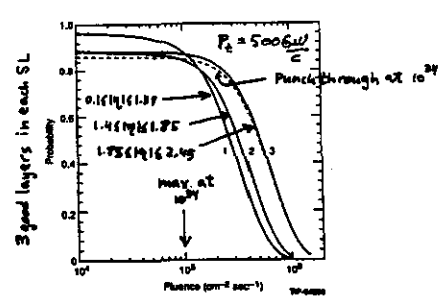

266

Improvements

- **Coverage:**

  Use CT [and Cal] at lower luminosity
  chambers $\eta = 0$ and 1.3
  optimize alignment paths

- **Resolution:**

  reduce material in SL2
  reconstruct energy loss in Cal
  use CT for isolation muon
  vertex constraint ($\approx$ 200 μm)

- **Access:**

  optimization of chamber attachments
  system engineering

267

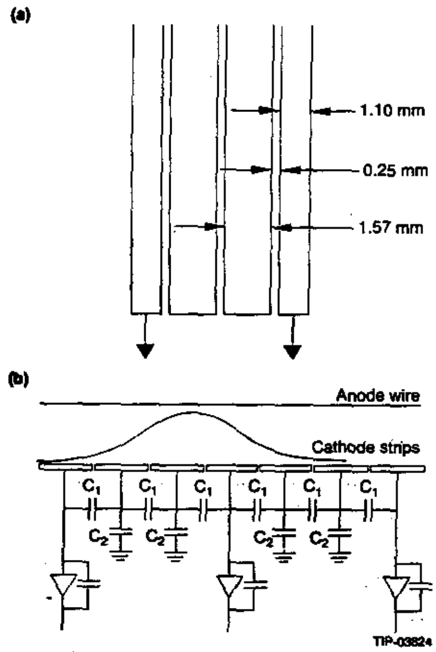

291

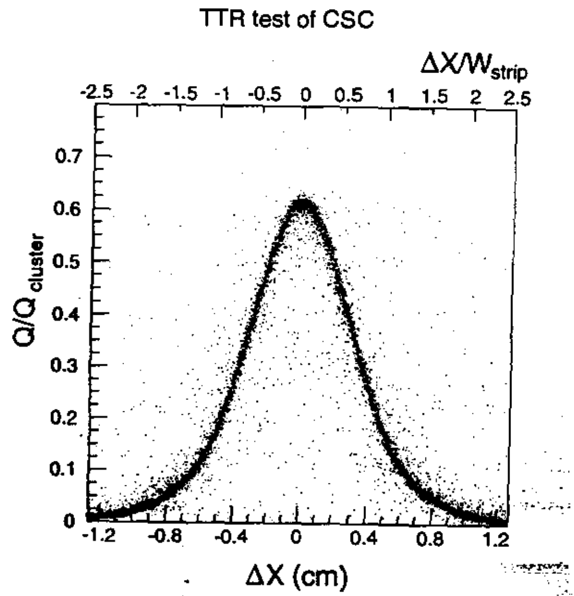

292

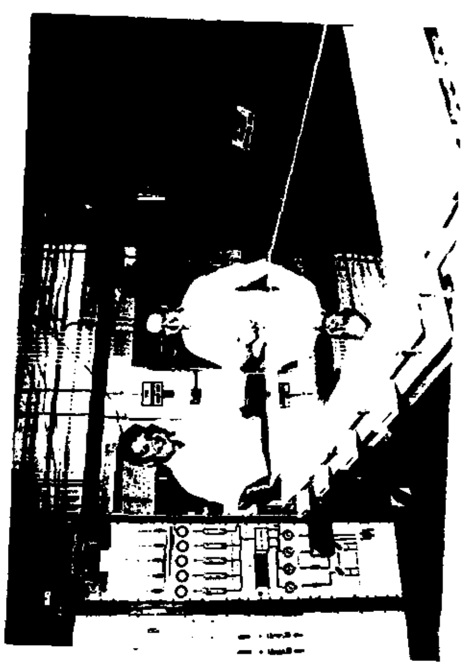

293

CSC ADVANTAGES.

1. Intrinsic resolution of CSC technique is much better than GEM requirement, and measured to be less than 75 microns.

2. Both measurement strips and survey marks for alignment are done on the same board by the process of lithographic etching, so there is no loose in precision due to reference mark transfer.

3. Non-bend coordinate measurement with the precision of few centimeters comes from anode wire or coarse strip readout.

4. Fast timing and position information for use in the Level 1 trigger can be extracted from the CSC in a natural way using simple electronics. The assignment of the proper bunch crossing is 99% efficient for the six-layer chamber, filled with the fast gas.

5. CSC has good double track resolution. Spatial resolution in the presence of second track is simulated to be under 100 microns when tracks are separated by at least 7.5 mm; for smaller separation the resolution degrades but always remains below 450 microns.

6. The chamber can handle particle rates as high as 500 cm-2s-1 with integration time of 300 ns and strip size of 300X0.5CM2, which is more than required for GEM conditions.

7. Since the CSC operates at the gas gain of 5x10**4, thus drawing a small anode current, the effects of the chamber aging are small.

8. The requirements for the gas mixing and delivery system are not tough, because the precise coordinate measurement does not depend crucially on the gas mixture.

9. The major component of the chamber - chathode strip boards - could be mass-produced in the industry, and the remaining steps of chamber assembly are well within capabilities of traditional facilities, which meets tight GEM construction time schedule.

294

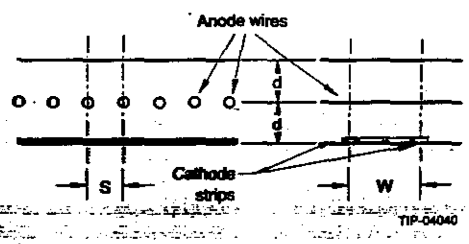

295

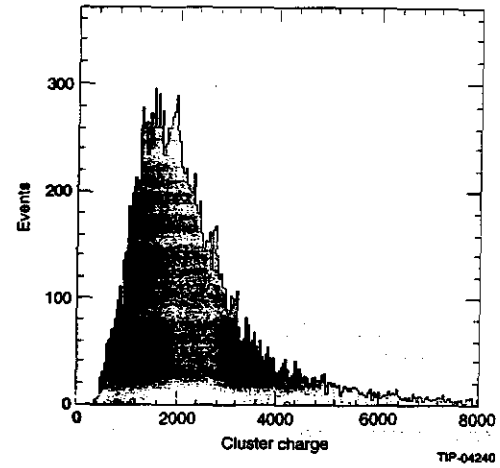

296

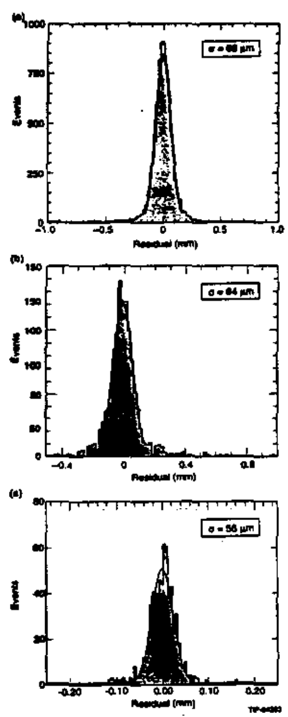

297

The results of the CSC prototypes tests

Prototype	σ_x, <2°	σ_x <6°
BNL 0.5×0.5 m²	46 μ	66 μ
BNL 1.8×1.2 m²	—	<95 μ
DUBNA 1.5×1.0 m²	60 μ	64 μ
HOUSTON 1.0×0.5 m²	38 μ	56 μ
PNPI 0.5×0.5 m²	43 μ	—

298

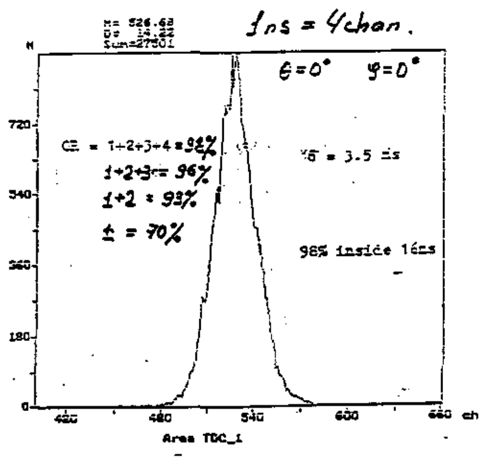

Fig. 4.3.1.12

299

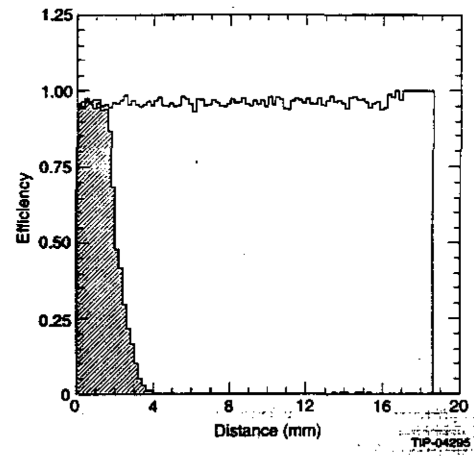

300

CEM has to manufacture ~1500 chambers

960 - Barrel CSCs

480 - endcap CSCs

Maximum size 3.5×1.4 m²

6 layers

Production strategy:

MOST precision parts in industry:

(strip boards glued on honeycomb panels)

NOW working with industry to reduce costs

Assembly in "chamber factories" (3-4 of them, in US and abroad)

working on tooling to reduce costs

301

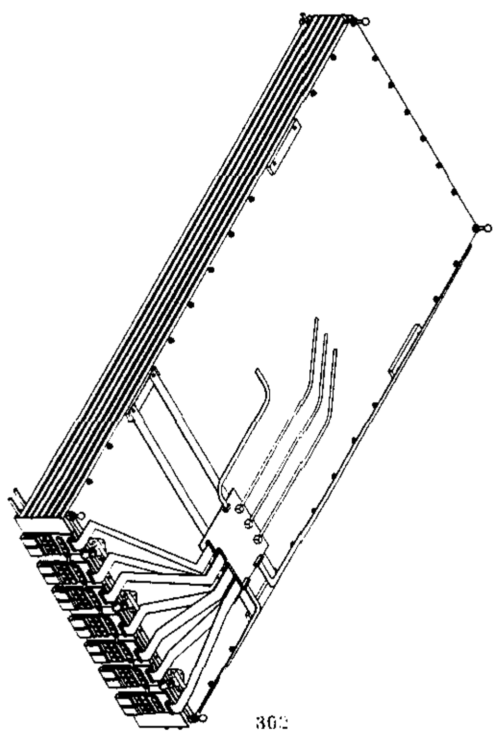

302

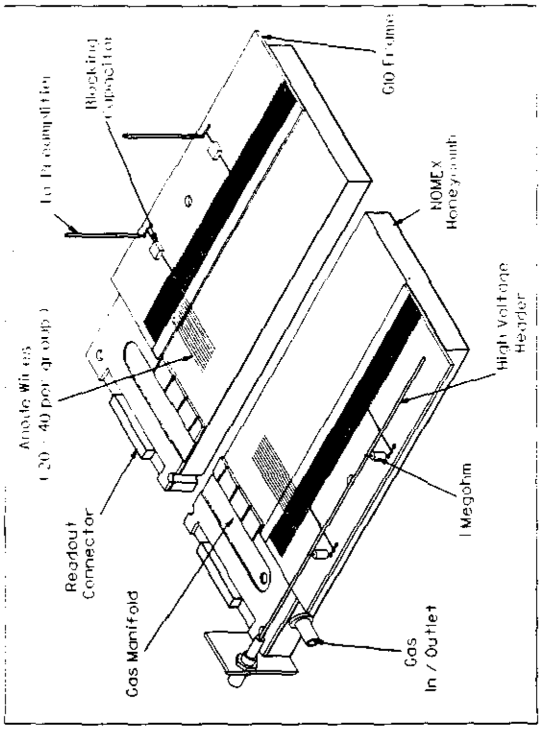

303

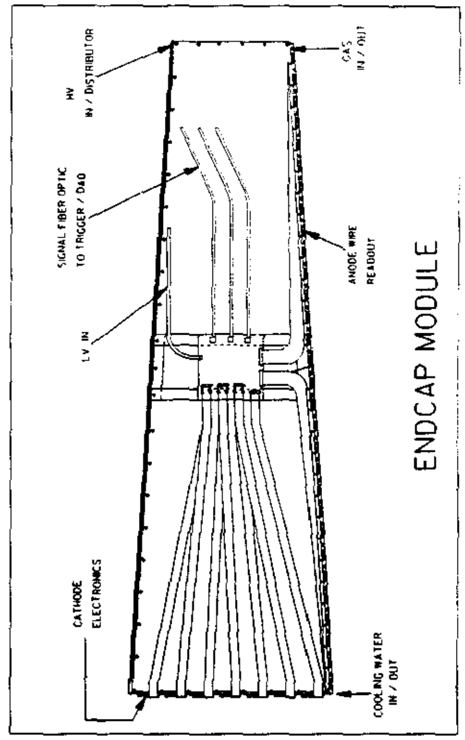

304

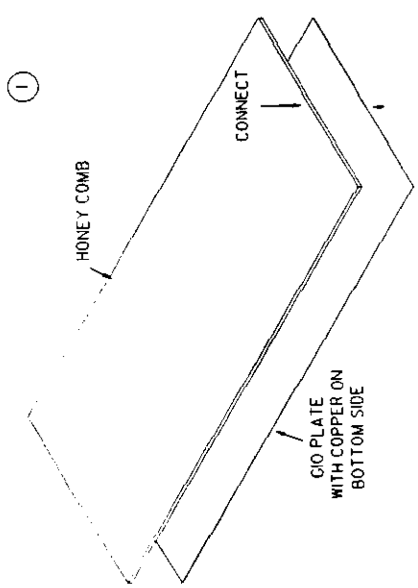

305

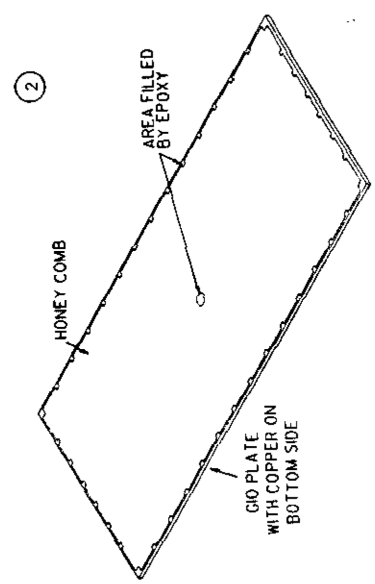

306

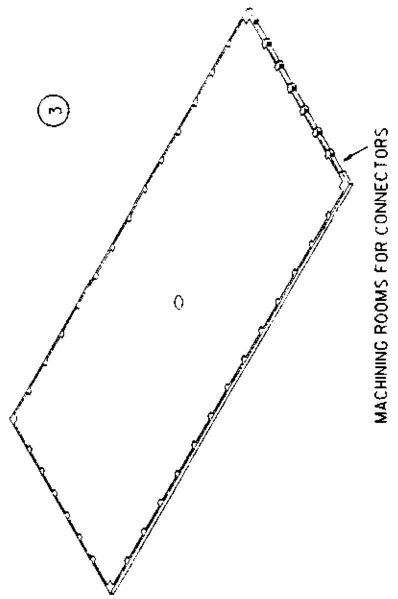

307

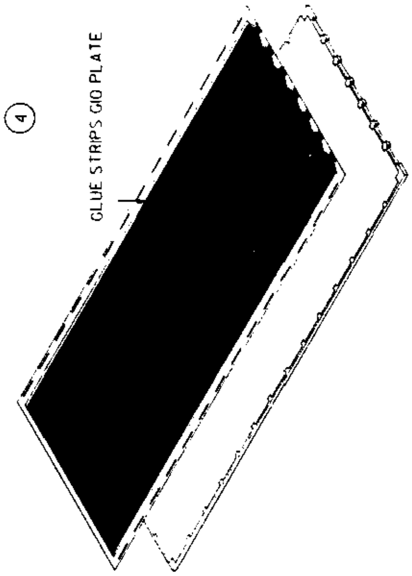

308

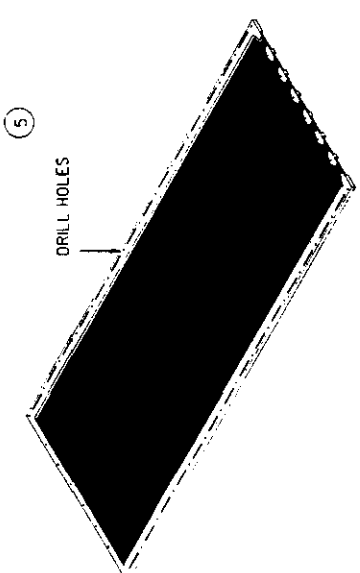

309

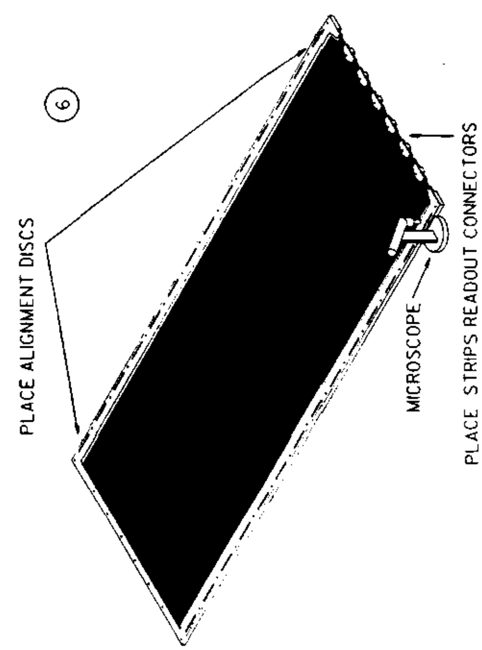

310

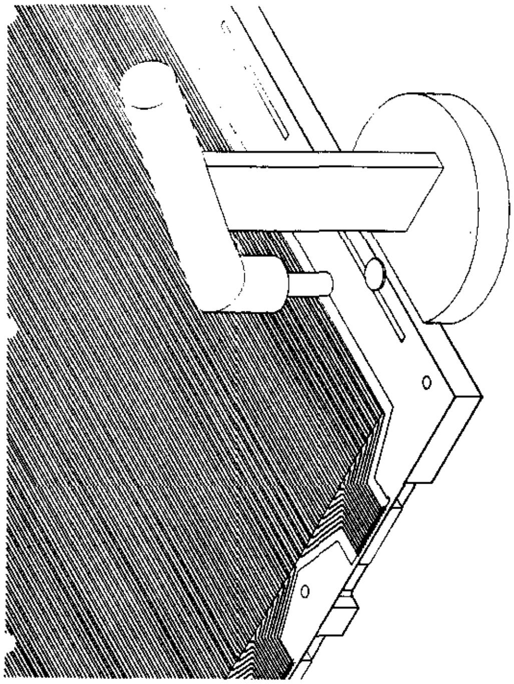

311

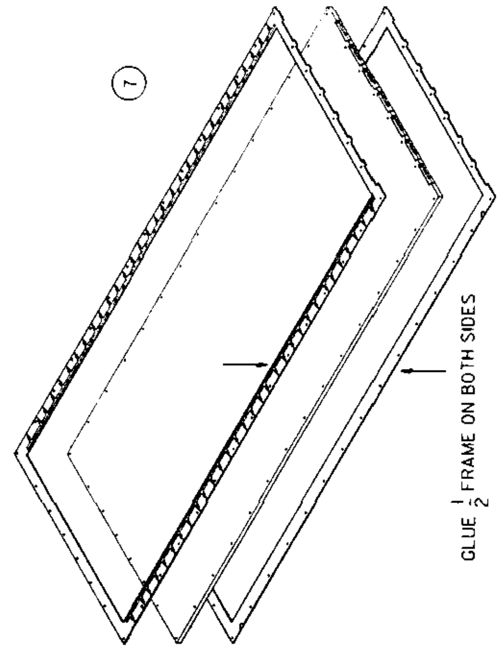

312

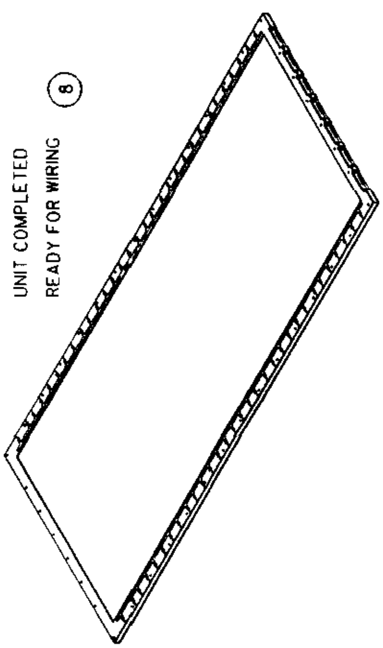

313

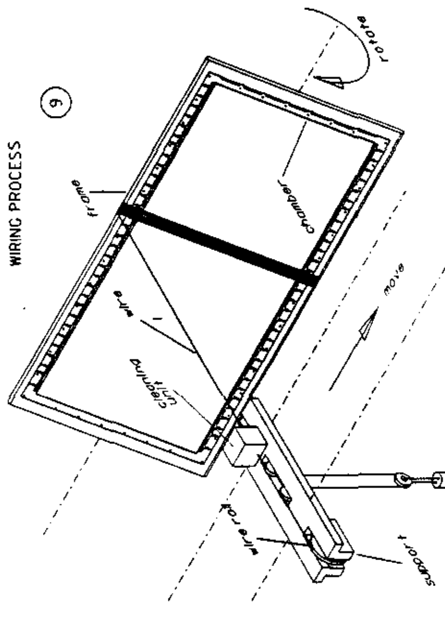

314

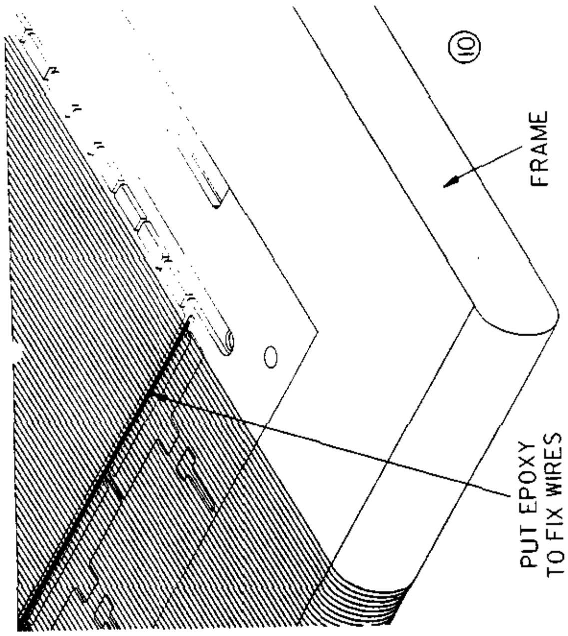

315

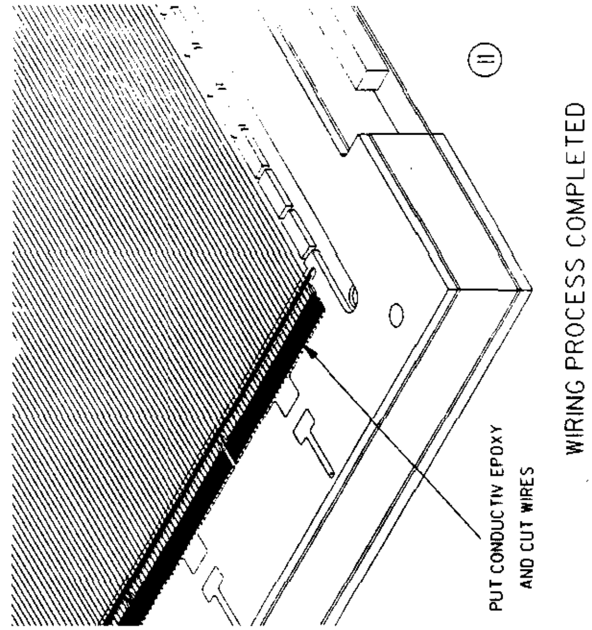

316

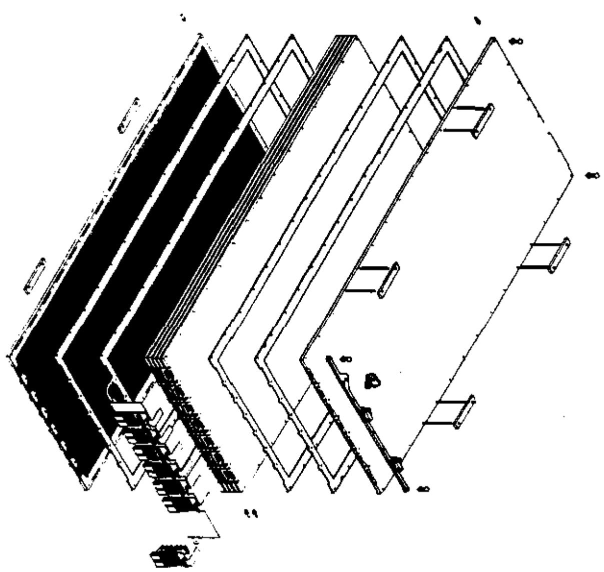

317

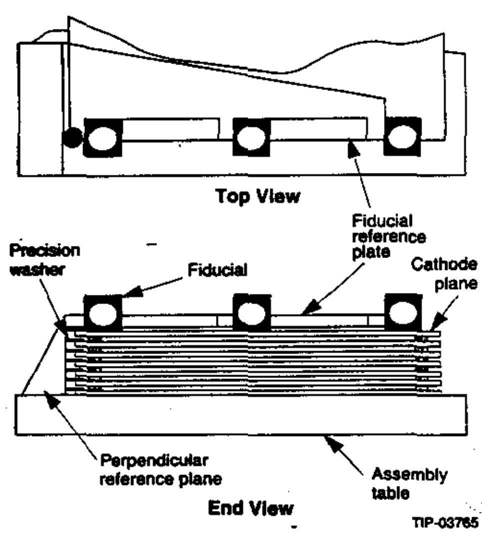

318

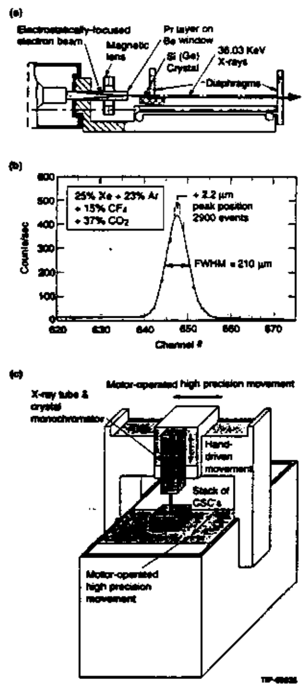

319

CSC material audit

	Mat.	Density g/cm³	c X_0	thick. cm	MASS kg	norm X_0
Hexel Core	Nomex	0.0288	1406	2×7	11.165	0.00995
Circuit Board	G10	1.7	19.4	0.05×14	32.873	0.0361
Skin Layer	Cu	8.96	1.47	0.0017×14	5.885	0.0162
Frames	G10	1.7	19.4	17.8	50.345	0.9175

Total mass ≈ 100 kg
Total area = 2.76 m^2
Mass/area = 36.24 kg/m^2
Frame area = 0.166 m^2 (6.03%)
X_0 through center ≈ 0.0622
X_0 through frame ≈ 0.9335

320

Remaining essential R&D

Results from our prototype program and R&D efforts thus far are very encouraging. The goals of our R&D program for the coming year will concentrate on the following points:

• verification of the detailed performance of a CSC in a magnetic field. We will build small detectors and test them in various magnetic field configurations to validate the Monte Carlo predictions of the Lorentz drift and geometric contributions to chamber resolution.

• development of preproduction modules. This effort will test construction techniques, the internal alignment of chambers within a module, and the electrical performance in an integrated six-chamber module.

• construction of a three-module tower with a truss support structure, as planned for the final muon system. This will test the structural support concept and validate the engineering calculations of structure rigidity and deformation. It will also provide a realistic test bed for the alignment systems proposed for the final system.

— Design strategy: input from all participants.
"Chamber committee" - centered at the SSC with broad participation of all GEM institutes
Working sessions: June - December 1993

321

"False Sagitta Correction Method"
(developed in GEM)

Strategy:
- relax tolerances for chamber positioning
- direct measurement of interesting value – Sagitta Correction Function $F_s(\theta,\varphi)$
- interpolation of $F_s(\theta,\varphi)$

$$S_{real} = S_{meas} + F_s(\theta,\varphi)$$

322

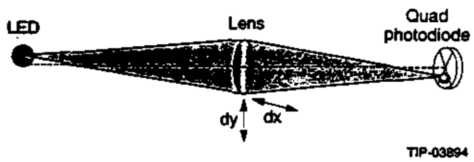

325

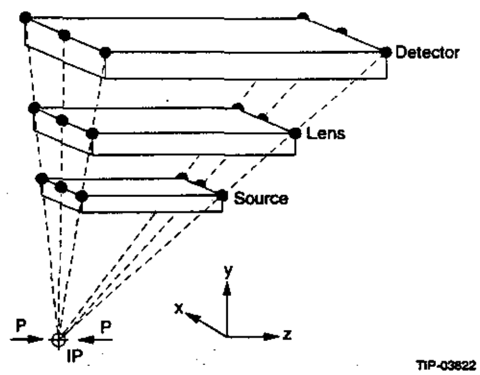

324

Need quadratic interpolation!

6-point monitors

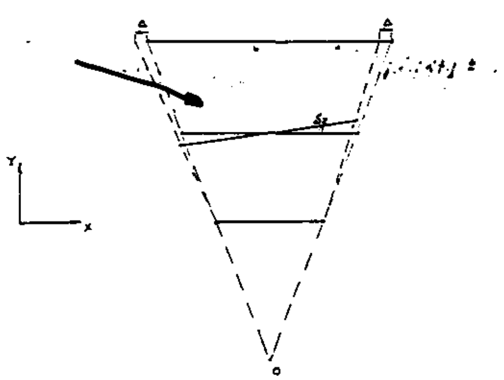

Fig.4 Insufficiency of 4-Point Option

327

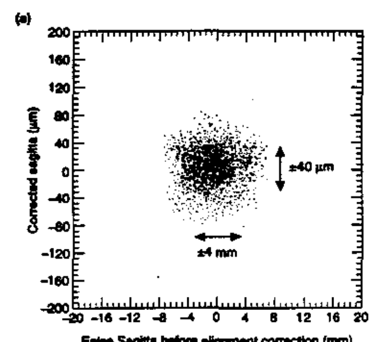

Shifts ± 3mm, Rotations ± 3mrad, ΔT ± 5°C, chamber torsion ± 3mrad, nonprojectivity ± 3cm

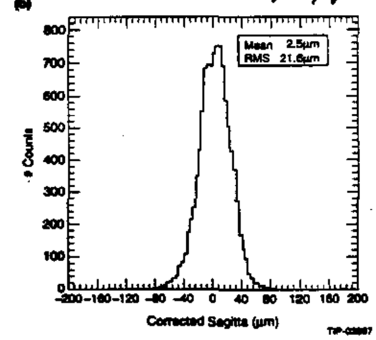

326

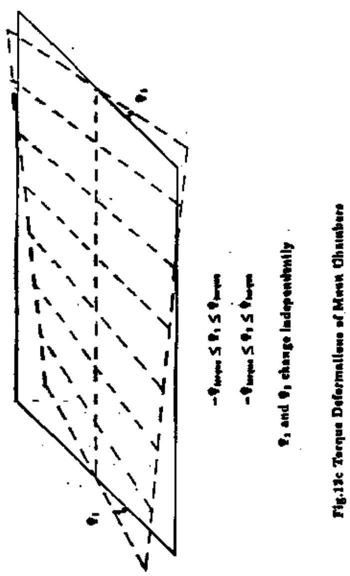

327

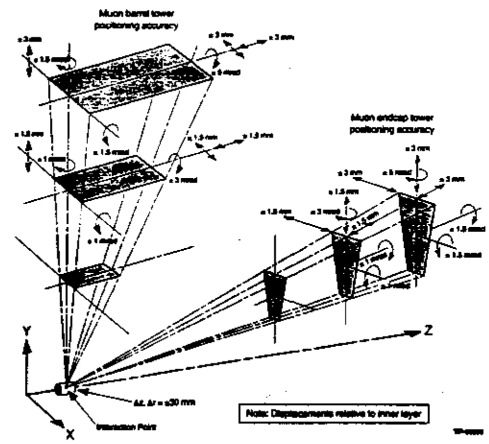

328

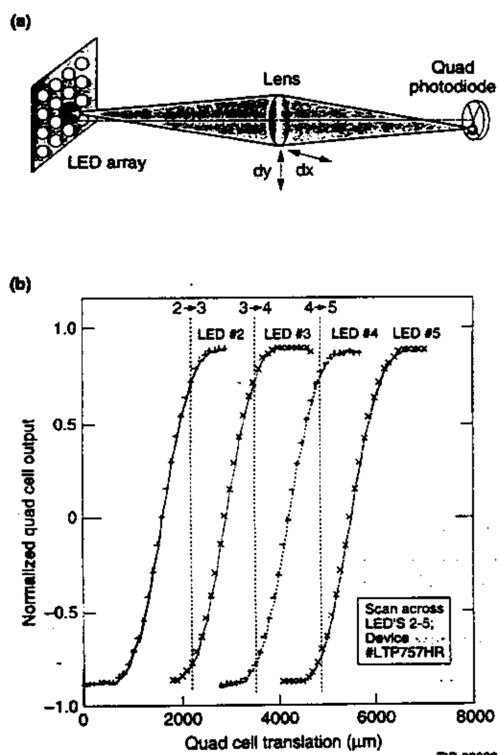

329

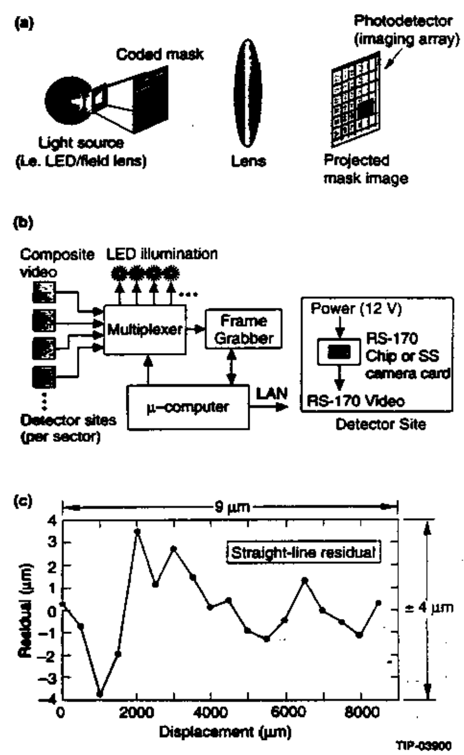

330

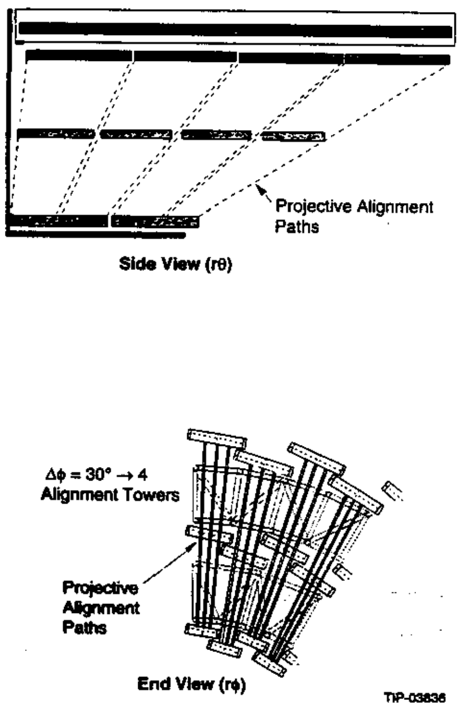

331

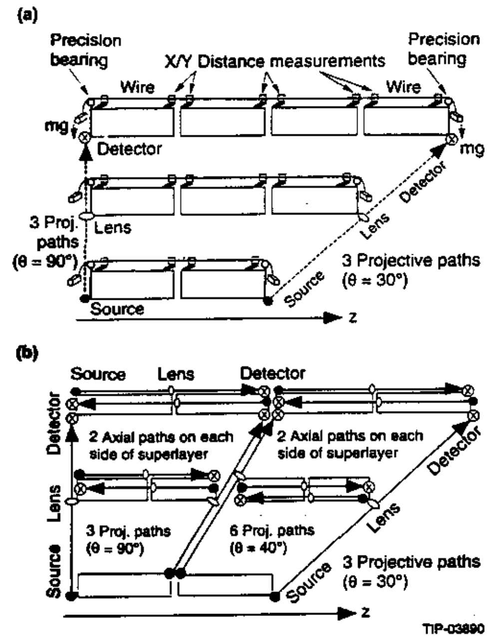

332

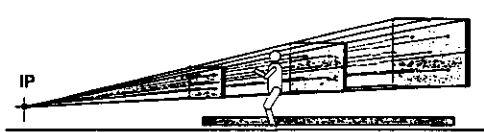

Proposed projective alignment lines of sight

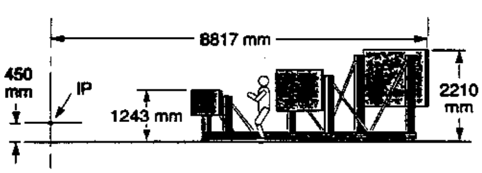

Mechanical design and fixturing

TIP-03893

333

Muon Subsystem
Layout of Chambers
&
Support Structure

Frank Nimblett
10 May 1993

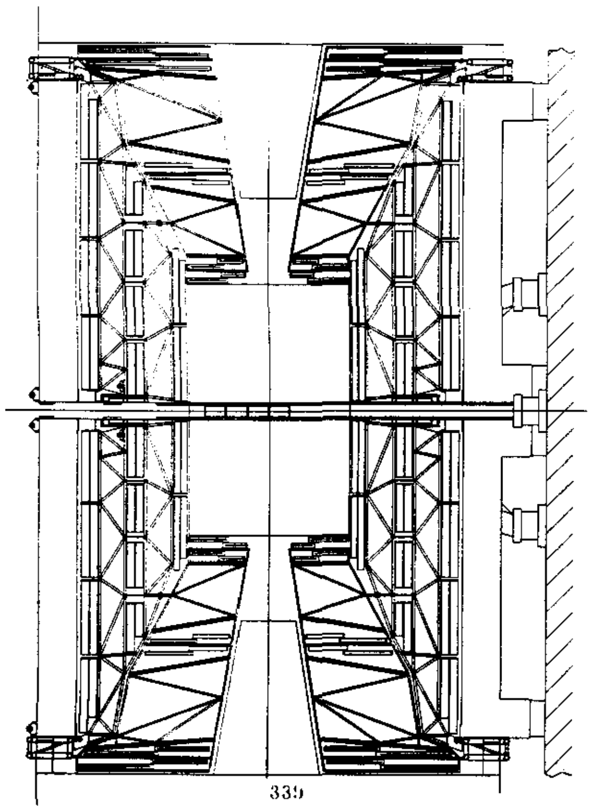

339

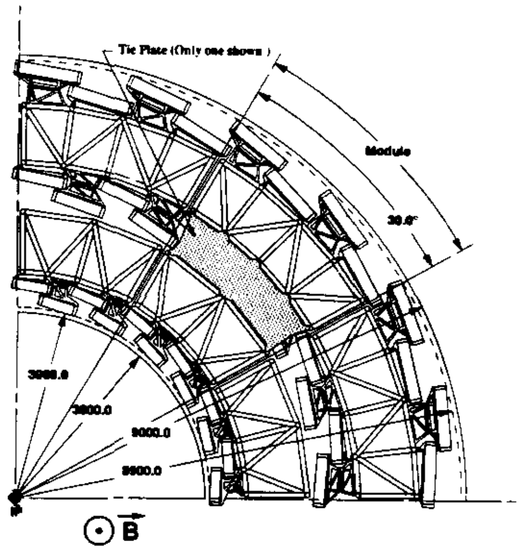

Figure 4.1b: Muon System End View (1/4 Section)
View from North End of UG Hall

340

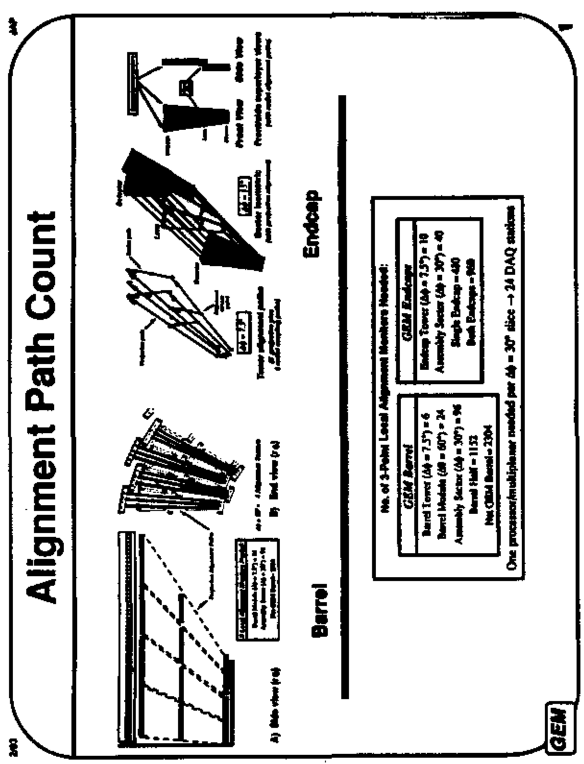

341

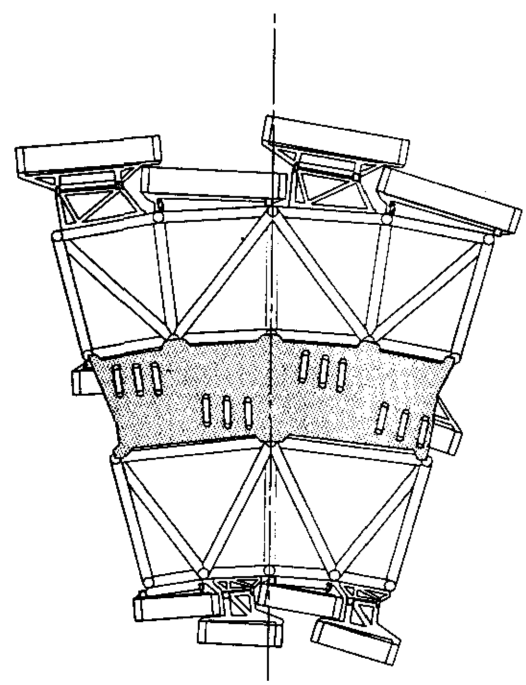

Figure 4.3.x.y: Barrel Module Section

342

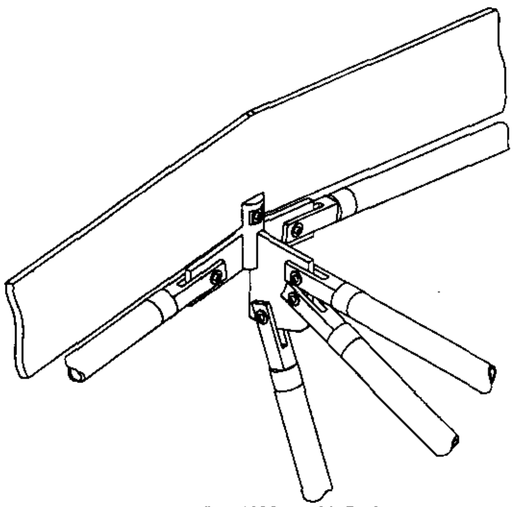

Figure 4.3.3.5: Truss Joint Detail

343

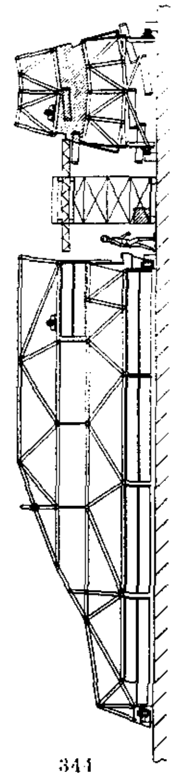

344

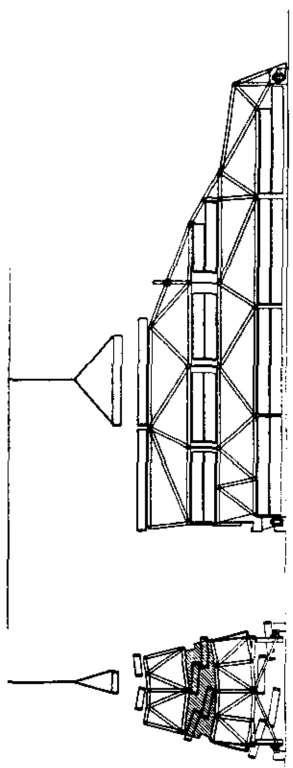

345

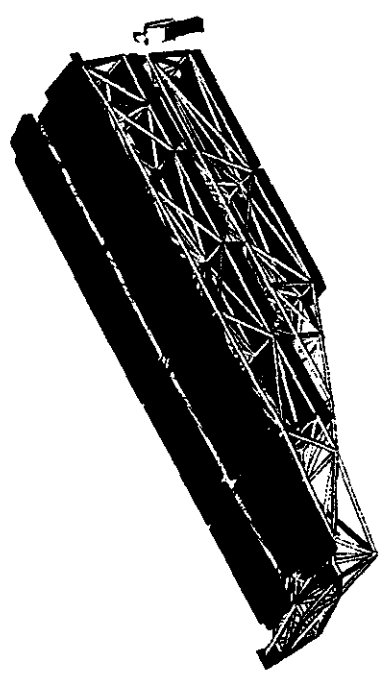

346

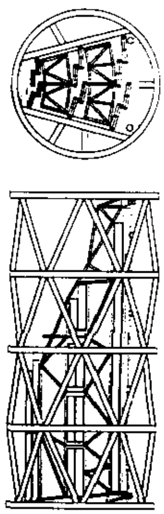

Module Installation Fixture

347

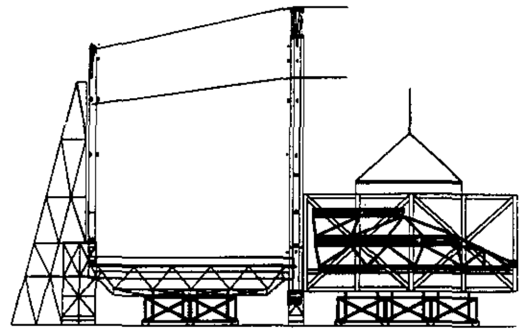

Figure 4.5.3: Initial Module Assembly Into Barrel Monolith

348

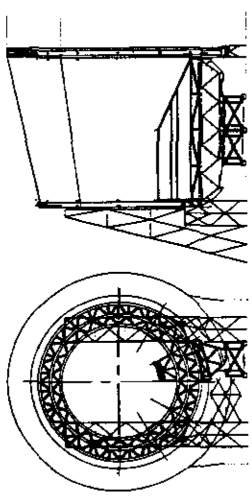

Initial Module Assembled Between End Support Rings

349

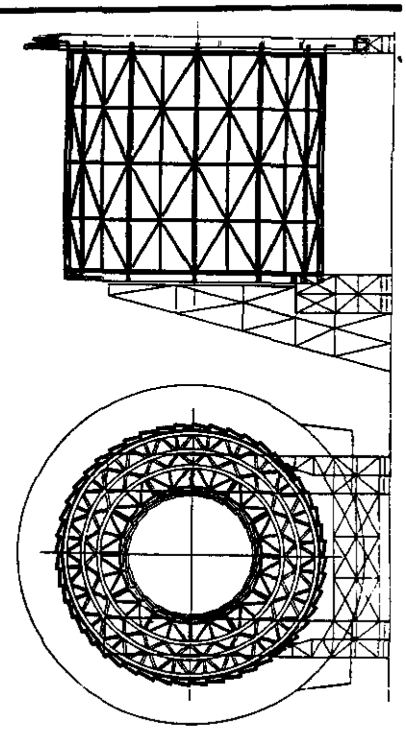

350

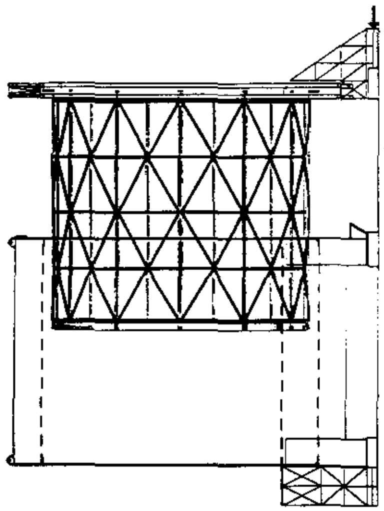

Barrel Monolith Installation Into Magnet

351

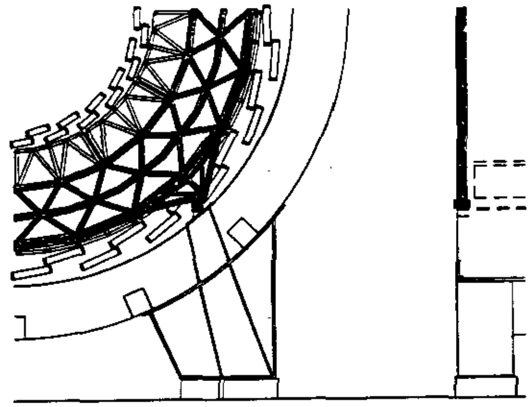

Figure 4.3.3.8b: CDS to Magnet Interface

352

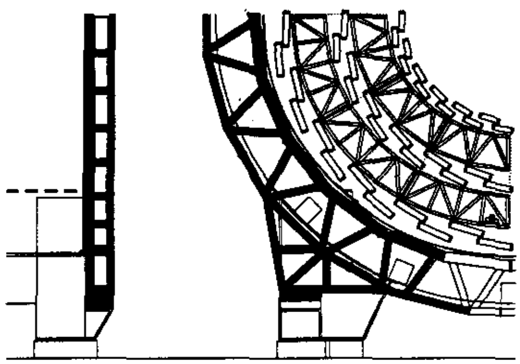

Figure 4.3.3.9b: FFS Ring to Magnet Interface

353

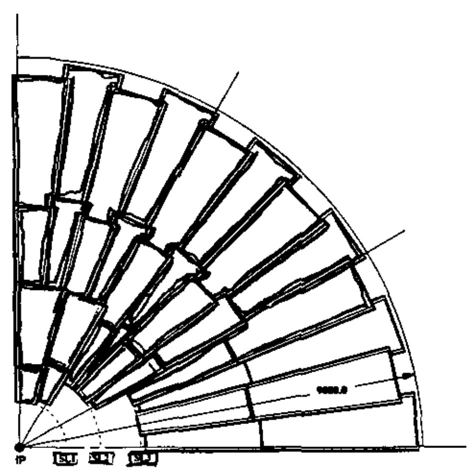

Figure 4.1c: Endcap Muon Chamber Layout
(1/4 Section) View from IP

354

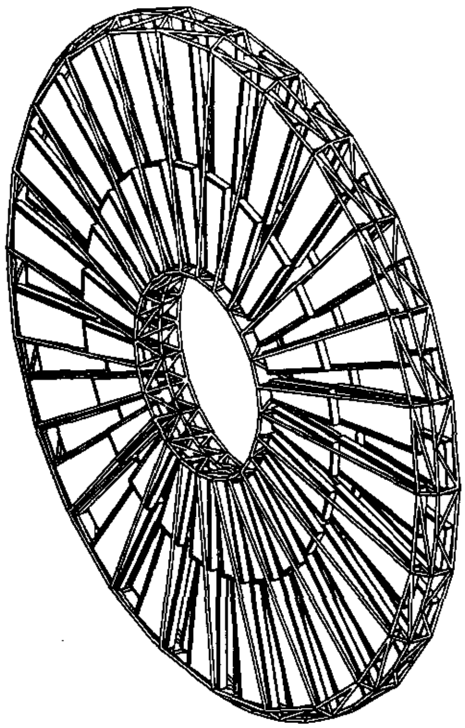

Figure 4.3.3.7: Endcap Outer Superlayer Wheel Structure

355

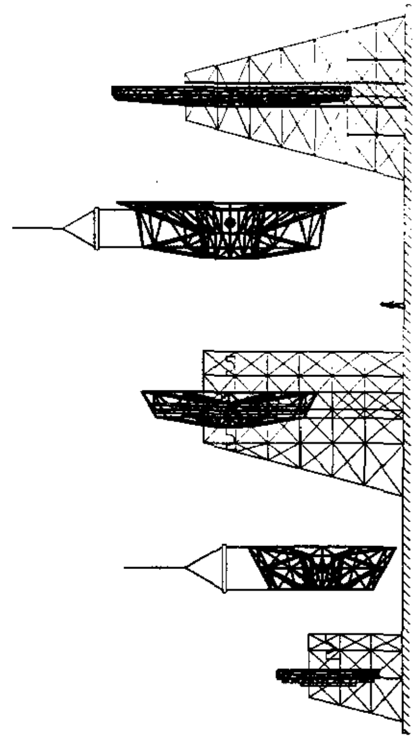

356

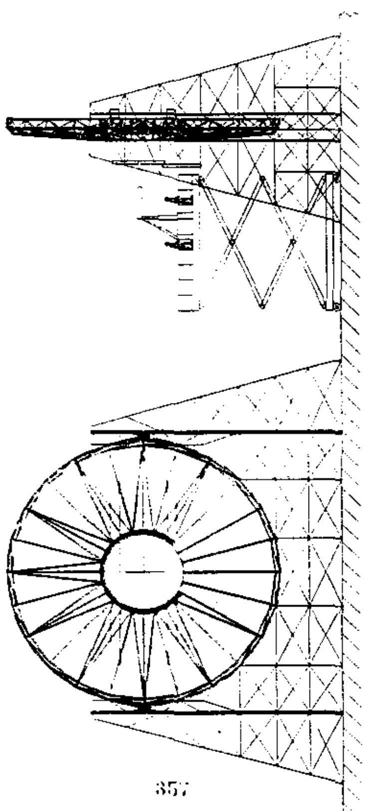

357

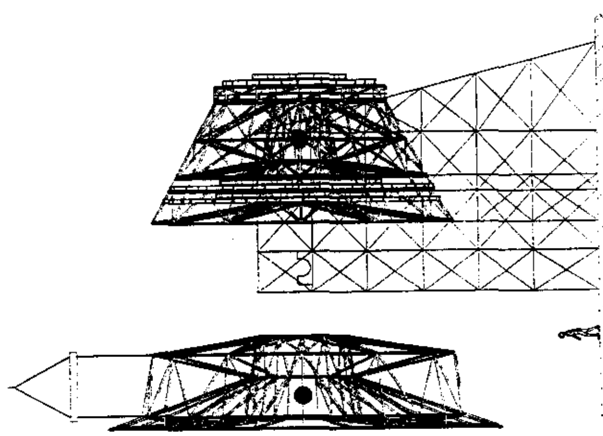

358

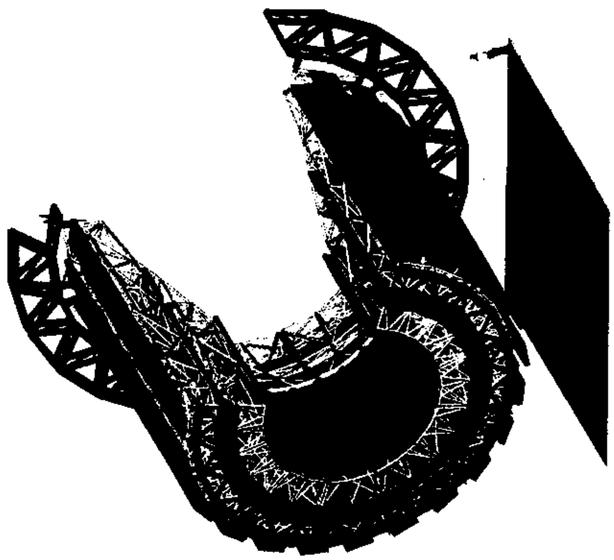

359

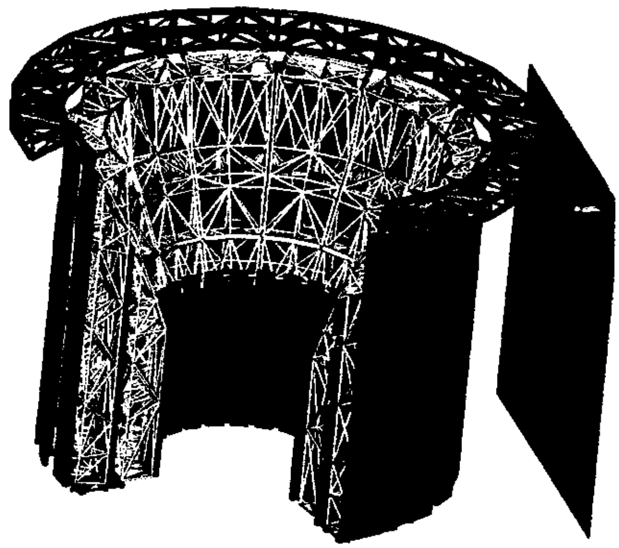

360

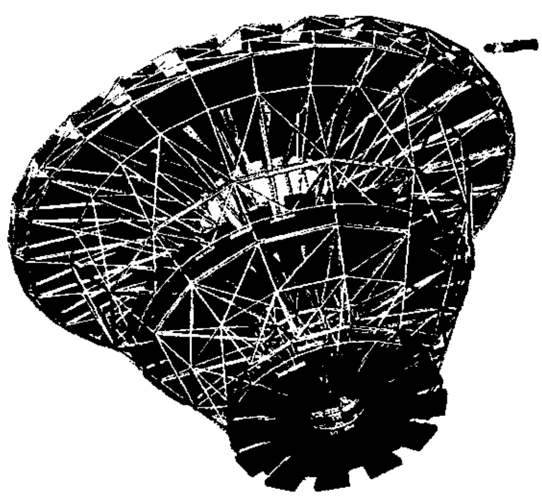

361

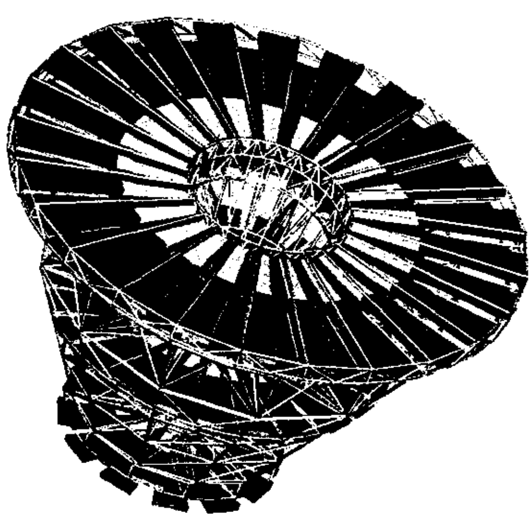

362

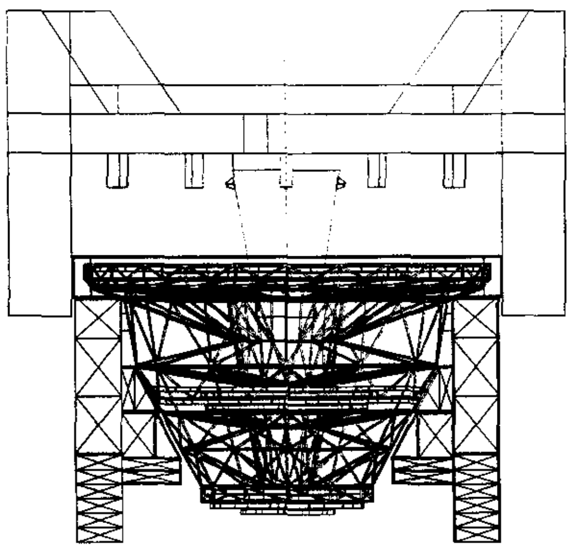

363

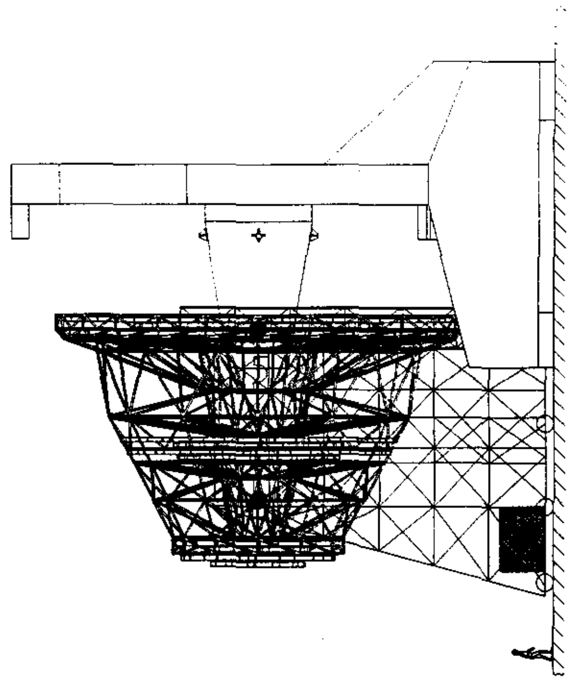

364

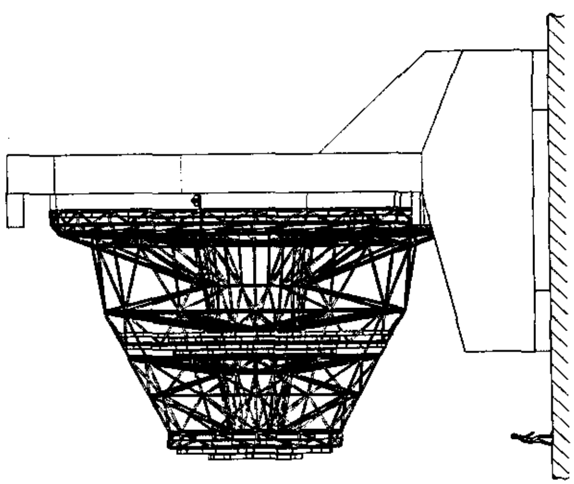

365

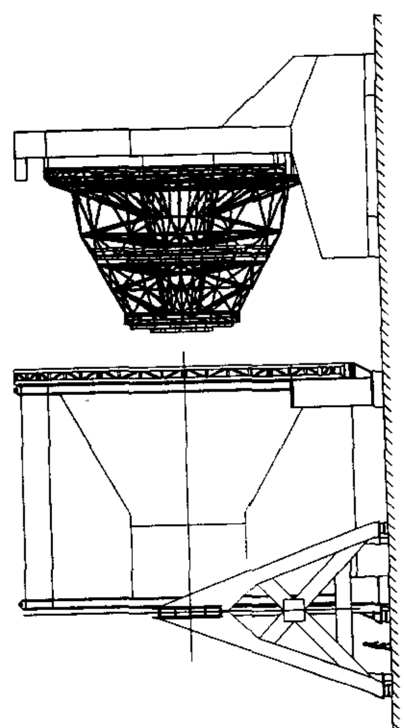

366

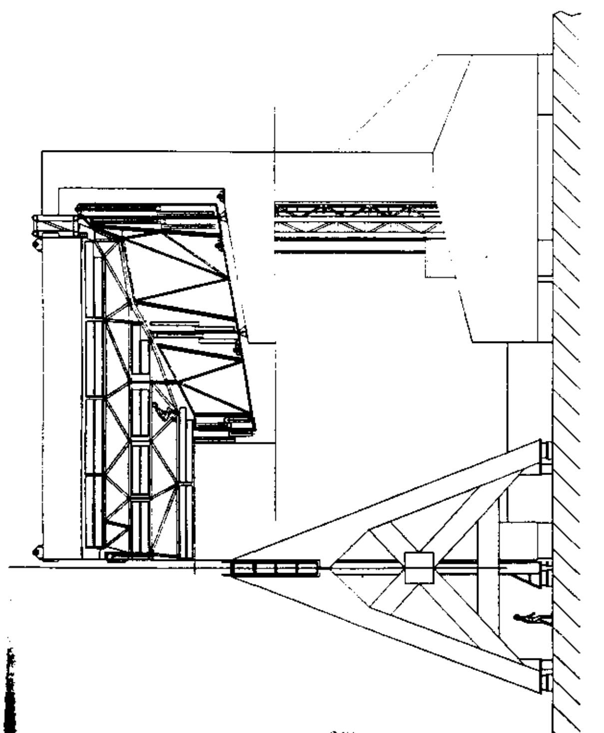

367

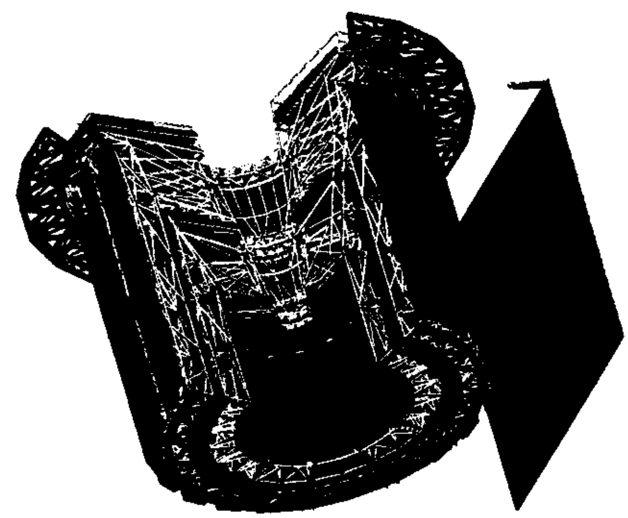

368

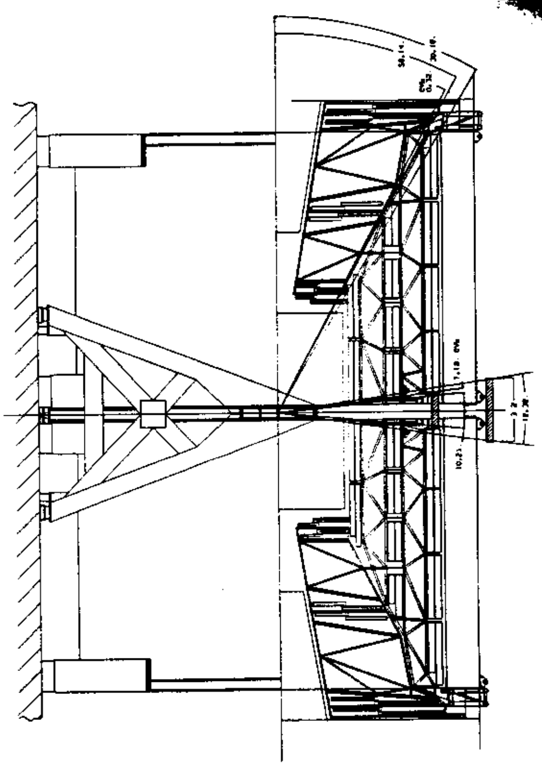

369

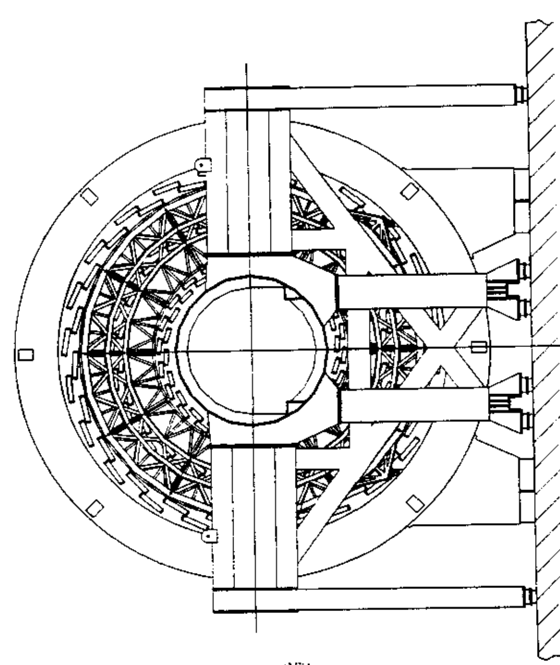

370

CENTRAL TRACKER REPORT

San Diego May 10, 93

1. Reasons for choice of Technologies
2. Rationale for choice of Detector Parameters
3. Physics Performance
4. Silicon Detector Design — Dave Lee
5. IPC Detector Progress — Jim Musser

373

Reasons for choice of Technologies

1 Inner Tracker $10\ cm \le R \le 35\ cm$

- Considered the following technologies:
  - a) Silicon microstrip detectors
    choice for baseline design
  - b) Silicon pixel detectors
    immature, high costs likely
  - c) Long drift length silicon det.
    immature, radiation hardness uncertain
- Reasons for choice of silicon microstrips
  - a) Ideal for element closest to interaction point
    - Fine segmentation ⇒ low occupancy
    - High radiation resistance
  - b) Very high spatial resolution
    - Precise vertex position and impact parameter measurement
  - c) Mature technology
    - Well understood performance, radiation hardness, cost etc.

374

2. Outer Tracker $40\ cm \le R \le 90\ cm$

- Considered following technologies
  - a) Interpolating Cathode Pad Chambers
    choice for baseline design
  - b) Straw tubes
  - c) Scintillating Fibers
- Reason for choice of IPC's
  - a) Pad sizes ~ few cm^2 are natural
    - Low occupancy even at 10^{34}
    - Other two technologies imply considerably higher occupancy
  - b) Pads approximate 3 dimensional points
    - this is important in high rate, high multiplicity environment of SSC
    - Other two technologies project all tracks onto a plane
  - c) IPC's not a new technology
    - Demonstrated to work in BNL Heavy Ion Expts.

375

Rationale for choice of Detector Parameters

a) Inner Radius of Silicon Det.
   10 cm

b) Outer Radius of Silicon
   22 cm barrel, 26 cm forward

c) Silicon microstrip pitch and strip length
   50μ pitch strips, 18 cm long

d) IPC Pad size and channel count
   $\Delta\eta \cdot \Delta\phi \approx 0.0007$, ~ 400,000 pads total

e) Outer radius of central tracker
   95 cm radius (including poly eth. shield)

f) Number of layers of Silicon & IPC's
   6 layers of Silicon, 8 layers of IPC's

g) Stereo Angles in Silicon and IPC's
   ± 5 mrad in Si, ± 50 mrad in IPC's

376

a) Inner Radius of Silicon Detector

- Vertex and Impact Parameter resolution improve with smaller inner radius
- Radiation Dose increases at smaller radii as $1/R^2$

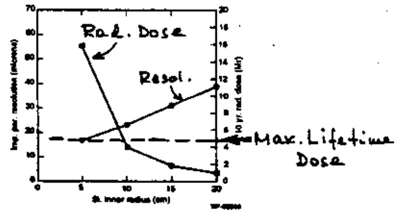

- Expected Lifetime Dose tolerance of ~ 5 Mrads means inner radius ≳ 10 cm

377

6-3

b) Outer radius of Silicon

- Vertex and Impact Parameter Resolution improve with increased outer radius (at R_{in} = 10 cm)
- Silicon Area, and therefore cost (~ 2 M\$/m²) increases rapidly as outer radius increases

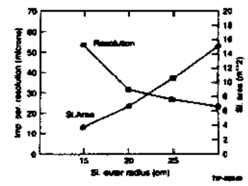

- Resolution vs. outer radius curve flattens out around 20 to 25 cm ∴ this seems like a sensible outer radius

Figure 6.1-6

378

6-4

c) Silicon microstrip pitch & strip length

- Microstrip pitch of 50 μm is now quite standard and provides adequate impact parameter resolution and low occupancy.

  Smaller pitch would increase electronics costs considerably
- Strip length of 18 cm allows simpler mechanical design for 36 cm long barrel and 16 cm forward (10 cm ≤ R ≤ 26 cm)
  - Reduces no. of support & cooling rings
  - All electronics and cooling at ends of barrel, outer edge of forward discs
  - Reduces cabling & simplifies
  - Reduces radiation length in Si detector

  Strips longer than 18 cm are difficult due to signal to noise

379

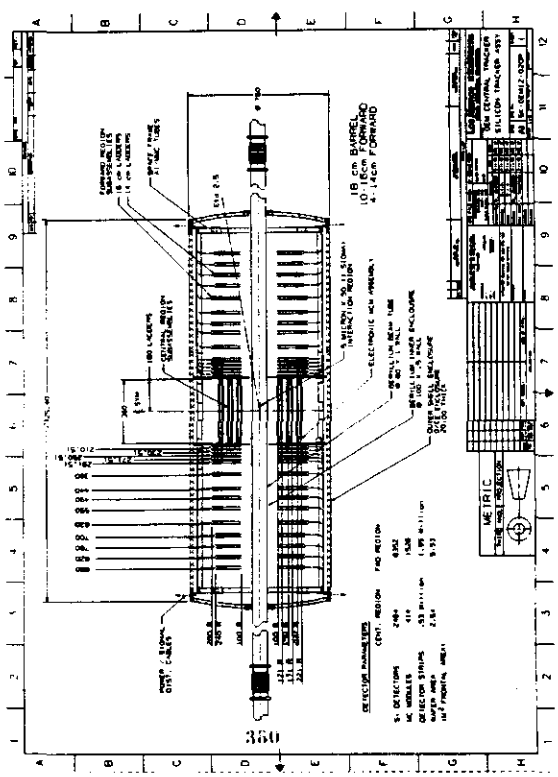

380

d) Pad size and channel count in IPC's

- Pad width (in "ϕ" direction) of 2.5mm required to give 50μ resolution via interpolation between pads
- Pad sizes vary around $\Delta\eta \cdot \Delta\phi \approx 0.0007$ to give occupancy $\leq 10\%$ at $\mathcal{L} = 10^{34}$

  Experience with other trackers indicate lots of problems at occupancies above 10%
- These pad sizes imply a total no. of pads of ~ 400,000

  Smaller pads, and ∴ larger no. of channels, would be nice, but not necessary, and would increase electronics costs significantly.

361

e) Outer Radius of Central Tracker

- Momentum resolution improves like ~ R^2.

  From the point of view of Tracker alone, larger radius would be better. Cost of tracker, if we keep no of layers and channel count fixed, would not increase much with radius
- Cost of Calorimeter & muon system increases sharply with tracker radius

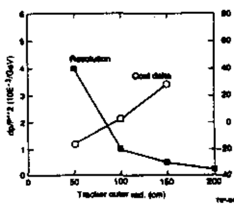

- Inner radius of ~ 1 m for EM Calorimeter makes tower sizes convenient mechanically at chosen η and ϕ segmentation.
- Tracker radius of 95cm was chosen by overall cost vs. performance optimization of GEM as a whole

362

6-5

f) Number of Layers of Si and IPC Detector

- More layers improve momentum resolution, but only slightly
- Main consideration in choice of 6 layers of Si and 8 layers of IPC's was the Pattern Recognition efficiency. With fewer layers track finding efficiency decreases.
- IPC's might be standalone at 10^{34}; will need all 8 layers for good e/γ separation.

  Would be hard to squeeze more layers into the space available. Also costs of more layers would be prohibitive.

363

g) Choice of Stereo Angles in Si & IPC's

- Larger stereo angles ⟹ better z resolution

  ±5 mr in Si ⟹ $\delta z \sim 2$ mm

  ±50mr in IPC's ⟹ $\delta z \sim 0.7$ mm

  - At 10^{33}, Si + IPC combined gives vertex $\delta z \sim 1$mm for each track
  - At 10^{34}, IPC alone gives vertex $\delta z \lesssim 2$mm for each track
- Larger stereo angles mean higher probability of multitrack ambiguities

  With ±5 mr in Si and ±50 mr in IPC we expect multiple tracks that are ambiguous to occur

  ~ 1% of the hits at 10^{33}

  ~ 10% of the hits at 10^{34}

  in both Si and IPC's.

364

h) Reason for 20 chambers / layer in barrel IPC's and 10 chambers/disc in EndCap IPC's

Number of chambers determined by keeping degradation of resolution due to non-normal incidence to be less than 50 μ.

365

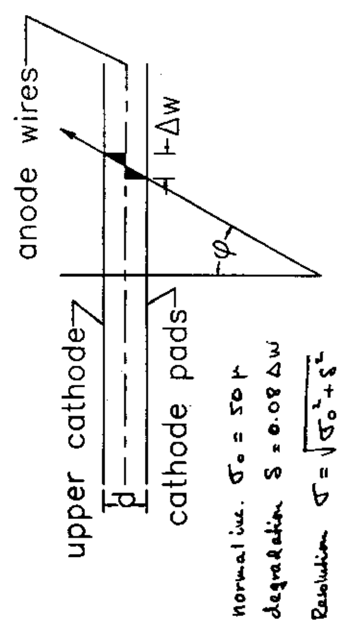

normal inc. $\sigma_0 = 50\,\mu$

degradation $S = 0.08\,\Delta W$

Resolution $\sigma = \sqrt{\sigma_0^2 + S^2}$

20 chambers/layer ⇒ keeps $\phi \le \pm 9°$ ⇒ keeps $S \le 50\,\mu$

366

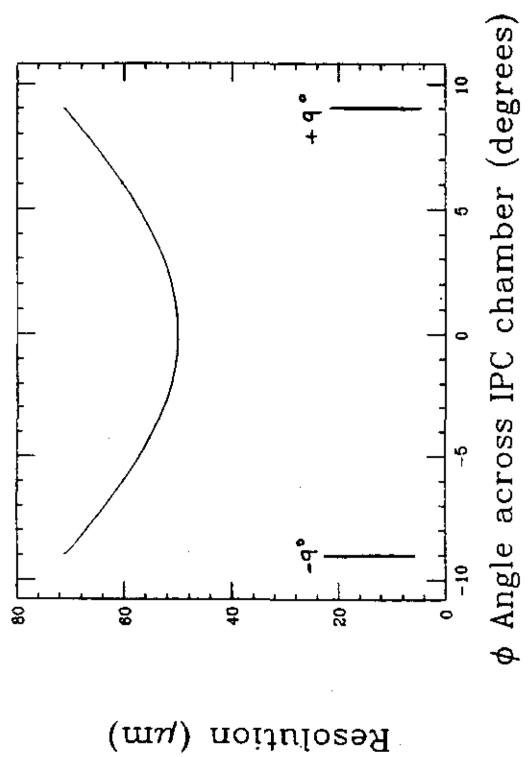

367

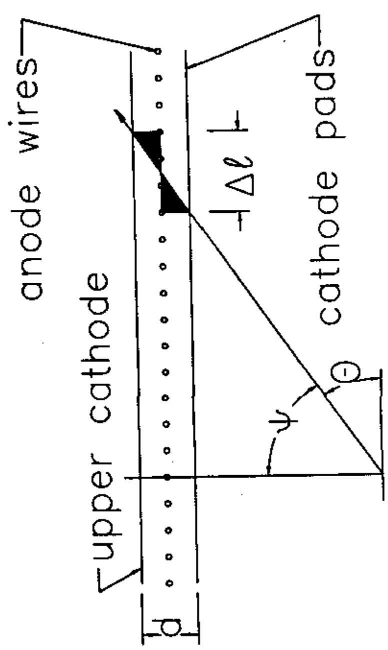

368

Degradation of Resolution due to non-normal incidence in "Z" direction and Stereo angle of pads

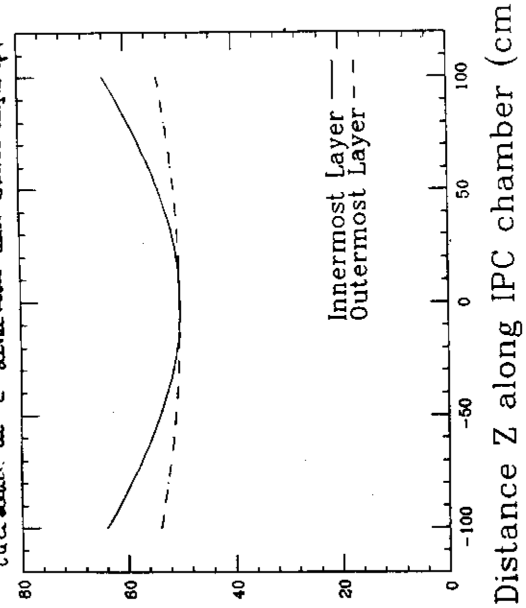

389

82	71	82
64	50	64
82	71	82

a) Resolutions in the innermost IPC layer

74	71	74
54	50	54
74	71	74

a) Resolutions in the outermost IPC layer

390

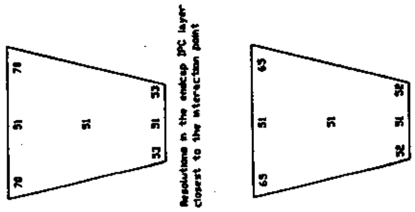

a) Resolutions in the endcap IPC layer closest to the interaction point

a) Resolutions in the endcap IPC layer farthest from the interaction point

391

6.1.1 Physics Goals of the Central Tracker

The physics goals for the central tracking in GEM can be divided into two categories. The first are those features that are required to support the primary objectives of GEM, namely the detection of gammas, electrons, and muons at high p_T. Some examples of these are:

- Identify the primary vertex of an event of interest, so that it can be separated from other pileup events in the memory time of the detector.
- Separate electrons and gammas using the presence or absence of a charged track pointing to an electromagnetic shower in the calorimeter.
- Help with electron-hadron separation by providing a momentum measurement that can be compared with the energy deposition in the calorimeter.
- Help with rejection of fake muon backgrounds by matching the muon momentum measured in the central tracker with the momentum measured in the muon chambers.
- Determine the electron sign up to ~ 600 GeV/c.
- Provide track information for e, μ, or γ isolation cuts, and to help with rejection of conversions and Dalitz pairs.
- Separate close together multi-charged particle tracks from single-charged particle tracks, which will be useful in tagging τ-decays and γ-conversions.

Physics performance of Central Tracker

How well do we do on these goals?

392

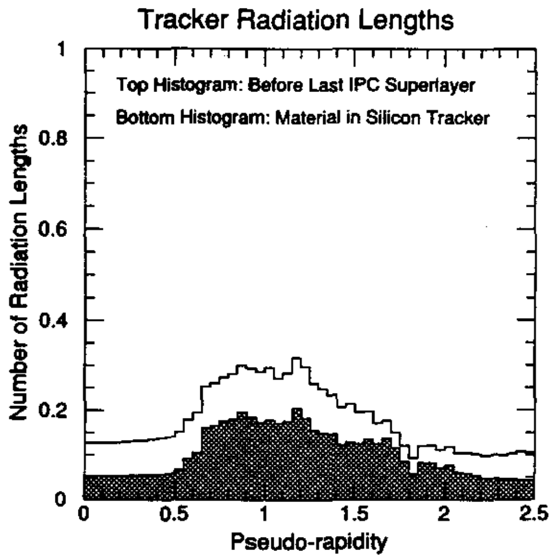

393

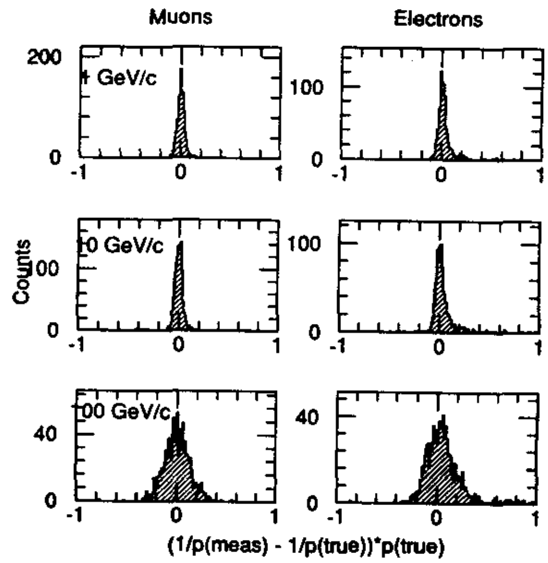

5

394

1. Vertex position measurement

Example - $H^\circ \rightarrow \gamma + \gamma$

Need vertex z position to $\pm$ 5 mm to get γ direction to use in $\gamma\gamma$ mass calculation

a) Reconstruct vertex from high P_t tracks

$\sigma_z \approx 1$ mm

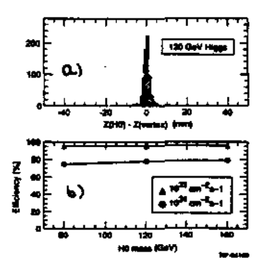

b) Efficiency of finding correct vertex within 5 mm of true vertex position

Efficiency ~ 95% at $\mathcal{L} = 10^{33}$

~ 80% at $\mathcal{L} = 10^{34}$

395

2. Electron/Gamma Separation

a) Separate γ signal from background $e^\pm$

- Example: $H^\circ \rightarrow \gamma + \gamma$ with M_H near M_{Z°

  background $Z^\circ \rightarrow e^+ e^-$

- Use full GEANT simulation of GEM including Central Tracker material, dead regions, efficiencies, pileup backgrd etc

- Select EM showers in calorimeter:
  - E_T of shower $\geq$ 20 GeV
  - (E in EM cal)/(E in EM + E in Had) ≥ 0.95
  - Isolation cut $\Sigma E(R \leq 0.3) - E_{shower} \leq 10$ GeV

- The above cuts do not distinguish γ from $e^\pm$

  Now use Central Tracker
  - Find location of prod. vertex from other charged tracks in event

    Use γ impact point in calorimeter
  - Define Road in tracker from γ to vertex straight line with a width of 1.5 cm
  - Cut on no. of hits in this Road

- • Can reject $e^\pm$ by a factor of 200

  and thus $Z^\circ \rightarrow e^+e^-$ by 4×10^4 !

396

NOTE: Do NOT require pattern recognition or track reconstr.!

ELECTRON/GAMMA SEPARATION

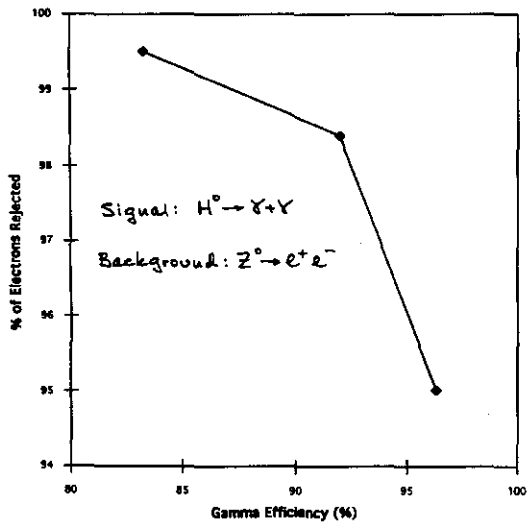

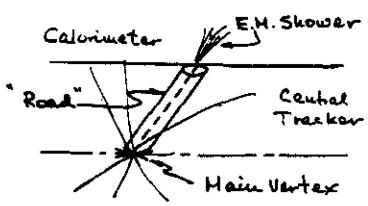

b) Electron signal, background γ's

- Example: $H^\circ \to Z + Z^* \to e^+e^-e^+e^-$ / $e^+e^-\mu^+\mu^-$

  $m_H \sim 150$ GeV

  Background: $p + p \to$ jets $\to \pi^\circ$ or γ
- Use full GEANT Simulation
  - Select E.M. Showers in Calorimeter
    same cuts as above
  - Define road in Tracker, look for hits
    same as above
  - Cuts to select electrons
    6 or more hits in road
    reconstruct P from curvature
    $P_{curv}/E_{cal} = 1 \pm \Delta$
- These cuts reduce γ and π° background by a factor of ~100
  - Remaining background mostly true $e^\pm$ from $\pi^\circ \to \gamma$'s, $\gamma \to e^+e^-$ pair
  - Can look for pair $e^\mp$ to selected $e^\pm$ in Central Tracker

    Should be able to get another factor of 10 rejection from this

Identify $e^\pm$ Signal

Backgrounds: $\gamma \to e^+e^-$
$\pi^\circ \to \gamma\gamma$, $\gamma \to e^+e^-$
$\pi^\circ \to \gamma e^+e^-$

a) e^+e^- pair separated

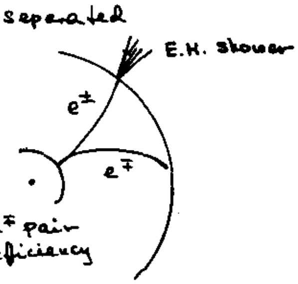

can detect $e^\mp$ pair with 97% eficiency

b) close together e^+e^- pair in same pads

can reject as multiple tracks by total charge with good efficiency

- 3 TRACKS CAN BE IDENTIFIED USING AVERAGE OF CHARGE OVER EIGHT LAYERS

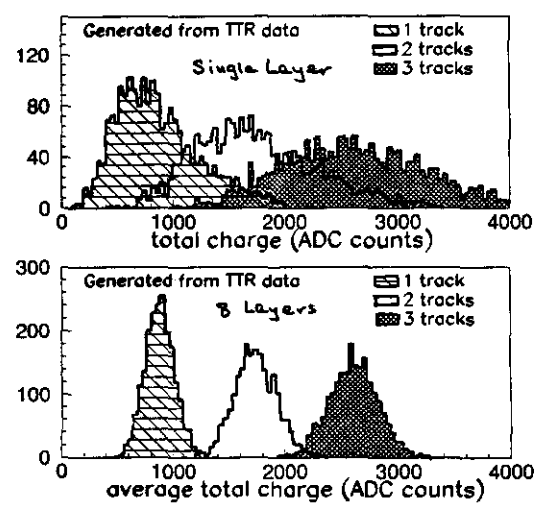

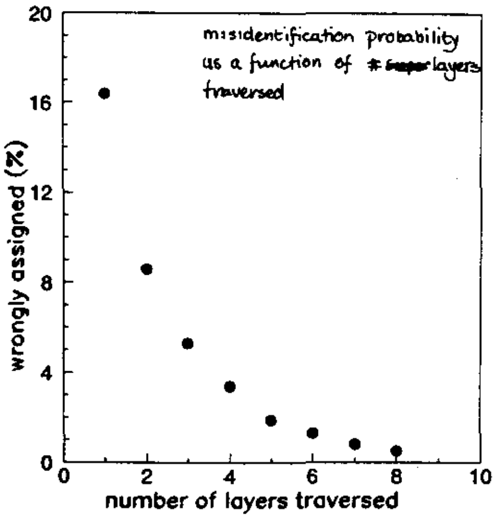

401

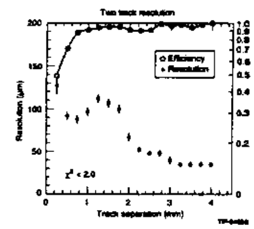

402

6-2c

3. Electron / Hadron or Electron / jet Separation

a) Uses both the calorimeter and the Central Tracker

- Calorimeter:
  - Energy distribution between E.M. and Hadronic Calorimeters
  - Isolation cuts
- Central Tracker:
  - Matching position of charged track to shower pos. in calorimeter
  - Energy / Momentum comparison
  - Help with isolation cuts

b) Used full GEANT Simulation to study

- Signal: $H^0 \to Z + Z^* \to e^+e^-\ e^+e^-$ or $e^+e^-\mu^+\mu^-$
- Background: $p + p \to 2$ jet events
- Select E.M. showers in calorimeter same cuts as before
- Look for hits in Road in Central Tracker same as before
- Reconstruct track, do E/p comparison

403

Summary of Electron Identification

Background	Probability of Misidentification as $e^\pm$
γ	10^{-3}
π^0	10^{-3}
$\pi^\pm$	8×10^{-4}
jet (non isolated)	2×10^{-4}
jet (isolated)	10^{-5}

404

4. Help with Muon Identification

Comparison of momentum of track in Muon system with momentum in Central Tracker can reduce fake muon background by a factor of ~5.

a) Quantitative study using full GEANT simul.

- signal: $t + \bar{t} \to W^+ b W^- \bar{b} \to e^{\pm} + \mu^{\mp} + \mu_{incl} + X$

  where $e^{\pm}, \mu^{\mp}$ are isolated

  $\mu_{incl.}$ is in a b-decay jet

- Background: $p + p \to 2$ jets

  with fake muons coming from

  i) hadrons that decay into muons

  ii) secondary hadrons from interactions in calorimeter penetrating to Muon Syst.

- Select muon candidates in Muon Syst. with

  i) $|\eta| \le 2.5$

  ii) isolated $e^{\pm}, \mu^{\mp}$ with $P_{\perp} \ge 30$ GeV/c

  iii) non-isolated μ_{incl} with $P_{\perp} \ge 5$ GeV/c

- Match muon candidate with track in Central Tracker, form χ^2

$$\chi^2 = \left(\frac{\Delta P}{\sigma_P}\right)^2 + \left(\frac{\Delta \theta}{\sigma_\theta}\right)^2$$

- Accept as muon if $\chi^2 \le 10$

405

Muon Identification

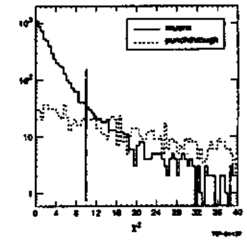

$$\chi^2 = \left(\frac{\Delta P}{\sigma_P}\right)^2 + \left(\frac{\Delta \theta}{\sigma_\theta}\right)^2$$

where $\Delta P = P_{Muon\,syst} - P_{Central\,Tracker}$

$\vec{\Delta\theta} = \vec{\theta}_{Muon\,syst} - \vec{\theta}_{Central\,Tracker}$

σ_P, σ_θ are combined errors

Cut at $\chi^2 \le 10$ reduces fake muon background by a factor of 5

406

Bing Zhou

b) Dependence of Fake Muon Background Rejection Factor on Central Tracker Momentum Resolution

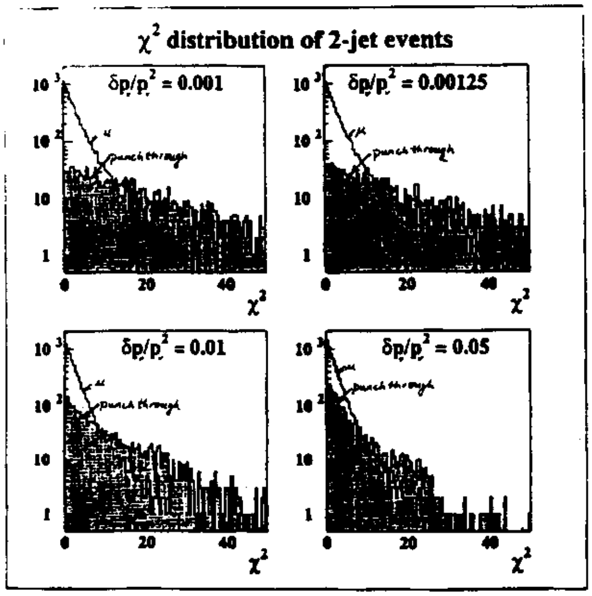

Obtain a factor of 5 reduction in μ punchthru background by comparing $P_T(\mu\,syst)$ with P_T(Cent.Trac)

407

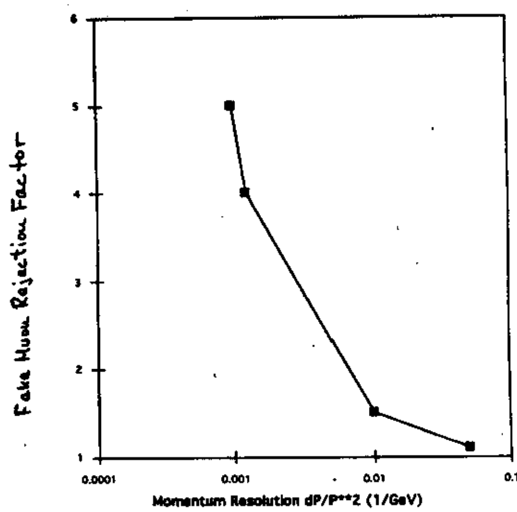

408

Improvement of Muon momentum resolution of Muon System using Central Tracker info.

a) At low momenta, combine Muon Syst + Central Tracker

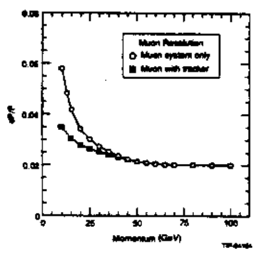

b) At high momenta, use of vertex point from Central Tracker improves Muon System momentum resolution by 10 to 30%

(study by Larry Rosenson)

409

Charge Separation at 95% Conf Level

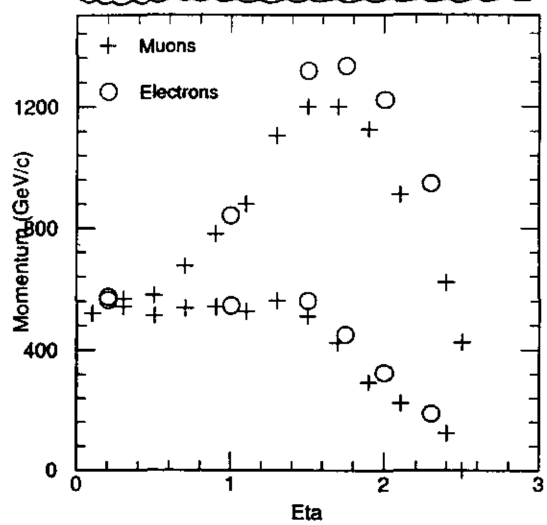

410

W-W Scattering

From John Bagger

$P + P \rightarrow W + W + X \rightarrow \ell^{\pm} \ell^{\pm} X$

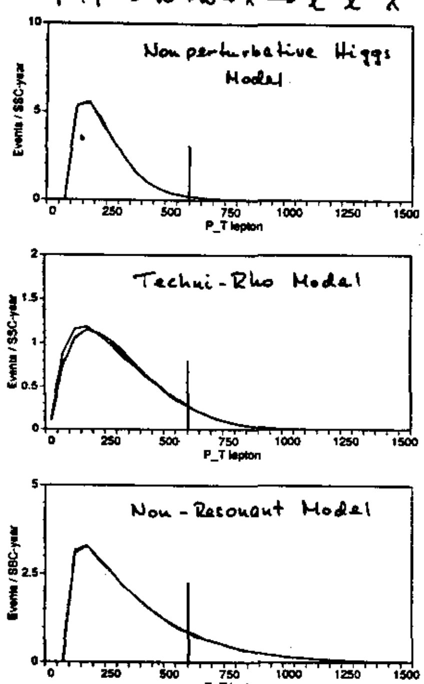

411

6. Help with Isolation Cuts

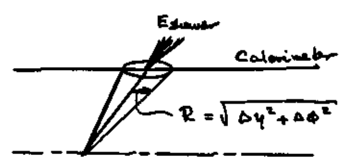

Typical Isolation Cut

$$\sum E_T(R \le 0.3) - E_{shower} \le E_{cut}$$

a) In calorimeter, can not make E_{cut} too small because of noise

b) Central Tracker is efficient for charged tracks around a few GeV/c, so can help to reduce E_{cut}

c) A study for isolation cuts for γ's in $H \rightarrow \gamma\gamma$ shows that we can reduce backgrounds by ~ factor of 2 by using Central Tracker

412

7. Tau Identification

Use $\tau \to 3$ charged tracks

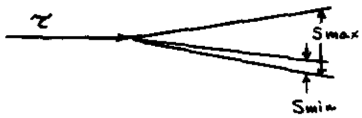

a) For low momentum τ's ($P_t \leq 100$ GeV or so) all 3 tracks are sufficiently separated to reconstruct all 3 tracks

typically need $S_{max} \geq 5$ mm (2 pads)

$S_{min} \geq 2.5$ mm (1 pad)

efficiency $\geq 60\%$ for $P_t \leq 100$ GeV/c

b) For high momentum τ's decay products often hit same pads. In this case

- we can tell we have multiple tracks from total charge deposition in IPC chambers
- can get total energy of τ from calorimeter.

413

6-30

$\tau \to 3$ charged tracks

Efficiency for reconstructing all 3 tracks

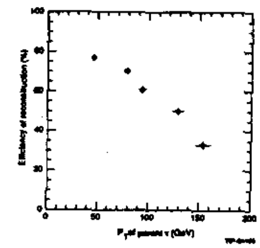

414

$\tau \to 3$ charged tracks

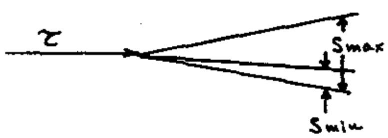

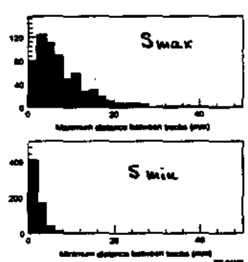

Separation between τ decay products at outermost IPC layer for P_t of $\tau = 150$ GeV/c

415

6-

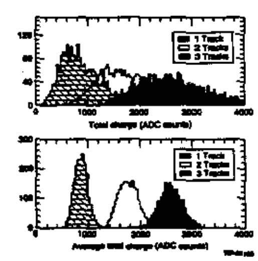

416

6-19

D.M.Lee, Los Alamos

STATE-OF-THE-SILICON TRACKER SYSTEM

- **UPDATE - IMPROVEMENTS and MODIFICATIONS**
- **MECHANICAL OVERVIEW and PROGRESS**
- **ELECTRONIC OVERVIEW and PROGRESS**

420

IMPROVEMENTS and MODIFICATIONS

SILICON TRACKER

1. **18 cm Ladder Length**
2. **0° Silicon Ladder Tilt Angle**
3. **Radiation Length Reduction**
4. **Reduced Number of Cooling Rings**
5. **Modified Cooling Ring**
6. **Modified Ladder Support**
7. **± 5 mradian Stereo**

421

GEM
Silicon Tracker Parameters

Silicon Area	8 m^2
Electronic Channels	2.5 x 10^6
Electronic Readouts	~2000
Bunch Crossing	16 ns
Data Transmission Rates	60 Mbit/s
Radiation Levels	.4 Mrad/ SSCY @ 10 cm, Charged
	a few x 10^{12}/ cm^2-SSCY, neutron
Stability	10 microns
Heat Dissipation	< 5 kWatts
Radiation Length	less than 10%
Lifetime	5 - 10 year

422

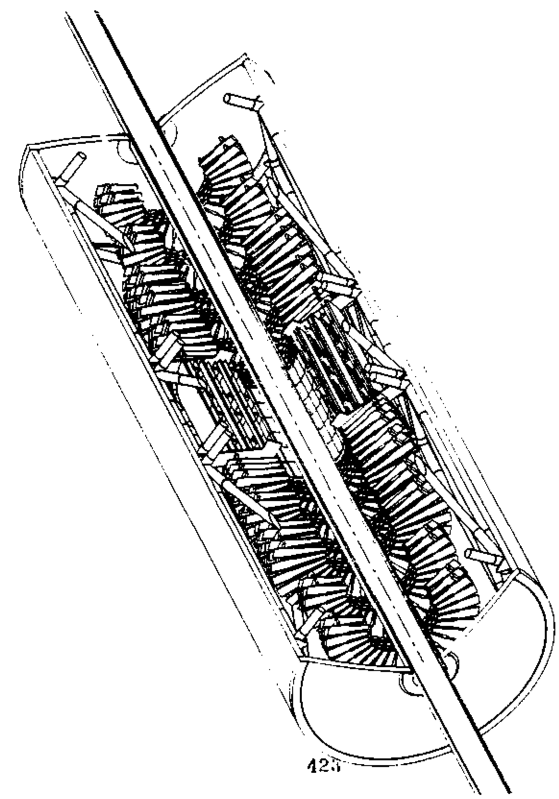

423

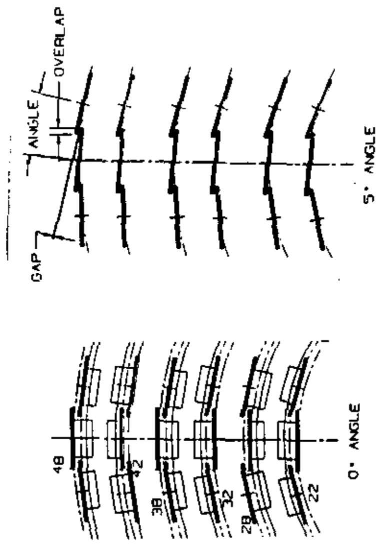

424

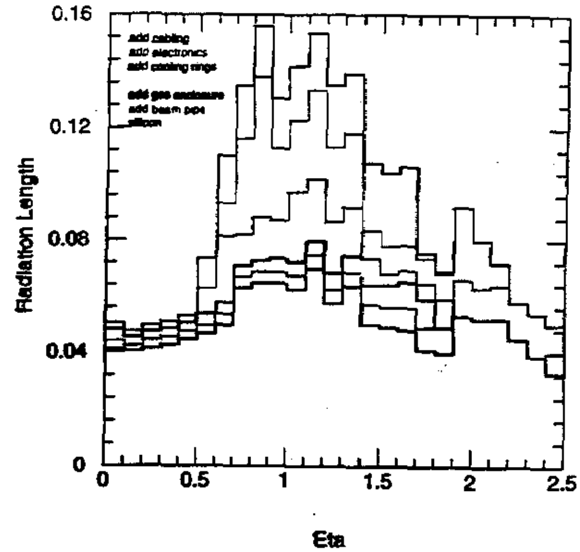

425

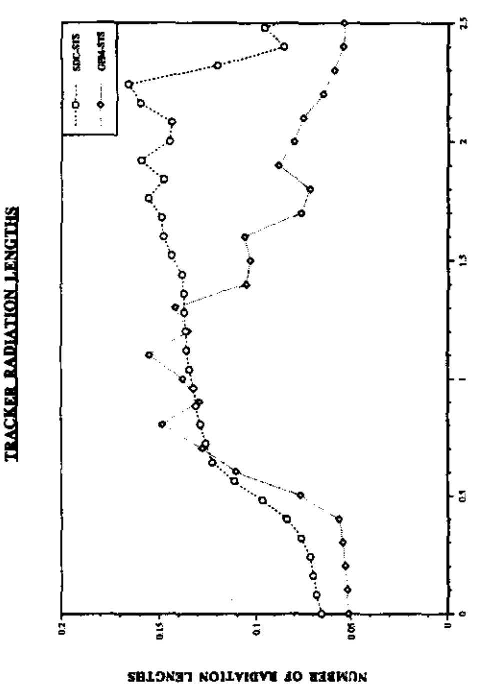

426

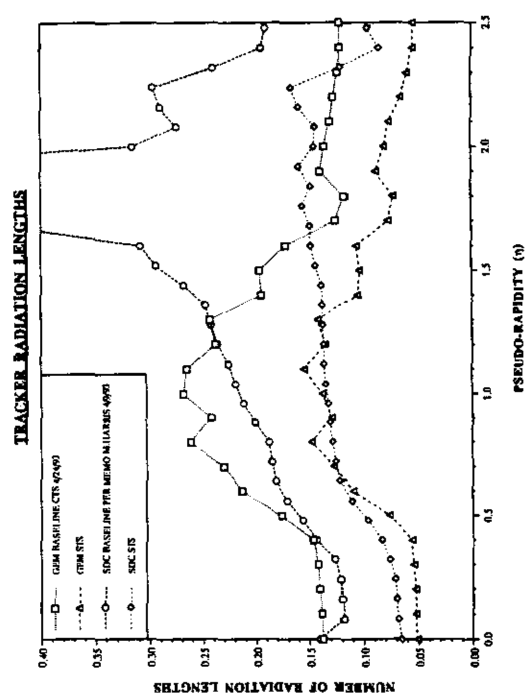

427

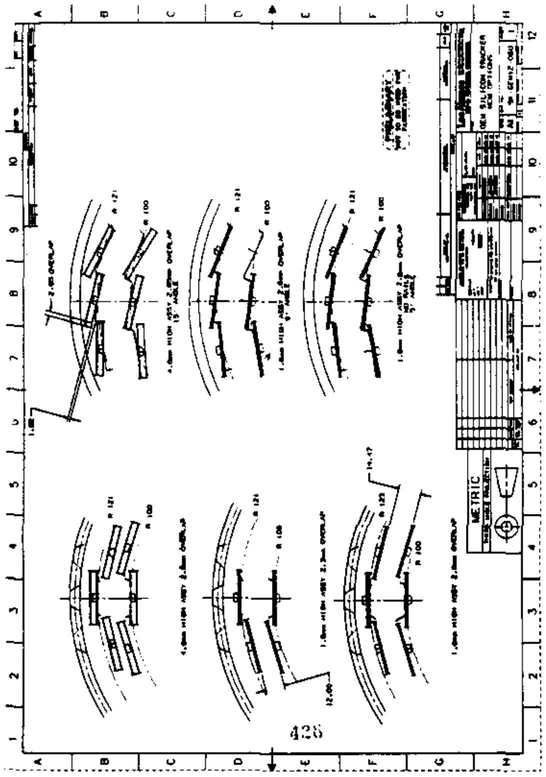

428

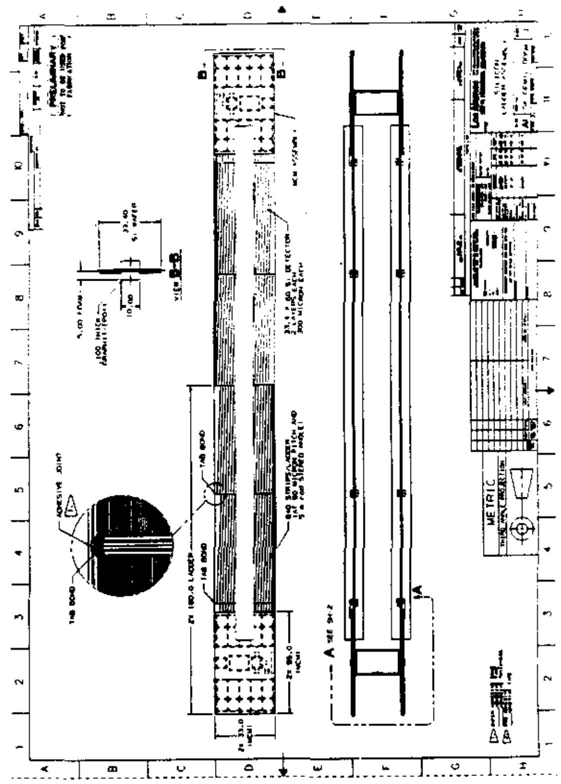

429

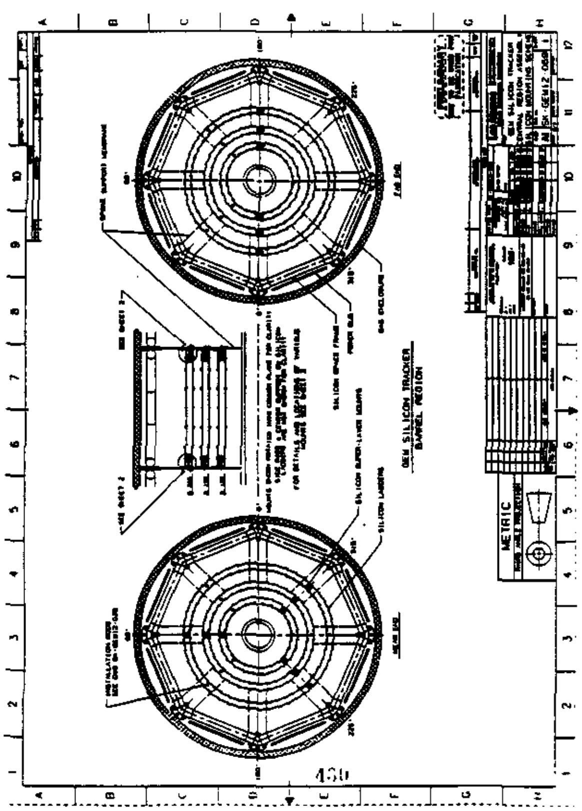

430

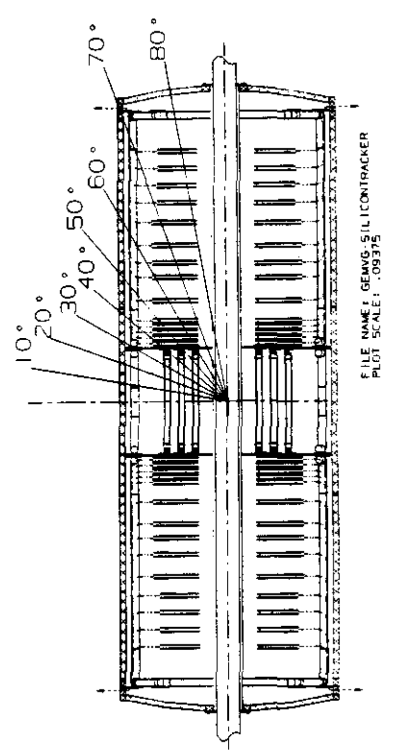

431

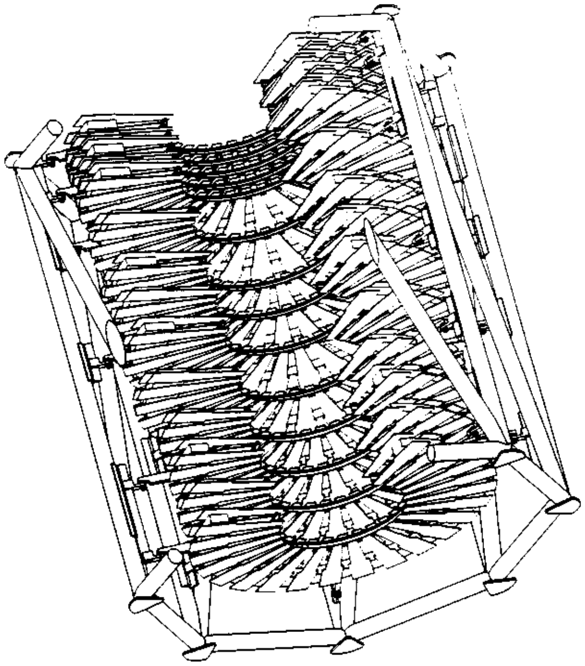

432

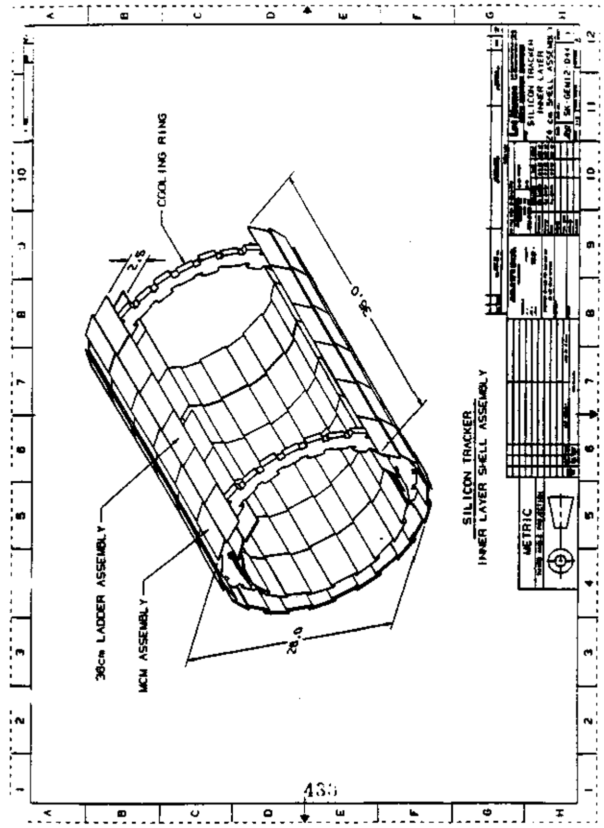

433

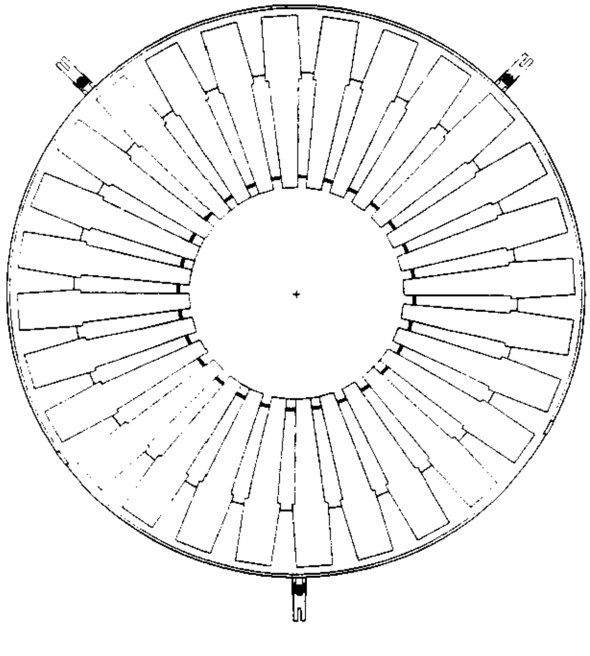

434

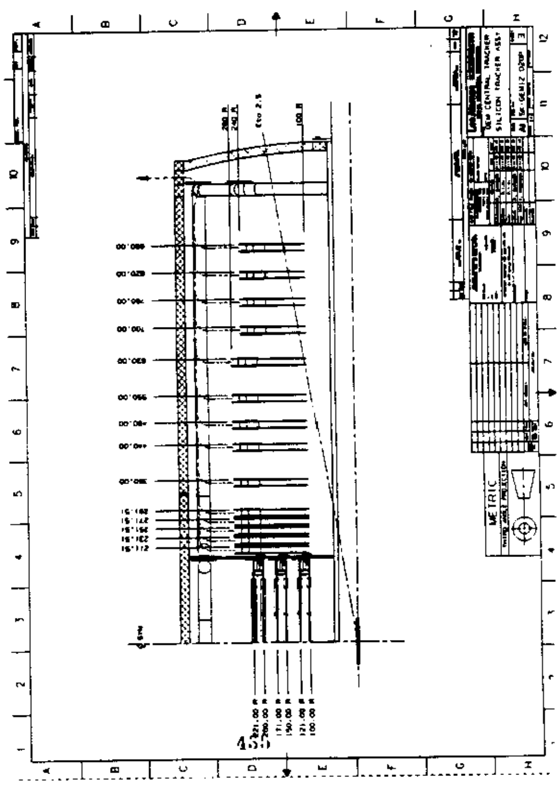

435

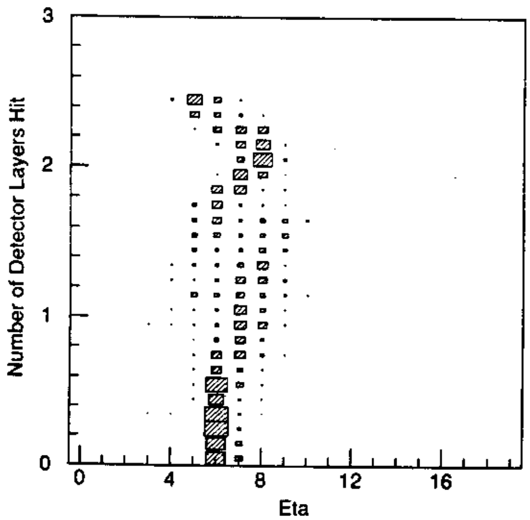

436

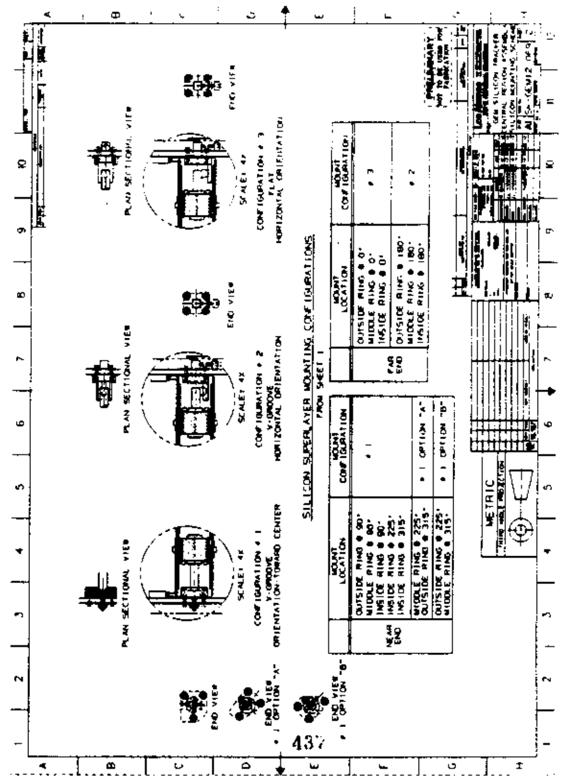

437

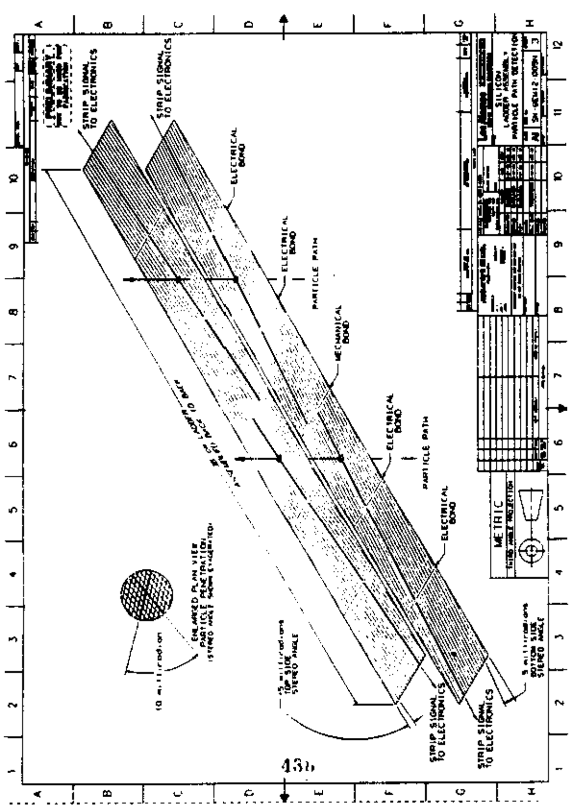

438

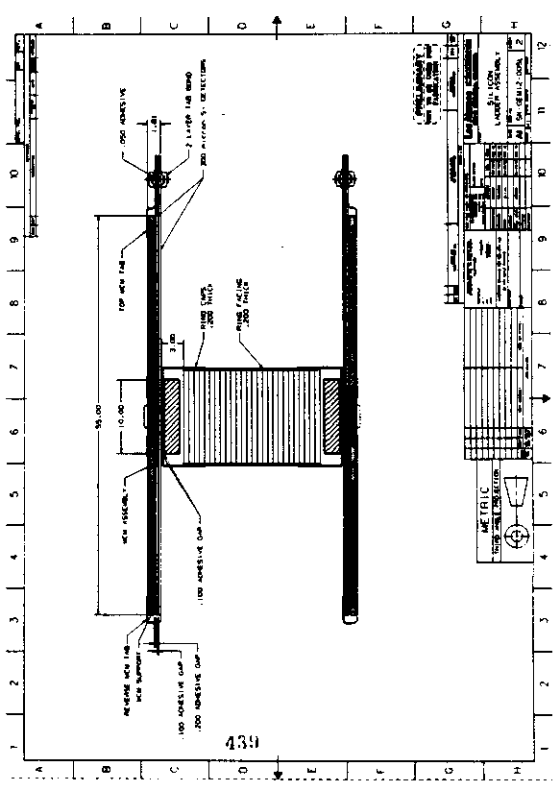

439

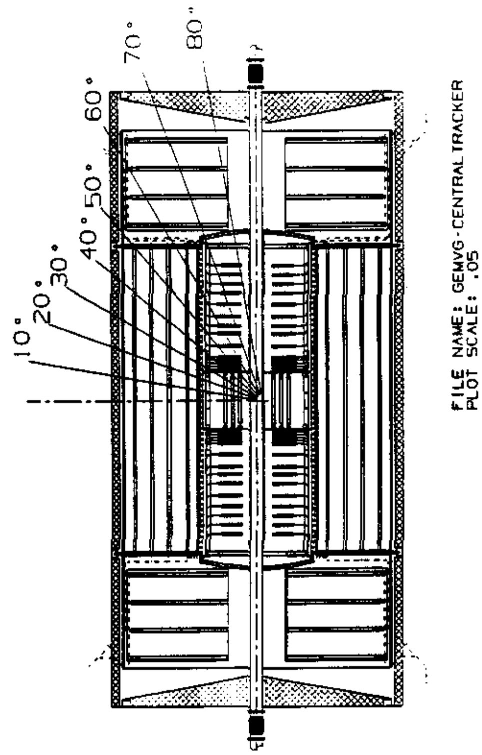

440

ELECTRONICS

1. **Bipolar Amplifier/shaper/discriminator**
   - **Design Complete**
   - **SemiCustom ASIC Fabricated and Tested**
2. **Digital Readout**
   - **Design Complete**
   - **VHDL Hardware Description Language in Progress**
3. **Multichip Module (MCM)**
   - **Prototype Design Complete**
   - **Design Layout Complete**

441

Electronics Design Requirements

Signal Level:	**24000 electronics**
Noise Level:	**< 2500 electronics**
Power:	**2 - 3 mW/channel**
Speed:	**60 MHz**
Output Data Rate:	**< 60 Mbps/ladder**
Radiation Resistance:	**> 5 mrad**
	> 10^{14} neutrons/cm^2

Low Mass MCM or Equivalent

Low Cost

Good Heat Transfer

442

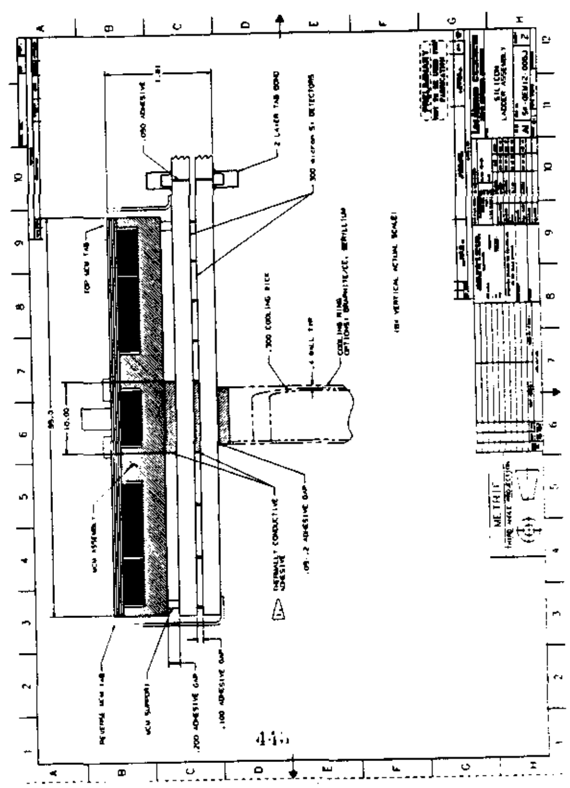

443

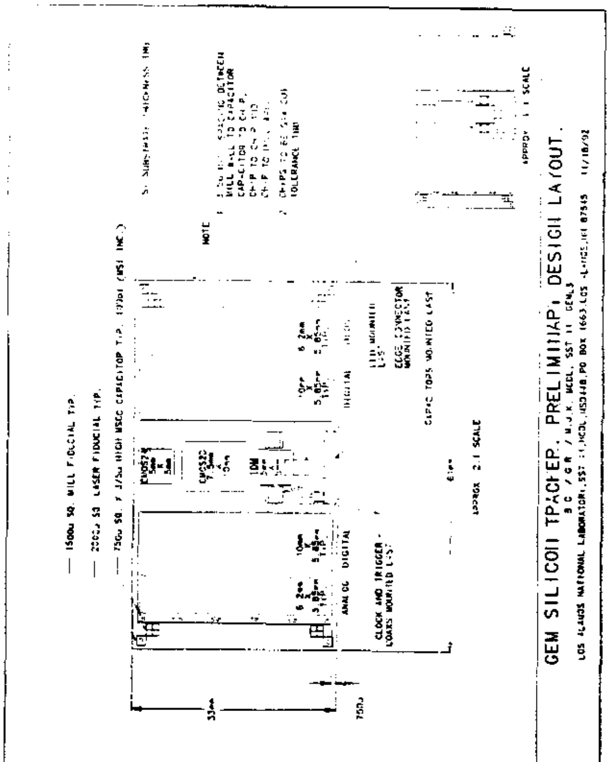

444

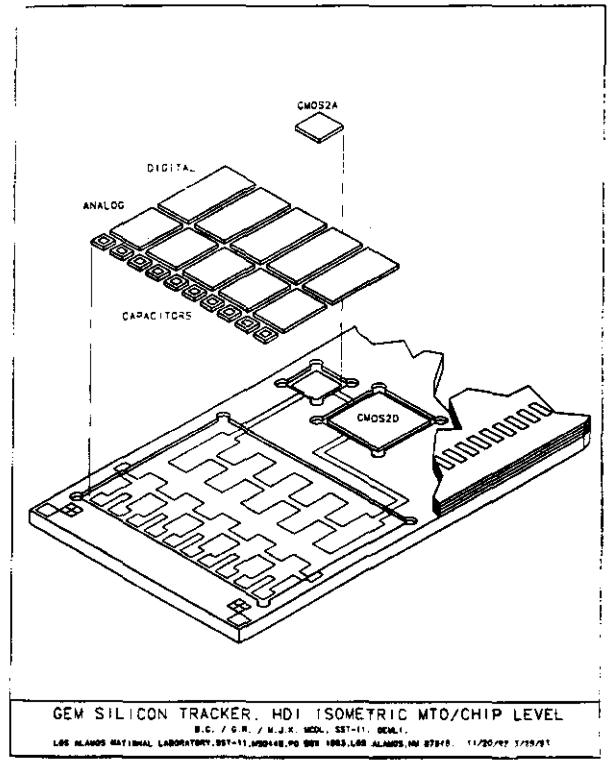

445

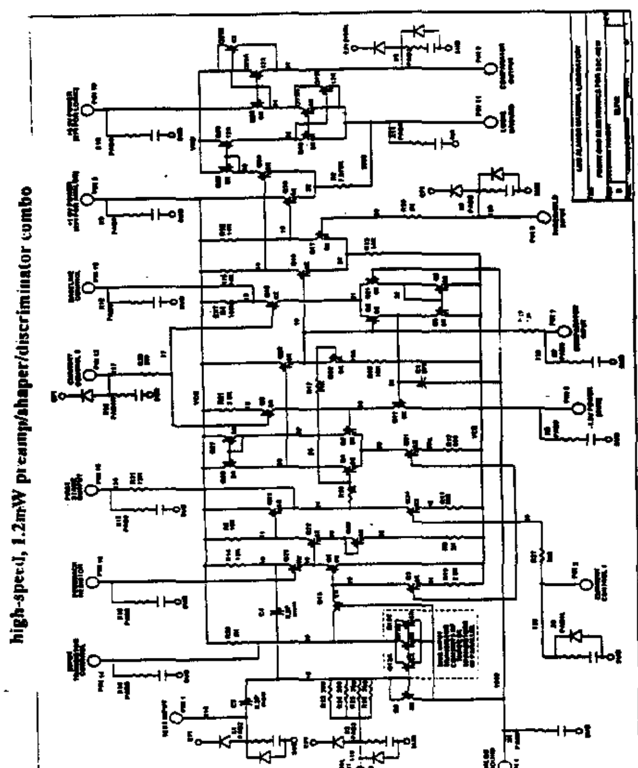

446

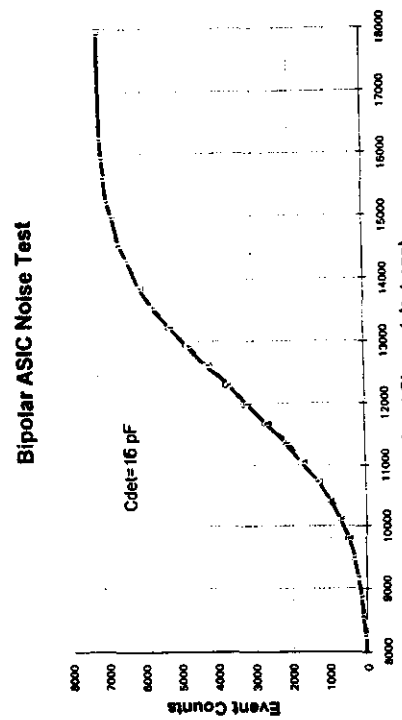

447

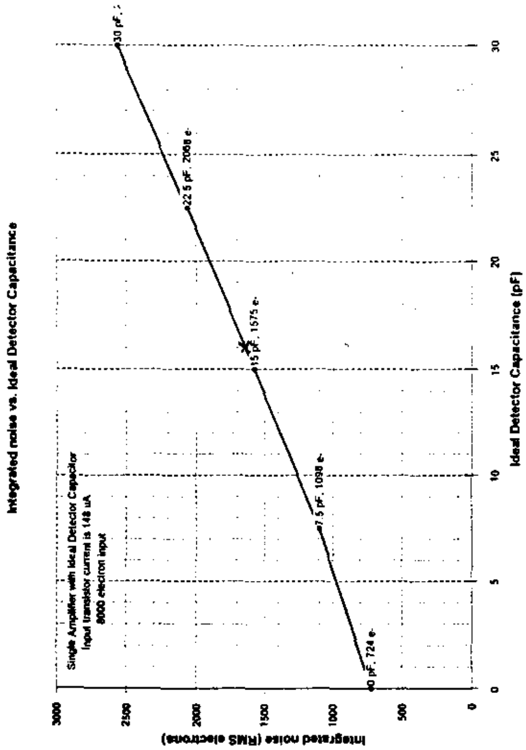

448

Future Activities - Electronics

1. Collaborate with Kipnis of SDC on Cost Sharing with Westinghouse Foundry for Full Custom Bipolar Fabrication - August

2. Collaborate with Grillo of SDC on Cost Sharing with Harris Foundry for Prototype CMOS Digital Circuit - July

3. Prototype Multichip Module (MCM) (Internal LANL Funds - CRADA) - Sept

4. Collaborate with Nickerson of SDC on Fiber Optic Readout

5. Refine Power Cables

449

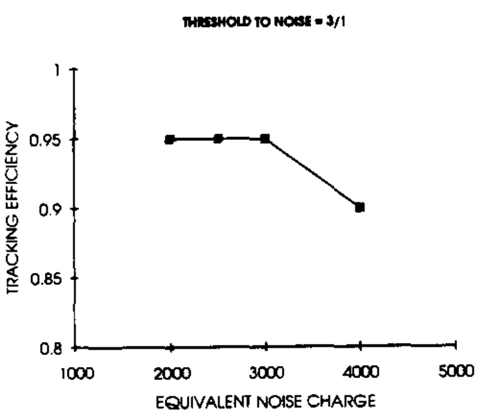

450

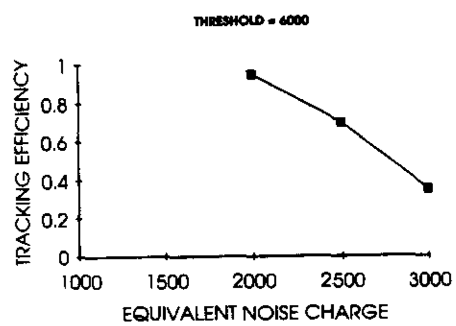

451

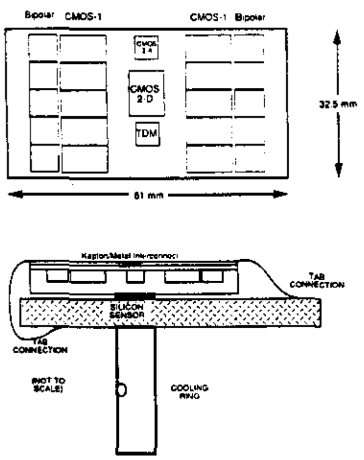

452

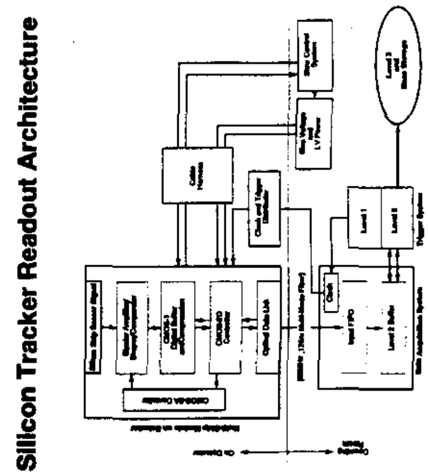

453

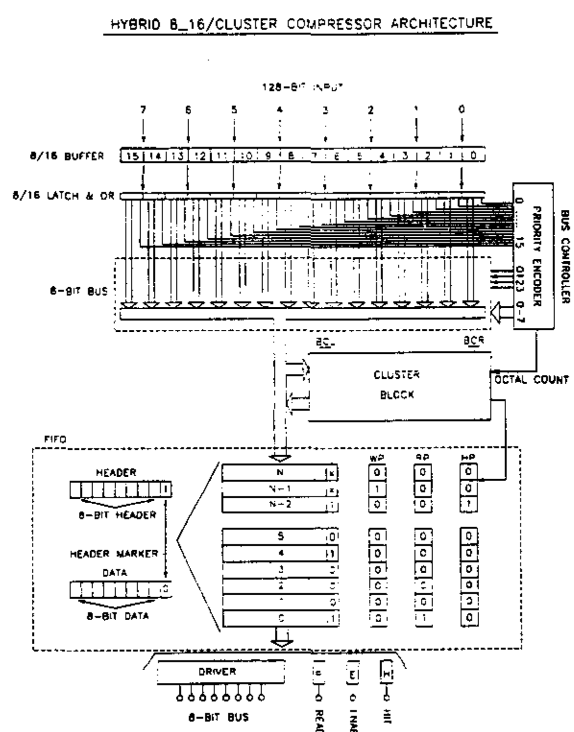

451

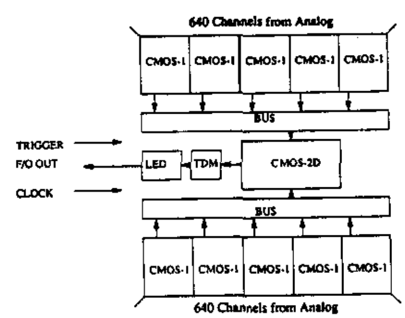

455

IPC Prototype Muon Test Stand Results

Position Residuals vs Angle

Angle defined as the angle between the particle trajectory and the normal, projected onto the precision measurement direction.

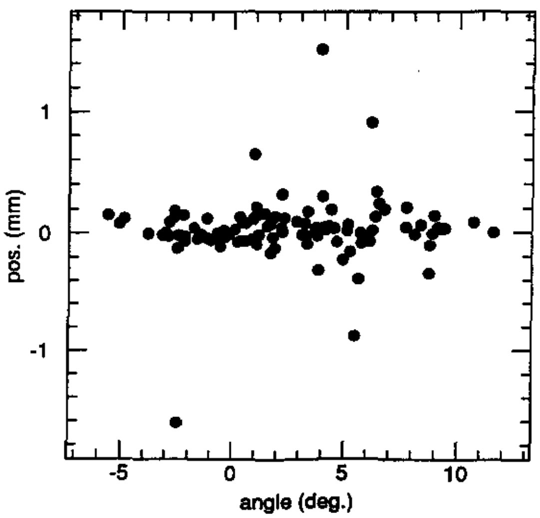

459

IPC Prototype Muon Test Stand Results

Expected vs Measured Position in Chamber P3

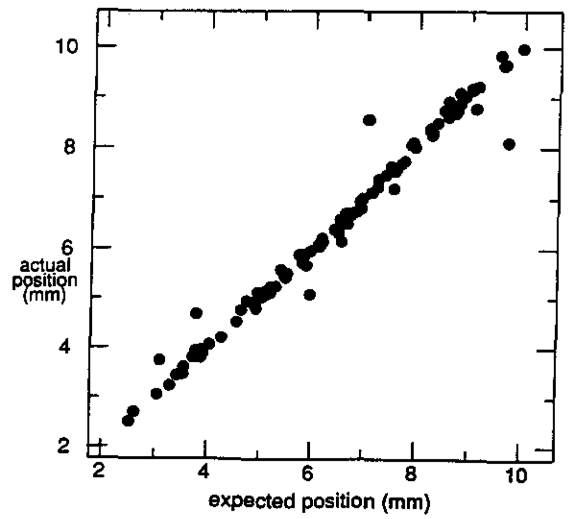

460

IPC Prototype Muon Test Stand Results

Data Cuts:

Minimal data cuts employed - no cut on 'fiducial region'

Three 'good' pad measurements are required for each of the three chambers. Good is defined as a non-saturated ADC value, not consistent with pedestal.

IPC Prototype Muon Test Stand Results

Angular Distribution of Accepted Events

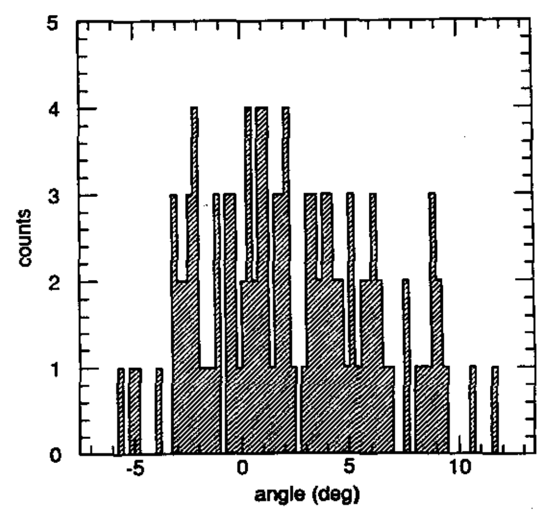

462

IPC Prototype Muon Test Stand Results

46

IPC Prototype Muon Test Stand Results

Angular Acceptance /Distribution

Angular acceptance of telescope = +/- 12 degrees.

However, some channels dead (bad plated through holes)
Due to small channel count, this effect leads to large angular dependent losses.

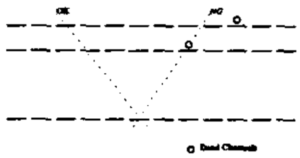

To pass data cuts, require 3 'good' measurements on each plane - results in effective angular acceptance of -6 to 12 degrees

IPC Prototype Muon Test Stand Results

Multiple Coulomb Scattering

Only material between first and second chamber relevant.
2x0.5 mm G10 boards + 2x0.25 Oz Cu = $6.5\times10^{-3}\ X_0$

Contribution from Multiple Scattering = 25 microns.
(*not subtracted out of result presented here)*

Relationship between observed position residuals and single chamber measurement error.

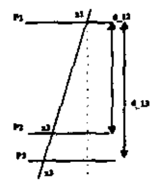

$(x_2-x_1)/d_{12}=(x_3-x_1)/d_{13}$

$(x_2-x_1)*d_{13}/d_{12}+x_1=x_3 \qquad d_{13}/d_{12}=a$

$\Delta=x_3^{meas}-x_3^{pred}=x_3^{meas}-ax_2+(a-1)x_1$

$\delta\Delta=\delta x_3\oplus a\delta x_2\oplus(a-1)\delta x_1$

$\delta\Delta=\delta x\sqrt{(1+a^2+(a-1)^2)}$

$\delta x=\delta\Delta/(\sqrt{2}\sqrt{(a^2-a+1)})$

For a=1.261

$\delta x=\delta\Delta/1.63$

IPC Prototype Muon Test Stand Results

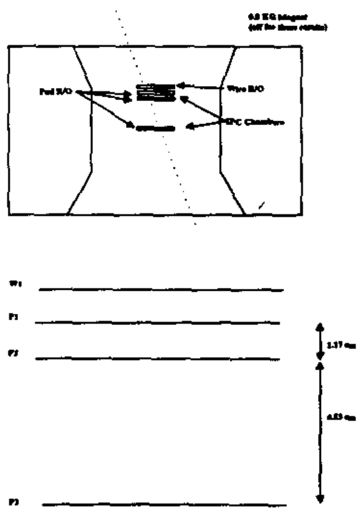

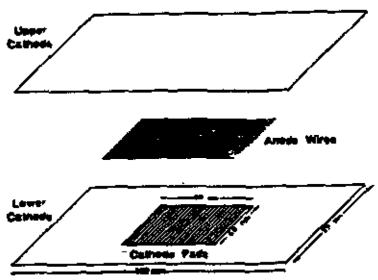

Figure 3
IPC Prototype

IPC Prototype Muon Test Stand Results

- 3 chambers with pad readout + 1 chamber with readout in orthogonal direction to correct for misalignment.
- Determine position resolution by extrapolating track determined in bottom two pad chambers to top chamber, and comparing with position measured in top chamber.
- Misalignment in precision tracking direction corrected by using global fit to pad data (minimizing position residuals) Misalignment in orthogonal direction corrected using data from wire readout chamber. (shortage of electronics precluded wire readout on more that one chamber)
- Tests conducted with fast front end electronics (25ns peaking time), and CO_2/CF_4 gas mixture.

467

IPC Electronics Status

Radiation Length of Low Voltage Cabling

Cross Sectional Area of Aluminum needed per chamber = 14 mm^2. (4x10 gauge + 2x18 gauge) (20 chambers per layer)

Aluminum:
Radiation length - uniform spreading over 2π
0.6×10^{-3} X_0 /layer

Radiation length - local
0.02 X_0/layer

Be:
Radiation length - uniform spreading over 2π
0.2×10^{-3} X_0 /layer

Radiation length - local
7×10^{-3} X_0/layer

468

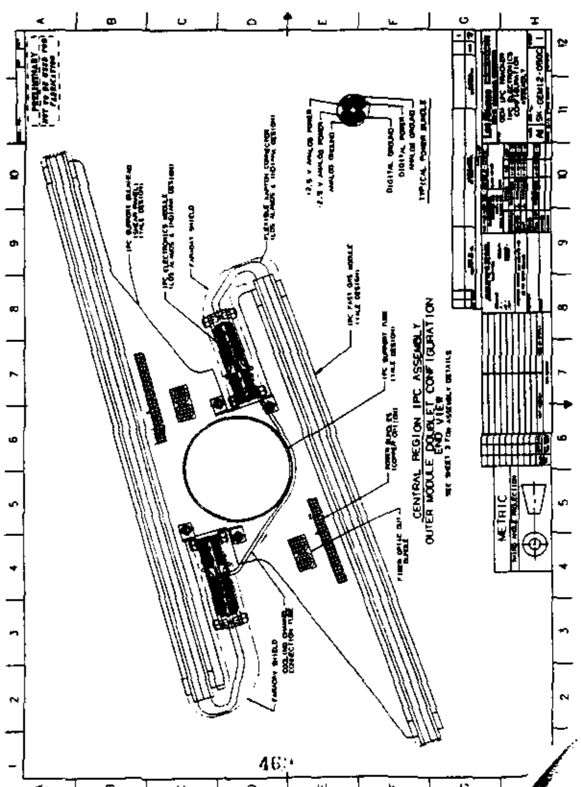

469

IPC Electronics Status Report

Basic Approach

Power supply bank mounted on gangway provides +5V, +-2.5V through 40m runs to patch box . Smaller gauge wire used for run from this point to electronics.

Inner Cabling

Conductor Figure of merit - X_0/ρ

Cu	8.5
Al	1.0
Be	0.3

Copper is out - Aluminum most practical solution, but Be remains possibililty.

Design based on 0.2V maximum voltage drop in 4 m cable. (remainder of cable to supplies @ 40m assumed o have negligable drop.)

470

IPC Electronics Status Report

Low Voltage Cabling

Power Budget Estimate (per chamber)

Preamp/Shaper/SCA - +/- 2.5 V & analog gnd
+2.5V - 7.7 A
-2.5V - 7.7 A

FADC - +5V & dig gnd., 2V reference
+5V - 6.4 A

Readout Controller - +5V & dig gnd
+5V - 2 A
FO Transmitter - +5V & dig gnd
+5V 2 A

Total per chamber pair ------

+5V	**10.4 A**
+ 2.5V	**7.7 A**
- 2.5V	**7.7 A**

IPC Electronics Status Report

- Rad-Hard Pre-amp/shaper and Analog memory now in fab.
  Delivery date - June 18.
  Preparations are being made for device testing after delivery. (Will use facilities at SSCL for SCA tests)
- Readout Controller FPGA prototype now 'complete'. Write address generation tested to 60 Mhz.
- Design/Layout of full IPC readout front end prototype now underway, using rad-hard custom ICs, and FPGA Controller.
- Design of power distribution/ cabling well underway. Options under consideration include Aluminum and Be -based on-chamber power distribution.

IPC Readout Prototype

Calibration System

Calibration Sequence controlled by on-board microcontroller. Controller injects known charge onto a calibration cap. located on input of each pre-amp.

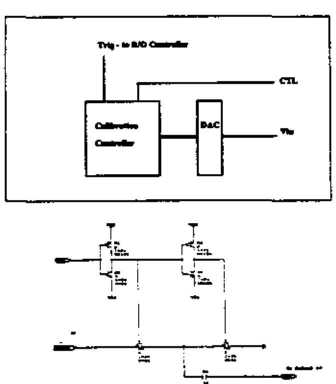

Full Calibration sequence consists of the generation of a set of pulse heights for each SCA cell. (i.e. pulse is moved through SCA by setting relative time between pulse and read address reset.)

IPC Readout Prototype

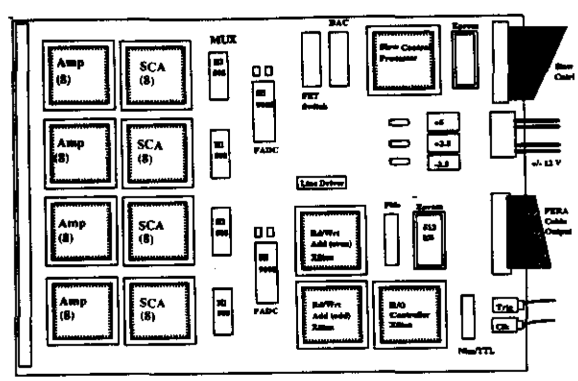

- 32 Channels per board
- Readout via FERA bus to dual port memory - later FO link
- Rad Hard parts used for front end Amp/SCA/FADC
- Controller implimented on FPGA chipset (done)
- Slow Control -
  Set Threshold for Zero Suppression
  System Reset
  Set Trigger Latency
  Control Calibration

IPC Readout Architecture

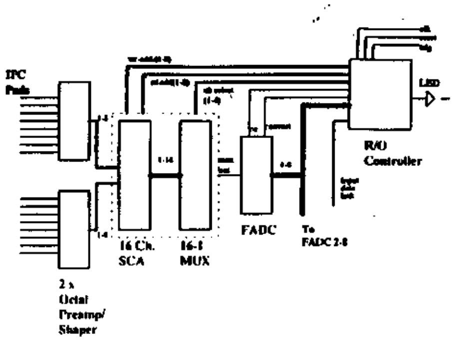

8 channel preamp/shaper

16 channel x 150 cell switched cap. array
16-1 analog multiplexer

15 Mhz 8-10 bit FADC (one/16 channels)

Readout Supervisor - (one per 128 channels)
Address generator + Readout Controller+
Zero Suppression + Fiber Link

IPC Electronics Status Report

- Rad-Hard Pre-amp/shaper and Analog memory now in fab.
  Delivery date - June 18.
  Preparations are being made for device testing after delivery. (Will use facilities at SSCL for SCA tests)

- Readout Controller FPGA prototype now 'complete'. Write address generation tested to 60 Mhz.

- Design/Layout of full IPC readout front end prototype now underway, using rad-hard custom ICs, and FPGA Controller.

- Design of power distribution/ cabling well underway. Options under consideration include Aluminum and Be -based on-chamber power distribution.

IPC Prototype Muon Test Stand Results

Position Resolution

Single chamber resolution (after making 'statistics' correction)= 60 microns, averaged over -6 to +12 degree acceptance.

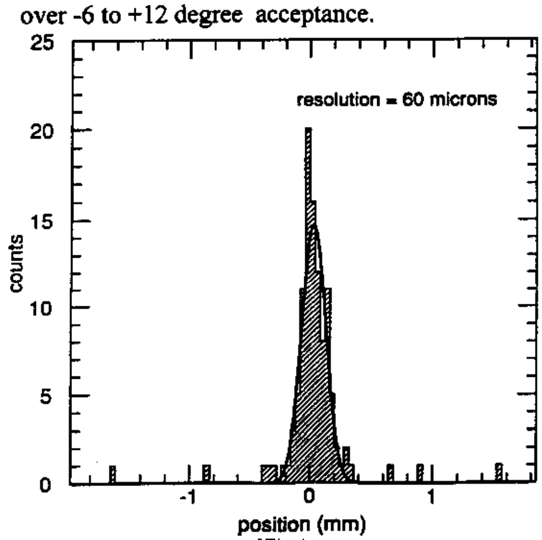

GEM TDR COST/SCHEDULE SUMMARY

AND

"PLANNING FOR A STRETCHOUT"

Gary Sanders

May 10, 1993

DRAFT PLANNING ASSUMPTIONS

EXTERNAL MILESTONES AND ASSUMPTIONS:

1. Collider commissioning April 1, 2002
2. SAB, NAB, Underground Hall, Utility Building dates do not change.
3. Test Beams at SSCL delayed 2 years.
4. Fermilab fixed target schedule slips to Spring, 1995.

SSCL Stretchout Exercise

1. 1999 completion is still the official baseline for all parts of SSC Project, including both detectors.

2. Within this baseline, the GEM surface assembly building dates have slipped a few months principally due to the failure of PB/MK to maintain the design schedule. The underground hall schedule has slipped 6 months to save construction dollars on both halls. GEM has provided official notice to the Laboratory that if this 6 month slip is adopted (it will be) GEM will require about $10 million more from the Laboratory to pay for premium shift work to try to maintain the installation schedule.

3. However, a multiyear stretchout will almost certainly take place, but the details must follow Congressional action.

4. SSCL is carrying out a strawman replanning following informal DOE guidance. Assumptions are a 3 year delay to 2002, nearly level Project funding for the next 3-4 years. The latter is a severe constraint. SSCL has chosen to fast-track the conventional construction (but not the Campus), the low rate production of superconducting magnets, and construction activities outside the US. Warm machines and test beams will be delayed from 6-36 months.

5. SSCL requested that GEM and SDC provide replans on April 1, 15, and 30. The April 1 request focused on the extent to which GEM costs would grow in this stretchout.

6. Barish, Willis, Sanders and Harris consulted and developed a response.

DRAFT PLANNING ASSUMPTIONS

GEM ASSUMPTIONS:

1. Add time in schedule so all R&D can be incorporated into production technique.
2. Set all installation and assembly to nonpremium shift labor as feasible.
3. Make our full-scale prototyping activity encompass a full 5% solid angle wedge of the detector.
4. Award magnet prime contract but fund only the design completion and cold mass R&D in the near years. Force funding profile down to permit all other subsystems to proceed within the level funding assumption in FY94-FY95. Replan magnet for a roughly 2 year delay in completion.
5. Complete Central Detector Support and Scintillating Barrel Calorimeter for first installation in Underground Hall. Make this activity into a self-contained project.
6. Hold very high priority of FNAL test beam in Spring, 1995. Complete liquid calorimeter module with highest priority. Make this activity into a self contained project leading to the full 5% wedge of the GEM detector.
7. Plan for the FNAL test beam and SSCL test beam activities to be in sequence as much as possible, rather than building two parallel overlapping activities as driven by the original compressed schedule.
8. Maintain the basic assembly and installation sequence of the 1999 baseline plan.
9. Continue R&D and design completion activities on the subdetectors, but take advantage of the stretchout to eliminate parallel and overlapping efforts. Thus, plan each program stage to benefit from the previous stage. Run a very lean program to stay within profile.
10. Take maximum advantage of technology development and price/performance improvements by postponing selection, production and purchase of final electronics and on-line computing and networking hardware as much as possible.

INITIAL REPLAN RESPONSE

1. It was felt that the Collaboration and Executive Committee had to discuss, review and participate in setting the guidance for the replan insofar as deciding the order of construction, items to be stretched out, etc. SSCL has been informed that no detailed replan will be submitted until this has taken place.

2. However, it was felt that submitting a figure for cost growth could not be postponed as SSCL was planning the total cost growth for the Project. A simple exercise was carried out to estimate the growth due to "marching army" costs and to necessary additional R&D which allowed us to use the extra time to reduce GEM project risks. No attempt was made to minimize the figure given to SSC. The growth was estimated at $120 million over the $552 million FY93.

3. GEM management has drawn up a list of suggested planning assumptions for further discussion in the Collaboration and Executive Committee.

OTHER INFORMATION ITEMS

1. SSCL hiring freeze and direction of attrition into technical hires of high priority.

2. Space at SSCL.

3. Reduction of FY93 budget!!! $34 million --> $25 million!

4. Reduction of FY94 funding?

5. $5 million + GEM university funding completed for FY93 (TNRLC provided about 65%). This has some items added from original plan (TDR preparation, FNAL test beam preparation,...).

DISCUSSION...

1. Discussion in general terms at this meeting, during the session and off-line with GEM Management.

2. Discussion at the GEM Executive Committee.

3. Following these, we will carry out a replan exercise:

   a. Complete detail of 1999 baseline. One day workshops called as needed.
   b. Top-level replan exercise by June. This will be circulated for discussion in June.
   c. Consideration by Collaboration Council and Executive Committee at meeting late June.

4. No detailed replan will be provided to SSCL until:

   a. A formal written request from the SSC Laboratory is received by GEM Management for a specific rebaseline with definite guidance. No response will be made to poorly defined requests or to oral or "last minute" requests.
   b. The GEM Collaboration Council and Executive Committee has reviewed the replan.

Any new GEM baseline should address the cost growth and funding shortfall in the GEM project.

GEM 3 YEAR STRETCH-OUT
COMPARISON OF PMB PROFILE & GEM ESTIMATE
(CONSTANT FY93 DOLLARS)

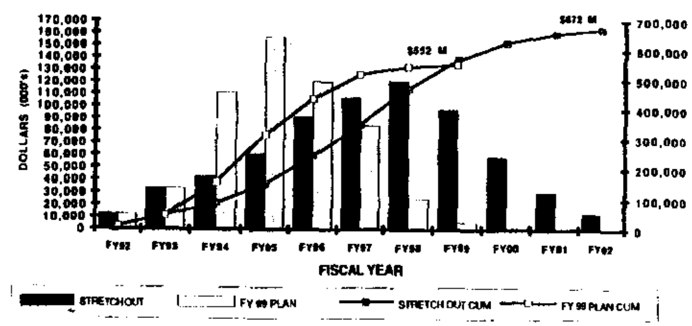

	FY92	FY93	FY94	FY95	FY96	FY97	FY98	FY99	FY00	FY01	FY02	TOTAL
FY 99 PLAN	13,100	34,000	111,400	157,100	120,100	84,300	25,875	6,200				551,875
FY 02 PLAN	13,100	34,000	43,100	61,300	91,000	107,100	121,150	97,250	58,700	30,000	13,350	671,550

FINAL AGENDA FOR PHYSICS MEETINGS AT UCSD, TUESDAY, MAY 11, 1993

Tuesday AM Session -- 8:00AM - 12:00PM

The main purpose of the morning session is to prepare our physics case to the PAC and to be sure nothing important has been left out.

NOTE: THE ALLOTTED TIMES ARE APPROXIMATE AND SOME MAY BE SUBTRACTED FROM THE TUESDAY MORNING SESSIONS TO GIVE ENOUGH TO THE AFTERNOON SESSIONS.

A. Higgs Physics (2 hours)

1. H -> gamma gamma, without and with associated lepton.
   (R. Zhu)

2. H -> l+ l- l+ l- for M_H = 100 - 800 GeV at L = 10^33 and 10^34;
   "WW" scattering.
   (S. Mrenna)

3. H -> l+ l- nu nu.
   (X. Shi)

4. Statistics and systematics; H -> lljj; SUSY Higgs; CP Nonconsevation.
   (H. Yamamoto)

B. Ultrahigh Luminosity Physics (30 minutes)

1. Z' -> e+e-
   (S. McKee)

C. Global simulation package for GEM (30 minutes)
   (J. Womersley)

D. Planning for PAC Presentations -- B. Barish, et al. (1 hour)

Tuesday PM Session -- 1:00PM - 5:30PM

The purpose of the afternoon session is to discuss issues of "detector optimization".

A. Trigger, Muon Reconstruction, Jet Resolution and all that (2 hours)

1. Optimizing trigger thresholds
   (H. Uijterwaal -- 15 min.)

2. Muon trigger model

(V. Balagura -- 15 min.)

3. Update on results from muon reconstruction: resolution, efficiency, coverage, physics performance; H->4mu, Z'
(T. Wenaus -- 30 min.)

4. Pattern recognition
(P. Dingus -- 20 min.)

5. Jet resolution
(M. Shupe -- 20 min.)

6. Forward calorimeter design parameters
(K. Shmakov -- 20 min.)

B. Using the CT and CAL to optimize MU acceptance and measurement (2.5 hours)

Two questions will be addressed:
By using calorimeter and central tracker
1) How to improve the muon acceptance?
2) How to improve the muon momentum measurement?

These questions should be addressed for L = 10^34 as well as 10^33 wherever appropriate.

(Note: Times below are approximate. Extensive discussion is expected.)

(1) General discussion of coverage of muon system and how the CT and calorimeter might help.

(F. Taylor (or volunteer) -- 10 min.)

(i) How to identify muons (MIPs) in the calorimetry? How often would hadronic background would be identified as a MIP?

(H. Ma, M. Shupe -- 15 min.)

(ii) How well can we match the HCAL MIP with the CT track? How clean will the muon track be found in the CT?

(S. McKee -- 10 min.)

(iii) If only two SLs find muon track, what will be the muon momentum resolution? Can we use the event vertex to improve the resolution?

(T. Wenaus, S. Mckee -- 15 min.)

(2) Discussions on improvement of the muon momentum measurement:

(i) How best to use the calorimeter information to reconstruct the energy lost in the calorimeter.

(V. Gavrilov -- 15 min.; Y. Efremenko -- 15 min.)

(ii) How to use the CT to fix the vertex of the muon track and to improve the momentum resolution of the muons ?
What are the limitations?

(M. Brooks 10 min.)

$H \to ZZ/ZZ^* \to \ell\ell\ell\ell$ Searches
140GeV $< M_H <$ 800 GeV

The $H \to ZZ \to \ell\ell\ell\ell$ decay provides the cleanest Higgs signal at the SSC.

- With four isolated leptons in the final state, most of the QCD background can be rejected by an isolation cut.
- For $M_H > 2M_Z$, both $\ell\ell$ pairs have an invariant mass of M_Z, so the Z mass constraint can also be used to reject background. If $M_H < 2M_Z$, only one such constraint applies.

High resolution of the EM calorimeter and the muon system is important for rejecting backgrounds and precise reconstruction of the Higgs mass peak.

The background processes considered are:

- $ZZ/ZZ^* \to \ell\ell\ell\ell$.
- $Q\bar{Q}Z \to \ell\ell\ell\ell + X$, where $Q = b$ or t.
- $t\bar{t} \to W^+bW^-\bar{b}$, in which the two W-bosons decay semileptonically and the b-jets fake an isolated lepton.

The $ZZ/ZZ^* \to \ell\ell\ell\ell$ background is irreducible. Since the cross section of $gg \to ZZ^*$ is not yet available in either PYTHIA or ISAJET, its contribution was accounted for by multiplying the contribution of $q\bar{q} \to ZZ^*$ by 1.65.

For $M_H < 2M_Z$, the following cuts were applied:

- $|\eta^\ell| < 2.5$ and $p_T^\ell > 10$ GeV. For electrons, the region $1.01 < |\eta^\ell| < 1.16$ was excluded.
- Lepton isolation with $R = 0.35$ and $E_T^{cut} = 5$ GeV
- Lepton identification and track matching.
- 10 GeV $\leq M_{\ell\ell}^{(l)} \leq$ 100 GeV and 70 GeV $\leq M_{\ell\ell}^{(h)} \leq$ 100 GeV to suppress the continuum background, where $M_{\ell\ell}^{(l)}$ and $M_{\ell\ell}^{(h)}$ are the low and high invariant masses of two $\ell\ell$ pairs.

Results for 10 fb^{-1}

Signal = .95 $\times \sigma_{\ell\ell\ell\ell}$(fb) $\times$ 10 fb^{-1}

Background = 4 $\Delta M_{\ell\ell\ell\ell}$(GeV) $\times$ R_{back}(fb GeV^{-1}) $\times$ 10 fb^{-1}

- The resolution is quite good in the four-electron channel, but one needs muons to increase the significance.
- The most difficult mass is 170 GeV, where the signal is 5.7σ
- In the four-muon channel, resolution is degraded by multiple scattering of the relatively low-energy muons in the second superlayer.

For $M_H = 140$ GeV, the $\mu\mu\mu\mu$ energy resolution is:

- 1.59 GeV
- 1.39 GeV from the muon system alone.

Signal and Background for $H \to ZZ^* \to \mu\mu\mu\mu$ and $H \to ZZ^* \to \ell\ell\ell\ell$

M_H (GeV)	140	150	160	170	180
$H \to eeee$					
ΔM_H (GeV)	1.05	1.06	1.13	1.23	1.33
σ_{accep}	1.2	1.7	.86	.62	1.6
Background (fb/GeV)	.025	.025	.025	.025	.040
$H \to \mu\mu\mu\mu$					
ΔM_H (GeV)	1.59	1.62	1.73	1.84	2.22
σ_{accep} (fb)	.81	1.1	.56	.36	.92
Background (fb/GeV)	.016	.016	.016	.016	.026
$H \to ee\mu\mu$					
ΔM_H	1.36	1.46	1.56	1.71	1.77
σ_{accep} (fb)	1.89	2.60	1.38	.89	2.43
Background (fb/GeV)	.038	.038	.038	.038	.062
$H \to \ell\ell\ell\ell$					
Significance	11	13	8.1	5.7	10.5

Significance if 4-muon acceptance increases by 40%

M_H (GeV)	140	150	160	170	180
$H \to \ell\ell\ell\ell$					
Significance	11.5	14.5	8.7	6.1	11.2

Significance if 4-muon mass resolution also decreases by 29%

M_H (GeV)	140	150	160	170	180
$H \to \ell\ell\ell\ell$					
Significance	12.3	15.4	9.4	6.7	12.0

For a heavy Higgs decaying into $\ell\ell\ell\ell$, the following cuts were applied:

- $|\eta^\ell| < 2.5$ and $p_T^\ell > 10$ GeV.
- Lepton isolation with $R = 0.3$ and $E_T^{cut} = 5$ GeV.
- Lepton identification and track matching.
- At least one Z with $p_T > \frac{1}{4}\sqrt{M_{ZZ}^2 - 4M_Z^2}$.
- $|M_{\ell\ell} - M_Z| < 10$ GeV for both lepton pairs.

$H \to ZZ \to \ell\ell\ell\ell$ Searches

$2M_Z < M_H < 800$ GeV

M_H (GeV)	200	400	600	800
Signal (fb)				
σ_H	85	56	16	5.3
Mass Bin (GeV)	±4.7	350–450	500–800	600–1200
σ_{accep}	21	14	4.3	1.5
Background (fb)				
ZZ	3.0	2.3	1.0	.6
Significance				
Significance	38	28	9.7	4.7

Models

There are 2 models which have been considered

① A left-right model:

$$SU(2)_L \otimes SU(2)_R \otimes U(1) \rightarrow SU(2)_L \otimes U(1)$$

② A model in which the grand unification group breaks down as:

$$SO(10) \rightarrow SU(5) \otimes U(1) \rightarrow SU(2)_L \otimes U(1)$$

Couplings are given by:

$$g_{uL} = \beta \qquad g_{uR} = \beta + \gamma$$
$$g_{dL} = \beta \qquad g_{dR} = \beta - \gamma$$
$$g_{\nu L} = -3\beta \qquad g_{\nu R} = -3\beta + \gamma$$
$$g_{eL} = -3\beta \qquad g_{eR} = -3\beta - \gamma$$

Model ① $\beta = 0.0528$ $\gamma = -0.3630$

Model ② $\beta = 0.0979$ $\gamma = -0.1958$

Widths are then given by:

$$\Gamma(Z' \rightarrow f_i \bar{f}_i) = \frac{2\alpha M_{Z'} C_i}{3 \sin^2 2\theta_w} \left(g_{iL}^2 + g_{iR}^2 \right)$$

$C_i = 3$ for quarks, 1 for leptons

$\Gamma_{①}(Z' \rightarrow e^+e^-) = \underline{105\ GeV}$ $\Gamma_{②}(Z' \rightarrow e^+e^-) = \underline{68\ GeV}$

501

Methodology

The user program fsisgl_zee.f was modified to do the Z' analysis.

Signal and min-bias events were generated with PYTHIA 5.6. Beam crossings were simulated by using GFA and including a Poisson distributed number of min-bias events with mean 16.

The assumed luminosity was 10^{34} and calorimeter noise was assumed gaussian (3 times 10^{33} noise).

The analysis for each event has 3 parts:

① Analyze charged track list and find vertex.

② Analyze EM bumps and find electron candidates.

③ Reconstruct $M_{e^+e^-}$

The following analysis will focus on the SO(10) model.

502

Charged Tracks

For each event all charged tracks were examined. A measured track list was constructed by requiring for each track:

① The track be an original particle track and not a secondary.

② The track be isolated in the tracker
dETA = 0.0677 (1.5 pads)
dPHI = 0.0116 (2.0 pads)

③ The track be reconstructed by the central tracker.

From the measured track list a vertex list is then constructed. Vertices are found by finding the maxima of:

$$f(z) = \sum_i \exp\left(-\tfrac{1}{2}\left((z - z_i)/\sigma_i\right)^2\right)$$

Tracks are then grouped by vertices and a P_T weighting is used to find the signal vertex.

503

EVENT 462 34/500 ≥ 5n

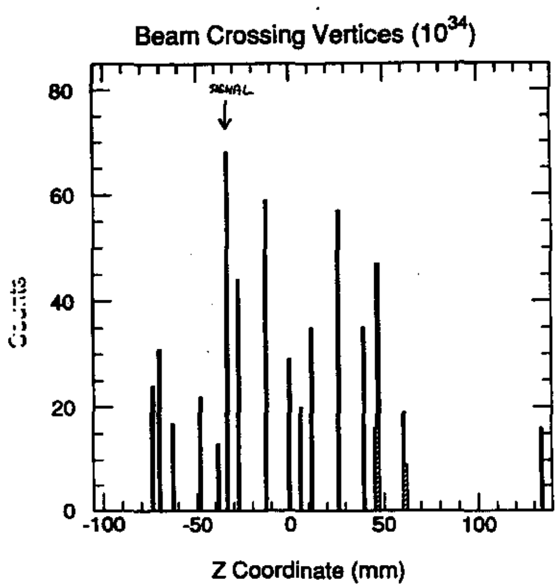

504

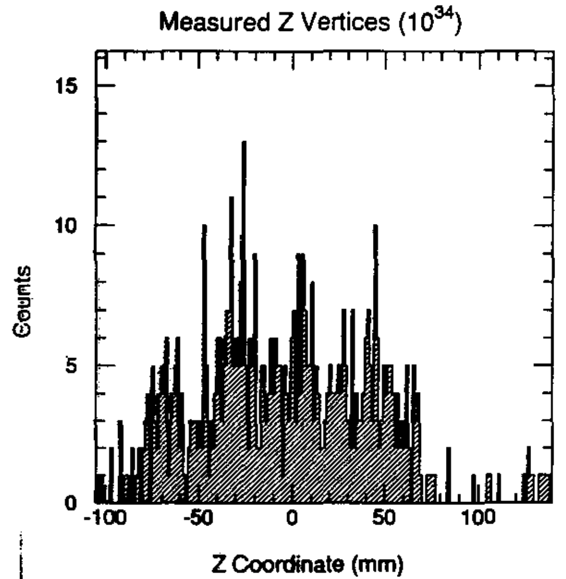
Measured Z Vertices (10^{34})
Counts
Z Coordinate (mm)

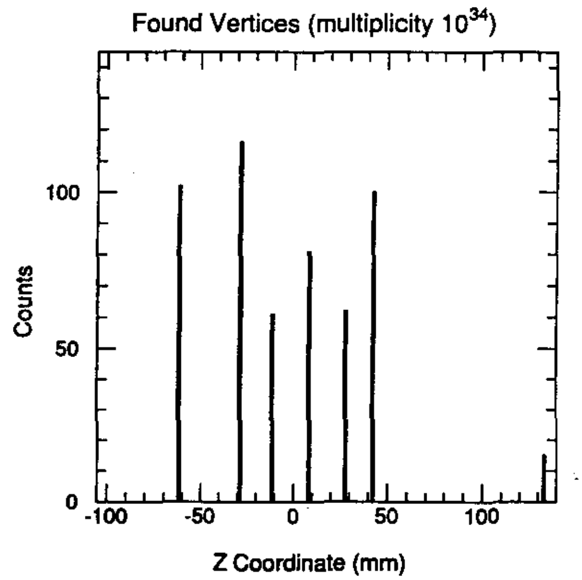
Found Vertices (multiplicity 10^{34})
Counts
Z Coordinate (mm)

EVENT 300

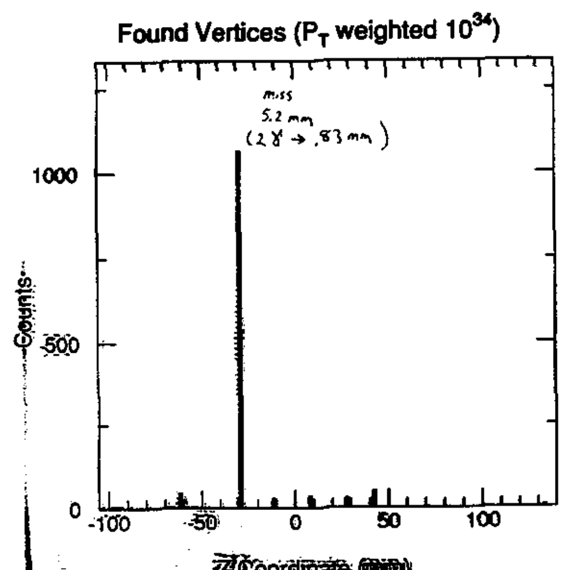
Found Vertices (P_T weighted 10^{34})
miss
5.2 mm
(2.8 → .83 mm)
Counts
Z Coordinate (mm)

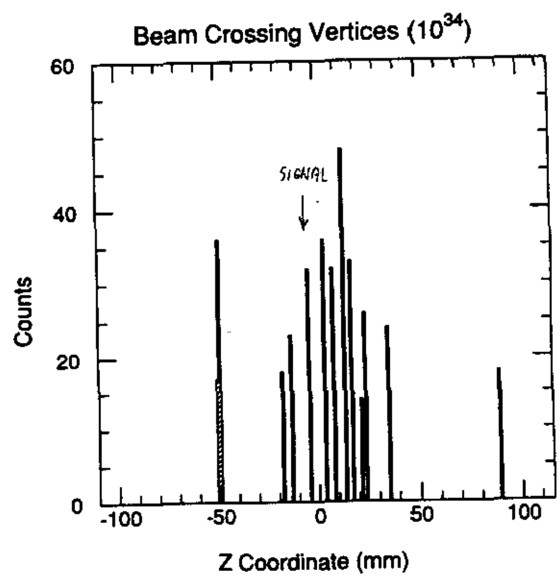
Beam Crossing Vertices (10^{34})
SIGNAL
Counts
Z Coordinate (mm)

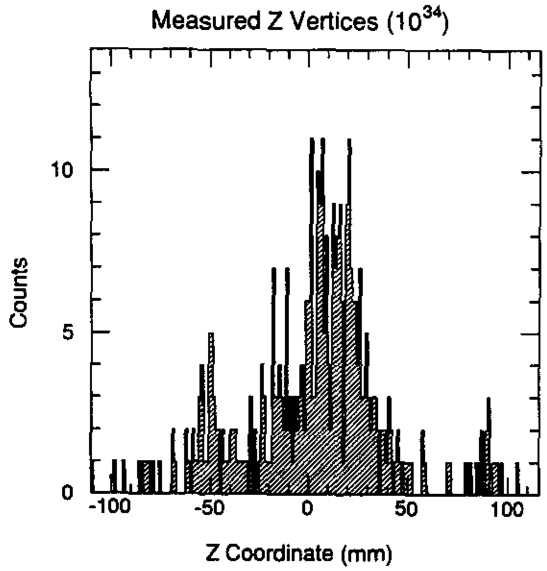

509

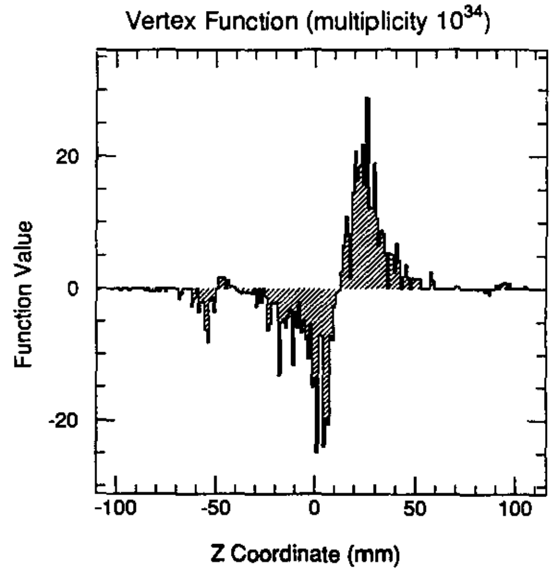

510

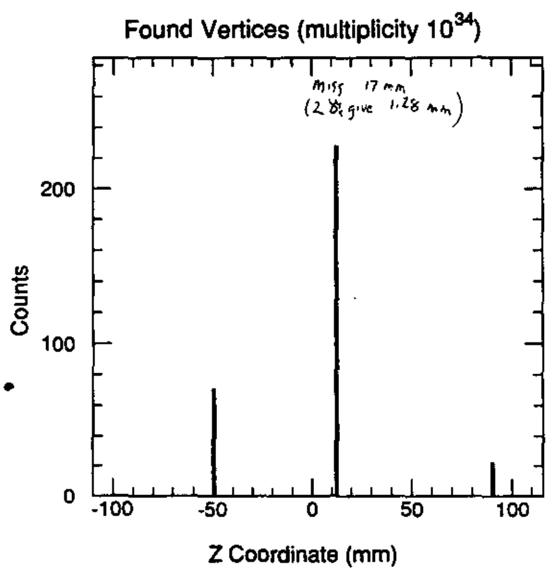

511

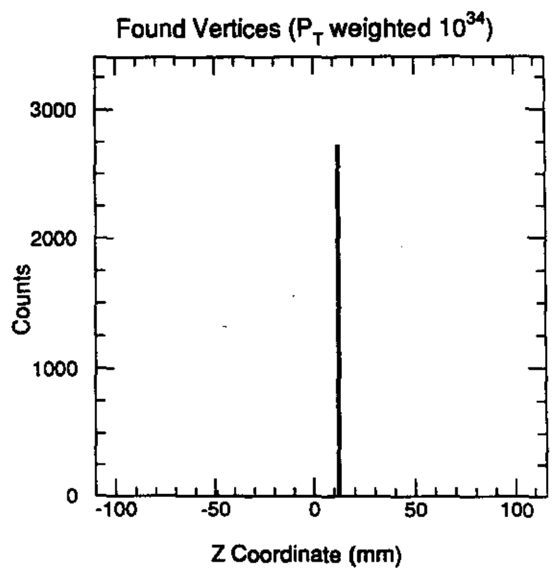

512

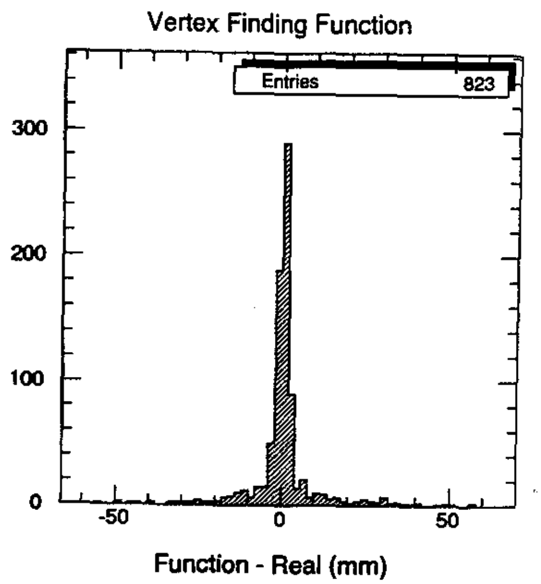

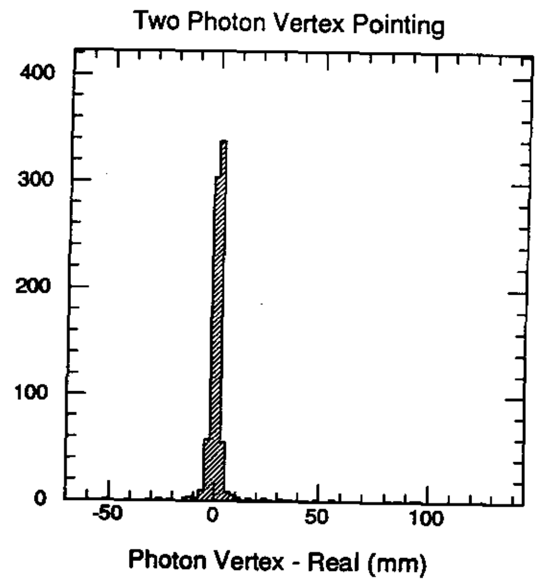

513

514

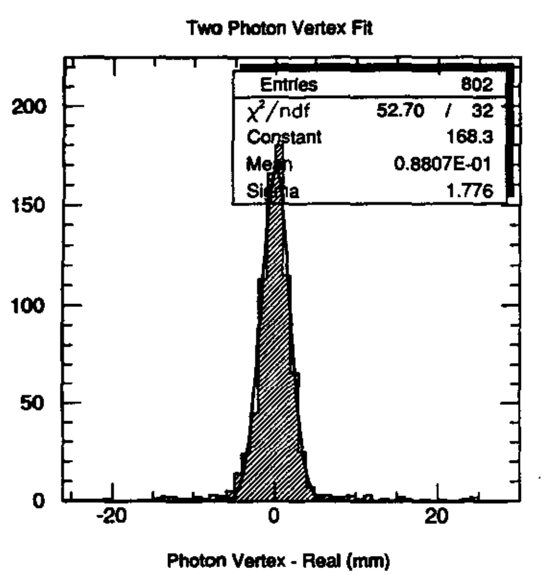

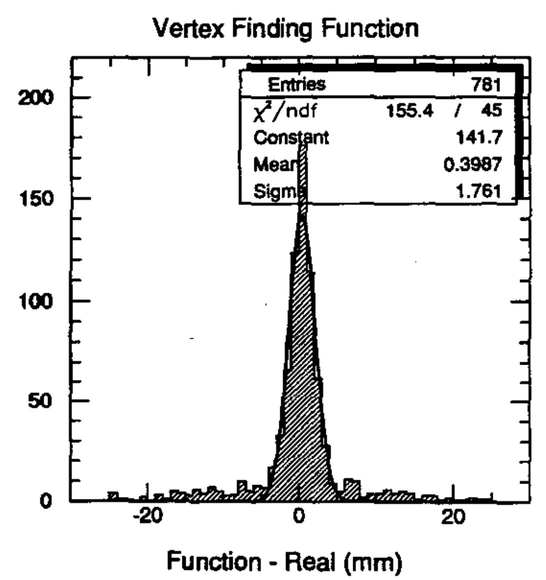

515

516

EC Bumps

The list of EC bumps is scanned. Each bump must meet the following requirements:

1. $|\eta| < 2.46$
2. $E_T > 250$ GeV
3. $|\eta| < 1.01$ OR $|\eta| > 1.16$ (transition region)
4. $E_{HAD}(3\times3) < 10\%\ E_{EM}(5\times5)$
5. A charged track must point to the hit EC cell (dETA = 0.125, dPHI = 0.02). This is equivalent to a cone of 0.05
6. Total calorimeter energy in a cone of 0.5 must not be greater than $1.1 \times E_T$ (isolation)

Every bump passing these criteria is classified as an electron.

517

Reconstruction

The Z' mass is reconstructed from the largest E_T electron candidates. As was shown the vertex can also be found using these electrons. The invariant mass is given by:

$$M_{Z'} = \sqrt{2E_1E_2(1-\cos(\theta_{12}))}$$

AND

$$\frac{\Delta M_{Z'}}{M_{Z'}} = \frac{1}{2}\sqrt{\left(\frac{\Delta E_1}{E_1}\right)^2 + \left(\frac{\Delta E_2}{E_2}\right)^2 + \left(\cot\left(\frac{\theta_{12}}{2}\right)\Delta\theta_{12}\right)^2}$$

Since we have $\frac{\Delta E}{E} \sim 0.4\%$ and $\Delta\theta_{12} \sim 0.003$ we have

$$\frac{\Delta M_{e^+e^-}}{M_{e^+e^-}} \approx 0.003 \text{ or } \Delta M \sim 12.5\ \text{GeV/c}$$

518

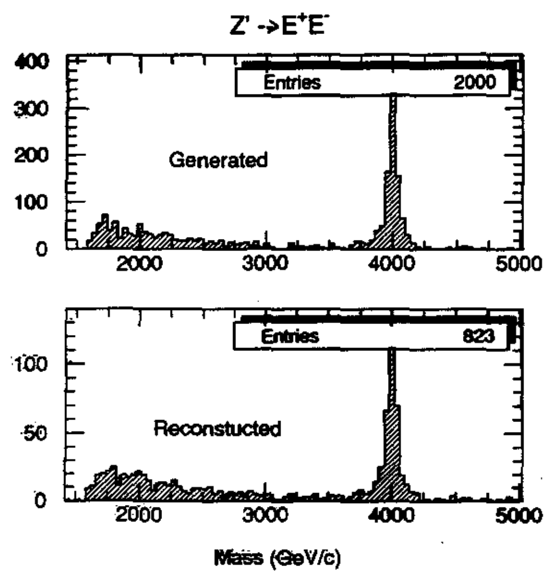

519

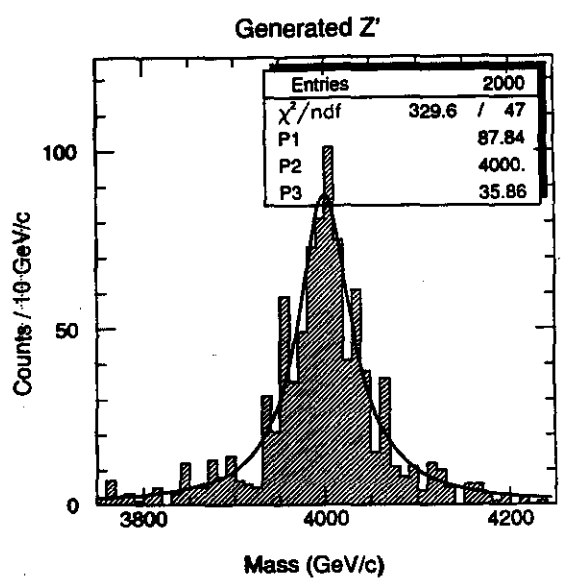

520

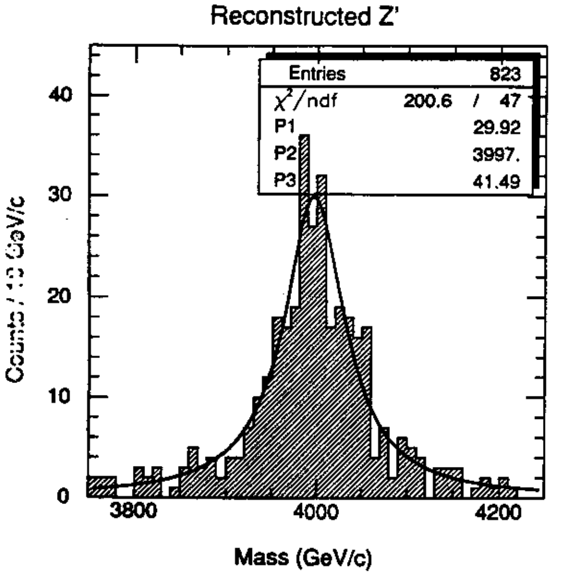

CUTS

Physics backgrounds arise from either mis-identifying jets as electrons or from isolated, high mass e^+e^- pairs from $t\bar{t}$.

The cross section for QCD jets with $|\eta| < 2.46$ and $3750 < M_{jj} < 4250$ is about 700 pb. W + jet $\rightarrow e$ + jet is about 25 pb. The $t\bar{t} \rightarrow e^+e^- + X$ with $M_{t\bar{t}} > 1.4$ TeV and $P_T(t,\bar{t}) > 100$ GeV is 1.4 pb.

Since the cross section for the Z' is about 5 fb we need to suppress this background

The EC bump requirements discussed above do a good job of suppressing the background, especially the calorimeter isolation and charged track requirement.

$R(e/\text{jet}) \sim 4 \times 10^{-4}$ (isolation + 50 GeV track)

~~$t\bar{t}$ background is eliminated if $M_{t\bar{t}} > 3500$ required~~

Signal

2000 events of the SO(10) model were analyzed including the $\gamma^*/Z0/Z'$ interference from 1600 – 5000 GeV/c^2.

(16.7%)	1667	Geometrical
(7.1%)	1548	$E_T > 250$ GeV
(15.5%)	1308	Not out of $1.01 < |\eta| < 1.16$
(27.6%)	947	Isolated in calorimeter
(13.1%)	823	1 and only 1 charged track $P_T > 50$

Focusing on the mass region $3750 < M < 4250$

	738	Geometrical
(8.1%)	678	$E_T > 250$ GeV
(16.1%)	569	Not in $1.01 < |\eta| < 1.16$
(30.0%)	398	Isolated in calorimeter
(12.5%)	349	1 and only 1 charged track $P_T > 50$

Total cross section was 12.97 fb

2000 events represent 1.54 years at 10^{34}

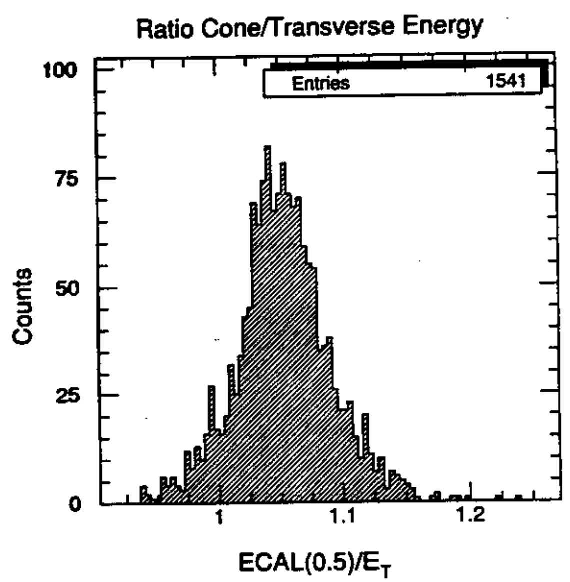

$H^0 \to l^+ l^- \nu \bar{\nu}$ at 800 GeV and its systematic error.

Xiaorong Shi

Caltech

at

GEM Collabration Meeting

UCSD

May 11. 1993

Decay Process

$H^\circ \rightarrow ZZ$
- $Z \rightarrow \nu\bar{\nu}$
- $Z \rightarrow e^+e^-$ or $\mu^+\mu^-$

Signature:

(1) A pair of high P_T lepton with $M_{\ell\ell} \sim M_Z$

$|M_{\ell\ell} - M_Z| < 10$ GeV

(2) Large $\not{E}_T$

529

Back Ground to the Signal

* Z + jet from

$f + \bar{f} \rightarrow Z + g$

$f + g \rightarrow Z + f$

$\quad \hookrightarrow \ell^+\ell^- \qquad \sigma = 1000 \times \sigma_{signal}$

* $t\bar{t}$ production with $t \rightarrow e X$

$Br(t \rightarrow e) \doteq 10\%$

$\sigma = 2 \cdot 10^4 \cdot \sigma_{signal}$

This study confirms previous studies that background from $t\bar{t}$ is negligible.

* $f\bar{f}$ or $gg \rightarrow ZZ$ Irreducible
  - $Z \rightarrow \nu\bar{\nu}$
  - $Z \rightarrow \ell^+\ell^-$

530

$E_T^Z > 250$ GeV

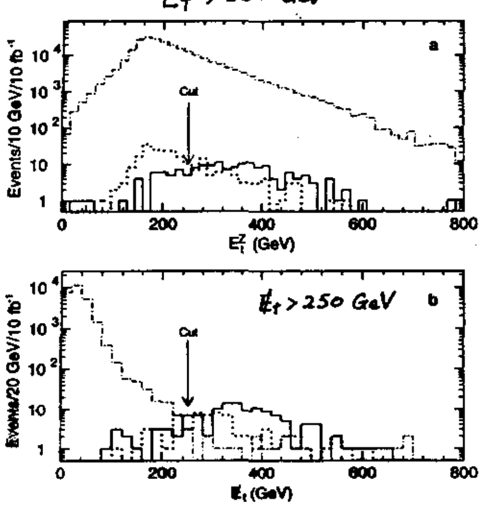

531

Result of $H^\circ \rightarrow \ell\ell\nu\nu$ in TDR

The shape of the signal & background the same ?

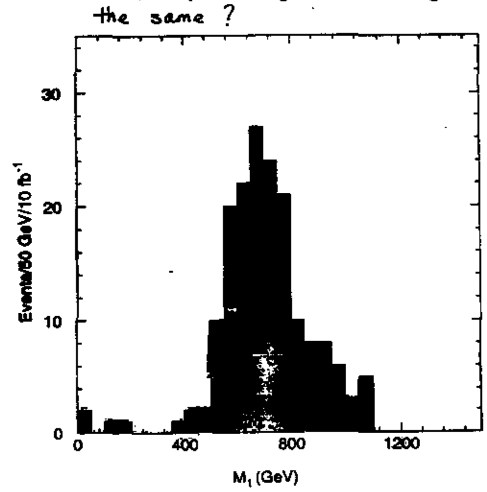

$N_{sig} = 105$

$N_{bgd} = 91$

} in $400 < M_t < 1200$ GeV

Significance $= \frac{105}{\sqrt{91}} = 11$

532

Distribution of M_t w/o cut P_t^Z, $\not{E}_T$

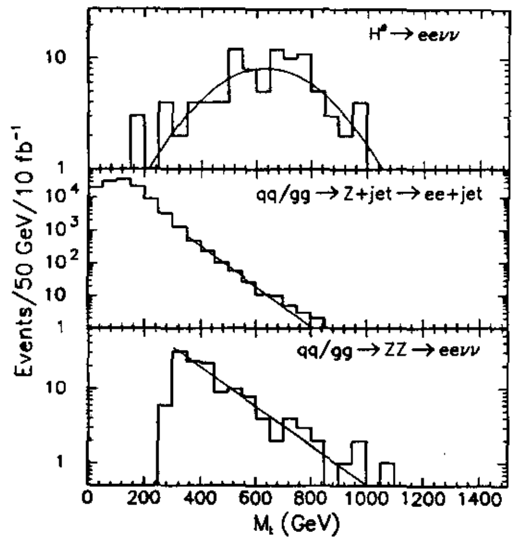

Distribution of $\not{E}_T$ vs. P_T^Z

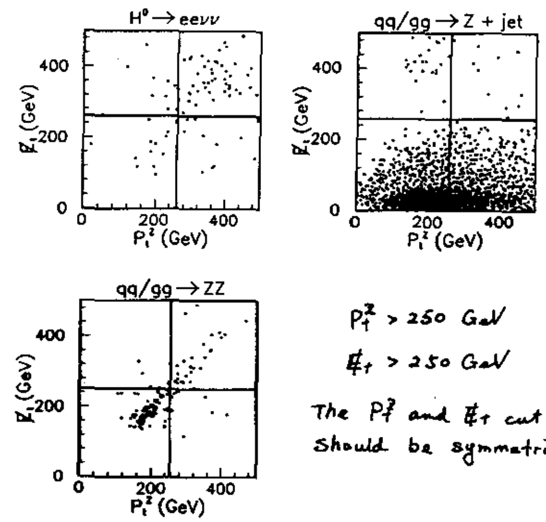

$P_T^Z > 250$ GeV

$\not{E}_T > 250$ GeV

The P_T^Z and $\not{E}_T$ cut should be symmetric.

Change of Cuts & Significance

$H^0 \to ee\nu\nu$

Cut : P_T^Z , $\not{E}_T$

Cut (GeV)	N_{sig}	N_{Z+jet}	N_{ZZ}	$\frac{N_{sig}}{\sqrt{N_{Zjet}+N_{ZZ}}}$
175	78	90	66	6.2
200	74	53	54	7.2
225	69	29	40	8.3
250	63	17	31	9.1
275	55	13	24	9.0
300	48	11	17	9.0

With Cut = 250 GeV

% in tail				
1%	63	19	31	8.9
10%	63	40	32	7.4
25%	65	73	33	6.3
50%	66	124	36	5.2
75%	68	171	37	4.7
100%	72	225	39	4.4

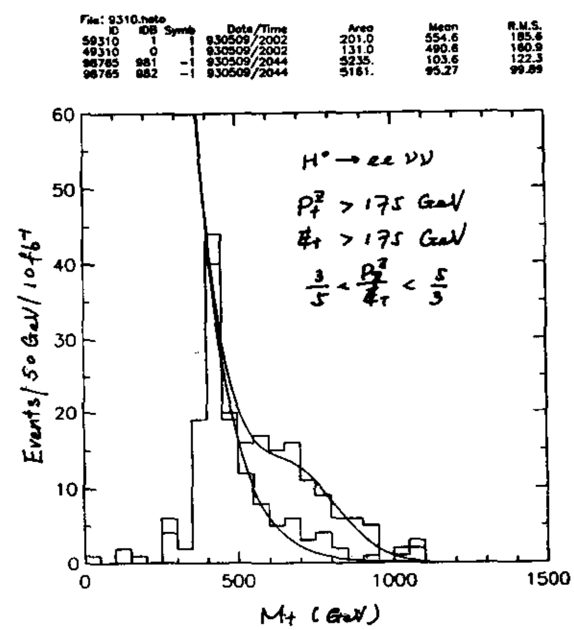

Can not lower cut because $\hat{t} > 150$ GeV in generator.

MINUIT χ^2 Fit to Plot 5931080

File: 9310.hsto

Plot Area Total/Fit 170.00 / 170.00 — Fit Status 2

Func Area Total/Fit 162.17 / 162.17 — E.D.M. 1.236E−05

χ^2 = 10.1 for 16 − 6 d.o.f., — C.L.= 43.1%

Errors		Parabolic	Minos	
Function 1: Exponential				
NORM	1470.8	±2592.	−0.0000E+00	+0.0000E+00
SLOPE	1.00000E−02	±5.6221E−06	−0.0000E+00	+0.0000E+00
OFFSET	54.339	±176.3	−0.0000E+00	+0.0000E+00
Function 2: Gaussian Distribution (sigma)				
AREA	70.357	±16.18	−0.0000E+00	+0.0000E+00
MEAN	693.29	±34.24	−0.0000E+00	+0.0000E+00
SIGMA	131.48	±27.00	−0.0000E+00	+0.0000E+00

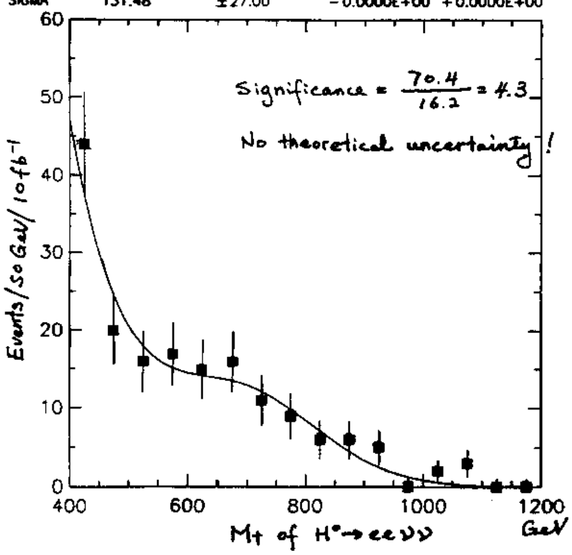

537

Conclusion

Include $H^0 \to \mu\mu\nu\nu$ channel
the significance of $H^0 \to \ell\ell\nu\nu$
is greater than 5 with $10 fb^{-1}$.

The key is $\not{E}_T$ under control.

536

Difficulties of

Hugo S[illegible]n / CIT
La Jolla CA
May 11, 1993

Higgs Physics

@ gem

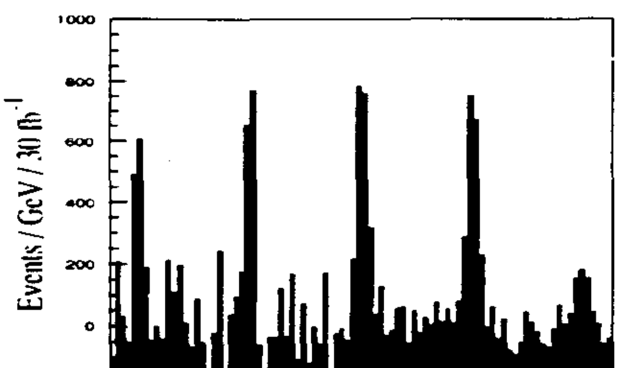

List of Topics

- not so beautiful, experimentally or theoretically -

1. 800 GeV Higgs search by $\ell\ell$ jet jet mode
   on behalf of S. Shevchenko / CIT @ CERN
   - Not the discovery channel, but not a junk.
2. Parton Distribution Function
   - Welcome back EHLQ.
3. Significance - game of statistics and systematics
   - "Not again !!!"
   - "Please, honestly this is the last."
4. Minimal Supersymmetric Standard Model
   - I know some people don't like it. I hate it, too complicated.
5. Study under way
   - Never ending story.

---

include 'Disclaimer.inc'

I am biased, I want to sell GEM, I want to sell t t / W + H mode, I want to be optimistically realistic. All the opinions are my own, not GEM's.

Color copies available, $10/copy + $5 shipping and handling + sales tax if applicable. Cash only, not tax deductible. No educational discount available.

545

800 GeV Higgs search by $\ell\ell$ jet jet mode

by S. Shevchenko / Caltech

1. Selection

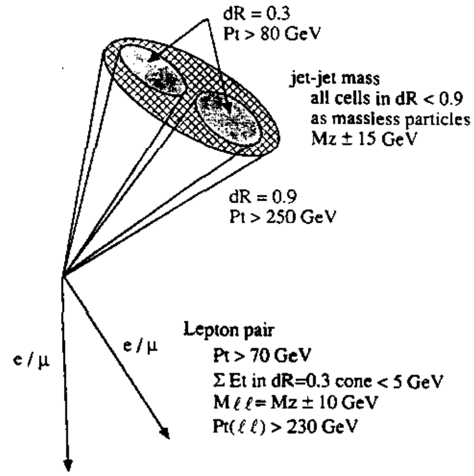

Cross sections which pass these cuts (fb)

Higgs	tt	Z + jets	ZW/ZZ
11	0.3	42	0.8

546

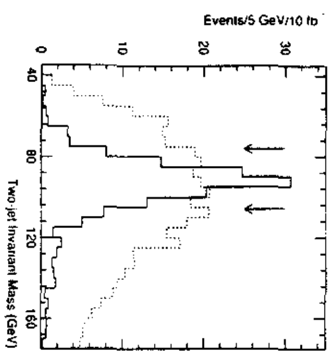

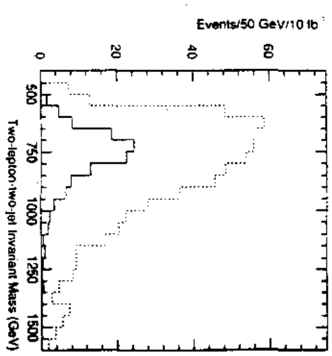

547

2. Significance of the signal

a) Significance estimation without direct MC input
   - Use MC to understand the background qualitatively, but not quantitatively.
     Reasonable background / event selection do not make fake structures, or things are smooth.
   - Use the event sample itself to estimate the background. Less sensitive to the understanding of the various efficiencies / effects.
   - Use Minuit to fit the distribution with reasonable signal and background shape to get the significance.

b) Fit the jet-jet mass by smooth background and gaussian gives 2-3 sigma indication of existence of Z

c) $\ell\ell$ jj mass study - use sideband for the BG estimation

1. dN/dM(Mjj=100-120, BG) ~ dN/dM(Mjj=80-100, BG)
2. Signal is BW
3. dN/dM(Mjj=80-100,observed) is fit by a1 * background + a2 * signal BW(width fixed)
   3 backgrounds
   case-1 dN/dM(Mjj=100-120)
   case-2 dN/dM(100-120)+dN/dM(60-80)
   case-3 dN/dM(60-80)
   3 signal width
   140, 160 and 180 GeV
5. Significance is insensitive to the signal width in this range
6. Worst significance - 2.3

548

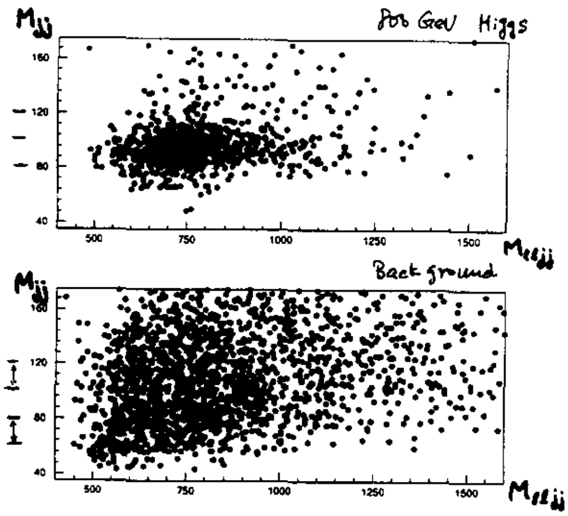

549

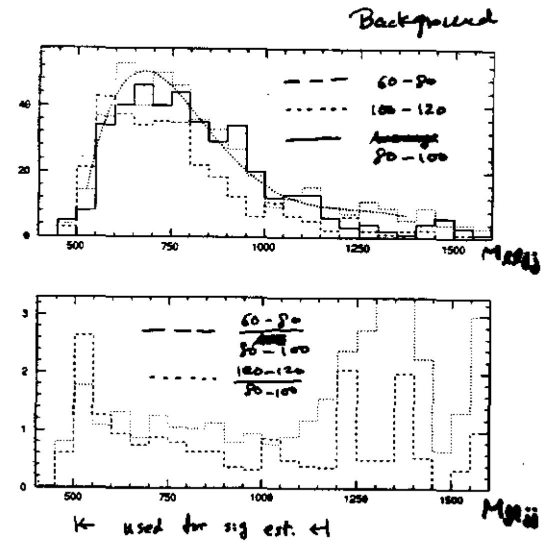

550

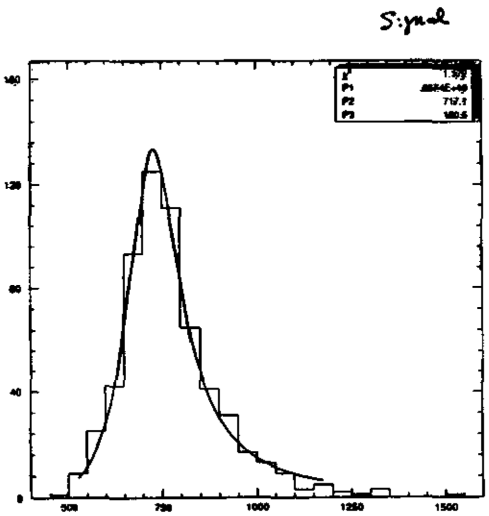

551

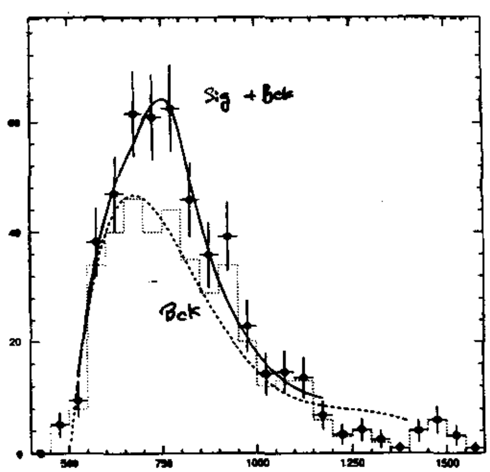

552

3. Forward Jet tagging

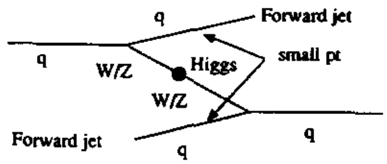

a) Simulation done in the particle level, not GEMFAST

b) Forward calorimeter
   i) η : 3 - 5
   ii) segmentation in η , ϕ : 0.2 or 0.3 (no diff)
   iii) energy resolution : 100% / $\sqrt{E} \oplus 5$ %

c) forward jet tagging
   i) rapidity region of forward jet : 2.5-4.5
   ii) jet energy > 2000 GeV
   iii) Pt of forward jet > 50 GeV
   iv) jet cone size : 0.6

d) Events after cut

i) Signal	24	eff = 2.1%
ii) background	32	eff = 1.3E-4
iii) significance	4.2	
	3.6 if 10 % uncertainty	

Structure Functions

1. EHLQ - good old boy @ 1984
   (H/K)MRS - European favorite @ 1988 - 1992
   CTEQ - New American hero @ 1992 -

2. New vs Old

   • Signal

	H + X	t t / W + H + X
(H/K)MRS/EHLQ	0.85	0.90
CTEQ / EHLQ	1 ± 0.1	1.1

   • $\gamma\gamma$ background $d\sigma / dm(\gamma\gamma)$ = A(pb) x exp(-B m)

	A	B
EHLQ	0.91 ± 0.03	0.030 ± 0.002
CTEQ	1.04 ± 0.04	0.030 ± 0.002
HMRSB	0.81 ± 0.03	0.029 ± 0.002
MRS S0	0.94 ± 0.03	0.030 ± 0.002

3. Significance Uncertainty (S / $\sqrt{B}$) for Higgs process
   ~ 10-15 %

4. We decided to stick to good old friend EHQL, with uncertainty of 20 %.

Comming soon 93-394

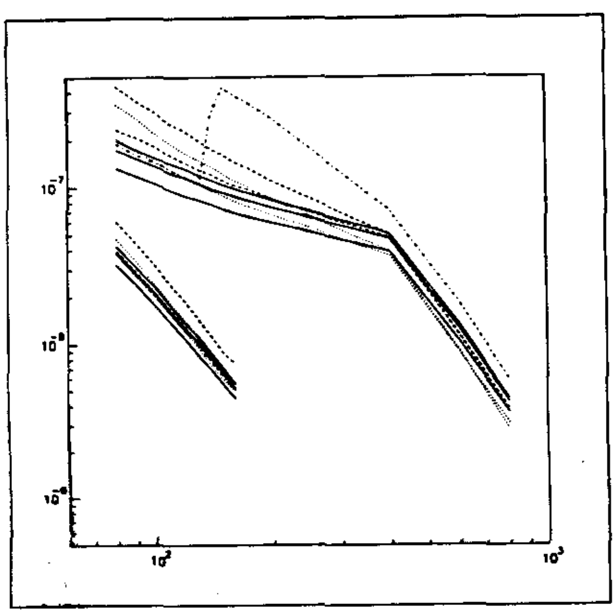

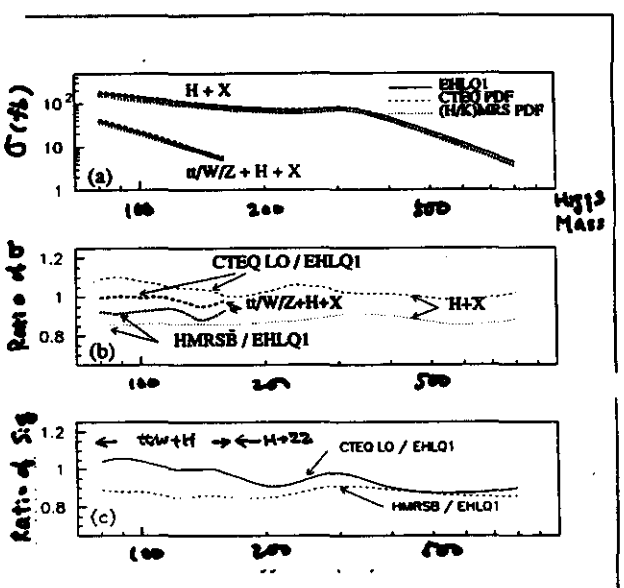

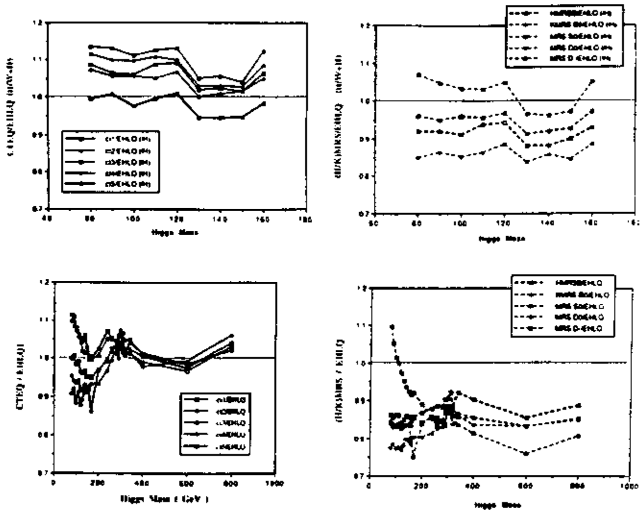

557

Significance of Higgs Signal

We use significance to represent how well the Higgs signal can be identified with background present. According to the Gaussian statistics, a probability of 1.35×10^{-3} is mapped to 3σ, and 2.85×10^{-7} is mapped to 5σ, etc.

In case of high background statistics, the significance (S) of a Higgs peaks can be estimated by dividing the number of signal events counted in a mass interval of $M_H \pm 2\Delta_{M_H}$ by the square root of the corresponding background events, where Δ_{M_H} is the reconstructed Higgs mass resolution. We thus have

$$S = \frac{N_S}{\sqrt{N_B}} = \frac{\int \mathcal{L}dt\ A_S\ 0.955\sigma_H}{\sqrt{\int \mathcal{L}dt\ A_B\ 4\Delta_{M_H}\ R_B}}, \tag{3}$$

where A_S and A_B are the acceptance of the signal and the background respectively, and R_B is the background rate at the Higgs mass. It is clear from Equation 3 that a better mass resolution or a better acceptance is equivalent to a shorter discovery time. Note, this significance is not sensitive to the choice of mass interval, in which the integration is performed. The significance obtained by summing the signal within $\pm 2\Delta_{M_H}$ is very close to summing only $\pm\Delta_{M_H}$, if the mass is Gaussian distributed.

For low statistics, Equation 3 is not adequate to define the significance. Since the probability of observing n events ($P_n(\lambda)$) with an expectation value of λ follows Poisson statistics, $P_n(\lambda) = \frac{\lambda^n e^{-\lambda}}{n!}$, the probability that the signal fluctuates down to even zero is not negligible for a small λ. Taking into account fluctuations of both signal and background, the probability of missing signal or signal caused by background fluctuation can be defined by a convolution of two Poisson distributions [21]. Assuming expected signal and background events are N_S and N_B, this probability (P) is given by

GEM 126

$$P = \sum_{n=0}^{\infty}[P_n(N_B + N_S) \times \sum_{m=n}^{\infty} P_m(N_B)]. \tag{4}$$

The first term in Equation 4 is the the normalized probability of observing n events when the expected number is N_s+N_b, and the second term is the probability that the background, with the expected number of N_b, fluctuates to the observed number and above. For the high statistics case, as demonstrated in reference [21], this probability is mathematically converted to the probability expressed by the significance corresponding to Equation 3 for a Gaussian distribution.

This definition, however, is too conservative to be used to estimate the significance, since 5σ is required to establish a signal but not the same safety margin is needed to avoid missing the signal. In this section, Equation 5 is used to estimate significance for low statistics (< 20 events), which defines the probability (P) the signal is caused by background fluctuation for fixed N_s and N_b:

GEM TOR

$$P = \sum_{m=N_s+N_b}^{\infty} P_m(N_B). \tag{5}$$

Equation 5, however, does not handle non integer N_s+N_b. When using this equation care should be taken to make a linear interpretation of two probabilities obtained by summing the Poisson series starting from two integers closest to N_s+N_b. Equation 4 does not have this problem. The difference between different definition of significance is clearly seen in the following example. Assuming $N_s = 5$ and $N_b = 1$, Equation 3 gives a significance of 5σ, while Equation 4 and 5 give 1.5σ and 3.2σ respectively.

558

2.3.4 $H \to \gamma\gamma$ Searches for 80 GeV < M_H < 160 GeV

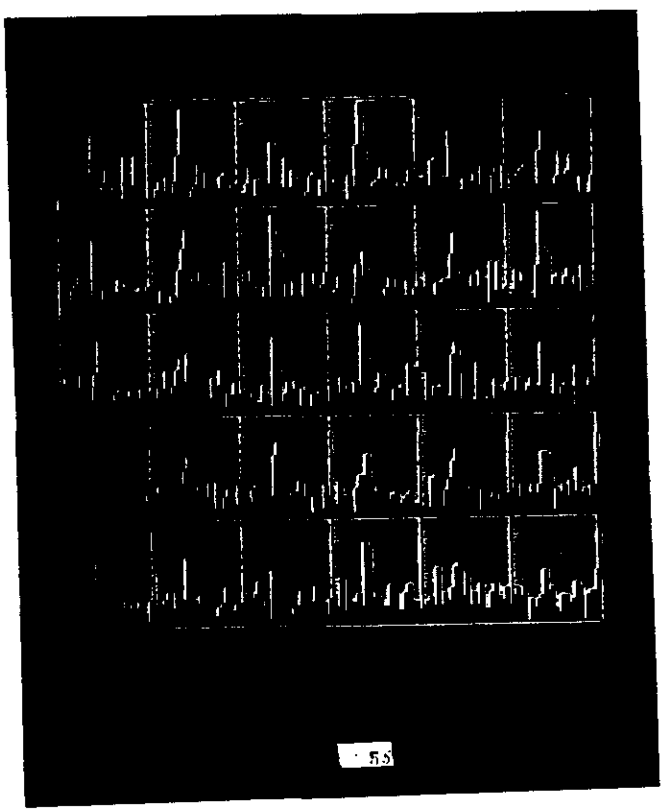

55

1000 exp. fit by bck + Gaussian
data GEM 93 ~ 1.5 year

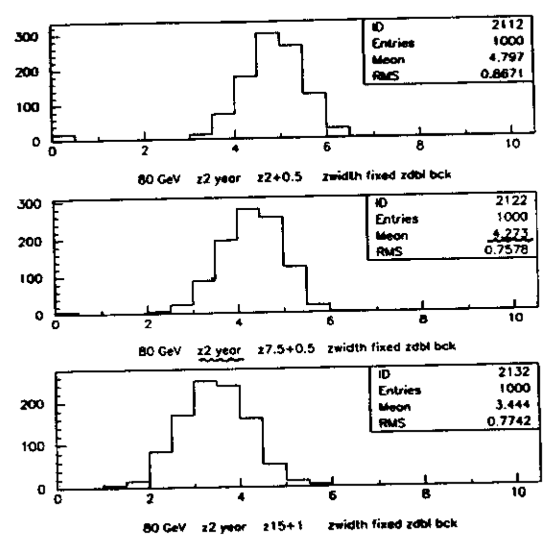

559

Educated guess of Significance - Not so scientific number -

		$\gamma\gamma$	$\gamma\gamma\ell$	Combined
80 GeV	TDR	3.9	4.5	6.3
	Hiro	3.5	3.5*	5.3

⇒ Different statistics (single vs double Poisso)
Include possible bck fluctuation masking

*) Can be worse if some new backgrounds join the game. We cannot make the cut tighter. Saga of low statistics (e.g., mass constraints cannot improve significance by reducing Z+γ background).

		$\ell\ell\ell\ell$	$\ell\ell jj$	$\ell\ell\nu\nu$	Combined
800 GeV	$S/\sqrt{B}$	4.7	5.4	11	
	TDR	4.2	1	4.2	
	Hiro	4	2	7*	9

⇒ Different systemtics (universal 0.25B vs process by process study)

*) Can be worse if missing Et is out of control.

Higgs Signal

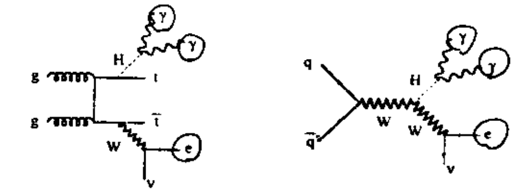

Background

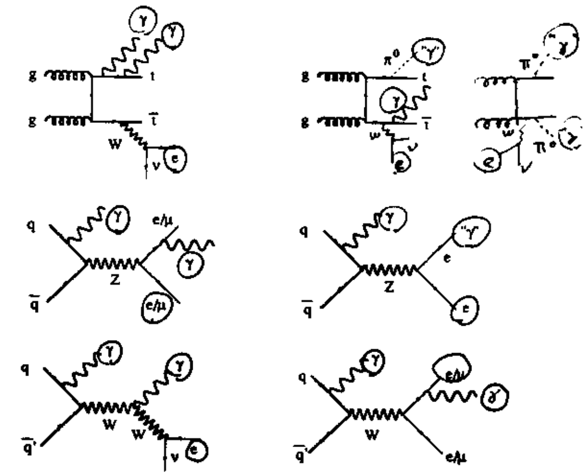

Minimal Supersymmetric Standard Model

Ref. Z. Kunszt & F. Zwirner '90

$\sigma(h^0, H^0, A^0)_{SSC} = 3 * \sigma(h^0, H^0, A^0)_{LHC}$

Detailed calculation needs analytic form of BR($H\to\gamma\gamma$)
PYTHIA($pp\to h^0, H^0, A^0$) does not simulate bbH ???

Limited case study from the figures in Ref
(M_t = 150 GeV, M_{sq} = 1 TeV, $M_{h,H,A}$ = 80-160 GeV)

h^0 : small tanβ, negligible
large tanβ , 88 GeV - M_Z, 100 fb ~ 2σ

H^0 : tanβ > 3, M_{A0} < 70 GeV, 200-300 fb > 2.5σ

tanβ	3	10	30	30
MH0 GeV	100	93	91.35	91.5
σ(prod) fb	230	210	300	180
σ(obs) fb	56	36	52	32
Signif	4.5	3.1	4.2	2.5

A^0 : small tanβ , hopeless, large tanβ , strong signal
tanβ = 30

MA0	80	90	100	120	140	160
σ(prod) fb	230	1300	2600	1800	1100	750
σ(obs) fb	52	230	640	460	280	200
Signif	3	18	51	48	39	34

Study under way

1.Higgs polarization using 4 lepton decay mode

2.CP violation

$Z' \longrightarrow e^+e^-$

A Study of GEM's Ability to Measure the Z'

11 May 1993

Shawn McKee
Liz Simmons

Results for 10 fb^{-1}

All $M_H < 800$ GeV are straightforward to discover.

For 800 GeV Higgs boson, one would seek confirmation in other channels.

However, one can should study the significance of a 800 GeV Higgs faced with the uncertainty in the ZZ background normalization.

568

Estimation of Systematic Uncertainty

- Scale background shape $\times$ 1, $\times$ 1.5, $\times$ 2.
- Fit $\ell\ell\ell\ell$ spectrum from 240–600 GeV
- Use fit to estimate background from 600-1200 GeV
- Reevaluate significance and determine dependence on slope.

569

Significance Study for $M_H = 800$ GeV

Scaling	Significance	Slope Uncertainty
1×	4.8	4.6
1.5×	4.2	4.1
2×	3.8	3.7

With 10 fb^{-1}, the situation is under control.

570

W^+W^+ Scattering with GEM

- We do not know the physics of Symmetry Breaking (SB).
- W_L, the manifestation of SB, should couple strongly to any new physics.
- Something must happen to unitarize $\mathcal{M}(W_LW_L \rightarrow W_LW_L)$.
- For $E_W \gg M_W$, $\mathcal{M}(W_LW_L \rightarrow W_LW_L) \rightarrow \mathcal{M}(ww \rightarrow ww)$, where w is the would-be Goldstone boson.

The simplification is calculational AND conceptual.

571

For $M_W = M_Z$, the symmetry group of the w self-interactions is $SU(2)_L \times SU(2)_R \to SU(2)_V$.

- If $w \approx \pi$, then $\mathcal{M}$ is unitarized by a Spin-1, Isospin-1 resonance – like the techni-rho.
- If w behaves like a linear Σ model, unitarization occurs through a Spin-0, Isospin-0 field – like the Higgs.

- Signal is $pp \to W_L W_L X$
- Main Background is $pp \to W_T W_T X$ and $pp \to W_T W_L X$.

Insensitive to new physics and can be calculated in the SM with $M_H = 100$ GeV.

- Heavy quark backgrounds $t\bar{t}, t\bar{t}W, t\bar{t}Z$.
- $\alpha^2\alpha_s^2$ background $q\bar{q} \to q\bar{q}WW$

Focus on $W^+W^+ \to \ell^+\nu\ell^+\nu$ signal.

- Distinctive final state (not studied in TDR).
- Absence of α^2 continuum background.
- Branching ratio is 4.7 %.

$W_L W_L$ vs Backgrounds

- Spectator quarks always associated with signal
  - $E(jet) \sim 1$ TeV, $P_t(jet) \sim M_W/2$
  - Tagging spectator quark suppresses some backgrounds.
- P_t spectrum of initial W is sharper for signal.
  - $W_L W_L \sim \frac{1}{P_t^4}$.
  - $W_T W_T \sim \frac{1}{P_t^2}$.

  There are two consequences of this.
  - Spectator quark from signal has small P_t, large y. *Veto central jets.*
  - Final $W_L W_L$ system has limited net P_t, and $W_L \to \ell^+\nu$ produces a harder ℓ^+ spectrum than $W_T \to \ell^+\nu$. *Demand back-to-back leptons.*

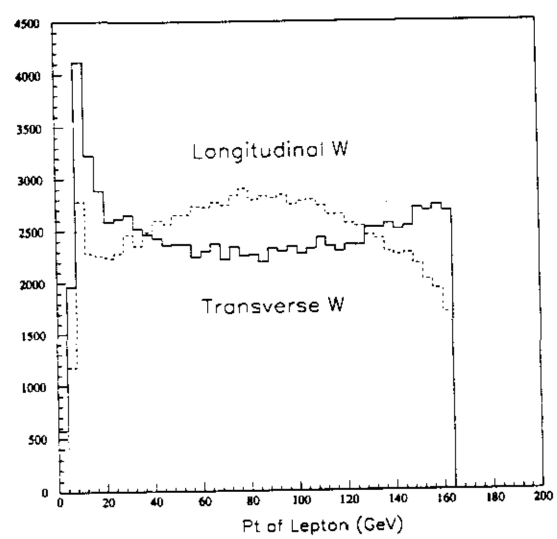

Bagger, Barger, Cheung, Gunion, Han, Ladinsky, Rosenfeld, Yuan

Parton Level Cuts

Leptonic Cuts	Central Jet Veto Cuts
$\|y(\ell)\| < 2.0$	$P_t(jet) > 60$ GeV
$P_t(\ell) > 100$ GeV	$\|y(jet)\| < 3.0$
$\Delta \vec{P}_t(\ell) > 200$ GeV	
$\cos\phi_{\ell\ell} < -.8$	
$M(\ell\ell) > 250$ GeV	

Parton Level Results (fb)

$\sqrt{s} = 40$ TeV and $m_t = 140$ GeV

W^+W^+	Leptonic Cuts	Veto Cuts
EW($M_H = 1$ TeV)	2.4	0.98
EW($M_H = .1$ TeV)	1.4	0.29
QCD	0.24	0.01
$t\bar{t}W$	0.75	0.05

576

Work in Progress

- Study must be performed at a GEMFAST level. This means hadron level.
- J.Thomas and E.Wang showed that the electron channel is difficult for GEM because of increased backgrounds from charge mis-measurement. We must emphasize the high energy muon capabilities of GEM.
- Parton level study assumes $t\bar{t} + jets$ backgrounds can all be eliminated by an isolation cut.
- Parton level study only implemented jet veto, not tagging. If isolation does not work, this might improve the situation.

577

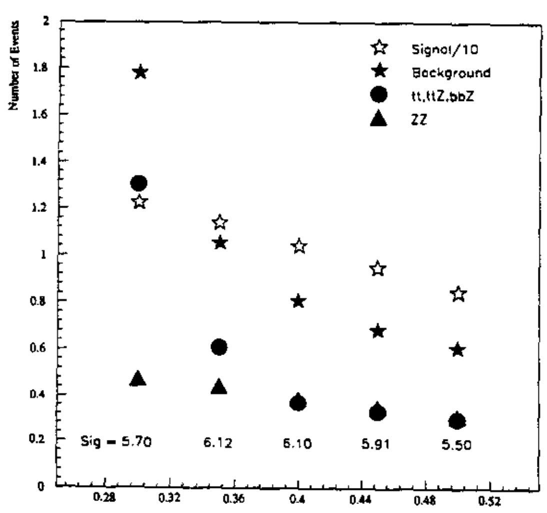

578

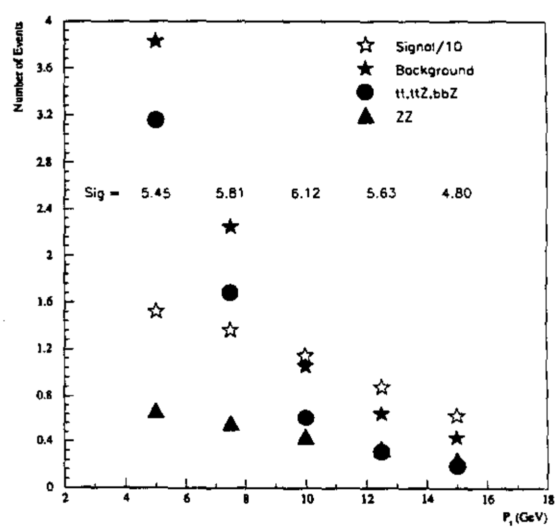

579

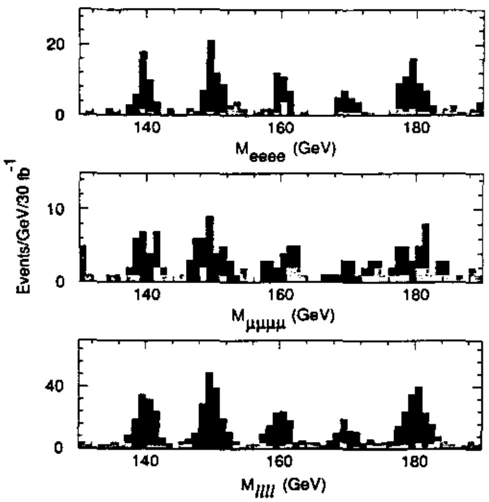

580

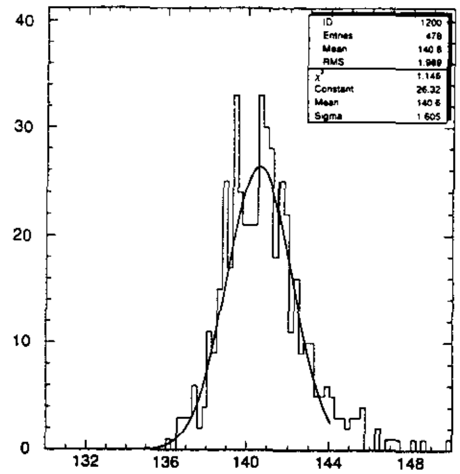

581

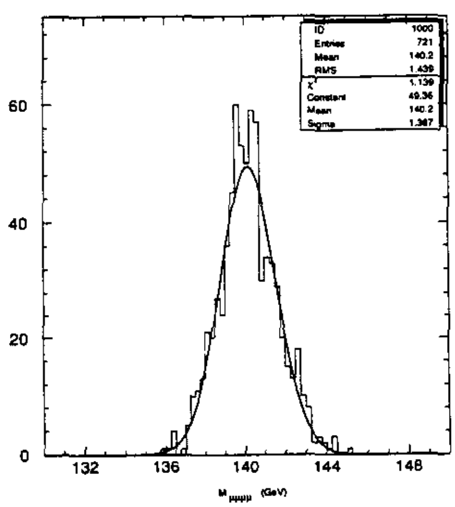

582

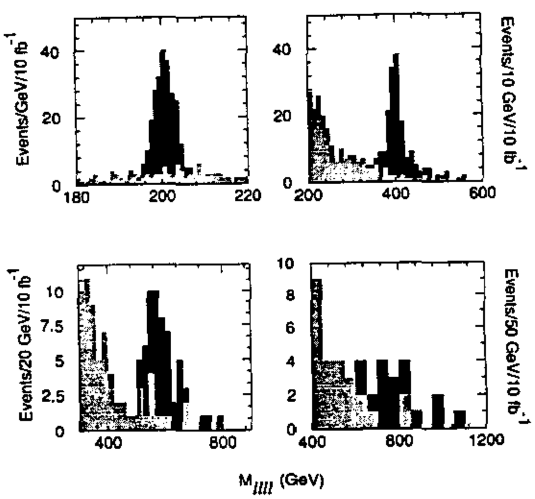

583

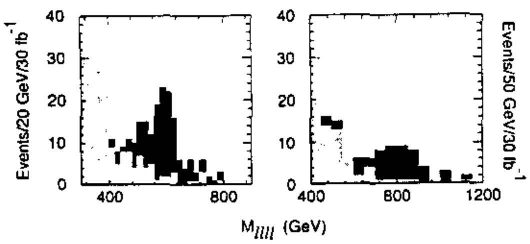
Events/20 GeV/30 fb^{-1}
Events/50 GeV/30 fb^{-1}
M_{llll} (GeV)

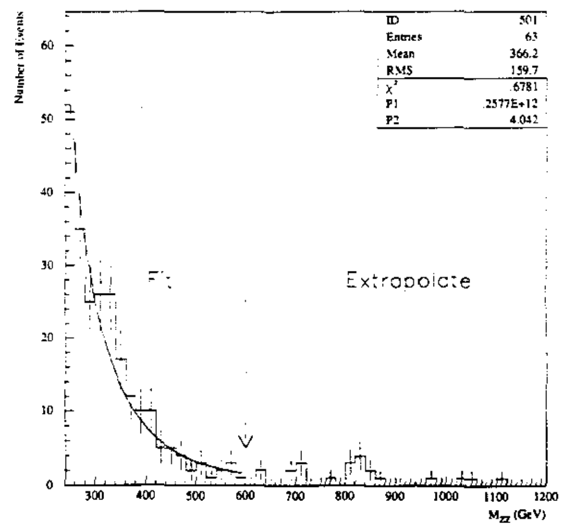
Number of Events
ID 501
Entries 63
Mean 366.2
RMS 159.7
χ^2 .6781
P1 .2577E+12
P2 4.042
Fit
Extrapolate
M_{ZZ} (GeV)

585

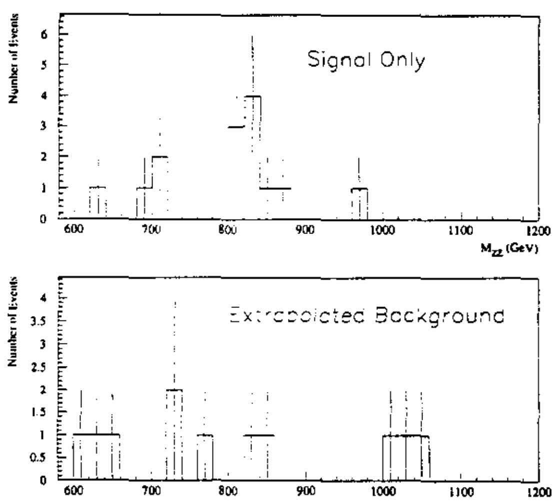
Number of Events
Signal Only
Extrapolated Background
M_{ZZ} (GeV)

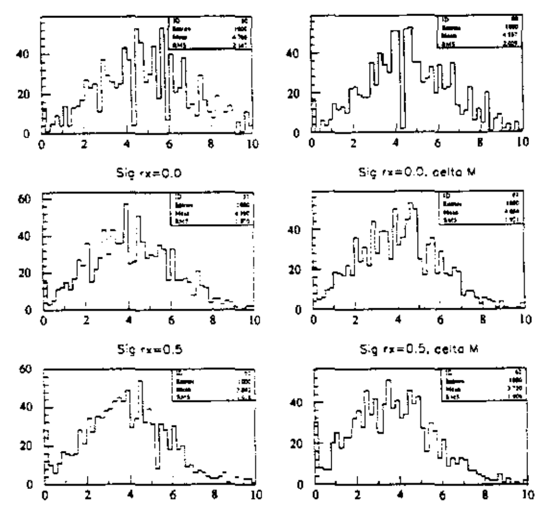
Sig rx=0.0
Sig rx=0.0, delta M
Sig rx=0.5
Sig rx=0.5, delta M
Sig rx=1.0
Sig rx=1.0, delta M

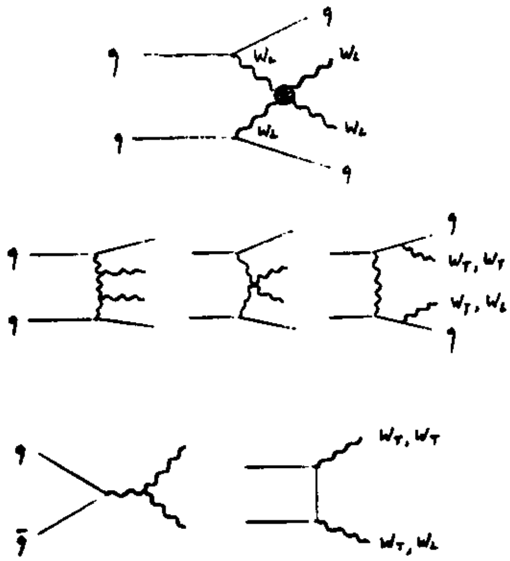

588

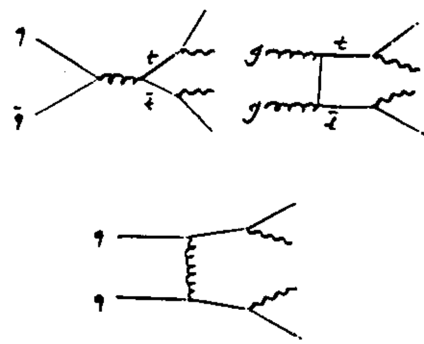

589

Report the discussions on "detector optimization"

- Subsystem optimization suggestions
  - Muon chamber
  - Trigger design
  - Calorimetry
  - Central Tracker
- Integrated performance
  - using CT and Cal. for muon measurement
  - e/jet rejection at 10^{34} (cal. + CT)
  - "OR" — trigger efficiency
- Tool — Global Simulation package

Signal and Background for $H \to ZZ^* \to \mu\mu\mu\mu$ and $H \to ZZ^* \to \ell\ell\ell\ell$

M_H (GeV)	140	150	160	170	180
$H \to eeee$					
ΔM_H (GeV)	1.05	1.06	1.13	1.23	1.33
σaccep	1.2	1.7	.86	.62	1.6
Background (fb/GeV)	.025	.025	.025	.025	.040
$H \to \mu\mu\mu\mu$					
ΔM_H (GeV)	1.59	1.62	1.73	1.84	2.22
σaccep (fb)	.81	1.1	.56	.36	.92
Background (fb/GeV)	.016	.016	.016	.016	.026
$H \to ee\mu\mu$					
ΔM_H	1.36	1.46	1.56	1.71	1.77
σaccep (fb)	1.89	2.60	1.38	.89	2.43
Background (fb/GeV)	.038	.038	.038	.038	.062
$H \to \ell\ell\ell\ell$					
Significance	11	13	8.1	5.7	10.5

V. Gavrilov

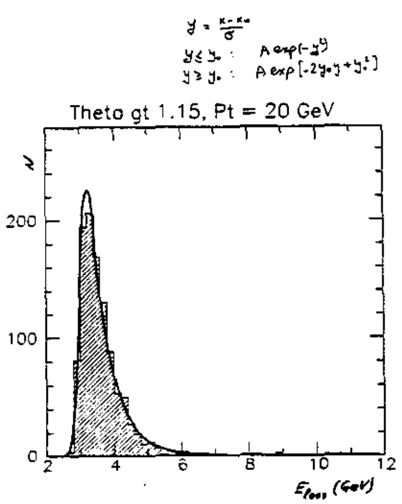

594

V. Gavrilov

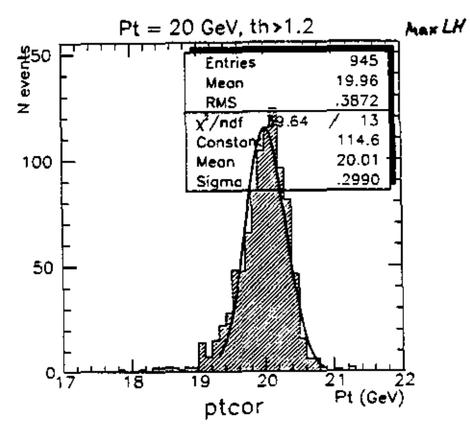

595

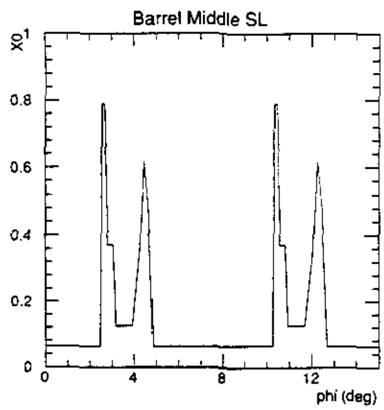

UNIFORM CHAMBER MATERIAL

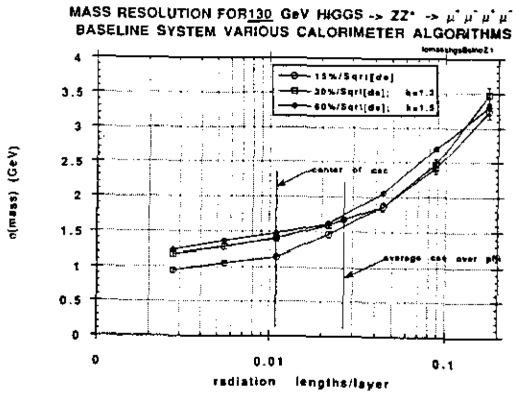

			if $A_{cut}/\mu = 0.91$
M_{H_0}	170 GeV	170 GeV	170 GeV
σ_{M_H}	1.84 GeV	1.53 GeV	1.53
$N_{2\sigma}$	3.42	3.42	4.8
$B_{2\sigma}$	1.18	0.99	1.39

significance on $H \to \ell\ell\ell\ell$ changing:
5.7 → 6.7

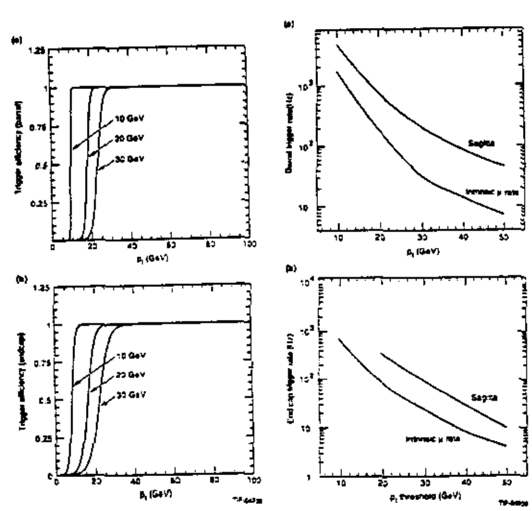

FIG. 4-15. Trigger efficiency versus muon p_T for various thresholds in a) the barrel and b) the endcap.

FIG. 4-16. Integrated trigger rate versus p_T threshold for a) the barrel and b) the endcap

4-24 4-25

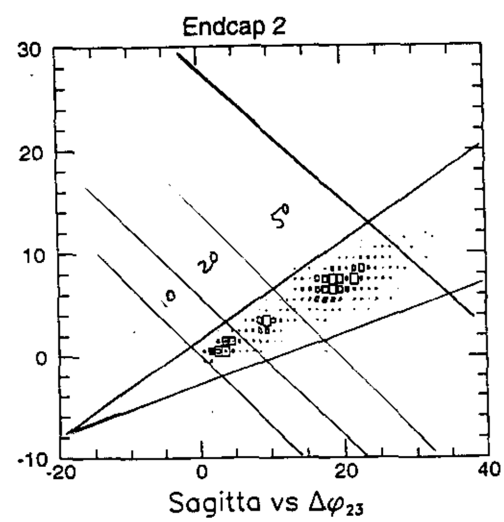

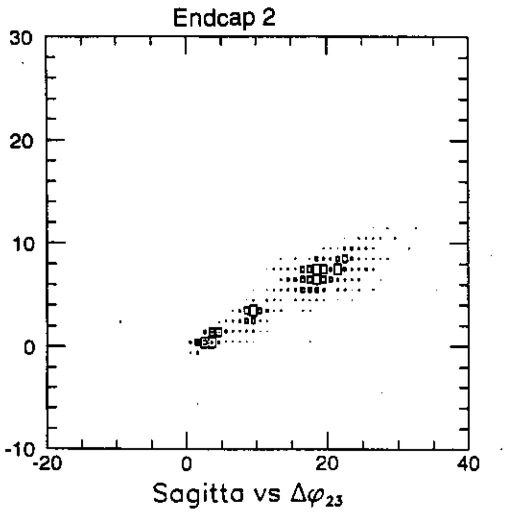

Sagitta vs $\Delta\varphi_{23}$

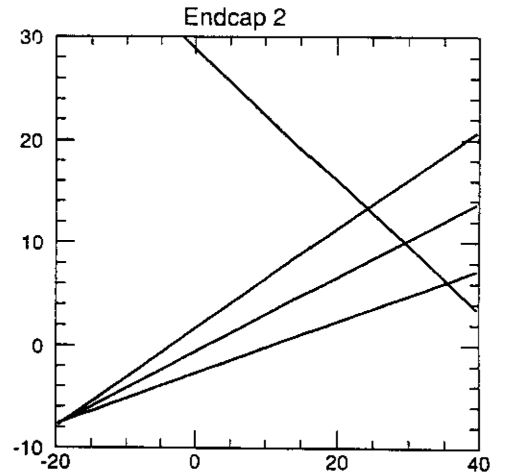

File: 9310.hsto

ID	IDB	Symb	Date/Time	Area	Mean	R.M.S.
59310	1	1	930509/2002	201.0	554.6	185.6
49310	0	1	930509/2002	131.0	490.6	160.9
98765	981	-1	930509/2044	5235.	103.6	122.3
98765	982	-1	930509/2044	5161.	95.27	99.89

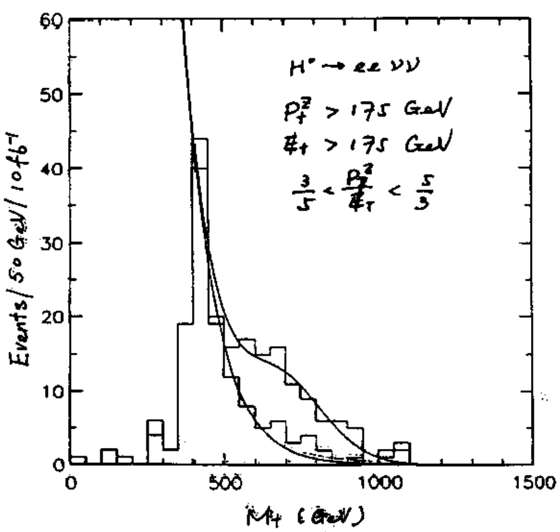

Can not lower cut because $\hat{t} > 150$ GeV in generator.

Change of Cuts & Significance

$H^0 \to ee\nu\nu$

Cuts: P_T^Z, $\not{E}_T$

Cut (GeV)	N_{sig}	N_{Z+jet}	N_{ZZ}	$\frac{N_{sig}}{\sqrt{N_{Zjet}+N_{ZZ}}}$
175	78	90	66	6.2
200	74	53	54	7.2
225	69	29	40	8.3
250	63	17	31	9.1
275	55	13	24	9.0
300	48	11	17	9.0

with Cut = 250 GeV

% in tail				
1%	63	19	31	8.9
10%	63	40	32	7.4
25%	65	73	33	6.3
50%	66	124	36	5.2
75%	68	171	37	4.7
100%	72	225	39	4.4

Change of Cuts & Significance

$H^0 \rightarrow ee\nu\nu$

Cuts: P_T^Z, $\not{E}_T$

Cut (GeV)	N_{sig}	N_{Z+jet}	N_{ZZ}	$\frac{N_{sig}}{\sqrt{N_{Zjet}+N_{ZZ}}}$
175	78	90	66	6.2
200	74	53	54	7.2
225	69	29	40	8.3
250	63	17	31	9.1
275	55	13	24	9.0
300	48	11	17	9.0

With Cut = 250 GeV

% in tail				
1%	63	19	31	8.9
10%	63	40	32	7.4
25%	65	73	33	6.3
50%	66	124	36	5.2
75%	68	171	37	4.7
100%	72	225	39	4.4

604

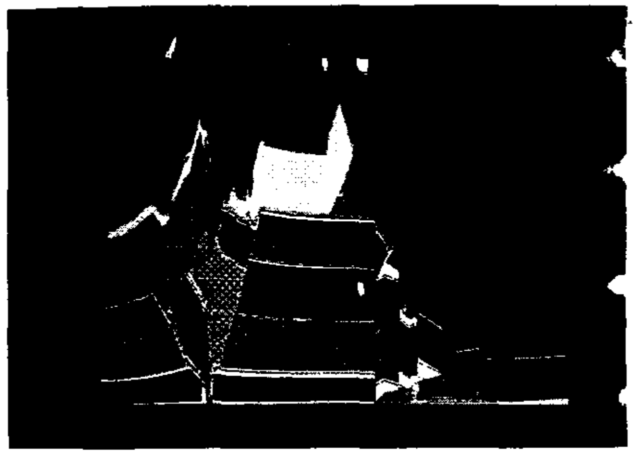

605

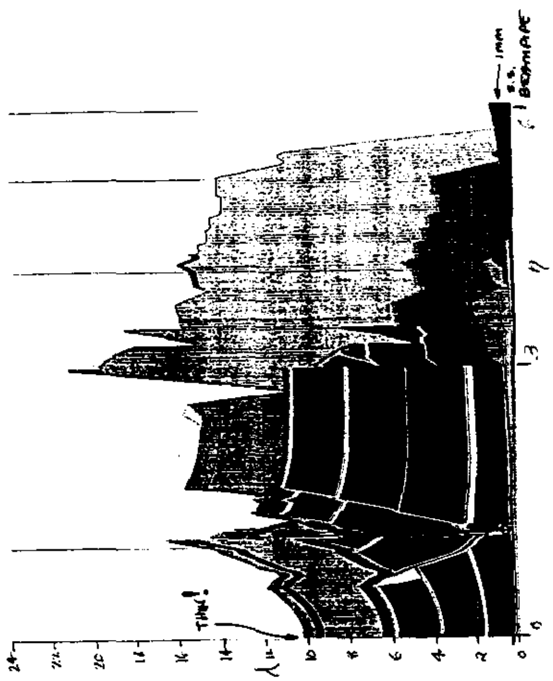

606

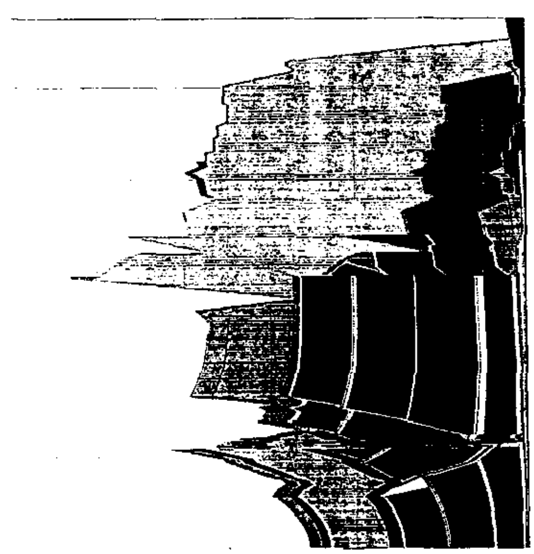

607

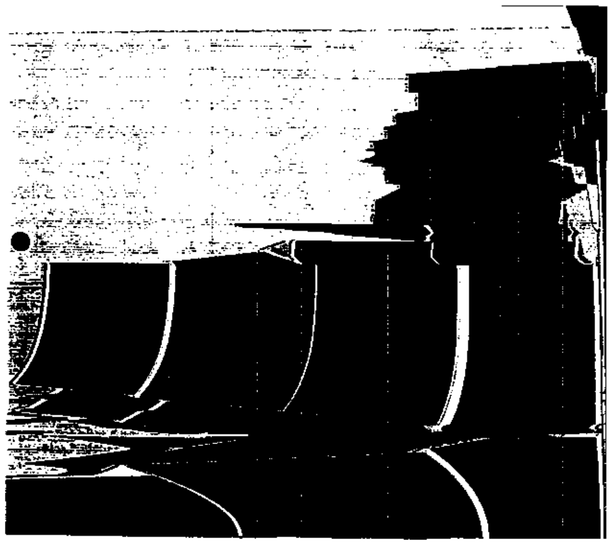

668

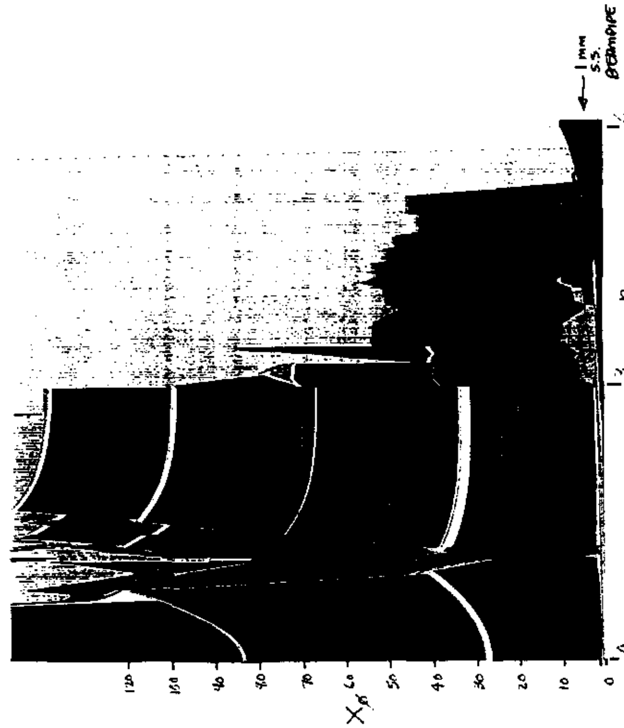

669

(1)

PATTERN RECOGNITION IN THE GEM MUON SYSTEM

Is Dependent on the Physical Layout of Muon Chambers; Active volume, Dead Materials in μ system, Distance of μ System from Calorimeter.

All of these Factors Determine the Nature of the Correlated Background both for Isolated Muons and for Muons in or near Jets.

I will only consider Correlated Background, First for 3 samples of Isolated Muons, then for Muons in "b" Jets. The talk will proceed as follows:

1) Describe the Nature of the Correlated Background and its Relation to the Physical Layout of the μ-System

2) [illegible]

(2)

3) Then give a more Technique oriented estimate of a Track Reconstruction Efficiency Based on Track Finding using all the information available.

4) Then finally we will give the P_T Resolution of the Tracks we have Found in the Presence of these Backgrounds; and make suitable comparison with other results.

613

MATERIALS – 1.9 cm Nomex
– 0.5, 0.7, 1.0 cm $CF_4 CO_2$ (SL 1, 1, 3)
– 0.05 cm G10
– 0.0017 cm Cu

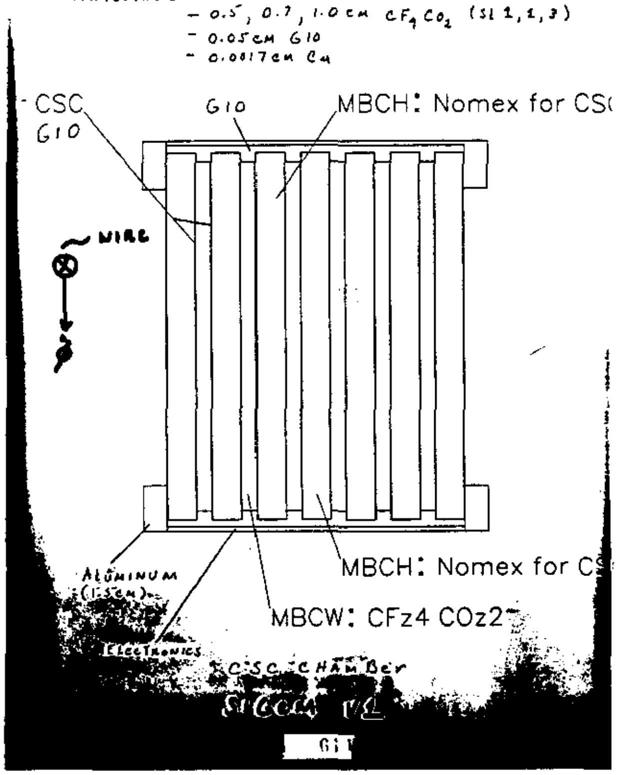

614

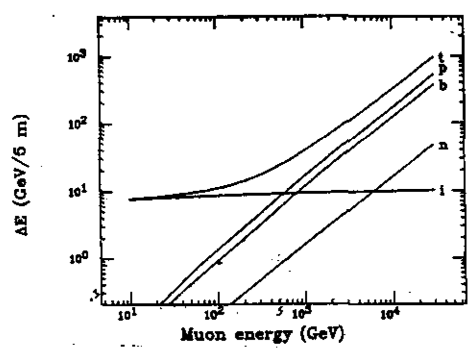

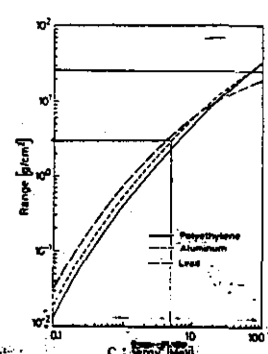

(3)

THE BACKGROUND

THE BACKGROUND CONSISTS OF EM DEBRIS PRODUCED BY μ'S BOTH AT THE TOP OF THE CALORIMETER AND IN THE MATERIAL OF THE MUON SYSTEM.

FROM THE CALORIMETER WE HAVE γ'S, $e^{+/-}$ FROM THE μ SHOWERING.

$e^{+/-}$ ARE NOT VERY PENETRATING. A 100 MeV e^- goes ABOUT 3.5 CM ON THE AVERAGE IN Cu.

FOR 100 MeV γ'S PRODUCED BY μ SHOWERING IN Cu AFTER 3.5 cm,

$\frac{I}{I_0} = e^{-(3.5(\ldots))} = 41\%$

ONLY ABOUT 40% OF THESE PHOTONS ESCAPE INTO THE μ-SYSTEM.

SO THAT ONLY THE LAST FEW CM OF THE CALO ARE IMPORTANT FOR SHOWER PARTICLES ASSOCIATED WITH THE μ. THIS BECOMES MORE IMPORTANT THE HIGHER THE μ ENERGY.

FOR p_μ ~ 400 GeV IONIZATION LOSS = BREMSSTRAHLUNG

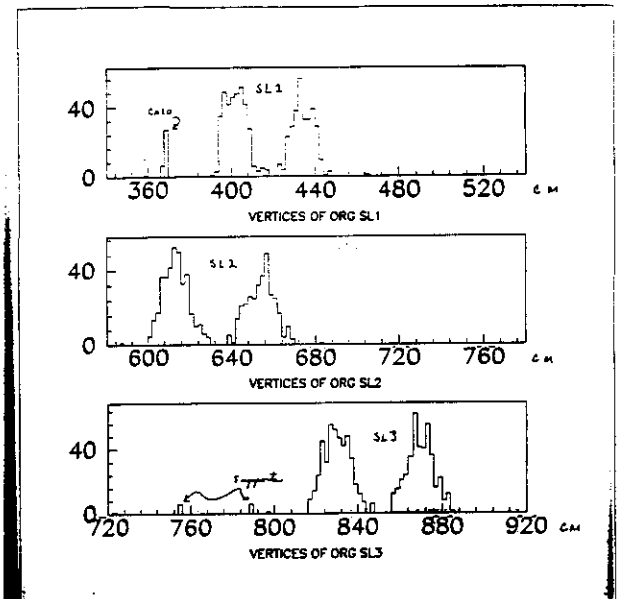

1 TeV P_T in THE BARREL

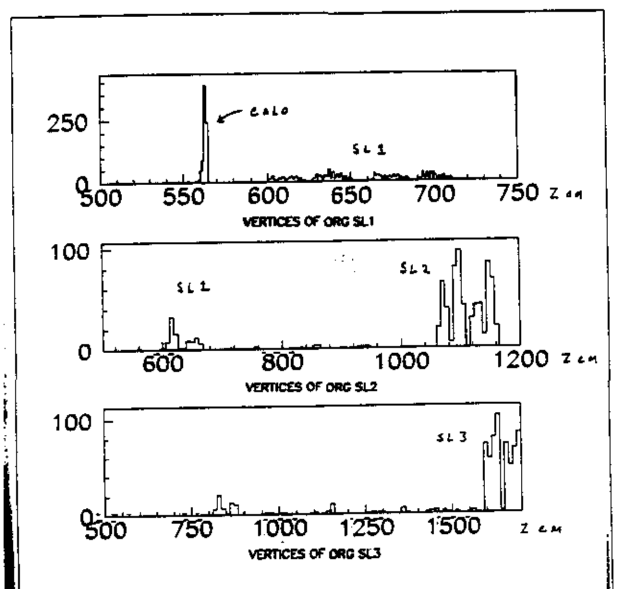

1 TeV P_T, ENDCAP

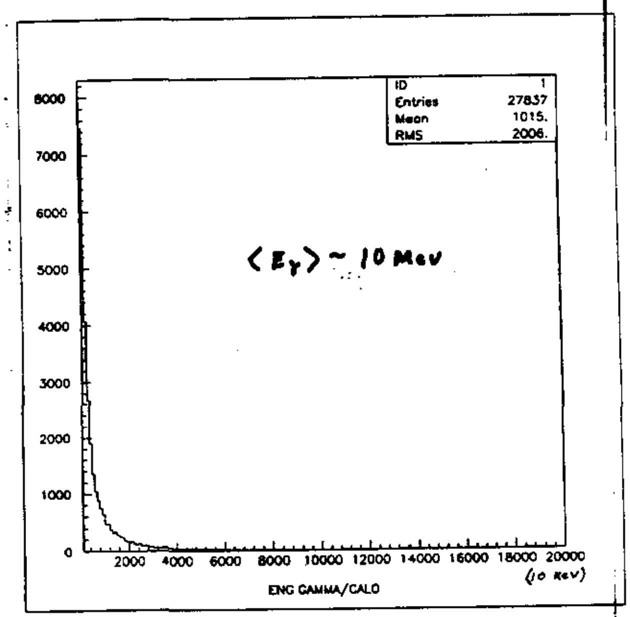

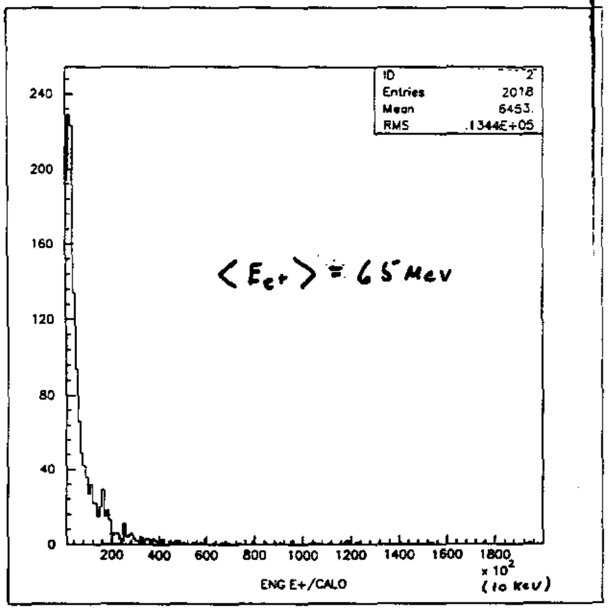

4

THE MOST DANGEROUS ASSOCIATED EM BACKGROUND IN THE BARREL IS γ'S, THEY ARE PRODUCED WITH THERE MOMENTUMS CLOSE TO THAT OF THE μ;

$$\frac{\vec{K}_\gamma}{|K|} \sim \frac{\vec{P}_\mu}{|P_\mu|} , \quad \theta \sim \frac{1}{\gamma_\mu}$$

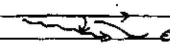

FOR 1 TeV P_T SAMPLE ONLY ABOUT 10% OF THE Bg ON FIRST S.L. IS FROM THE CALO, ON THE 1st SL IN THE ENDCAP IT IS MORE THAN 50% !

THIS IS BECAUSE IN THE BARREL THE $\vec{B}$ FIELD SWEEPS CHARGED PARTICLES AWAY. FOR THE 20 cm MINIMUM gap IN THE BARREL 50 MeV IS NEED TO get FROM CALO TO 1st SL; TO get WITHIN 1 cm (= 2 PADS) OF the μ (BOTH STARTING TogeTHER on Top of CALO) 500 MeV IS NEEDED.

THE AVERAGE ENERGIES OF CHARGED PARTICLES EXITING THE CALO ARE;

$e^+ \Rightarrow \langle E \rangle \simeq 65$ MeV, $e^- \Rightarrow \langle E \rangle \sim 60$ MeV

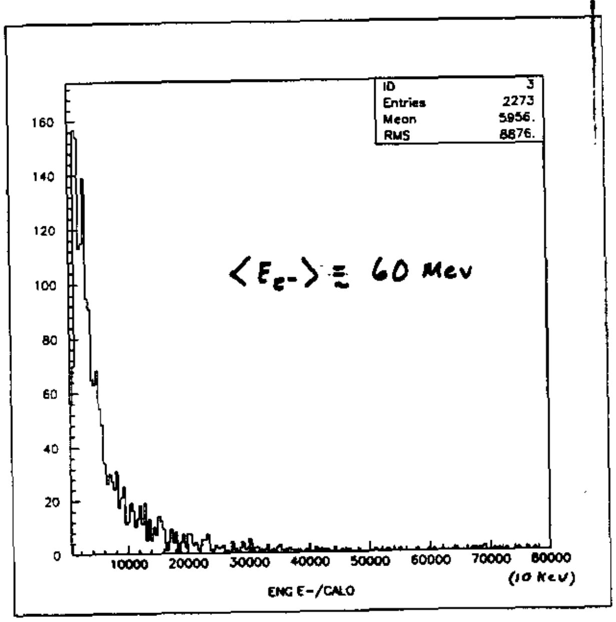

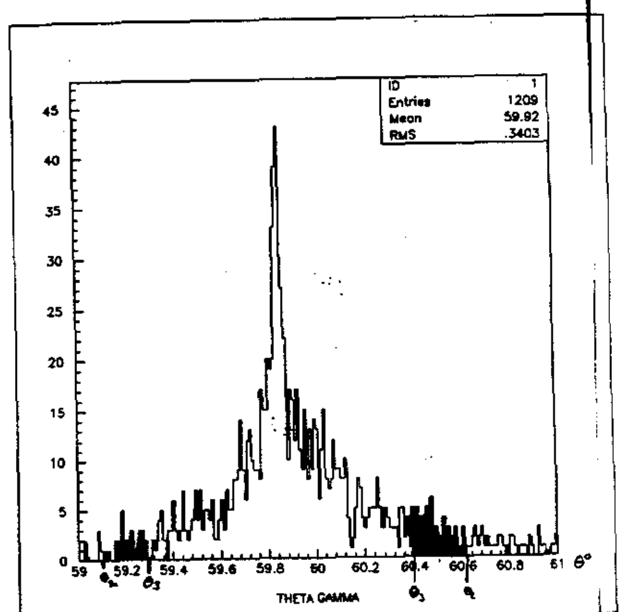

1 TeV μ @ θ = 60°

■ = EXTRA γ's SEEN ON SL2 COMPARED TO SL3 FOR TWO PAD WIDTHS

(5)

FOR THE γ'S WE EXPECT BECAUSE OF THE SHARP ANGULAR DISTRIBUTION NO MORE THAN A 10-15% DIFFERENCE BETWEEN CONVERSIONS ON SL2, SL3.

WE FIND FOR $E_{e^+} < 20$ MEV THAT THIS IS TRUE FOR THE 1 TEV P_T SAMPLE. HOWEVER WE FIND OVER THE ENTIRE ENERGY RANGE ALMOST TWICE THE NUMBER OF CONVERSIONS ON BARREL SL2 THAN SL3.

WE FIND % CONVERSIONS FOR THE 1 TEV SAMPLE:

	SL1	SL2	SL3
BARREL	20%	9.2%	9%
ENDCAP	53%	24%	18%

MOST OF THE EM BACKGROUND PRODUCED CLOSE TO THE MUON IS VERY LOW ENERGY ~ < 100 KEV, WHICH IS MOSTLY PRODUCED IN THE GAS.

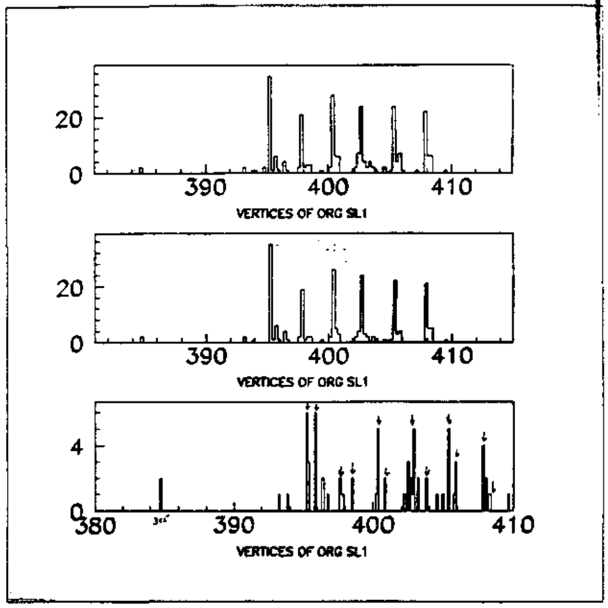

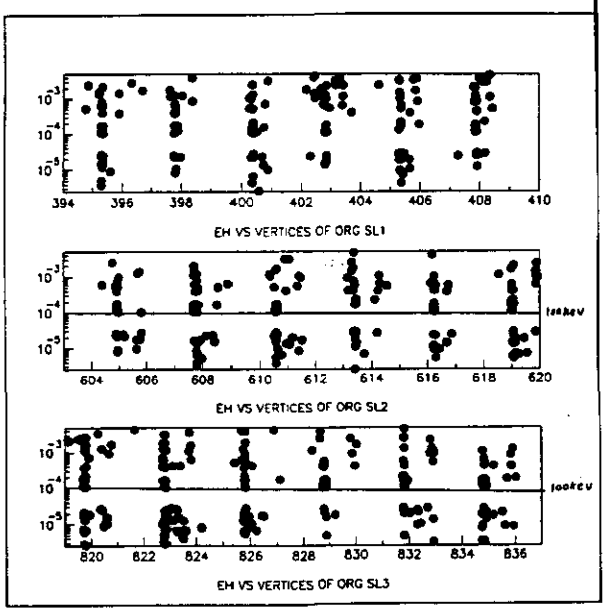

1 Tev G θ = 60°

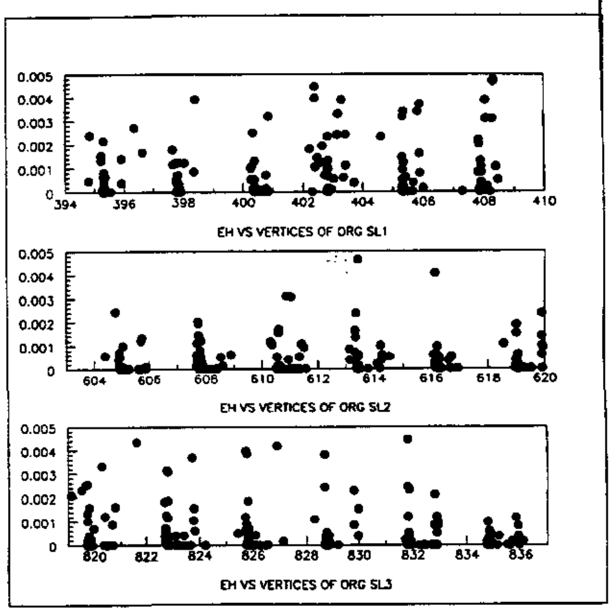

1 Tev G θ = 60°

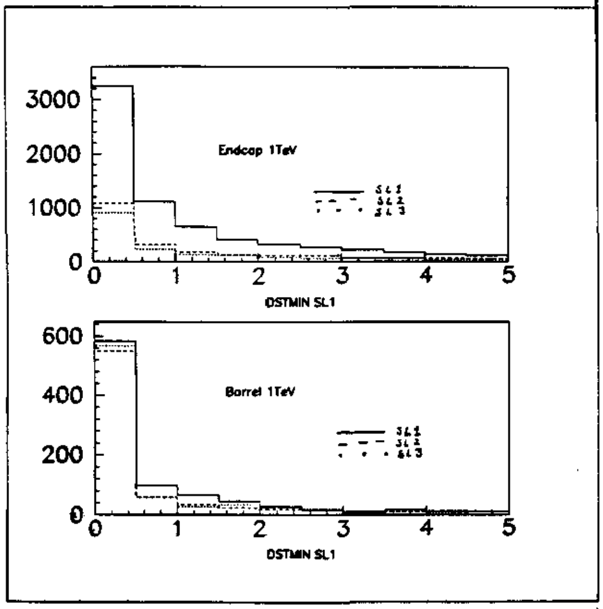

628

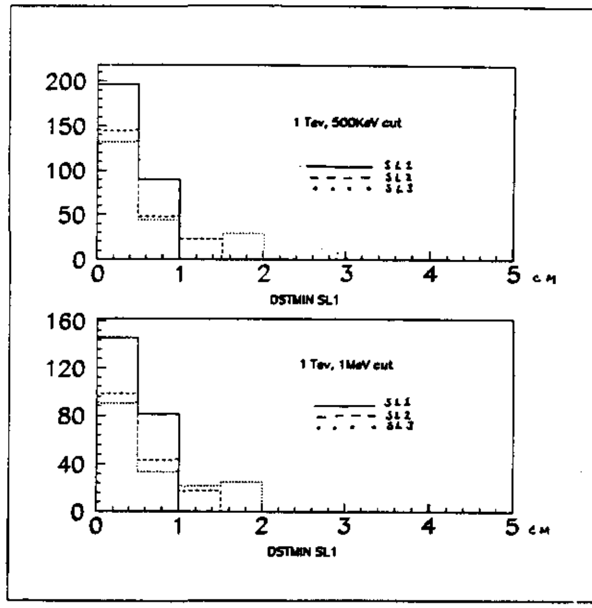

629

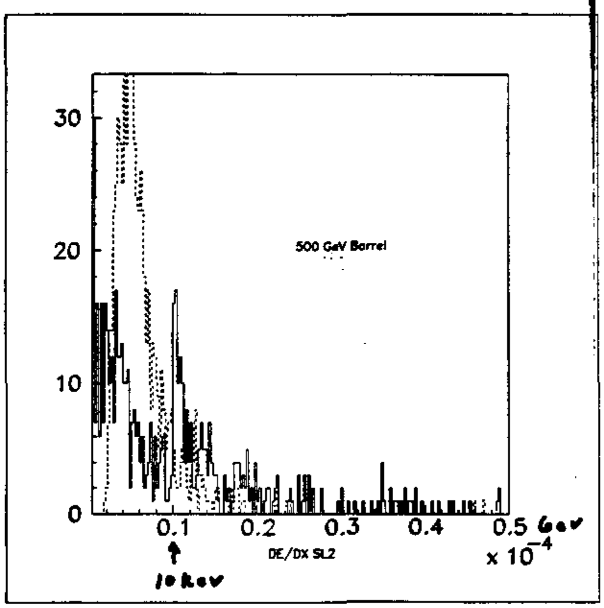

630

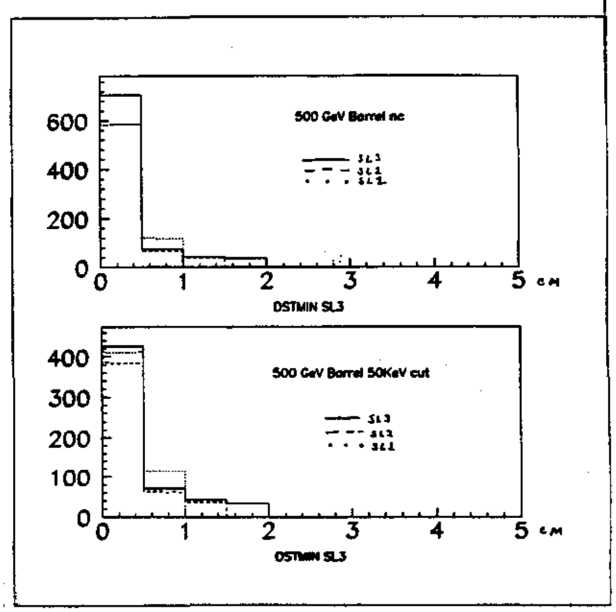

631

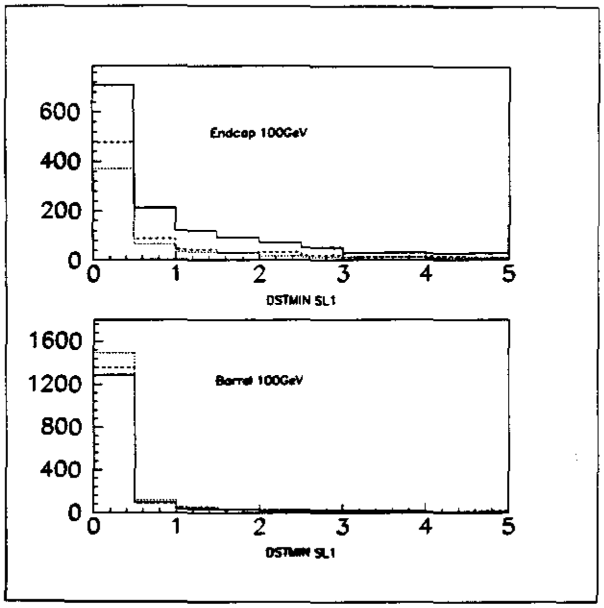

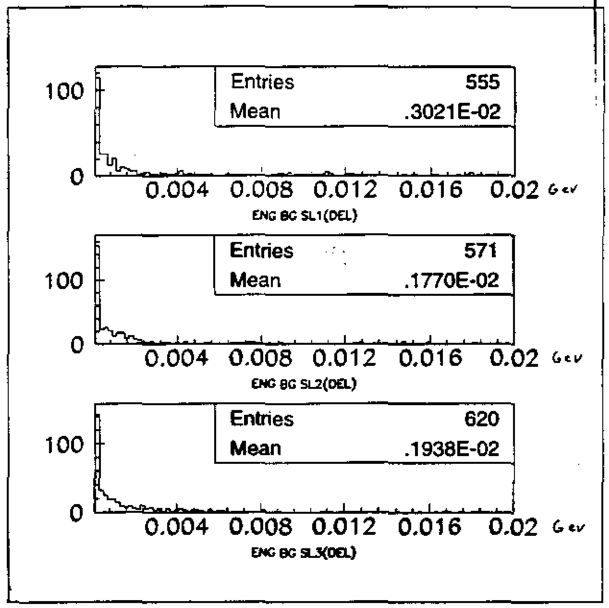

1 Tev P_T

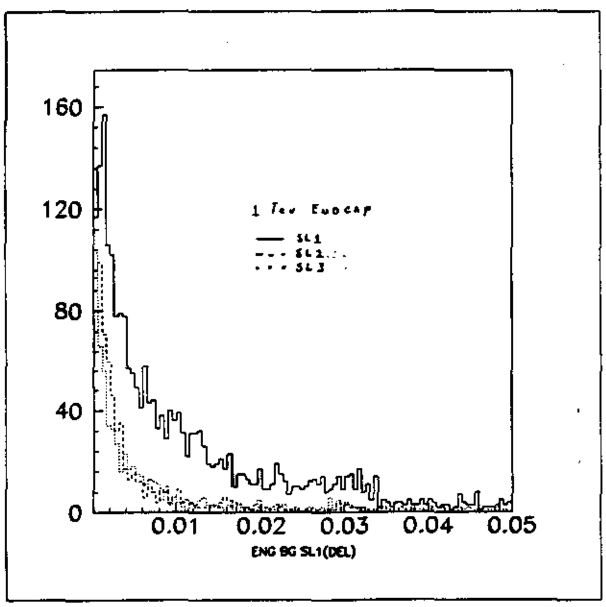

(5)

Pattern Recognition

We will now define some standard interval with which we will use to define our ability to reconstruct a track;

0.02cm < Δ < 2·PAD

where Δ ≡ distance in the direction of the wire in the middle of the gas volume

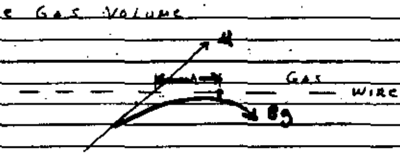

Between the energy weighted centroid of both particles.

From the single track" resolution in the presence of another track (⇒ This will be known as the "Two Track Resolution") we have determined the interval

Δ ≡ to be the interval where, given the "pitch size ≡ PAD", the measurement persion of the μ is spoiled.

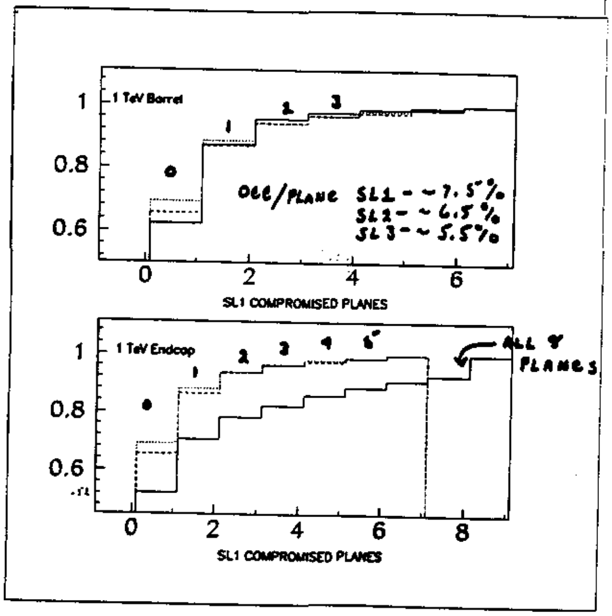

$P(3,3,3)|_{Barrel} \sim (0.98)\,.97 = 0.93$

$P(5,3,3)|_{END} \sim (0.97)\,.95 = 0.83$

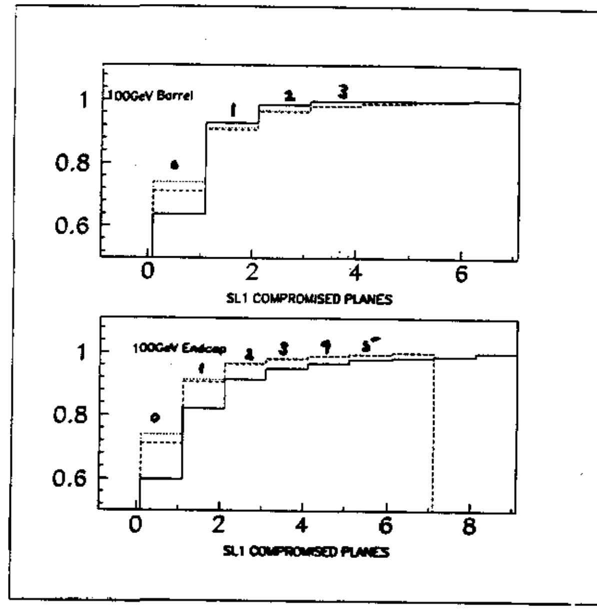

Barrel $P(3,3,3) = .98 = 0.96$

Endcap $P(5,3,3) = .98(.97) = 0.93$

(6)

WE THEN DEFINE THE CRITERION THAT WE MUST FIND EITHER 3:6 OR 5:8 "GOOD" μ HITS ON PLANES/SUPERLAYER GIVING A WAY OF MAKING TRACK STUBS ON SL'S. THE 3 POINTS WILL GIVE US A STUB WHOSE FIT TO A LINE RESULTS IN RESIDUALS THAT APPROX. OUR PLANE-PLANE MEASUREMENT PERSION.

THIS WILL, WHEN 3 TRACK STUBS ARE FOUND THAT BELONG TO A TRACK, GIVE AN "UPPER LIMIT" TO THE TRACK RECONSTRUCTION EFFICIENCY.

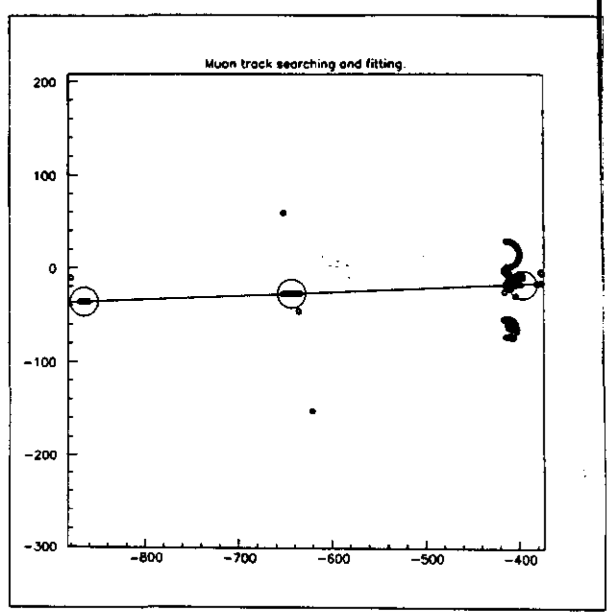

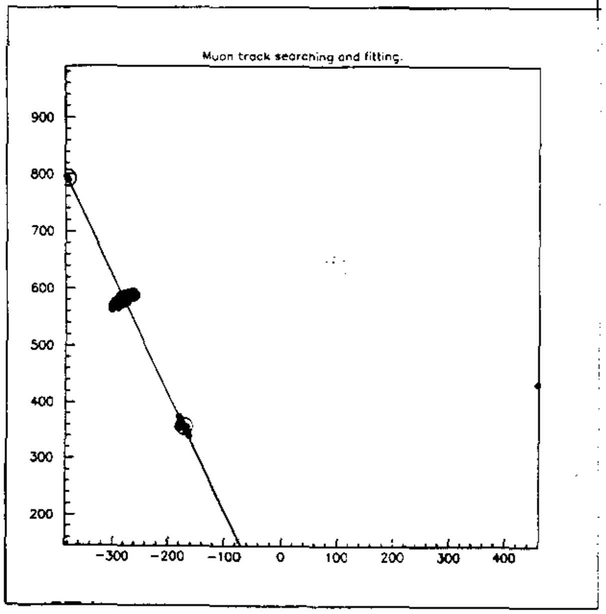
Muon track searching and fitting.

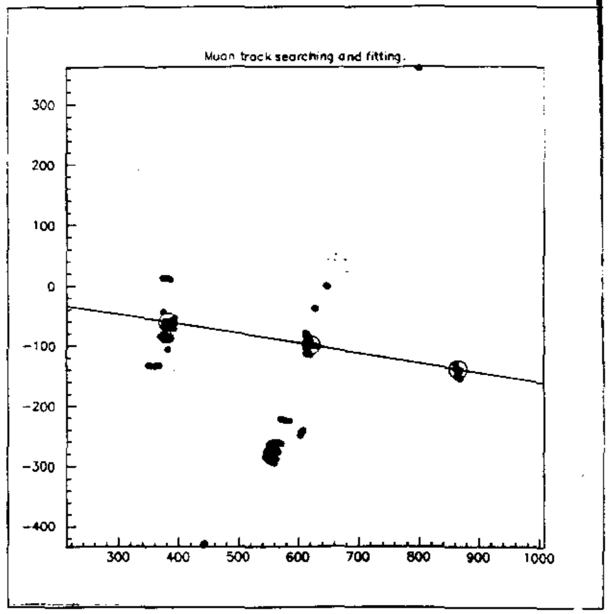
Muon track searching and fitting.

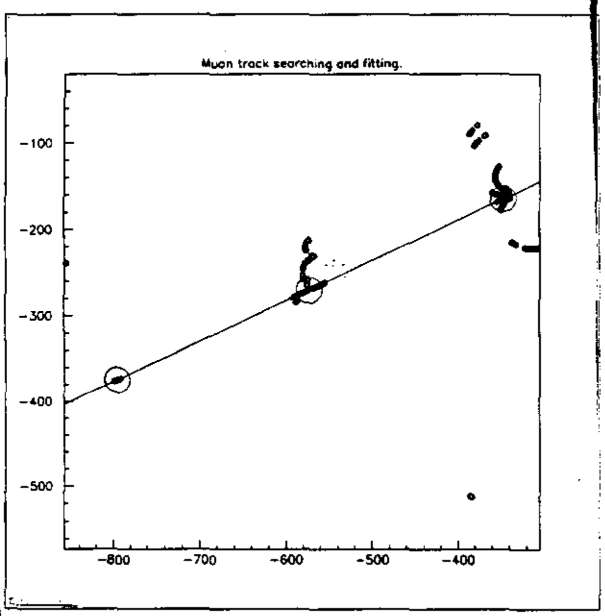
Muon track searching and fitting.

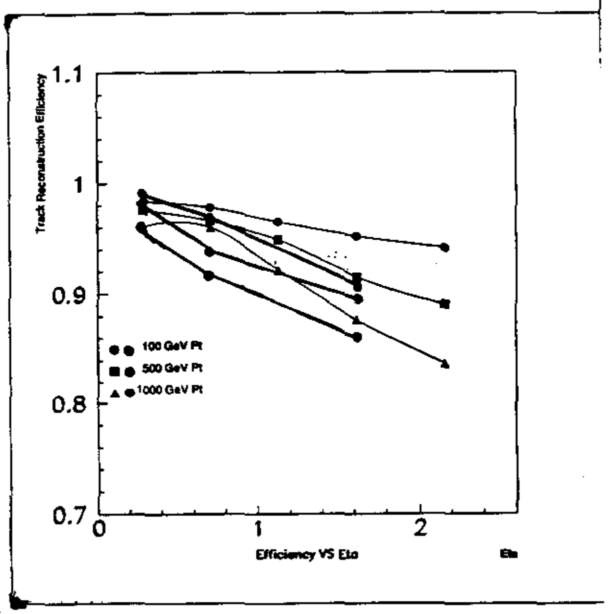
Track Reconstruction Efficiency
100 GeV Pt
500 GeV Pt
1000 GeV Pt
Efficiency VS Eta
Eta

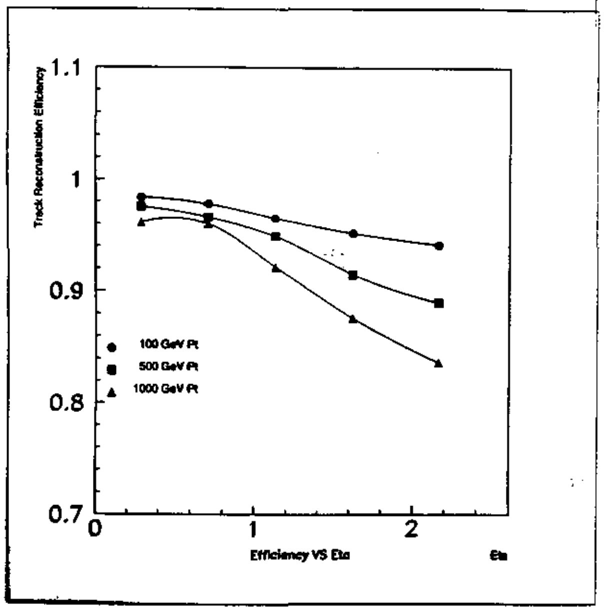

644

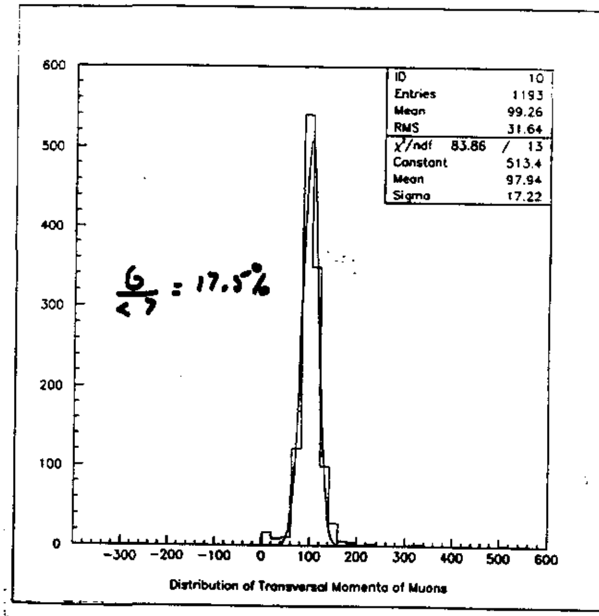

645

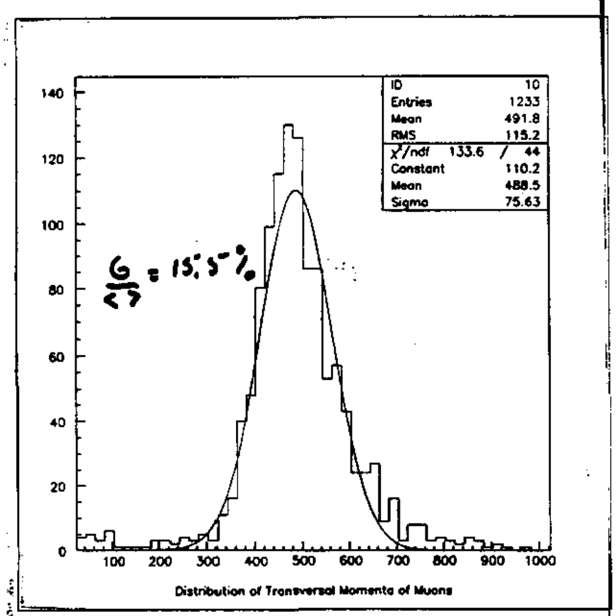

646

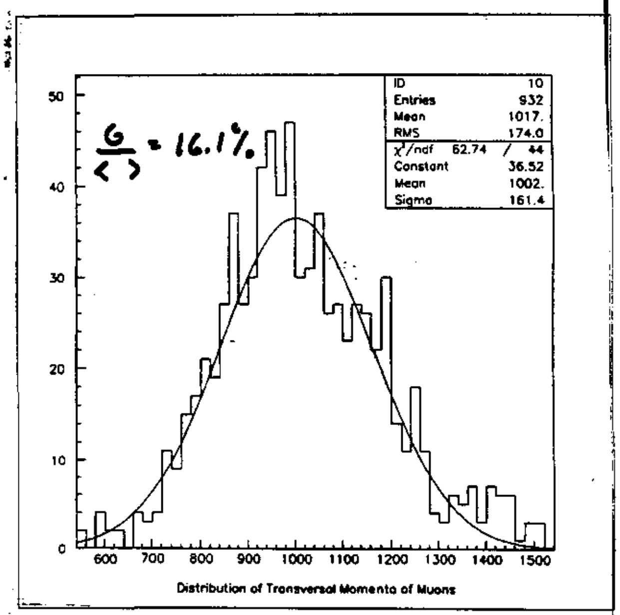

647

(7)

MUONS IN b JETS:

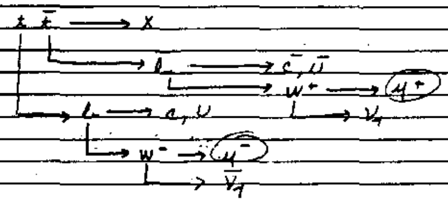

WHERE THE $M_t = 250$ GeV
$P_{t_{1}} = 200$ GeV

MAKE CONE AROUND HOTTEST μ
FROM A $b(\bar{b})$
WHERE:
$r = \sqrt{\Delta\eta^2 + \Delta\phi^2} = 1.0$

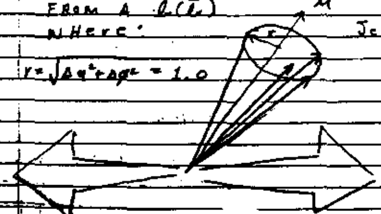

648

PUT ALL PARTICLES IN THE CONE INTO SIGMA

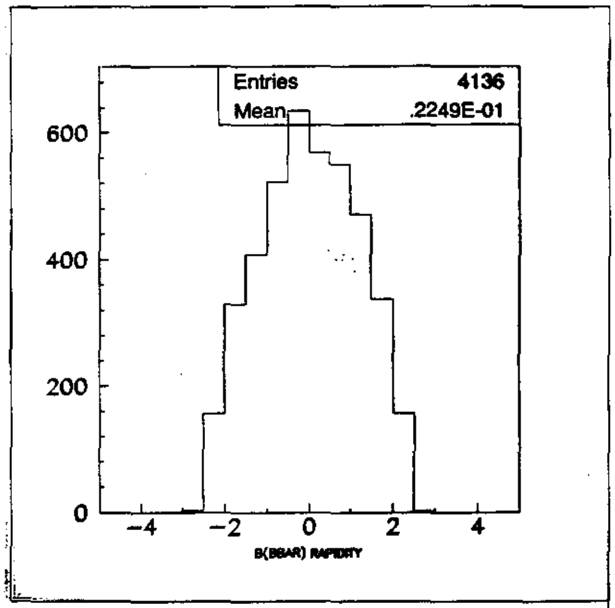

649

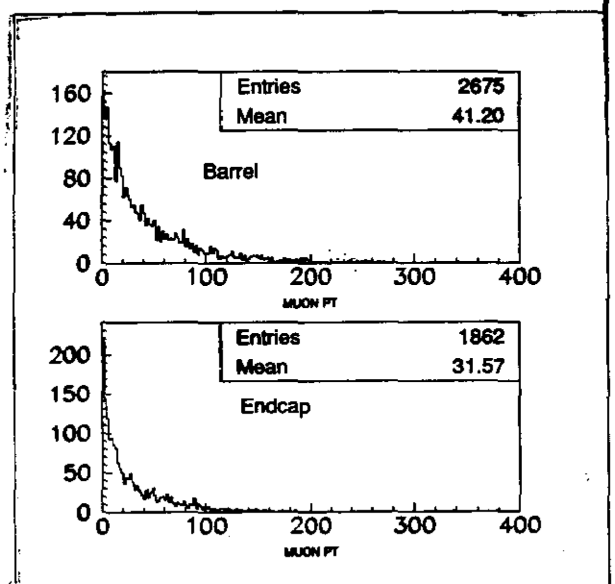

650

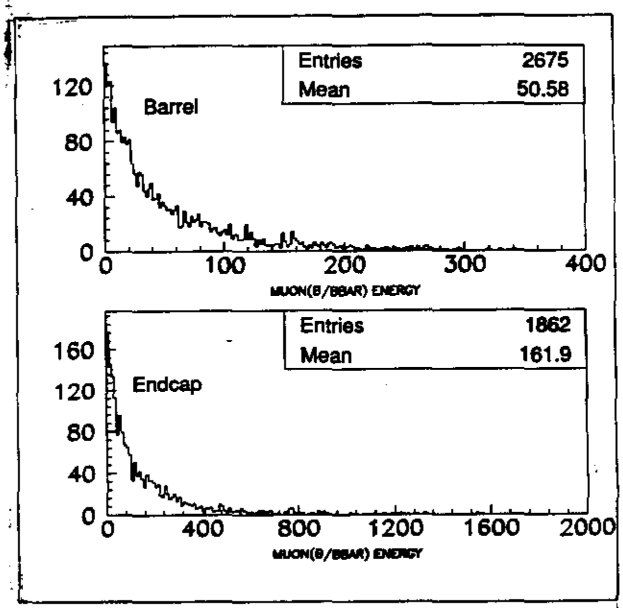

651

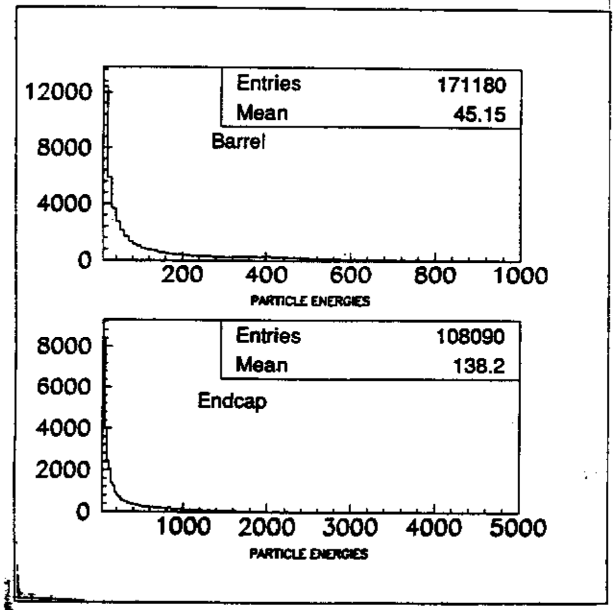

Energies of Particles in a cone around γ, $\sqrt{\Delta\eta^2+\Delta\phi^2}=1$

652

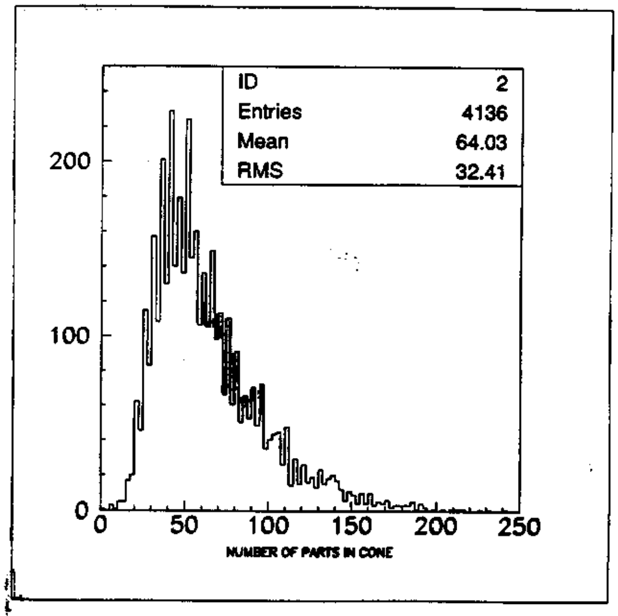

653

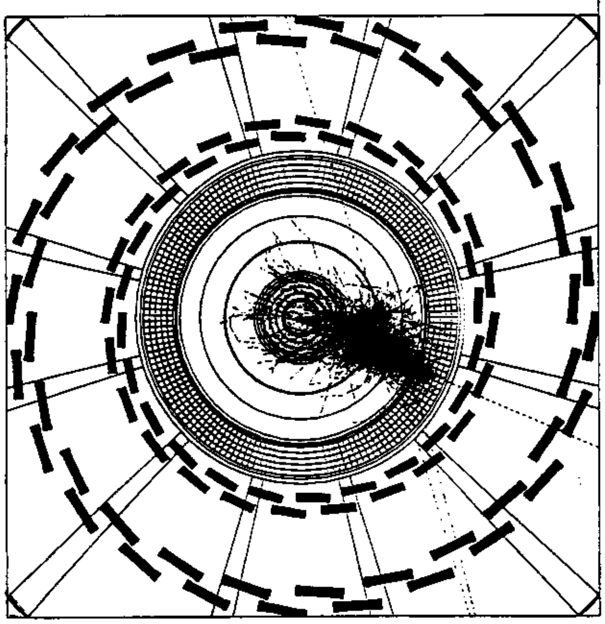

500 GeV γ with an 800 GeV π in the cone around γ

654

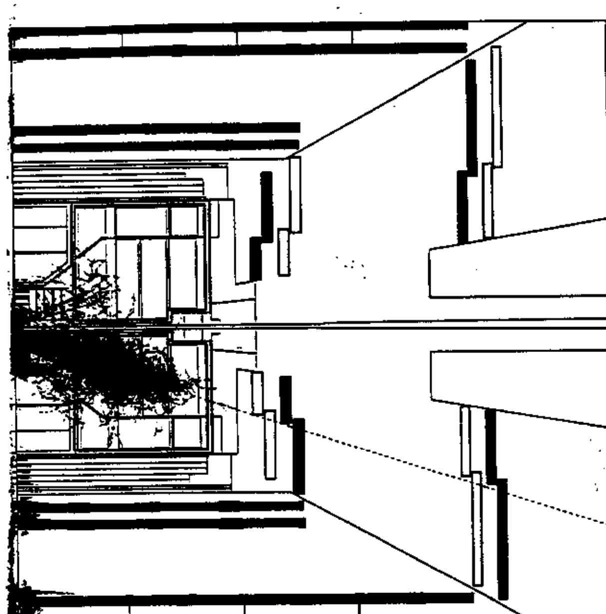

135 GeV γ with 795 GeV π^+ in the cone ($C = \sqrt{\Delta\eta^2+\Delta\phi^2} = 1.0$) around γ

65

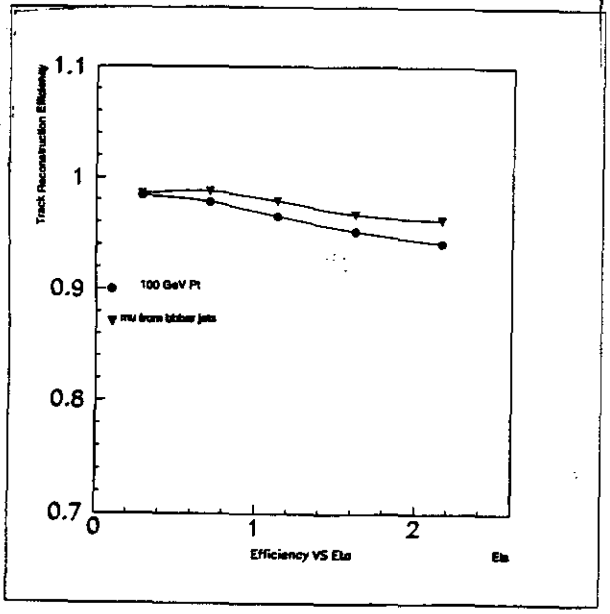

656

(8)

KALMAN FILTER TRACK FIT

ERRORS + RESOLUTIONS

ERRORS:

ALIGNMENT => CHAMBER PLANE-PLANE 50 μm
SUPERLAYER - SUPERLAYER 25 μm

CHAMBER SINGLE LAYER RESOLUTION =>

AS PER TDR => IN PITCH DIRECTION { FUNCTION OF ϕ_{TW} / FUNCTION OF θ / FUNCTION OF S.L.

IN WIRE DIRECTION => ± 5 cm PER PLANE

TWO TRACK RESOLUTION => AS PER J. THOMAS SCALED TO SIZE OF THE PAD ON A SUPERLAYER

657

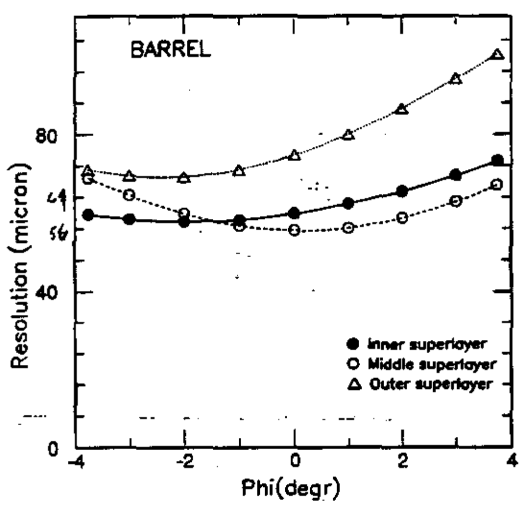

4_3_1_5a.ps

658

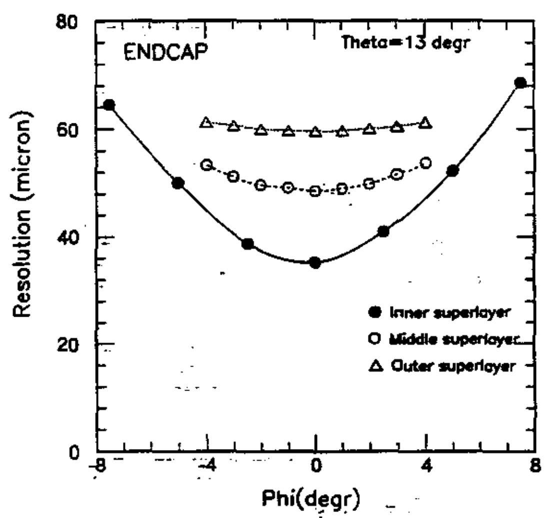

4_3_1_6a.ps

659

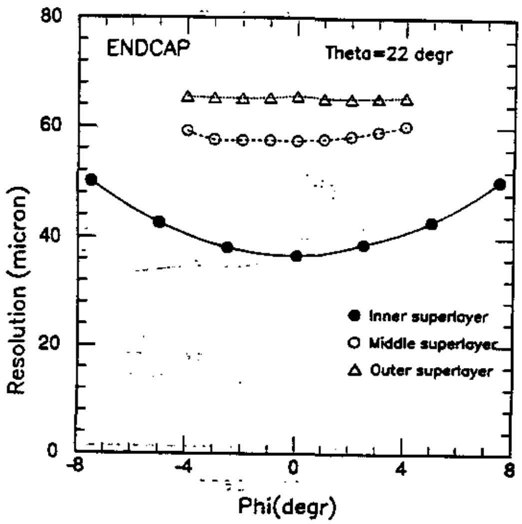

24-3-1-68.ps

660

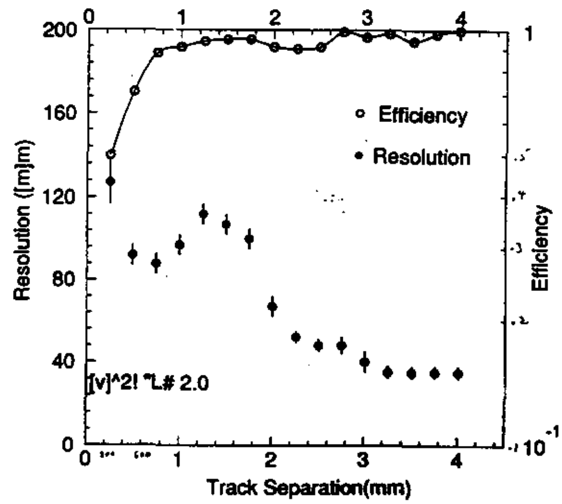

(For 2.5mm PADs)

661

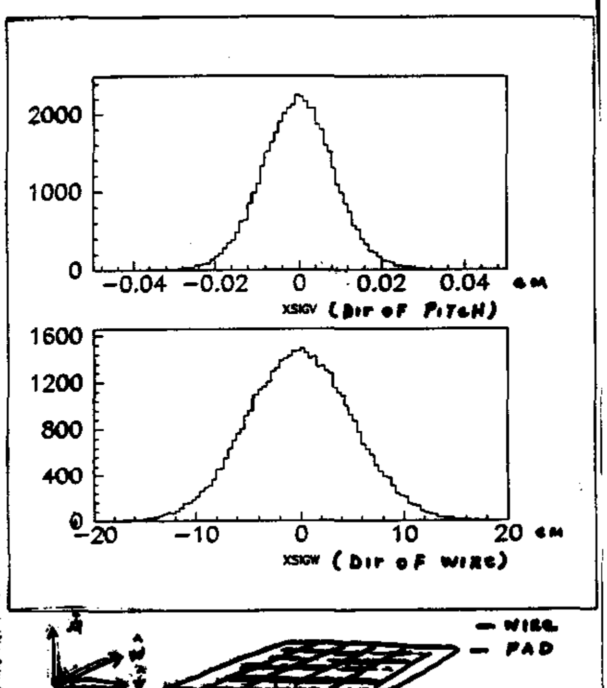

662

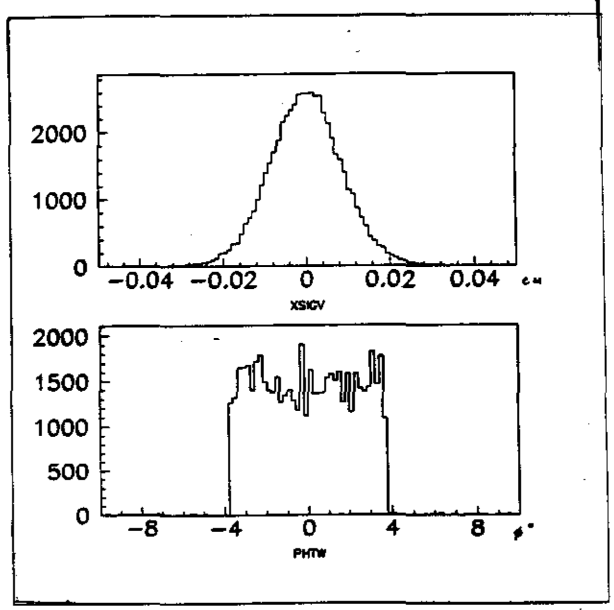

663

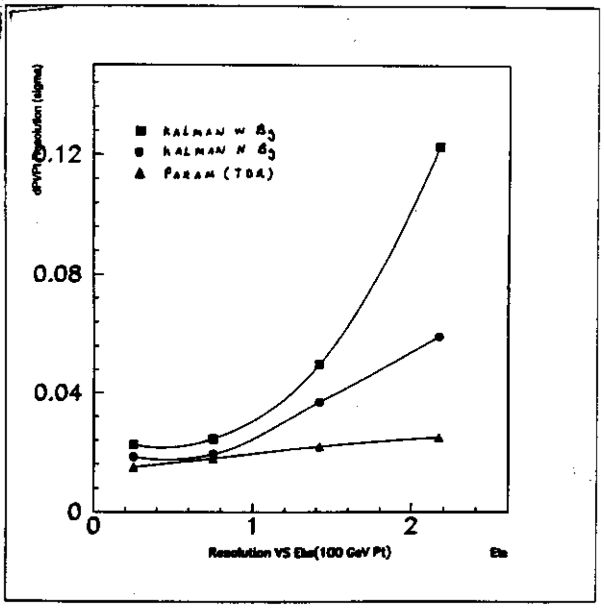

664

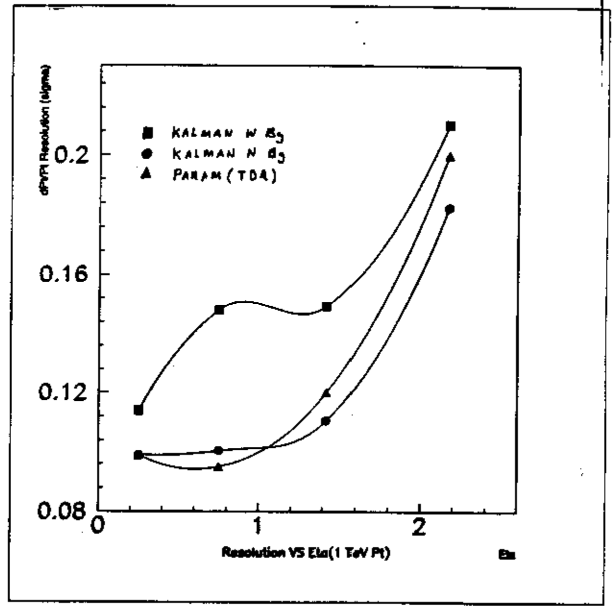

665

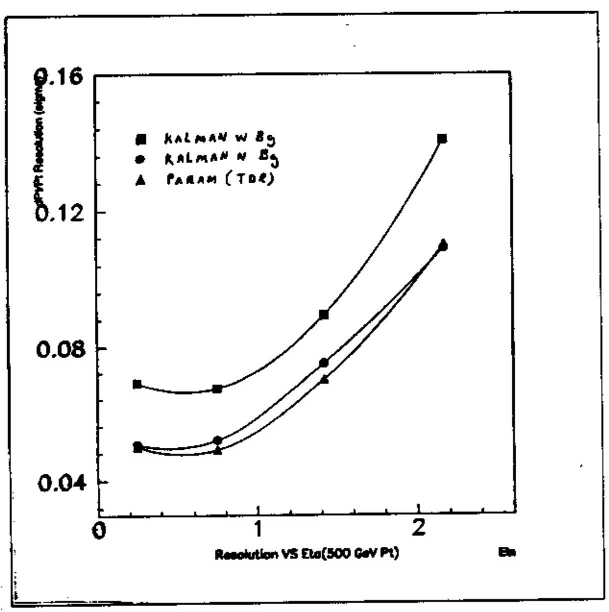

666

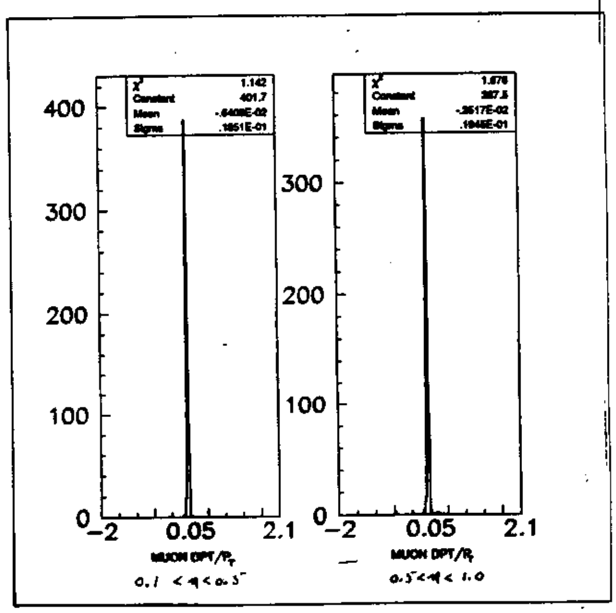

100 Gev P_T

667

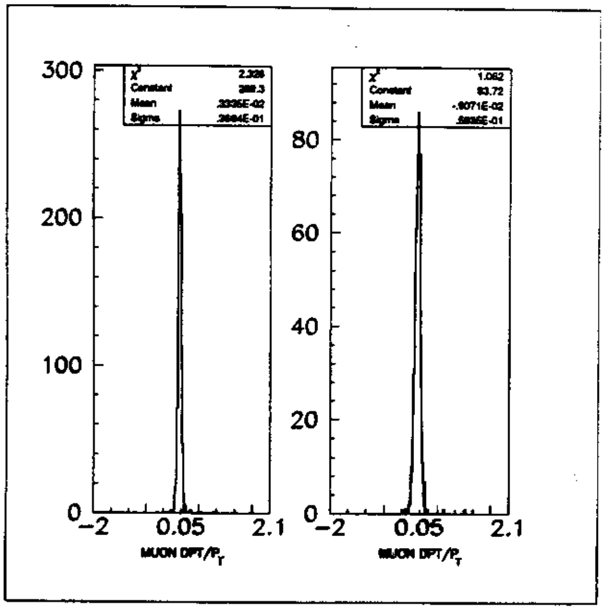

100 GeV P_T

668

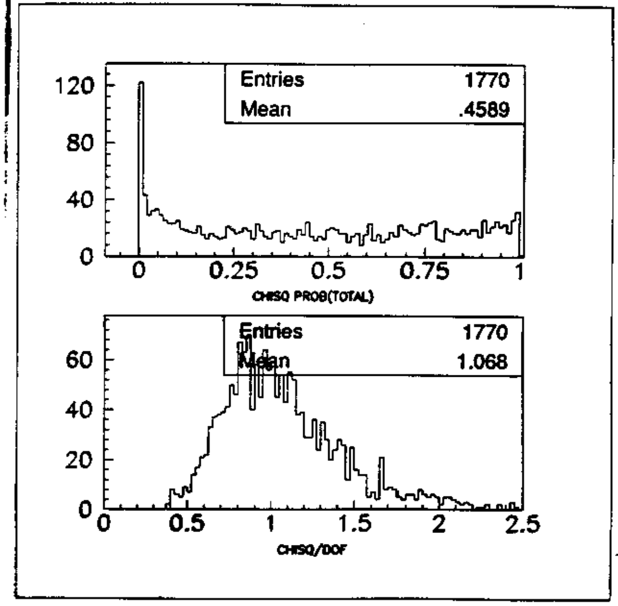

100 GeV P_T

669

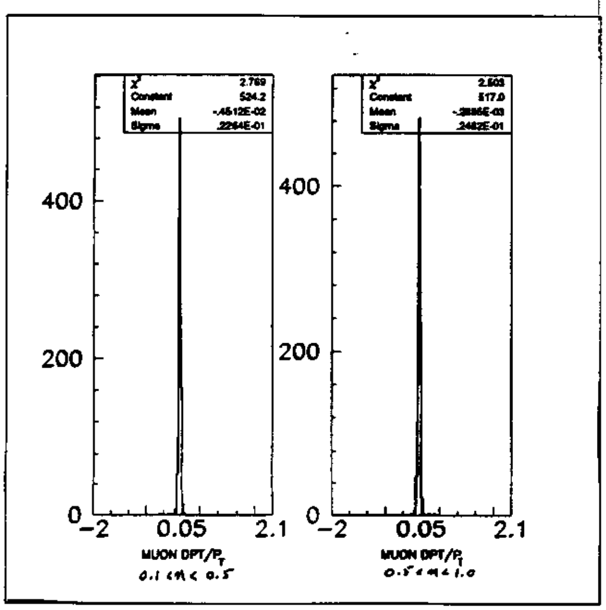

100 GeV P_T,
with Two Track

670

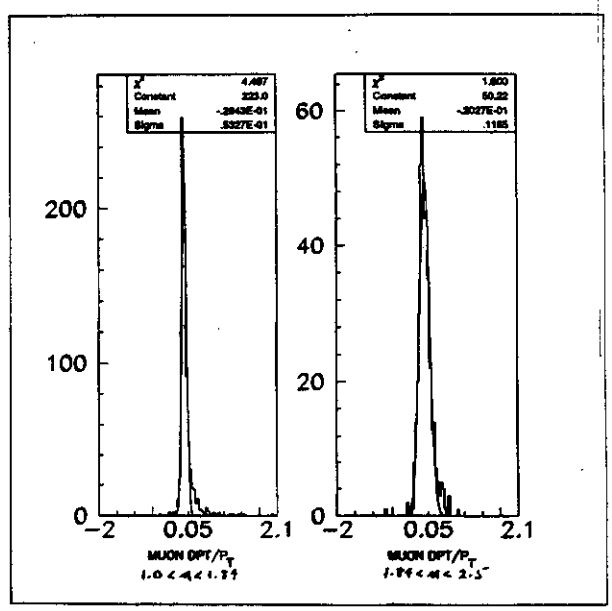

100 GeV P_T,
with Two Track

671

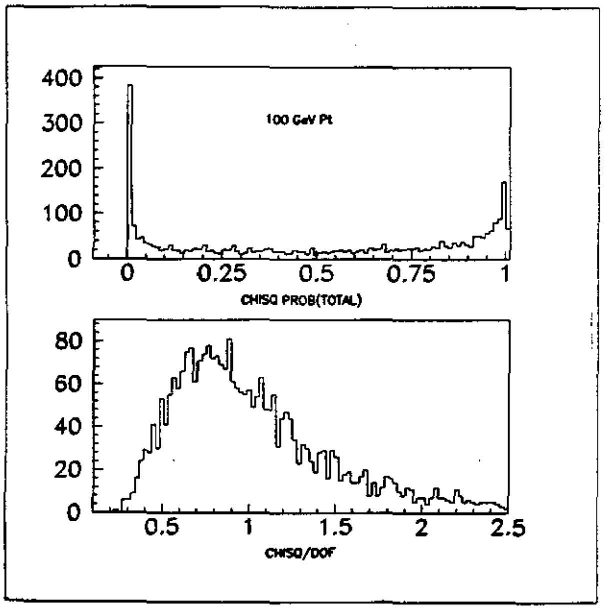

672

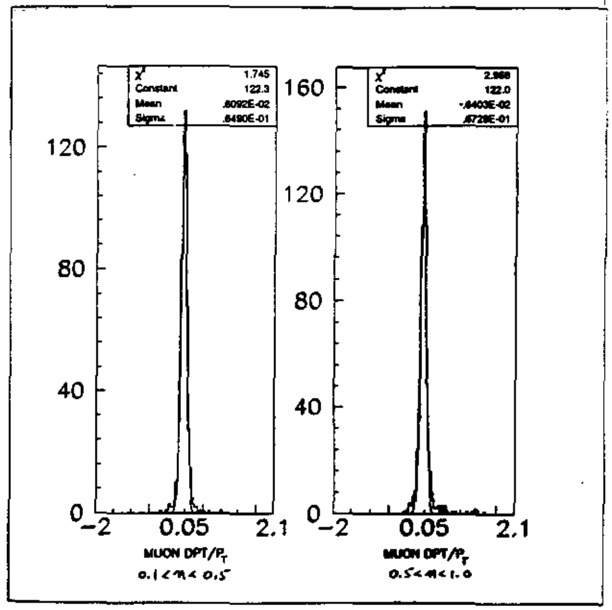

500 GeV P_T,
WITH TWO TRACK

673

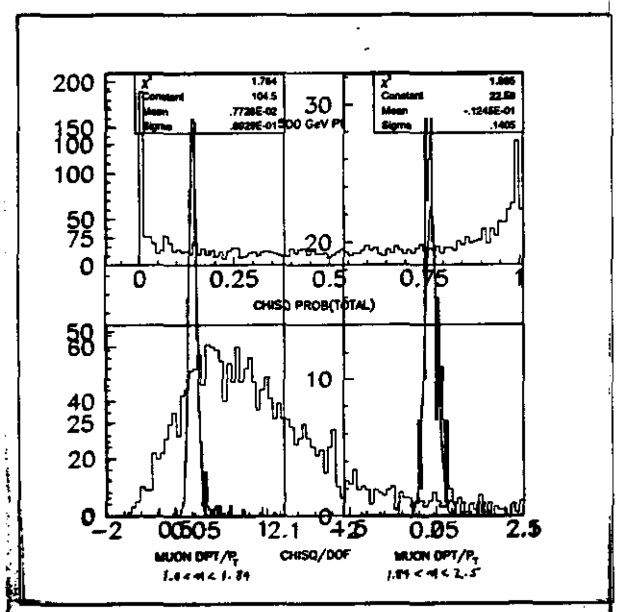

500 GeV P_T,
WITH TWO TRACK

674

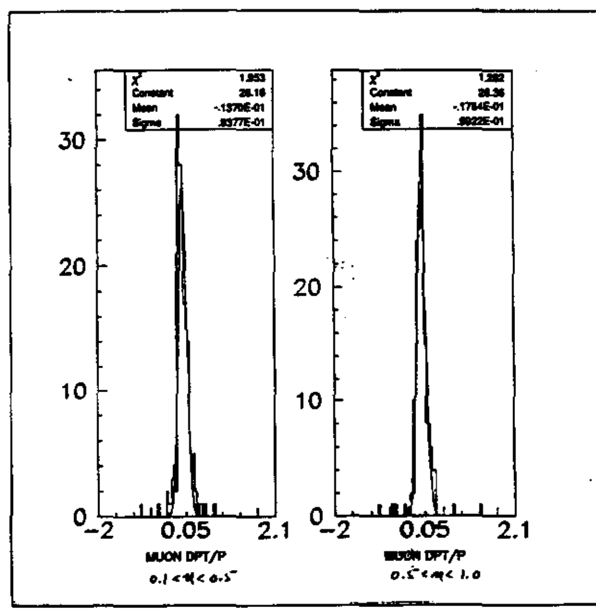

1 TeV P_T

675

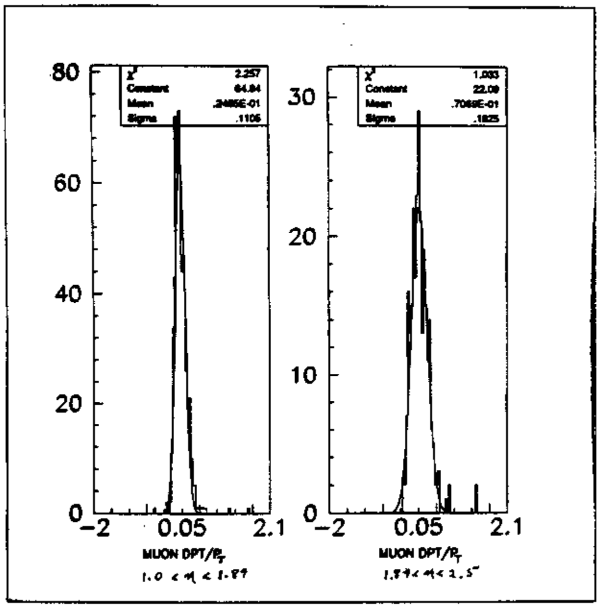

1 TeV P_T

676

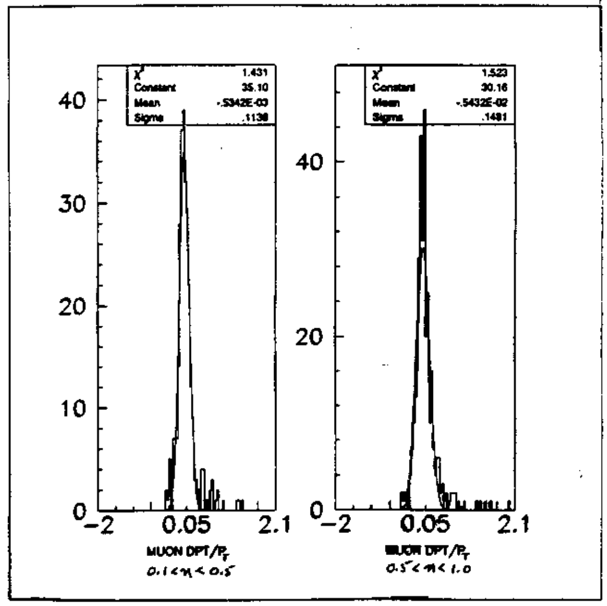

1 TeV P_T ,
with two track

677

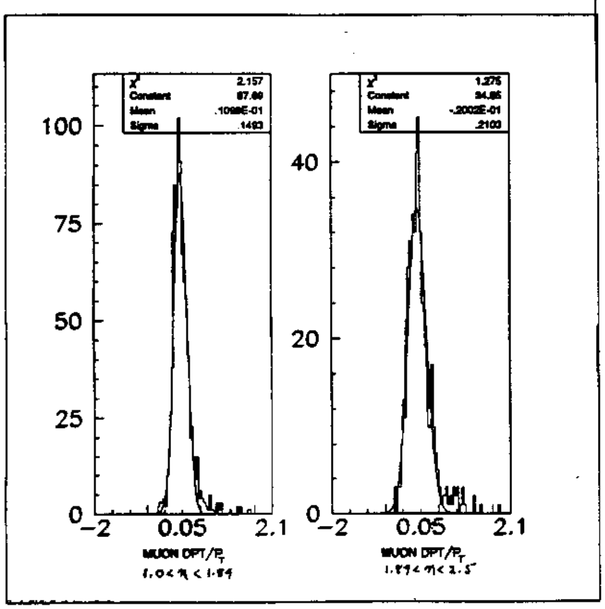

1 TeV P_T ,
with two track

678

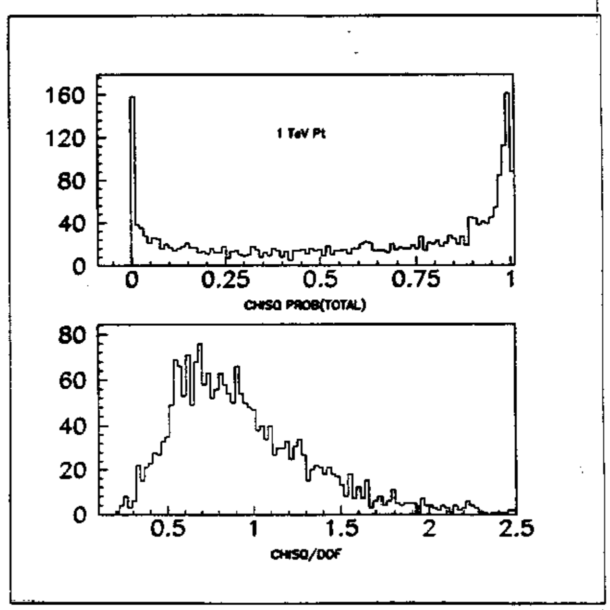

679

(9)

Try To Calculate Resolution:

For 1 Tev P_T => No Mult-Scatter
=> % Energy loss is negligable

$$\Delta S = \sqrt{\left(\frac{\partial S}{\partial x_i}\right)^2 \Delta x_i^2} = \sqrt{\left(\frac{\partial S}{\partial x_i}\frac{\partial x_i}{\partial x_{ij}}\right)^2 \Delta x_{ij}^2}$$

i = Superlayer j = Plane

$$S = \left[\frac{\bar{x}_1 + \bar{x}_3}{c} - \bar{x}_2\right]_{\text{Bend Plane}}$$

$$\Delta S^2 = \sqrt{\frac{\Sigma \Delta_{1j}^2}{c^2 N_1^2} + \frac{\Sigma \Delta_{2j}^2}{N_2^2} + \frac{\Delta_{3j}^2}{c^2 N_3^2}}$$

$$\frac{\Delta P}{P} = \frac{8\, \Delta S\, P}{.3 \times B \times l^2}$$

=> Barrel (Take $\bar{\Delta} \sim 70\mu m$) => $\frac{\Delta P}{P} \sim 7.3\%$ (9.5)
$\theta = 60°$

680

Endcap (" $\bar{\Delta} \sim 62\mu m$) => $\frac{\Delta P}{P} \sim 14\%$ (13.9)
$\theta = 20°$

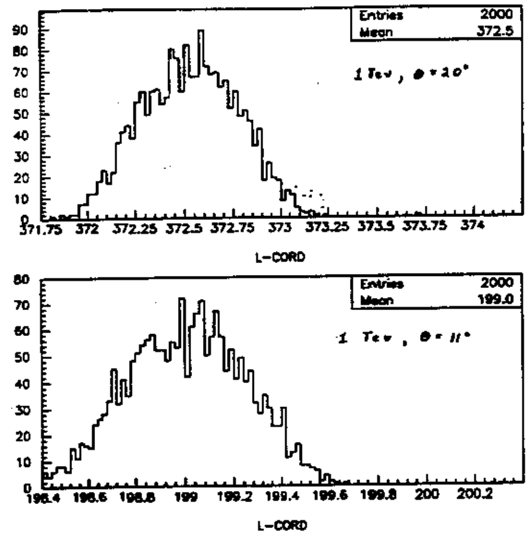

681

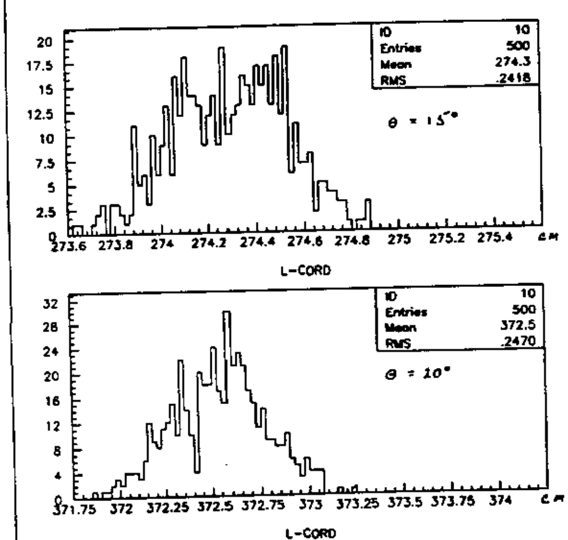

682

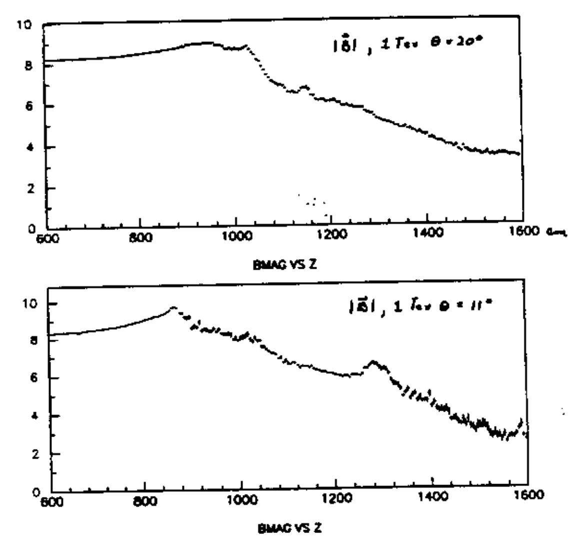

683

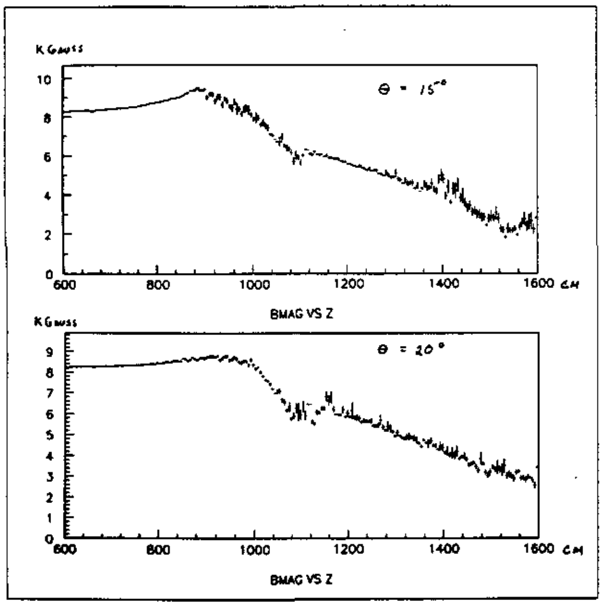
K Gauss
10
8
6
4
2
0
600
800
1000
1200
1400
1600 cm
BMAG VS Z
K Gauss
9
8
7
6
5
4
3
2
1
0
600
800
1000
1200
1400
1600 cm
BMAG VS Z

684

JETS IN GEM

- SOURCES OF RESOLUTION
- CURRENT CALORIM., + OPTION
- MIXTURE DESCRIPTION (UARMIX)
- SEGMENTATION
- π + JET (TDR) RESPONSE
- WEIGHTING SCHEMES
- NEW APPROACH TO JETS
  (RESULTS BY NEXT WEEK)
- BAD SPOTS IN THE DETECTOR.
  (WATCH THOSE HAYSTACKS)

M. SHOPE
UNIV. OF ARIZONA
MAY 11, 1993

E_T Resolution

Sources

1) Hadronic Energy Resolution
   (e/h + ...)
2) Angle resolution
3) Dead material (EM/had separate manifestations)
4) Lack of coverage (beam hole, η = 1.1 cc/ec transition, ...)
5) Shower leakage out the back
6) p_T cross-over
7) Dead cells/hot cells
8) Weighting schemes
9) Extra min-bias events on top of trigger event

688

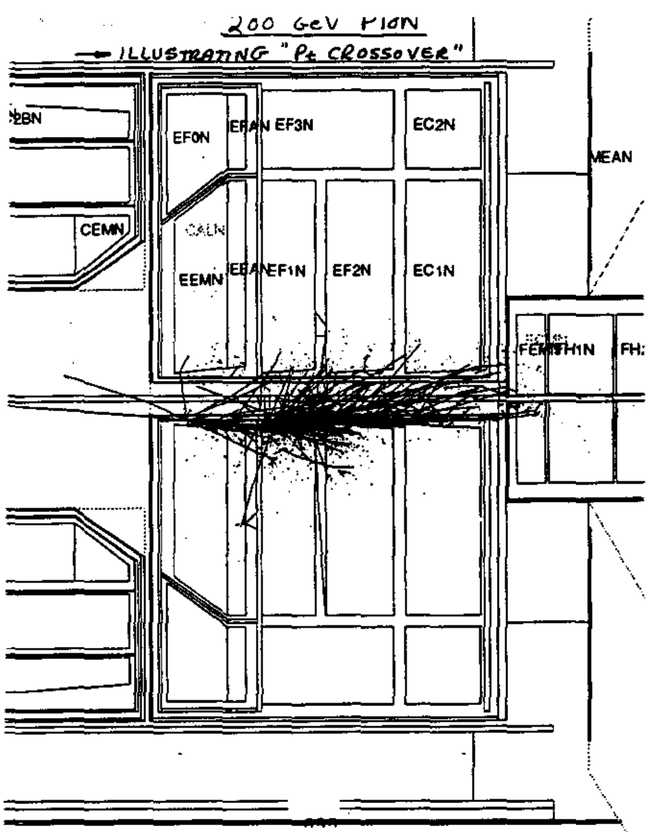

689

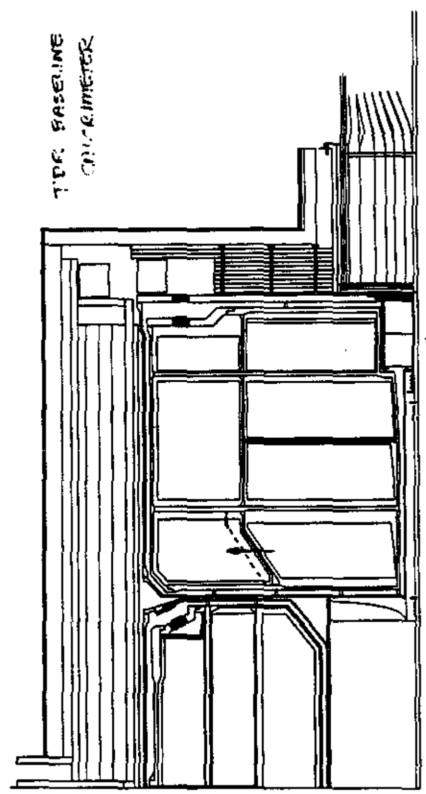

691

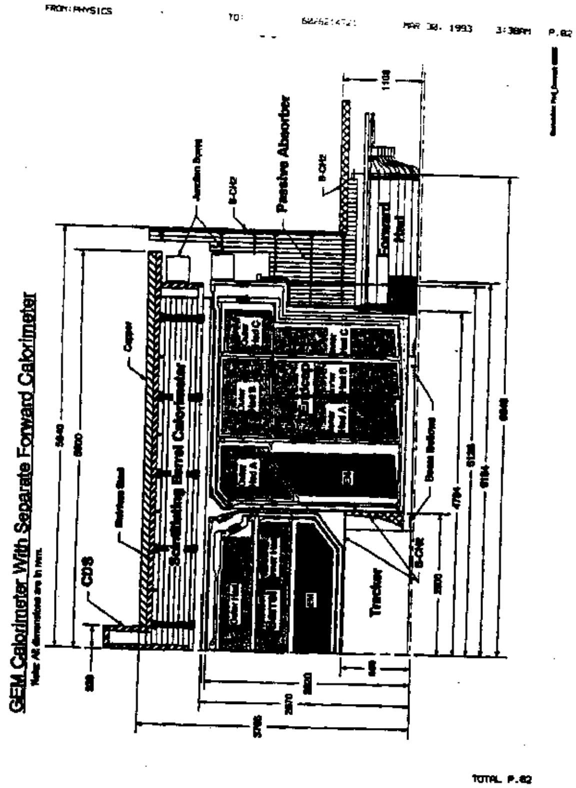

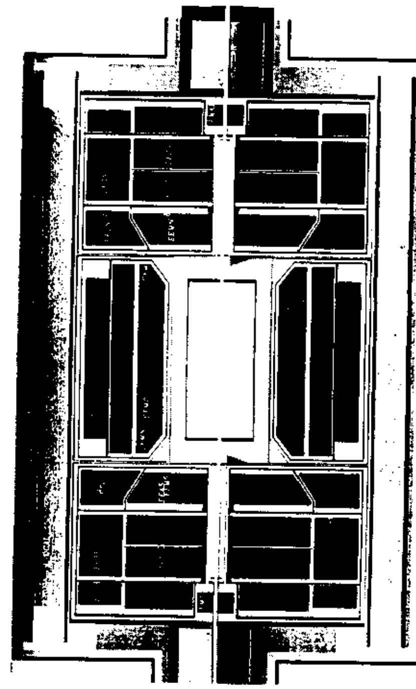

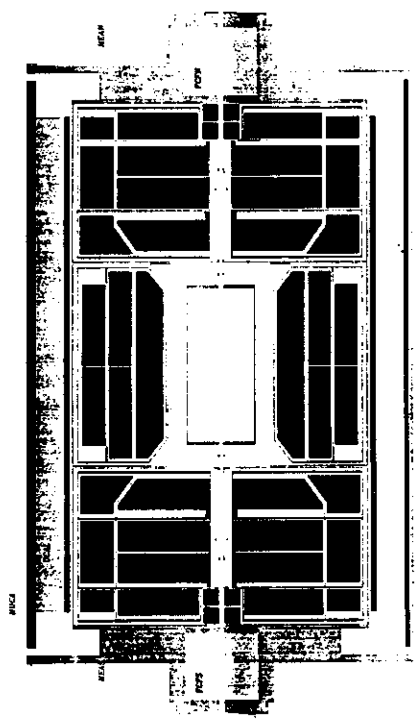

SOFTWARE CELLS
"CAL TOWERS"

⇨ TO SPEED UP GEANT, REDUCE THE NUMBER OF VOLUMES.

⇨ USING MIXTURES ALLOWS VOLUMES TO FOLLOW ONLY "MAJOR" SEAMS AND CRACKS.

IN THE CURRENT FCAL SIMULATION:

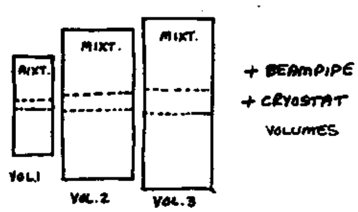

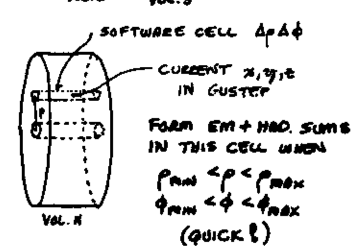

⇨ AVOIDS 100's OF GEANT VOLUMES.

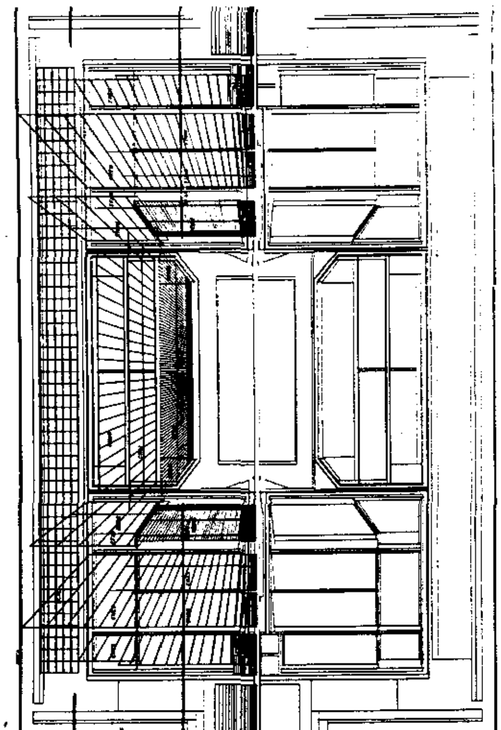

696

ENERGETICS OF SAMPLING CALORIMETERS

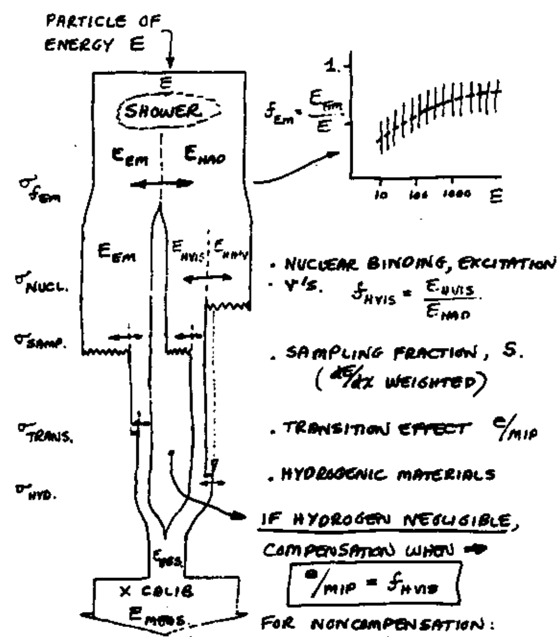

- NUCLEAR BINDING, EXCITATION
- ν's. $f_{HVIS} = \frac{E_{HVIS}}{E_{HAD}}$
- SAMPLING FRACTION, S. (dE/dx WEIGHTED)
- TRANSITION EFFECT $e/_{MIP}$
- HYDROGENIC MATERIALS

IF HYDROGEN NEGLIGIBLE, COMPENSATION WHEN ⇒ $e/_{MIP} = f_{HVIS}$

FOR NONCOMPENSATION: $e/h = e/_{MIP} / f_{HVIS}$ ($e/_S = 1.6$)

697

ENERGETICS OF GEANT MIXTURES

UA2MIX TECHNIQUE.

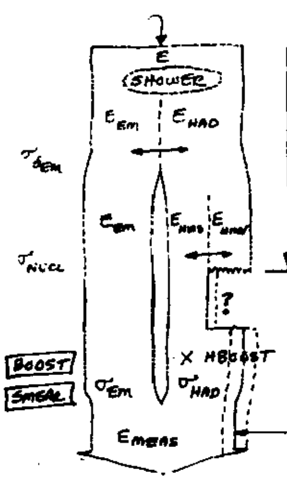

SIMULATES REAL BEHAVIOR TO HERE.

- NO SAMPLING FRACTION, S.
- NO TRANSITION EFFECT, $e/_{MIP}$.
- PROPER SIM. OF HYDROGENIC MATERIALS ⇒ "CALOR89." (GCALOR)

① EM ENERGY REMAINS CALIBRATED.

② COMPENSATION ⇒ HBOOST = $1/f_{HVIS}$ (~2)

NON COMPENSATING ⇒ HBOOST = $(h/e)/f_{HVIS}$ (EG. $\frac{2}{1.6}$)

③ σ_{EM} INCLUDES σ_{SAMP}, σ_{TRANS} ⇒ "TEST BEAM"

σ_{HAD} INCLUDES σ_{SAMP}, σ_{HYD} ⇒ "TESTBEAM ⊖ σ_{NUCL}"

698

MIXMAKER

```
***** MAKING MIXTURE FROM PROPORTIONS BY   VOLUME:  LKREM_1.0PB4
 # OF COMPS:    5  DENSITY:     4.190  SAMP.FRAC:     0.394
 RAD.LEN.(CM):     2.064  ABS.LEN.(CM):   37.328 DEDX:     1.350
        COMPONENT              INPUT         FRAC BY WT        INDX
SS                             0.04000        0.12686           13
G10                            0.01600        0.01385          108
LEAD                           0.10000        0.45451           22
KAPTON                         0.04000        0.01778          107
LIQUID_KRYPTON                 0.40000        0.38699           17

     ELEMENTS BY FRACTIONAL WEIGHT.  # =      7
          SS                          0.126863      13
          LEAD                        0.454511      22
          LIQUID_KRYPTON              0.386995      17
          CARBON                      0.019963       6
          HYDROGEN                    0.003358       2
          SILICON                     0.003885      10
          OXYGEN                      0.004426       8
  SIG-EM  SIG-HAD  CTERM   CNOISE   BOOST  ETOH:
 0.0600  0.6000  0.0040 25.0000  2.2200  1.8000

***** MAKING MIXTURE FROM PROPORTIONS BY   VOLUME:  LKRHAD_9CUS
 # OF COMPS:    4  DENSITY:     7.383  SAMP.FRAC:     0.051
 RAD.LEN.(CM):     1.744  ABS.LEN.(CM):   18.173 DEDX:     1.411
        COMPONENT              INPUT         FRAC BY WT        INDX
COPPER                         0.93400        0.15889           15
COPPER                         4.50000        0.76554           15
G10                            0.50000        0.02052          108
LIQUID_KRYPTON                 1.20000        0.05505           17

     ELEMENTS BY FRACTIONAL WEIGHT.  # =      6
          COPPER                      0.924431      15
          LIQUID_KRYPTON              0.055046      17
          SILICON                     0.005756      10
          OXYGEN                      0.006558       8
          CARBON                      0.007027       6
          HYDROGEN                    0.001182       2
  SIG-EM  SIG-HAD  CTERM   CNOISE   BOOST  ETOH:
 0.1600  0.6000  0.0200120.0000  2.0100  1.6000
```

INPUT

OUTPUT

EXPLICIT HYDROGEN FOR NEUTRON STUDIES

699

GEANT SETTINGS FOR FCAL SIMULATION:

- VERSION ~~3.14TE~~ 3.15
- GHEISHA
- STANDARD CUTS
  - EM 1.0 MeV
  - HADRONIC 10. MeV
  - } O.K. NO CUT DEPENDENCE.
- MIXTURE W/LAr (FOR EXAMPLE)

		f_{VOL}	f_{WT}	
ρ = 18.24	TUNGSTEN	.841	.937	ρ = 17.31, λ = 11 cm
	NICKEL	.067	.034	
	COPPER	.029	.015	
	STAINLESS	.021	.009	
	LIQ. ARGON	.042	.003	

- $\vec{B}$ FIELD .8 TESLA. (PURE SOLENOIDAL)

NOTE: $\lambda_{GEANT} = \lambda_{PDG} \pm 10\%$

THIS NEEDS INVESTIGATION?

70[illegible]

PARAMETER VALUES IN CURRENT STUDY

MIXTURE	$f_{HAD\ VIS}$ (GEMFAST)	(NEW)	e/h	e/h (WIGMANS)
CC				
ACC LKr Pb	.450	(.454)	1.8	
FH LKr Pb	.498	(.461)	1.6	(1.46)
EC				
ACC LAr Pb	.500	(.472)	1.8	
FH LAr Cu	.500	(.465)	1.8	
FC				
FC LAr W	.515	(.454) (PETER LOCH SIMULATION)	1.4	
FC HAD SCILIQ	—	(.420)		

70[illegible]

50 GeV PIONS

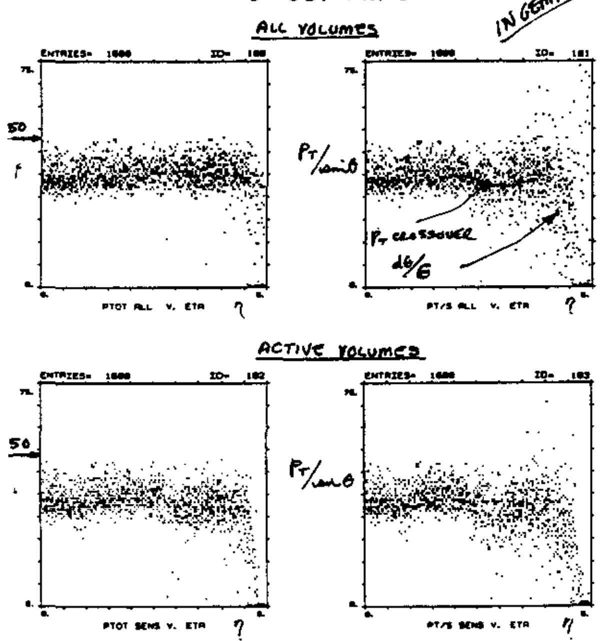

(NO SMEARING)

702

50 GeV PIONS

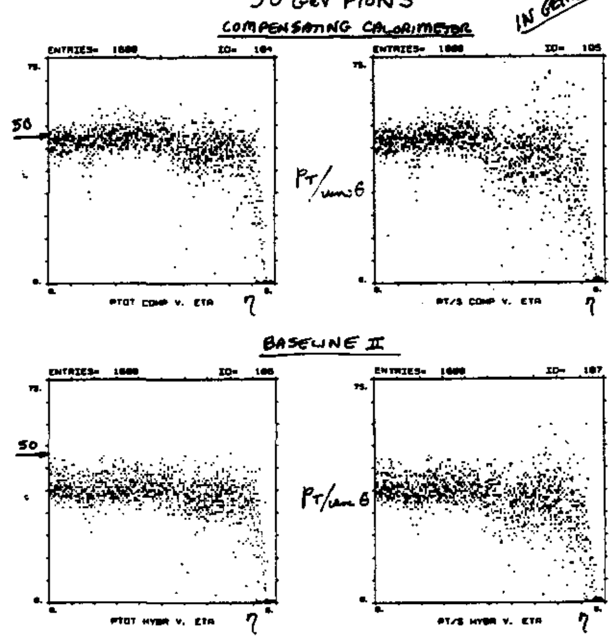

(NO SMEARING)

703

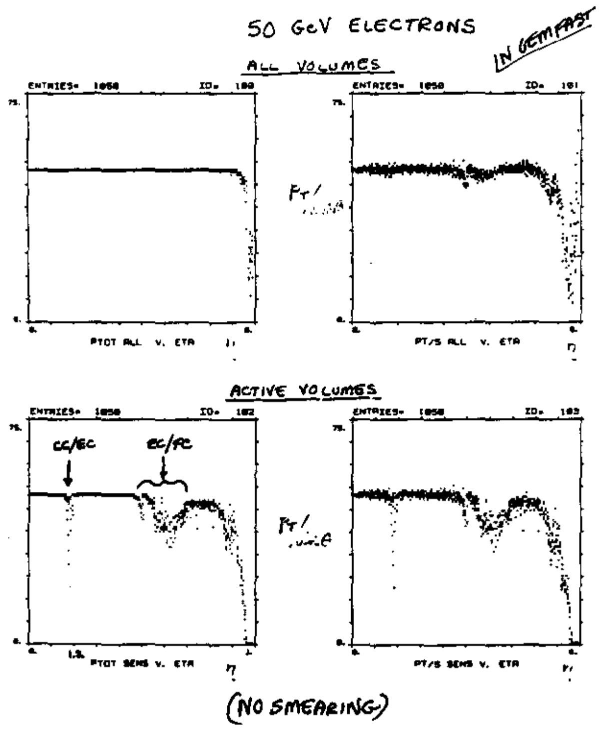
50 GeV ELECTRONS
IN GEMFAST
ALL VOLUMES
PTOT ALL V. ETA
PT/S ALL V. ETA
ACTIVE VOLUMES
CC/EC
EC/FC
PTOT SENS V. ETA
PT/S SENS V. ETA
(NO SMEARING)

704

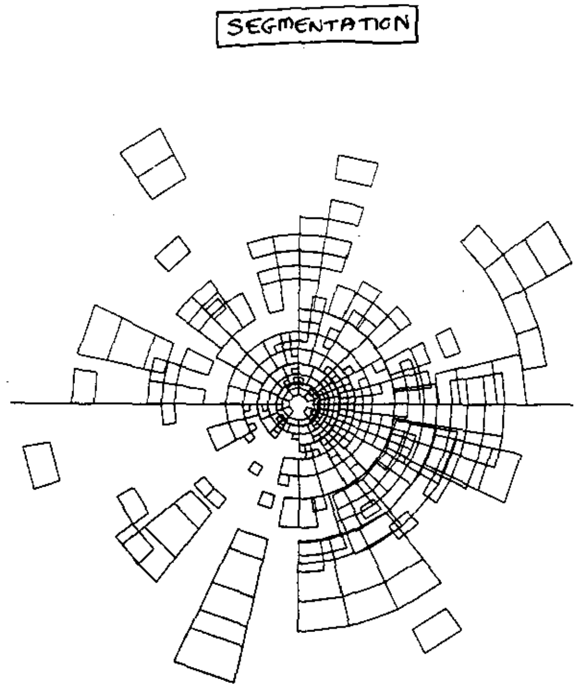
SEGMENTATION

705

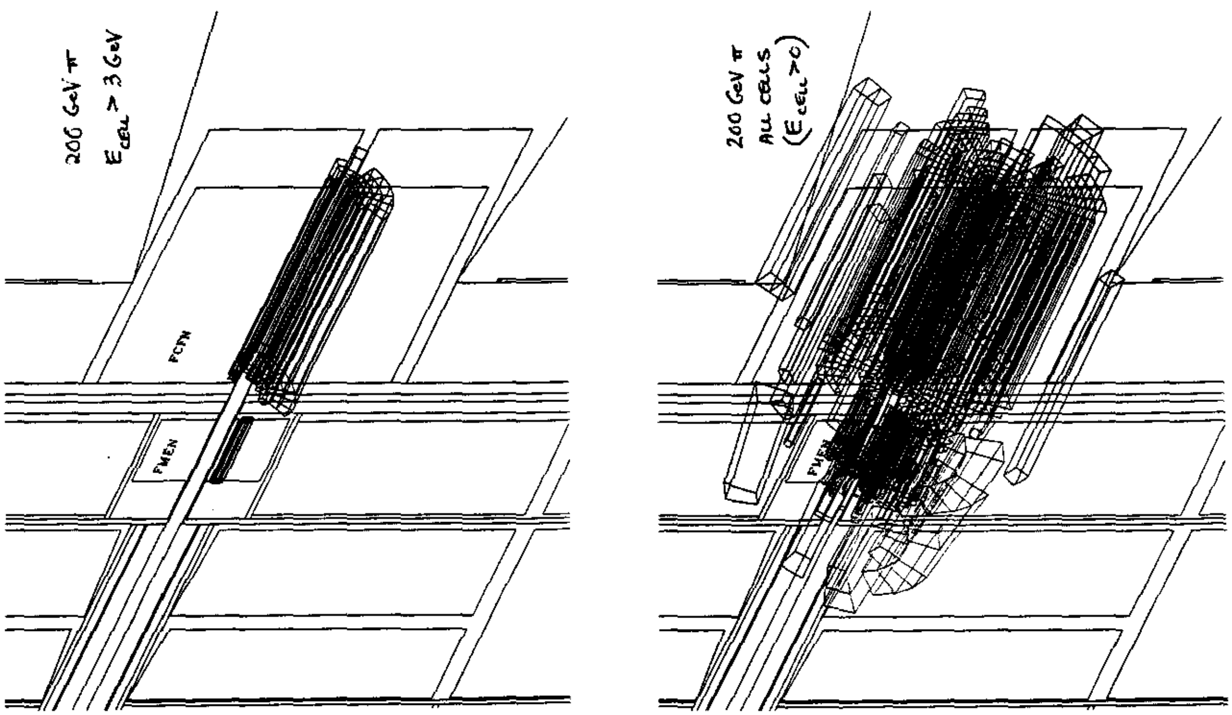
200 GeV π
E_{CELL} > 3 GeV
FMEN
200 GeV π
ALL CELLS
(E_{CELL} > 0)

706

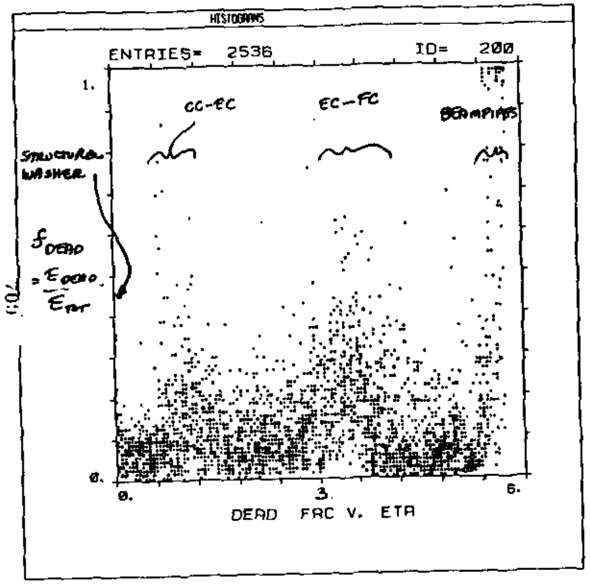

BASELINE
50 GeV π's

EFFECT OF
DEAD MATERIALS

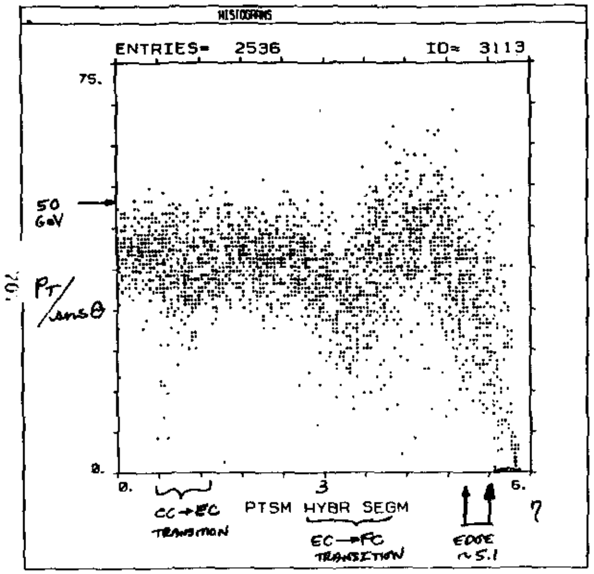

BASELINE
MAR 10, 1993

50 GeV π
CURRENT BASELINE
(2 DAYS OF
STATISTICS)

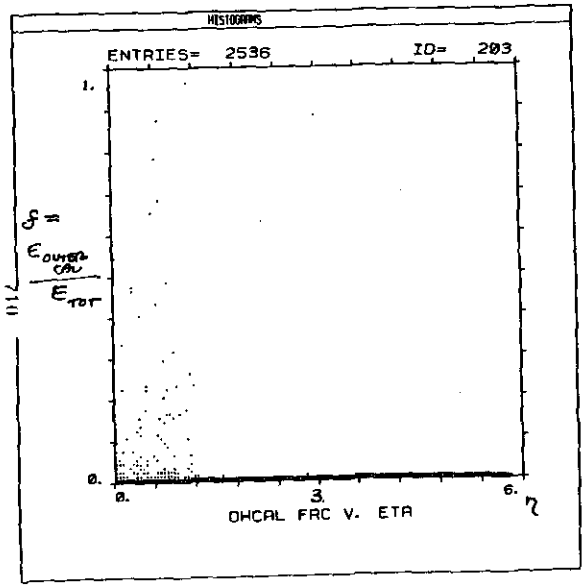

BASELINE
50 GeV π

ENERGY IN OUTER
CALORIMETER.

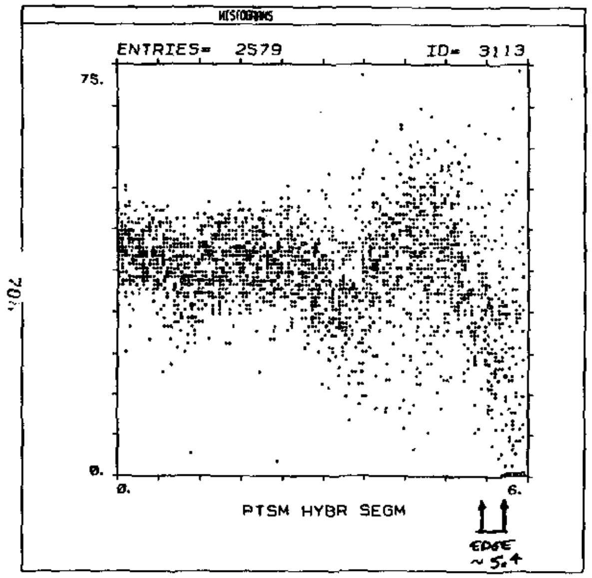

SMALL PIPE

50 GeV π
SMALLER BEAMPIPE

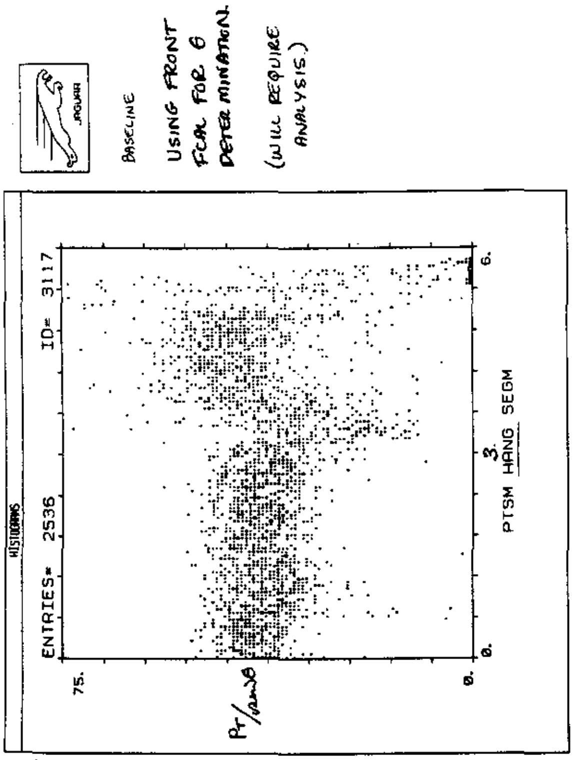

711

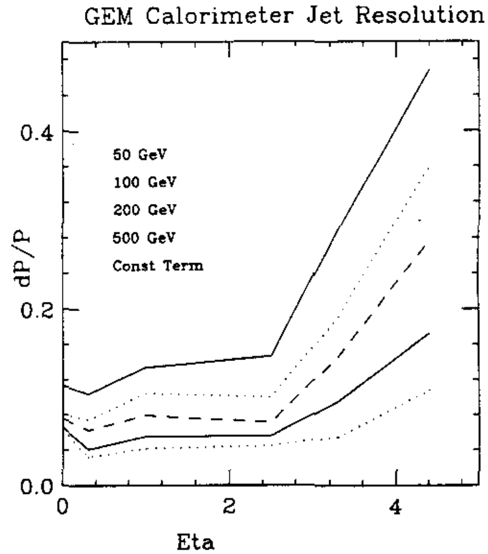

712

WEIGHTING SCHEMES- 2 LAYER AND n LAYER

FOR SINGLE HADRON SHOWERS:

- ENERGY INDEPENDENT WEIGHTS CAN IMPROVE LOSS OF RESOLUTION DUE TO e/h DIFFERING LAYER TO LAYER
- ENERGY DEPENDENT WEIGHTS FIX THE ABOVE, AND NONLINEARITY DUE TO $f_{em}(E)$

FOR JETS:

SAME AS ABOVE, BUT ADDITIONAL IMPROVEMENT BECAUSE FLUCTUATIONS TO PROMPT π^0's APPEAR AS ENERGY IN "1ST" OR "EARLY" LAYER(S).

WEIGHTING SCHEME USED HERE:

(WOMERSLEY, MOORE, SAVIN)

RECONSTRUCTED ENERGY: $E_{RECON.} = \sum_{l=1}^{L} W_l E_l$

L = # OF LAYERS

W_l = WEIGHT FOR LAYER l. IF $W_l = f(E_{RECON})$, MUST ITERATE.

E_l = ENERGY OBSERVED IN LAYER l

713

HOW WEIGHTS ARE DETERMINED:

MINIMIZE: $\sum_{i=1}^{N\ EVENTS} (E_{TRUE} - E_{RECON})^2$

FOR SIMULATIONS: $E_{TRUE} = E_{GENERATED}$ (π, JET...)

IN REAL LIFE: $E_{TRUE} = E_{TESTBEAM}$ (π, P, ...)
OR
= "E_{JET}"

E_{JET} IS GOTTEN FROM
① TESTBEAM RUNS ON π, P, e, γ, ...
\+ ② APPLICATION OF A THEORETICAL FRAGMENTATION FUNCTION. (UNCERTAINTIES) [ISAJET, PYTHIA, ...]

LAYERS USED HERE: (EG.) ★ WEIGHTS ARE η DEPENDENT ★

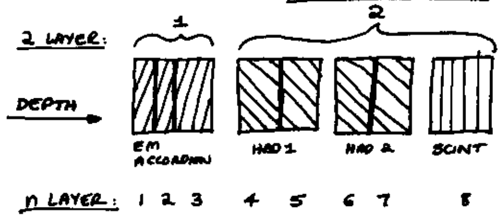

714

NOT CURRENT

JET ENERGY SCAN AT $\eta = 0$ (JETSET)
BASELINE II HYBRID

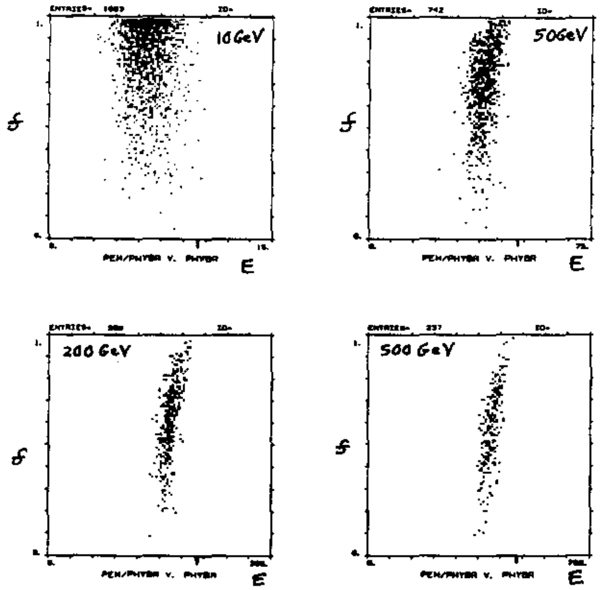

$f = \frac{\text{ENERGY IN EM SECTION}}{\text{TOTAL ENERGY}}$

715

TWO LAYER WEIGHTS USED FOR PIONS:

ETA	E INDEP	10.00	50.00	100.00	200.00	500.00
0.0100	1.2212	1.4058	1.3095	1.2493	1.1865	1.1655
	1.4183	1.4458	1.4502	1.4220	1.4420	1.4004
	1280	618	273	164	135	90
0.3000	1.2341	1.3978	1.2397	1.2387	1.2143	1.1888
	1.2917	1.2845	1.3674	1.3003	1.2755	1.2911
	1251	615	255	182	121	78
1.0000	1.2839	1.4892	1.3739	1.3266	1.2440	1.2186
	1.3697	1.4153	1.3666	1.3945	1.4014	1.3608
	1218	576	254	186	119	83
2.5000	1.2686	1.4530	1.3247	1.2833	1.2585	1.2057
	1.2965	1.3551	1.3496	1.3500	1.2883	1.2835
	1334	649	267	197	122	99
3.3000	1.7156	1.7321	1.8258	1.7107	1.8124	1.5880
	1.3200	1.5047	1.3864	1.3538	1.2854	1.3013
	1290	590	290	205	117	88
4.4001	1.1734	1.2086	1.1741	1.1638	1.1741	1.1490
	1.2602	1.5032	1.3604	1.3114	1.2674	1.2026
	1187	549	257	186	142	53

716

TWO LAYER WEIGHTS USED FOR JETS:

ETA	E INDEP	50.00	100.00	200.00	500.00
0.0100	1.1611	1.2689	1.2018	1.1493	1.0915
	1.5027	1.5181	1.5012	1.5070	1.5423
	923	359	271	181	112
0.3000	1.1691	1.2803	1.1918	1.1557	1.1041
	1.3817	1.4788	1.4643	1.3854	1.4030
	885	350	241	163	131
1.0000	1.2272	1.3931	1.3012	1.2308	1.1494
	1.5606	1.6207	1.6267	1.5980	1.5727
	961	363	256	206	136
2.5000	1.2376	1.4467	1.3080	1.2544	1.1496
	1.4494	1.5179	1.4866	1.4002	1.4789
	958	380	273	173	132
3.3000	1.6862	1.3032	1.6265	1.5945	1.8760
	1.5514	2.0959	1.7333	1.6171	1.4439
	942	338	275	194	135
4.4001	1.2771	1.5503	1.4873	1.3421	1.1677
	1.4042	1.4556	1.4688	1.4117	1.3483
	961	376	277	185	123

717

NEW APPROACH, FOR MORE REALISTIC JETS

IN ORDER TO GENERATE JETS WITH REALISTIC DISTRIBUTIONS OF η, p, AND Q^2:

1. RUN ISAJET TO GENERATE QCD (TWOJET) EVENTS WITH p_T IN NARROW RANGES: 100 – 101, 500 – 501, etc.
2. RUN A FIXED CONE JETFINDER, WITH $R_{cone} = .7$ AND P_T MIN JET $= 15$ GeV, TO FIND JETS FROM PARTICLE 4-VECTORS.
3. REMOVE ALL PARTICLES ~~WITHIN~~ BEYOND $R = .9$ OF A JET (ALLOWS FOR SPLASH-IN).
4. PROPAGATE JET PARTICLES THROUGH DETECTOR (GEANT)
5. RUN JETFINDER ON CALORIMETER CELLS. MATCH UP WITH GENERATED JETS, AND PLOT $\Delta\eta$ VS η, $\Delta\phi$ VS η, $\frac{\Delta E}{E}$ VS η, $\frac{\Delta P_T}{P_T}$ VS η, etc.

APPLY WEIGHTS HERE.

718

UNWEIGHTED

P_T hard scatt = 100 GeV/c

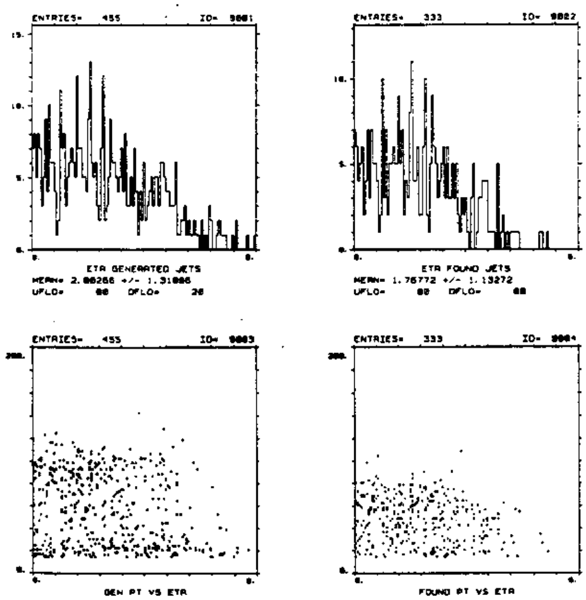

719

P_T hs = 100 GeV/c

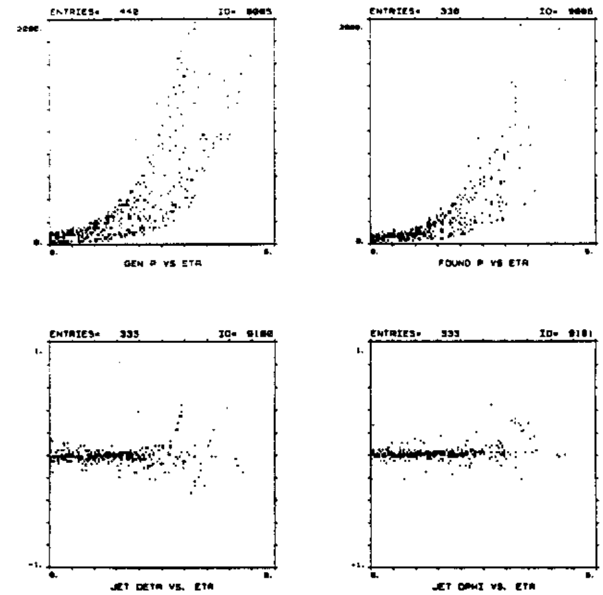

720

P_T hs = 100 GeV/c

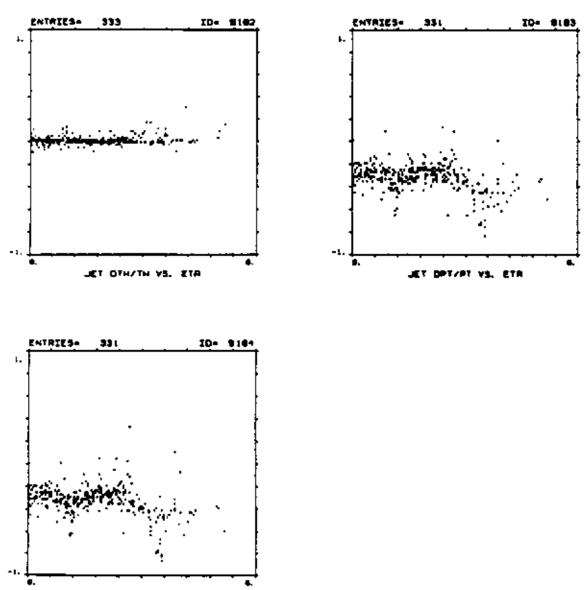

721

UNWEIGHTED

$P_{T_{hs}}$ = 500 GeV/c

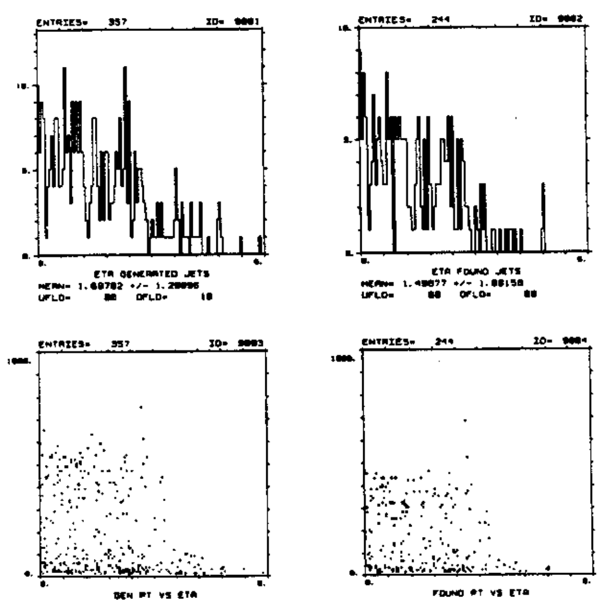

722

$p_{T\,hs}$ = 500 GeV/c

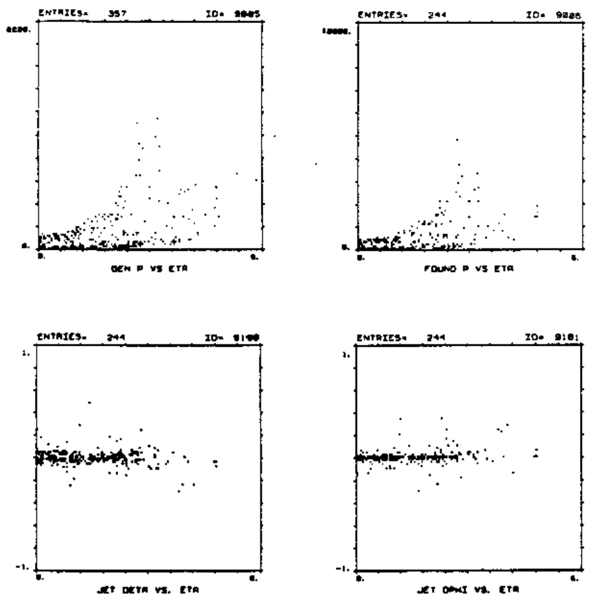

$p_{T\,hs}$ = 500 GeV/c

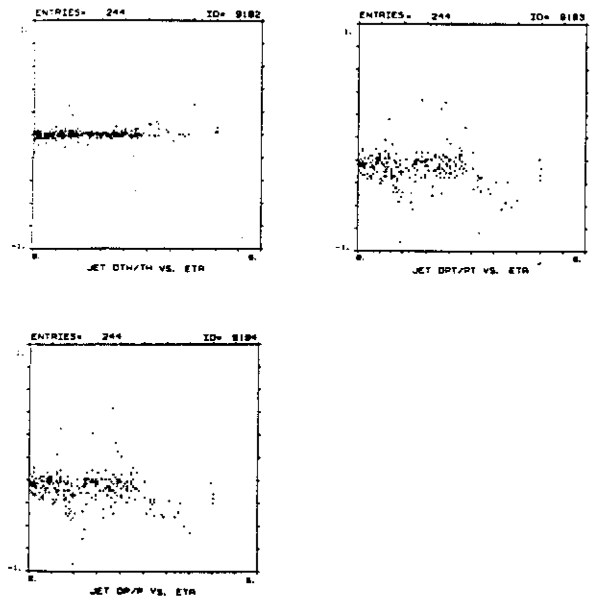

72.

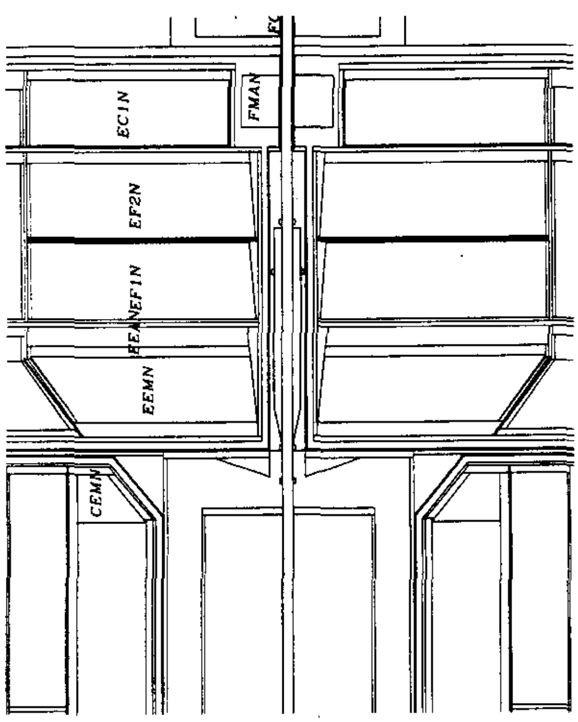

72

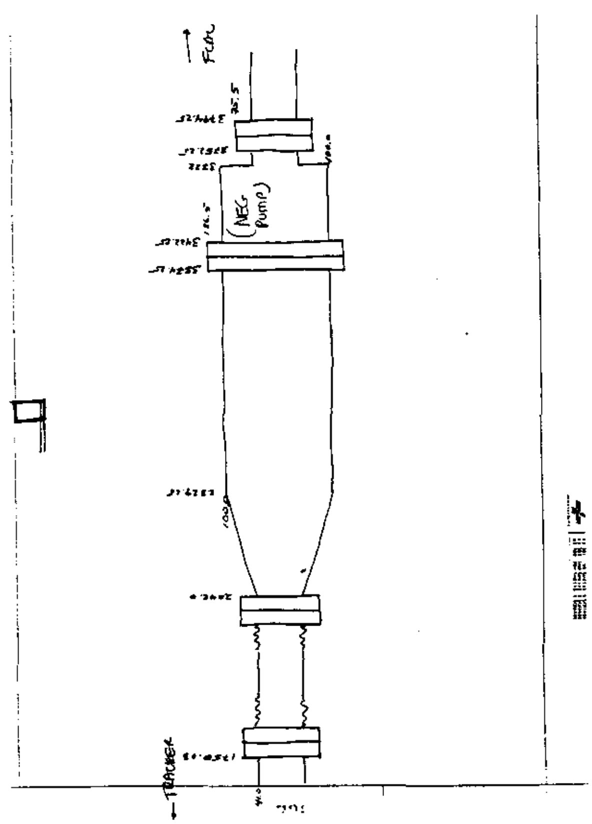

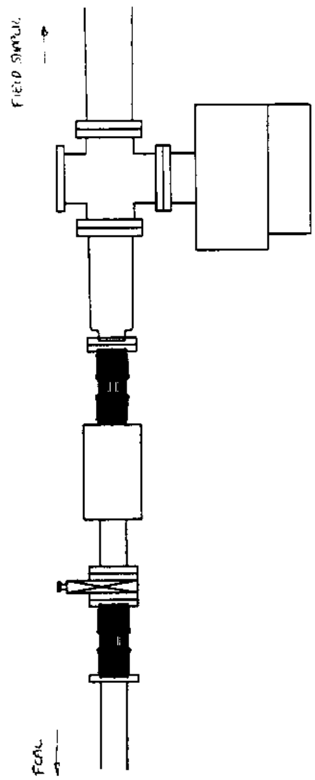

727

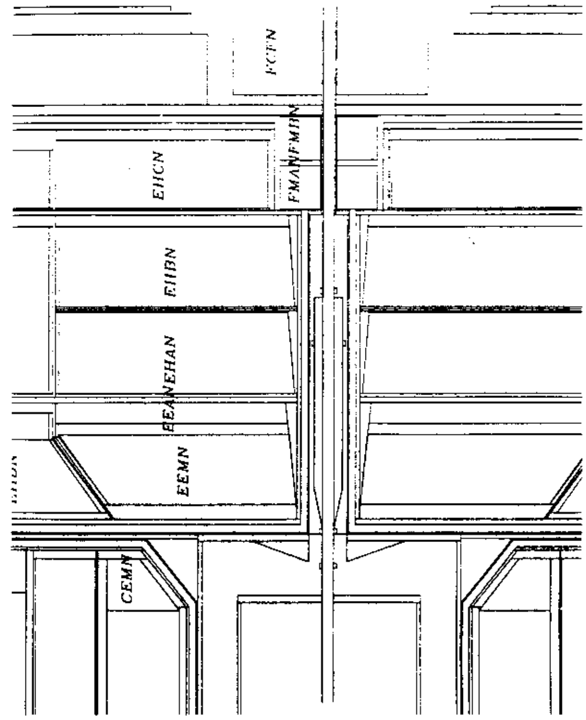

728

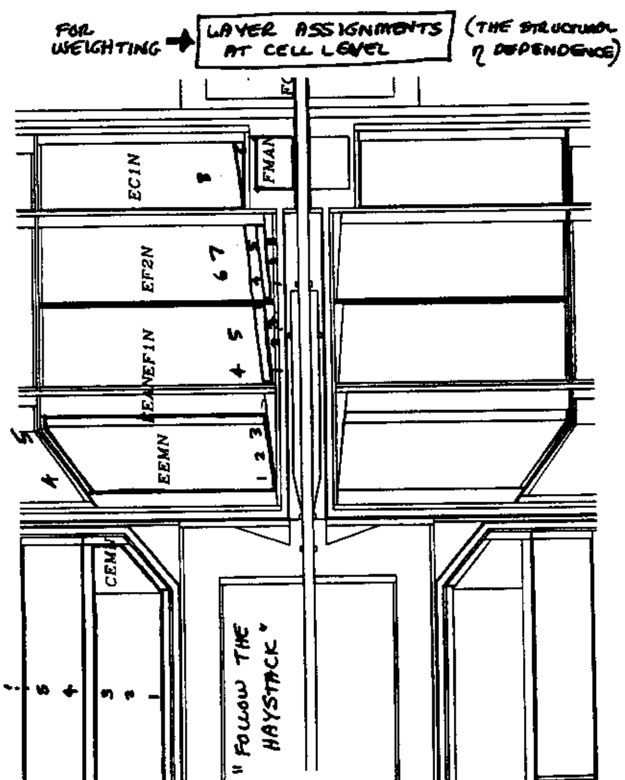

729

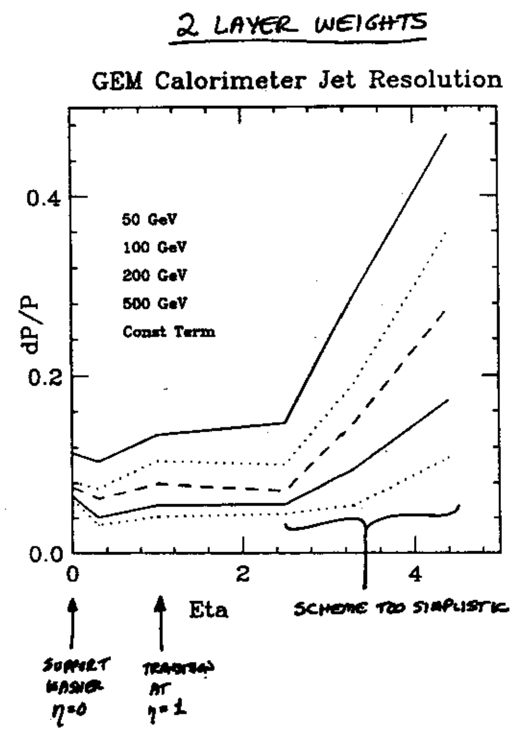

730

GEM FCal Technology Choice

Options

	TDR	Opt 1	Opt 2	Opt 3	...
"EM"	LAr	LAr	QF	LAr	
Hadronic	LScint	QF	QF	LAr	

'93 Beam Tests

LAr (EM)	BNL → CERN	UAz
LScint (Had)	BNL	TA&M
QF (Had)	BNL	Fairfield/ORNL
QF (?)	CERN	Gorodetsky

Other R&D

→ High Rate/Rad Damage — LAr: UAz; QF: ORNL

Time Scale of Decision

Was to be Fall '93

In time for Fermilab tests in '97

731

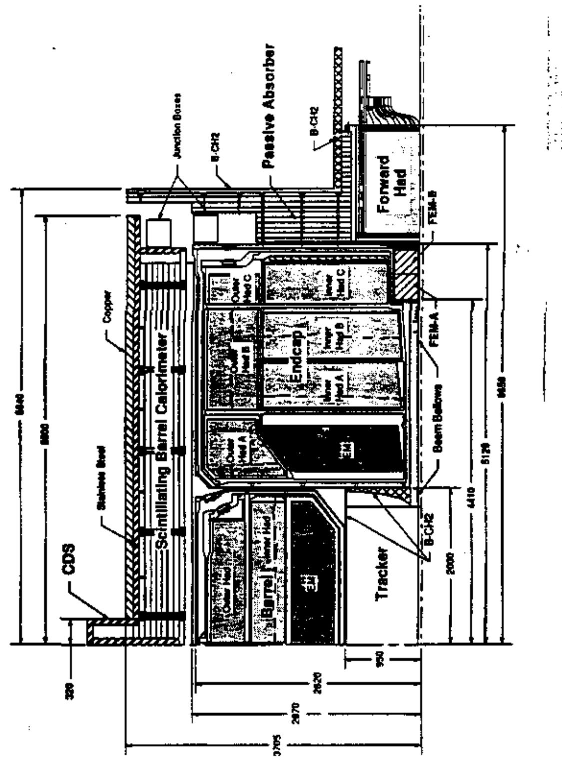

732

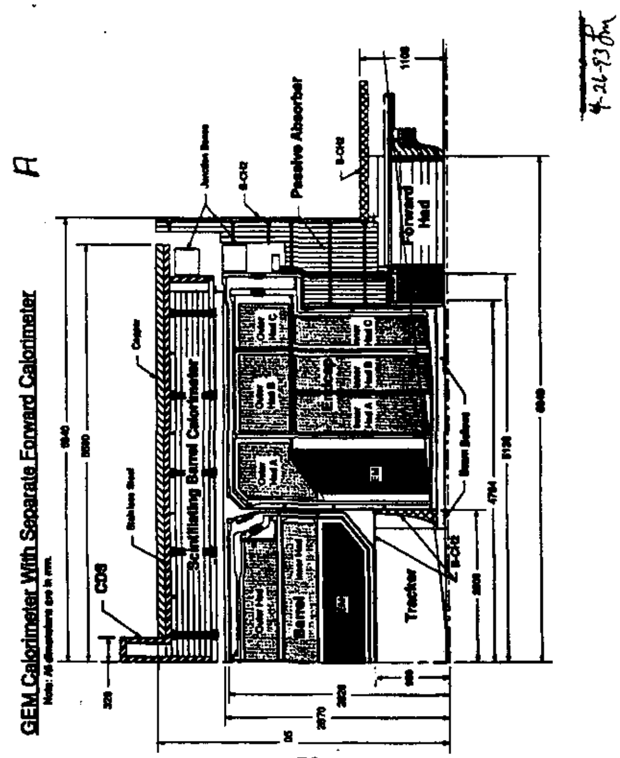

GEM Calorimeter With Separate Forward Calorimeter

Note: All dimensions are in mm.

733

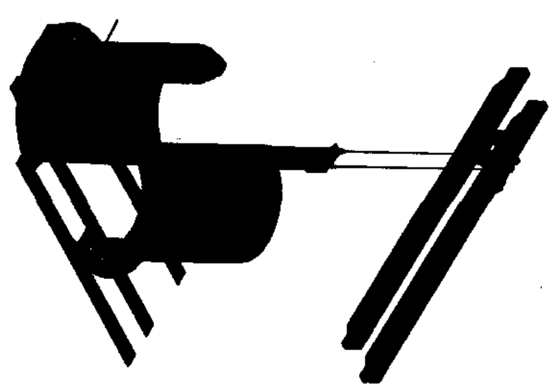

734

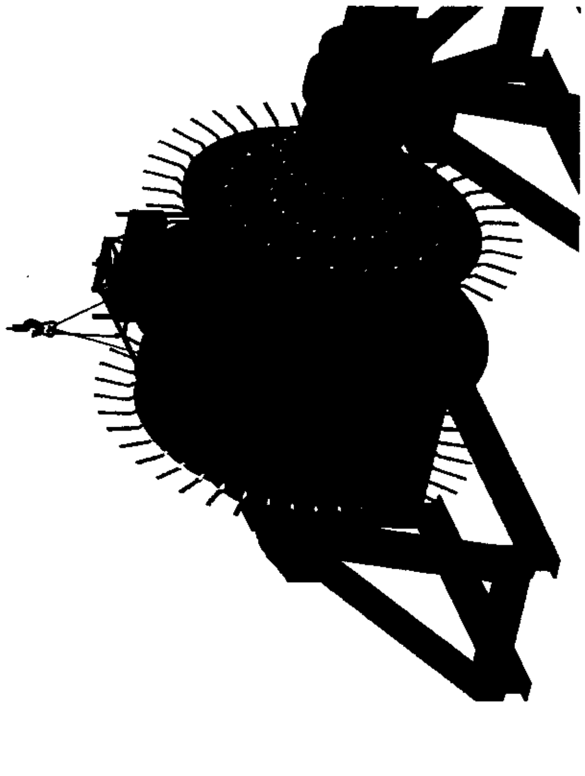

735

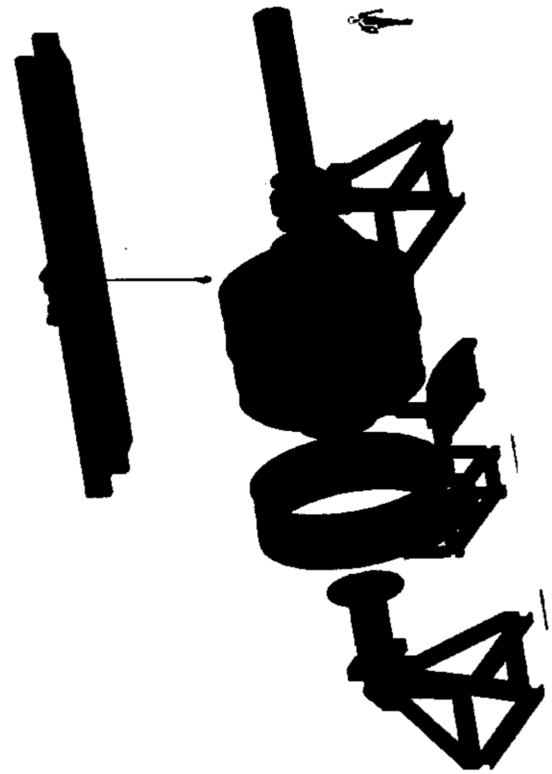

736

JET RESOLUTION
CONCLUSIONS

① 2 LAYER WEIGHTING SCHEMES GET THE DESIRED JET RESOLUTION, BUT ONLY IN THE MOST UNIFORM PART OF THE CALORIMETER.

② n LAYER WEIGHTS ARE BEING SET UP FOR A TEST AT ALL η, BUT ARE TRICKY TO IMPLEMENT. RESULTS: 1-2 WKS. (BEFORE PAC)

③ GREAT CARE IS NEEDED TO MINIMIZE DEAD MATERIAL IN THE FOLLOWING REGIONS:
- Ⓐ SUPPORT WASHER AT $\eta=0$
- Ⓑ $\eta=1$ TRANSITION
- Ⓒ $\eta=3-3.8$ CRYOSTAT WALLS !
- Ⓓ BEAMPIPE FLANGES, $\eta \approx 4$.

(④ FOR NEUTRONS, BEAMPIPE SHOULD FLARE A LITTLE IMMEDIATELY BEHIND FCAL.)

737

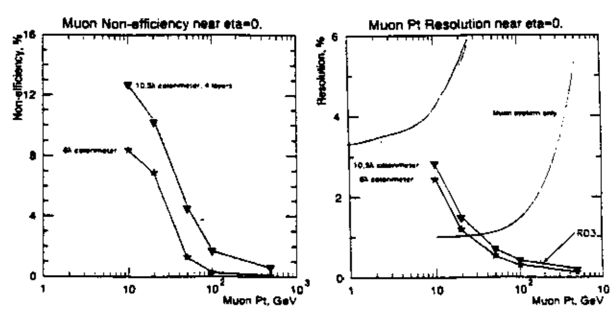

738

Fig 17

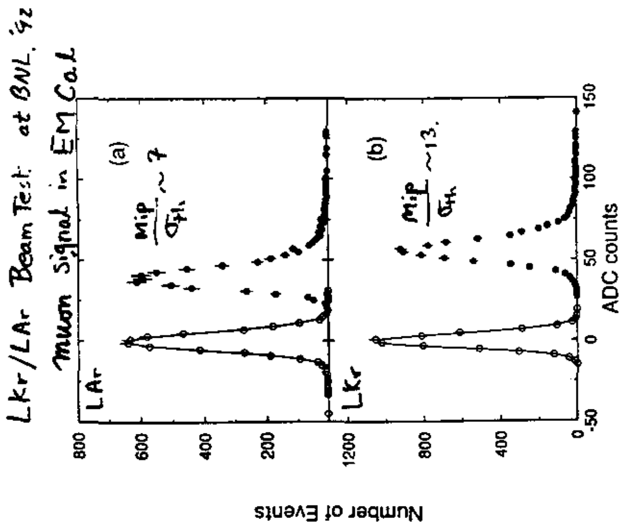

739

CALORIMETERS RESOLUTIONS FOR MUON ENERGY LOSS (TDR)

$$\frac{\sigma E}{E} \simeq \frac{a\%}{\sqrt{E}} + \frac{C}{E} \leftarrow \text{noise, pileup}$$

$\mathcal{L} = 10^{33} cm^{-2} s^{-1}$

		Thick (λ)	a%	C (MeV)/# towers
Barrel	EM	1.3	6	50 / 4
	LH	4.5	~35	180 / 2
	SH	4.5	?	22 / 1
	Absor.	1-2	–	–
Endcap	EM	1.5	8	90 / 4
	LH	10	~35	215 / 2
	Absor.	≲5	–	–

740

For $H^0 \rightarrow \mu^+\mu^-\mu^+\mu^-$

If require 3 well measured μs and identify the 4th μ using CT and Calorimeter

- Isolated high P_T track
- Isolated MIP in Calorimeter

Acceptance gain : 78%

50% ⟹ 89%

741

Reconstruction of high P_T fake muon tracks

- Conspiracy of random hits (n/γ) to form track segments (≥3 layers) in superlayers

rate for track segments in 3 superlayers	rate for track segments in 2 superlayers
$< 10^{-5}$ per $100 fb^{-1}$	$< 10^{-1}$ per $100 fb^{-1}$

- Catastrophic multiple scattering through the muon system by lower P_T tracks OR overlap of lower P_T track and random n/γ hits

Number of fake tracks per $100 fb^{-1}$

min P_T	track segments in 3 superlayers	track segments in middle, outer superlayer only	track segments in any 2 Superlayers
1 TeV/c	3	30	90
3 TeV/c	0.3	10	30

Rate of REAL high P_T muons of $P_T > 1 TeV/c$ is 2×10^4 per $100 fb^{-1}$

Fake high P_T tracks will contribute negligible background to high mass Z' [illegible] requirement) and W' [illegible]

742

e/jet rejection at 10^{34}

- current status : $R(e/\text{jet}) \sim 4\times10^{-4}$
  - Isolation
  - 50 GeV Track in front of 5x5

→ Good enough for $Z' \to e^+e^-$

($\sigma_{2jet} \sim 700\,pb$, $\sigma_{Z'} \sim 5\,fb$)

- For $W' \to e\nu$

($\sigma_{2jet} \sim 700\,pb$, $\sigma_{W'} \sim 30\,fb$)

need $R(e/\text{jet}) \lesssim 2\times10^{-5}$

743

SUMMARY

Recent Reductions in Central Tracker Thickness

Physics Analysis is Progessing (eg. B-jet tagging)

ASIC Preamp Prototype Tests Demonstrate Design Performance

18 cm Silicon Strip Tests Underway

747

To Forward Calorimeter Design Parameters

Konstantin Shmakov
ITEP/ORNL

May 11, 1993

1. **Standard Model E_T^{miss} Background and Detector acceptance**
2. **Requirements for δP/P, δE/E and δx**
3. **Cu or W absorber ?**
4. **How to go to small E_T^{miss} measurements? Veto in very forward region**

748

Standard Model Background

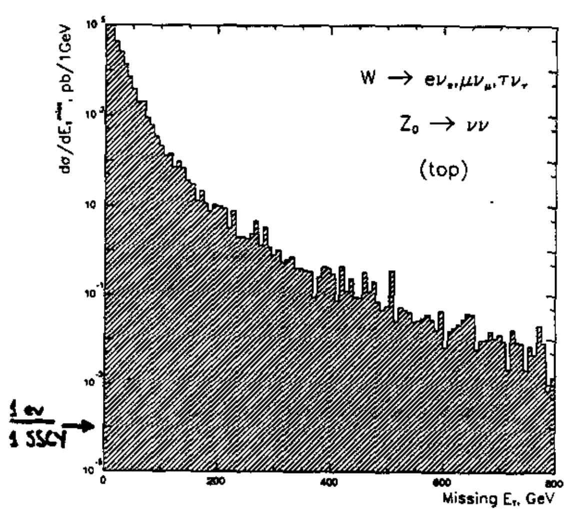

749

Missing $\not{E}_T$

Standard Model Background:

$Z_0 \to \nu\nu$ (~40%)
$W \to \mu\nu, e\nu$ (~30%)
$W \to \tau\nu$ (~20%)
t-quark (~10%)

- a few jets (2, 3)
- Low jet activity

Supersymmetric particles:

$\tilde{g} \to q\bar{q} + \tilde{\chi}_i^0$ (neutralino)
$\tilde{g} \to q\bar{q}' + \tilde{\chi}_i^\pm$ (chargino)
$\tilde{g} \to g + \tilde{\chi}_i^0$ (neutralino)

- many jets (>3)
- high jet activity

'Originally 1-2 orders of magn. below the Standard Model Background

750

Assumptions :

① Instrumental $\not{E}_T$ Background is to be below SM ν-s (not real events)

② The contribution of the Instrumental backgrounds can be considered independently from SM -ν-s background (no correlation)

751

SM Background and Detector acceptance

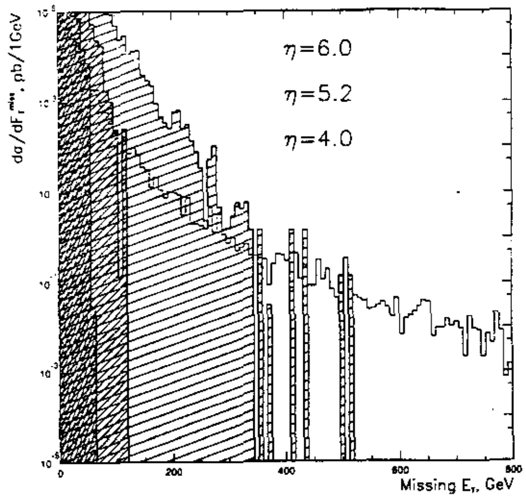

75?

Detector acceptance Background / SM Background

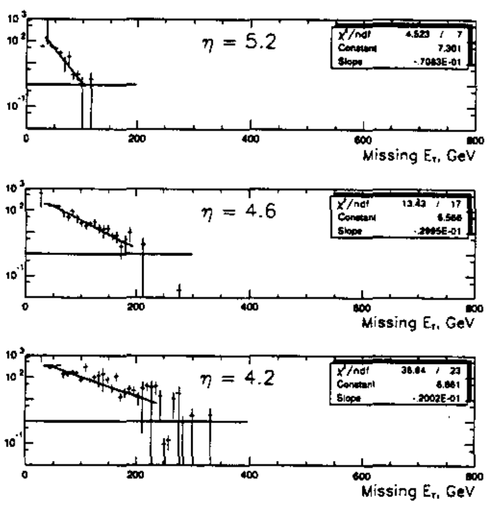

753

Missing Et of EQUAL Standtard Model and eta-Leakage contribution

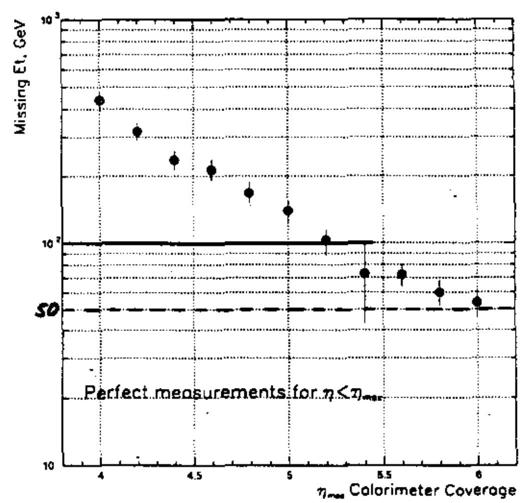

75·

- Acceptance above $\eta = 5.2$ is required to measure 100 GeV $\not{E}_T$ physics
  (current design $\eta = 5.5 - 5.7$)

- Acceptance above $\eta = 6.$ is required to measure 50 GeV $\not{E}_T$ physics

(what's the mass of lightest SUSY particle?)

755

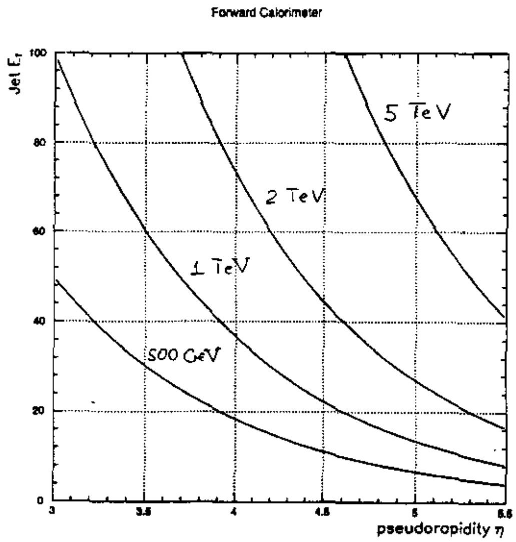

just $E_T = E \sin\theta \approx 2E\, e^{-\eta}$

756

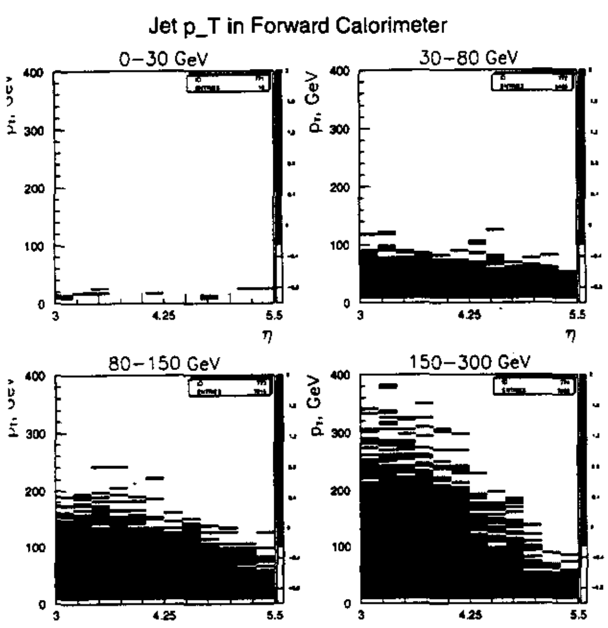

757

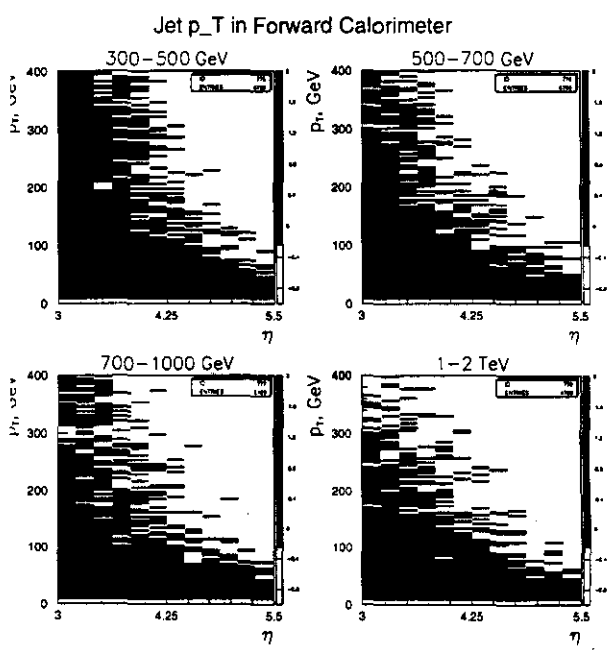

758

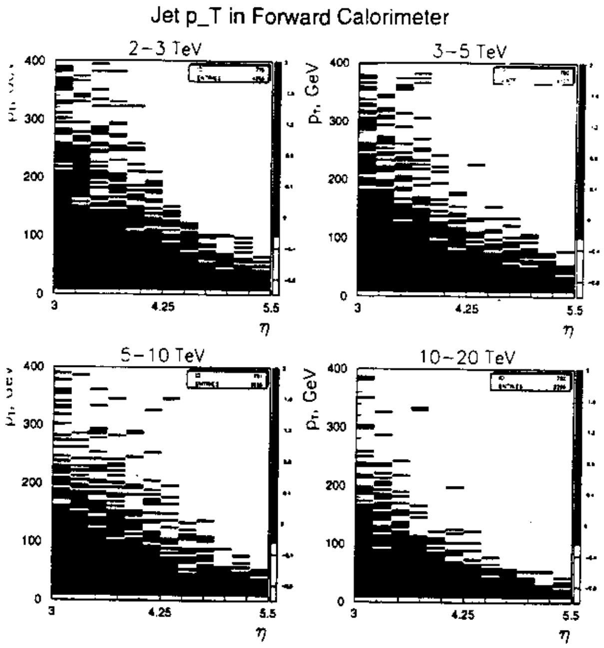

759

Requirements for $\frac{\delta p_T}{p_T}$ are not constant, they should be **η - dependent**

Natural parameters:

$$\frac{\delta p_T}{p_T} = \frac{\delta E}{E} (+) \frac{\delta\theta}{\theta}$$

$\frac{\delta\theta}{\theta} \rightarrow \frac{e^{+\eta}}{2}\delta\theta$, $\delta\theta \rightarrow$ const

$\frac{\delta E}{E} \rightarrow$ const at high energy

position accuracy $\rightarrow \delta\theta = \delta R/z = \frac{f(E)}{\sqrt{E}} (+)$ const

constant term in energy resolution $\rightarrow \frac{\delta E}{E} = \frac{A}{\sqrt{E}} (+) B = \frac{100-200\%}{\sqrt{E}} (+)$ 5-10%

760

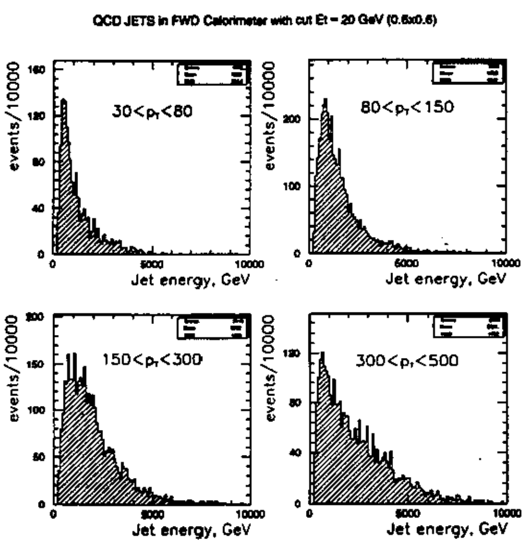

761

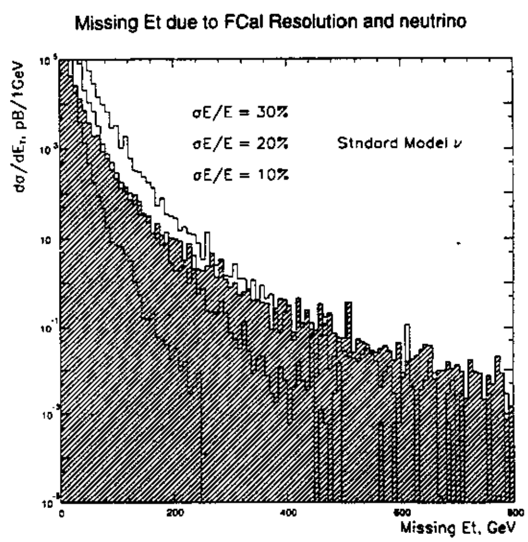

$\sigma E/E = 100\%/\sqrt{E}$ (+) const

$3 < \eta < 5.5$

762

Missing Et of EQUAL Standard Model and Forward Calorimeter contribution

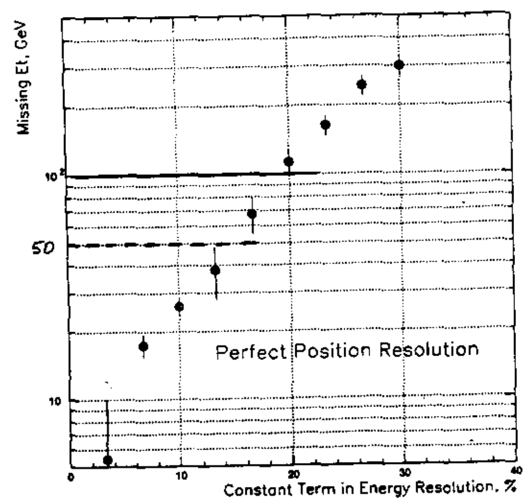

765

Missing Et due to FCal Position Accuracy and neutrino

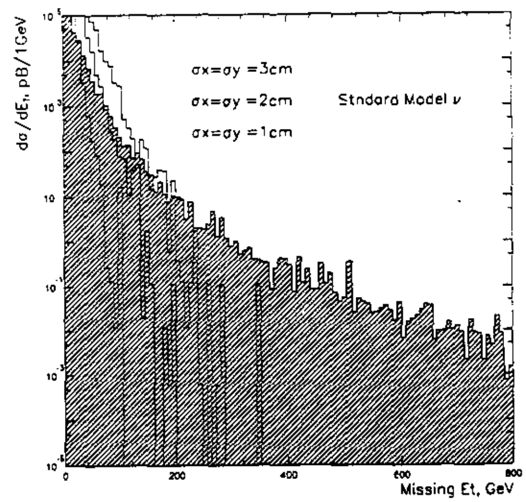

perfect energy resolution

764

Missing Et of EQUAL Standard Model and Forward Calorimeter contribution

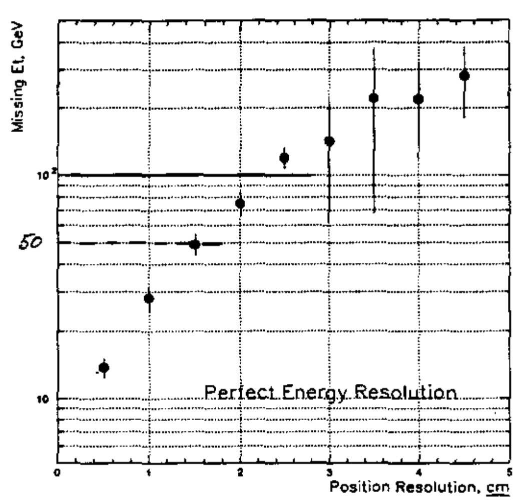

763

Missing Et of EQUAL Standard Model and Forward Calorimeter contribution

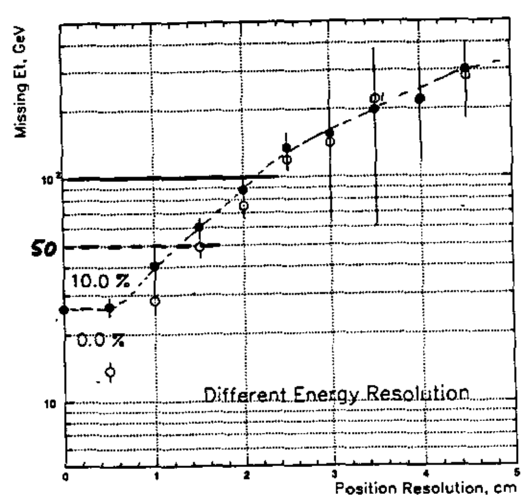

76

- 100 GeV $\not{E}_T$ physics :

$\delta x = \delta y = 2.$ cm

$\delta E / E = 16\%$

- 50 GeV $\not{E}_T$ physics :

$\delta x = \delta y = 1.$ cm

$\delta E / E = 10\%$

767

Nongaussian tails in Resolution?

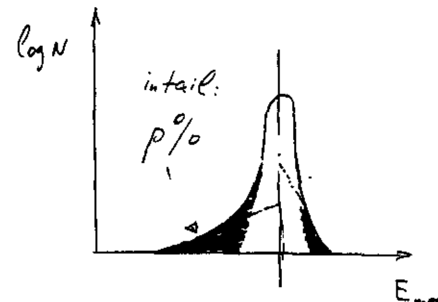

tail: $n_{tail} \sim e^{-\delta E / \lambda(GeV)}$

$p\% = \int n_{tail} / \int N$

Gaussian peak: $\frac{100\%}{\sqrt{E}}$ (+) 10%

768

E_T where Tails (En. Resolultion) Contribution = SM Background

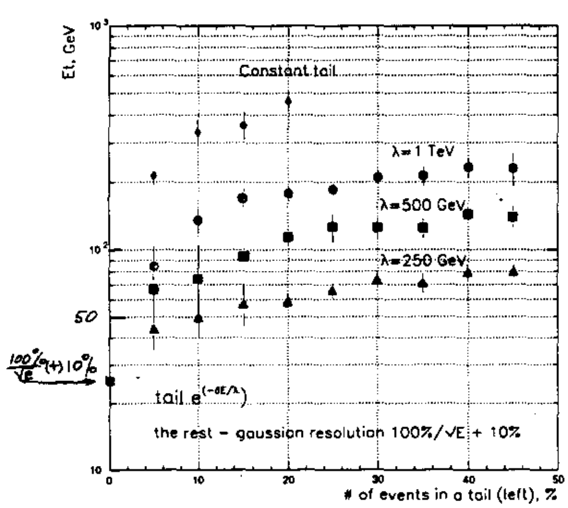

769

Tails (exponential):

- 100 GeV $\not{E}_T$:

$p < 15\%$

$\lambda < 500$ GeV

- 50 GeV $\not{E}_T$:

$p < 10\%$

$\lambda < 250$ GeV

770

Cu or W ?

- A. Savin ITEP/ORNL
GEANT 3.15 Monte Carlo with "idealized" calorimeter :

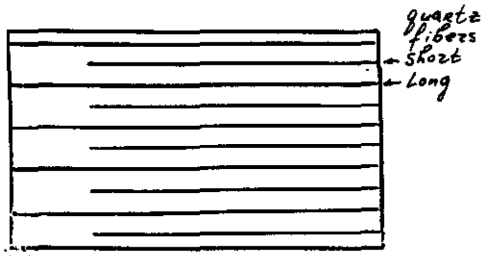

- "compensation"
- $\delta E/E$
- $\delta x/x$
- $\delta p_T/p_T$

77

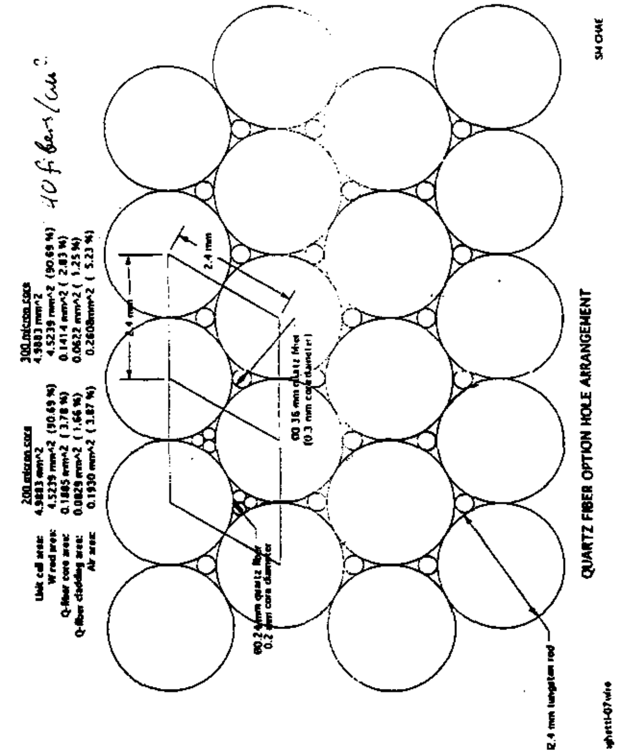

77

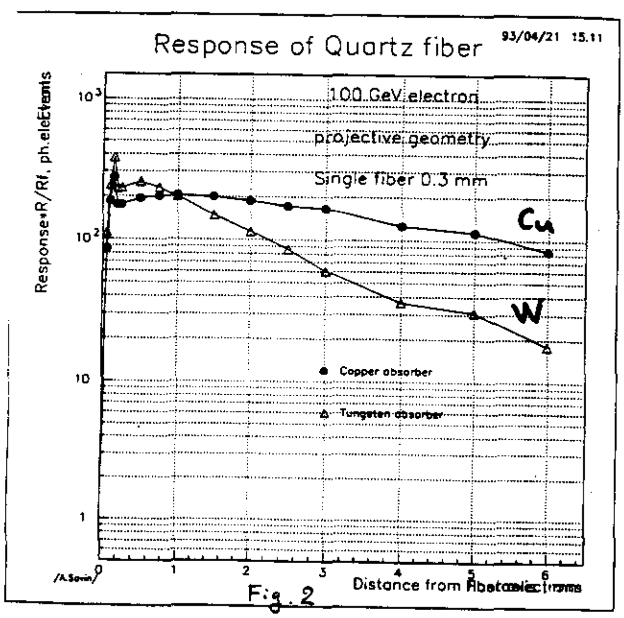

Fig. 2

Distance to the electron impact point, mm

77

- "Compensation"

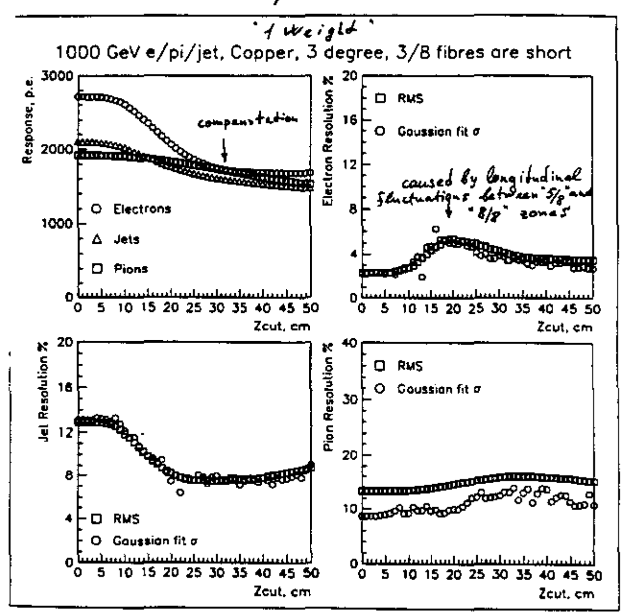

77

"Packing fraction"

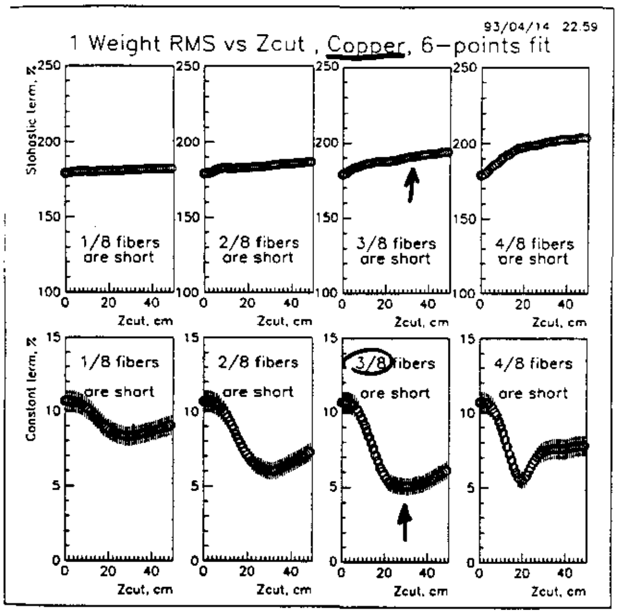

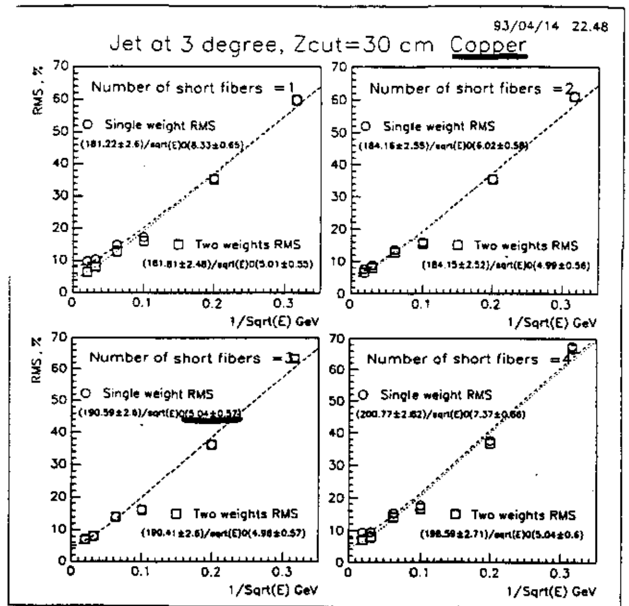

$$\frac{\delta E}{E} = \frac{190\%}{\sqrt{E}} (+)\ 5\%$$

775

776

... And Summarized.

.... then fitted by $\frac{A}{\sqrt{E}} \oplus B$ ....

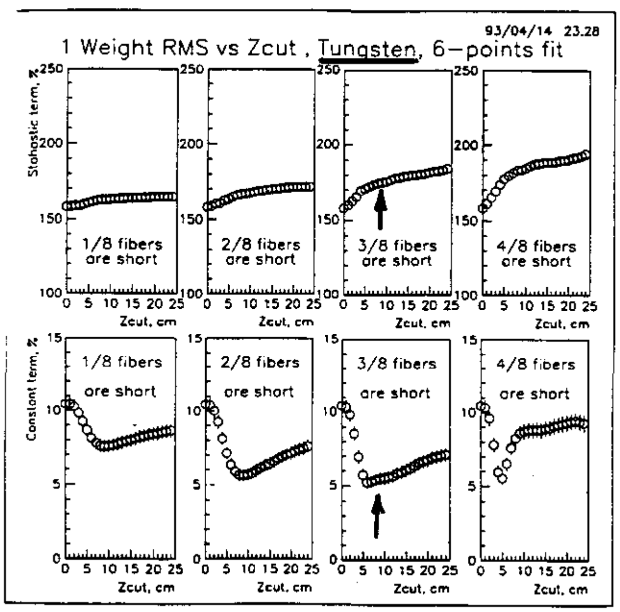

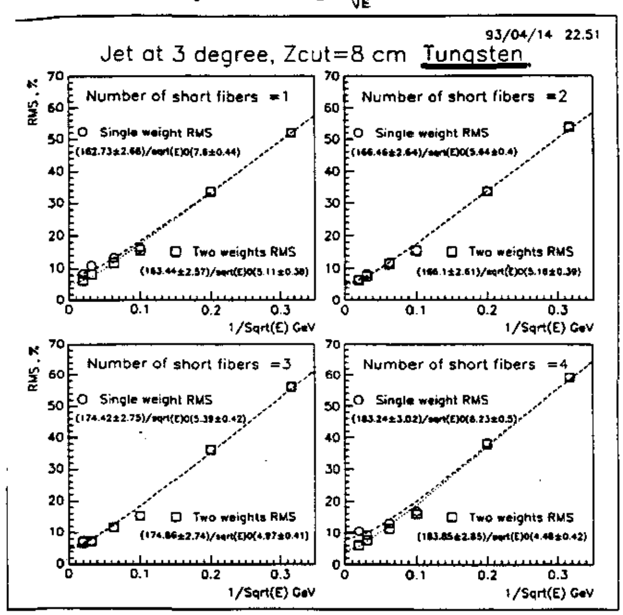

$$\frac{\delta E}{E} = \frac{175\%}{\sqrt{E}} (+)\ 5\%$$

777

778

- W and Cu calorimeters with effective "compensation" can give about the same energy resolution:

$$\frac{170-190\%}{\sqrt{E}} \oplus 5\%$$

(without leakages – idealized calorimeters)

Cu, position resolution

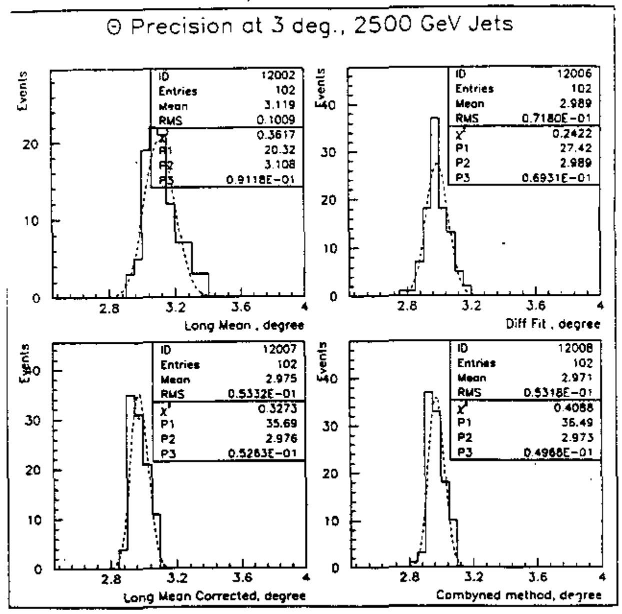

↓ 0.091° = 0.70 cm
0.05° = 0.38 cm

780

Cu, Position Resolution

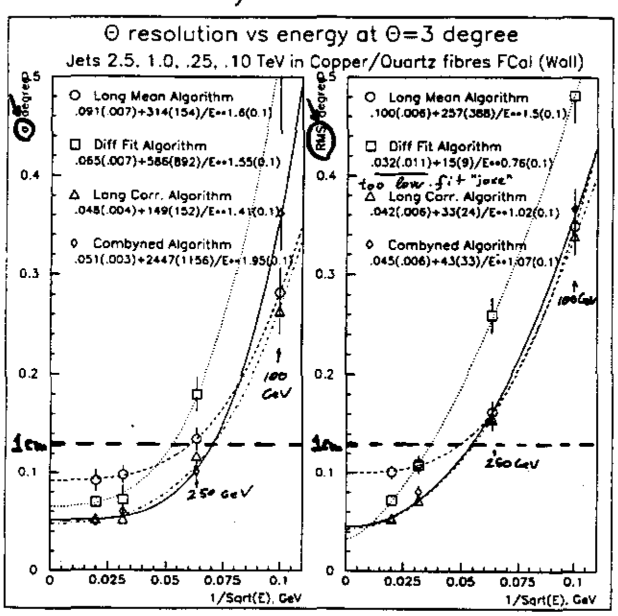

781

- W and Cu calorimeters can give about < 1 cm position resolution

(without side leakages – idealized calorimeter)

782

Idealized Cu Forward Calorimeter, Instrumental missing E_T

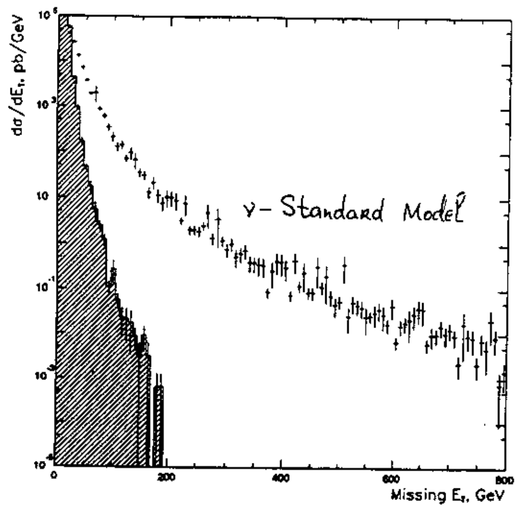

783

Idealized W Forward Calorimeter, Instrumental missing E_T

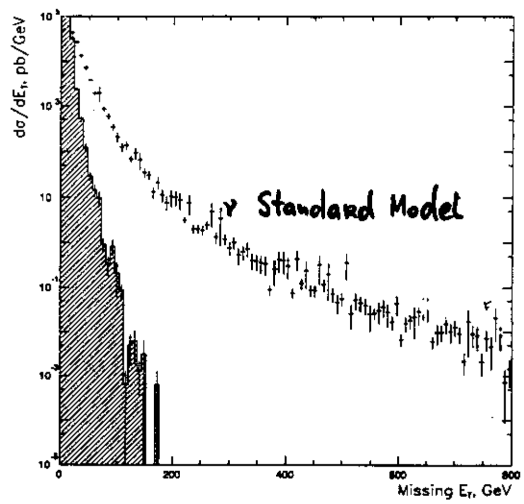

781

$\delta p_T / p_T$

Method I:

- measure E
- measure θ

$> \; p_T = E \sin\theta$

Method II:

- reconstruct p_T of the event without reconstructing E and θ.

785

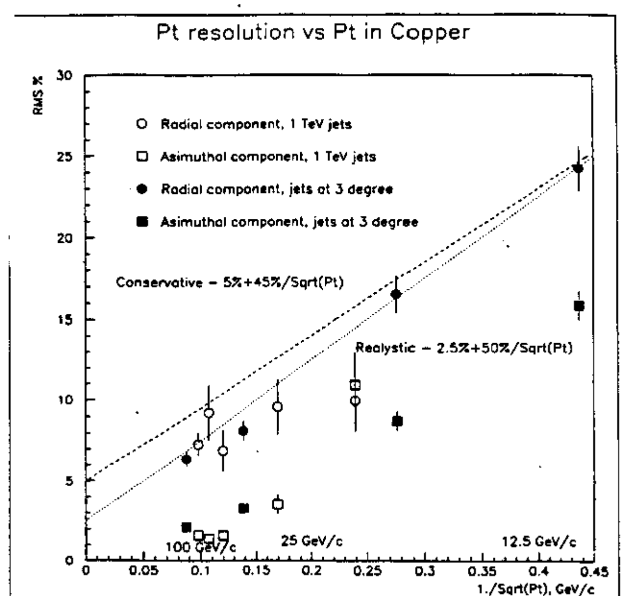

$\frac{1}{\sqrt{p_T}}$

786

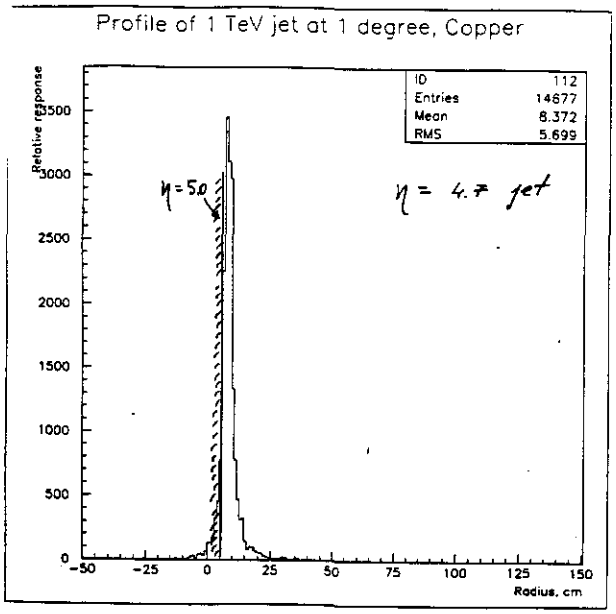

787

Real Calorimeter:

1) Reconstruct the energy and position of jets taking into account leakages

2) To use inner rings of the calorimeter for "veto" only!

3)! To extend the inner part of the calorimeter up to $\eta = 6$. No energy or position resolution is required in the region $5 < \eta < 6.(\ldots)$!
Only veto for $\not{E}_T$ events.

788

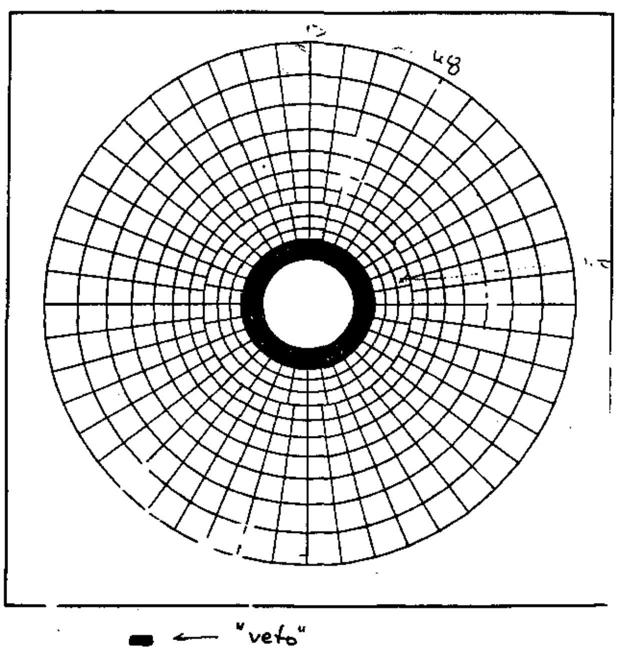

789

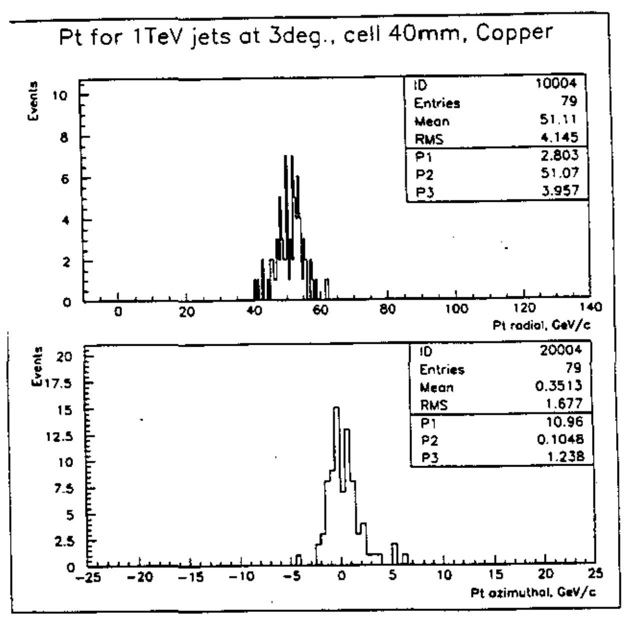

790

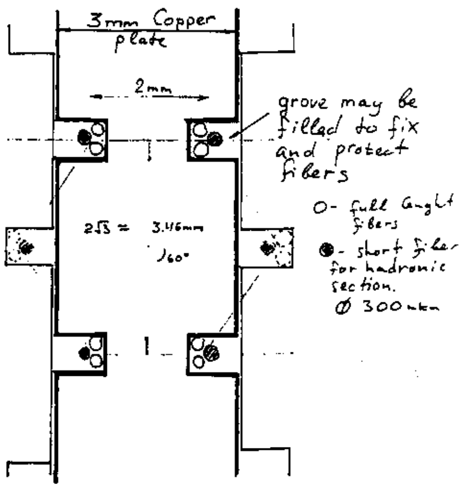
3mm Copper plate
2mm
grove may be filled to fix and protect fibers
$2\sqrt{3} \approx 3.46$mm
60°
O- full lenght fibers
●- short fiber for hadronic section.
Ø 300 mkm

75:

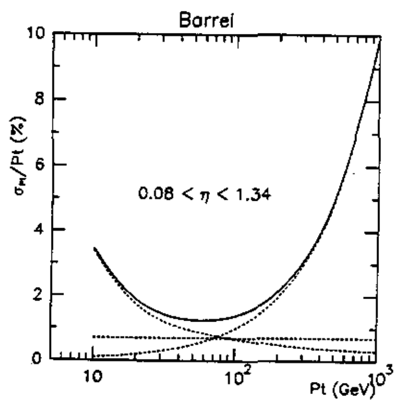

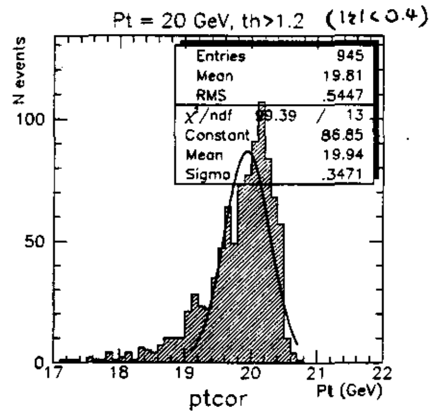

L3
PL B271 (1991) 453

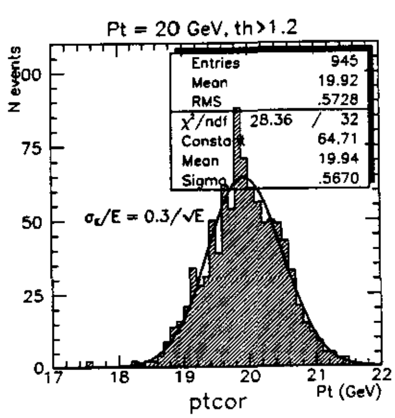

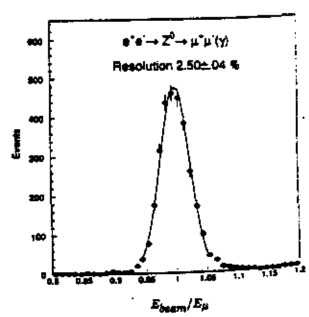

Fig. 1. Muon energy (E_μ) resolution from $Z^0 \to \mu\mu(\gamma)$ events.

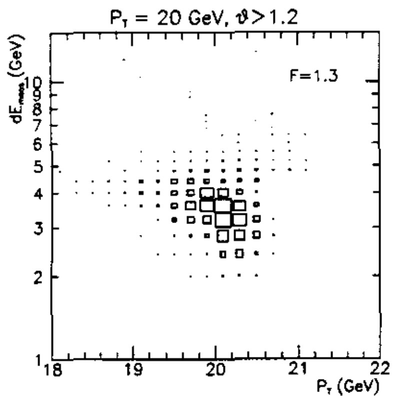

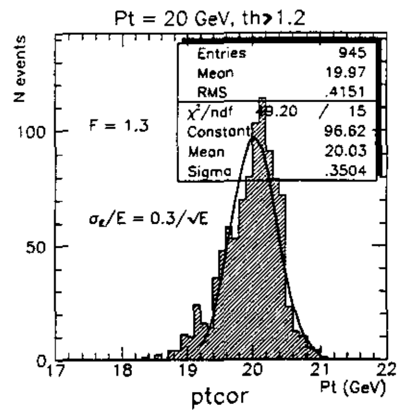

$LH(dE^*) = R(dE_{meas} - dE^*) \cdot W(dE^*; p_\mu, \eta_\mu)$

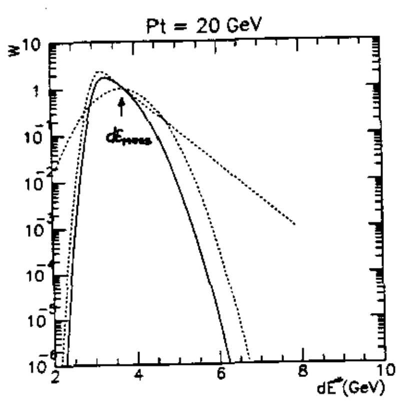

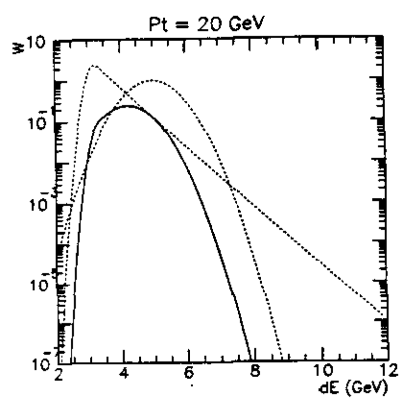

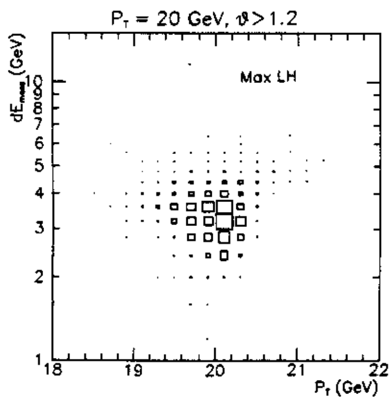

80

$P_T = 20$ GeV $|\eta| < 0.4$

"Toy" calorimeter $\frac{\sigma_E}{E} = \frac{30\%}{\sqrt{E}}$

	"σ" (GeV)	RMS (GeV)
Cal only	0.57	0.57
F=1.3	0.35	0.42
Max LH	0.30	0.39

80

CONCLUSION

Adequate description of Calorimeters in SIGEM will allow:

- to take advantage of Max LH for muon E_{loss} corrections
- to joint optimally muon tracks in CT and muon chambers
- to provide accurate simulations of $H \to 4\mu$, $H \to 2\mu 2e$ mass distributions

805

D. LISSAUER

Calorimeter group Meeting
May 11th.

I. Preparation for PAC. — D. Lissauer
- Agenda
- List of questions.

II. Em design Update — M. Seman.

III. Hadronic Barrel Update — F. Lobkowicz.
Simulation. — M. Shupe

IV. Hadronic EndCap Update — P. Mockett.

V. Feed through Update — P. Mockett

VI. Forward Calorimeter — J. Rutherfoord

VII. Test Beam Program — P. Slattery.

VIII. Material Certification — J. Forden

IX. Scintillator Cal. — Y. Kamyshkov

.....DRAFT ..... DRAFT.....

AGENDA FOR THE CALORIMETER PAC REVIEW
May 25 and 26.

I. Overview Session: May 25 9:00-12:30

1)Calorimeter System. W.Willis 9:00 a.m

(Note: This will be a recap of the presentation in the general session to allow for more questions)

Including
- Physics
- Calorimeter Concept
- Technology choices
- Calorimeter Overview
- Optimization

2) Liquid Calorimeter V.Radeka 9:45 a.m

(Including the Forward Liquid)

Including:
- Design Considerations
- Optimization summary
- Status of the design, R&D, open questions
- Electrodes and readout
- Calibration
- Outline of the rest of the presentations

Break 10:30 a.m

3) Scintillation Calorimeter Y.Kamyshkov 11:00 a.m

(Including the Forward Scintillation cal.)

Including:
- Design Considerations
- Technological solutions.

811

4)Engineering System L.Mason 11:30 a.m

Including:
- Support including CDS
- Cryostat
- EM concept Barrel and endcap.
- Hadronic Module
- Cryogenic and Vacuum systems.
- Installation.

(emphasis on how the whole system comes together)

Lunch 12:30 -2:00 p.m

II. Calorimeter Session: May 25 2:00-5:00 p.m

1) EM Design Considerations and simulation results M.Seman 2:00 p.m

Including:
- Accordion structure
- Electronics placement, Segmentation,
- Cable routing,
- Design Optimization: Massless Gap, segmentation, pointing, total depth, density.
- Argon.vs.Krypton
- Endcap- why did we select the lens design.?

2) Liquid Hadronic F.Lobkowitz 3:00 p.m

Including: Design Considerations, e/π , Cu.vs.Pb, Jet Resolution.

812

3) Forward Calorimeter: J.Rutherfoord 3:45 p.m

Including
- Location. Why locate so close to the interaction point?
- Technology Choice, R&D, test beam
- Production Plan

4) Liquid Hadronic :(Standby presentation) P.Mockett (30 min)

Including: Design Considerations, Box construction, H.V , Signal connections

5) Hadronic module structure:(Standby: presentation) K.Barnstable (20 min)

Including:
- Individual plate analysis
- Box Analysis

6) Barrel and Endcap Structure. (standby presentation) B.Easom (30 min)

Including:
- Individual plate stress analysis,
- Barrel 2x assembly concept and stress analysis
- Endcap assembly concept
- Spacers requirements

7) Production of Calorimeter (Standby presentations)

Press, Bending machine, Absorber production S.Bellavia (20 min)

Electrodes, motherboards, cables D.Makowiecki (20 min)

813

III. Calorimeter Systems and Operations: May 26 9:00-12.30.

1) Scintillation Calorimeter M.Rennich 9:00 a.m

2) Trigger W.Cleland 9:30 p.m

Including:
- Trigger sums hierarchy
- Level I
- Level II.

Break 10:15 a.m

3) Cryogenics and Vacuum Subsystems M.Wilson 10:45 a.m

Including:
- Cool down procedure
- Fluid rates
- Purification
- Operation
- Safety, Control.

VAC. BEAM LINE

4) Assembly at the SSC: W.Wisniewski 11:15 a.m

Including:
- Assembly at the SSC
- Access questions
- Installation

5) Electronics: (standby presentation) J.Parsons (30 min)

Including:
- Electronic Readout chain
- Placement, power and space requirements
- Dynamic Range.

814

6) Cryostat: (standby presentation) L.Mason or B. Humphreys (20 min)

Including:
- Design criteria
- Stress analysis
- Production and assembly scenario.

7) Feedthroughs: (standby presentation) P.Mockett (20 min)

Including:
- Hermetic Seal Solution
- IBM Solution
- Decision process, strengths and weaknesses of each solution
- Design Criteria.
- Reliability
- Electrical properties

Lunch 12:30-2:00

IV. Parallel Calorimeter Session (closed) 2:00-5:00 p.m

Calorimeter Questions anticipated from the PAC

(person responsible underlined)

I. EM

A. General

- ● 1. From the recent CDF results on 2 photons (PRL 70, 2233(1993)) is GEM emphasis on $H^0 \to \gamma\gamma$ prudent?
- 2. Describe the method of tensioning the straps in the EM barrel. They seem captured?
- 3. Show how the background from π^0 conversions and Dalitz decays is eliminated.

B. Optimization

- ● 1. Justify the choice of krypton: significance of the $H^0 \to \gamma\gamma$, pointing resolution, jet rejection? For example show all with all argon.
- 2. Show the thermal and pileup noise vs. η and shaping time and luminosity.
- ● 3. Prove that the number of channels can not be significantly reduced by increasing the tower size. Show the effects on pointing resolution, jet rejection as a function of the strip width, tower size.
- 4. Prove that three longitudinal layers are needed - not two: pointing, jet rejection...
- 5. Prove that the depth of the EM section is optimal for 20 GeV to 6 TeV. Show the effect of adding energy from the first hadronic layer.
- ● ● 6. Justify the design of the endcap. Show alternatives studied and give reasons for selection. (Dydak's question left over from December): show the cost impact of the large number of different electrodes needed. Seman, Makowiecki, Eason

C. Performance

1. Failure analysis: what is the effect on physics of losing one channel completely. How many channels can be lost? What is the probability of losing a channel?
2. What mechanical tolerances are required on plate thickness, nominal absorber position to achieve the energy resolution?
3. Prove that the constant term will be less than 0.4%.
4. Show how you will achieve the dynamic range.
5. Has the simulation of the energy resolution used the actual amount of dead material due to the tracker, cryostat, liquid etc.?
6. What is the effect of the magnetic field on π^0 rejection?
7. Show the energy resolution vs. x and y in the endcap. How much is the performance impaired near the steps? Energy resolution? Pointing? Jet rejection?

II. Hadronic calorimeter

A. Optimization

1

- ● ● 1. Justify the use of lead in the barrel and copper in the endcap.
  Single particle done (Moore GEM note), $H \to \ell\ell jet + jet$ in progress: Lobkowicz. Note our lead is enclosed - not like SLD.
- ● ● 2. Justify the use of 9 mm thick plates in the barrel and 27 mm plates in endcap. Effect on EM resolution: Lobkowicz, Leltchouk, Klimenko
- 3. Justify the depth of the transition from liquid to scintillator.
  EM only, Need new drawing showing real feedthroughs, muon response?
  9 λ Kr cost: Bearable. V. Radeka
- 4. Justify the transition from barrel to endcap where a single jet may have to traverse sections with as many as 5-6 different sampling ratios.
  Test beam goals. (Ar/Kr not tested) Shupe
- 5. Show the energy resolution vs. η and depth of the calorimeter. How does the missing energy resolution depend on the depth of the calorimeter? Shupe

B. Performance

1. Describe and justify the procedure of longitudinal weighting. Does it depend on the number of longitudinal layers? Shupe
2. Show that the EST does not affect the jet resolution. Gordon
3. Show that the steps in the endcap EM do not deteriorate the hadronic performance - specifically do the jets broaden in the region of the steps? Shupe
4. Show how the hadronic towers map to the EM towers in the endcap. Takai

III. Forward calorimeter

- A. Justify the choice of copper for the FEM and tungsten for the FHAD.
- ● ● B. Justify the use of two different technologies for the forward calorimeter.
- C. Show the expected signal/noise vs. η - thermal and pileup.

IV. Cryogenics concerns

- A. No liquid krypton calorimeters have been operated in an experiment - only in tests. Show how the krypton purity will be maintained.
  List examples with shaping times used: BINP, NA48, Short shaping helps. Rahm, Wilson
- B. Show the cooling scheme for taking heat from the preamps. Describe the cooling scheme for the krypton and argon cryostats. Will it be a closed system? Effect of excluders. Mason
- C. Show a failure mode analysis for: loss of krypton; rupture of a cold vessel; leak at a feedthrough; (include fires!) Humphreys, Wilson
- D. How long does the cooldown take? What is the steady state LN_2 required/day? Mason
- E. Show the thermal effects on dimensions. Can the installation be done both warm and cold?
- F. Show a plot of the response vs. depth in the barrel due to density (temperature) effects. Mason
- G. Show the time required to certify the signal feedthroughs: pins in ceramic vs. IBM. Mockett
- H. Effect of magnet quench: load effects and heating effects:

V. Assembly and access

- A. Where is access required and how often? How long does it take to achieve an access. Wisniewski

2

VI. Other

- A. Describe the setting of the absolute energy scale. Relation of calibration, test beam response. EM: Radeka, Hadronic: Lobkowicz, Mockett
- B. Describe the installation sequence for a single channel: testing, installation of motherboard, cabling, feedthrough, testing: up to what point are repairs possible? Makowiecki
- C. What happens after the cryostat is welded shut and cooled down if repairs are required? What can be done in 1 year? Mason
- D. Show the program for certifying all components for radiation hardness.
  Outgassing after radiation? Arizona - Forden
- E. LKr has a large cross-section for thermal neutrons (~200 barns). Is this of any benefit or harm?
- F. Describe the high voltage system and feedthroughs. How many channels will there be? 4/EM module, hadronic? Makowiecki
- G. How much cooling is required for junction boxes? Makowiecki

3

STATUS OF EM ENDCAP DESIGN
AND SIMULATION
(M. SEMAN)

1) DO WE NEED MASSLESS GAP ?

2) PRELIMINARY RESULTS ON ENERGY RESOLUTION

TO BE DONE :

1) MORE DETAIL STUDY OF "STEPS"

2) POSITION RESOLUTION

3) POINTING RESOLUTION

4) π° (JET) REJECTION

5) IMPACT ON JET MEASUREMENT

82

(ENDCAP QUESTIONS)

1) WHY THIS APPROACH ?

2) DO WE NEED MASSLESS GAP ?

3) ENERGY RESOLUTION (x, γ) (STEPS ?)
CORRECTION ON LEAKAGE ?

4) POSITION RESOLUTION

5) POINTING RESOLUTION

6) π° - REJECTION
JET REJECTION

7) IMPACT ON JET MEASUREMENT

82

TOP VIEW

$\sigma/\sqrt{E}$(%); E = 80 GeV

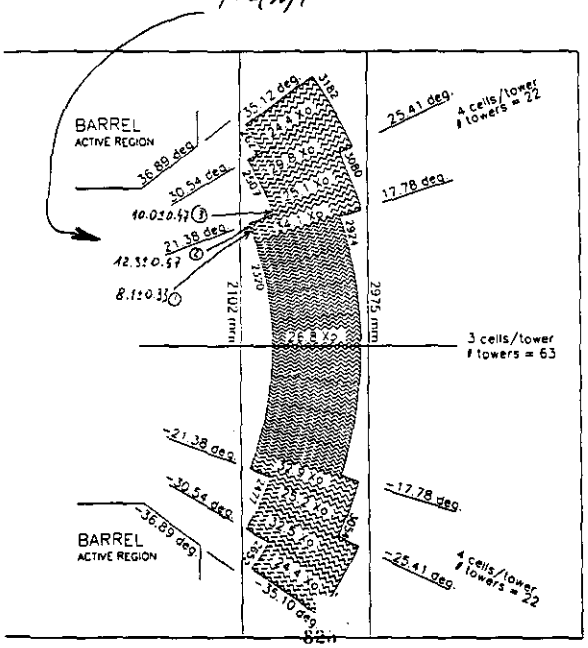

$\sigma/\sqrt{E}$ (%)

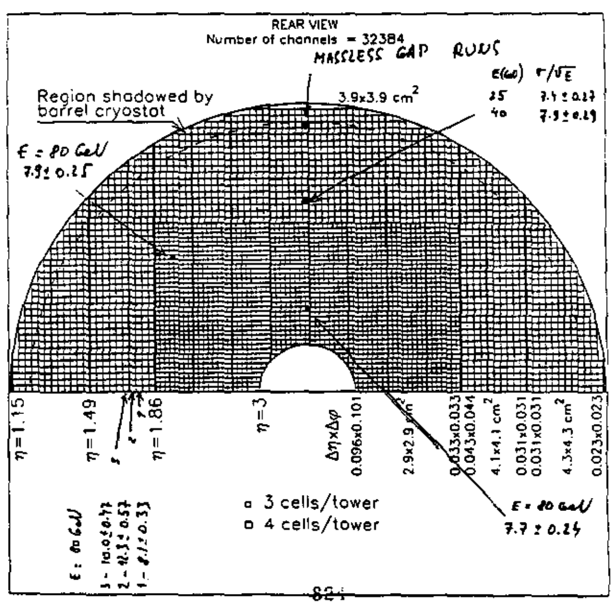

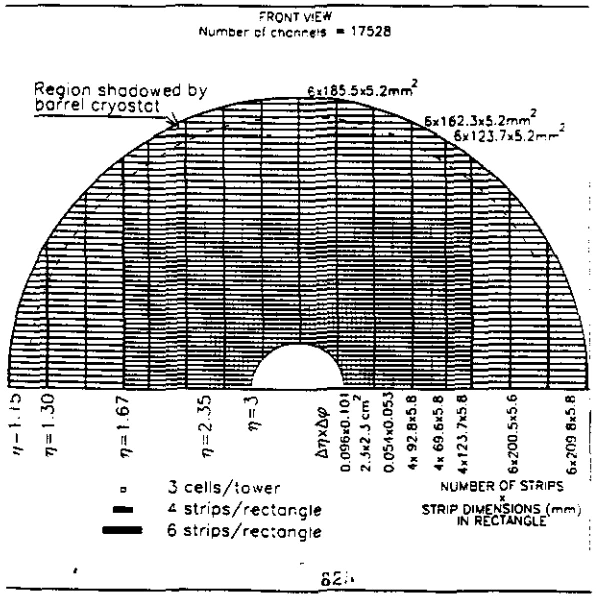
FRONT VIEW
Number of channels = 17528
Region shadowed by barrel cryostat
6x185.5x5.2mm²
6x162.3x5.2mm²
6x123.7x5.2mm²
η=1.30
η=1.67
η=2.35
η=3
ΔηxΔφ
0.096x0.101
2.3x2.3 cm²
0.054x0.053
4x 92.8x5.8
4x 69.6x5.8
4x123.7x5.8
6x200.5x5.6
6x209.8x5.8
3 cells/tower
4 strips/rectangle
6 strips/rectangle
NUMBER OF STRIPS
x
STRIP DIMENSIONS (mm)
IN RECTANGLE

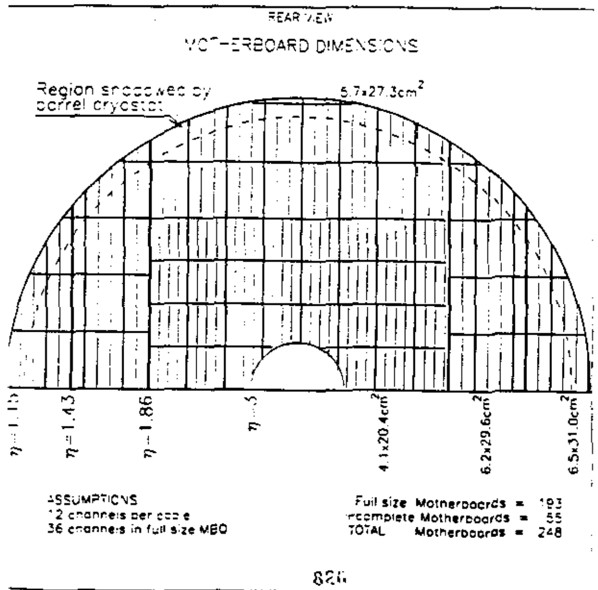
REAR VIEW
MOTHERBOARD DIMENSIONS
Region shadowed by barrel cryostat
5.7x27.3cm²
η=1.43
η=1.86
4.1x20.4cm²
6.2x29.6cm²
6.5x31.0cm²
ASSUMPTIONS
12 channels per cable
36 channels in full size MBO
Full size Motherboards = 193
Incomplete Motherboards = 55
TOTAL Motherboards = 248

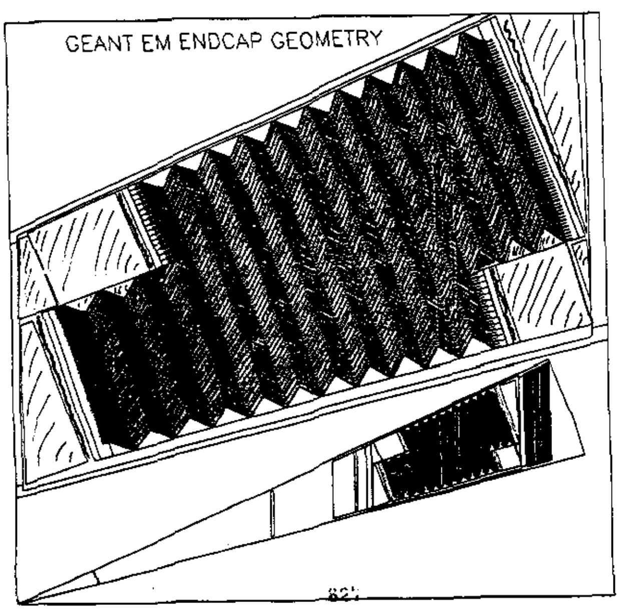
GEANT EM ENDCAP GEOMETRY

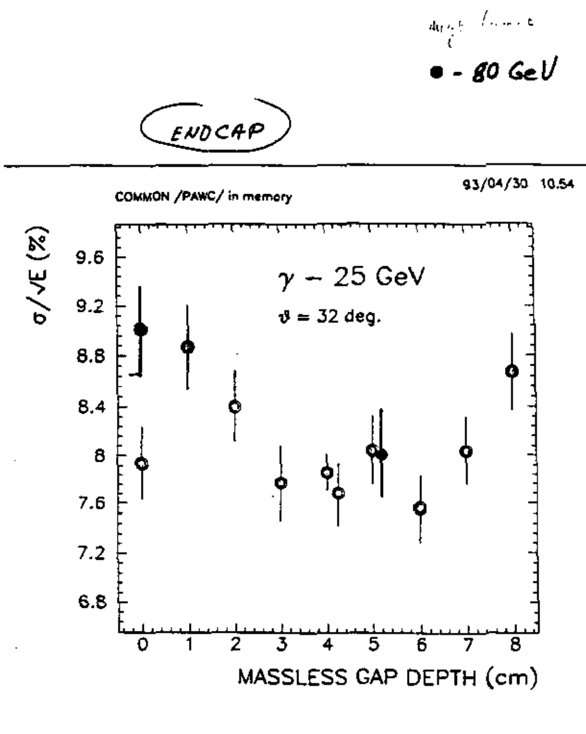
• - 80 GeV
ENDCAP
COMMON /PAWC/ in memory
93/04/30 10.54
σ/√E (%)
γ – 25 GeV
ϑ = 32 deg.
MASSLESS GAP DEPTH (cm)

BARREL

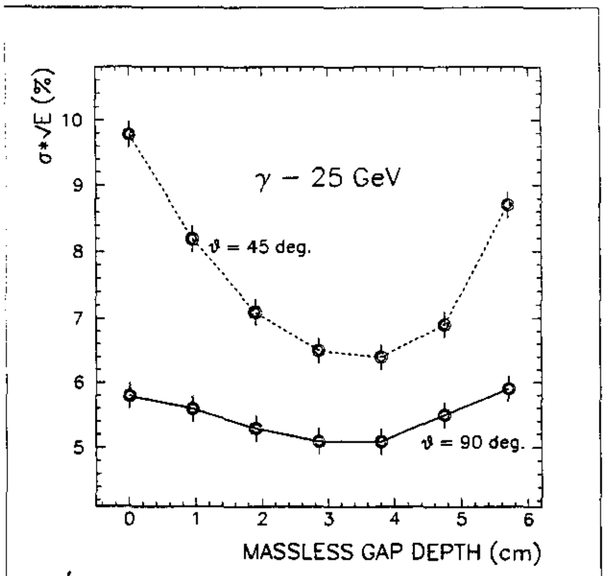

829

Hadronic Endcap Module

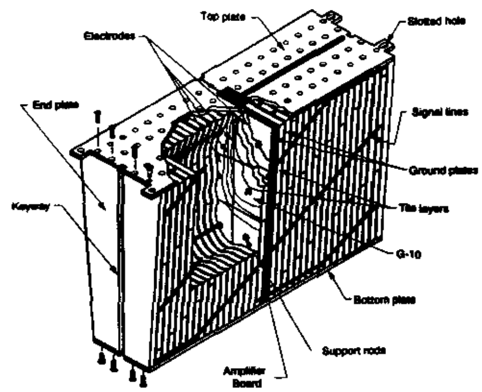

830

S.V. May 11

Barrel Hadron. Modules

Absorber: Pb (Cu?)
Gap: 2 mm LKr

Transformer: 3:1, Electrostatic

$\Delta\eta \times \Delta\varphi = \frac{\pi}{40} \times \frac{\pi}{40} \sim 0.08 \times 0.08$

? layers in depth, $-1 \leq \eta \leq +1$

Shaping: 100-200 nsec

Questions:

1) Massless gaps
2) Outer Had – thickened Cryostat
3) "Feedthru corner"
4) Brass or Alu for Endplate?

833

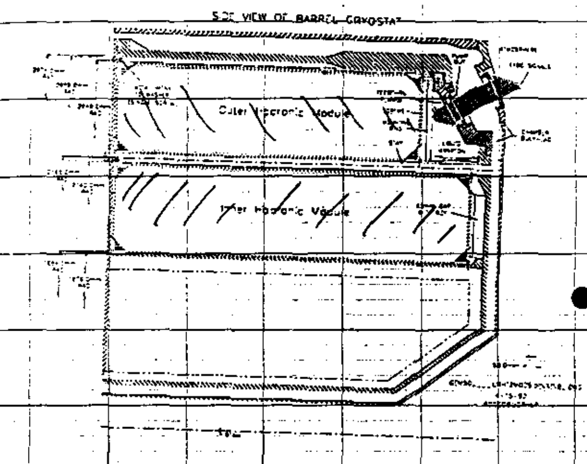

Figure 2-2: The hadronic modules inside the barrel cryostat (Side view)

834

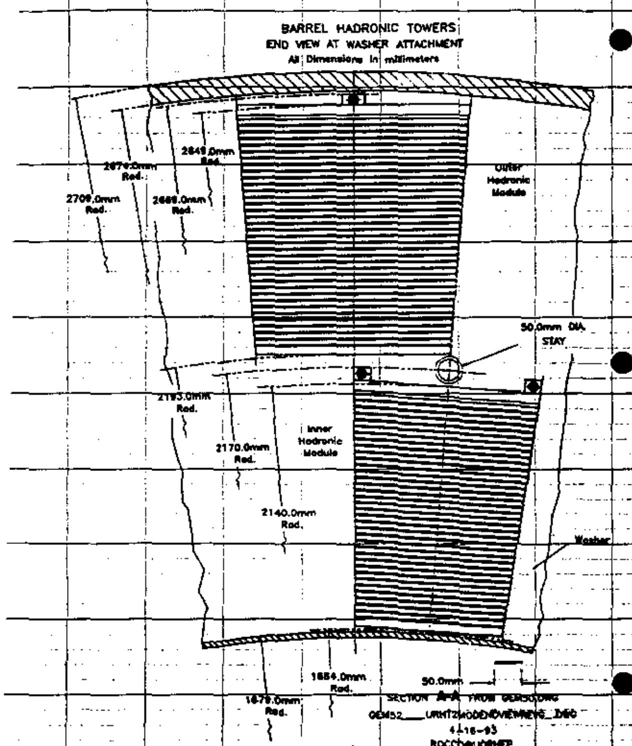

835

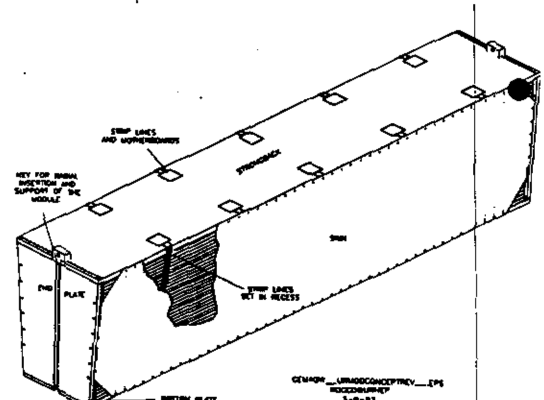

Figure 6-1: An assembled inner hadronic module, with identification of the individual elements.

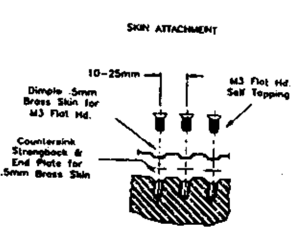

Figure 6-2: Fastening the skin to the Strongback, Endplate or Bottom plate.

836

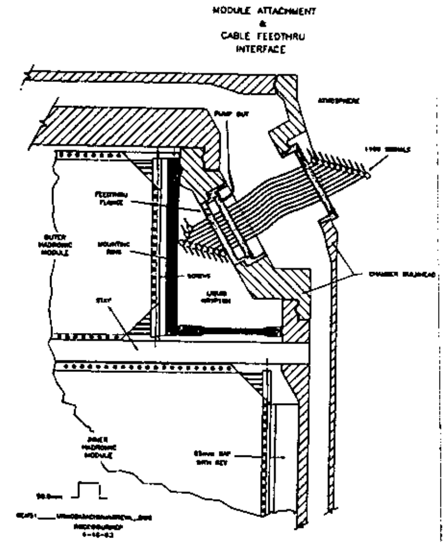

Figure 7-1: Detail of inner barrel cryostat near the feedthrus, showing the ring on which the outer hadronic modules will be mounted.

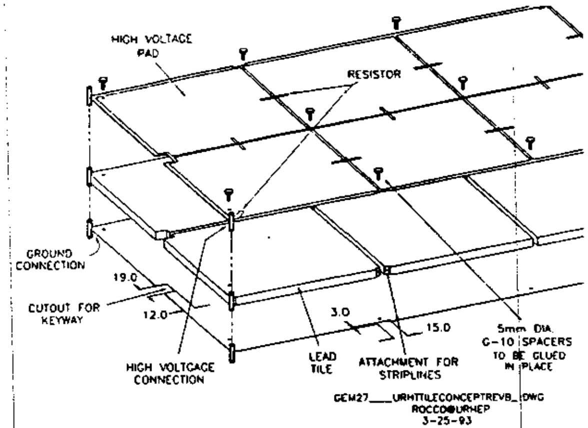

Figure 4-1: Exploded view of one end of a tile absorber layer, showing spacers, as well as the notches for cable connections and keyways for attaching the layer to the endplates

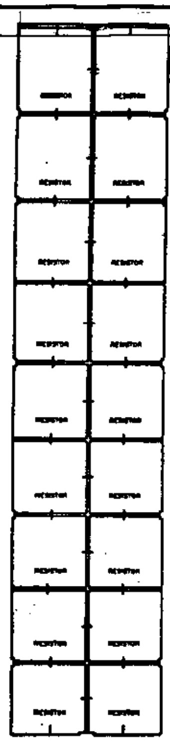

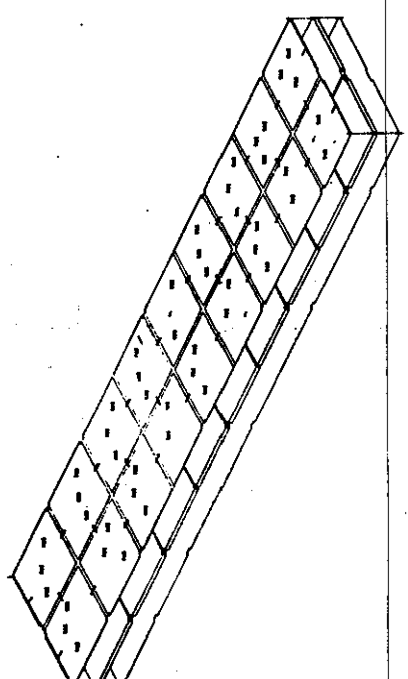

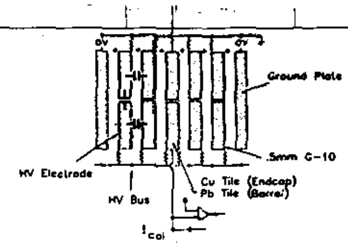

Figure 3-1: The chosen Cell structure using a Electrostatic Transformer of 3:1

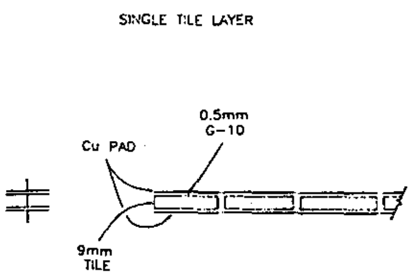

Figure 3-2: A Tile Absorber layer, with the *G-10* boards and pads; on the side we are showing the electric equivalent circuit.

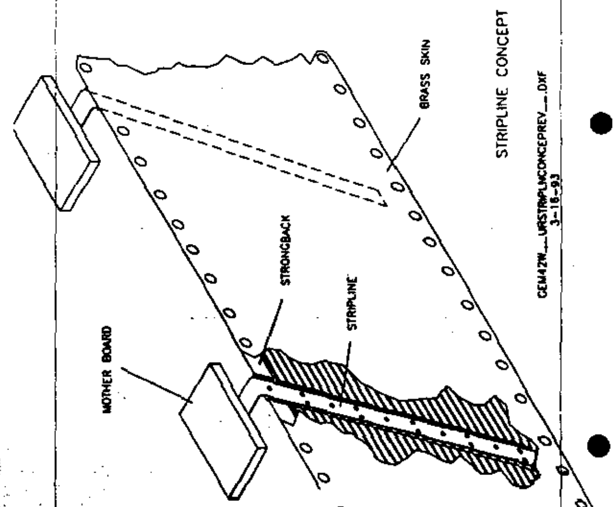

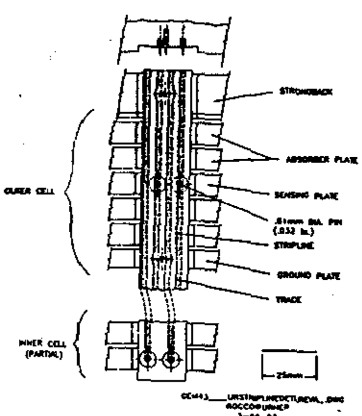

Figure 4-2: Connection to the readout cable which connects tiles to the preamplifier

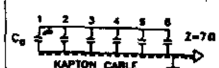

Figure 5-1: Equivalent circuit diagram for reading out six cells. We assume a perfect termination of the cable at the amplifier input.

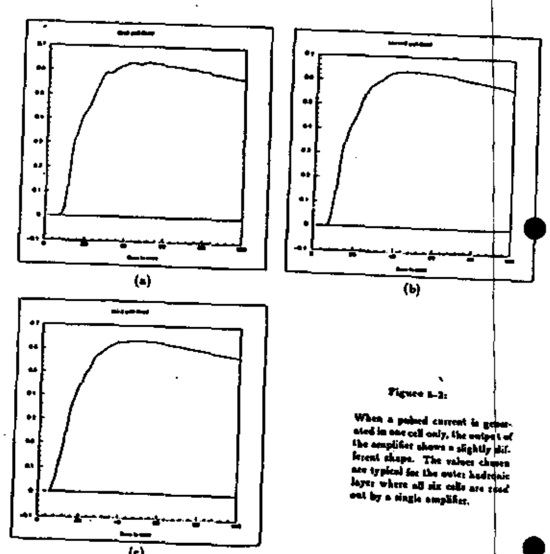

(a) (b) (c)

Figure 5-2:

When a pulsed current is generated in one cell only, the output of the amplifier shows a slightly different shape. The values chosen are typical for the outer hadronic layer where all six cells are read out by a single amplifier.

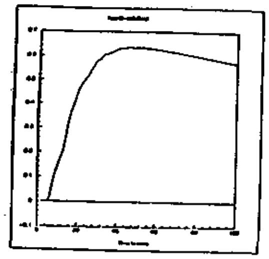

(d)

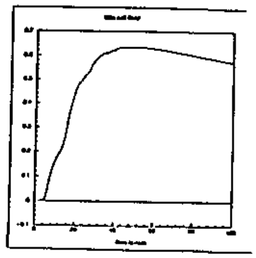

(e)

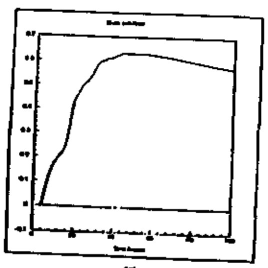

(f)

Figure 6-3:

When a pulsed current is generated in one cell only, the output of the amplifier shows a slightly different shape. The values chosen are typical for the outer hadronic layer where all six cells are read out by a single amplifier.

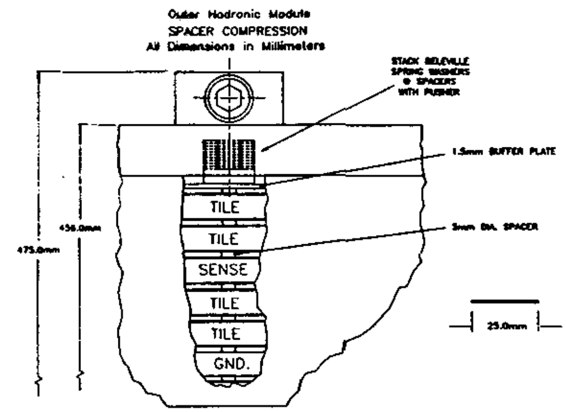

Figure 6-5: Compression of a module stack. A set of Belleville washers pushes a plunger which acts through a thin buffer plate directly on the spacers.

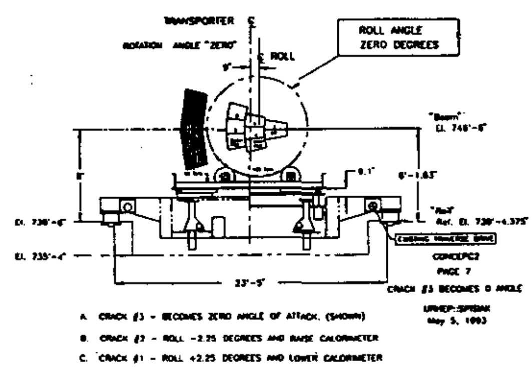

Figure 13-1: The test beam cryostat and its transporter. Two EM barrel modules, and three each of inner and outer hadronic modules are shown. Behind it one sees the scintillating warm calorimeter layer. This setup is planned for the MWEST area at Fermilab.

The GEM Test Beam Program at MWest

Overview

- Calorimeter Testing and Calibration
  - Barrel and End Cap Calorimetry
  - End Cap and Forward Calorimetry
  - Both LAr and LKr Testing
- Muon Tracker Testing
- Central Tracker Testing
- DAQ and Trigger Development

During the initial test beam run the emphasis will be on carrying out a coordinated test of the various GEM subsystems. During subsequent running, the goal will be to carry out an integrated test of a sector of the GEM detector.

851

MWest Hall Overview

- Floor Space: 200×63 ft^2
- Crane: 25 tons; 30 ft hook height
- Beam:
  - Momenta ≤ Primary Protons
  - Significant Bending (2.4 mr & 4.8 mr)
  - Cherenkov Counter
- Cryogenics:
  - Storage Tanks: LN_2 & LAr
  - Extensive Cryo-plumbing
  - Complete ODH System (incl. runoff pit)
- Multi-zone Radiation Interlocks
- Large Aperture Magnet:
  - Field ≤ 1.2 T
  - H=50 in; W=36 in; L=66 in
- Transverse Rails (400 tons) spanning 3 ft deep trench
- Internal & External Counting Areas
- Reusable Equipment:
  - Tracking Chambers (E706; E672; E704)
  - PREP Electronics
  - Computers

852

The Fermilab MWEST Area – Not Drawn to Scale

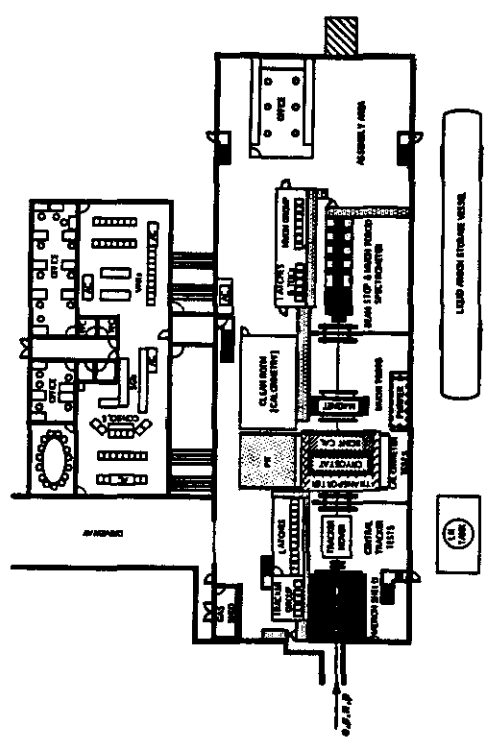

853

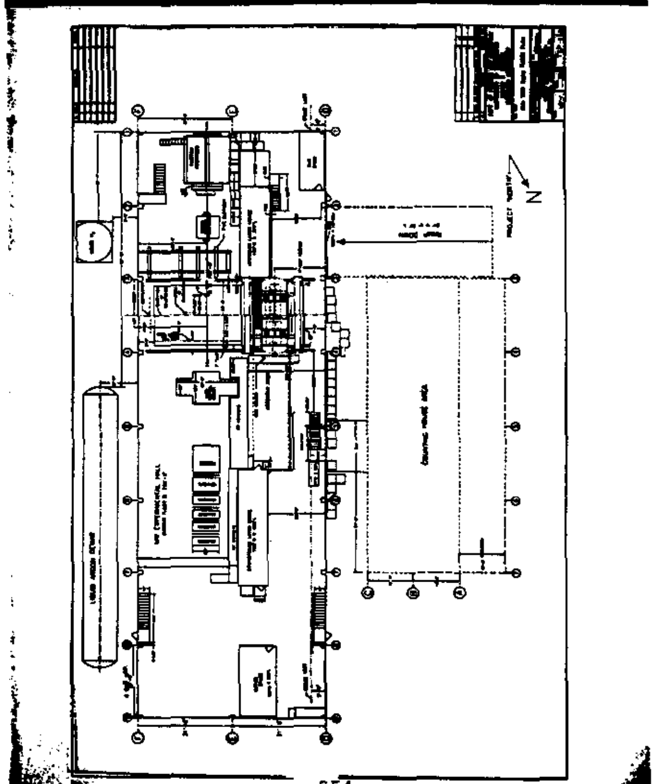

854

MWest Beam Overview

- Accumulate Data at a Variety of Momenta:
  - Primary Protons: ~800 GeV/c
  - Secondary Beams: ±10, ±25, ±50, ±100, ±200, ±300, ±400 & ±500 GeV/c
- Precision Momentum Tagging: ~0.2 %
- Electron Enrichment
- Electron Tagging:
  - Cherenkov Counter
  - Synchrotron Radiation Detector
- Muon Enrichment (Close Collimators)
- Primarily Low Intensity Running: ~10 Hz – 10 kHz
- Limited "Pinged" Beam Running: ~10^9 Hz for ~1 ms

Data Acquisition Considerations

From the data acquisition perspective, there is an almost total dichotomy between the MWest test beam program and GEM itself:

- Near term decisions regarding DAQ hardware and software must be made in the case of the test beam program, since its success requires an operational data acquisition system at all times – including (perhaps especially) during its startup phase.

- Near term decisions regarding DAQ hardware and software must not be made in the case of GEM itself, since the relevant technology is changing so rapidly (and radically) that any decision made today will inevitably be a mistake from the perspective of the technology of the SSC era.

Nevertheless, the MWest program is an ideal test bed for trying out and perfecting DAQ concepts and configurations. Thus, the program will be used for this purpose, keeping in mind at all times that there must be an operational data acquisition system in place throughout the life of the program.

J. Dunlea (University of Rochester) will be responsible for coordinating the effort to achieve an appropriate balance between near term requirements and long term goals.

The GEM Calorimeter

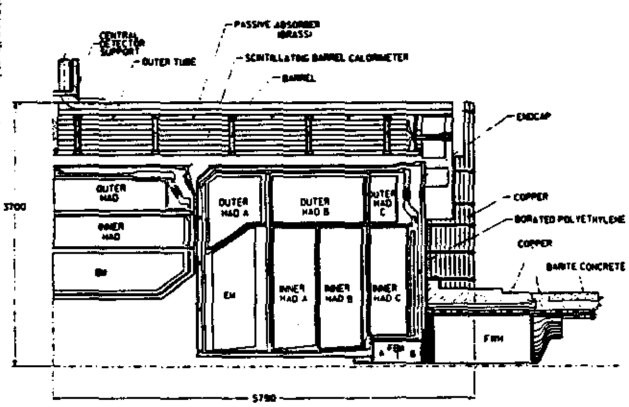

Calorimeter Testing and Calibration

Goals

- Perform full-scale engineering studies of all calorimeter subsystems: mechanical, electrical and cryogenic
- Achieve full system integration of the electromagnetic and hadronic cryogenic calorimetry and of the external scintillating calorimetry
- Carry out a full system test of the calorimeter readout and calibration systems
- Measure the response of the scintillating calorimeter and determine the reproducibility of its performance from module to module
- Study the calorimeter's resolution at the highest energies available
- Investigate the calorimeter's single particle response in the vicinity of representative cracks
- Study the calorimeter's single particle response across the barrel to end cap transition
- Investigate the calorimeter's response to high energy muons
- Investigate the calorimeter's single particle response in the forward direction (relative to the GEM axis)

Optimize the calorimeter's design where this is possible, modify existing modules when this is necessary, and understand the characteristics of the final calorimeter.

Resolution of the GEM LKr Calorimeter
(Full GEANT Monte Carlo Simulation)

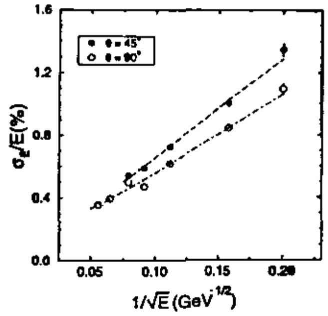

MWest Momentum Tagging

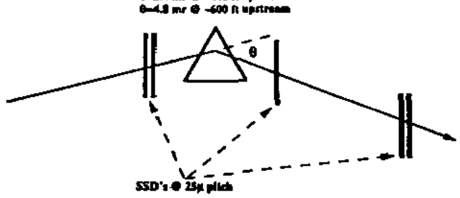

System will be provided by the University of Pittsburgh group of E. Engels, Jr. & P. Shepard using apparatus and electronics from E706 plus four new silicon wafers.

Electron Tagging in MWest

The GEM electromagnetic calorimeter has excellent electron/hadron discrimination (~10^{-4}) by virtue of its very fine segmentation – in both ϕ and η.

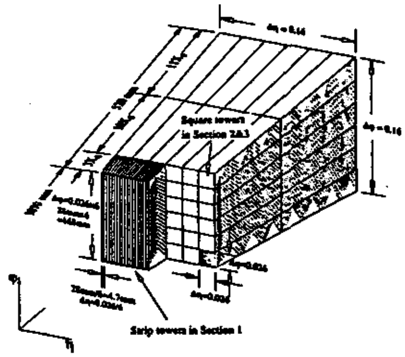

To improve the electron-to-hadron signal-to-noise, the MWest beam will be provided with:

- Electron Enrichment {R. Tokarek}
- Electron Tagging
  - Cherenkov Counter ($p \lesssim 75$ GeV/c) {Existing}
  - Synchrotron Radiation Detector ($p \gtrsim 75$ GeV/c) {H. Fenker}

Calorimeter Test Beam Apparatus

- Calorimeter Transporter (Rochester)
  - Horizontal Motion on Existing Rail System
  - Vertical Motion on a "Lowboy" Carriage
  - Rotational Motion: ±90°
  - Tilting Motion: ±4°
  - Supports ~150 tons
- Test Cryostat (SSCL)
  - Double Walled (Flanged) Aluminum Cylinder
  - Internal Bath Box to Minimize LKr
  - Length: ~26 ft; Radius: ~100 in
  - Loaded via Rails on an Insertion Bridge
  - Weight When Loaded: ~100 tons

The schedule for producing these devices is very tight. Fermilab safety committees should be established for both units as soon as possible so that the requisite dialog can commence.

Calorimeter Testing
Beam on Barrel Calorimeter Center Line

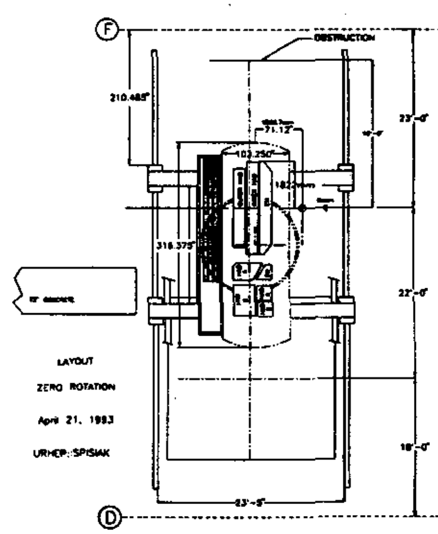

Calorimeter Testing
Beam at Barrel Calorimeter Extreme

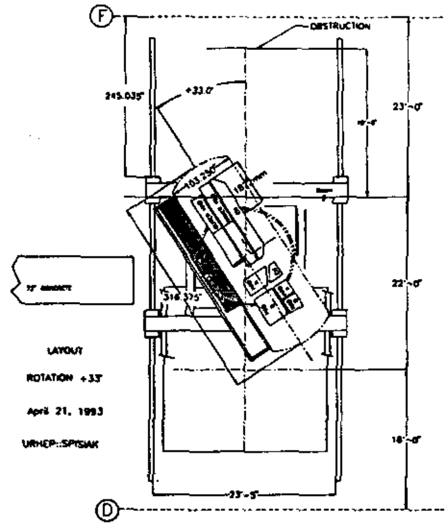

Calorimeter Testing
Beam at End Cap Calorimeter Extreme

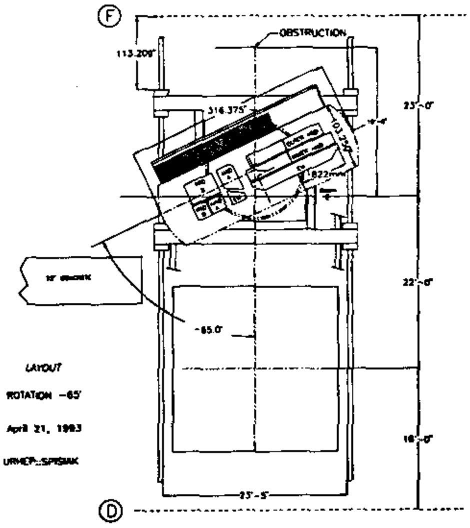

Calorimeter Testing
Beam on EM Center Line

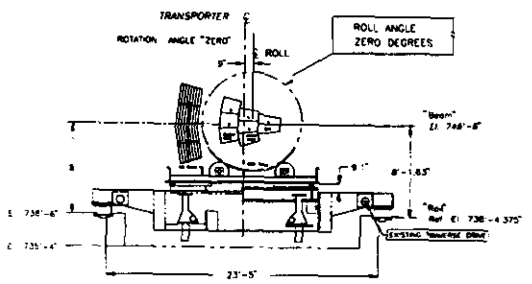

Calorimeter Testing
Beam on Inner Hadronic Crack

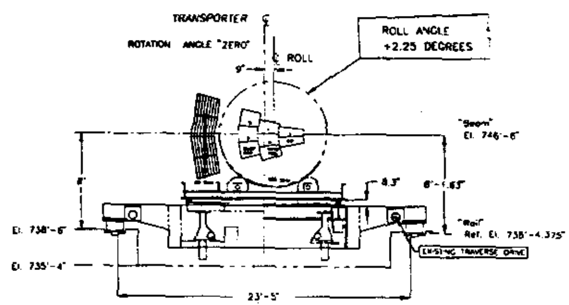

Calorimeter Testing
Beam on Outer Hadronic Crack

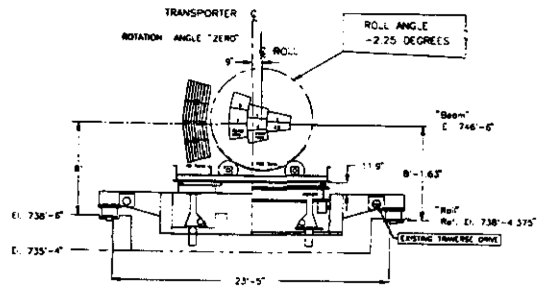

867

Layout of the MWest Experimental Hall

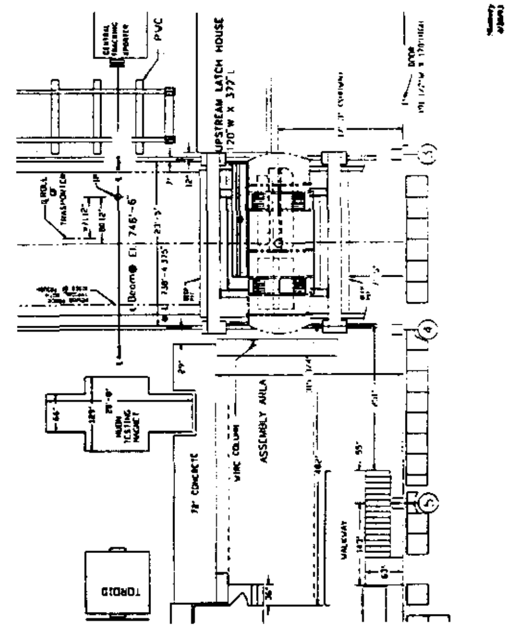

868

Loading the Test Cryostat

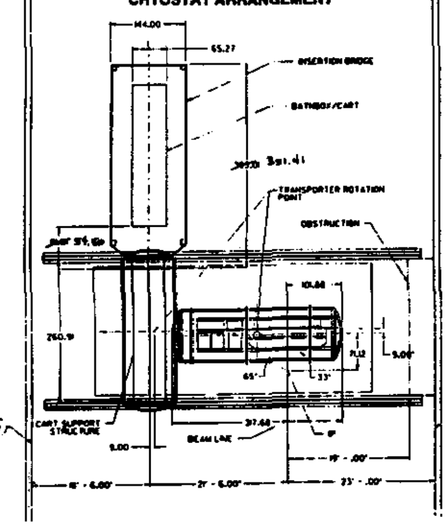

869

Loading the Bath Box

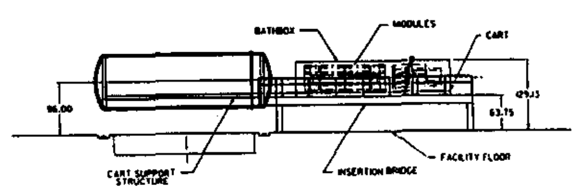

870

Calorimeter Testing in MWest

Open Questions

- What is the schedule for providing calorimeter readout electronics for the Fermilab beam tests? We need a multi-year plan that is consistent with the most probable Fermilab running schedule – next fixed target run in early 1995 and a follow-on run in 1997.
- Should the MWest test cryostat be constructed with a thin window? A relatively narrow window would suffice to shadow the barrel calorimetry. This option should be costed out before a final decision is reached.

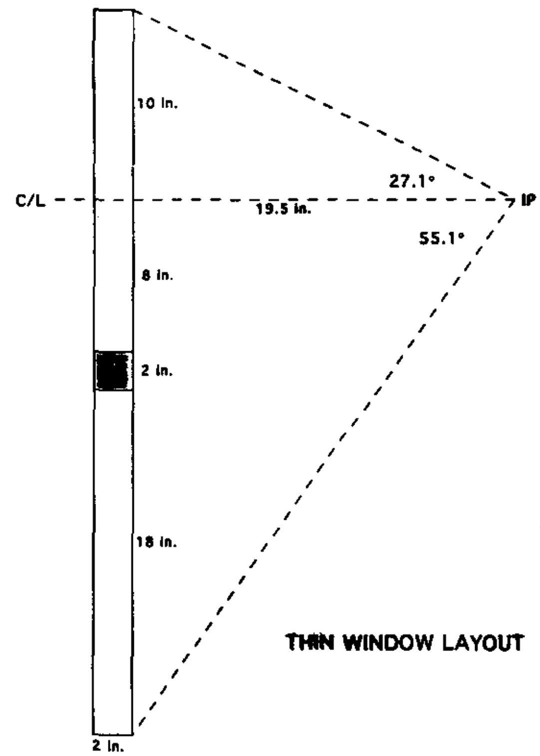

THIN WINDOW LAYOUT

San Diego Meeting Agenda
May 12, 1993

Plenary Session

Morning Session (Chair: Xiaorong Shi)

8:30	Electronics,DAQ	Marlow (30)
9:00	Computing	
	Introduction	Sheer (5)
	Future Directions in GEM Computing	Word (25)
	GEM Detector Simulations	Womersley (20)
	Common GEM/SDC Computing Issues	Hilgart (10)
10:00	Break	
10:15	Physics with GEM report	
	Physics at the SSC	Lane (5)
	GEMGEN	Sheer (15)
	GEMFAST	Skwarnicki (15)
	Higgs Physics	Zhu (25)
	Top, H^+ Physics	Yanagisawa (15)
	Jet Physics, e/h	Womersley (15)
	Physics at 10^{34}	Lane (15)
	$\not{E}_T$, SUSY	Vaniachine (15)
	Detector Optimization	Zhou (20)
12:35	Lunch	

Afternoon Session (Chair: George Yost)

1:45	The incompleteness of the Higgs Sector and the Super Collider	J. Kuti
2:45	Summaries of Working Groups'	
	Calorimetry	TBA
	Muons	Taylor
	Tracker	Brau
4:15	Break	
4:30	N and Gamma Leakage in the Forward Calorimeter Region	Moore
4:50	Summary of the Meeting	Barish
5:30	Adjourn	

Session Highlights
Electronics / Trigger / DAQ

San Diego GEM Meeting

May 12 1993

D. Marlow

San Diego 5/93

GEM Elect/Trig/DAQ Meeting Agenda

8^{30}	~~Gavritov~~ Balagora * ✓	Charge Sharing in the Muon Trigger
8^{55}	Wixted	CSC Readout Update
9^{20}	Mills	SiVtx PAC practice
9^{40}	Hohn	SiVtx PAC practice
10^{00}	Clemen ✓ *	Cal Readout + Trigger Issues
10^{30}	Uijterwaal ✓ *	Trigger MC Update
10^{55}	Bowden ✓ *	DAQ Design Update
11^{25}	Bronson ✓ *	DAQ studies
1^{00}	Dunlea	Test Beam DAQ
1^{30}	Marlow	PAC Review

V. Balagura
ITEP/SSCL
May 12, 1993

Muon trigger model

- Description of the model

real strips
↓
virtual strips
↓
virtual clusters

883

- resolution and efficiency curves
- Sagitta or $\Delta\varphi$?

Trigger based on the cutting of the road in 3-dimensional space $\varphi_1 \otimes \varphi_2 \otimes \varphi_3$ combines all available information for the trigger
⇒ includes naturally <u>both sagitta and $\Delta\varphi$ methods.</u>

884

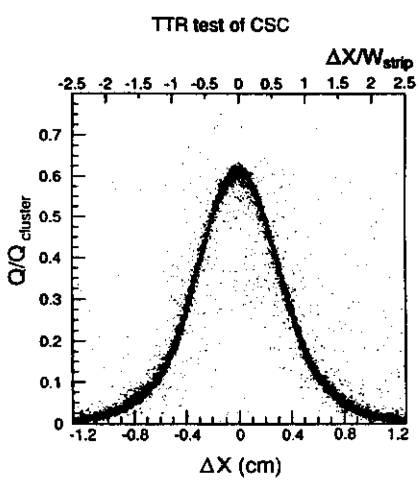

Distribution of charge induced on strips

$$Q_{threshold} = 0.5 \cdot Q^{(dE/dx)}_{threshold}$$

885

Definition of the tower associated with virtual strip

Barrel   Endcap

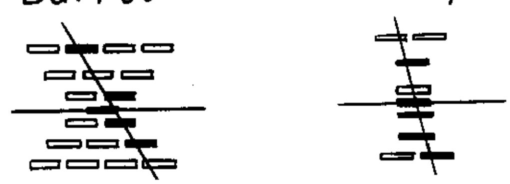

virtual strip ≡ tower with at least 4 strips in different layers with

$$Q > Q_{threshold}$$

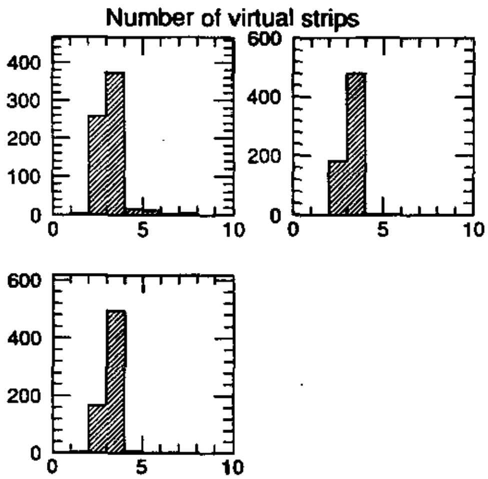

Endcap

887

Definition of the virtual cluster

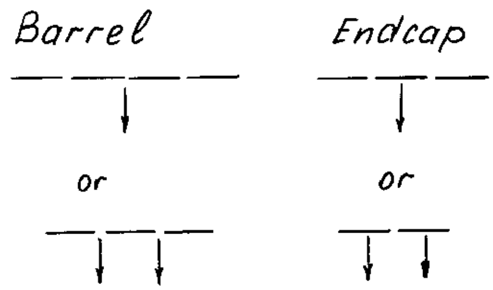

888

Barrel

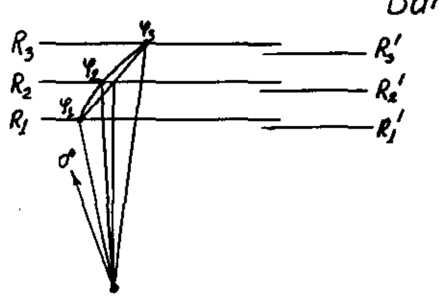

$$\Delta\varphi_{23}^{(str)} = (\varphi_2 - \varphi_3)/(R_2 - R_3) * (\langle R_2\rangle - \langle R_3\rangle)/\Delta\varphi_{str}^{c}$$

$$Sagitta^{(str)} = \frac{\varphi_2 R_2 - \frac{(\varphi_1 R_1 + \varphi_3 R_3)}{2}}{(R_3 - R_1)^2 \Delta\varphi_{str}^{(2)}} (\langle R_3\rangle - \langle R_1\rangle)^2$$

Endcap : $Sagitta^{(str)} = \frac{\varphi_2 - (0.3\varphi_1 + 0.7\varphi_3)}{\Delta\varphi_{str}^{(2)}}$

889

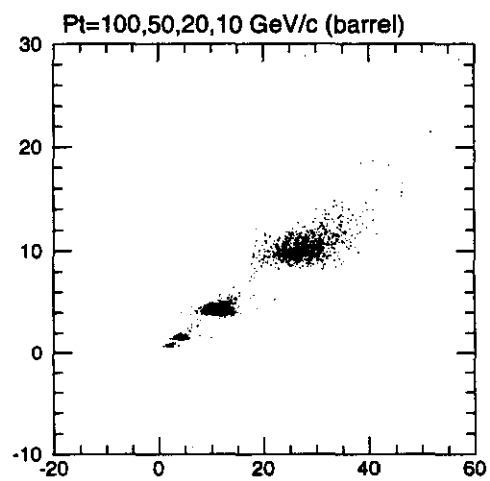

Sagitta vs $\Delta\varphi_{23}$

890

Mark Clemen

- Accordion Data Analysis (Upul Samarakara)
- Trigger Rates - 1st level calorimeter
  - Simulation
  - Endcap Layout
  - Modifications
    - EM Sum Size
    - EM vs SPEM lateral veto
    - Cable Layout Problems

891

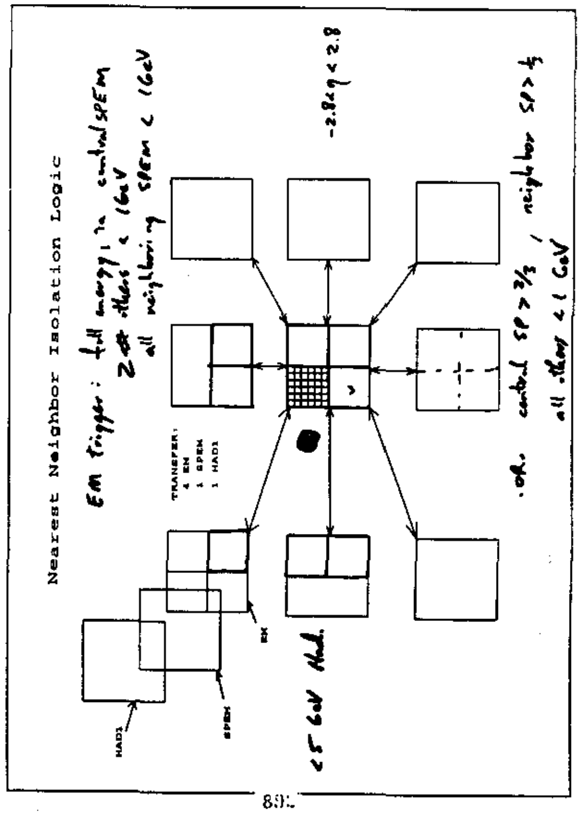

892

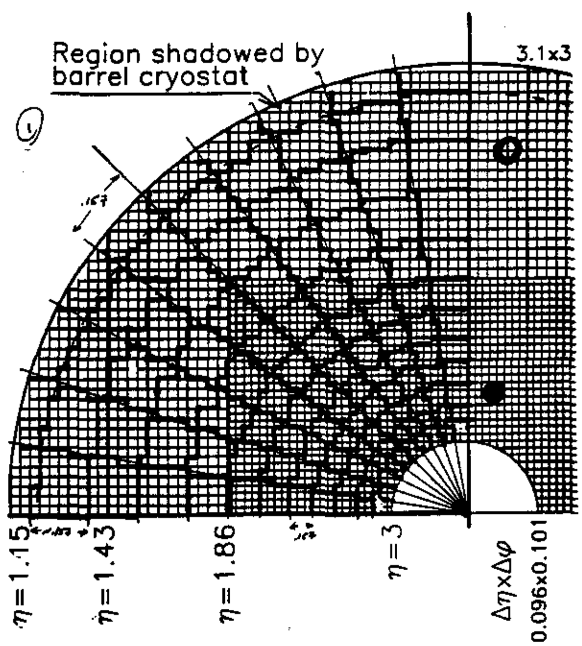

893

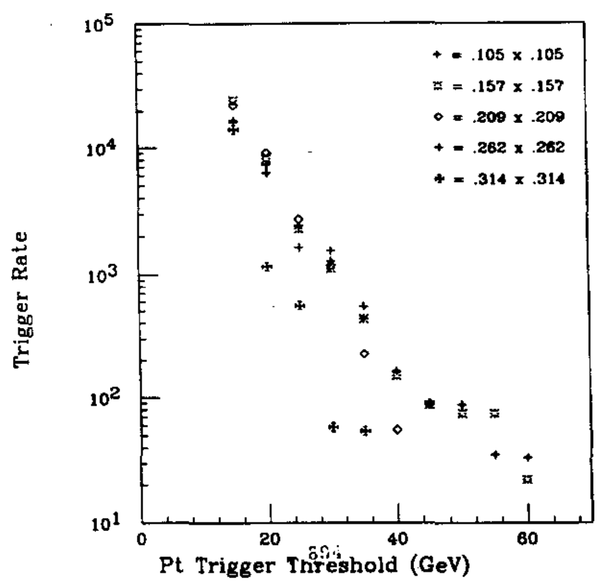

894

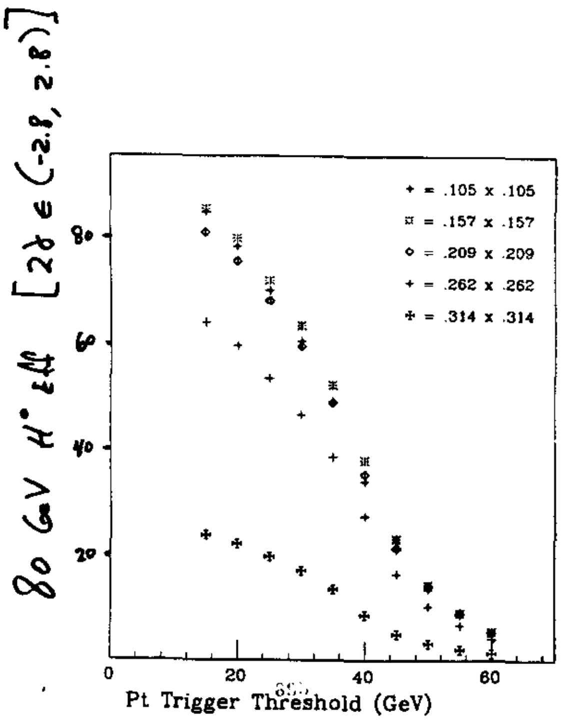
80 GeV H° eff [2γ ∈ (-2.8, 2.8)]
+ = .105 x .105
¤ = .157 x .157
◇ = .209 x .209
+ = .262 x .262
✣ = .314 x .314
Pt Trigger Threshold (GeV)

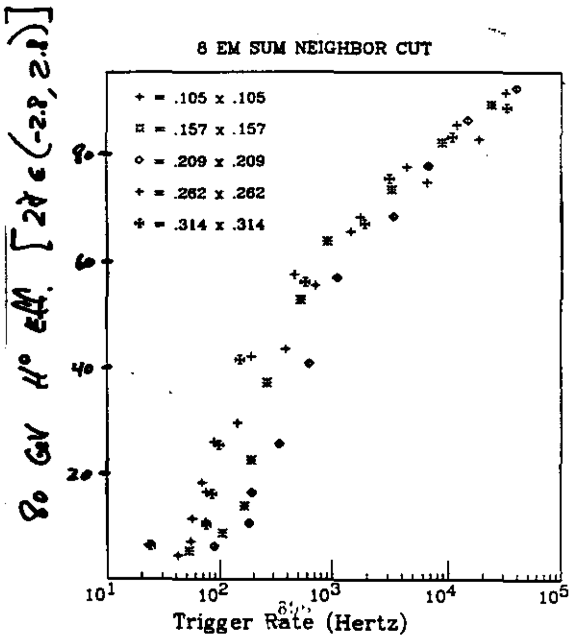
8 EM SUM NEIGHBOR CUT
80 GeV H° eff. [2γ ∈ (-2.8, 2.8)]
+ = .105 x .105
¤ = .157 x .157
◇ = .209 x .209
+ = .262 x .262
✣ = .314 x .314
Trigger Rate (Hertz)

Optimising the trigger thresholds.

(Trigger simulations update)

Henk Uijterwaal, SSCL, May 11, 1993.

Contents:

Details can be found in GEM TN 93-332.

Status of the trigger simulations.

* Version v104 (or PAC review version) of libtrf was released on pdsf on 5/4/93. The code will not be changed, except for urgent bug-fixes, until 6/1/93.
* Modifications w.r.t. v103:
  - Switch to gemfast vII204. Older versions of gemfast are not supported anymore.
  - Routines to print the trigger primitives have been added.
  - Fixes in the analog CA-L1 algorithm to avoid double counting of the number of e/γ-candidates. This caused the differences in trigger-rates between the two CA-L1 algorithms; the rates and efficiencies for the two algorithms are now equal within statistical errors.
  - The global L1 routine uses the optimized thresholds.
  - CA-L2 e/γ finder has been tuned for maximal e/π rejection based on single particles. The effect on physics still has to be studied.
* The next version of gemgen will have an option to generate only $P(1.6)$ minimum bias events per crossing instead of $1+P(1.6)$ events per crossing. This will make the background rate calculations more realistic.

The present calculation overestimates detector activity (E_T) and thus the rate by a factor of up to 2. Down scaling of the rates by a factor 1.6/2.6 is not completely accurate. The new gemgen solves this problem.

E_T for minimum bias interactions.

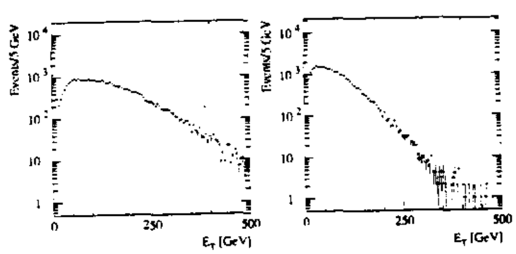

Left: $|\eta|<6.0$ (main + forward cal), Right $|\eta|<3.0$ (main cal only).

Data points: $1+P(1.6)$ interactions/crossing, the model used for these studies.

Yellow Area: $P(1.6)$ Interactions/crossing.

The model used for these studies overestimates the background activity by a factor of up to 2.

Optimising the trigger thresholds.

* The thresholds presented in the TDR were preliminary and have 2 known problems:
  1) The minimum bias rate is too high (24.8 kHz before down scaling, 15.3 kHz after down scaling). The plots presented in this talk show the non-down scaled rates.
  2) The trigger efficiencies for low mass H events is too low. (O(80)%).
* These problems can be solved by tuning the trigger thresholds. Procedure:
  1) Plot the trigger rates as a function of the thresholds in the trigger conditions.
  2) Raise the thresholds for trigger conditions that contribute more than 1 kHz to the rate. (Reduces background but also physics acceptance).
  3) Lower the thresholds for trigger conditions that contribute less than 1 kHz to the rate. (Increases physics acceptance but also background rates.)
  4) Calculate the trigger rates/efficiencies. (The trigger rates for the different conditions are correlated, the plots do not show the correlation's).
  5) Repeat 1-4 until there is no improvement in the rates or efficiencies.
* This talk shows the results of a few loops through step 1 to 4. Further improvement is still possible but fine-tuning of the thresholds is not too interesting at this stage of the experiment.

Trigger rates for Minimum Bias Events.

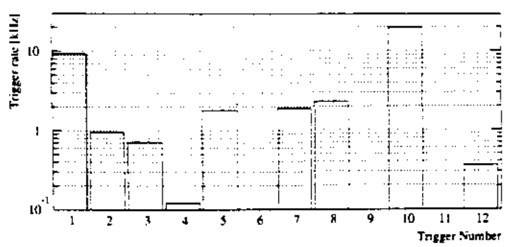

Trigger rates for the 12 trigger conditions based on $5 \cdot 10^5$ minimum bias events.

1 jet trigger rate.

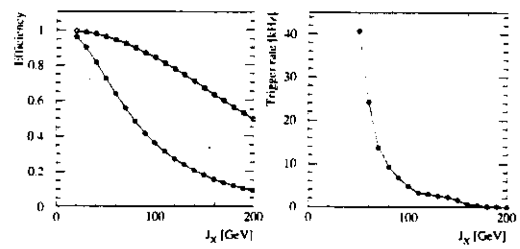

Left: 1 Jet trigger rate for $t\bar{t}$ - production (•) and $H^0 \to ee\,jet\,jet$ (∘).
Right: corresponding minimum bias rates.

E_T missing trigger rate.

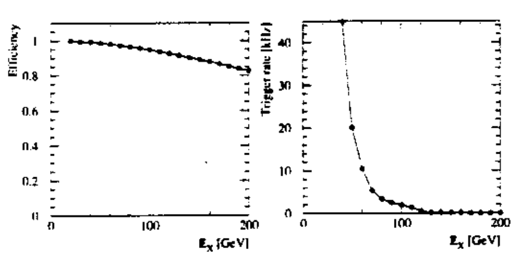

Left: ET Missing trigger rate for SUSY Right: minimum bias rates.

Photon trigger rates.

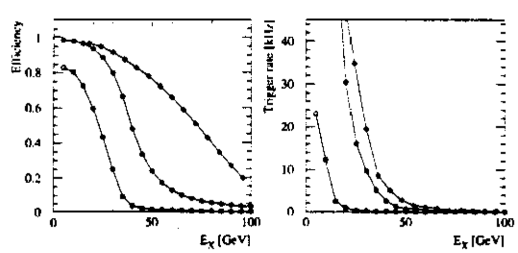

Left: Trigger rate for $H \to \gamma\gamma (m_H = 80 GeV)$.

Right: Corresponding minimum bias trigger rates.

- • : Single e/γ-trigger.

o: Two e/γ-trigger

+: Single e/γ-trigger OR two e/γ-trigger at 1/3 of the single e/γ threshold.

New Trigger Thresholds.

These plots and similar ones for the other 9 trigger conditions suggest the following modifications to the thresholds:

#	Condition	Comment	Modifications
1	J_{125}	Single Jet Trigger	Increased from 80.
2	4 of J	Multi Jet event	
3	E	High P_T e/γ	Lowered from 50.
4	M	High P_T μ	The lowest possible value?
5	2 of E	2 e/γ	Lowered from 16.
6	2 of M	2 μ	
7	E	Missing E_T	Increased from 100
8	E and E	e/γ and missing E_T	
9	M and E	μ and missing E_T	Lowest possible threshold.
10	-	Jet and missing E_T	Removed
11	M and 3of J	μ and 3 jets	Lowest possible threshold.
12	E and 3of J	e and 3 jets	Lowest possible threshold.

Efficiencies/Rates.

- The new thresholds reduce the background rate from 24.8 kHz to 15.6 kHz. (9.6 kHz after down scaling).
- The $H \rightarrow \gamma\gamma$ efficiency at 80 GeV is increased by 10%.
- The efficiency for heavy particles (SUSY, 800 GeV H') is still at the 99% level.

This is a clear improvement over the old set of thresholds.

Electron/μ triggers.

- The trigger for $H^0 \rightarrow eeee$ or $H' \rightarrow \mu\mu\mu\mu$ looks for a pair of leptons. So only 2 of the 4 leptons have to be found at Level 1. This allows for some trigger efficiency without affecting the physics performance for this process.

  But in case of $H' \rightarrow ee\mu\mu$ the trigger cannot recover, if an electron or muon is missed by level 1, the event will not be accepted by the electron/muon pair trigger.

- This problem can be solved by adding an electron-muon trigger like E and M to the list of triggers:

- This trigger is background free and accepts 35% (out of a possible 50%) of the $H' \rightarrow ee\mu\mu$ events for $m_{H'} = 140\,GeV$

Electron/μ trigger rate.

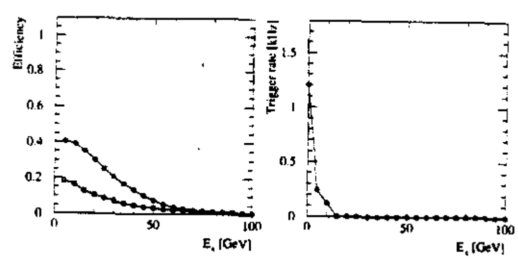

Trigger : E and M

Left: Trigger rates for $H \rightarrow llll\,(m_{H'} = 140\,GeV)$ (•) and $t\bar{t}$ - production (o).

Right: Corresponding minimum bias rates.

The new set of Triggers.

#	Condition	Comment
1	J	Single Jet Trigger
2	4 of J	Multi Jet event
3	E	High P_T e/γ
4	M	High P_T μ
5	2 of E	2 e/γ.
6	2 of M	2 μ
7	E	Missing E_T
8	E and E	e/γ and missing E_T
9	M and E	μ and missing E_T
10	-	Obsolete
11	M and 3of J	μ and 3 jets
12	E and 3of J	e and 3 jets
13	M and E	e and μ

Process	M_{H^0} (GeV)	# Generated events	Fraction Accepted	Fraction Accepted
$H^0 \to \gamma\gamma$	80	10000	88.05 %	92.01 %
	110	10000	94.44 %	97.13 %
	140	10000	96.63 %	98.17 %
$H^0 \to \tau\tau$	140	10000	41.11 %	
$H^0 \to Z^0Z^* \to \ell^+\ell^-\ell^+\ell^-$	140	10000	86.36 %	
$H^0 \to Z^0Z^* \to e^+e^-e^+e^-$	140	10000	86.94 %	
$H^0 \to Z^0Z^* \to \mu^+\mu^-\mu^+\mu^-$	140	10000	86.74 %	
$H^0 \to Z^0Z^* \to e^+e^-\mu^+\mu^-$	140	10000	85.88 %	
$H^0 \to Z^0Z^0 \to e^+e^-\mu^+\mu^-$	400	10000	99.84 %	
$H^0 \to Z^0Z^0 \to e^+e^-$ jet jet	800	10000	99.81 %	
$H^0 \to Z^0Z^0 \to e^-e^+\nu\bar{\nu}$	800	5000	98.34 %	
$H^0 \to Z^0Z^0 \to \mu^-\mu^+\nu\bar{\nu}$	800	5000	93.32 %	
$t\bar{t} \to H^0 \to \ell\gamma\gamma + X$	80	9981	96.81 %	
$t\bar{t}$-production.		10000	77.00 %	
SUSY. $\tilde{g}\tilde{g}$-production.		10000	99.99 %	
$W^\pm \to e\nu$		10000	35.34 %	
$W^\pm \to \mu\nu$		10000	31.66 %	
$Z^0 \to e^+e^-$		10000	88.10 %	
$Z^0 \to \mu^+\mu^-$		10000	88.10 %	

Table 7: Physics efficiency for the Level 1 trigger criteria suggested in table 6. The fourth column lists the trigger efficiency when the standard generator cuts were used, the fifth column the efficiency when more restrictive generator cuts were used. (See table 1).

Conclusions.

- The background rate for this set of triggers is 15.6 kHz before down scaling, 9.6 kHz after down scaling. This rate does not include about 2 kHz of false muon triggers.
- The physics efficiencies (except for $H^0 \to \tau\tau$) are close to or well above the 90% level. The efficiencies for "analysable" events are even higher.
- These numbers are an improvement over the previous results and even closer to the design goal for the Level 1 trigger.

The next steps are:

- Better estimate for the minimum bias background using the new gemgen.
- Level 2 trigger simulations.
- Triggers for $L=10^{34} cm^{-2} s^{-1}$

Mark Bowden

Overview of the GEM Data Acquisition System

Preliminary

System Architecture

The baseline GEM Data Acquisition system is designed to support a bandwidth of approximately 10 GBytes/sec (figure 1). This implies a maximum event size of 1 MByte at the expected Level 1 rate of 10 KHz (or 100 KBytes at the highest allowable Level 1 rate of 100 KHz). If necessary, this bandwidth can be increased by a factor of four through the simple addition of output channels.

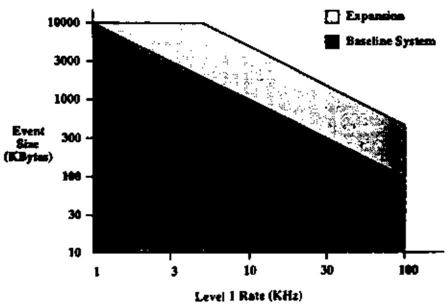

Figure 1 Data Acquisition System Operating Range

The basic system architecture is shown in figure 2. Most of the Data Acquisition system is located in the Electronics Room and is connected to the front-end electronics through independent fiber data links. Up to 12000 front-end modules are supported. Following a Level 1 Trigger Accept, all digitized data from the front-end system is transmitted to the Event Data Collectors (EDCs) where it is buffered during the Level 2 Trigger decision. This approach allows a relatively long latency and greater flexibility in the design of the Level 2 Trigger. Level 2 will initially be implemented in software using the general-purpose processors of the Level 3 system. As the algorithms are refined, some portion may be transferred to hardware. The architecture allows any combination of hardware or software implementations.

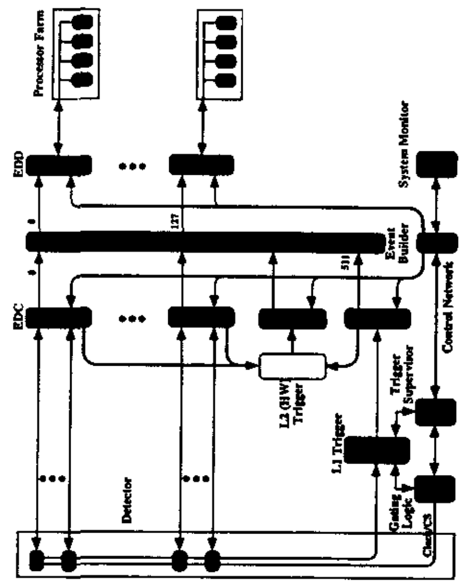

Figure 2 GEM Data Acquisition System

Simulation of the GEM Data Acquisition System

Jim Branson

May 1993

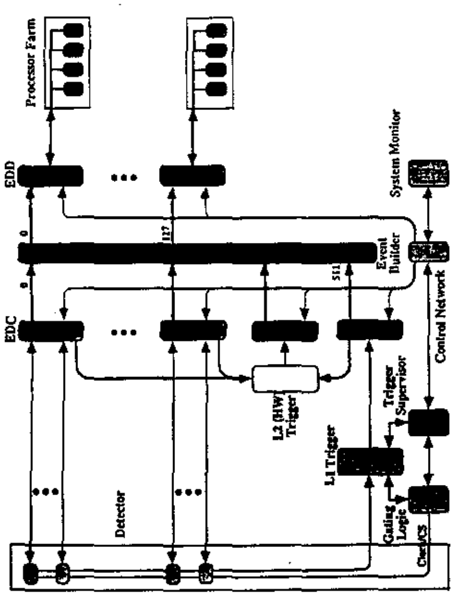

Figure [] GEM Data Acquisition System

THE SIMULATION

- 512 EDCs. Minimal Simulation: We assume the EDC can keep data flowing at 100 kbyte/s into the output fiber (when requested). (memory use)
- 128 EDDs. Moderate Simulation: EDDs have a queue of requests from processor. They perform one task (such as a message to EDCs or processor) per 4 microsecond time interval. (memory use)
- 512 Processors. Moderate Simulation: Processors have an event queue and run trigger tasks when data are available. Level-2 tasks run to completion. Level-3 tasks may be suspened. Processors send messages to EDDs (one action per 4 microsecond time step).
- Switch. Minimal Simulation: The (barrel) switch has 512 input fibers and 128 output fibers. We simulate 65536 virtual links with 1/512 the capacity of one fiber (about 200 kbyte/s). We just keep track of the backlog in each of the virtual links.
- 128 Links from EDD to (4) Processors Minimal Simulation: Again we just keep track of the backlog on each link.
- Trigger Supervisor Moderate Simulation: Every millisecond, the supervisor polls the processors (for queue size) and distributes events to those least busy.

IMPORTANT PARAMETERS

Mean Level-1 Rate	100 khz
Mean Event Size	200 kbyte
Data per EDC	12 EDCs have 38% of data
Level-2 Data	9% of data per step, $\frac{RMS}{Mean} = 6$
Fiber Link Speeds	100 megabyte/s
Level-2 Rejection	0.23 per step (4 step)
Time Step	4 microseconds
Mean Level-2 Task Time	1 millisecond
Mean Level-3 Task Time	0.1 seconds

EVENT SIZE

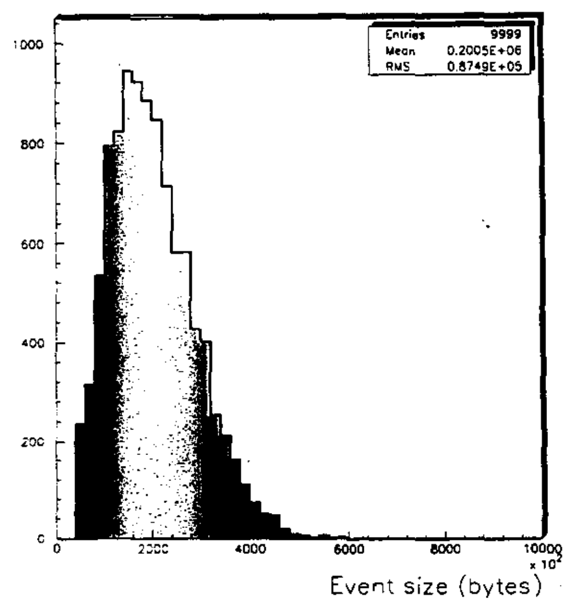

SIZE IN 12 LARGEST EDCS

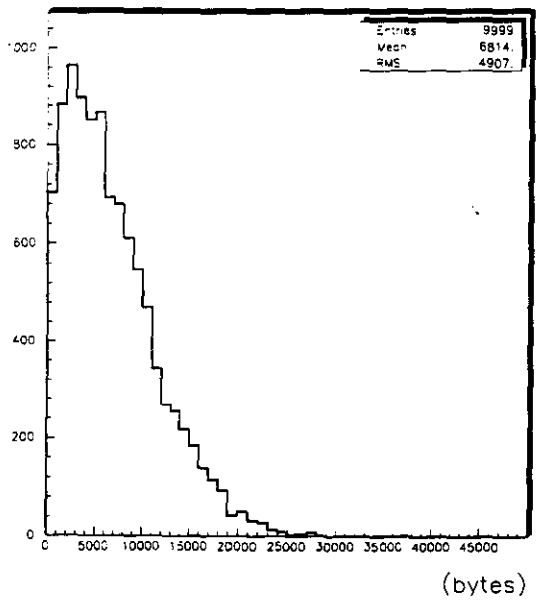

924

BYTES TRANSFERED PER EDC

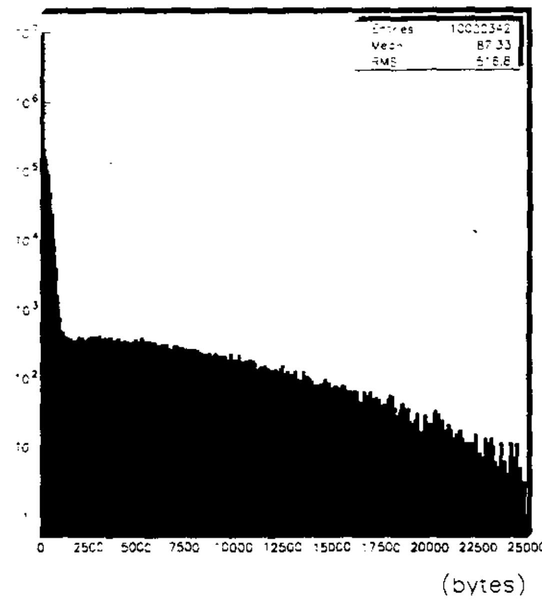

925

BYTES TRANSFERED PER EDC*

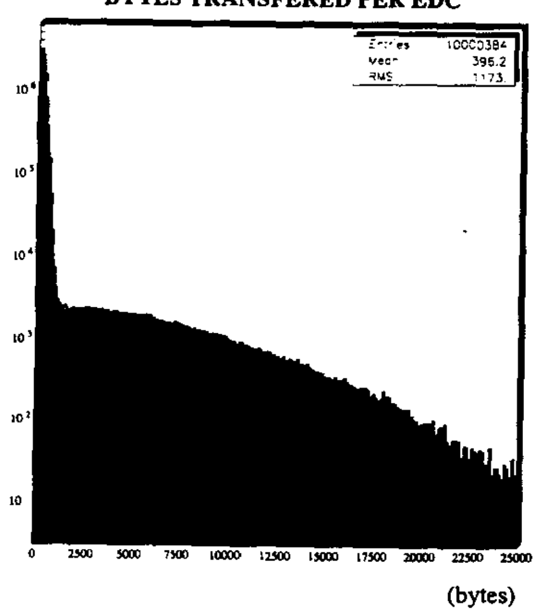

926

LATENCY IN EDC

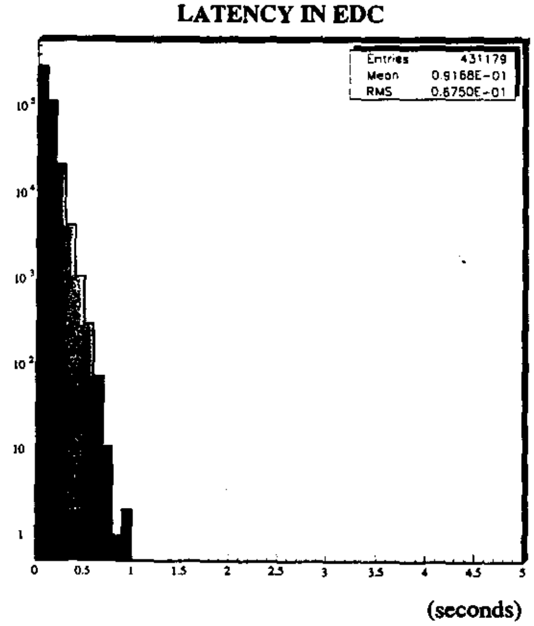

927

LATENCY IN EDC* (50 khz full xfer)

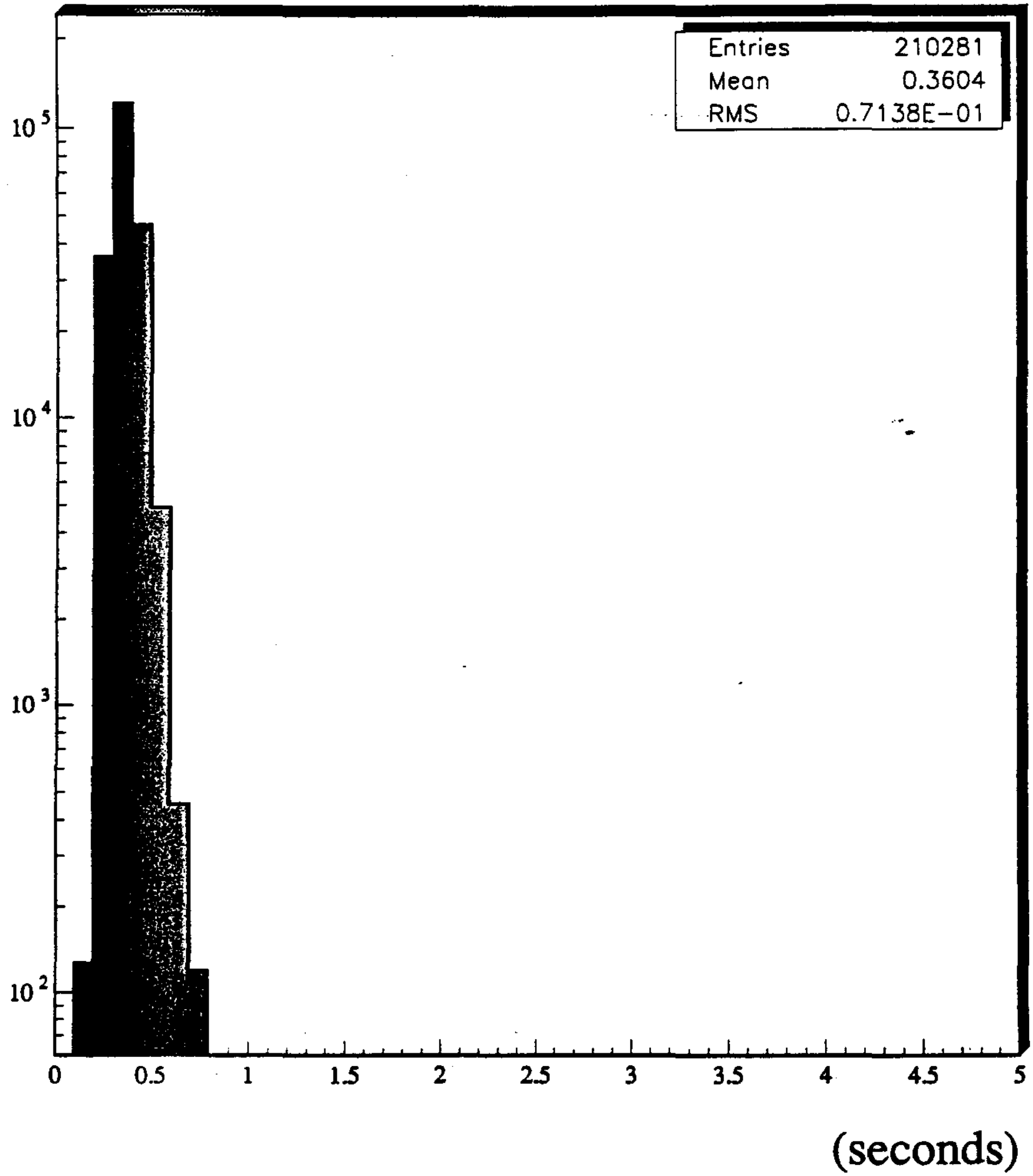

LATENCY FOR EVENTS PASSING LEVEL 2

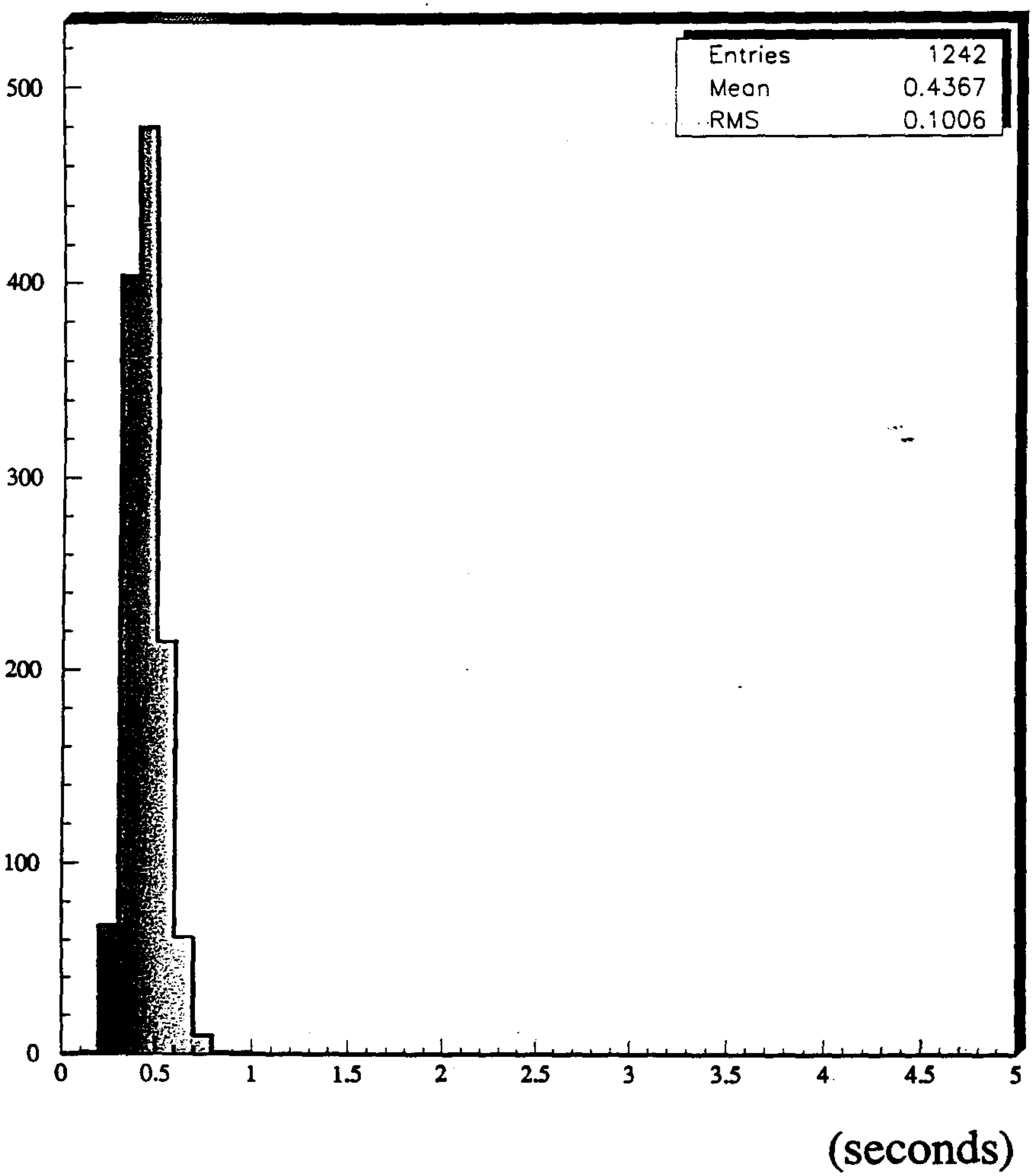

VIRTUAL LINK BUSY FRACTION

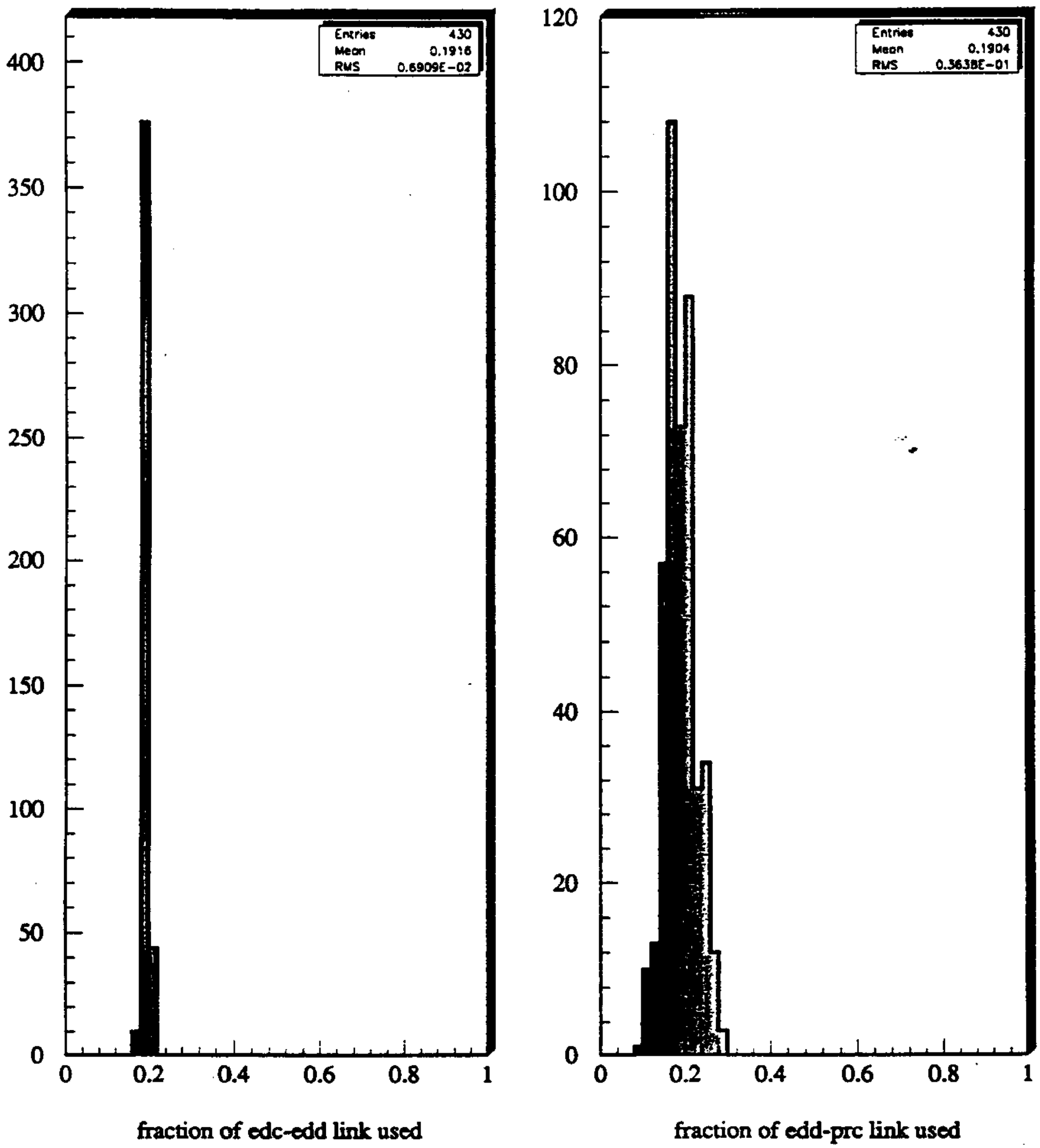

VIRTUAL LINK BUSY FRACTION*

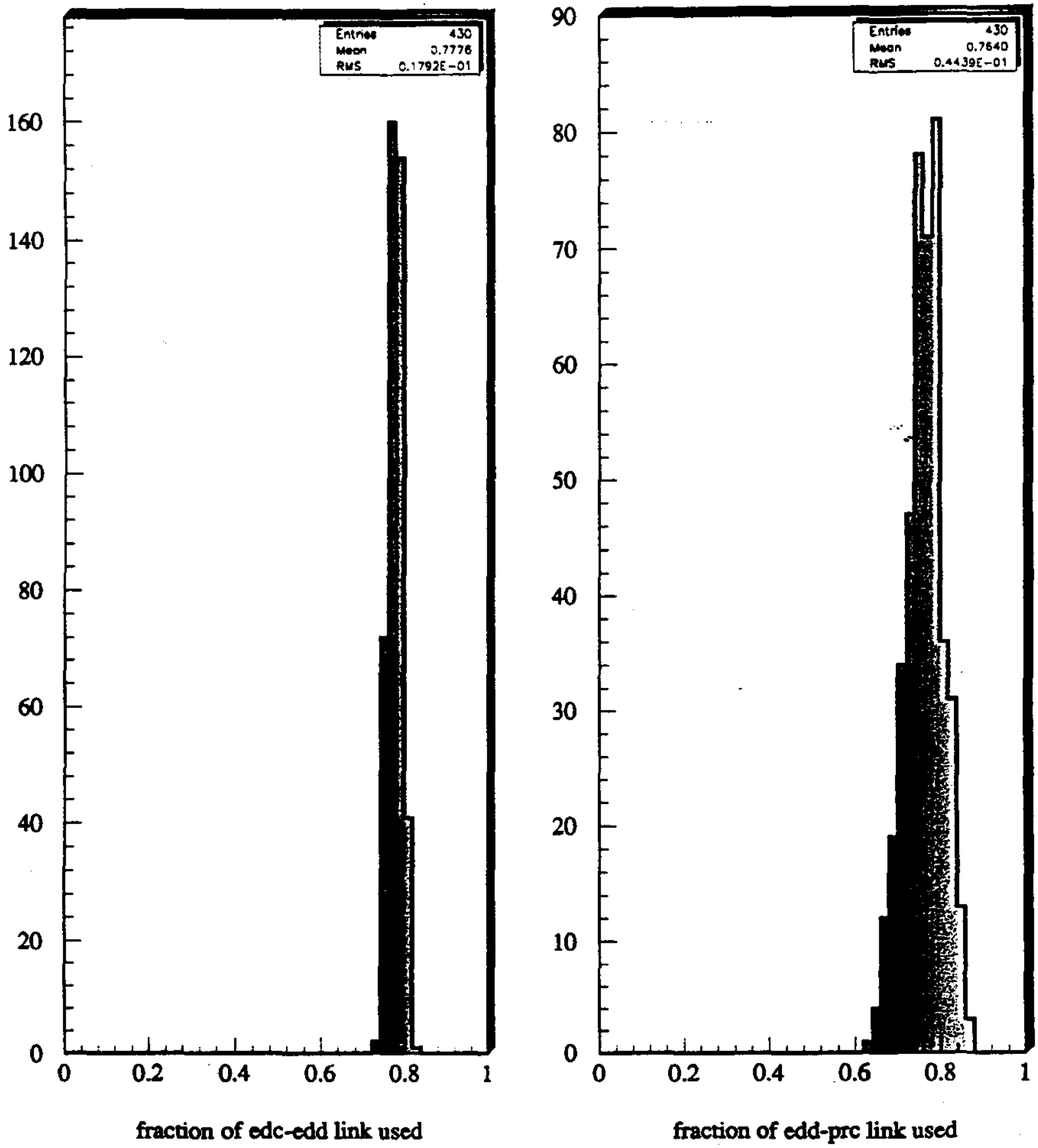

LATENCY IN EDC* (50 kHz full xfer)

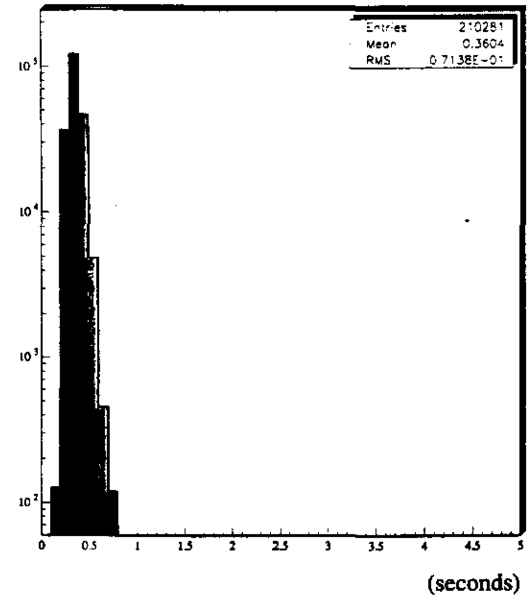

928

LATENCY FOR EVENTS PASSING LEVEL 2

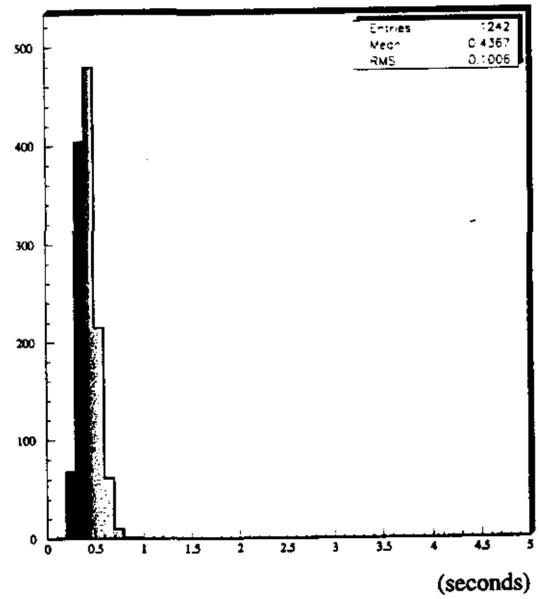

929

VIRTUAL LINK BUSY FRACTION

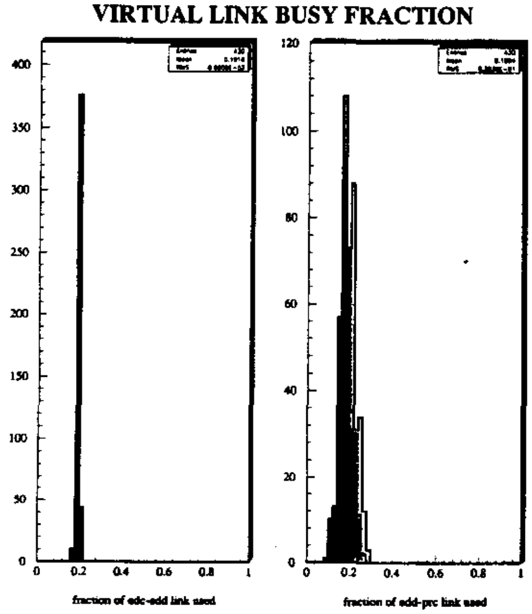

930

VIRTUAL LINK BUSY FRACTION*

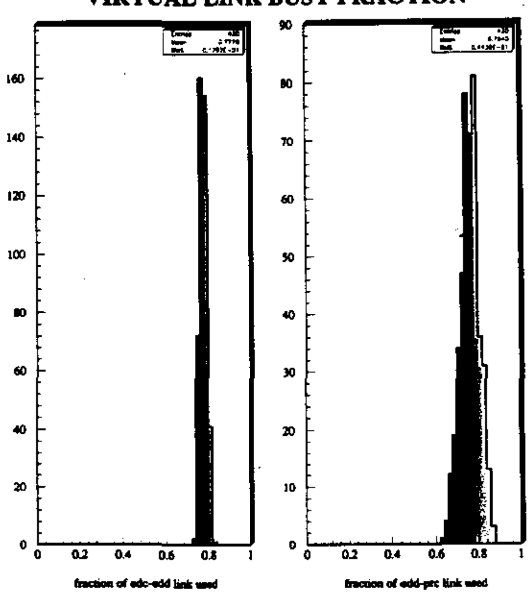

931

VIRTUAL LINK BACKLOG TIMES

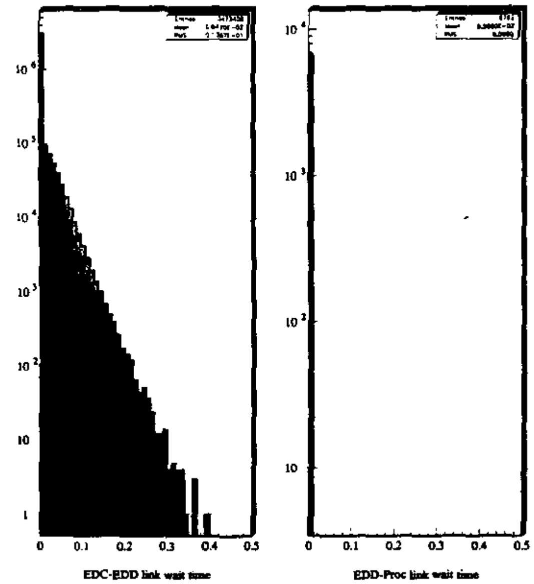

932

VIRTUAL LINK BACKLOG TIMES*

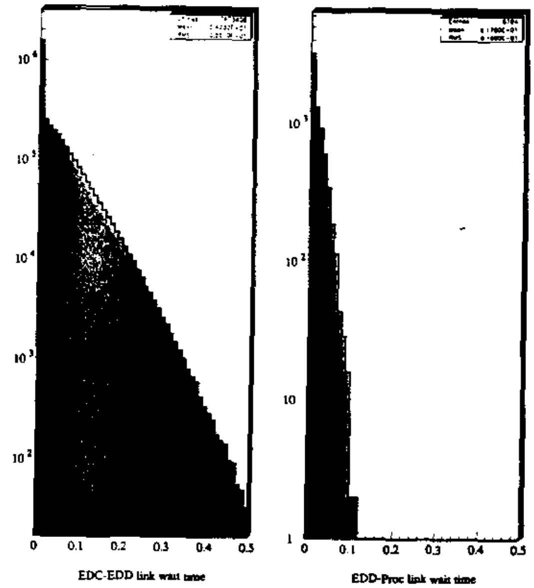

933

EDC MEMORY USAGE

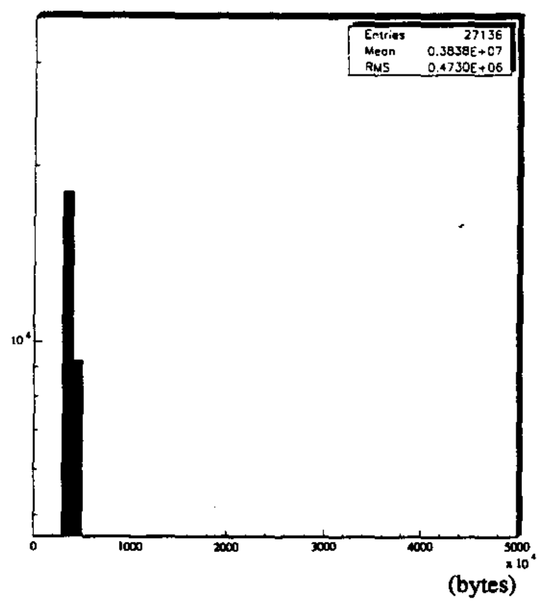

934

EDC MEMORY USAGE*

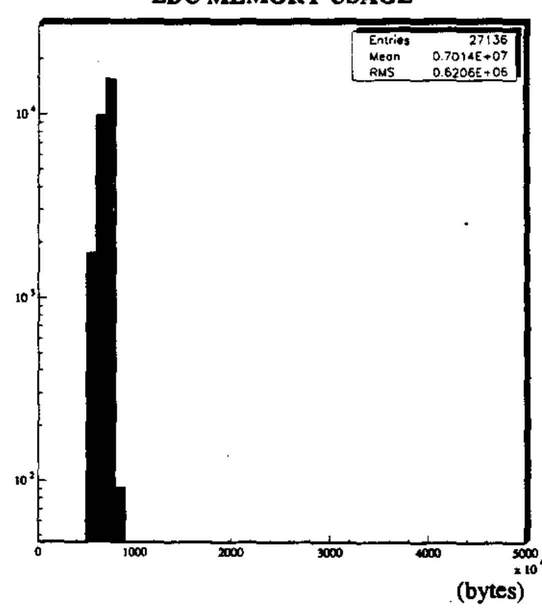

935

EDD MEMORY USAGE

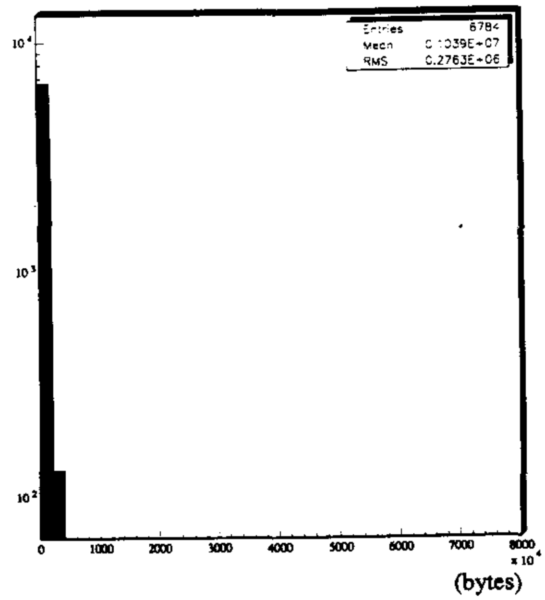

936

EDD MEMORY USAGE *

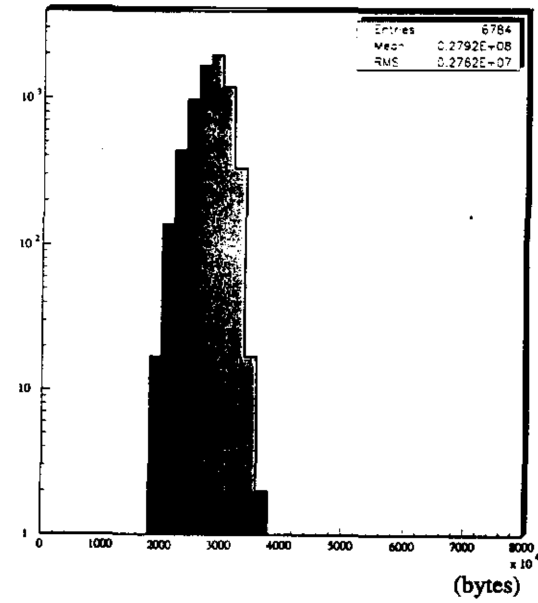

937

EVENTS IN PROCESSOR QUEUE

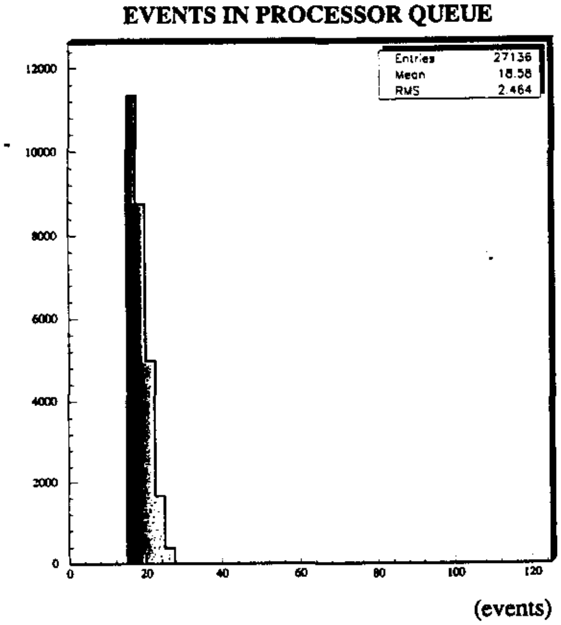

938

EVENTS IN PROCESSOR QUEUE *

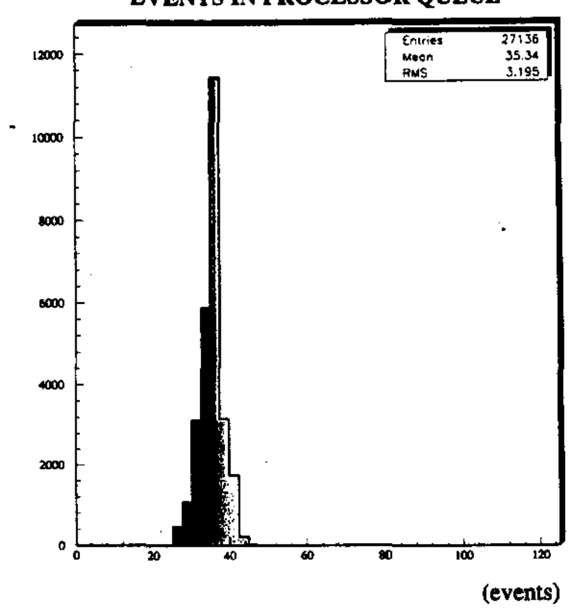

939

Performance Under Various Conditions

	Mean Latency	Maximum Latency	Link Use Fraction	Mean EDC Memory	Mean EDD Memory	Mean Queue Processor
Virtual Level 2 Mode						
5 khz rate	0.06	0.4	0.01	0.2	0.2	0.6
100 khz rate	0.09	0.7	0.19	3.8	1.4	19
200 khz rate	0.14	1.2	0.38	11.4	4.0	50
100 khz rate 400 kb size	0.27	2.0	0.38	21.7	8.5	53
Full Transfer Mode						
2 khz rate	0.08	0.2	0.03	0.1	1.2	0.3
25 khz rate	0.15	0.5	0.39	1.5	5.9	7
50 khz rate	0.30	0.7	0.78	7.0	27.9	35

Full Transfer mode fails at a 62 khz rate with 128 EDDs.

With 256 EDDs, full transfer works at 100 khz.

CONCLUSIONS

Virtual level-2 mode works in principle. It reduces switch requirements by about a factor of 8 (using my parameters). With the same switch average latency is lower than in the full transfer mode. Maximum latency increases a bit.

At 100 khz level-1 rate, the switch is running at 19% capacity. This leaves about a factor of 4 as a performance contingency.

The model assumes that the average amount of data in each EDC is the same and that all EDCs are equally requested for level-2. We must attempt to achieve good balance. A factor of 2 imbalance will use up a factor of 2 in performance.

A simple calculation shows that level-2 tasks must run on a processor in a few milliseconds. We must now test the level-2 algorithms.

Memory requirements for EDCs and EDDs seem moderate.

Processor queues of order 50 or more are needed. This means that the system will be processing about 25,000 events simultaneously.

GEM Computing

• Introduction	I.Sheer	5'
• Future Directions	G.Word	20'
• Full Simulation	J.Womersley	20'
• GEM & PRCD	J.Hilgart	10'

Computing Chapter in the TDR

- concentrates on gross features rather than details
- is aimed at people with computing backgrounds *as well as* physicists
- suggests possible projects for both the collaboration and PRCD/SSCL

Table 8-6. Technology and cost projections.

Parameter	1993	1997	1998	1999	2000	2003
Single CPU power (kSSCUP) (midrange)	0.10	0.38	0.54	0.75	1.05	2.89
Number of CPUs per box	1	2	2	4	4	8
CPU cost per box (k$)	6	7	6	11	9	13
Memory size (GB)	0.06	0.3	0.5	1	1	3
Memory Cost (k$/GB)	100	35	27	21	16	7
Disk Cost (k$/GB)	2	1	0.8	0.6	0.5	0.3
Mass (slow) memory cost (k$/GB)	25	7	5	3.5	2.4	0.9
Mass storage media cost (M$/PB)	2	0.41	0.38	0.34	0.31	0.23
Mass storage bandwidth cost (M$/GB/s) (including robots)	20	10	8	7	6	3
Number of boxes for 1 MSSCUP	10,000	1,302	930	332	237	43
Cost/MSSCUP (M$)	130	24	19	11	6	1.5

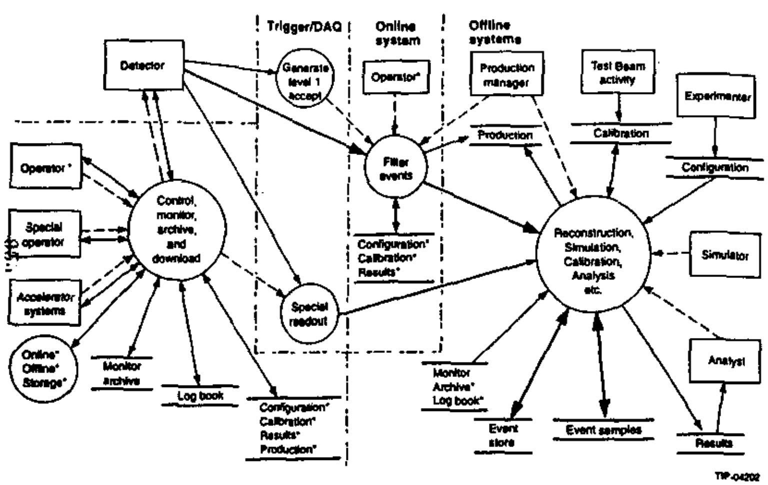

FIG. 8-1. System model for GEM computing. Rectangles represent external entities, circles represent processes, double bars represent stores, solid arrows represent data flows, and dashed arrows represent commands. The primary data flows are indicated by a thick arrow. A label with an asterisk (*) indicates that the entity appears in more than one place in the diagram.

Table 8-2. Overall model for expected rates; system capabilities will exceed these rates. Rates are given for the end of the operating year, while integrated quantities (integrated luminosity, total storage) are calculated assuming an exponential increase in luminosity each year until a constant value is reached in 2003. For *explanations, see text.*

Parameter/Year	1999	2000	2001	2002	2003
Peak luminosity (cm^{-2} s^{-1})	10^{30}	10^{31}	10^{32}	10^{33}	10^{33}
Total live time (s)	10^{6}	10^{7}	10^{7}	10^{7}	10^{7}
Integrated luminosity (pb^{-1})	1	40	400	4,000	10,000
Level 1 trigger level	100 μb	100 μb	100 μb	100 μb	100 μb
Level 1 trigger rate (maximum)	100 Hz	1 kHz	10 kHz	100 kHz	100 kHz
DAQ event size	1 MB	0.6 MB	0.3 MB	0.3 MB	0.3 MB
Peak data rate out of DAQ	100 MB/s	600 MB/s	3 GB/s	30 GB/s	30 GB/s
Event filter (Level 2/3) factor	1	10	100	500	500
Level 2 computational load (SSCUP)[a]	10^{3}	10^{3}	10^{4}	10^{5}	10^{5}
Level 3 computational load (SSCUP)	0	10^{4}	3×10^{4}	1.3×10^{5}	1.3×10^{5}
RECO rejection factor	1	1	1	2	2
RECO computational load (SSCUP)	2×10^{4}	2×10^{5}	3×10^{5}	4×10^{5}	4×10^{5}
Event rate stored	100 Hz	100 Hz	100 Hz	100 Hz	100 Hz

Table 8-2. Overall model for expected rates; system capabilities will exceed these rates. Rates are given for the end of the operating year, while integrated quantities (integrated luminosity, total storage) are calculated assuming an exponential increase in luminosity each year until a constant value is reached in 2003. For explanations, see text. (Cont.)

Parameter/Year	1999	2000	2001	2002	2003
Equivalent cross section	100 μb	10 μb	1 μb	100 nb	100 nb
Initial data per event	1 MB	0.9 MB	0.6 MB	0.6 MB	0.6 MB
Rate of initial data to storage	100 MB/s	90 MB/s	60 MB/s	60 MB/s	60 MB/s
Additional event data	1.6 MB	1.6 MB	1.6 MB	1.6 MB	1.6 MB
Peak event data rate	110 MB/s	150 MB/s	130 MB/s	130 MB/s	130 MB/s
Annual event storage	0.26 PB	1 PB	0.9 PB	0.9 PB	2.2 PB
Simulation computational load (SSCUP)	1.5×10^{5}	3×10^{5}	6×10^{5}	6×10^{5}	6×10^{5}
Annual simulation storage	0.14 PB	0.25 PB	0.4 PB	0.4 PB	0.4 PB
Annual test beam data	0.01 PB	0.01 PB	0.01 PB	0.01 PB	0.01 PB
Total annual storage	0.5 PB	1.3 PB	1.3 PB	1.3 PB	2.6 PB
Peak rate to storage	125 MB/s	170 MB/s	155 MB/s	155 MB/s	155 MB/s

Table 8-7. Estimated lines of code in the final GEM system.

Category	Lines of Code
GCS software	100k
On-line software	50k
Generators (GEM-specific code)	20k
Simulation (GEM-specific code)	150k
Reconstruction	200k
Physics analysis	50k
Event display and graphics	40k
Database	50k
Framework	50k
Utilities	100k
Special OS interfaces and drivers	50k
Event filters	50k

Table 8-8. Estimated manpower profile for software development, in FTE by year.

Source	1993	1994	1995	1996	1997	1998	1999	2000
PRCD	4	10	20	40	40	40	30	20
GEM Project	1	4	8	12	16	16	16	12
DAQ	1	3	6	6	6	6	6	6
SSCL Physics	2	4	8	8	10	10	10	12
Collaboration	25	30	35	40	50	50	55	60

Future Directions in GEM Computing

Highlights from the TDR

Gary Word
SSCL

May 12, 1993

SSC Collaboration Meeting
at UCSD

GEM Computing Subsystem

Responsibility:

"To ensure that computing systems are available to fulfill the overall goals of GEM."

Includes:

- event filters
- control systems
- monitoring systems
- reconstruction
- simulation
- calibration
- database systems
- analysis systems
- mass storage
- communication systems for machines and people

962

Management Structure:

[CS ⇒ Computing Subsystem]

CS Leader	– Ken McFarlane
CS Project Manager	TBD
CS Chief Engineer	TBD
CS Steering Committee	TBD

Jan, '93, Ken formed the Acting CS Steering Committee

SSCL/PRO	K. McFarlane, chair
	I. Sheer
	J. Womersley
	G. Word
SSCL/PRCD	L. Cormell
	L. Roberts
	J. Hilgart
LLNL	T. Wenaus
UW	T. Burnett
CalTech	H. Newman
	R. Mount
BU	T. Johnson

963

At Jan., '93 Acting Steering Comm. Workshop:

"Be bold! Give us the computing environment that you think best!"

– Barry Barrish

964

Committee made specific recommendations, as reflected in TDR.

Comments are sought by the committee.

- e-mail to mcfarlan@sscvx1
- post to newsgroup ssc.gem.comp
- attend comp. mtgs. around Collab. Council mtg.
- attend (in person or via video- or audio-conference) monthly Steering Committee mtg.

965

In TDR section:

8.7 Software Implementation Model

8.7.1 Standards and Integration

Integration ⇒ same standards for off-line & online

Standards:

"For software, the standards that would be used for a current implementation are:

1. OS - variant of UNIX
2. GUI - X, Motif
3. file system - NFS, later DFS
4. languages - F77, C, C++
5. network protocol - TCP/IP
6. code management - CVS
7. Data Model, Data Description Language - to be defined
8. coding standards & practices - to be defined"

966

8.7.1 Standards & Integration, Cont.

"On the language issue, Fortran 90 is omitted since it is felt that C and C++ will provide the functionality beyond F77 that is needed to support GEM computing, and will have wide industry support. The implementation will provide a framework in which processes written in FORTRAN can access needed data structures."

967

8.8 Development Projects

- GEM projects may overlap with PRCD, SDC or PASS projects.

8.8.1 Detector Simulations

Parameterized - gemfast, gemgen

Detailed - SIGEM

Mixture - UAEMIX

Gemfast, gemgen & SIGEM "will be supported at the SSCL until a replacement is developed."

"We aim to develop a global simulation package that... incorporates [these packages] but places [them] in a unified, coherent structure."

(PRCD help requested for maintenance, portability.)

968

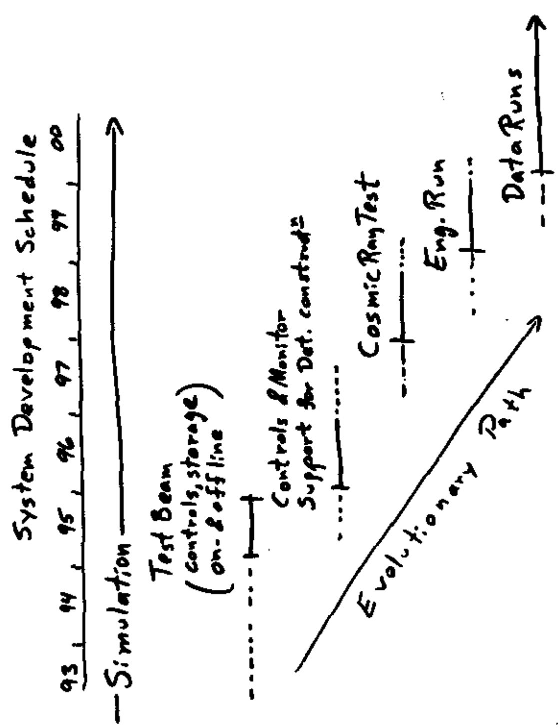

969

8.8 Development Projects
- GEM projects may overlap with PRCD, SDC or PASS projects.

8.8.1 Detector Simulations
Parameterized — gemfast, gemgen
Detailed - SIGEM
Mixture - UAZMIX

Gemfast, gemgen & SIGEM "will be supported at the SSCL until a replacement is developed."

"We aim to develop a global simulation package that ... incorporates [these packages] but places [them] in a unified, coherent structure."
(PRCD help requested for maintenance, portability.)

970

Test Beam ('95 @ FNAL)
- 2nd Major near-term focal point
- gemfast/UAZMIX/SIGEM will be used for simulations

All five computing subsystem groups are expected to focus on support of the Test Beam effort. Assistance from PRCD is expected.

971

Computing Subsystem Groups
1) Global Control System (GCS) Group
Produces a GC System which controls and monitors detector.
2) Online System Group
Responsible for systems which filter events and apply calibration constants.
3) Software Framework Group
Responsible for coordination of all GEM computing tasks and provides common tools.
4) Detector Subsystems Group
Responsible for detector-subsystem specific code and calibration constants.
5) Global Physics Tasks Group
Makes sure the physics is valid.

972

Critical Path Items:
- development of requirements
- development of a data model
- selection of data management techniques and database approach
- development of a basic framework

973

8.8.3 Software Framework Project

- Bulk of effort provided by PRCD.
- Prototype framework to be developed for the test beam work.
- Specific elements are:
  - Data modelling/management/structures
  - Interprocess Communication & Control
  - Remote Procedure Calls (RPC)
  - Parallel Processing support
  - Mixed Language Programming
- A C++ pilot project will be established, in cooperation with PRCD, which will address development of:
  - basic C++ classes
  - method of object persistence
  - method of object transport between processes

974

Computing Subsystem Groups

Reporting to CS Project Manager:
- Global Control System
- Online Computing

} T. Kozlowski

Reporting to CS Leader (K. McFarlane):
- Software Framework
  - John Hilgart
  - Tony Johnson
  - Irwin Sheer
  - Torre Wenaus
  - Gary Word
- Detector Subsystems
  - Muon - Roger McNeil
  - Cal - John Womersley
  - CT - Shawn McKee

975

- Global Physics Tasks
  - Irwin Sheer
  - Torre Wenaus
  - John Womersley
  - Tomasz Skwarnicki

Collaborators interested in joining or assisting the Computing subsystem should contact McFarlane at mcfarlan@sscvx1.ssc.gov

976

J. Hilgart

Common GEM/SDC Computing Issues

- Issues where informal cooperation and agreement exist
- Current SSCL Comp. Dep. projects
- Future SSCL Comp. Dep. projects

980

Informal GEM/SDC cooperation

- GEM observes and advises at SDC computing working group meetings. Fermilab, Houston, → joint meetings
- Operating System - emphasize UNIX
- Code management - use rCVS
- Code distribution - use rdist complemented by afs
- Explore WWW for easy interactive information queries, e.g.,
  - GEM tech. note titles of '92
  - meeting calender
  - collaborator data base

Informal coop, cont

- Document preparation
  - MS Word, Tex, FRAME co-exist
  FRAME expertise growing at SSCL

98?

Current Common Projects

- PDSF upgrade is imminent
  2000 → 4000 SSCUPs
  - new batch system
  - equipment installation
    HP
    SUN
    SGI
- Application Servers using afs file servers
  - Put software in one place
  - Bonus: automatically exports SSCL afs filesystems outside the lab
  - CERNlib and generator support
  - Public Domain utility software
  - Common login scripts

Current Projects, cont.

- PASS - petabyte Access Storage Solutions
  - Investigate functionality and suitability of different kinds of data bases and storage hardware
    - HEP traditional home-grown
    - Relational data base
    - object oriented data base
  - Reach PByte in stages
    - 100 MByte ✓
    - 10 GBytes, next few months
    - 1 TByte, ~1 year
- Desktop televideo conferencing
  - Feedback to vendors our requirements
  - Audio, video, shared whiteboard on a X-Windows workstation

964

Future SSCL CD projects

- C++ - Fortran interfaces
- object data bases
  - meta data bases of event data
  - non-event data bases, e.g., geometry
- PDSF
  - Tertiary storage acquisition in preparation for test beam data of '95
  - automatic file migration software
- Analyze test beam requirements for computing in order to identify modules
- Pick several modules to work on

965

Future projects, cont.

In the course of developing these modules, address

- Analysis and design framework (software methodology)
- Core software concepts (SDC), including parallel programming
- GEM's concerns:
  - Basic OO class libraries
  - Object persistence
  - Object transport
  - remote procedure calls
  - inter-process communication
- QA, conformance to standards

966

GEM & SDC are developing common solutions for most of their common computing issues

967

Tomasz Skwarnicki
SMU

GEM PHYSICS SIMULATIONS FOR TDR

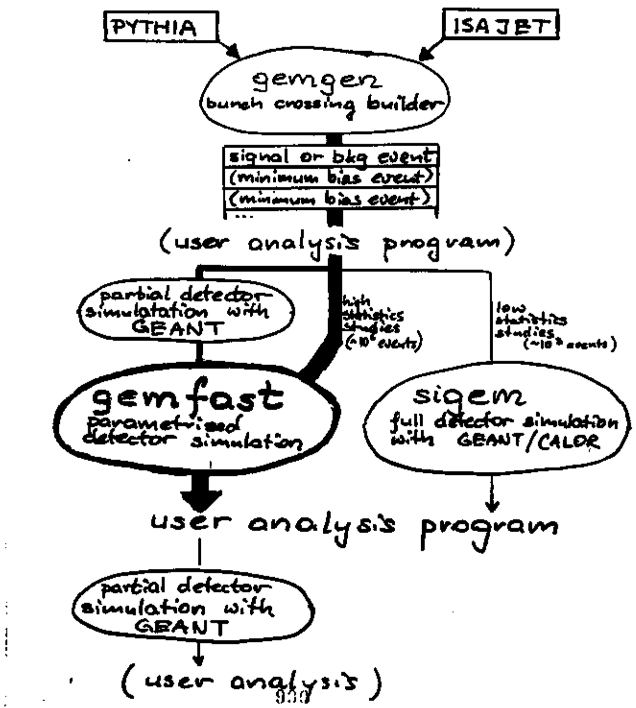

990

People directly involved in gemfast development:

21 People
12 Institutions

Muons:
- Torre Wenaus
- Peter Dingus
- TS
- (Roger McNeil)
- (John Sullivan)

() previous versions

Central region calorimeters:
- TS
- Hong Ma
- Sasha Vanyashin
- Rob Carey
- Sasha Sabin
- Mike Shupe

Forward Calorimeter:
- Mike Shupe

Central Tracker:
- Shawn McKee
- Melynda Brooks
- Scott Nutter
- TS
- Irwin Sheer
- Jenny Thomas

Trigger:
- Henk Uijterwaal
- Ken McFarlane
- (Charles Allen)
- Peter Dingus

Coordination/integration:
- TS
- Bing Zhou
- Ken Lane
- Ken McFarlane

991

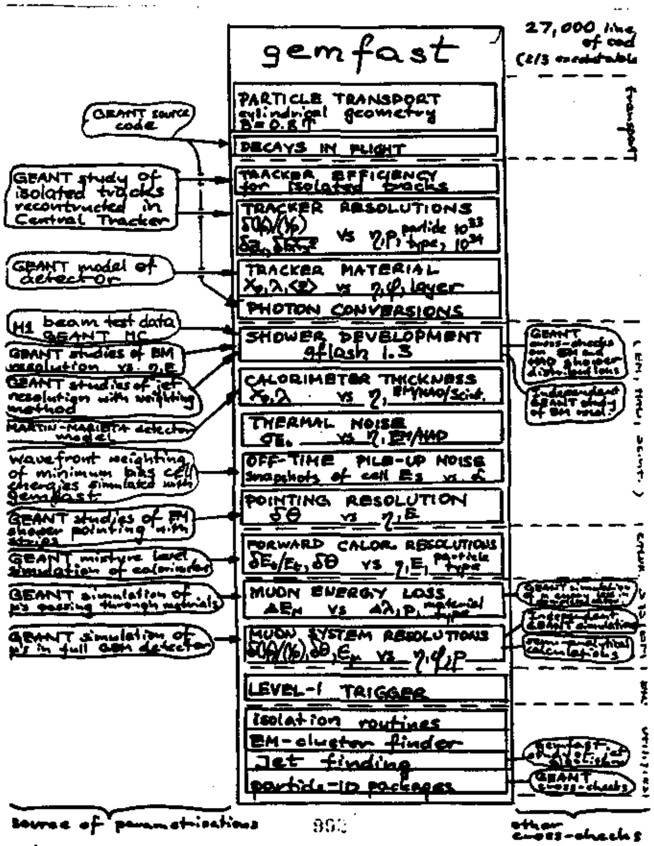

992

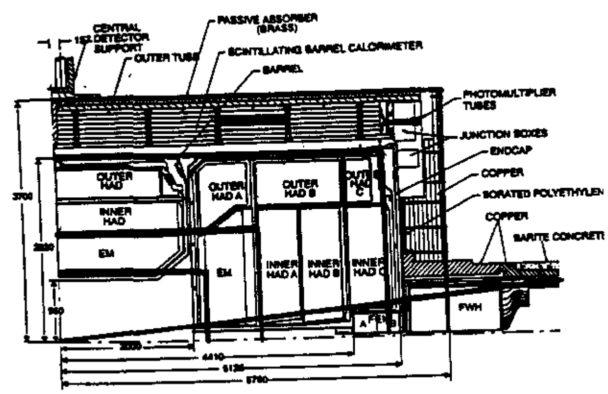

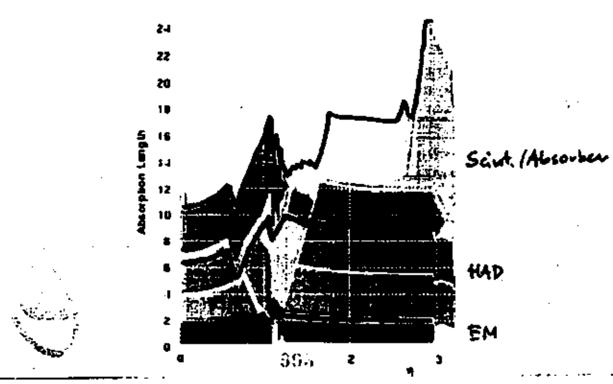

993

Muon energy loss

Peter Dingus

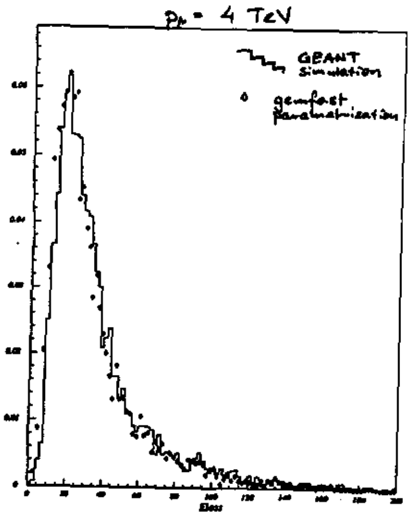

994

Muon system acceptance

Torre Wenaus

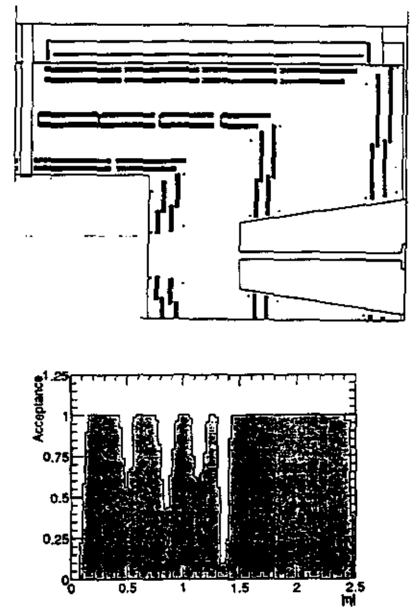

995

Muon system resolution

Torre Wenaus

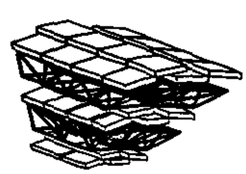

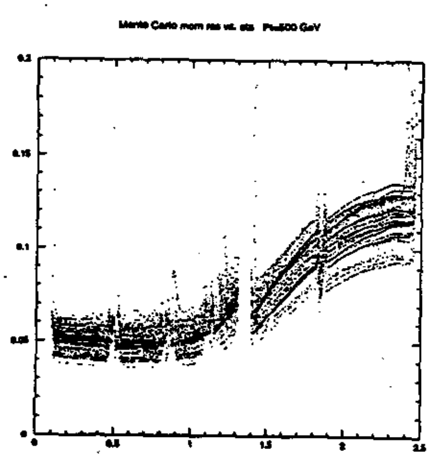

996

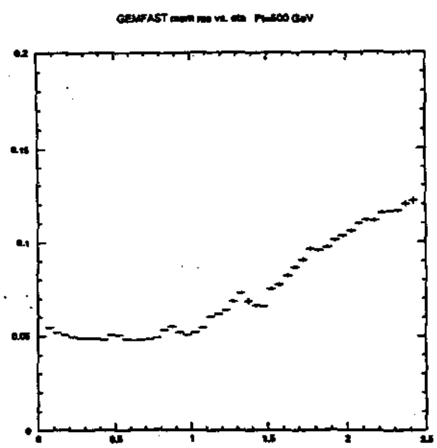

997

gemfast segmentation of central region calorimeters

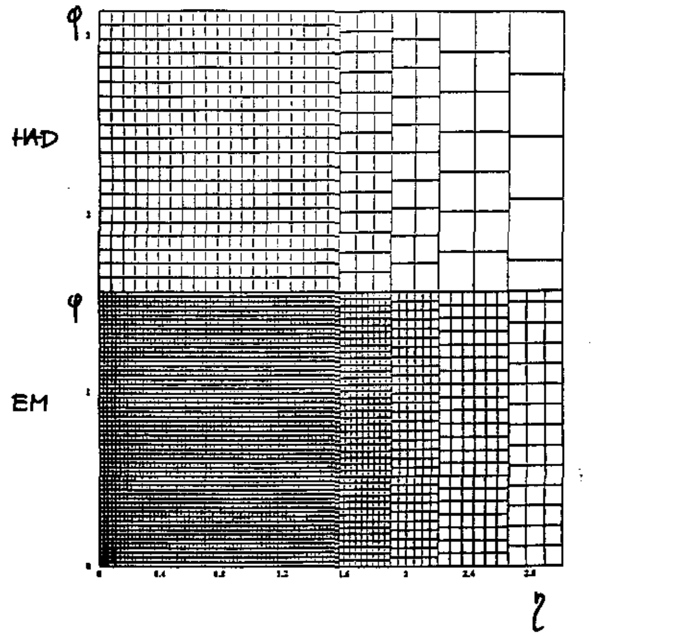

998

gflash 1.3

→ H1 beam test data

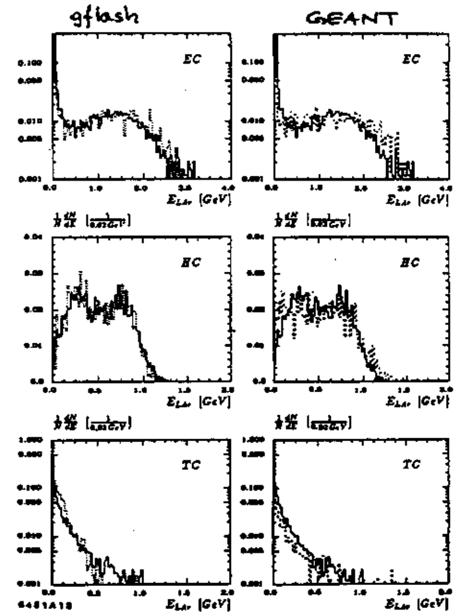

Figure 14: Energy distributions in the modules EC, HC, and TC for 30 GeV π^- showers: experiment (—), GFLASH (···), and GEANT (– – –).

999

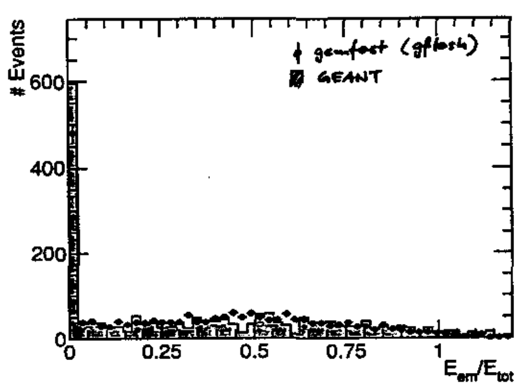

1000

gemfast/gflash

Hong Ma

Transverse Hadronic shower profiles

p_T = 100 GeV

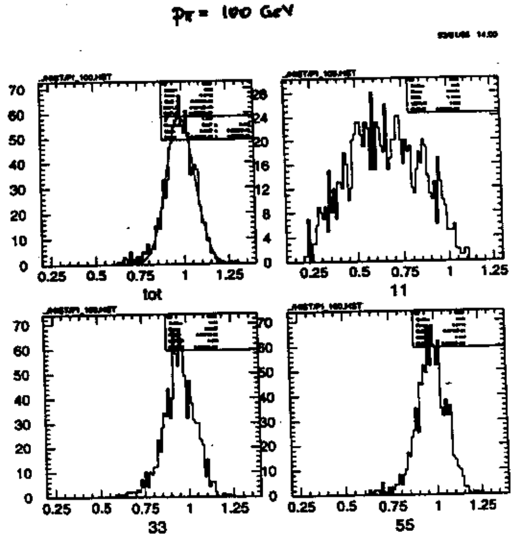

1001

GEANT

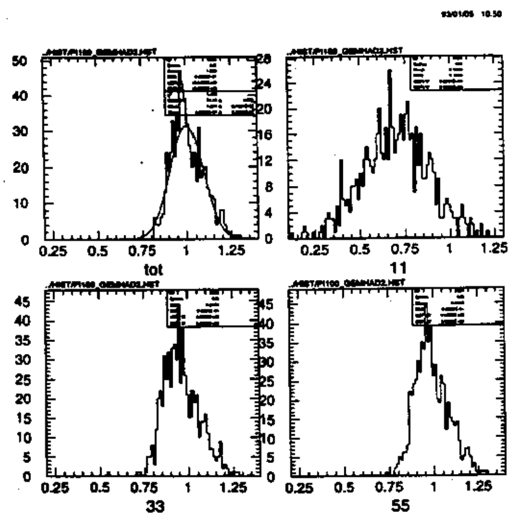

1002

Off-time pile-up simulation

Sasha Vanyashin
TS
(Cleland)

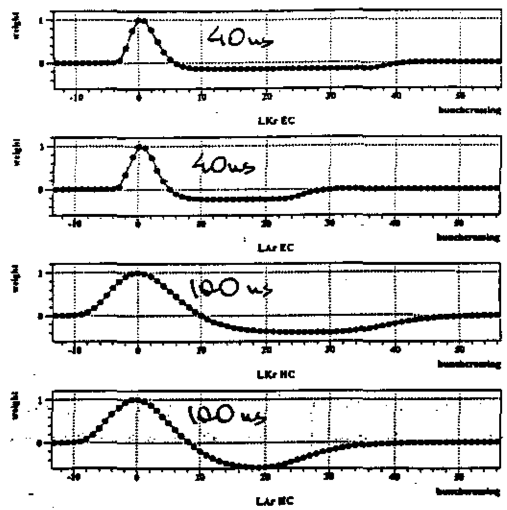

1003

0.16×0.16 EM trigger tower

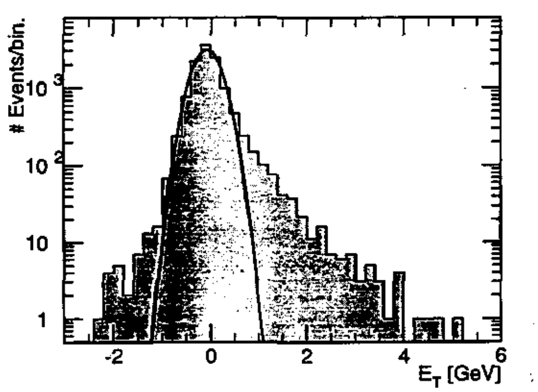

1004

Forward Calorimeter

UA2MIX MC
Mike Shupe

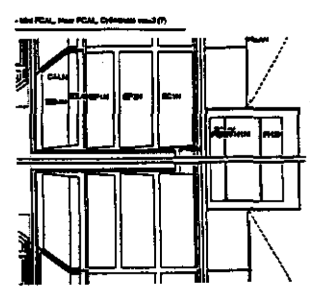

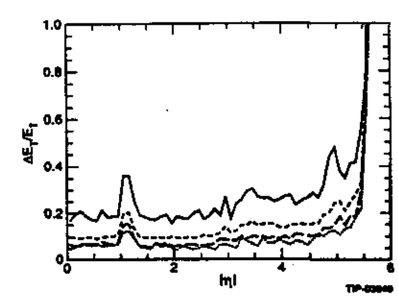

1005

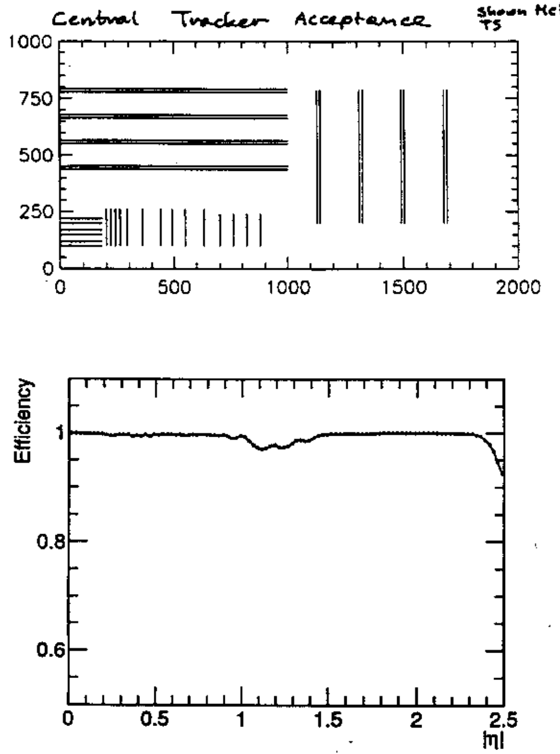

1006

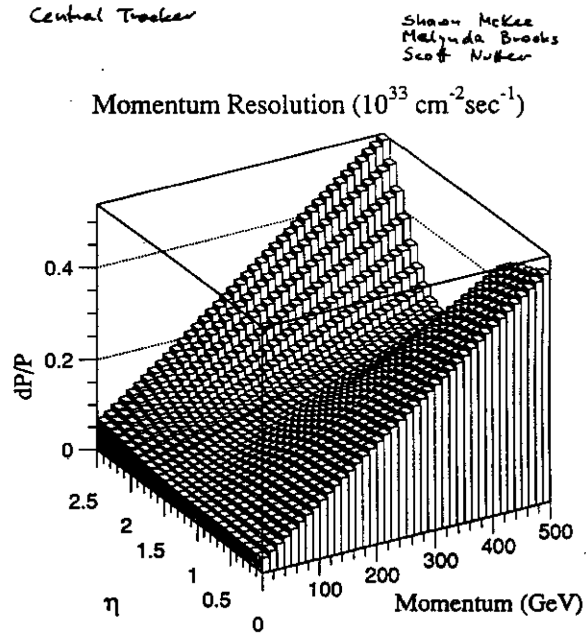

1007

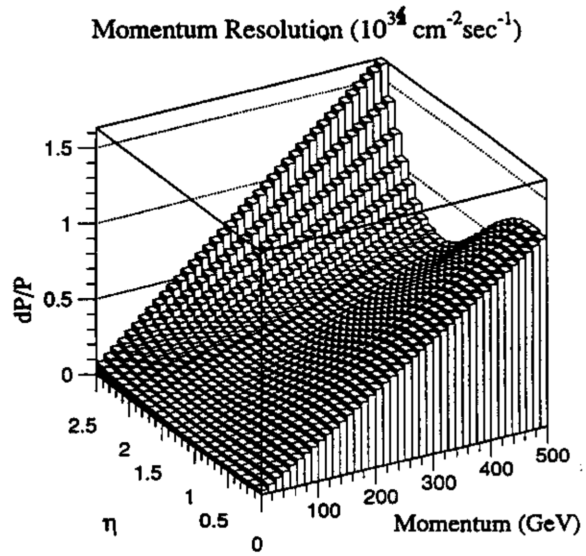

1008

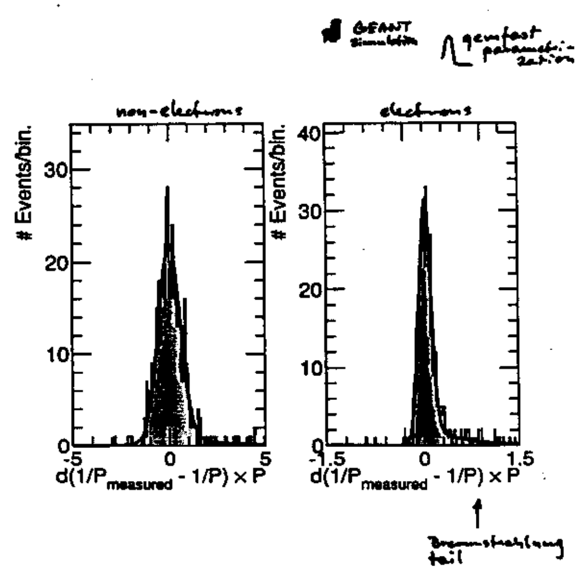

1009

$\gamma \to e^+e^-$

Sharon McKee
TS
Jenny Thomas

Trigger simulation
(Level-1)

Henk Uijterwaal
Ken McFarlane

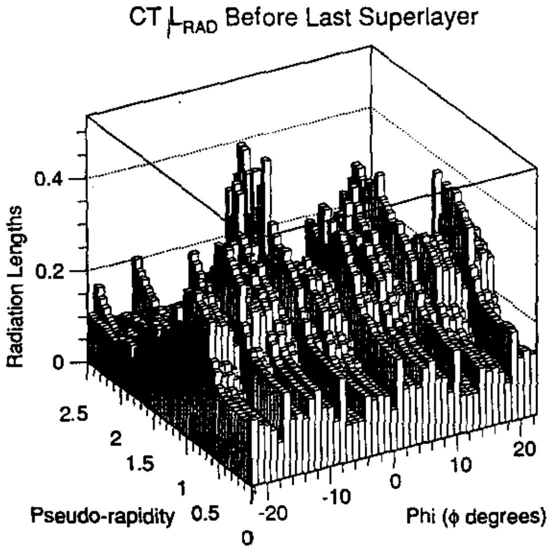

1070

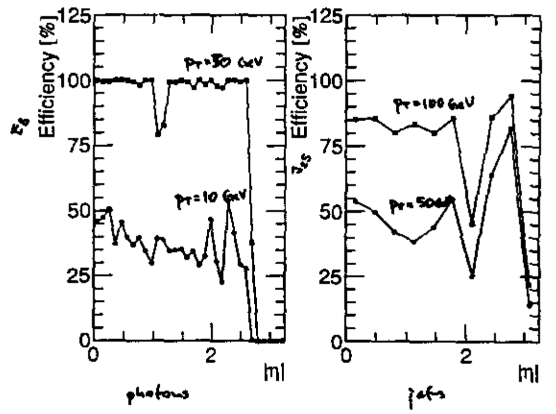

1071

Higgs Physics
@ gem

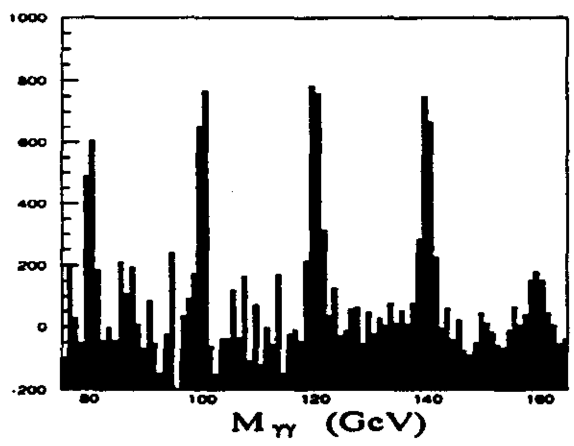

Standard Model Higgs Physics

Renyuan Zhu
on behalf of Caltech Group

GEM General Meeting, San Diego
May 12, 1993

- Higgs Searches with GEM,
- GEM's Strength — $H \rightarrow \gamma\gamma$,
- Uncertainties.

Caltech Team

√ • S. Mrenna: H→ $\ell\ell\ell\ell$;

• S. Shevchenko: H→ $\ell\ell$jj

√ • X. Shi: H→ $\ell\ell\nu\nu$;

√ • H. Yamamoto: H→ $\gamma\gamma$;

√ • R. Zhu: Coordinate Higgs Section and H→ $\gamma\gamma$.

H $\to \gamma\gamma$ with GEM

Renyuan Zhu
Caltech

Physics Meeting, San Diego
May 11, 1993

- The analysis;
- Comparison with GEM-TN-92-126.

Standard Model Higgs Physics

Renyuan Zhu
on behalf of Caltech Group

GEM General Meeting, San Diego
May 12, 1993

- Higgs Searches with GEM,
- GEM's Strength — H→$\gamma\gamma$,
- Uncertainties.

1018

Caltech Team

- S. Mrenna: H→ $\ell\ell\ell\ell$;
- S. Shevchenko: H→ $\ell\ell jj$
- ✓ X. Shi: H→ $\ell\ell\nu\nu$;
- H. Yamamoto: H→ $\gamma\gamma$;
- ✓ R. Zhu: Coordinate Higgs Section and H→ $\gamma\gamma$.

1019

H → $\gamma\gamma$ with GEM

Renyuan Zhu
Caltech

Physics Meeting, San Diego
May 11, 1993

- The analysis;
- Comparison with GEM-TN-92-126.

1020

$H \rightarrow \gamma\gamma$
Compared to GEM TN-92-126

- HoC is included, PDF is under control;
- Exact calculation of jet-jet background (quark and gluon);
- $|\cos\theta^*|$ cut optimized for sum of all background: no further improvement with additional max(E_T^γ) > 40 GeV cut.
- Improved analysis on vertex determination with event topology;
- Realistic Detector Effect:
  - cracks and segmentation in detector;
  - pile-up/thermal noises;
  - GEANT based R(γ/jet);
  - GEANT based R(γ/e).
- Better uncertainty analysis.

1022

Standard Model Higgs production & Decay Branching Ratio

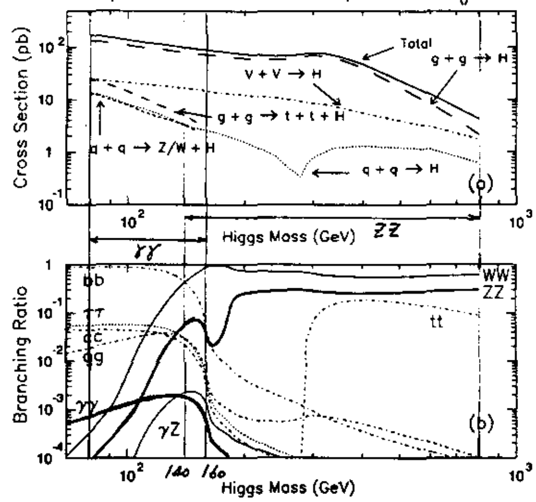

Figure 4: Higgs production cross-section (a) from three direct production mechanisms: gg, VV and $q\bar{q}$ and two associated production mechanisms: (Z/W)H and $t\bar{t}H$ and Higgs decay branching ratios to $\gamma\gamma$, ZZ^*/ZZ, WW^*/WW, $b\bar{b}$, $c\bar{c}$, $\tau^+\tau^-$, gg and γZ (b) are plotted as a function of Higgs mass.

1023

Lowest Order Higgs Production Cross-Section × Decay Branching Ratio (fb)

Assuming M_t = 140 GeV, EHLQ-1 PDF, and no high order corrections.

M_H	Γ_H	$\sigma_{H(\gamma\gamma)}$	$\sigma_{tH(\gamma\gamma)}$	$\sigma_{H(4\ell)}$	$\sigma_{H(\ell\ell jj)}$	$\sigma_{H(\ell\ell\nu\nu)}$
80	.0030	124	8.4			
90	.0034	144	8.0			
100	.0037	169	7.8			
120	.0049	211	6.9			
140	.0097	180	4.2	26		
150	.019	128	2.6	32		
160	.097	52.6	0.87	15		
170	.380			9.2		
180	.620			22		
200	1.4			85		
400	30			56		
600	112			16		
800	266			5.3	110	32

1024

γ/e/μ ID: Isolation Cut

- γ and electron:

$$\sum_{r<R} E_T - E_T^{\gamma/e} < E_T^{mean} + E_T^{cut} \text{ GeV}$$

were $E_T^{\gamma/e}$ is reconstructed transverse energy of γ or e by using 5 × 5 cells in EMC, E_T^{mean} is the mean energy measured in the isolation cone (R), and E_T^{cut} is the threshold determined by studying the behaviour of the sum of pile-up and thermal noise in the isolation cone (W. Cleland and A. Vanyashin).

- Muon:

$$\sum_{r<R} E_T - \Delta E < E_T^{mean} + E_T^{cut} \text{ GeV}$$

where ΔE is the measured energy in calorimeter, along muon track.

1025

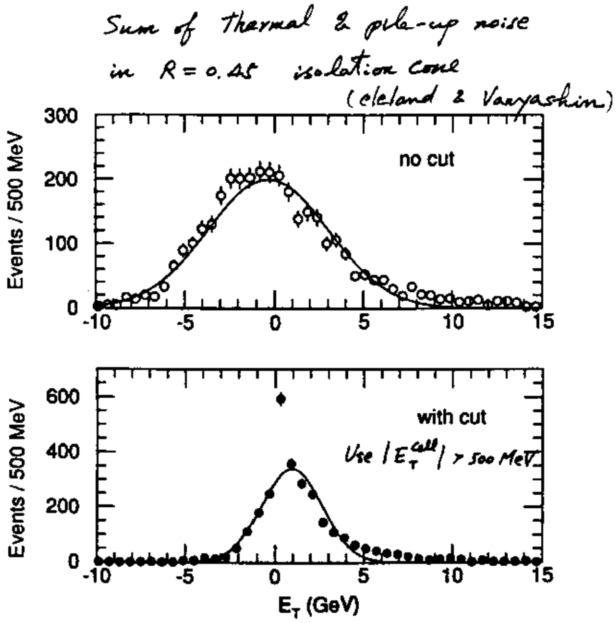

EM Accordion Segmentation

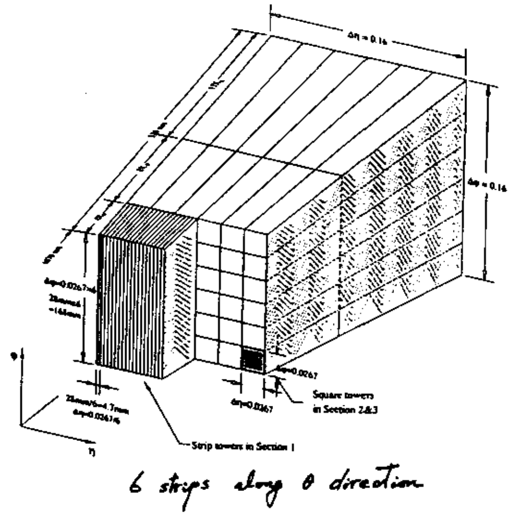

Figure 3: Schematic of three longitudinal segments of the EMC and six strips in the first segment.

Higgs Physics with GEM

- Intermediate Mass Higgs ($80 < M_H < 2M_Z$):
  - $H \rightarrow \gamma\gamma$ (80 GeV $< M_H <$ 160 GeV);
  - $(t\bar{t}/W)H \rightarrow \gamma\gamma \ell X$ (80 GeV $< M_H <$ 140 GeV);
  - $H \rightarrow ZZ^* \rightarrow \ell^+\ell^-\ell^+\ell^-$, (140 GeV $< M_H < 2M_Z$).
  - Key: Precision EMC with good photon ID and precision Muon System.
- Heavy Higgs ($2M_z < M_H <$ 800 GeV):
  - $H \rightarrow ZZ \rightarrow \ell^+\ell^-\ell^+\ell^-$,
  - "Gold Plated".
- Very Heavy Higgs ($M_H \approx$ 800 GeV):
  - $H \rightarrow ZZ \rightarrow \ell^+\ell^-\ell^+\ell^-$,
  - $H \rightarrow ZZ \rightarrow \ell^+\ell^-\nu\nu$, and
  - $H \rightarrow ZZ \rightarrow \ell^+\ell^- jj$.
  - Key: Understand systematic uncertainties.

Significance

- High Statistics: $S = N_S/\sqrt{N_B}$ *used in TDR*
  where N_S and N_B are expected signal and background.
- High Statistics Resonance Hunting:

$$S = \frac{\int \mathcal{L}dt\ A_S\ 0.955\sigma_H}{\sqrt{\int \mathcal{L}dt\ A_B\ 4\Delta M_H\ R_B}} \propto \sqrt{\frac{\int \mathcal{L}dt}{\Delta M_H}}$$

where A_S and A_B are the acceptance for signal and background, σ_H is Higgs cross-section, ΔM_H is Higgs mass resolution, and R_B is the background rate at the Higgs mass.

- Low Statistics:

$$P_{high} = \sum_{m=N_S+N_B}^{\infty} P_m(N_B)$$ *used in TDR*

for fixed N_S and N_B, where $P_n(\lambda) = \lambda^n e^{-\lambda}/n!$ following Poisson statistics with λ the expected value.

- Low Statistics with all Possible Fluctuation:

$$P_{low} = \sum_{n=0}^{\infty} [P_n(N_B + N_S) \times \sum_{m=n}^{\infty} P_m(N_B)]$$

Mathematically, P_{low} can be converted to a Gaussian probability defined by $N_s/\sqrt{N_B}$ if N_B is high.

For N_S=5, N_B=1: $N_S/\sqrt{N_B}$=5, S_{high}=3.2 ans S_{low}=1.9.

GEM's Sensitivity to Standard Model Higgs

M_H	$\int \mathcal{L}dt$	$\gamma\gamma$	$\gamma\gamma\ell$	$\ell\ell\ell\ell$	$\ell\ell jj$	$\ell\ell\nu\nu$	Combined
80 GeV	30 fb^{-1}	3.9σ	4.5σ				6.3σ
90 GeV	30 fb^{-1}	4.9σ	4.9σ				7.2σ
100 GeV	10 fb^{-1}	4.6σ	2.9σ				5.8σ
120 GeV	10 fb^{-1}	7.8σ	2.7σ				8.5σ
140 GeV	10 fb^{-1}	9.0σ	2.3σ	11σ			15σ
150 GeV	10 fb^{-1}	7.3σ		13σ			15σ
160 GeV	10 fb^{-1}	3.2σ		8.1σ			8.9σ
170 GeV	10 fb^{-1}			5.7σ			5.7σ
180 GeV	10 fb^{-1}			10σ			10σ
200 GeV	10 fb^{-1}			38σ			38σ
400 GeV	10 fb^{-1}			28σ			28σ
600 GeV	10 fb^{-1}			9.7σ			9.7σ
800 GeV	10 fb^{-1}			4.7σ*	5.4σ*	11σ*	-
800 GeV	10 fb^{-1}			4σ**	2σ**	7σ***	9σ**

* Statistical only.

** Including systematic uncertainty.

*** Including systematic uncertainty, assuming $\not{E}_t$ is under control.

10 fb^{-1} will cover 100 GeV < M_H < 800 GeV.

30 fb^{-1} is needed to cover 80 GeV < M_H < 100 GeV.

1030

H→ $\gamma\gamma$ Two-Photon Mass Resolution

$$\frac{\Delta M_{\gamma\gamma}}{M_{\gamma\gamma}} = \frac{1}{2}\sqrt{(\frac{\Delta E_1}{E_1})^2 + (\frac{\Delta E_2}{E_2})^2 + (\cot\frac{\theta}{2}\Delta\theta)^2}$$

where E_1 and E_2 are energies of two photons and θ is the opening angle between them.

$$\frac{\Delta E}{E} = (\frac{a}{\sqrt{E}} \oplus b \oplus \frac{c}{E})\%$$

Improvement: for $|\eta| > 1.9$, 3 x 3 rather and 20 ns shaping, rather than 5 x 5 and 40 ns shaping is used.

M_H (GeV)	80	100	120	140	160
a=6/8.5 b=0.4	0.66	0.77	0.84	0.91	1.0
a=14/17 b=1.0	1.3	1.5	1.7	1.8	2.0
a=9/14 b=1.0	1.1	1.3	1.4	1.6	1.7

This mass resolution does not degrade if Higgs vertex $\delta z < 5$ mm and the the cog of γ shower $\delta x < 2$ mm (GEM TN-92-126).

1031

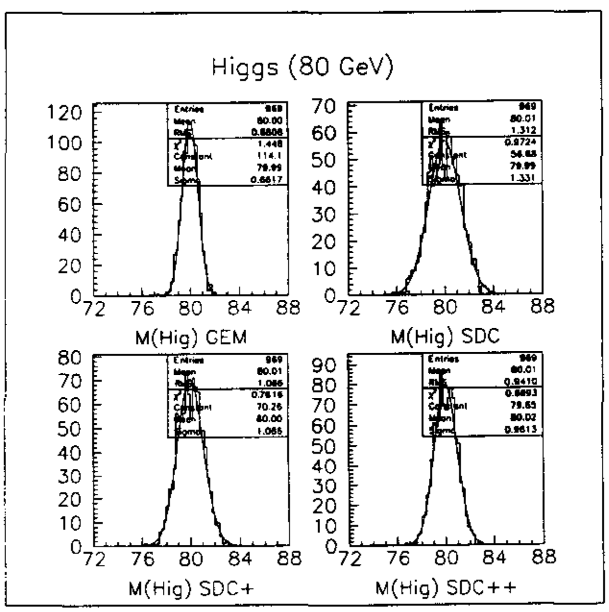

1032

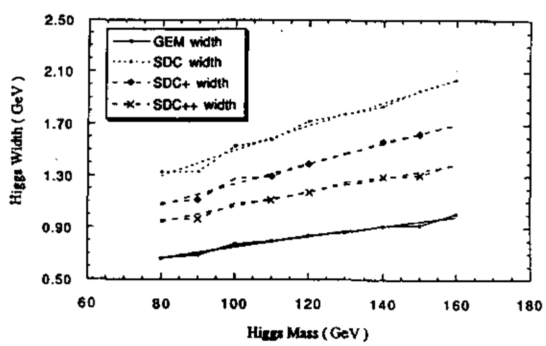

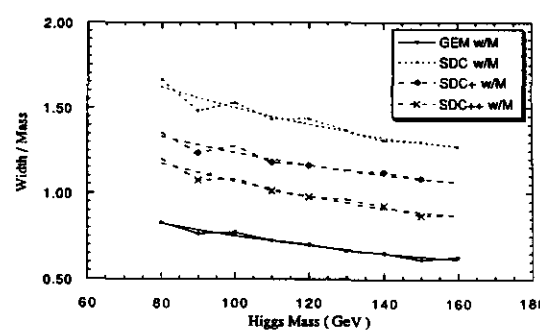

1033

H→ $\gamma\gamma$
Higgs Vertex Determination at 10^{33}

1. Use event topology, *e.g.* select vertex with the highest p_T-weighted charge multiplicity: 95% correct (I. Sheer).
2. Use calorimeter pointing alone: $[(d \text{ and } d+10)/\sqrt{E} + 0.5]$ mrad for barrel and endcaps

d (mrad)	40	50	60	80
a=6/8.5 b=0.4	1.2	1.2	1.3	1.4
a=14/17 b=1.0	2.0	2.0	2.1	2.2
a=9/14 b=1.0	1.6	1.6	1.7	1.8

3. Use pointing and select the closest CT vertex: 87% correct, i.e within 5 mm to the real vertex.
4. Use pointing and select the highest charge multiplicity in vicinity: 97% correct.

A conservative assumption of 95% is used in analysis.

GEM TDR CT chapter (I. sheer)

9/2

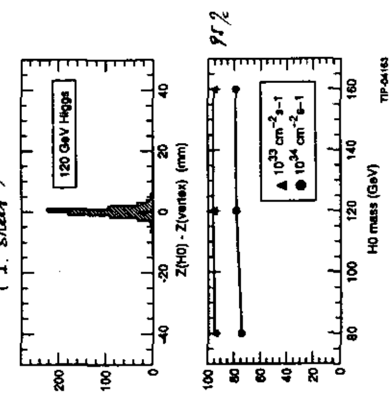

FIG. 6-23. (a) The difference in mm between the z coordinate of the true H^0 production vertex and the reconstructed primary vertex selected by choosing the vertex made up of tracks with the highest Σp_T for a 120-GeV standard model Higgs. (b) Vertex tagging efficiency as a function of the standard model Higgs mass and luminosity.

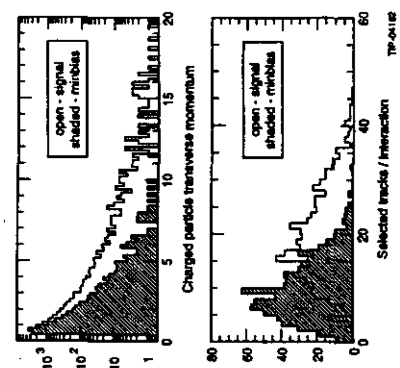

FIG. 6-22. (a) The transverse momentum spectrum for $p_T > 0.5$ GeV isolated charged tracks from standard model Higgs production (open histogram) for $M_H = 120$ GeV, and minimum bias events (hashed histogram) produced using the PYTHIA Monte Carlo. (b) The number of these tracks per event from standard model Higgs production (open) and minimum bias events (hashed).

H→ $\gamma\gamma$
Event Selection Cuts

1. $|\eta^{\gamma}| < 2.5$ and $p_t^{\gamma} > 20$ GeV,
2. Photon Isolation with R = 0.45, $E_T^{cut} = 4$ GeV,
3. Photon identification with shower shape to reject jet background,
4. Electron rejection,
5. $|\cos\theta^*| < 0.7$, where θ^* is the polar angle of photon in the center of mass system of two photons, to reject direct photon and jet background.

H→ $\gamma\gamma$
All Background

$$\begin{aligned}\sigma_{\text{``}\gamma\gamma\text{''}} &= \sigma_{\gamma\gamma} \quad (direct-photon)\\ &+ \sigma_{ee}\, R^2(\gamma/e) \quad (Drell-Yan)\\ &+ \sigma_{\gamma-jet}\, [R(\gamma/jet) + R(e/jet)R(\gamma/e)] \quad (\gamma-jet)\\ &+ \sigma_{2jet}\, [R(\gamma/jet) + R(e/jet)R(\gamma/e)]^2 \quad (jet-jet)\end{aligned}$$

where $\sigma_{\gamma\gamma}$ is the direct photon background, R(e/jet) and R(γ/jet) are the probability of a jet faking an isolated electron and photon respectively, and R(γ/e) is the probability of an electron faking a photon.

Since R(e/jet) is known to be in an order of 10^{-5},

$$\begin{aligned}\sigma_{\text{``}\gamma\gamma\text{''}} &= \sigma_{\gamma\gamma} \quad (direct-photon)\\ &+ \sigma_{ee}\, R^2(\gamma/e) \quad (Drell-Yan)\\ &+ \sigma_{\gamma-jet} R(\gamma/jet) \quad (\gamma-jet)\\ &+ \sigma_{2jet}\, R^2(\gamma/jet) \quad (jet-jet)\end{aligned}$$

H→ γγ
Signal and Direct Photon Background

- High order QCD corrections (HOC) increase Higgs production via gluon fusion by a factor of 1.5 (A. Graudenz, M. Spira and P. Zerwas, Phys Rev Lett **70** (1993) 1372.)
- HOC to direct photon background is calculated to NLL (B. Bailey, J. Owens and J. Ohnemus, Phys. Rev. **D46** (1992) 2018), including
  - Born ($q\bar{q}\to\gamma\gamma$) and $O(\alpha_s)$ corrections,
  - box diagram ($gg\to\gamma\gamma$),
  - single and double bremsstrahlung, and
  - the exact 2→3 kinematics for $q\bar{q}\to\gamma\gamma g$, $qg\to\gamma\gamma q$ and $g\bar{q}\to\gamma\gamma\bar{q}$.
- HOC to the $gg\to\gamma\gamma$ background is unknown. Since it is 1/3 of the NLL, a "K" factor of 1.5 reduces the significance by 8%.

1038

NLL γγ Background (B. Bailey, J. Owens) Phys. Rev. Lett 70(93)137

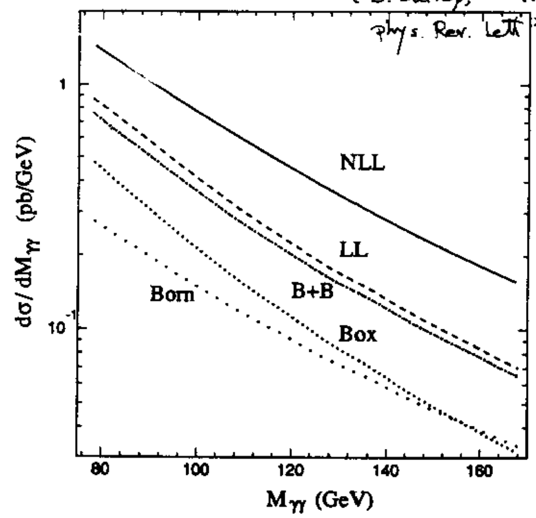

1039

|cos θ*| cut to reduce NLL γγ & γjet Background: optimized at 0.7

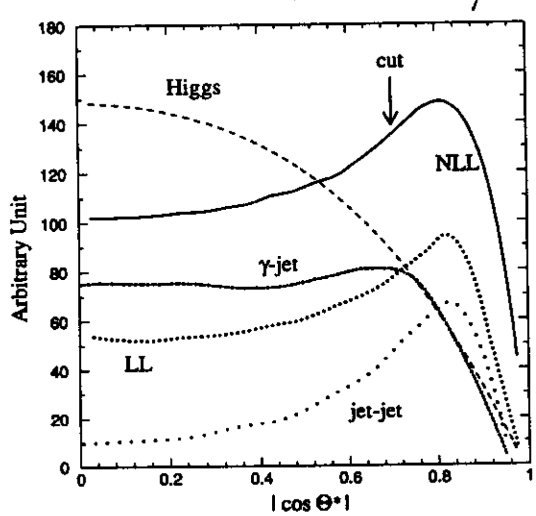

1040

H→ γγ
Signal and Direct Photon Backg. (Cont.)

H→γγ Signal (fb)							
M_H (GeV)	80	90	100	120	140	150	160
σ_{prod}	169	199	233	291	255	182	71.2
After cuts 1–4	47	45	74	96	88	64	25
After cuts 1–5	38	35	57	74	66	48	19
Direct Photon Background Rate (fb/GeV)							
$M_{\gamma\gamma}$ (GeV)	80	90	100	120	140	150	160
After cuts 1–2*	1840	1360	1020	600	370	300	240
After cuts 1–4	1010	560	560	330	210	160	130
After cuts 1–5	650	330	310	170	100	77	63

* Theoretical x-section scaled by $(B+B)_{pythia} \times NLL/(B+B)_{B\&O}$

1041

$H \rightarrow \gamma\gamma$

$R(\gamma/jet)\ (10^{-4})$

Rejection as function of $M_{``\gamma"\gamma}$ calculated by using GEANT Simulation for γ-quark and γ-gluon final states (H. Ma).

$M_{``\gamma"\gamma}$ (GeV)	80	100	120	140	160
Quark Jet					
After Isolation	20	18	15	13	12
After γ ID	4.1	3.9	3.7	3.6	3.4
Gluon Jet					
After Isolation	5.9	5.3	4.8	4.3	3.9
After γ ID	1.2	1.1	1.0	0.91	0.83

Rejection is used for jet-jet background according to parton species (qg, qq and gg).

1042

γ - quark Background

(H. Ma)

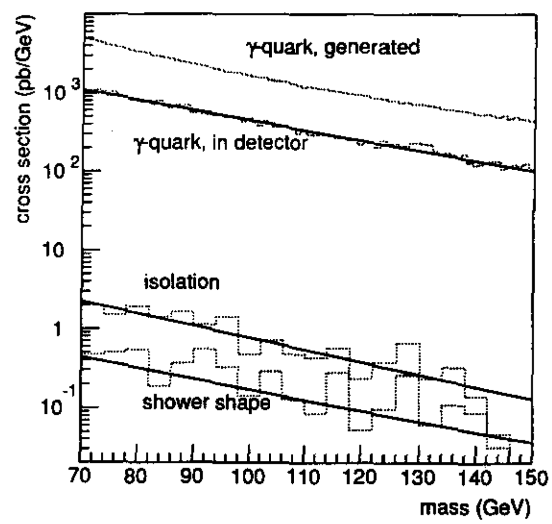

1043

γ - gluon Background

(H. Ma)

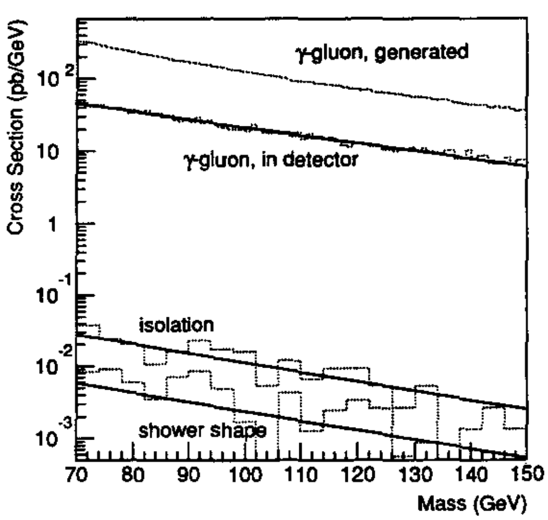

1044

$H \rightarrow \gamma\gamma$

Jet Background

$M_{\gamma\gamma}$ (GeV)	80	90	100	120	140	150	160
$qg \rightarrow \gamma q$							
After cut 1 (pb/GeV)	1170	880	660	370	210	160	120
After cuts 1-2 (fb/GeV)	1590	830	780	380	190	130	91
After cuts 1-3 (fb/GeV)	320	180	170	92	50	36	27
After cuts 1-5 (fb/GeV)	260	140	130	65	32	23	16
$q\bar{q} \rightarrow \gamma g$							
After cut 1 (pb/GeV)	53	41	32	20	12	9.2	7.2
After cuts 1-2 (fb/GeV)	21	11	11	6.1	3.4	2.5	1.8
After cuts 1-3 (fb/GeV)	4.3	2.4	2.4	1.3	0.7	0.5	0.4
After cuts 1-5 (fb/GeV)	3.2	1.7	1.6	0.8	0.4	0.3	0.2
jet-jet							
After cut 1 (μb/GeV)	8.3	6.8	5.6	3.8	2.5	2.1	1.7
After cuts 1-2 (pb/GeV)	4.4	2.4	2.3	1.2	0.6	0.5	0.3
After cuts 1-3 (fb/GeV)	190	110	110	60	34	25	19
After cuts 1-5 (fb/GeV)	95	46	39	16	6.8	4.4	2.9
Sum of All Jet Background							
Total (fb/GeV)	360	190	170	82	40	28	19

γ-q, γ-g and 2jets are 40, 0.5 and 15% of NLL.

Remain uncertainty: fragmentation — a factor of 2 or 4.

1045

H→ γγ
R(γ/e) — Drell-Yan Background

R(γ/e) calculated by using a hit level GEANT simulation for CT (M.J. Wang and A. Sumarokov):

e Acceptance	5%	1.6%	0.5%
γ Acceptance	96%	92%	83%

Rejection of R(γ/e) = 0.5% is used in $M_Z \pm 7.5$ GeV, and R(γ/e) = 5% everywhere. The corresponding loss of γ identification efficiency is included in analysis.

1046

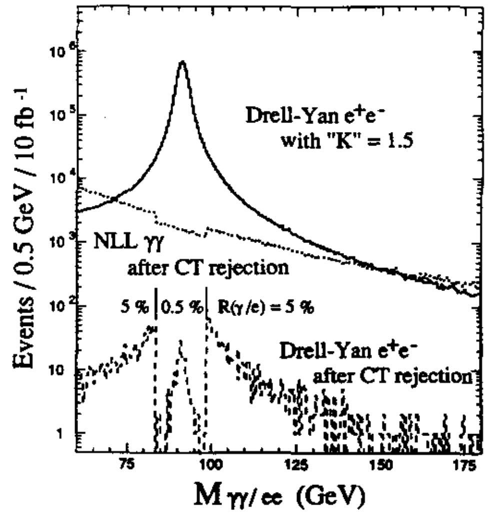

1047

H → γγ

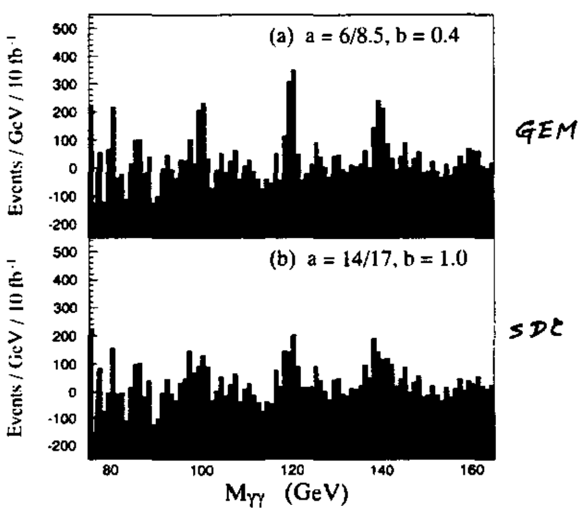

1048

H→ γγ
Significance

M_H (GeV)	80	90	100	120	140	150	160
ΔM_H (GeV)	0.66	0.69	0.79	0.84	0.91	0.93	0.99
σ_H (fb)	38	35	57	74	66	48	19
R_B (fb/GeV)	1010	520	480	250	140	110	82
GEM Significance							
10 fb^{-1}	2.2	2.8	4.6	7.8	9.0	7.3	3.2
30 fb^{-1}	3.9	4.9	7.9	14	16	13	5.5
Significance for a=14/17 b=1.0							
10 fb^{-1}	1.6	2.0	3.2	5.5	6.3	5.1	2.2
30 fb^{-1}	2.8	3.5	5.6	9.5	11	8.8	3.8

Fragmentation Uncertainty (lower bond):
γ-jet background: ×2, and jet-jet background: × 4.

1049

$H \to \gamma\gamma$

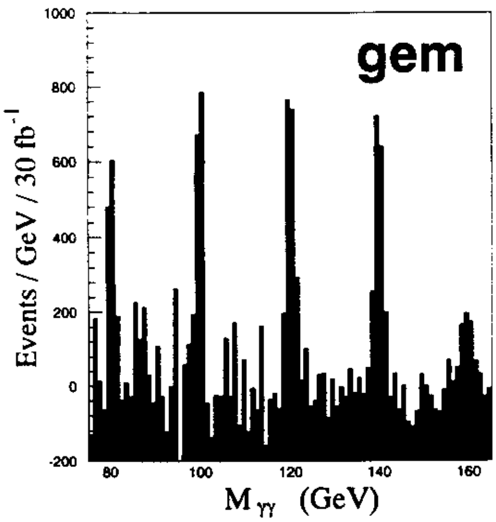

1050

Significance of $H \to \gamma\gamma$

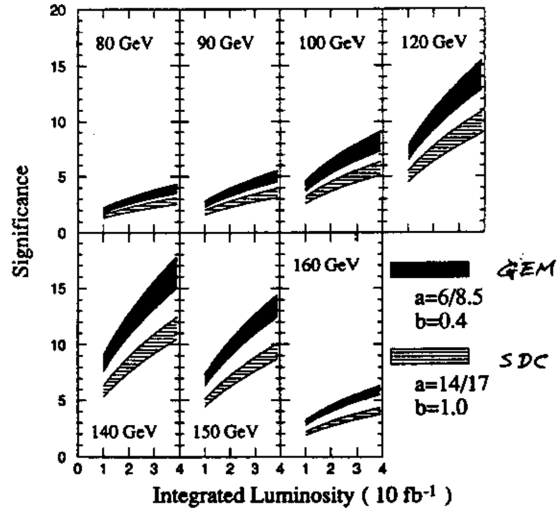

1051

$H(t\bar{t}/W) \to \gamma\gamma\ell X$

Background

1. $t\bar{t}\gamma\gamma$ or $b\bar{b}\gamma\gamma \to \ell\gamma\gamma$,
2. $q\overline{q'} \to W\gamma \to \ell\gamma\gamma$,
3. $q\overline{q'} \to W\gamma \to \ell\gamma\gamma$,
4. $q\bar{q}/gg \to Z\gamma \to \ell^+\ell^-\gamma\gamma$,
5. $q\bar{q}/gg \to Z\gamma \to e$"$\gamma$"$\gamma$, and
6. $t\bar{t}$.

Cuts

1. $|\eta_\ell| < 2.5$ and $p_t^\ell > 20$ GeV,
2. $|\eta_\gamma| < 2.5$ and $p_t^\gamma > 20$ GeV,
3. Photon and lepton identification, including isolation with $E_T^{cut} = 5$ GeV and $R = 0.45$ and 0.3 for photon and lepton respectively.
4. $p_t^{\gamma\gamma} > 40$ GeV.

1052

$(t\bar{t}/W)H \to \ell\gamma\gamma X$

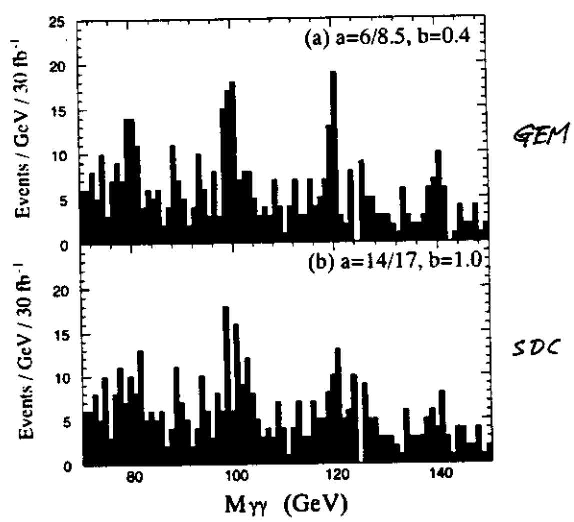

1053

$H(t\bar{t}/W) \rightarrow \gamma\gamma\ell X$

Signal & Background

$H(t\bar{t}/W) \rightarrow \gamma\gamma\ell X$ Signal (fb)					
M_H (GeV)	80	90	100	120	140
σ_{prod}	8.4	8.0	7.8	6.9	4.2
After cuts 1–3	0.95	1.0	1.0	0.82	0.61
After cuts 1–4	0.74	0.82	0.86	0.74	0.58
Background Rate, R_B (fb/GeV)					
$M_{\gamma\gamma}$ (GeV)	80	90	100	120	140
$t\bar{t}\gamma\gamma$	.019	.018	.018	.017	.016
$W\gamma\gamma$	.010	.010	.009	.008	.008
$W\gamma \rightarrow \ell\gamma\gamma$	.027	.025	.023	.020	.016
$Z\gamma \rightarrow \ell^+\ell^-\gamma\gamma$	.068	.068	.064	.046	.027
$Z\gamma \rightarrow e$ "γ" γ	.031	.024	.019	.012	.008
$t\bar{t}$	.044	.044	.041	.029	.016
Total	.20	.19	.17	.13	.09

1054

Significance of $(t\bar{t}/W)H \rightarrow \ell\gamma\gamma X$

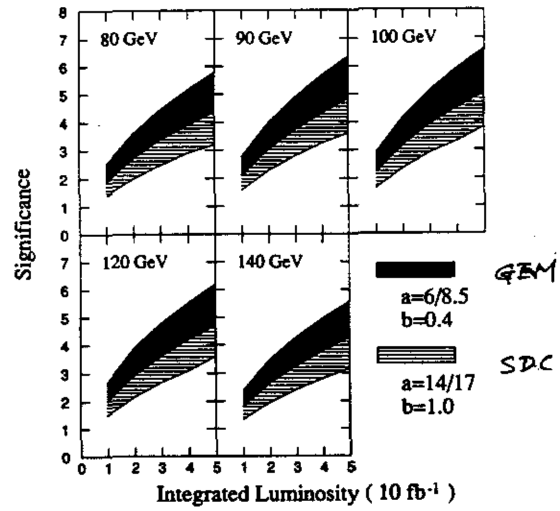

1055

$H(t\bar{t}/W) \rightarrow \gamma\gamma\ell X$

Significance

M_H (GeV)	80	90	100	120	140
ΔM_H (GeV)	0.66	0.69	0.77	0.84	0.91
σ_H (fb)	0.74	0.82	0.86	0.74	0.58
σ_{bac} (fb/GeV)	0.20	0.19	0.17	0.13	0.09
GEM Significance					
10 fb^{-1}	2.5	2.8	2.9	2.7	2.3
30 fb^{-1}	4.5	4.9	5.1	4.8	4.3
Significance for a=14/17 b=1.0					
10 fb^{-1}	1.9	2.1	2.2	2.0	1.8
30 fb^{-1}	3.4	3.8	3.9	3.6	3.3

1056

$\gamma/e/\mu$ Identification

- γ/e Identification:
  - Lateral shower shape, HCAL veto for γ or e, and matching momentum, position and angle measured in CT and in the EMC for electron;
  - A photon likelihood function from strips, shower size and ϕ pointing from 2nd and 3rd segments (H. Ma, See next Slide).
- Muon Identification:
  - Matching positions, angles and momenta of the track measured in the muon system and in the CT.

$$\frac{|p_{CT} - p_\mu - \Delta E|}{\sqrt{\sigma_{CT}^2 + \sigma_\mu^2 + \sigma_{\Delta E}^2}} < \text{cut}$$

1057

Photon ID with Strips

- Likelihood function defined by SYM, ASYM, W2, W3, H3, H4 and H5 from the strips:

  E1 = Energy in the highest energy strip — center;

  E3 = Energy sum in 3 strips around the center;

  E_{right} = energy sum in 3 strips right to the center;

  E_{left} = energy sum in 3 strips left to the center;

  SYM = $(E_{right} + E_{left})/E3$;

  ASYM = $|E_{right} - E_{left}|/E1$;

  W2 = distance between the center and the second highest energy strip, in unit of strip numbers; and

  W3 = distance between the center and the third highest energy strip, in unit of strip numbers.

  H3 (H4,H5) = The energy in the third (fourth, fifth) highest energy strip normalized to the energy in the two highest energy strips.

- Shower size in θ and ϕ defined as the energy weighted second moment of the shower in the second and third segments, and
- ϕ pointing obtained from 2nd and 3rd segments.

$H \to ZZ^* \to \ell^+\ell^-\ell^+\ell^-$

Significance

M_H (GeV)	140	150	160	170	180
$H \to e^+e^-e^+e^-$					
ΔM_H (GeV)	1.05	1.06	1.13	1.23	1.33
σ_{accep} (fb)	1.2	1.7	.86	.62	1.6
R_B (fb/GeV)	.025	.025	.025	.025	.040
$H \to \mu^+\mu^-\mu^+\mu^-$					
ΔM_H (GeV)	1.59	1.62	1.73	1.84	2.22
σ_{accep} (fb)	.81	1.1	.56	.36	.92
R_B (fb/GeV)	.016	.016	.016	.016	.026
$H \to e^+e^-\mu^+\mu^-$					
ΔM_H	1.36	1.46	1.56	1.71	1.77
σ_{accep} (fb)	1.9	2.6	1.4	.89	2.4
R_B (fb/GeV)	.038	.038	.038	.038	.062
$H \to \ell^+\ell^-\ell^+\ell^-$					
Significance	11	13	8.1	5.7	10

$H \to ZZ \to \ell^+\ell^-\ell^+\ell^-$

Cuts

- $|\eta^\ell| < 2.5$ and $p_t^\ell > 10$ GeV
- Lepton ID, including isolation with R = 0.3 and $E_T^{cut} = 5$ GeV,
- $Max(p_T^Z) > \sqrt{M_{ZZ}^2 - (2M_Z)^2}/4$, and
- $|M_{\ell\ell} - M_z| < 10$ GeV for both lepton pairs.

Significance

M_H (GeV)	200	400	600	800
Signal (fb)				
σ_{prod}	85	56	16	5.3
Mass Bin (GeV)	±4.7	350–450	500–800	600–1200
σ_{accep}	21	14	4.3	1.5
Background (fb)				
ZZ	3.0	2.3	1.0	.6
Significance				
Significance	38	28	9.7	4.7

GEM

$H \to ZZ \to \ell\ell\ell\ell$

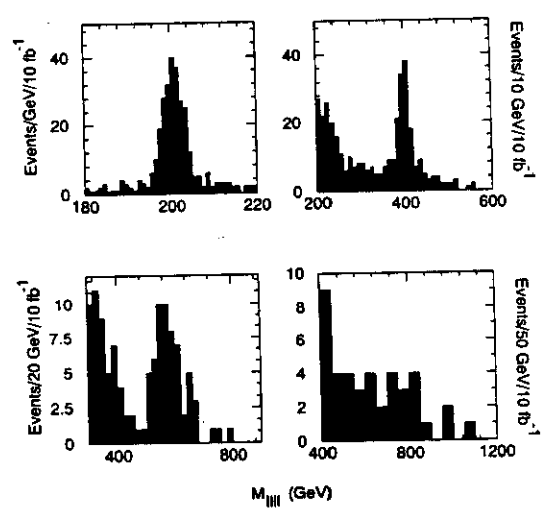

$H \to \ell^+ \ell^- \ell^+ \ell^-$

(30 pb^{-1})

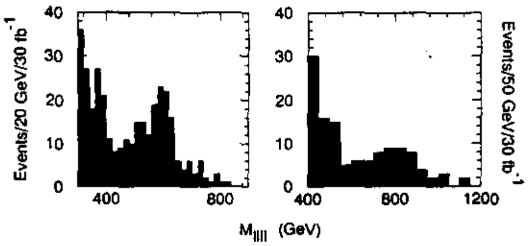

$H \to ZZ \to \ell^+\ell^-\nu\nu$

Background

- $q\bar{q}/gg \to ZZ$,
- $q\bar{q} \to Zg$ and $qg \to Zq$ with $Z \to \ell^+\ell^-$,
- $q\bar{q} \to t\bar{t}$ and $gg \to t\bar{t}$ with $t \to b\ell^+\nu$ and $\bar{t} \to \bar{b}\ell^-\bar{\nu}$.

Cuts

1. $|\eta^\ell| < 2.5$ and $p_t^\ell > 20$ GeV,
2. Lepton ID, including isolation with R = 0.3 and $E_T^{cut} = 5$ GeV.
3. $|M_{\ell\ell} - M_Z| < 10$ GeV,
4. $E_t^Z > 250$ GeV, and
5. $\not{E}_t > 250$ GeV.

Plot M_t: $M_t^2 = 2E_t^Z \not{E}_t(1 - \cos\Delta\phi_{Z\nu})$ where $\Delta\phi_{Z\nu}$ is the difference of the azimuthal angle of energy vectors of two Z's. Count events between 400 and 1200 GeV.

GEM $H \to \ell^+\ell^-\nu\nu$

Transverse Mass

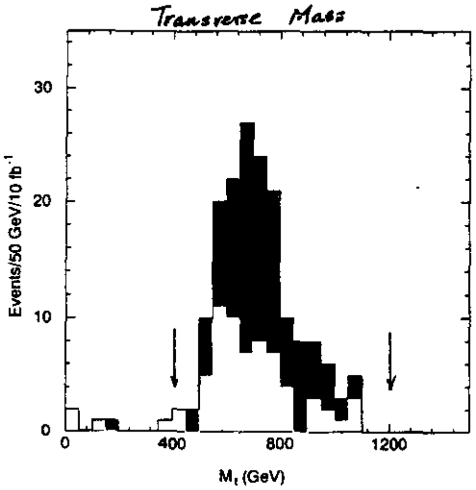

$M_t^2 = 2E_t^Z \not{E}_t (1 - \cos\Delta\phi_{Z\nu})$

400 GeV $< M_t <$ 1200 GeV

$H \to ZZ \to \ell^+\ell^-\nu\nu$

Signal & Background

	Signal	ZZ	Z + jet	$t\bar{t}$
$e^+e^-\nu\bar{\nu}$ Channel				
σ_{prod}	16.0	36.7	3.3×10^4	2.0×10^5
After cuts 1–3	9.5	13.8	1.2×10^4	53.5
After cuts 1–4	7.4	4.2	3.1×10^3	0.36
After cuts 1–5	6.2	3.2	2.2	0.0
$\mu^+\mu^-\nu\bar{\nu}$ Channel				
	Signal	ZZ	Z + jet	$t\bar{t}$
σ_{prod}	16.0	36.7	3.3×10^4	2.0×10^5
After cuts 1–3	6.5	9.4	8.1×10^3	36.2
After cuts 1–4	5.0	2.9	2.1×10^3	0.24
After cuts 1–5	4.2	2.2	1.5	0.0

Significance

- Statistically: $N_S = 106$, $N_B = 91$: 11σ;
- Systematically: Losen cuts to normarize background rate: 7σ;
- Uncertainty on $\not{E}_t$: 1% tail with twice resolution — no change.

H→ZZ→$\ell^+\ell^-$jj

Background

- pp → ZW or ZZ with one Z→ee or $\mu\mu$,
- pp → Z+jets with Z→ee or $\mu\mu$, and
- pp → tt with t→bW and W→eν or $\mu\nu$.

Cuts

1. For leptons, we request
   - $|\eta^\ell| < 2.5$ and $p_t^\ell > 70$ GeV,
   - Lepton identification, include isolation with R = 0.3 and $E_T^{cut} = 5$ GeV,
   - $|M_{\ell\ell} - M_Z| < 10$ GeV, and
   - $p_t^{\ell\ell} > 230$ GeV.
2. For jets, we request
   - Two reconstructed jets with $|\eta^j| < 2.5$ and $p_t^j > 80$ GeV,
   - $|M_{\ell\ell} - M_Z| < 15$ GeV.
3. Use reconstructed $\ell\ell jj$ invariant mass window between 600 and 1000 GeV.

1063

H → ZZ → ℓℓjj

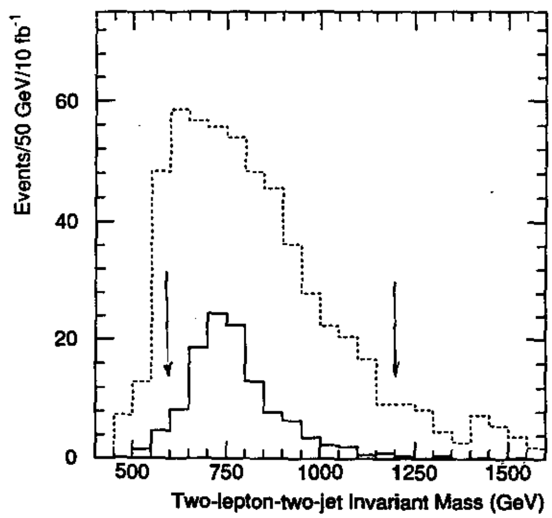

600 < $M_{\ell\ell jj}$ < 1000 GeV

1064

H→ZZ→$\ell^+\ell^-$jj

Signal & Background (fb)

Cut	Higgs	tt	Z+jets	ZW/ZZ
After Cut 1	41	130	3240	20
After Cuts 1–2	12	0.5	65	1.5
After Cuts 1–3	11	0.3	42	0.8

Significance

- Statistically: $N_S = 110$, $N_B = 430$: 5.3σ;
- Systematic: Side band analysis: $S = 2\sigma$;
- Central jet veto and $|\cos\theta^*|$ cut were found not useful after p_T cut;
- Forward jet tagging was studied in hadron level by using PYTHIA: tag one jet with E > 2000 GeV and $p_t > 50$ GeV in $2.5 < |\eta| < 4.5$ and leptons with $p_t > 50$ GeV in $|\eta| < 2.5$: $N_S = 170$, $N_B = 7500$. After applying all cuts: $N_S = 24$, $N_B = 32$. The forward jet tagging increases N_S/N_B.

1065

Uncertaities in Significance (%)

	80 GeV 30 pb⁻¹		800 GeV 10 pb⁻¹		
Item	$\gamma\gamma$	$\gamma\gamma\ell$	$\ell\ell\ell\ell$	$\ell\ell\nu\nu$	$\ell\ell jj$
Statistics	20	30	30	15	15
HoC	20	20	20	20	20
PDF	10	10	10	10	10
Background	20	40	20	25	65
Detector	20	20	20	40	20
Total	40	60	50	50	75
N_S	1100	22	15	100	110
N_B	80000	6	6	90	430
Significance*	3.9	4.5	4.7	11	5.3
Significance**	3–3.5	3–3.5	3–4	6–8***	1.5–2.5

* Statistical only.

** Including systematic uncertainty.

*** Including systematic uncertainty, assuming $\not{E}_t$ is under control.

Conclusion

Low Mass Higgs (M_H = 80 – 100 GeV)

Needs 30 pb⁻¹

1066

$H \to ZZ^* \to \ell^+\ell^-\ell^+\ell^-$

Background

- $pp \to ZZ/ZZ^* \to \ell^+\ell^-\ell^+\ell^-$,
- $pp \to q\bar{q}Z \to \ell^+\ell^-\ell^+\ell^- X$, where $q = b$ or t,
- $pp \to t\bar{t} \to W^+bW^-\bar{b}$, when two W's decay semileptonically and b's fake an isolated lepton.

Cuts

- $|\eta^\ell| < 2.5$ and $p_t^\ell > 10$ GeV,
- Lepton ID, including isolation with $R = 0.35$ and $E_T^{cut} = 5$ GeV,
- 10 GeV $\le M_{\ell\ell}^{(l)} \le$ 100 GeV and 70 GeV $\le M_{\ell\ell}^{(h)} \le$ 100 GeV $\Rightarrow$ suppress continuum background, where $M_{\ell\ell}^{(l)}$ and $M_{\ell\ell}^{(h)}$ are low and high invariant masses of two $\ell^+\ell^-$ pairs.

1070

GEM $H \to ZZ^* \to \ell\ell\ell\ell$

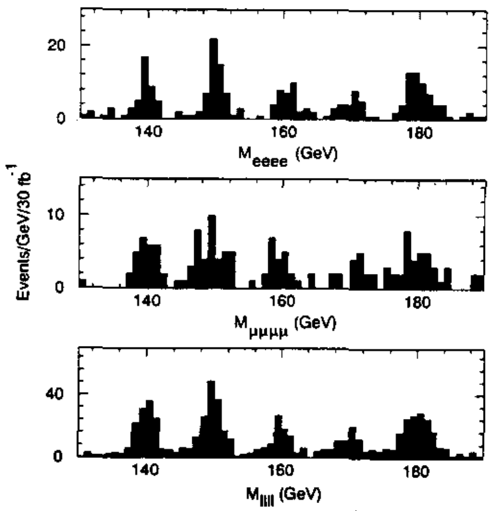

107·

PDF Dependence

To understand uncertainties caused by PDF's, the following latest PDF's were studied:

- five sets of (H/K)MRS, among which HMRS(B) is the commonly used PDF in Europe, and
- five sets of CTEQ which is a recent product of the Coordinated Theoretical/Experimental Project on QCD Phenomenology and Tests of the Standard Model in the U.S.

The result indicates that the Higgs cross-section differs by 20%, but the significance differ by 10% with EHLQ-1, in the middle, almost identical to the result using CTEQ LO (H. Yamamoto).

107..

PDF Dependence (H. Yamamoto)
X-section : 20%, significance : 10%

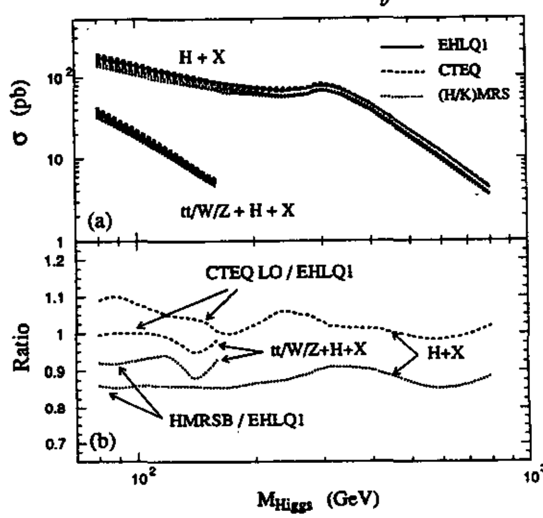

107..

Heavy Flavor Physics

5/12/93 at La Jolla

Chiaki Yanagisawa
Stony Brook

§. Introduction

Standard top decay. $t \to Wb$

- Discovery of heavy top quark ($m_t = 250\ GeV/c^2$)
- Top mass measurement ($m_t = 140\ GeV/c^2, 250\ GeV/c^2$)

Non-standard top decays.

- $t \to H^+ b$ $\quad H^+ \to \tau^+ \nu_\tau$ ($H^+ \to c\bar{s}$)

⋮

§. Standard top decay

$t\bar{t} \to$ tri-lepton (Chiaki Yanagisawa)

Signal

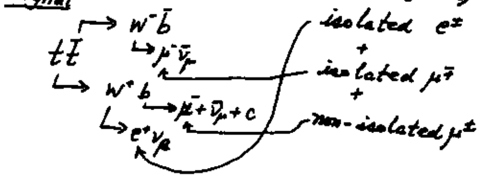

- Isolated e^+e^- or $\mu^+\mu^-$ pairs are not used to avoid contamination from $Z(\to \ell\bar{\ell}) +$ jets
- If only one isolated lepton is required, that will increase the contamination from $W(\to \ell\nu)+$jets.

Cuts

Isolated $\mu^\pm$

$|\eta| < 2.4$, $p_T > 40\ GeV/c$, $E_t(R=0.4) - E_t(R=0.1) < 2\ GeV$

Isolated $e^\pm$

$|\eta| < 2.4$, $E_t^{em}(R=0.2) > 40\ GeV$,

$E_t(R=0.4) - E_t^{em}(R=0.2) < 10\ GeV$, $0.8 < \frac{E_t(R=0.2)}{p_t(CT)} < 1.2$

Non-isolated $\mu^\pm$

$|\eta| < 2.4$, $p_T > 20\ GeV/c$, $E_t(R=0.4) - E_t(R=0.1) > 10\ GeV$

Background

W + jets	Z + jets	WZ
< 9%	negligible	negligible

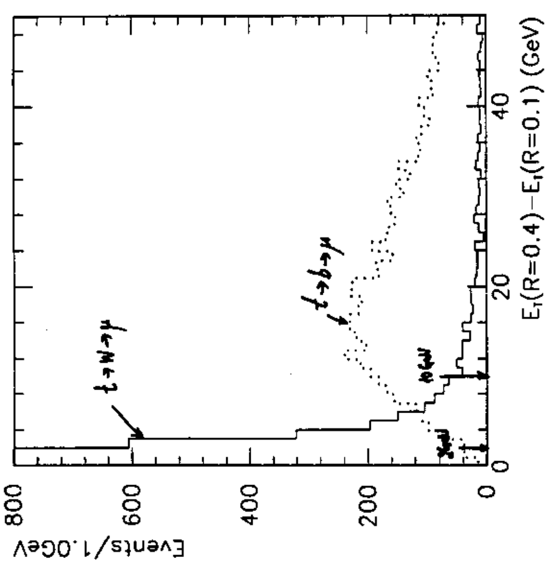

Mass measurement

- The leptons from W and b which come from the same top quark still retain information of the top mass.

$t \to W^+ b$, $b \to \mu^+ + \bar{\nu} + c$, $W^+ \to \mu^+ \nu$

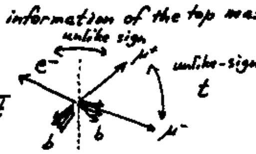

- The leptons from the same top tend to be in the same hemisphere.

$\phi_{\ell^{iso}, \mu^{non\text{-}iso}} < 90°$

to reduce the probability to pick up μ from c quark. $\quad \bar{t} \to \bar{b} \to \bar{c} \to \mu^-$

$t \to b \to \mu^-$

- Linear relation between $\langle m_{\ell^{iso}\mu^{non\text{-}iso}} \rangle$ and m_t
- # of events expected for SSCY ($10\ fb^{-1}$)

4.5k, 2.4k, 1.4k for $m_t = 200, 250, 300\ GeV/c^2$

- $\Delta m_t = \pm 2.3 \pm 2.3 \pm 3.4\ GeV/c^2$

stat. ↑ uncertainty in b fragmentation ↑ uncertainty in p_T^{top} dist.

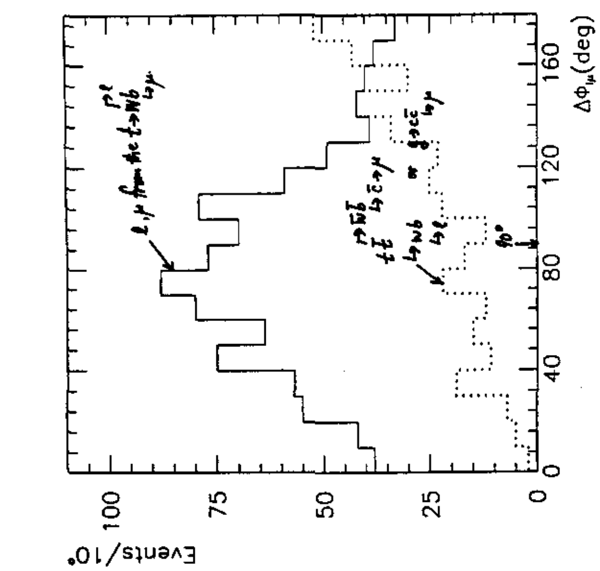

1060

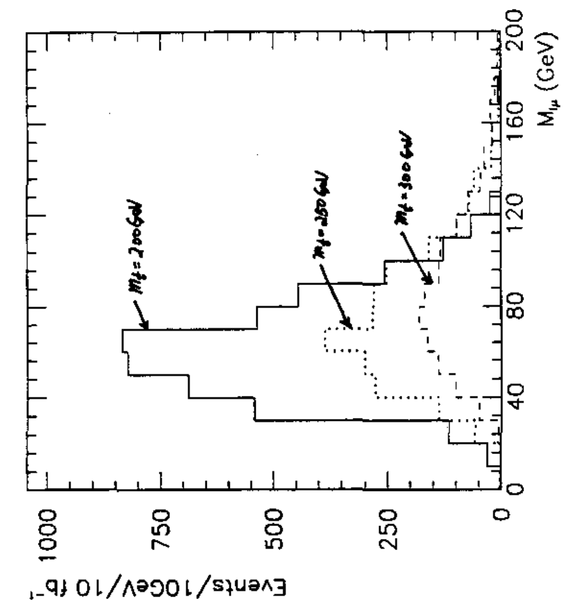

1061

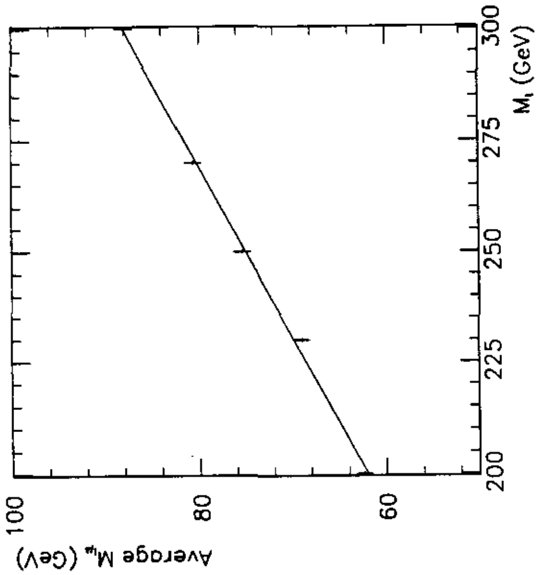

1062

$t\bar{t} \to \ell + n \geq 3$ jets ($m_t = 140$ & 250 GeV/c^2)

(Chiaki Yanagisawa)

Signal

$t\bar{t} \to W^- \bar{b}$, $W^- \to q\bar{q}'$

$t\bar{t} \to W^+ b$, $W^+ \to \ell^+ \nu$

isolated $\ell^\pm$ + at least 3 jets

Cuts

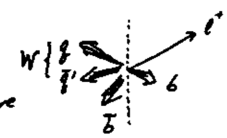

Isolated leptons

The same as before

Jets

- $p_T > 30$ GeV (for $m_t = 140$ GeV), 50 GeV (for $m_t = 250$ GeV)
- $\phi_{e,jet} > 90°$
- Three most energetic jets
- p_T(3-jet) > 200 GeV (for $m_t = 140$ GeV), 300 GeV (for $m_t = 250$ GeV)

Background

W + jets

- negligible for $m_t = 140$ GeV/c^2
- 15% to the 3-jet mass distribution for $m_t = 250$ GeV/c^2.

1063

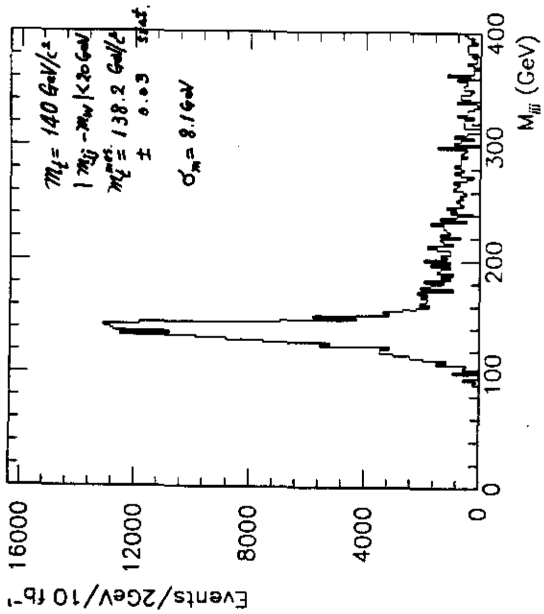

1084

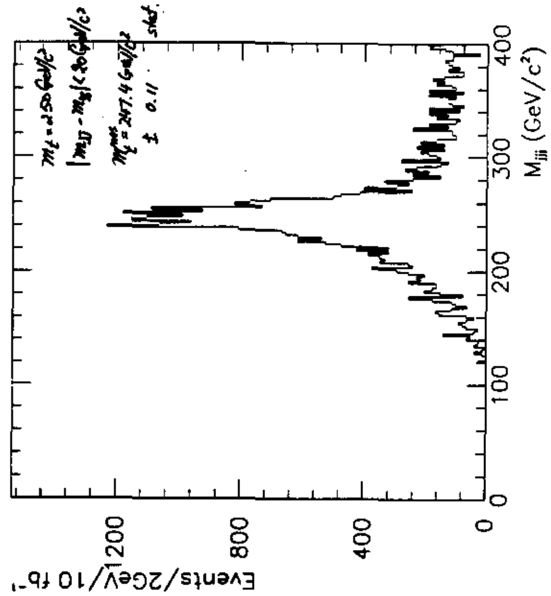

1085

§. Non-standard top decays.

$t \to H^+ b$, $H^+ \to \tau^+ \nu$ (Mohammad Mohammadi, David Skrzyniarz)

<u>Signal</u>

$t\bar{t} \to H^- \bar{b}$, $H^- \to \tau^- \nu$, $\tau^- \to$ had. ν

$\hookrightarrow W^+ b$, $W^+ \to \ell^+ \nu$

Isolated lepton + τ jet (1 or 3 prong) + b jet (30% eff.)

Since $H^- \to \tau^- \nu$ looks like $W^- \to \tau^- \nu$, the basic strategy is to look for an excess of τ i.e. violation of lepton universality.

<u>Cuts</u>

- Isolated $e^\pm$
  $|\eta| < 2.4$, $E_t(R=0.3) > 50$ GeV, $E_t^{em}(R=0.2) > 40$ GeV
  $E_t(R=0.4) - E_t^{em}(R=0.2) < 10$ GeV, $0.8 < \frac{E_t(R=0.2)}{p_t(CT)} < 2.0$
- Isolated $\mu^\pm$
  $|\eta| < 2.4$, $p_t > 20$ GeV/c, $E_t(R=0.4) - E_t(R=0.1) < 2$ GeV
- τ jet ($p_t > 1$ GeV/c & $\Delta R_{tr\text{-}jet} < 0.1$)
  $|\eta| < 2.4$, 1 or 3 prong, $E_t(R=0.3) > 50$ GeV
  Leading track: $p_t > 15$ GeV/c, $\Delta R_{tr\text{-}jet} < 0.1$
  $E_t(R=0.4) - E_t(R=0.1) < 10$ GeV, $\phi_{\ell\text{-}\tau jet} > 100°$
- b-jet (tagged)
  $|\eta| < 2.4$, Scalar $E_t > 30$ GeV, $\phi_{\ell\text{-}bjet} < 100°$

1086

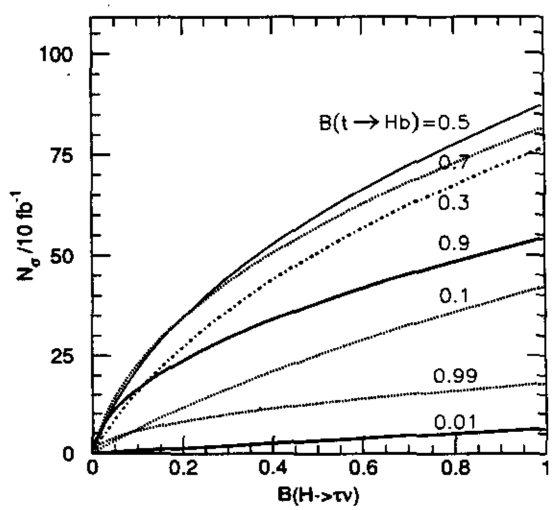

1087

Minimal SUSY (MSSM)

Two Higgs doublets

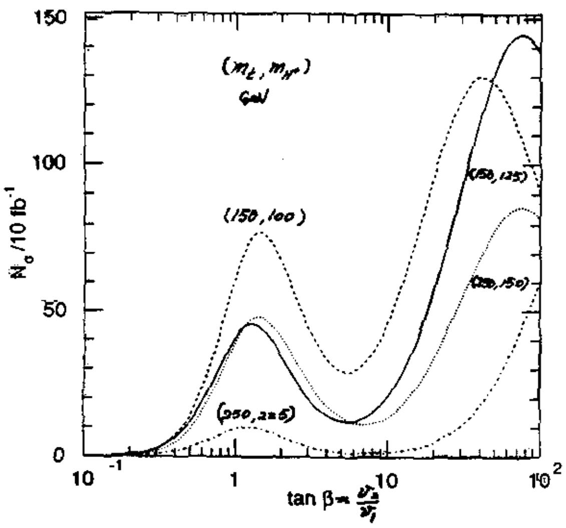

1088

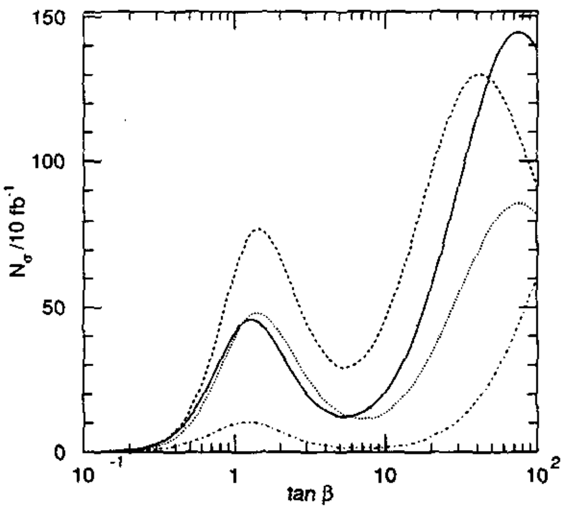

1089

TDR study

- Compositeness signal (Λ = 25,30 TeV), QCD background (ΣE_T > 9 TeV) and QCD normalization region (ΣE_T > 4.8 TeV) samples generated with PYTHIA 5.6 for 10 fb-1.
- Require $|\eta(\text{jet})| < 1.1$
- Trigger efficiency ~ 100%
- Jet finding with fixed cone R=0.9.
- Include non-gaussian response in **gemfast** (using a second gaussian of three times the width and 1% of the amplitude of the calorimeter resolution)

J. Womersley SSCL

Hadronic energy resolution

This table summarizes my present understanding of hadronic and jet energy resolution calculations in the GEM calorimeter.

		Single hadrons		Jets	
		Sampling Term	Constant Term	Sampling Term	Constant Term
UAZMIX - Mike Shupe					
(GEANT mixture geometry, e/h = 1.0 in EM, 1.6 in Pb/Kr HAD, 1.8 in Ar/Cu HAD, HAD energy smeared by 0.6/sqrt(E), 2 energy-dependent weights) Truncated fit, 50-500 GeV (100 & 500 only)					
eta=0	wall FH1-FH2	63	9	44	6
eta=0.3	good spot in CC	31	8	57	3 ←
eta=1.0	CC-EC	100	7	80	4
eta=2.5	good spot in EC	52	8	75	5
eta=3.3	EC-FC	86	9	172	6
eta=4.4	FC	86	7	303	11
CALOR89 - Brent Moore					
(slab geometry, no scintillator, eta=0, 6 energy-dependent weights)					
Single Pions,	Pb	56 (64)	6.5 (6.0)		
	Cu	56 (58)	9.0 (11)		
from fits (from hist rms)					
GEANT - Sasha Savin					
(eta=0, six energy-dependent weights)				60	3.9
GEMFAST					
Tuned to agree with Savin's result		70	5?	60	4

J. Womersley SSCL

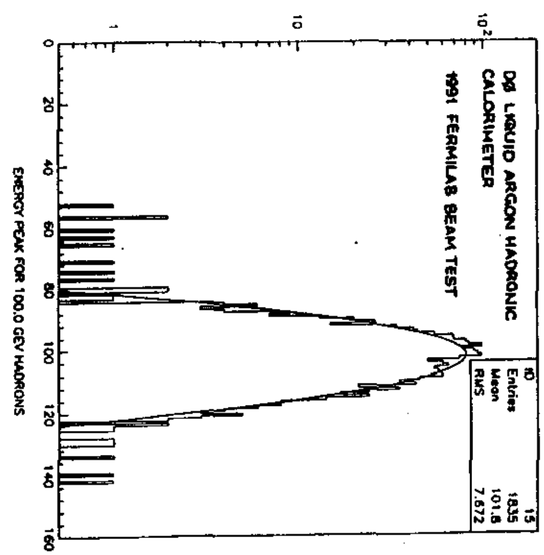

Jets at high transverse momentum

- Measure the high-p_T jet cross section as a test of QCD: deviations would be a signal of quark substructure.
- If quarks are composite at a scale Λ, then the four-fermion contact interaction leads to an excess of jets at high p_T (but $p_T << \Lambda$).
- Experimentally, one normalizes the jet p_T spectrum to QCD at low to moderate p_T values and then looks for an excess of events at high p_T. *(This avoids limitations from collider luminosity measurement, ΔL ~10%)*
- Systematic limitations arise from:
  - — uncertainty in parton distribution functions
  - — incomplete knowledge of the calorimeter jet energy response

J. Womersley SSCL

Systematic limitations

• Uncertainty in PDF's

Assuming perfect knowledge of the calorimeter energy response, the results obtained with three sets of PDF's were compared: CTEQ-1L, EHLQ-1, and MT-2.

• Calorimeter response

Since e/h ≠ 1, the calorimeter measurement of jet energy is not linear. The nonlinearity was modelled in GEANT (UAZMIX), and pion response normalized at 200 GeV (as in a test beam). The response then varies by up to 10% (depending on the weighting scheme) over the interval 10—5000 GeV.

In both cases the resulting uncertainty in jet rates is small (few %).

→ effects do not seriously compromise the value of Λ that can be reached. Λ = 25 TeV remains "easy".

J. Wamersley SSCL

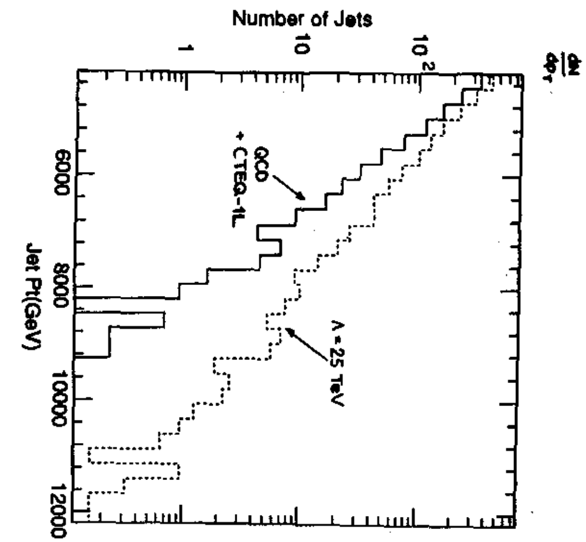

Table 2-15: Number of jets expected with 10 fb^{-1} for various E_T^{cut}, substructure scales and parton distributions.

E_T^{cut}(GeV)	4500	5000	5500	6000
CTEQ-1L Distributions				
Λ = ∞	704	339	155	74
30 TeV	905	489	278	164
25 TeV	1226	724	447	276
EHLQ-1 Distributions				
Λ = ∞	663	326	155	76
30 TeV	802	439	255	146
25 TeV	1106	669	407	251
MT-2 Distributions				
Λ = ∞	703	326	155	77
30 TeV	918	498	276	159
25 TeV	1328	803	507	309

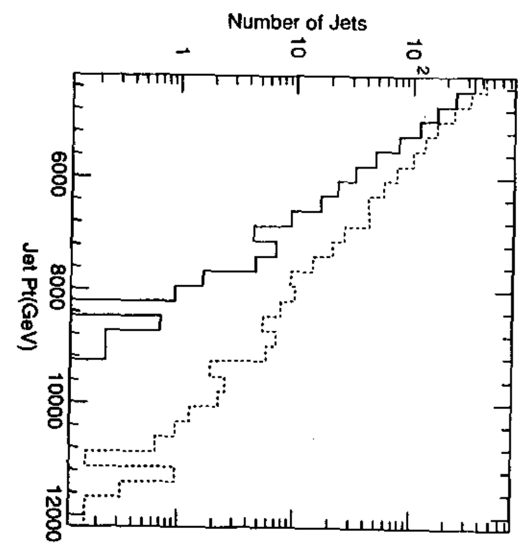

Table 2-16. Number of jets expected with 10 fb^{-1} in different energy-weighting schemes as described in the text. The CTEQ-1L entries are from Table 2-15.

E_T^{cut} (GeV)	4500	5000	5500	6000
CTEQ-1L Distributions				
$\Lambda = \infty$	704	339	155	74
25 TeV	1226	724	447	276
Energy-independent Weights				
$\Lambda = \infty$	718	349	167	79
25 TeV	1257	739	468	286
Energy-dependent Weights				
$\Lambda = \infty$	676	321	148	70
25 TeV	1189	701	435	267

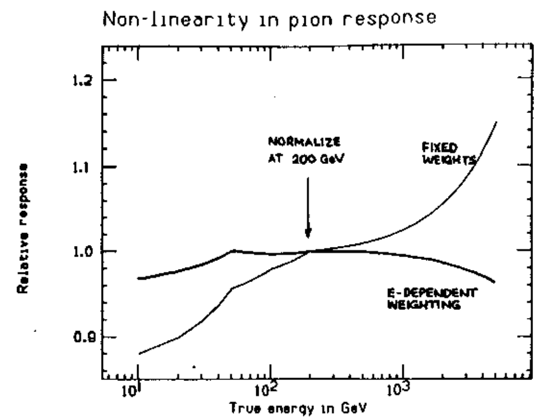

Possible future work

- investigate effects of other possible systematics in calorimeter response e.g. cell-to-cell miscalibrations, 5% offset in scintillator energies, etc.
- do a real analysis involving fitting the p_T distributions to get a better feel for the errors
- studies at high luminosity
  estimate $\Lambda \sim 45$ TeV with 100 fb^{-1}

J. Womersley SSCL

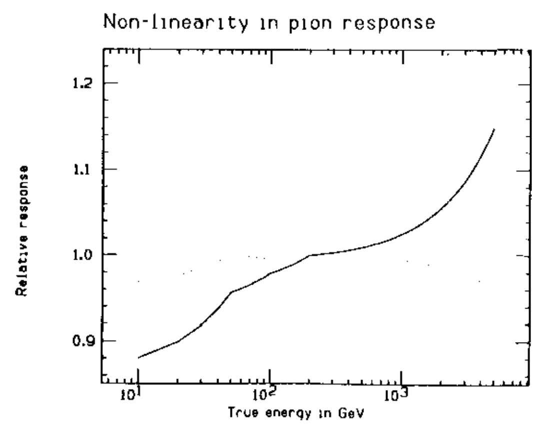

Physics at the SSC

- Electroweak Symmetry Breaking:

  $M_\gamma = 0$, but $M_W, M_Z \neq 0$.

  $\Lambda_{EWSB} \simeq 2^{-1/4} G_F^{-1/2} = 246.22$ GeV

  New physics must occur near 1 TeV

  $\hat{\sigma}_{EWSB} \simeq$ 1nb - 1fb ⟹ SSC design parameters

  $\sqrt{s} \simeq 40$ TeV ; $\mathcal{L} = 10^{33} - 10^{34}$ ($\to pp$)

- Flavor Symmetry + Flavor Symmetry Breaking
  - 3 identical generations of $q_i = \binom{u_i}{d_i}$, $\ell_i = \binom{\nu_i}{e_i}$ except that
  - $m_q \neq 0$, $m_\ell \neq 0$; $m_{q'} \neq m_q$, $m_{\ell'} \neq m_\ell$

  If $\Lambda_{FSB} \ll 100$ TeV, $\sigma_{FSB} \sim$ 1nb - 1fb

  Again ... $\sqrt{s} \simeq 40$ TeV ; $\mathcal{L} = 10^{33} - 10^{34}$

- The Unknown!

  $Q = \binom{U}{D}$, $L = \binom{N}{E}$, ... ?

  $W'^{\pm}$, Z'^{0}, ... ??

  Axigluons, ... ???

Whatever the new physics is, it's scale $\Lambda \gtrsim 1$ TeV

⟹ $\hat{\sigma} \leq \frac{\pi}{\Lambda^2} \sim$ 1nb

(geometrical)

The popular scenarios for EWSB, FSB:

- Elementary Higgs boson models – H^0; h^0, $H^\pm$
- Supersymmetric Higgs boson models – ditto + ditto
- Dynamical EWSB – TC + ETC – ρ_T, π_T, ...
- Dynamical flavor – Composite q/ℓ – Scale Λ.

None of the models of these scenarios is a satisfactory, compelling description of EW, flavor physics.

(i.e. they stink!)

That is wonderful, exciting!

Physics at $\mathcal{L} = 10^{34}$

- Isolated high-p_T leptons from Z', W', q/ℓ substructure, ρ_T, ...

  $\sigma \simeq 1\text{-}10\ fb$ $\quad M_{W',Z'} \simeq 5$ TeV; $\Lambda_{q/\ell} \simeq 20\text{-}30$ TeV; $M_{\rho_T} \simeq 1\text{-}2$ TeV

  → $\int \mathcal{L}dt \simeq 10^{34} \times 10^{7} = 100\ fb^{-1}$ for detailed studies.

- Precision EM (+CT!)

  → $\Delta M_{Z'}/M_{Z'} \simeq 0.3\%$, dominated by $\Delta E/E$

  → $\Gamma_{Z'}$ well-measured in $Z' \to e^+e^-$

- Robust MU – measurement outside CAL.

  → P_t/P_t up to $\gtrsim 5$ TeV; Q_μ-sign at 99% at 10^{34}.

  → Z', W', $\Lambda_{q/\ell}$ couplings probed by measuring $\bar{q}q \to \mu^+\mu^-$; $\mu^\pm\nu_\mu$ ang. dist'ns.

High-Luminosity Studies for the TDR

1. Distinguish two models with a 4-TeV Z'
   - by $\Gamma_{Z'}$ in $Z' \to e^+e^-$.
   - by angular distributions in $Z' \to \mu^+\mu^-$.
2. Distinguish two "models" of q/ℓ substructure — chiral couplings in $\Lambda_{q/\ell}$ via angular distributions in $\bar{q}q \to \mu^+\mu^-$.

(3. We also discussed $W'^\pm$, $\bar{q}q' \to \ell^\pm\nu_\ell$.)

$Z' \to e^+e^-$

- Two models with $M_{Z'} = 4$ TeV,

  $\sigma(Z_1) = 5.4\ fb$; $\Gamma_{Gen'd}(Z_1) = 124$ GeV

  $\sigma(Z_2) = 4.5\ fb$; $\Gamma_{Gen'd}(Z_2) = 94$ GeV

- Backgrounds –

  $pp \to jj \to$ "e" "e" $\quad (\sigma(\geq 250\ GeV) = 700\ pb)$

  $\to W^\pm j \to e^\pm$ "e" $\quad (\sigma(\geq 250\ GeV) = 25\ fb)$

  $\to \bar{t}t \to e^+e^- + X \quad (\sigma(M > 1.4\ TeV, p_T > 100\ GeV) = 1.4\ pb)$

Isolation : $\sum_{R<0.3} E_T - 1.1 \sum_{5\times5} E_T(EC) < 0$

→ $R(e/jet) \simeq 2\times10^{-3}$ (W̸J) (j̸j)

CT(!) : ≥ 1 track w/ $p_T > 50$ GeV in 5×5 EC.

→ Additional 1/5 → $R(e/jet) \simeq 4\times10^{-4}$ (j̸j)

- Acceptance : ~ 90% → Pix.

Leakage, pileup, brem, ... unimportant!

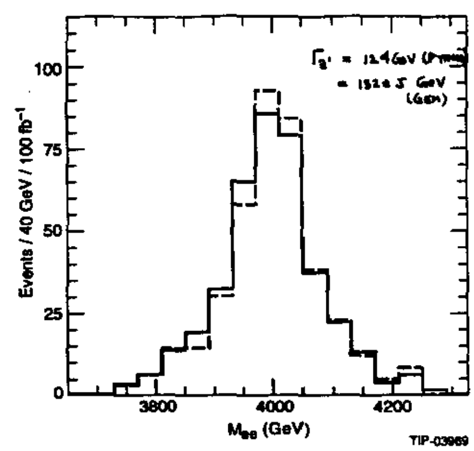

FIG. 2-44. The $M_{e^+e^-}$ distribution for a 4 TeV mass Z' of Model 1 as described in the text. Reconstructed (solid) and generated (dashed) distributions are shown.

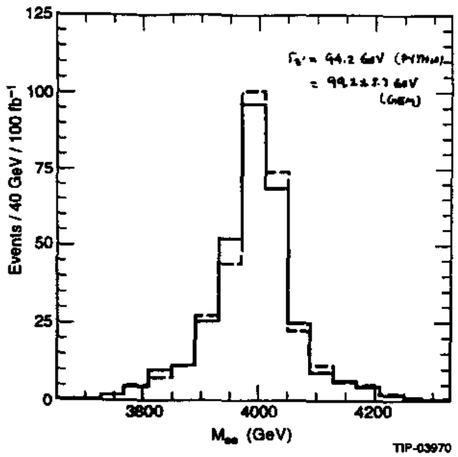

FIG. 2–45. The $M_{e^+e^-}$ distribution for a 4 TeV mass Z' of Model 2 as described in the text. Reconstructed (solid) and generated (dashed) distributions are shown.

1114

4.

$Z' \to \mu^+\mu^-$ AND $\bar{q}q \to \mu^+\mu^-$

- SAME TWO Z' MODELS WITH GENERATED $A_{FB}(Z_1) = 0.083$, $A_{FB}(Z_2) = -0.115$
- TWO $\mathcal{L}_{qq\ell\ell}$ MODELS WITH $\Lambda = 25$ TeV AND $\frac{dN}{d(\cos\theta)} \propto (1+\cos\theta)^2$ ("ISO") ; 1 (FLAT!) ("HNC")
- BACKGROUNDS –

  $\bar{t}t \to \mu^+\mu^-$ – ELIMINATED BY ISOLATION, $M_{\mu\mu}$ CUTS

  $\bar{q}q \to \mu^+\mu^-$ – NEGLIGIBLE FOR 4-TeV Z'
  – 20–25% OF SUBSTRUCTURE SIGNAL

  PUNCHTHROUGH, DECAY $\mu^\pm$, MISMEASURED LOW-P_T $\mu^\pm$ – ALL NEGLIGIBLE !

- ACCEPTANCE –

  GEOMETRIC – 70% OF $\mu^+\mu^-$ w/ $|\eta| < 2.46$
  $\eta \simeq 0$; 1.3 GAPS!

  RECONSTRUCTION – 85% PER $\mu \Rightarrow$ 70% FOR $\mu^+\mu^-$.
  RAISED TO ~ 95% BY ACCEPTING 1 "GOOD" + 1 "BAD" MUON

$\Rightarrow$ Pix

1115

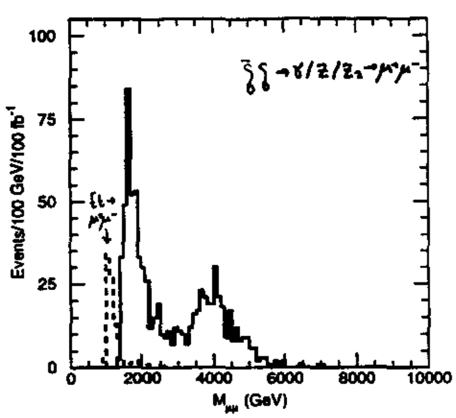

FIG. 2–47. The $M_{\mu^+\mu^-}$ distribution for the Drell-Yan continuum and $Z_2 \to \mu^+\mu^-$. The $t\bar{t} \to \mu^+\mu^- + X$ background before the invariant mass cut is also shown (dashed).

1116

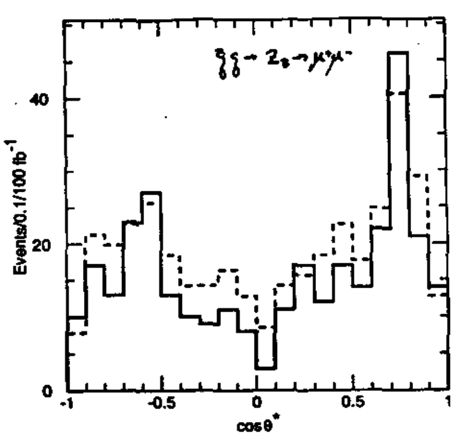

FIG. 2–48. Generated (dashed) and reconstructed (solid) cos θ^* distributions for $Z_1 \to \mu^+\mu^-$ events passing signal selections.

1117

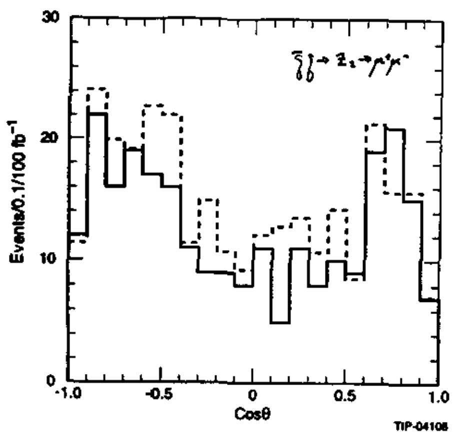

FIG. 2–49. Generated (dashed) and Reconstructed (solid) $\cos\theta^*$ distributions for $Z_2 \rightarrow \mu^+\mu^-$ events passing signal selections.

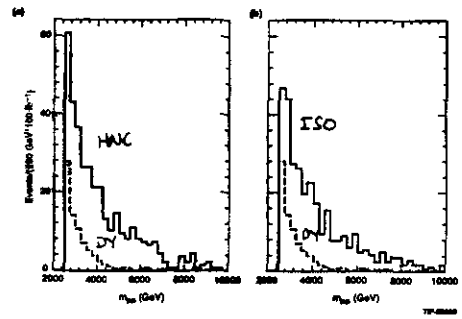

Fig. 2–50. The $M_{\mu^+\mu^-}$ distributions for the ISO (a) and HNC (b) substructure models defined in the text. The lower dashed histogram is the standard Drell-Yan distribution.

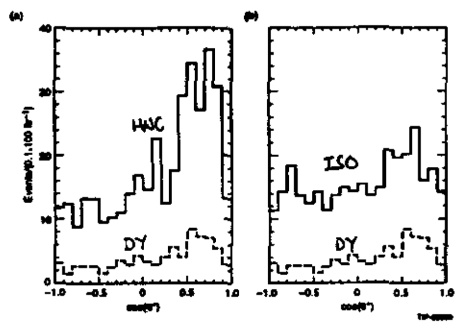

Fig. 2-51. The $\cos\theta^*$ distributions for the ISO (a) and HNC (b) substructure models defined in the text. The lower dashed histogram is the standard Drell-Yan distribution.

'Rocket' smokes 0's with 13 strikeouts

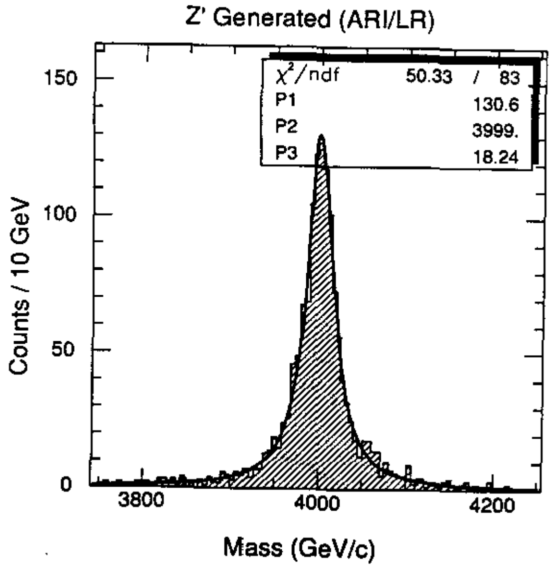

1122

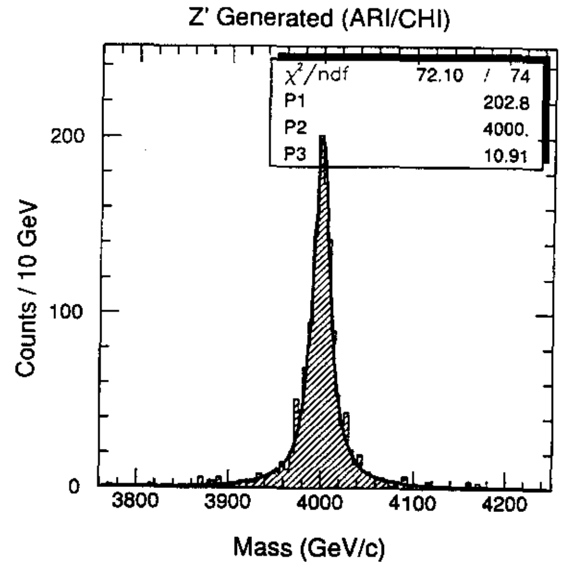

1123

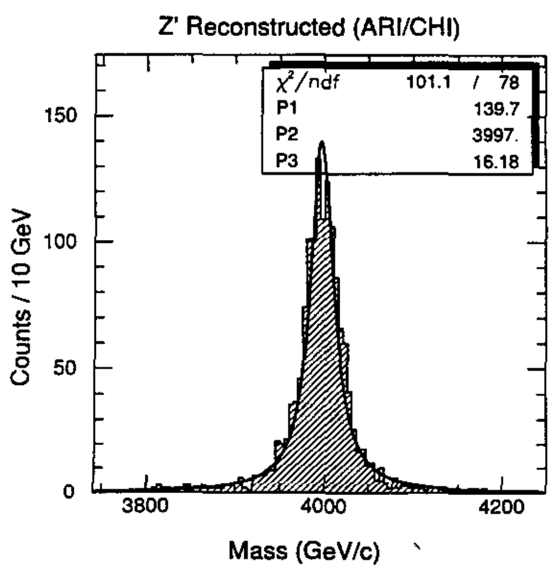

1124

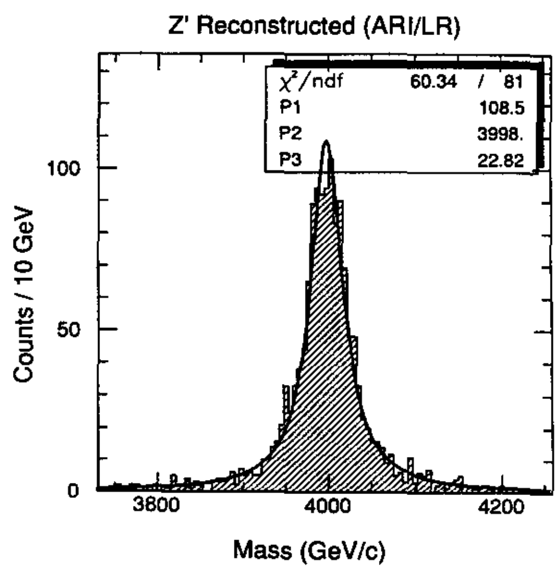

1125

F. Paige, A Vanyashin

Supersymmetry Signatures in GEM

- related to missing energy $\not{E}_T$

M ~ 300 GeV — lower limit of interest (Tevatron)

M ~ 2000 GeV — limited by statistics

FC GEANT Mike Shupe U.AZ

⇓

gemfast ($\Delta P_T / P_T$) ~ 10%-15%

nongaussian effects (DØ)

1128

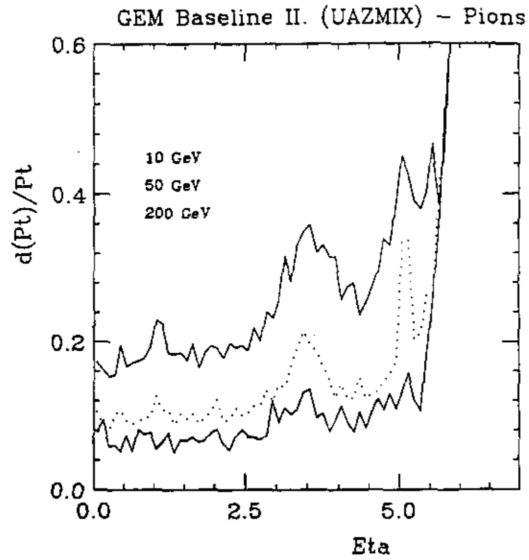

1129

handles:

- $\not{E}_T$ > 200 GeV
- N_{jet} cone 0.7
  - p_T > 75 GeV
  - p_T > 300 GeV
- S_T transverse sphericity
  - to ~~sele~~ reject QCD 2jet events
  - S_T > 0.2
- lepton veto:
  - no isol. e or μ p_T > 20Ge
  - Loose eid: $|E/p - 1| <$ 0.5 / 3.5p

1130

GEM report to PAC July, 92

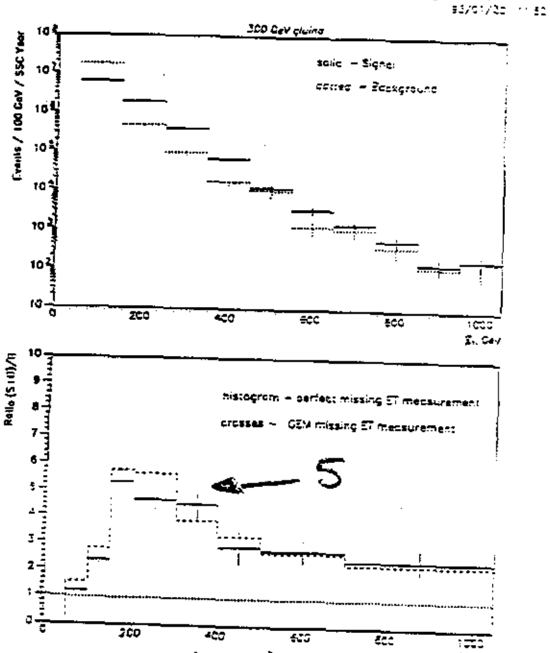

Baseline I

1131

Last edited by Paige, 5 April 1993, 21:00

Table 2.7-1: Choices of MSSM paramaters for the three cases considered. All the squarks and all the sleptons are taken to be degenerate for simplicity. All masses are in GeV. See Ref. 91 for the notation.

Parameter	Case I	Case II	Case III
$M_{\tilde g}$	300	350	2000
$M_{\tilde q}$	600	325	2500
$M_{\tilde l}$	500	200	1500
M_A	300	300	300
μ	−300	−300	−1000
$\tan\beta$	2	2	2

Case I has a light gluino and a heavier squark; it is generally similar to the models of Arnowitt and Nath[93] and to the case considered in the Letter of Intent.[98] Case II has a squark slightly lighter than the gluino and is generally similar to the models of Ross and Roberts.[92] Since $\tilde g \to \tilde q q$ dominates for $M_{\tilde g} > M_{\tilde q}$, the signatures in this case are similar to those for squark pair production. One might think that this case would be more difficult to detect because the events contain just two hard jets from $\tilde q \to \tilde\chi_1^0 q$, but the decays

300 GeV gluino:

```
MSSM MASSES:
M(UPL  ) =    600.000     M(DNL  ) =    600.000     M(STL  ) =    600.000
M(CHL  ) =    600.000     M(BTL  ) =    600.000     M(TPL  ) =    600.000
M(UPR  ) =    600.000     M(DNR  ) =    600.000     M(STR  ) =    600.000
M(CHR  ) =    600.000     M(BTR  ) =    600.000     M(TPR  ) =    600.000
M(NUEL ) =    500.000     M(EL-  ) =    500.000     M(NUML ) =    500.000
M(MUL- ) =    500.000     M(NUTL ) =    500.000     M(TAUL-) =    500.000
M(ER-  ) =    500.000     M(MUR- ) =    500.000     M(TAUR-) =    500.000
M(GLSS ) =    300.000     M(Z1SS ) =     48.430     M(Z2SS ) =    102.718
M(Z3SS ) =    303.965     M(Z4SS ) =    318.843     M(W1SS+) =    102.181
M(W2SS+) =    317.234     M(HL0  ) =     74.507     M(HH0  ) =    310.430
M(HA0  ) =    300.000     M(H+   ) =    310.403

OTHER MSSM PARAMETERS:
TAN(BETA) =       2.000    2*M1 =    300.000
```

325 GeV squark $M_{\tilde g} > M_{\tilde q}$

```
MSSM MASSES:
M(UPL  ) =    325.000     M(DNL  ) =    325.000     M(STL  ) =    325.000
M(CHL  ) =    325.000     M(BTL  ) =    325.000     M(TPL  ) =    325.000
M(UPR  ) =    325.000     M(DNR  ) =    325.000     M(STR  ) =    325.000
M(CHR  ) =    325.000     M(BTR  ) =    325.000     M(TPR  ) =    325.000
M(NUEL ) =    200.000     M(EL-  ) =    200.000     M(NUML ) =    200.000
M(MUL- ) =    200.000     M(NUTL ) =    200.000     M(TAUL-) =    200.000
M(ER-  ) =    200.000     M(MUR- ) =    200.000     M(TAUR-) =    200.000
M(GLSS ) =    350.000     M(Z1SS ) =     56.031     M(Z2SS ) =    116.985
M(Z3SS ) =    304.243     M(Z4SS ) =    318.267     M(W1SS+) =    116.620
M(W2SS+) =    316.960     M(HL0  ) =     67.345     M(HH0  ) =    309.893
M(HA0  ) =    300.000     M(H+   ) =    310.483

OTHER MSSM PARAMETERS:
TAN(BETA) =       2.000    2*M1 =    300.000
```

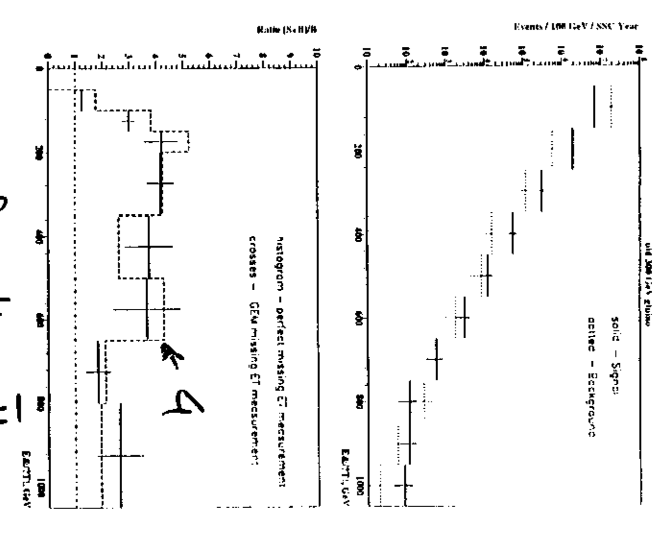

Baseline = larger beam pipe more detailed simulation

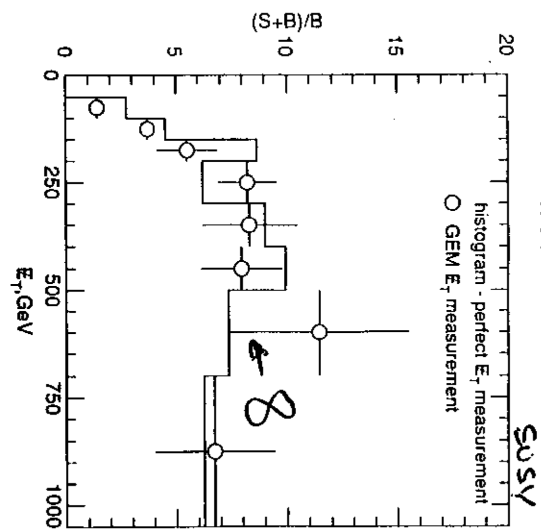

GEM TDR more detailed SUSY model

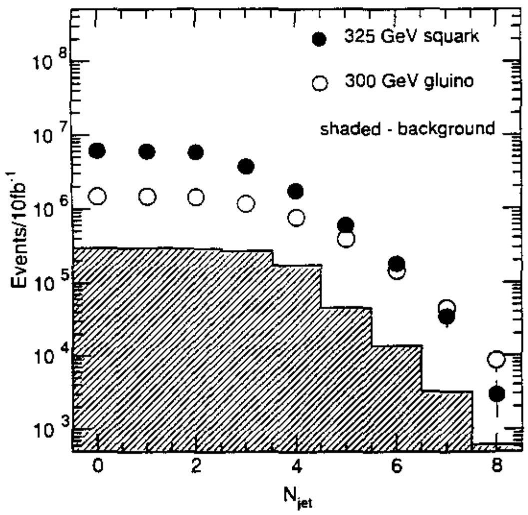

1136

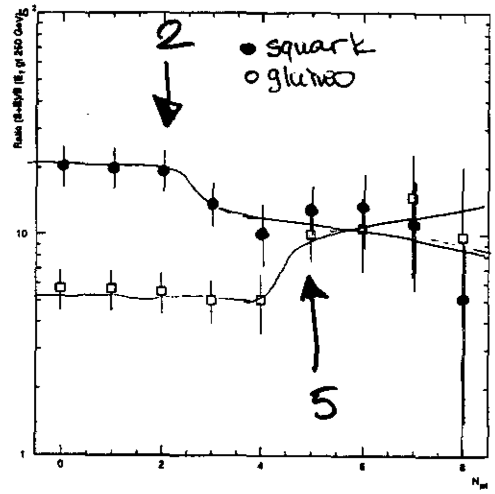

1137

$N_{jet} \geq 5$

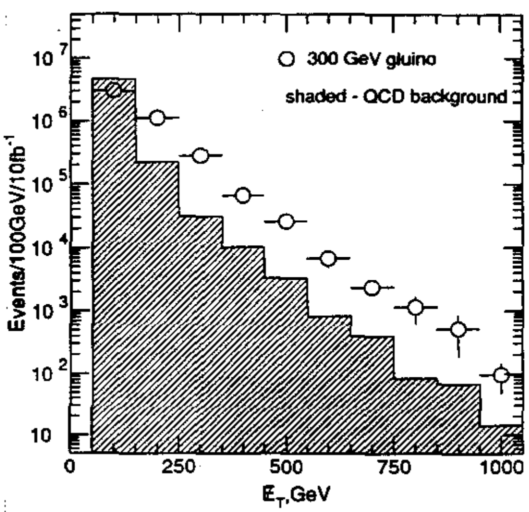

560 eV

70 keV

1138

$N_{jet} \geq 2$

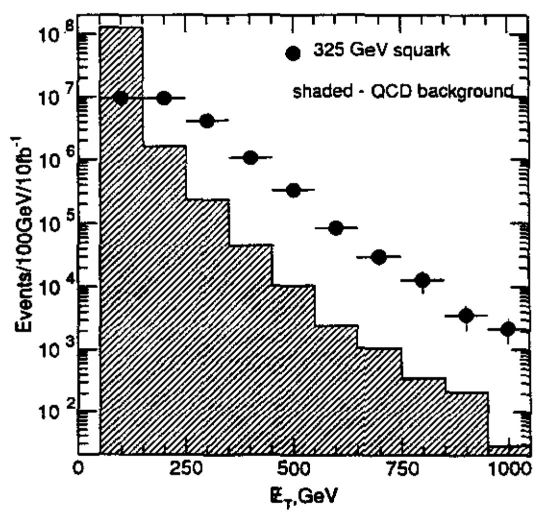

25 keV

1139

2000 GeV gluino

```
MSSM MASSES:
M(UPL  ) =   2500.000   M(DNL  ) =   2500.000   M(STL  ) =   2500.000
M(CHL  ) =   2500.000   M(BTL  ) =   2500.000   M(TPL  ) =   2500.000
M(UPR  ) =   2500.000   M(DNR  ) =   2500.000   M(STR  ) =   2500.000
M(CHR  ) =   2500.000   M(BTR  ) =   2500.000   M(TPR  ) =   2500.000
M(NUEL ) =   1500.000   M(EL-  ) =   1500.000   M(NUML ) =   1500.000
M(MUL- ) =   1500.000   M(NUTL ) =   1500.000   M(TAUL-) =   1500.000
M(ER-  ) =   1500.000   M(MUR- ) =   1500.000   M(TAUR-) =   1500.000
M(GLSS ) =   2000.000   M(Z1SS ) =    303.002   M(Z2SS ) =    608.510
M(Z3SS ) =   1001.908   M(Z4SS ) =   1004.892   M(W1SS+) =    608.518
M(W2SS+) =   1005.197   M(HL0  ) =     89.923   M(HH0  ) =    311.841
M(HA0  ) =    300.000   M(H+   ) =    310.483

OTHER MSSM PARAMETERS:
TAN(BETA) =      2.000      2*M1 =   1000.000
```

1140

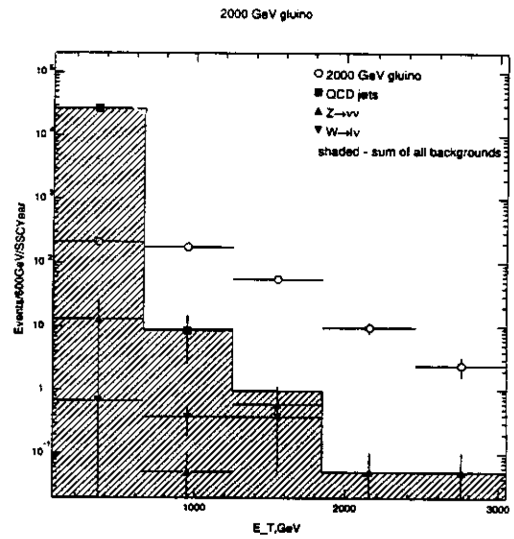

4 jets > 500 GeV

1141

same sign dileptons:
R Tracker is essential (Majorana)

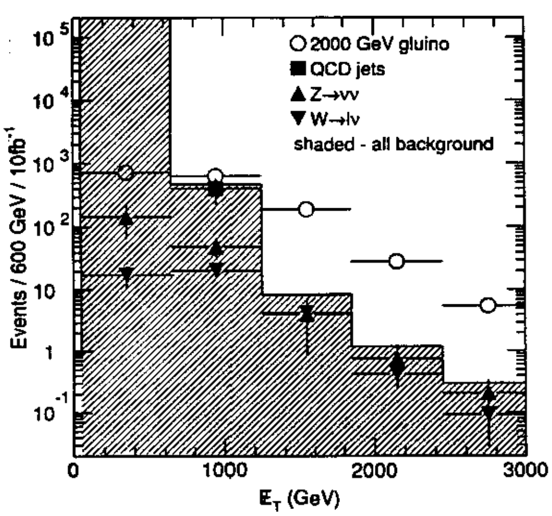

4 jets > 300 GeV

1142

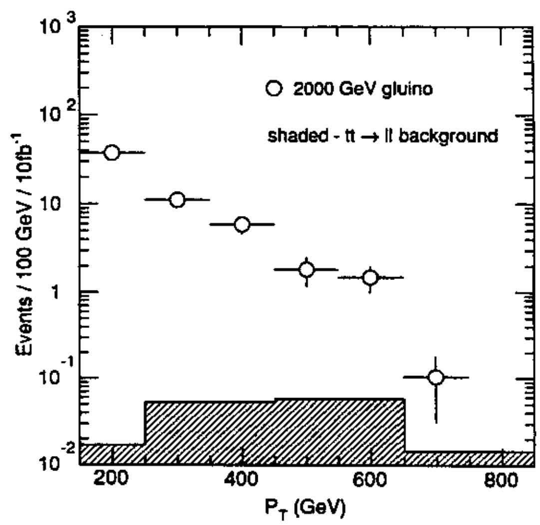

highest lepton
electrons – 4 times more statistics

1143

F.E. Taylor
5/12/93

Summary of Muon Meeting

- Working Meeting to go through PAC presentation
  - fine-tuned agenda of muon parallel session
- Joint Meeting with simulations group
  - how to use CT and calorimeter to cover muon chamber gaps
- Progress on muon simulation
  - Yuri Fisyak SIGEM 2.0
  - Torre Wenaus Hit Level MC results

May 6, 1993

Yu. Fisyak

SIGEM
GEANT SImulation for GEM detector
Version 2.0

Base line 1 → vrs. 0

—"— 2 → vrs. 1

TDR → vrs. 2

SIGEM structure

I have borrowed L3 idea about using GEANT for simulation of systems and subsystem as combination of different level detailization description of these system:

- Level 0 — NO detector or subdetector at all.
- Level 1 — System as a "dead" material
- Level 2 — Simplified description (= mixture level Calorimeter with GFLASH) with HITS
- Level 3 — Full description (Barrel accordion) with HITS

SIGEM consists of the following packages:

- si — SIGEM 2.00/00 930501 12.42 GEANT3/GEM SImulation program steering;
  - *SIGEM — Pilot for complete Simulation
  - SIGEM — High level steering routines for event Simulation
  - SIUSER — User routines for event Simulation
  - SIEVNT — routines control one event ← Kine
  - SISTEP — routine related to one step/hit
  - SIHSTA — histograms
  - SILUND — Pythia version for GEANT
  - SIDATA — FFREAD cards definition
  - SITRIG — trigger related topics
  - SIRUN — FFREAD Run cards for standard GEANT run
  - SICOM — Command (script) files for creation library and executable files
  - SIPYTH — Run cards for standard PYTHIA/JETSET

- xs — XSGEM 2.00/00 930501 12.31 eXperimental Setup of GEM detector, TDR version;
  - * XSGEM — General geometry routines for GEM experimental setup
  - * XSTRAK — Description of the central Track detector
  - * XSCALO — Description of the Central Calorimeter
  - * XSMUON — Description of the high precision Muon chambers
  - * XSMAGN — Description of the Solenoid
  - * XSFFSH — Description of the Flux CONcentrator
  - * XSPIPE — Description of the beam PIPE and beam QUADrupole regions
- ut — UTGEM 2.00/00 930501 12.34 GEM utility routines;
  - * UTBODY — General utility routines for simulation and reconstruction simulated data
  - * GEANT DEV — Specific GEM / GEANT3 / HBOOK4 interface F2
  - * DUTIL/DRPACK/DMPACK/DVPACK — double precision part of KERN lib R2
- tt — TTGEM 2.00/00 930501 12.56 GEM TiTle data base TDR version;

- * *TT GEM Pilot patch for GEM titles
- * TT GEM GEM materials, tracking media, standard rotation matrices and GEM as a whole
- * TT FIELD Field map
- * TT PIPE Beam pipe
- * TT TRAK Central tracker
- * TT CALO Calorimeter
- * TT MEMB Membrane
- * TT MUON Muon system
- * TT MSUPP Muon system support
- * TT FFSI Forward field shaper
- * TT MAGN Superconducting solenoid
- * TT QUAD Low beta quadrupole
- * TT SETS SETS and DETector definitions

- gf — GFLASH 1.41/00 930125 17.54 by Stefan Peters;
- gc — CALOR 1.00/00 930427 14.36 by C.Zeitnitz;
- re — REGEM 2.00/00 930501 12.46 GEM REconstruction.
  - * REFUTY Kalman Fit UTiliY
  - * RETSEG finding and fitting of track segments
  - * RETRAK GEM implimentation of GEANE package.

1156

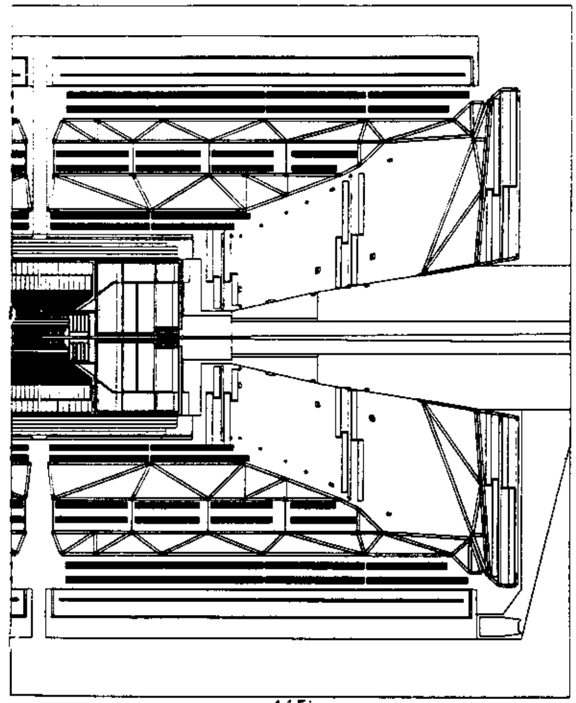

1157

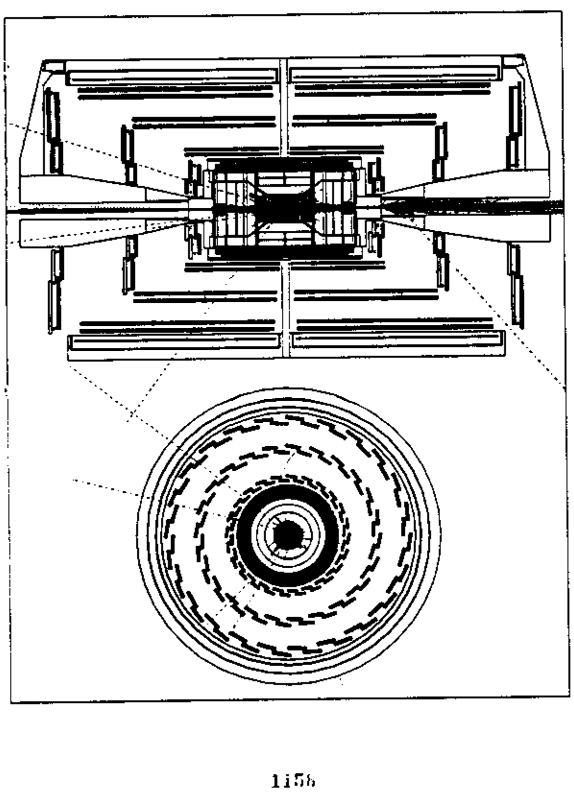

1158

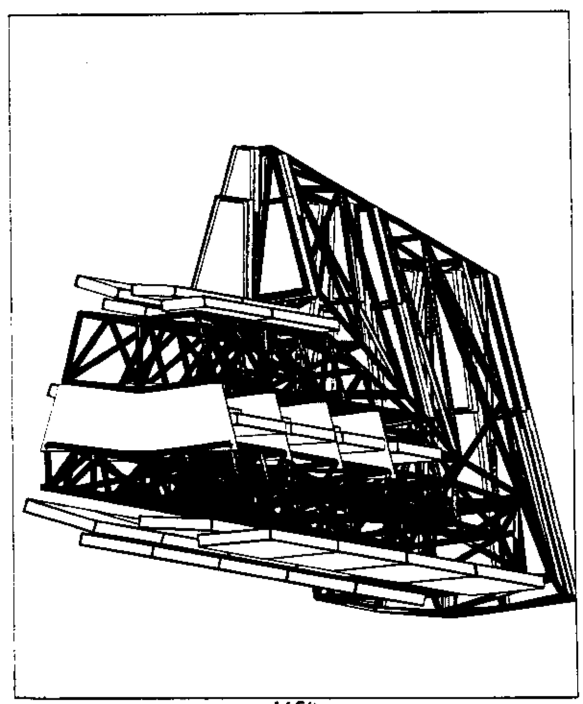

1159

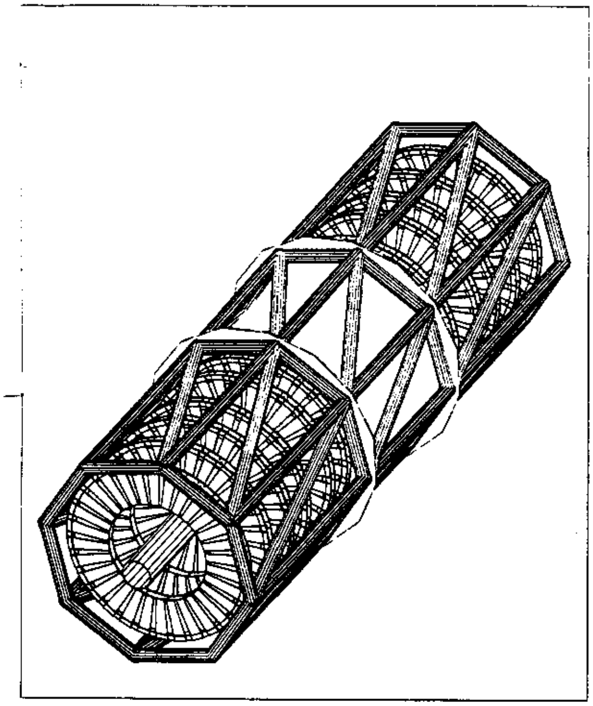

1160

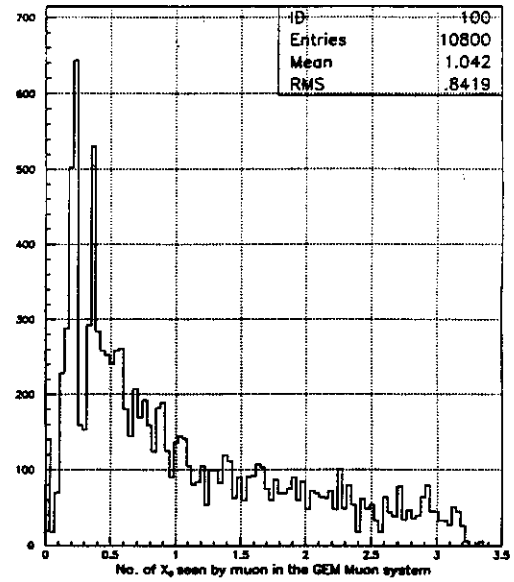

1161

SIGEM Page 6

Digitization has not yet implemented. For the muon system this topics is in the agenda. Hopely it will be done by (V.Balagura + ITEP) in the nearest one - two months.

SIGEM is installed and supported now on VAX/VMS, HPUX and SUN as interactive, debug and batch version. The examples of different detector view are shown in Figures.

The SIGEM status can be expressed as the following:

- There is up to date (TDR) version for the GEM muon system including the Draper support structure and some elements of chamber construction .
- The calorimeter factually corresponds to the November Base line 2 design. GFLASH is installed, debugged but not yet tested in the sense of comparison full GEANT simulation with GFLASH results.
- The Central Tracker model is mainly corresponds to the November Base line 2 design.

1162

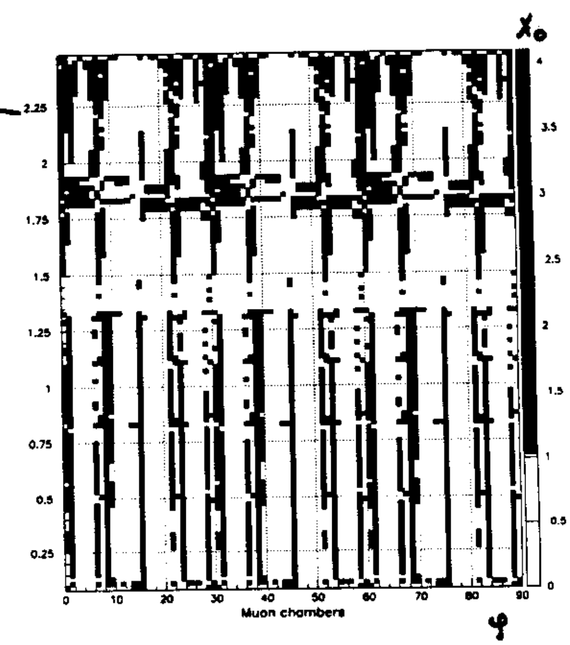

1163

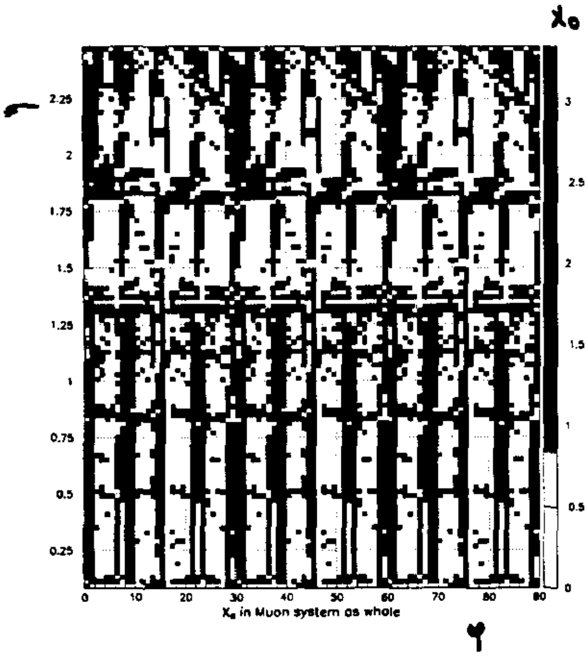
2.25
2
1.75
1.5
1.25
1
0.75
0.5
0.25
0 10 20 30 40 50 60 70 80 90
3
2.5
2
1.5
1
0.5
0
X0 in Muon system as whole

1164

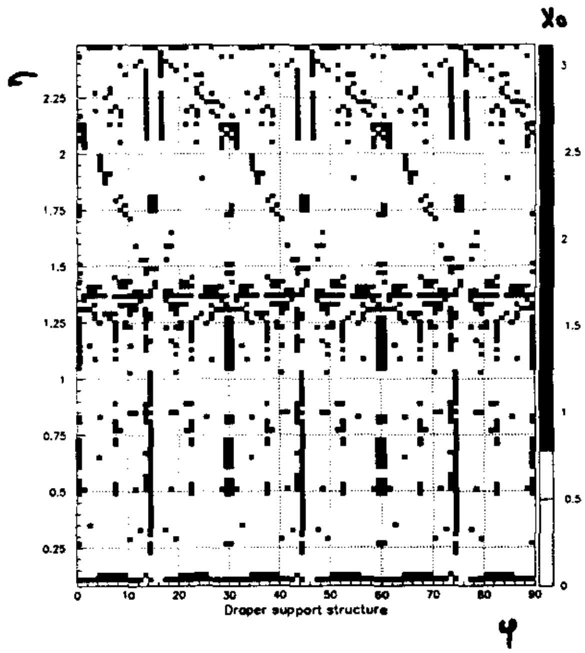
2.25
2
1.75
1.5
1.25
1
0.75
0.5
0.25
0 10 20 30 40 50 60 70 80 90
3
2.5
2
1.5
1
0.5
0
Draper support structure

1165

Central Tracker Report

J. Brau
May 12, 1993
San Diego

There will be a meeting of the Central Tracker group at San Diego on Tues., May 11, 1993 from 9:00am - 2:00pm. Location will be announced.

A G E N D A

9:00 - 9:30	General Discussion Agenda for May 24th PAC Review		— Material Rad. Lengths
RECENT R & D RESULTS:			
9:30 - 9:50	Silicon Detectors	J. Brau	— Prototype Tests
9:50 - 10:10	IPC's at Indiana	C. Bower	
10:10 - 10:30	IPC Prototypes	E. Wolin	
10:30 - 11:00	Test Beam Instrumentation	S. Alam	
11:00 - 11:20	Silicon Electonics	S. Hahn	— Preamp Prototype Fab
SOFTWARE PROGRESS:			
11:20 - 11:40	Melynda Brooks		— B-jet tagging, γ/e separation
11:40 - 12:00	Jenny Thomas		— calibration of alignment
12:00 - 12:20	Shawn McKee		— $Z' \to e^+e^-$ @ 10^{34}
12:20 - 12:40	Discussion		— Test beam plans

1170

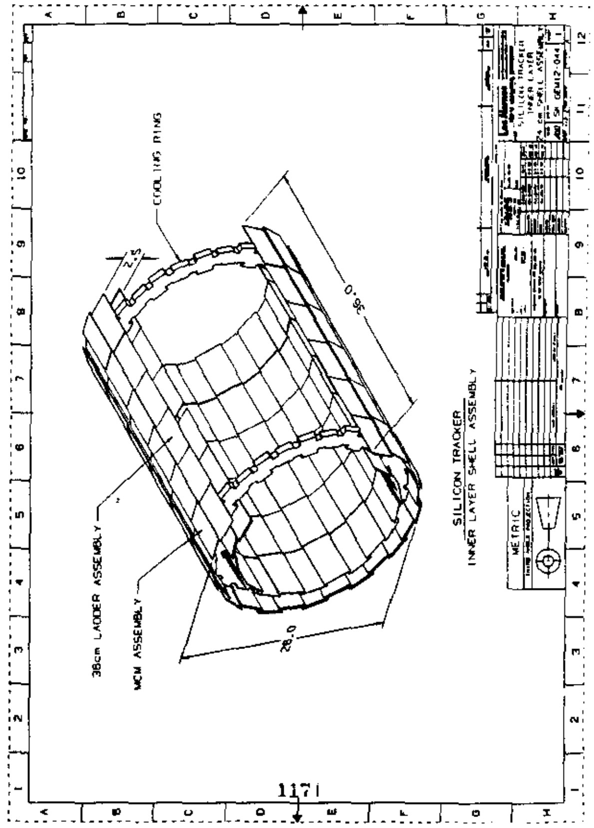

1171

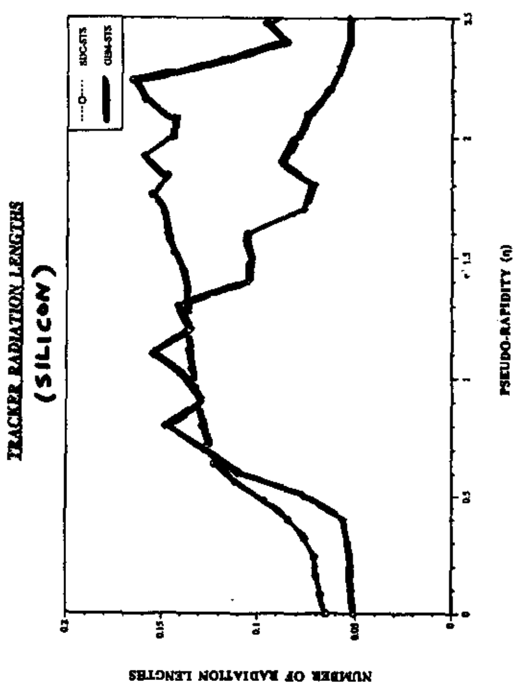

117?

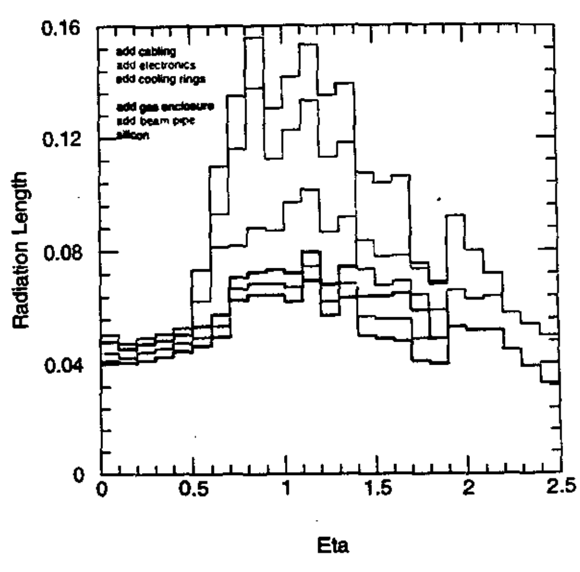

1173

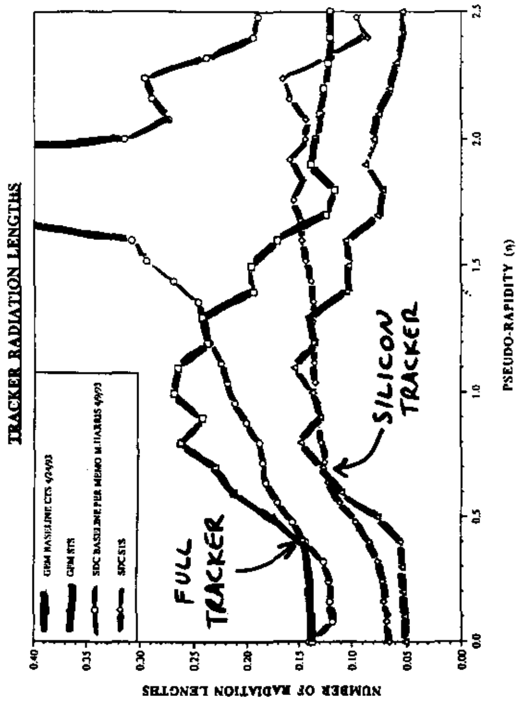

1174

Kollipara

Measured Strip Resistance on Hamamatsu Single-sided Detector

STRIP WIDTH (μm)	R (Ω/cm)	ρ (Ω/cm · μm) (R · width)
38	7.4	280
28	10.1	284
18	15.8	284
8	40.1	321
6	70	420

1175

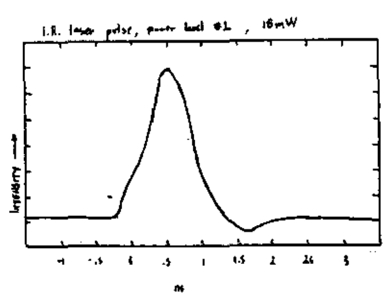

1176

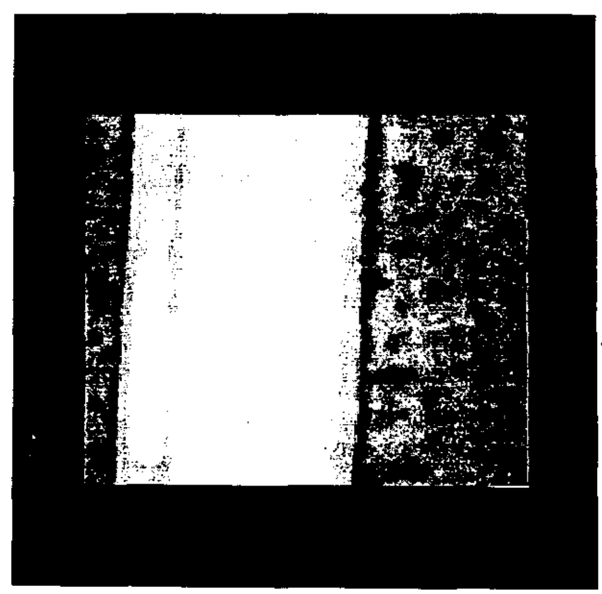

I.R. laser imaged onto Aluminum strip w/o slit, using 100X objective — (configuration used in tests)

117.

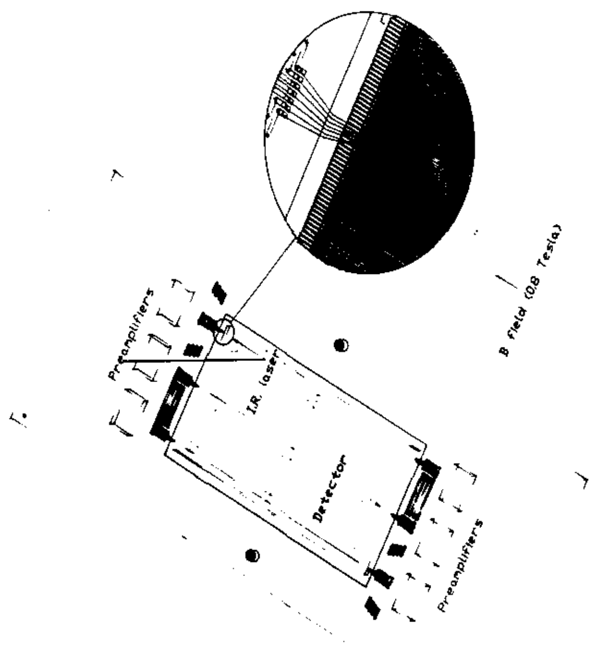
Preamplifiers
I.R. laser
Detector
Preamplifiers
B field (0.8 Tesla)

1176

Bipolar ASIC Noise Test

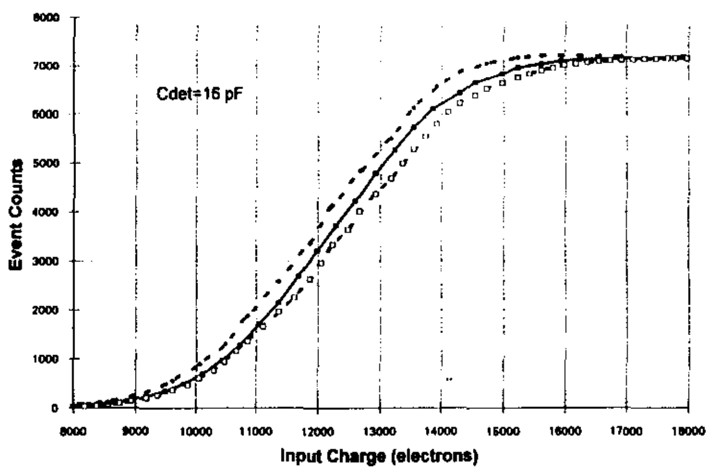

Conclusions

Things are progressing on schedule.

Bipolar

Prototype semi-custom chip produced
Packaged chip DC test under way
Wafer probing to be done
Full custom design to be submitted to Westinghouse with SDC

CMOS-1, 2

16-ch version layout to be done by July
VHDL-based design to be completed by October
FPGA implementation to be completed by October

MCM

Proof-of-principle fabrication to be completed by October

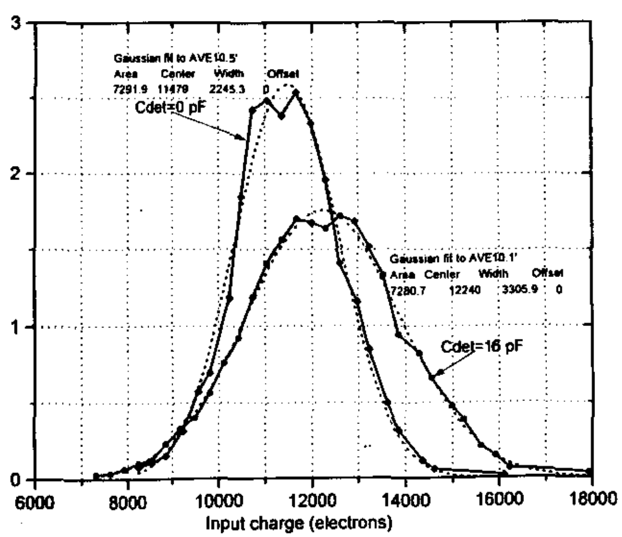

Prototype Test and Evaluation

Preliminary DC test (on packaged chips)
Power consumption: ~1.3mW/ch
Noise: ~1650 electrons RMS (Cd=16pF)
To be tested (wafer probe station being setup)
Noise, Time-walk
Radiation effects
Controllability

Full-Custom Design Features To Be Implemented
(*August '93 submission to Westinghouse sharing SDC Reticles*)

Reduce the positive feedback from the logic output pulse to the preamp input
Reduce impact from lower than expected PNP gains/leakages
Lower BLR cut-off frequency (additional 2pF)
Active load for input transistor
Increased open-loop gain on second stage: Darlington-pair or series-shunt
Use of current source for input transistor collector node
Built-in charge injection amplifiers for calibration
Reference current sources common to multiple chains
Threshold and housekeeping signal amplifiers

6.3.1.1

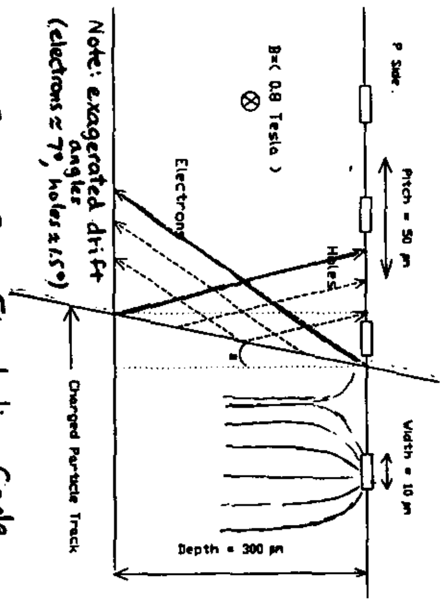

Santa Cruz Simulation Code (J.Leslie, A.Seiden, Y.Unno)

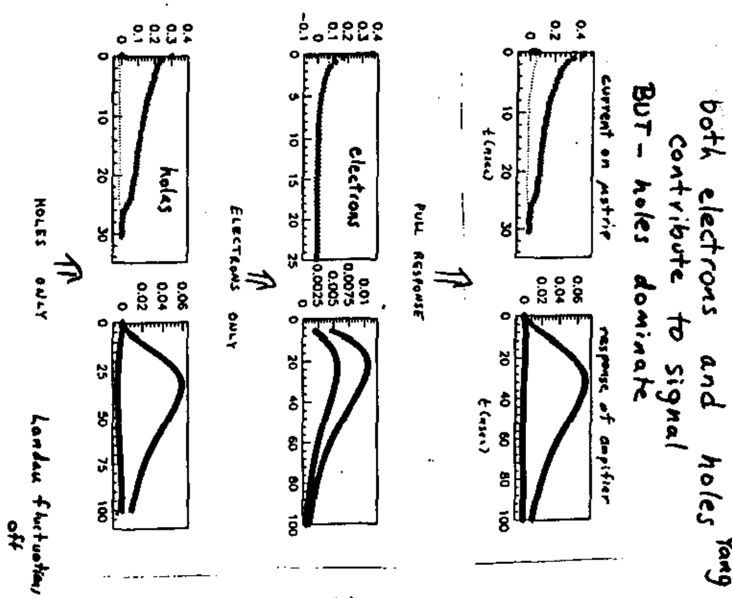

18cm Detector Length, Simulation Results

- increased detector capacitance: reduce inter-strip capacitance
- charge dispersion and delay for far-end injection: reduce strip line resistance
- increased leakage current
- tough to tackle noise, time-walk and power constraints

Noise (1.0pF/cm, 20 ohms/cm detector)
~2200 e- RMS, near-end injection
~2300 e- RMS, far-end injection

Interference noise, detector leakage current effects not considered

Time Walk (Leading edge trigger, 8k to 48k electrons input range, 6k equivalent threshold voltage): May have to use zero-crossing detection

24 ns, near-end
26 ns, far-end } These for 1/4 MIP; Much less for large signals

TDR93.XLS

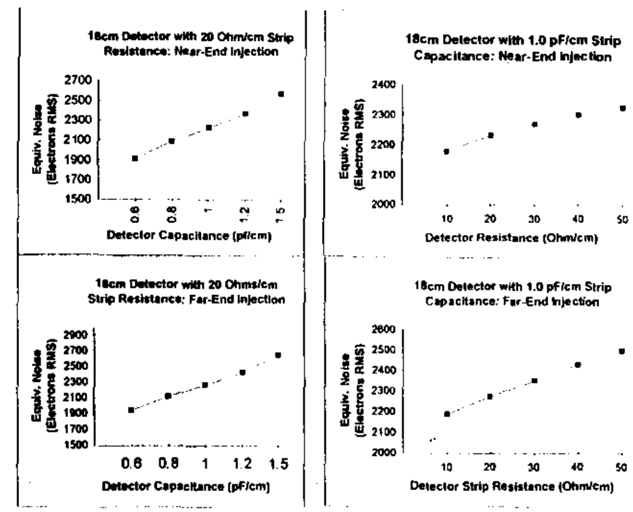

Page 2

Yang

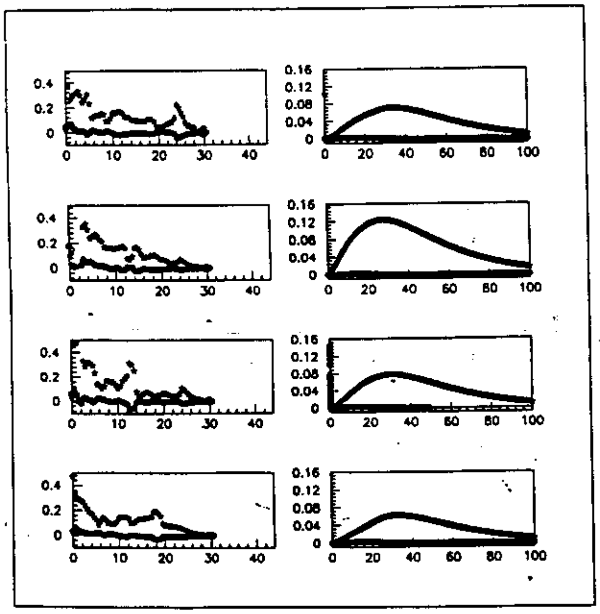

FIG. 2.

Yang

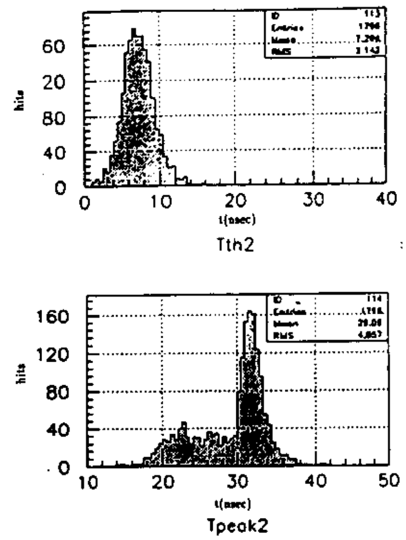

Figure 2. Timing of hits in microstrip detectors for two different time algorithms. The microstrip responses have been convoluted with a simulation of the preamplifier response having a 20 nanosecond shaping time. The upper figure results from using the time of threshold crossing with the threshold set to 1/4 mip. The lower figure results from using the peaking time of the convoluted pulse. 1000 particle crossings were simulated with 1796 hits (average 1.8 strips per crossing).

1155

Kollipara

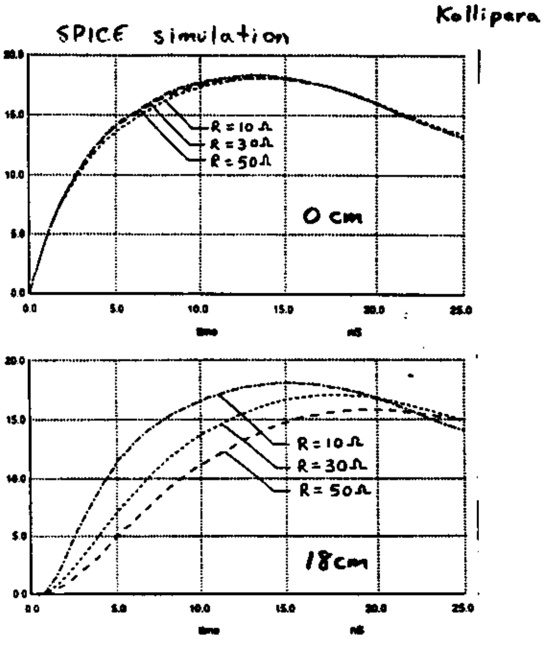

Figure 1. Calculated GEM preamplifier output waveforms as a function of strip resistance. The upper curves show the waveforms for 10 Ω/cm, 30 Ω/cm, and 50 Ω/cm where the charge is deposited at the end of the strip nearest the preamplifier. These curves show little dependence on strip resistance, as is expected. The lower curves show the waveforms for these strip resistances where the charge is deposited at the far end of the microstrip, 18 centimeters from the preamplifier. Here the effect of strip resistance is clear.

1194

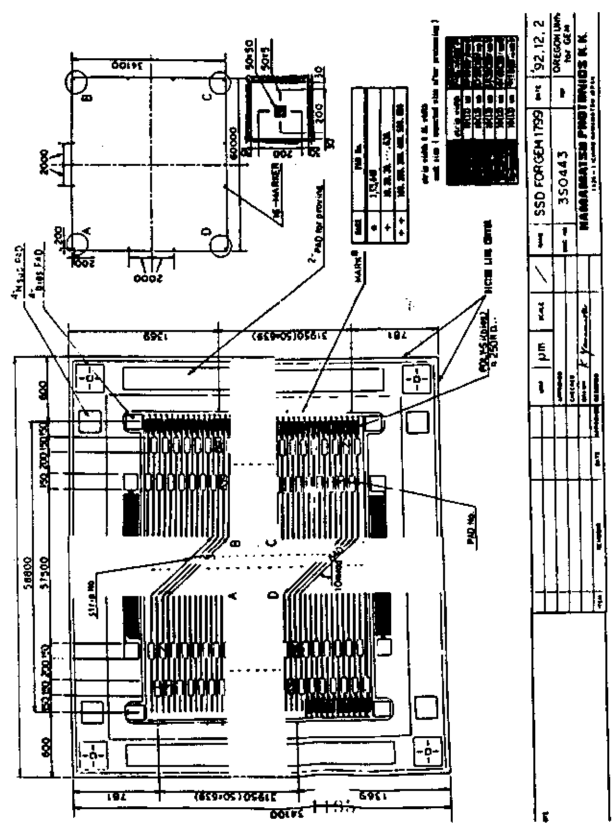

BROOKS

B-jet Identification

--Use "large" impact parameter of b-jets to separate them from other jets:

B-jet--Large impact parameter

Generic jet--average impact parameter

Separation is still difficult because:

1) Only an average of 5 particles/jet above 0.8 GeV/c
2) Impact parameter resolution at low momenta can be comparable to b-jet impact parameter.
3) Not all particles from jet have high impact parameter

1198

BROOKS

Cuts for B-jets

1) Look only at tracks found with pattern recognition (80-95% of tracks are found)

2) Look only at tracks with p_T>0.8 GeV/c

3) Cone cut on tracks of R<0.5

4) Impact Parameter has "correct"sign":

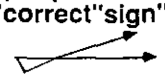

Ex: for tracks "above" axis, impact parameter should be "below" axis.

5) Three or more tracks must have impact parameter greater than 3σ, where σ is parameterized tracker resolution:

$\sigma=(24^{**}2 + (200/p_T)^{**}2 + (300^*\cos(\theta)/p_T)^{**}2)^{1/2}$

1199

BROOKS

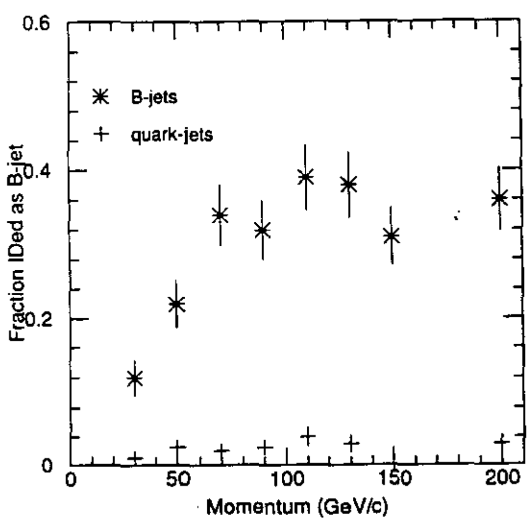

1200

BROOKS/LEE

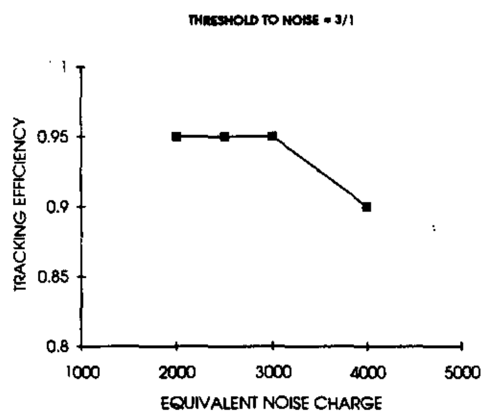

1201

Arodzero/Mason

LASER SOURCE FROM ≃0 cm
(fast, current sensitive preamp)

Printed: 27 APR 1993 at 12:51:00

hp running

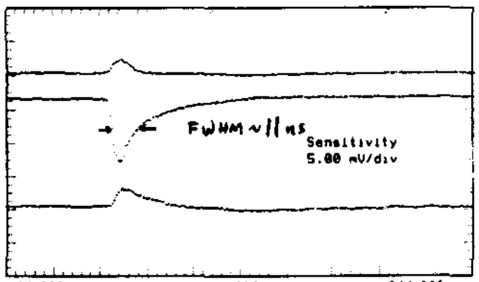

44.000 ns · 144.000 ns · 244.000 ns
#Avg · 20.0 ns/div · repetitive

1204

Arodzero/Mason

LASER SOURCE FROM 18 cm
(fast, current sensitive preamp)

Printed: 26 APR 1993 at 18:46:12

hp stopped

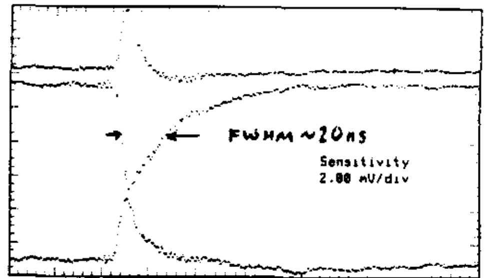

44.000 ns · 144.000 ns · 244.000 ns
#Avg · 20.0 ns/div · repetitive

1205

Arodzero/Mason

LASER ≈ 0 cm
(charge sensitive preamp ≈ GEM)

Printed: 07 MAY 1993 at 15:56:21

hp running

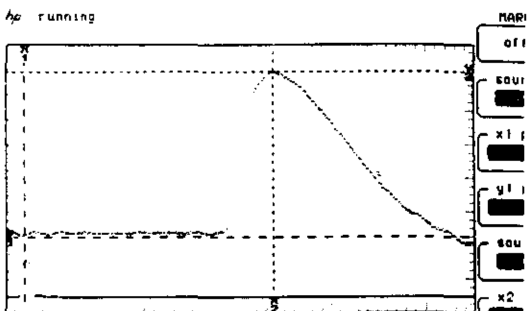

-8.000 ns · 92.000 ns · 192.000 ns
#Avg · 20.0 ns/div · repetitive

y2(2) 24.5312mV · x2(2) 107.200ns
y1(2) 0.00000 V · x1(2) 0.00000 s
delta y 24.5312mV · delta x 107.200ns
1/delta x 9.32836MHz

	Sensitivity	Offset	Probe	Coupling
Channel 2	5.00 mV/div	8.75000 mV	1:1	dc
Channel 4	1.00 V/div	3.50000 V	1:1	dc

Trigger Mode: Edge
On the Positive Edge of Channel4
Trigger Level(s)
Channel4 = 750.000 mV (noise reject OFF)
HoldOff = 100.000 ns

1206

Arodzero/Mason

LASER = 18 cm
(charge sensitive preamp ≈ GEM)

Printed: 07 MAY 1993 at 16:21:00

hp running

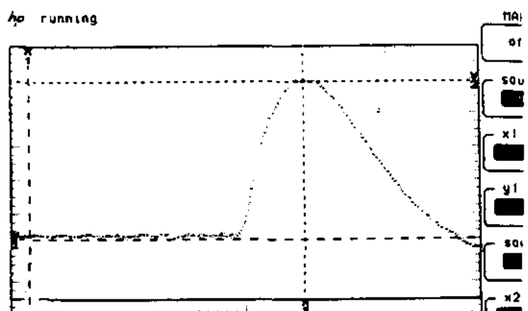

-8.000 ns · 92.000 ns · 192.000 ns
#Avg · 20.0 ns/div · repetitive

y2(2) 23.4375mV · x2(2) 116.800ns
y1(2) 0.00000 V · x1(2) 0.00000 s
delta y 23.4375mV · delta x 116.800ns
1/delta x 8.56164MHz

	Sensitivity	Offset	Probe	Coupling
Channel 2	5.00 mV/div	8.75000 mV	1:1	dc
Channel 4	1.00 V/div	3.50000 V	1:1	dc

Trigger Mode: Edge
On the Positive Edge of Channel4
Trigger Level(s)
Channel4 = 750.000 mV (noise reject OFF)
HoldOff = 100.000 ns

1207

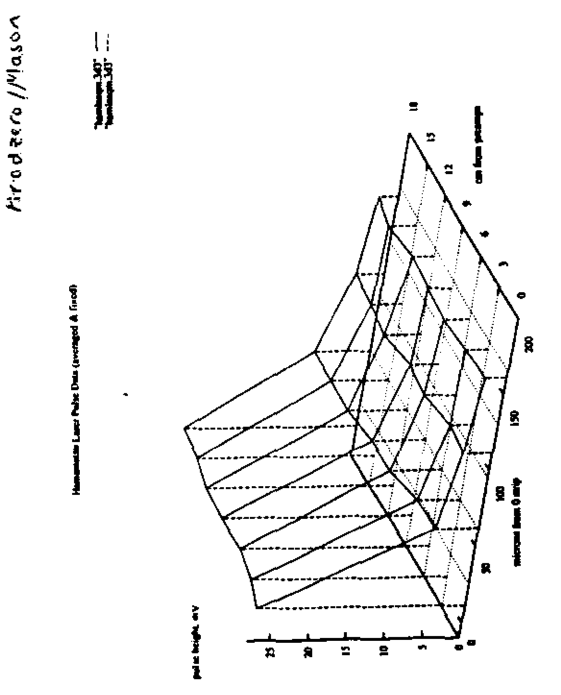

1205

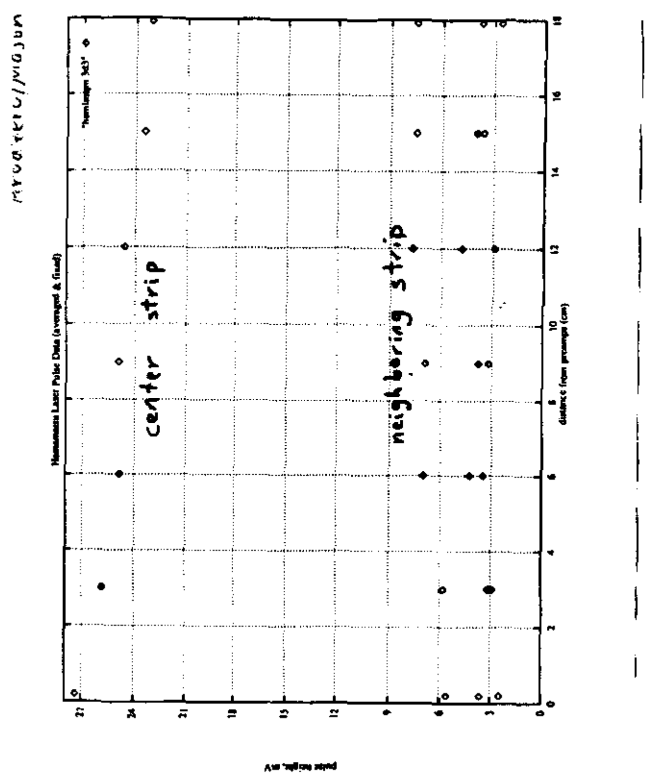

1209

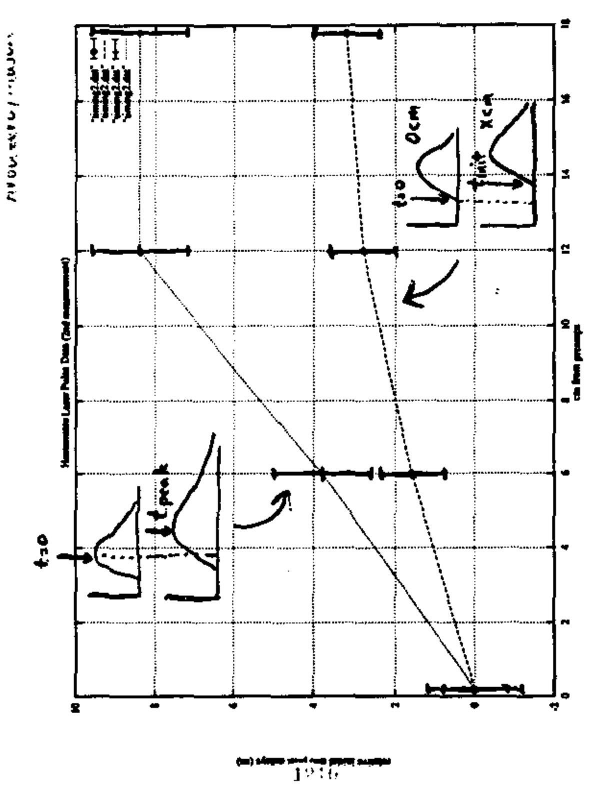

1210

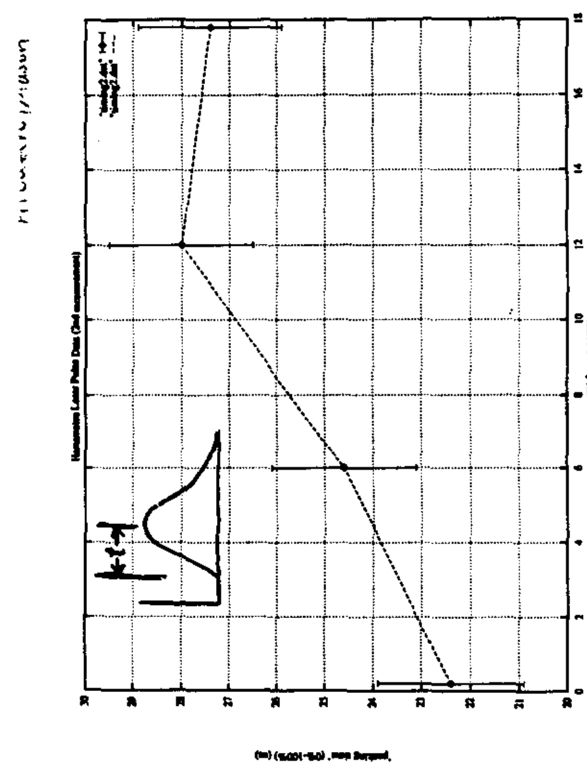

1211

OPTIMIZATION OF THE FORWARD REGION TO MINIMIZE NEUTRON AND PHOTON LEAKAGE

BRENT R. MOORE

UNIV. OF MISSISSIPPI

GEM COLLABORATION MTG.

SAN DIEGO, CA

MAY 12, 1993

MILIND DIWAN - SSCL

IOURI FISSIAK - SSCL

NIKOLAI MOKHOV - SSCL

LAURIE WATERS - LANL

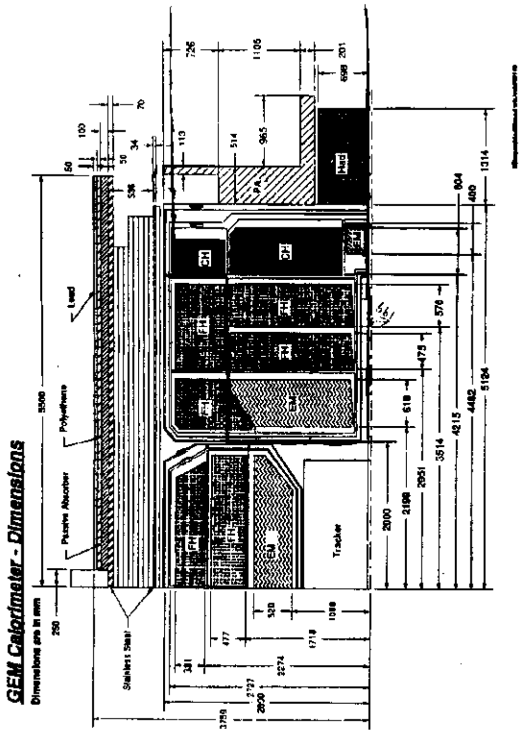

1216

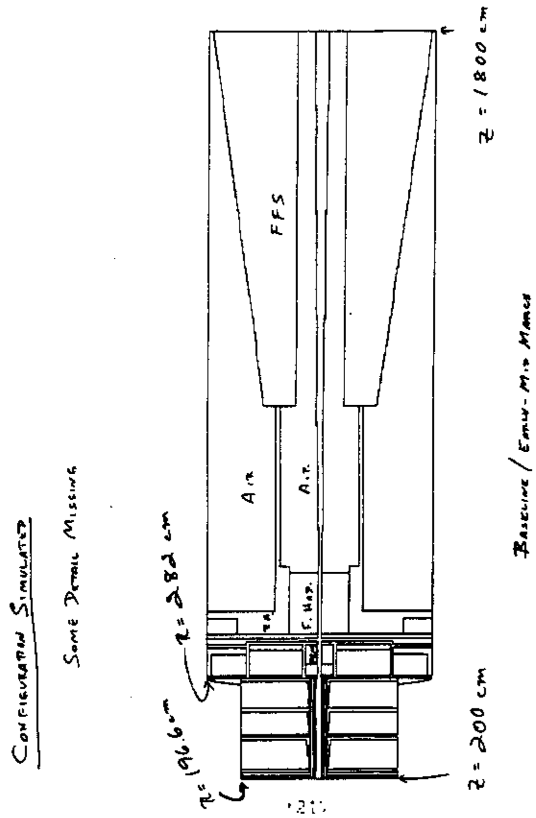

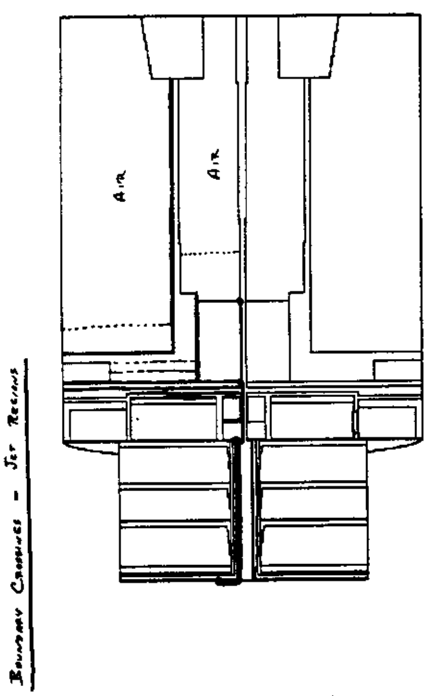

1000 DIJET EVENTS   20 TeV p ⟶ ⟵ 20 TeV p

10^8 Interactions/Second ⟶ 1000 Events = 10^{-5} seconds

	η Range	# Particles/Evt	Energy/Evt	
	X $\eta < 2.5$	33	0.04 TeV	(0.2 %)
Front	$2.5 < \eta < 4.4$	26	0.2	(1 %)
Middle	$4.4 < \eta < 5.6$	12	0.4	(2 %)
Under F-Had	$5.6 < \eta < 5.8$	2	0.2	(1 %)
	X $5.8 < \eta$	22	19.1	(96 %)
		95	20.0 TeV	

Transported 10 % of these Particles - Chosen Randomly

⇓

10^{-6} Seconds

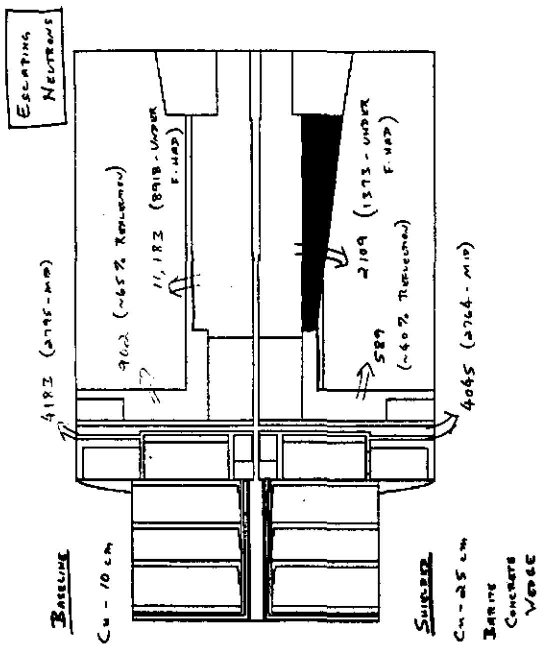

1220

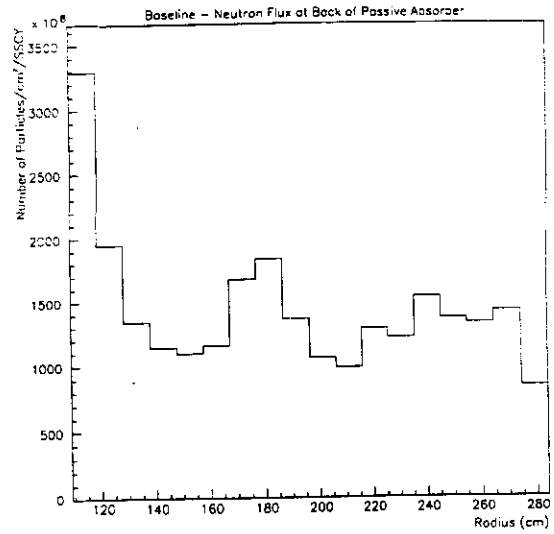

1221

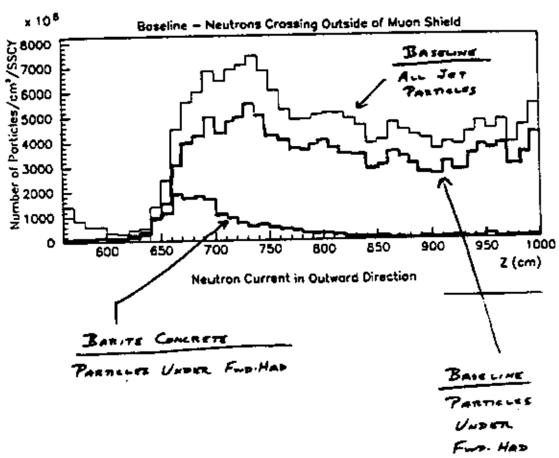

1222

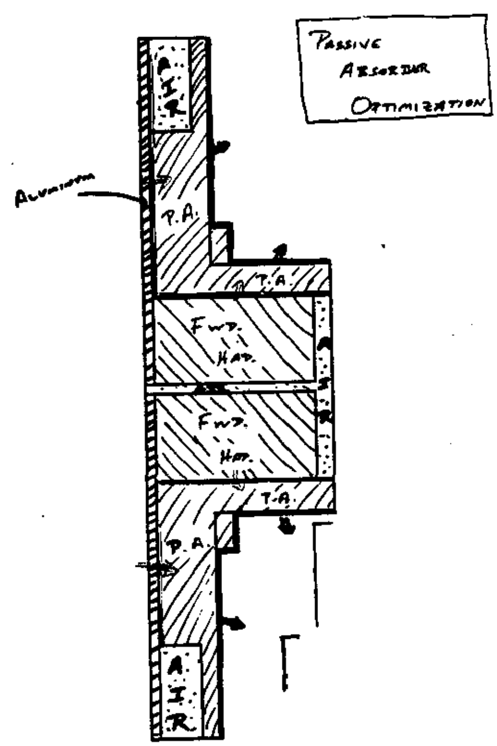

1223

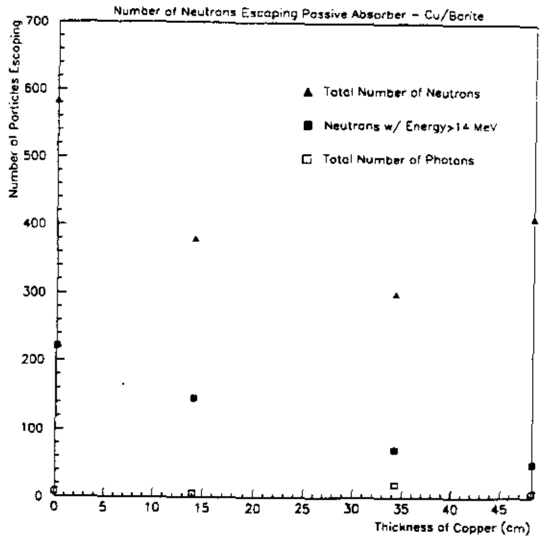

122.

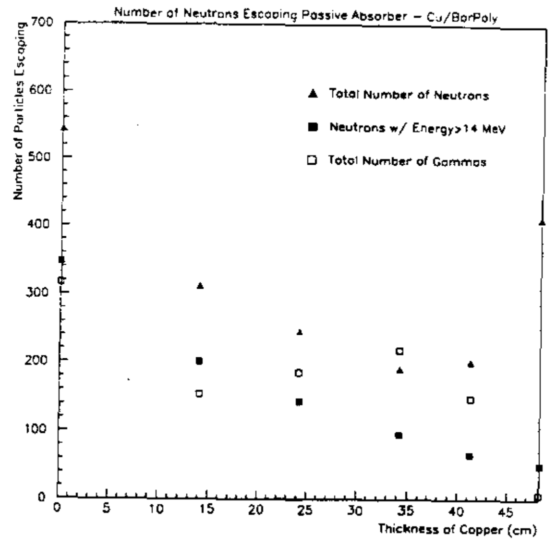

122.

Passive Absorber Leakage

Run	n > 14 MeV	0.1 < n < 14	Total n	γ > 1 MeV	0.1 < γ < 1	Total γ	—
Baseline Cu-No Block	59	379	540	5	15	20	1133
Cu 48.2	50	286	411	3	4	7	72½
Barite 48.2	221	274	584	2	7	8	925
B.Poly 48.2	348	166	544	5	197	316	76[illegible]
Cu 34.2 Barite 14.0	71	130	299	1	19	19	924
Cu 14.0 Barite 34.2	146	176	380	1	5	6	66[illegible]
Cu 14.0 B.Poly 34.2	200	103	312	11	142	153	361½
Cu 24.1 B.Poly 24.1	142	95	245	9	175	185	42.[illegible]
Cu 34.2 B.Poly 14.0	92	84	190	9	208	217	4[illegible]
Cu 41.2 B.Poly 7.0	66	82	201	7	141	148	34[illegible]
Cu 14.0 Barite 20.2 B.Poly 14.0	177	108	303	4	128	131	31[illegible]
Cu 14.0 B.Poly 20.2 Barite 16.0	163	188	397	6	11	18	8[illegible]
Cu 34.2 B.Poly 11.0 Cu 3.0	73	125	225	10	35	45	124[illegible]
Cu 34.2 B.Poly 8.0 Cu 6.0	64	142	232	2	13	16	6

122.

Conclusions

1 - Barite Concrete Wedge (Hollow Truncated Cone) Connecting PA and FFS Outside 25 cm thick Copper Cylinder is Recommended

2 - PA Materials and Thicknesses

Copper (No Block) - 1188

Copper (Block) - 726

Copper/Barite 14.0 34.2 - 644

Cu/B.Poly/Cu 34.2 8.0 6.0 - 625

3 - Forward Hadronic Calorimeter Projective on the Inside

4 - 5 cm Polyethylene on Inside of PA ?

W in front of Fwd. EM Reduces Escapes From Vacuum Gap (6183 → 1100)

122.

gemgen

A Generic Monte Carlo Generator Interface Package

- Motivation
- Overview
- Generator Interfaces
- Event Builder
- Pipeline Builder
- User Analysis Frame
- Examples

gem SCL

Irwin Sheer - Superconducting Super Collider Laboratory

1230

Motivation

- standardize generator output
- unbiased comparisons of different generators
- events which include signal and underlying minbias interactions
- pipelines of interleaved signal and pileup events.

gem SCL

Irwin Sheer - Superconducting Super Collider Laboratory

1231

Overview

- highly modular:
  - generator interfaces
  - event builder
  - pipeline builder
  - user analysis frame
- flexible:
  - many possible configurations
  - concurrent and/or sequential processes
  - customizable
  - expandable

gem SCL

Irwin Sheer - Superconducting Super Collider Laboratory

1232

Modularity

• gemisa (usrisa):	ISAJET interface
• gempyt (usrpyt):	PYTHIA interface
• gemspg (usrspg):	Single Particle/Jet Generator
• gemevb:	Event Builder
• gemplb:	Pipeline Builder
• usrgfa:	User Analysis Frame (Generator File Analysis)

gem SCL

Irwin Sheer - Superconducting Super Collider Laboratory

1233

Configurations

generator := gemisa, gempyt, or gemspg
(usrisa, usrpyt, or usrspg)

- interaction study:

- event study:

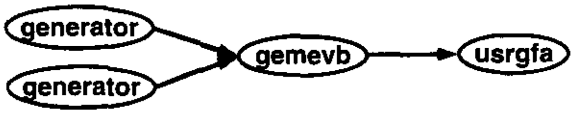

- pipeline study:

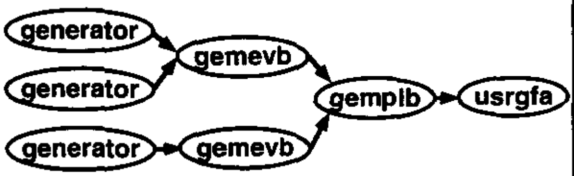

Irwin Sheer - Superconducting Super Collider Laboratory

1234

Concurrent and/or Sequential Operations

- concurrent:

- sequential:

- mixed:

Irwin Sheer - Superconducting Super Collider Laboratory

1235

Customization

- generator user hooks:
  - set defaults:

    subroutine usrdefs
    void usrdefs_()
  - initialize:

    subroutine usrinit
    void usrinit_()
  - event loop:

    subroutine usrevnt
    void usrevnt_()
  - termination:

    subroutine usrdone
    void usrdone_()

Irwin Sheer - Superconducting Super Collider Laboratory

1236

Expandability

Gemgen can be interfaced to any Monte Carlo generator whose output can be mapped into the standard /hepevt/ common block.

Irwin Sheer - Superconducting Super Collider Laboratory

1237

Generator Interfaces

- gemisa (usrisa): ISAJET interface
- gempyt (usrpyt): PYTHIA interface
- gemspg (usrspg): Single Particle/Jet Generator

Irwin Sheer - Superconducting Super Collider Laboratory

gem

gemisa

- run time parameter file:

```
*
* utg runtime parameters:
*
idebug_utg = 1    ! debug level
nprint_utg = 5    ! events to print using heplst
nskip_utg = 10    ! events to skip
mlist_utg = 1     ! heplst list mode
mxerr_utg = 10    ! maximum number of generator errors
mxsel_utg = -1    ! maximum number of events to select
timel_utg = 300   ! cpu time limit
iosel_utg = 1     ! select all events by default
ofile_utg = ' '   ! event output file
*
* isa runtime parameters
*
nprint_isa = 0    ! events to print using prtevt
nskip_isa = 0     ! events to skip
idtpf_isa = 0     ! decay table print flag
cseed_isa = '225694492122301.0' ! rand # seed
rnget_isa = ' '   ! rand # generator state get file
rnput_isa = 'random.dat' ! rand # generator state put file
dtble_isa = 'isajet.dat'  ! isajet decay table
jfile_isa = 'minbias.isa' ! isajet job file
end
```

Irwin Sheer - Superconducting Super Collider Laboratory

gem

gemisa

- ISAJET setup file:

```
TRUE MINIMUM BIAS SSC EVENTS
40000,100,0,0/
TWOJET
PT
5,100/
END
STOP
```

Irwin Sheer - Superconducting Super Collider Laboratory

gem

gempyt

- run time parameter file:

```
*
* utg runtime parameters
*
idebug_utg = 1    ! debug level
nprint_utg = 2    ! events to print using heplst
nskip_utg = 10    ! events to skip
mlist_utg = 1     ! heplst list mode
mxerr_utg = 10    ! maximum number of generator errors
mxsel_utg = -1    ! maximum number of events to select
timel_utg = 300   ! cpu time limit
iosel_utg = 1     ! select all events by default
ofile_utg = ' '   ! event output file
*
* pyt runtime parametes
*
sqrts_pyt = 40000.  ! center-of-mass energy
nevnt_pyt = 10      ! events to generate
nprint_pyt = 0      ! events to print using lulist
nskip_pyt = 0       ! events to skip
mlist_pyt = 1       ! lulist list mode
iseed_pyt = 19780503    ! rand # seed
rnget_pyt = ' '     ! rand # generator state get file
rnput_pyt = ' '     ! rand # generator state put file
jfile_pyt = 'H0_2gamma.pyt'  ! pythia job file
end
```

Irwin Sheer - Superconducting Super Collider Laboratory

gem

1241

gempyt

• **PYTHIA setup file:**

```
MSEL=16          ! H0 production
*
MDME(184,1)=0  ! supress H0 -> d d~
MDME(185,1)=0  ! supress H0 -> u u~
MDME(186,1)=0  ! supress H0 -> s s~
MDME(187,1)=0  ! supress H0 -> c c~
MDME(188,1)=0  ! supress H0 -> b b~
MDME(189,1)=0  ! supress H0 -> t t~
MDME(190,1)=-1 ! supress H0 -> l l~
MDME(191,1)=-1 ! supress H0 -> h h~
MDME(192,1)=0  ! supress H0 -> e- e+
MDME(193,1)=0  ! supress H0 -> mu- mu+
MDME(194,1)=0  ! supress H0 -> tau- tau+
MDME(195,1)=-1 ! supress H0 -> chi- chi+
MDME(196,1)=0  ! supress H0 -> g g
MDME(197,1)=1  ! allow H0 -> gamma gamma
MDME(198,1)=0  ! supress H0 -> gamma Z0
MDME(199,1)=0  ! supress H0 -> Z0 Z0
MDME(200,1)=0  ! supress H0 -> W+ W-
*
PMAS(C6,1)=140.    ! top quark mass
PMAS(C25,1)=80.    ! H0 mass
*
MDCY(C111,1)=0     ! inhibit pi0 decays
*
MSTJ(22)=4       ! decayed only if in cylinder
PARJ(73)=4.      ! cylinder radius (cm)
PARJ(74)=3500.   ! cylinder length (cm)
END
```


gemspg

• **run time parameter file:**

```
*
* utg runtime parameters
*
(suppressed)
*
* spg runtime parametes
*
nevnt_spg = 1000      ! number of events to generate
npart_spg = 1         ! number of particles per event
ipart_spg = 5         ! stdhep id of particle
iseed_spg = 19780503    ! rand # seed
moder_spg = 1         ! random  mode switch
modep_spg = 1         ! p or pt mode switch
nsppt_spg = 10        ! number of p or pt steps or points
nseta_spg = 10        ! number of eta steps or points
nsphi_spg = 10        ! number of phi steps or points
pptmn_spg = 1.        ! minimum p or pt
pptmx_spg = 100.      ! maximum p or pt
etamn_spg = -2.5      ! minimum eta
etamx_spg =  2.5      ! maximum eta
phimn_spg = 0.        ! minimum phi (degrees)
phimx_spg = 360.      ! maximum phi (degrees)
rnget_spg = ' '       ! random number state get file
rnput_spg = 'random.dat'    ! rand # state put file
jfile_spg = ' '       ! JETSET setup file
end
```


gemspg

• **JETSET setup file:**

```
*
* JETSET setup
*
PMAS(C6,1)=140.    ! top quark mass
PMAS(C25,1)=100.   ! H0 mass
*
MDCY(C111,1)=0     ! inhibit pi0 decays
*
MSTJ(22)=4       ! decayed only if in cylinder
PARJ(73)=4.      ! cylinder radius (cm)
PARJ(74)=3500.   ! cylinder length (cm)
END
```


Event Builder (gemevb)

- **reads 1 interaction from 'signal' stream**
- **reads a Poisson distributed random number of interaction from 'minbias' stream**
- **smears interaction vertices**
- **outputs event**

Pipeline Builder
(gemplb)

- reads n events from 'pileup' stream
- reads 1 event from 'signal' stream
- reads m events from 'pileup' stream
- outputs events

1246

User Analysis Frame
(usrgfa)

- user hooks for:

  - default setting
  - initialization
  - event processing
  - termination

- reads data from input stream
- data is avaliable to user via /hepevt/ common or hepevt_ struct
- selectively writes data to output stream

Framework for gemfast.

1247

Examples

- gemgen examples (/gem/demo/gemgen):
  - usrisa: customizable gemisa example
  - usrpyt: customizable gempyt example
  - usrspg: customizable gemspg example
  - usrgfa: example user analysis frame
- gemfast examples (/gem/demo/gemfast)

See README files and manpages or additional help

1248

SSCgen

A C++ object oriented re-implementation of gemgen

Coming soon to a computer near you...

1249